UNIVERSITAT ROVIRA i VIRGILI

Gold-Catalyzed Intermolecular Reactions of Alkynes with Alkenes: Novel Reactivities and Global Mechanistic Picture

María Elena de Orbe Izquierdo

DOCTORAL THESIS
2018

UNIVERSITAT ROVIRA I VIRGILI
GOLD-CATALYZED INTERMOLECULAR REACTIONS OF ALKYNES WITH ALKENES: NOVEL REACTIVITIES AND GLOBAL MECHANISTIC PICTURE
María Elena de Orbe Izquierdo

UNIVERSITAT ROVIRA I VIRGILI
GOLD-CATALYZED INTERMOLECULAR REACTIONS OF ALKYNES WITH ALKENES: NOVEL REACTIVITIES AND GLOBAL MECHANISTIC PICTURE
María Elena de Orbe Izquierdo

María Elena de Orbe Izquierdo

Gold-Catalyzed Intermolecular Reactions of Alkynes with Alkenes: Novel Reactivities and Global Mechanistic Picture

DOCTORAL THESIS

Supervised by Prof. Antonio M. Echavarren

Institut Català d'Investigació Química (ICIQ)

UNIVERSITAT ROVIRA I VIRGILI

Tarragona 2018

UNIVERSITAT ROVIRA I VIRGILI
GOLD-CATALYZED INTERMOLECULAR REACTIONS OF ALKYNES WITH ALKENES: NOVEL REACTIVITIES AND GLOBAL MECHANISTIC PICTURE
María Elena de Orbe Izquierdo

UNIVERSITAT ROVIRA I VIRGILI

I STATE that the present study, entitled "Gold-Catalyzed Intermolecular Reactions of Alkynes with Alkenes: Novel Reactivities and Global Mechanistic Picture", presented by María Elena de Orbe Izquierdo for the award of the degree of Doctor, has been carried out under my supervision at the Institut Català d'Investigació Química (ICIQ).

Tarragona, June 28th, 2018

Doctoral Thesis Supervisor

Prof. Antonio M. Echavarren Pablos

UNIVERSITAT ROVIRA I VIRGILI
GOLD-CATALYZED INTERMOLECULAR REACTIONS OF ALKYNES WITH ALKENES: NOVEL REACTIVITIES AND GLOBAL MECHANISTIC PICTURE
María Elena de Orbe Izquierdo

A mis padres

UNIVERSITAT ROVIRA I VIRGILI
GOLD-CATALYZED INTERMOLECULAR REACTIONS OF ALKYNES WITH ALKENES: NOVEL REACTIVITIES AND GLOBAL MECHANISTIC PICTURE
María Elena de Orbe Izquierdo

"El mar sería menos
si le faltara una gota"

Teresa de Calcuta

UNIVERSITAT ROVIRA I VIRGILI
GOLD-CATALYZED INTERMOLECULAR REACTIONS OF ALKYNES WITH ALKENES: NOVEL REACTIVITIES AND GLOBAL MECHANISTIC PICTURE
María Elena de Orbe Izquierdo

I would like to thank Prof. Antonio M. Echavarren for letting me pursue my PhD studies in his research group at the Institut Català d'Investigació Química (ICIQ) and for trusting me from the beginning. Not only have I learned about chemistry, but also about life.

I would like to thank Prof. Feliu Maseras for introducing me in the field of computational chemistry, which has been essential for this thesis, and for the fruitful collaboration. I thank the members of his research group Dr. María Besora, Ignacio Funes and Víctor Fernández for teaching me about DFT calculations and for crucial discussions on this regard. I am grateful as well to the system manager Martin Gumbau.

I would like to express my thanks to Prof. Kim D. Janda for giving me the unique opportunity to stay four months in his research group at The Scripps Research Institute in California, where I enjoyed working on fascinating projects about chemical biology, and for his hospitality. I thank all the members of his group for being so nice, particularly Dr. Jon Ashley, Dr Major Gooyit, Dr. Kensaku Anraku, Dr. Atsushi Kimishima, Dr. Candy Hwang and Dr. Cody Wenthur. Special thanks to whom I collaborated with: Dr. Pedro Miranda, Lauren Smith, Dr. Bin Andrew Zhou, Nicholas Jacob and Ryan Shirey. Also, thanks to Terri Normann for receiving me so kindly and the funniest roommates: Charity, Evan, Víctor, Dr. Taishi L. Kimura and Dr. Ana M. Gamo (you made the difference).

I would like to say thanks to the research support units at ICIQ: Nuclear Magnetic Resonance, High Resolution Mass Spectrometry (Dr. Noemí Cabello for her archeological findings), X-Ray Diffraction, CELLEX - High Throughput Experimentation, Chemical Reaction Technologies, Chromatography, and Informatics.

Regarding the members of Prof. Echavarren´s group, I would like to thank Sònia Gavaldà, the best administrative coordinator, for her help with all and for taking care of each of us. I want to thank Imma Escofet, the most efficient laboratory engineer and the personification of the diplomacy, for being always available to resolve any problem, for her ability to listen and for our discussions about both chemistry and life. I thank Carla Obradors for her warm welcome in Tarragona (and in San Diego) and together with Anna Homs, for their impeccable research work, which has been key for this thesis. I would like to say thanks to both of them as well as Morgane Gaydou, Yahui Wang, Ruth Dorel, Dr. Ricarda Miller, Dr. José M. Muñoz, Dr. Javier Carreras and Dr. Beatrice Ranieri for their tips, suggestions and answers to my questions at the very beginning. In general, I thank all the labmates for sharing laboratory tasks, seminars, and hours of work and fun too, in and out of ICIQ, in particular Bart Herlé, Alba González (Tarragona was just the starting point), Dr. Hanna Bruss, Dr. Miguel Peña (always ready to make the funniest comment), Hilary Kerchner and Jordan Boothe (amazing visiting students), Zhouting Rong, Dr. Jean-Simon Suppo, Giuseppe Zuccarello, Dr. Dagmar Scharnagel, Joan Guillem Mayans, Otilia Stoica…Furthermore, I am very grateful to with

whom I was fortunate to collaborate, especially Dr. Ophélie Quinonero, Laura Amenós, Mariia S. Kirillova and Margherita Zanini.

Thanks to Pilar Calleja for always transmitting optimism with a huge smile, to Xiang Yin for our philosophical conversations and pointing out that chem-is-try, and to Dr. G. Araceli Fernández (*recopada*) for radiating positivity and bringing people together to enjoy the life. Special thanks to Dr. Fedor Miloserdov, Dr. Philipp M. Holstein and Dr. Juan M. Sarria (*Juanito maravilla*) for great moments and wise advices. From both professional and personal perspectives, there are no enough words to express my MANY THANKS to the following wonderful people who are always available to help anyone: Dr. Oscar Pablo (and his personality) and Dr. Michael E. Muratore (and his dedication).

I am very grateful to the best friends I could have next to me in the laboratory: Sofía Ferrer and Ekaterina S. Smirnova. Sofía, the personification of the perseverance and the willpower, thanks for being an exceptionally good and patient person every single day. Katya, the most energetic person ever, MANY THANKS for ALL during these years: for being so attentive, for making me smile so often, for helping me in every situation…

In addition to the labmates, I have had the pleasure to meet and live unforgettable moments with friends such as Jeroen Rintjema (thanks for all your help and for great moments of sports and beyond), Rosie Somerville (swimming each morning solves everything), Dr. Sébastien Bouvet, Léa Lalou, Klaudia Michaliszyn, Sergio Sopeña (facing the challenge of organizing activities), Pablo Garrido, Pedro Benavente, Madalina Mihai…Thanks to all of them and to Blanca Vea-Murguía for making my time in Tarragona really enjoyable.

Marino, gracias por haberme hecho crecer mucho como persona y por hacer que estuviera más feliz en tantos momentos a lo largo de este camino en Tarragona.

También quiero agradecer el apoyo que me han regalado amigos y familiares desde kilómetros de distancia. Muchas gracias a Estefanía, Laura, Sara, Paloma Ballenato (mil gracias por hacer que cambie el chip tan fácilmente), Julia, Marina y Paloma Merino. Muchísimas gracias a la familia que soy tan afortunada de tener, por poder contar con ellos en cualquier momento, en especial a Dr. Ignacio de Orbe (por los consejos profesionales), M. Teresa, Mari Tere, Teresa (por ser la voz de la experiencia y por tus diseños de portada), Laura (por ser una magnífica *coach*), Gemma, Silvia e Irene (por dar siempre más del 100% por todos). Por último, lo más importante, infinitas gracias a mis padres, M. Ángeles y Javier, a quienes debo lo que soy y hasta donde he llegado, gracias por enseñarme los valores que definen mi día a día y el valor del trabajo, por animarme tanto y ayudarme incondicionalmente: esta tesis es también vuestra.

We thank Severo Ochoa Excellence Acreditation 2014-2018 (SEV-2013-0319 and Severo Ochoa predoctoral fellowship SVP-2014-068611 to M.E.d.O.), the European Research Council (Advanced Grant No. 321066), Agencia Estatal de Investigación (AEI/FEDER, UE, CTQ2013-42106-P and CTQ2016-75960-P), the Agència de Gestió d'Ajuts Universitaris i de Recerca (AGAUR, 2014 SGR 818 and 2017 SGR 1257) and CERCA Program / Generalitat de Catalunya for financial support.

UNIVERSITAT ROVIRA I VIRGILI
GOLD-CATALYZED INTERMOLECULAR REACTIONS OF ALKYNES WITH ALKENES: NOVEL REACTIVITIES AND GLOBAL MECHANISTIC PICTURE
María Elena de Orbe Izquierdo

At the time of writing this manuscript, part of the results described herein have been published in:

Intermolecular [2+2] Cycloaddition of Alkynes with Alkenes Catalyzed by Gold(I).
de Orbe, M. E.; Echavarren, A. M.
Org. Synth. **2016**, *93*, 115–126.
Featured article.

Cyclobutene vs 1,3-Diene Formation in the Gold-Catalyzed Reaction of Alkynes with Alkenes: The Complete Mechanistic Picture.
de Orbe, M. E.; Amenós, L.; Kirillova, M. S.; Wang, Y.; López-Carrillo, V.; Maseras, F.; Echavarren, A. M.
J. Am. Chem. Soc. **2017**, *139*, 10302–10311.

Broadening the Scope of the Gold Catalyzed [2+2] Cycloaddition: Synthesis of Vinylcyclobutenes and Further Transformations.
de Orbe, M. E.; Echavarren, A. M.
Eur. J. Org. Chem. **2018**, 2740–2752.
Selected as Very Important Paper. Front Cover.

In addition, other results which are not that related to the topic of this manuscript have been published in:

Broad-Scope Rh-Catalyzed Inverse-Sonogashira Reaction Directed by Weakly Coordinating Groups.
Tan, E.; Quinonero, O.; de Orbe, M. E.; Echavarren, A. M.
ACS Catal. **2018**, *8*, 2166–2172.

Synthetic molecules for disruption of the MYC protein-protein interface
Jacob, N. T.; Miranda, P. O.; Shirey, R. J.; Gautam, R.; Zhou, B.; de Orbe, M. E.; Hixon, M. S.; Hart, J. R.; Ueno, L.; Vogt, P. K.; Janda, K.D.
Bioorg. Med. Chem. **2018**, DOI: 10.1016/j.bmc.2018.07.019.

UNIVERSITAT ROVIRA I VIRGILI
GOLD-CATALYZED INTERMOLECULAR REACTIONS OF ALKYNES WITH ALKENES: NOVEL REACTIVITIES AND GLOBAL MECHANISTIC PICTURE
María Elena de Orbe Izquierdo

Table of Contents

Prologue 19
Abbreviations and Acronyms 21
Abstract 23
Short Summary 25
General Objectives 27

General Introduction
Gold in Homogeneous Catalysis 29
Gold Intermediates upon Activation of Multiple Bonds 32
Cycloisomerizations of 1,*n*-Enynes 35
Intermolecular Reactions of Alkynes with Alkenes by Gold(I) 39

Chapter 1. Cyclobutene *vs.* Diene Formation in Gold-Catalyzed Reactions of Alkynes with Alkenes
Introduction 47
Objectives 55
Results and Discussion 56
On the Methods of Quenching the Gold-Catalyzed Reactions 56
Arylalkynes Leading to Cyclobutenes and 1,3-Dienes 59
1,3-Butadiynes Leading to Cyclobutenes 64
Mechanism for the Formation of Cyclobutenes and Dienes 68
Deuteration and Monitoring Experiments 68
Theoretical Studies 70
Reaction of Phenylacetylene with α-Methylstyrene 70
Reaction of (*o*-Bromophenyl)acetylene with α-Methylstyrene 74
Reaction of 1-Phenyl-1,3-butadiyne 78
Key Cyclopropyl Gold(I) Carbenes: Generation and Reactivity 81
Activation of Acetylene by Gold(I) 85
Conclusions 87
Experimental Part 89

General Information 89
Synthetic Procedures and Characterization Data 90
Experimental Mechanistic Studies 125
Theoretical DFT Calculations 127
Computational Methods 127
Computed Structures and Energies 128

Chapter 2. Cyclobutenes by Gold-Catalyzed [2+2] Cycloaddition: Extension and Further Transformations

Introduction 151
Objectives 155
Results and Discussion 156
Synthesis of Vinylcyclobutenes 156
Reaction of Alkynes with Cycloheptatriene 161
Combining Cyclobutenes with Gold(I) Carbenes to Give Cyclopentenes 164
Transformations of Cyclobutenes by Cycloaddition or Ring Opening 174
Turning Cyclobutenes into 2,3-Dihydrofurans 177
Conclusions 182
Recent Related Results by Other Groups 184
Experimental Part 185
General Information 185
Synthetic Procedures and Characterization Data 185

Chapter 3. Novel Pathways in Gold-Catalyzed Reactions of Bromoalkynes

Introduction 221
Hydroarylation of Alkynes 221
Reactivity of Haloalkynes Under Gold Catalysis 226
State-of-art on the Synthesis of Skipped Enynes 227
Objectives 230
Results and Discussion 231
Optimization of the Synthesis of Skipped Enynes 231
Scope of the Synthesis of Skipped Enynes 238

Reaction of Bromoalkynes with Allenylsilanes 242
Allylation/Hydroarylation of Bromoalkynes 243
Mechanistic Insight into Gold-Catalyzed Reactions of Bromoalkynes 249
Experiments with σ-Gold and σ,π-Digold Alkyne Complexes 249
Mechanism of the Formation of Skipped Enynes 251
Mechanism of the Reaction of Bromoalkynes with Allenylsilanes 257
Mechanism of the Allylation/Cyclization Cascade 258
Extension to the Intramolecular Reaction of 1-Bromo-1,6-enynes 262
Towards the Enantioselective Synthesis of Skipped Enynes 263
Conclusions 273
Experimental Part 275
General Information 275
Synthetic Procedures and Characterization Data 275
Experimental Mechanistic Studies 296
General HTE Procedure for the Enantioselective Reactions 302
Theoretical DFT Calculations 303
Computational Methods 303
Computed Structures and Energies 303

General Conclusions 317
Appendix 319

UNIVERSITAT ROVIRA I VIRGILI
GOLD-CATALYZED INTERMOLECULAR REACTIONS OF ALKYNES WITH ALKENES: NOVEL REACTIVITIES AND GLOBAL MECHANISTIC PICTURE
María Elena de Orbe Izquierdo

Prologue

This Doctoral Thesis manuscript is divided into four main parts: a general introduction about gold catalysis and three chapters about the research results. Each chapter comprises five sections including a more specific introduction on the research topic, the objectives, the discussion of the results, the conclusions and, lastly, the experimental part.

The **General Introduction** explains the fundamentals of homogeneous gold catalysis, focusing on the activation of unsaturated C–C bonds as well as the intra- and intermolecular reactions of alkynes with alkenes.

The **Chapter 1** collects the investigations on the formation of cyclobutenes and dienes in the gold(I)-catalyzed reaction of aryl and alkynyl substituted alkynes with alkenes. An in-depth mechanistic study by both experimental and computational techniques is presented. Since this project was initiated with experiments of Verónica López-Carrillo, Laura Amenós, Mariia S. Kirillova, and Yahui Wang, some of their results are included for consistency. Most of this work, in collaboration with Prof. Feliu Maseras (ICIQ), was published in *J. Am. Chem. Soc.* **2017**, *139*, 10302–10311, and the key experimental procedure in *Org. Synth.* **2016**, *93*, 115–126.

The **Chapter 2** contains the extension of the gold(I)-catalyzed [2+2] cycloaddition of alkynes with alkenes to access 1-vinyl-, 3-vinyl- and 3-alkynylcyclobutenes. Moreover, it gathers the development of one-pot transformations of cyclobutenes into diverse skeletons. Most of these results were published in *Eur. J. Org. Chem.* **2018**, 2740–2752.

The **Chapter 3** discloses the discovery of novel gold-catalyzed reactions of bromoalkynes with allylsilanes to construct skipped enynes and skipped dienes. The detailed investigations on the mechanism of such processes are exposed. Dr. Ophélie Quinonero joined the project mainly for the studies on the scope of the transformations and Margherita Zanini is now continuing our investigations, therefore part of their results is also included for completeness. This work has not been published yet.

In addition, a summary of the thesis and the general objectives are detailed at the beginning of this manuscript. The manuscript ends with the general conclusions and an appendix showing the publications which were not covered herein.

Abbreviations and Acronyms

The abbreviations and the acronyms used in this manuscript follow the recommendations published in the "Guidelines for Authors" of *The Journal of Organic Chemistry*. Additional abbreviations and acronyms employed in this manuscript are listed herein:

APCI	Atmospheric pressure chemical ionization
BAr_4^F	Tetrakis[3,5-bis(trifluoromethyl)phenyl]borate
brsm	Based on recovered starting material
ee	Enantiomeric excess
ESI	Electrospray Ionization
IMes	1,3-Bis(2,4,6-trimethylphenyl)imidazole-2-ylidene
IPr	1,3-Bis(2,6-diisopropylphenyl)imidazol-2-ylidene
JohnPhos	(2-Biphenyl)di-*tert*-butylphosphine
L	Ligand
NTf_2	Bis(trifluoromethyl)imidate
SFC	Supercritical Fluid Chromatography
*t*BuXPhos	2-Di-*tert*-butylphosphino-2′,4′,6′-triisopropylbiphenyl
TMS	Trimethylsilyl
Tol	4-Methylphenyl
XPhos	2-Dicyclohexylphosphino-2',4',6'-triisopropylbiphenyl

UNIVERSITAT ROVIRA I VIRGILI
GOLD-CATALYZED INTERMOLECULAR REACTIONS OF ALKYNES WITH ALKENES: NOVEL REACTIVITIES AND GLOBAL MECHANISTIC PICTURE
María Elena de Orbe Izquierdo

Abstract

Gold catalysis is a powerful tool to build C–C bonds and create molecular complexity *via* the selective activation of alkynes. Despite the advances in intramolecular reactions of alkynes with alkenes, the intermolecular version remains a challenge since the final products are also alkenes which compete with the initial substrates leading to undesired oligomerizations. Among the few intermolecular reactions that have been reported, we found puzzling the fact that terminal electron-rich arylalkynes react with alkenes by [2+2] cycloaddition to afford cyclobutenes, whereas electron-deficient alkynes lead to 1,3-dienes or lactones. In order to shed light on these fundamental gold(I)-catalyzed processes, during this Doctoral Thesis we have explored the reactivity of a wider range of alkynes and investigated in detail the reaction mechanisms both experimentally and by DFT calculations.

We discovered that *ortho*-substituted arylalkynes react with alkenes in the presence of gold(I) catalysts to give also 1,3-dienes by a metathesis-type process. In contrast, we found that less sterically demanding 1,3-butadiynes undergo [2+2] cycloaddition with alkenes to build 1-alkynylcyclobutenes. DFT calculations showed that the key intermediates in these transformations are the cyclopropyl gold(I) carbenes, whose steric and electronic properties control their evolution through distinct pathways close in energy. On one hand, the formation of regioisomeric cyclopropyl gold(I) carbenes depends on the electronic nature of the initial alkyne: the gold carbene is generated at the alkyne carbon in β-position to electron-donating groups and in α-position to electron-withdrawing groups. On the other hand, mainly the steric effects among the substituents in the cyclopropyl gold(I) carbenes determine whether these intermediates undergo a stepwise rearrangement to construct 1,3-dienes or a ring expansion to form cyclobutenes. The intermediacy of cyclopropyl gold(I) carbenes was supported by independently generating them and examining their reactivity. This comprehensive mechanistic study laid the ground for designing novel reaction pathways.

Cyclobutenes are important frameworks in natural and biologically active products as well as versatile synthetic intermediates. In order to prepare cyclobutenes regioselectively, the

gold(I)-catalyzed [2+2] cycloaddition of alkynes with alkenes is a convenient straightforward approach. However, this methodology initially seemed to be restricted to the use of arylalkynes. After extending the reaction to 1,3-butadiynes, we additionally broadened the scope to 1,3-enynes and polyenes to access more functionalized 1-vinyl-, 3-vinyl- and 3-alkynylcyclobutenes. This methodology is complementary to the previously reported metal-catalyzed [2+2] cycloadditions to forge cyclobutenes. Furthermore, we developed one-pot procedures to convert the valuable cyclobutenes into a variety of architectures *via* cycloaddition, ring opening, expansion or contraction.

Finally, we designed a novel intermolecular reaction of bromoalkynes with allylsilanes catalyzed by gold(I) which renders a totally different outcome: skipped enynes *via* a cross-coupling-type process or skipped dienes *via* allylation/cyclization cascade. Based on experiments and theoretical calculations, the mechanism of these reactions was proposed to proceed *via* an unprecedented rearrangement through cyclic bromonium intermediates.

Short Summary

Gold catalysis creates molecular complexity via selective activation of alkynes. Intermolecular reactions of alkynes with alkenes remain challenging, since the alkenyl products compete with the substrates leading to oligomerizations. Herein, we examined the reactivity of diverse alkynes and the reaction mechanisms experimentally and computationally.

Gold(I)-catalyzed [2+2] cycloaddition of arylalkynes with alkenes furnish regioselectively cyclobutenes. Now we found that *ortho*-substituted arylalkynes give 1,3-dienes by a metathesis-type process, whereas less sterically demanding 1,3-butadiynes lead to 1-alkynylcyclobutenes. The key intermediates are cyclopropyl gold(I) carbenes, whose electronic and steric properties determine their evolution through pathways close in energy.

Cyclobutenes are important frameworks in bioactive products and versatile synthons. We expanded the gold(I)-catalyzed [2+2] cycloaddition to access more functionalized vinylcyclobutenes. Furthermore, we developed one-pot transformations of cyclobutenes into other valuable architectures.

Finally, we discovered an unprecedented rearrangement in gold(I)-catalyzed intermolecular reactions of bromoalkynes with allylsilanes to form 1,4-enynes via a cross-coupling-type process or 1,4-dienes via allylation/cyclization.

Breve Resumen

La catálisis de oro crea complejidad molecular mediante activación selectiva de alquinos. Las reacciones intermoleculares de alquinos con alquenos suponen un reto, al competir los productos alquenílicos con los sustratos dando oligomerizaciones. Aquí, examinamos la reactividad de diversos alquinos y los mecanismos experimentalmente y computacionalmente.

La cicloadición [2+2] de arilalquinos con alquenos catalizada por oro forma regioselectivamente ciclobutenos. Ahora encontramos que arilalquinos *orto*-sustituidos generan 1,3-dienos en un proceso tipo metátesis, pero 1,3-butadiinos menos estéricamente impedidos dan 1-alquinilciclobutenos. Los intermedios clave son ciclopropil carbenos de oro, cuyos efectos estéricos y electrónicos determinan su evolución por caminos próximos en energía.

Los ciclobutenos son importantes esqueletos en productos bioactivos y sintones versátiles. Así, expandimos la cicloadición [2+2] para sintetizar vinilciclobutenos más funcionalizados. Además, transformamos los ciclobutenos en otras valiosas estructuras.

Finalmente, descubrimos un mecanismo novedoso en reacciones intermoleculares de bromoalquinos con alilsilanos catalizadas por oro que proporcionan 1,4-eninos mediante un proceso de tipo acoplamiento cruzado o 1,4-dienos mediante ciclación.

General Objectives

The main objective of this Doctoral Thesis was the examination of gold-catalyzed intermolecular reactions of a wide range of alkynes with alkenes to access different architectures. In particular, we focused on the following three general goals:

- The detailed mechanistic study on the fundamental gold(I)-catalyzed intermolecular reactions of terminal alkynes with alkenes leading to cyclobutenes and dienes in order to lay the mechanistic foundations for further developments.
- The extension of the scope of the gold(I)-catalyzed [2+2] cycloaddition of alkynes with alkenes to furnish more functionalized cyclobutenes and the development of straightforward one-pot transformations of the cyclobutenes into a variety of skeletons.
- The design of novel pathways in intermolecular reactions of bromoalkynes with allylsilanes catalyzed by gold(I) and the investigations on the corresponding reaction mechanisms.

Each chapter of this manuscript provides a more detailed description of the corresponding objectives.

UNIVERSITAT ROVIRA I VIRGILI
GOLD-CATALYZED INTERMOLECULAR REACTIONS OF ALKYNES WITH ALKENES: NOVEL REACTIVITIES AND GLOBAL MECHANISTIC PICTURE
María Elena de Orbe Izquierdo

General Introduction

Gold in Homogeneous Catalysis

Since ancient ages, gold had been considered a merely precious and decorative inert metal. Only a few decades ago, the first examples of active gold species in organic reactions were described,[1] and in 1998, the group of Teles reported the first gold(I)-catalyzed transformation of alkynes in homogeneous conditions, namely the formation of acetals by addition of alcohols (Scheme 1).[2] After this groundbreaking discovery, gold catalysis has grown exponentially due to the unique ability of gold to selectively activate multiple bonds.

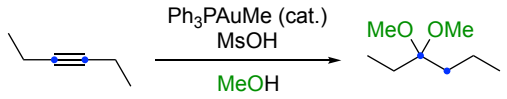

Scheme 1. First reaction of alkynes in homogeneous gold catalysis.

Nowadays, homogeneous gold catalysis is recognized as a powerful tool to construct C−C and C−heteroatom bonds and to efficiently access complex architectures. Gold-catalyzed transformations are characterized by their atom economy, mild conditions, high functional group tolerance, absence of additives and chemo-, regio- and stereoselectivities. Importantly, the reactivity of gold is orthogonal to that found for other transition metals.

The singular properties of this element are attributed to the relativistic effects.[3] Relativistic effects arise from the high speeds of electrons orbiting near a heavy nucleus. Consequently, the mass of the electrons increases, which leads to a decrease in the Bohr radius and a

1. (a) Hydrogenation of alkenes and alkynes by supported gold catalysts: Bond, G. C.; Sermon, P. A.; Webb, G.; Buchanan, D. A.; Wells, P. B. *J. Chem. Soc., Chem. Commun.* **1973**, 444–445. (b) Hydrochlorination of acetylene by supported gold(III) catalysts: Hutchings, G. J. *J. Catal.* **1985**, *96*, 292–295. (c) Gold(I)-catalyzed asymmetric aldol reaction: Ito, Y.; Sawamura, M.; Hayashi, T. *J. Am. Chem. Soc.* **1986**, *108*, 6405–6406. (d) Cyclization of 5-alkynylamines by gold(III) salts: Fukuda, Y.; Utimoto, K.; Nozaki, H. *Heterocycles* **1987**, *25*, 297–300. (e) Oxidation of CO catalyzed by gold particles: Haruta, M.; Kobayashi, T.; Sano, H.; Yamada, N. *Chem. Lett.* **1987**, *16*, 405–408. (f) Transformation of alkynes into ketones or acetals catalyzed by gold(III) salts: Fukuda, Y.; Utimoto, K. *J. Org. Chem.* **1991**, *56*, 3729–3731.
2. Teles, H.; Brode, S.; Chabanas, M. *Angew. Chem. Int. Ed.* **1998**, *37*, 1415–1418.
3. Gorin, D. J.; Toste, F. D. *Nature* **2007**, *446*, 395–403, and references cited therein.

subsequent contraction of the *s* and *p* orbitals. As a result, the electrons in the *d* and *f* orbitals are more shielded and experience a weaker nuclear attraction. This contraction is most significant for elements with filled 4*f* and 5*d* orbitals, reaching a maximum for gold. This phenomenon explains the highest electronegativity for gold among the transition metals (2.54) as well as its superior Lewis acidity. In particular, gold is a remarkably soft Lewis acid owing to the diminished electron-electron repulsion in the diffuse 5*d* orbitals, and therefore preferentially activates "soft" electrophiles such as π-bonds.

The lower energy gap between the *s*, *p* or *d* orbitals, also derived from the relativistic effects, leads to efficient *s*/*p* or *s*/*d* hybridizations, which justifies the tendency of gold(I) to form linear two-coordinated complexes.[4] The strong preference for this geometry together with the lower nucleophilicity of gold make its oxidative addition challenging and thus, its involvement in redox catalytic cycles ($E^0(Au^{III/I})$ = 1.41 V) less likely.[5] Nevertheless, gold(III) complexes are active in catalytic transformations and exhibit square planar geometries. From a practical perspective, the redox stability of gold(I) complexes allows to run the reactions catalyzed by this metal in air without precautions to exclude oxygen. Another distinctive feature of gold(I) in catalysis is the reluctance to undergo β-hydride elimination, as the filled 5*d* shell disfavors the interaction of β C−H bonds with gold.[6]

4. Gimeno, M. C.; Laguna, A. *Chem. Rev.* **1997**, *97*, 511–522.
5. Discussion: (a) Livendahl, M.; Goehry, C.; Maseras, F.; Echavarren, A. M. *Chem. Commun.* **2014**, *50*, 1533–1536. Different strategies to promote oxidative addition in gold catalysis: (b) Joost, M.; Zeineddine, A.; Estévez, L.; Mallet-Ladeira, S.; Miqueu, K.; Amgoune, A.; Bourissou, D. *J. Am. Chem. Soc.* **2014**, *134*, 14654–14657. (c) Guenther, J.; Mallet-Ladeira, S.; Estevez, L.; Miqueu, K.; Amgoune, A.; Bourissou, D. *J. Am. Chem. Soc.* **2014**, *136*, 1778–1781. (d) Cambeiro, X. C.; Ahlsten, N.; Larrosa, I. *J. Am. Chem. Soc.* **2015**, *137*, 15636−15639. (e) Wu, C. Y.; Horibe, T.; Jacobsen, C. B.; Toste, F. D. *Nature,* **2015**, *517*, 449–454. (f) Harper, M. J.; Arthur, C. J.; Crosby, J.; Emmett, E. J.; Falconer, R. L.; Fensham-Smith, A. J.; Gates, P. J.; Leman, T.; McGrady, J. E.; Bower, J. F.; Russell, C. A. *J. Am. Chem. Soc.* **2018**, *140*, 4440−4445.
6. Selected discussions and examples of β-hydride elimination in gold catalysis: (a) Mankad, N. P.; Toste, F. D. *Chem. Sci.* **2012**, *3*, 72– 76. (b) Klatt, G.; Xu, R.; Pernpointner, M.; Molinari, L.; Quang Hung, T.; Rominger, F.; Hashmi, A. S. K.; Köppel, H. *Chem. Eur. J.* **2013**, *19*, 3954–3961. (c) Castiñeira Reis, M.; López, C. S.; Kraka, E.; Cremer, D.; Faza, O. N. *Inorg. Chem.* **2016**, *55*, 8636–8645. (d) Rekhroukh, F.; Estevez, L.; Mallet-Ladeira, S.; Miqueu, K.; Amgoune, A.; Bourissou, D. *J. Am. Chem. Soc.* **2016**, *138*, 11920−11929. (e) Kumar, R.; Krieger, J.-P.; Gómez-Bengoa, E.; Fox, T.; Linden, A.; Nevado, C. *Angew. Chem. Int. Ed.* **2017**, *56*, 12862–12865.

Owing to the relativistic contraction of the 6*s* orbital in gold, the Au−L bond is strengthened so that the electronic and steric properties of gold complexes are easily tuned by the ligand.[7] Despite simple gold salts such as AuCl or $NaAuCl_4$ are able to catalyze many transformations, more sophisticated gold complexes have been used to induce greater reactivity and modulate selectivity. In general, complexes with phosphite ligands are more electrophilic than with phosphines, which still show higher electrophilicity than those bearing more donating *N*-heterocyclic carbenes (Scheme 2).[8] Moreover, sterically hindered ligands have demonstrated to be the most successful. A series of chiral ligands have enabled the development of enantioselective gold(I)-catalyzed reactions.[9]

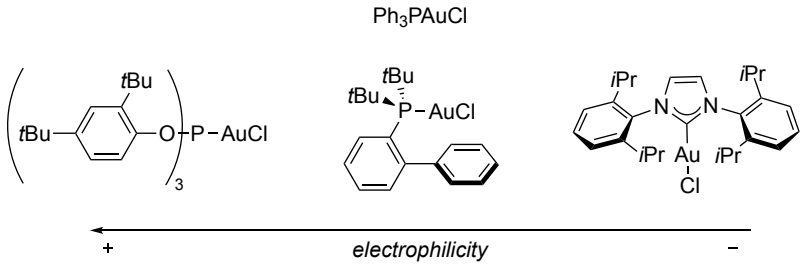

Scheme 2. Ligands frequently used in gold catalysis.

Neutral gold chloride complexes [LAuCl] normally exhibit poor reactivity. They are commonly used as precatalysts that need to be activated *in situ* by chloride abstraction. Silver(I) salts are often employed to generate more reactive species through AgCl release. However, the innocence of silver in gold catalyzed reactions has been questioned.[10] For this reason, it is more convenient to prepare neutral complexes [LAuX], where X^- is a weakly coordinating anion such as NTf_2^-, or cationic complexes [LAuL´]X, where L´ is a neutral weakly coordinating ligand (*i.e.*, MeCN or PhCN) and X^- is a counterion (*i.e.*, SbF_6^-, BF_4^-

7. (a) Gorin, D. J.; Sherry, B. D.; Toste, F. D. *Chem. Rev.* **2008,** *108*, 3351–3378. (b) Benitez, D.; Tkatchouk, E.; Gonzalez, A. Z.; Goddard III, W. A.; Toste, F. D. *Org. Lett.* **2009**, *11*, 4798–4801. (c) Wang, W.; Hammond, G. B.; Xu, B. *J. Am. Chem. Soc.* **2012**, *134*, 5697−5705.
8. Obradors, C; Echavarren, A. M. *Chem. Commun.* **2014**, *50*, 16–28.
9. (a) Zi, W.; Toste, F. D. *Chem. Soc. Rev.* **2016**, *45*, 4567–4589. (b) Li, Y.; Li, W.; Zhang, J. *Chem. Eur. J.* **2017**, *23*, 467−512.
10. (a) Homs, A.; Escofet, I.; Echavarren, A. M. *Org. Lett.* **2013**, *15*, 5782–5785. (b) Lu, Z.; Han, J.; Hammond, G. B.; Xu, B. *Org. Lett.* **2015**, *17*, 4534–4537. (c) Zhdanko, A.; Maier, M. E. *ACS Catal.* **2015**, *5*, 5994−6004.

or PF_6^-).[11] These complexes enter the catalytic cycle by associative ligand exchange with the reactive substrate.[12] Recently, the effect of counterions in gold catalysis has also been discussed.[13] Although complexes of type $[LAu]^+$ are sometimes invoked, the existence of these "naked gold" species has not been proven yet in the solid state or in solution.[14]

Gold Intermediates upon Activation of Multiple Bonds

Gold(I) is an π-electrophilic Lewis acid[15] and forms stable π-complexes with alkynes,[16] alkenes[17] and allenes,[18] which have been isolated, characterized spectroscopically and analyzed by X-ray crystallography (Scheme 3).[19] The metal coordinates to internal alkynes in an almost symmetrical η^2-fashion, with a significant degree of bending in the substituents. A similar almost symmetrical η^2-coordination has been observed in the case of symmetric alkenes. In contrast, gold binds preferentially to the less substituted carbon in terminal alkenes or the less substituted double bond in allenes. According to the reported bond lengths and angles, steric factors seem to control the unsaturation orientation.

11. Ranieri, B.; Escofet, I.; Echavarren, A. M. *Org. Biomol. Chem.* **2015**, *13*, 7103-7118.
12. (a) Komiya, S.; Albright, T. A.; Hoffmann, R.; Kochi, J. K. *J. Am. Chem. Soc.* **1976**, *98*, 7255–7265. (b) Dickson, P. N.; Wehrli, A.; Geier, G. *Inor. Chem.* **1988**, *27*, 2921–2925. (c) Schmidbaur, H.; Schier, A. *Organometallics* **2010**, *29*, 2–23.
13. (a) Jia, M.; Bandini, M. *ACS Catal.* **2015**, *5*, 1638–1652. Veenboer, R. M. P.; Collado, A.; Dupuy, S.; Lebl, T.; Falivene, L.; Cavallo, L.; Cordes, D. B.; Slawin, A. M. Z.; Cazin, C. S. J.; Nolan, S. P. *Organometallics* **2017**, *36*, 2861−2869.
14. (a) One complex of this type has been claimed without structural evidence: Weber, S. D.; Zahner, D.; Rominger, F.; Straub, B. F. *Chem. Commun.* **2012**, *48*, 11325–11327. (b) For a pertitent discussion see: Veenboer, R. M. P.; Collado, A.; Dupuy, S.; Lebl, T.; Falivene, L.; Cavallo, L.; Cordes, D. B.; Slawin, A. M. Z.; Cazin, C. S. J.; Nolan, S. P. *Organometallics* **2017**, *36*, 2861–2869.
15. Yamamoto, Y. *J. Org. Chem.* **2007**, *72*, 7817–7831.
16. (a) Brown, T. J.; Widenhoefer, R. A. *J. Organomet. Chem.* **2011**, *696*, 1216–1220. (b) Zuccaccia, D.; Belpassi, L.; Rocchigiani, L.; Tarantelli, F.; Macchioni, A. *Inorg. Chem.* **2010**, *49*, 3080–3082. (c) Flügge, S.; Anoop, A.; Goddard, R.; Thiel, W.; Fürstner, A *Chem. Eur. J.* **2009**, *15*, 8558–856.
17. (a) Brooner, R. E. M.; Brown, T. J.; Widenhoefer, R. A. *Chem. Eur. J.* **2013**, *19*, 8276–8284. (b) Brown, T. J.; Dickens, M. G.; Widenhoefer, R. A. *J. Am. Chem. Soc*. **2009**, *131*, 6350–6351.
18. Brown, T. J.; Sugie, A.; Leed, M. G. D.; Widenhoefer, R. A. *Chem. Eur. J.* **2012**, *18*, 6959–6971.
19. Brooner, R. E. M.; Widenhoefer, R. A. *Angew. Chem. Int. Ed.* **2013**, *52*, 11714–11724.

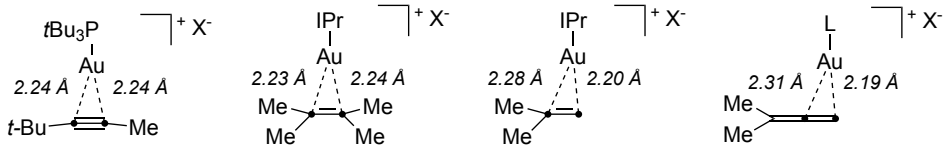

Scheme 3. Isolated and characterized gold complexes (X = SbF_6, L = JohnPhos).

The nature of the gold-unsaturation bond has been described by the Dewar–Chatt–Duncanson model.[20] In short, the bond is characterized by a substrate-to-metal σ-donation and a metal-to-substrate π-back-donation. This back-donation was found to be the moldable component depending on the ligand, metal-substrate distance and substrate rigidity towards deformation. The comparison between gold(I)-alkyne and gold(I)-alkene bonds revealed that they are essentially the same, although gold(I) coordinates preferentially to electron-rich alkenes leading to (η^2-alkene)gold(I) complexes.[21]

However, in the presence of other functional groups including alkenes, gold(I) selectively activates alkynes. In line with the analysis of the nature of the gold-unsaturation bond, there is no thermodynamic preference of gold for the coordination to alkynes correlated to the relative strength of the bonding. Instead, the alkynophilicity of gold(I) arises from the higher reactivity of the resulting (η^2-alkyne)-gold(I) complexes towards a nucleophilic attack.[22]

The attack of nucleophiles to the activated alkyne occurs generally in an outer-sphere *anti*-fashion leading to *trans*-alkenyl species (Scheme 4),[23] though few exceptions have been suggested.[24] A wide range of nucleophiles have been used in intra- and intermolecular processes, such as alcohols, thiols, amines, imines, sulfoxides, *N*-oxides and

20. Salvi, N.; Belpassi, L.; Tarantelli, F. *Chem. Eur. J.* **2010**, *16*, 7231–7240.
21. Jašíková, L.; Roithová, J. *Organometallics*, **2012**, *31*, 1935–1942. See also ref. 16a.
22. García-Mota, M.; Cabello, N.; Maseras, F.; Echavarren, A. M.; Pérez-Ramírez, J.; López, N. *ChemPhysChem* **2008**, *9*, 1624–1629.
23. (a) Kennedy-Smith, J. J.; Staben, S. T.; Toste, F. D. *J. Am. Chem. Soc.* **2004**, *126*, 4526–4527. (b) Hashmi, A. S. K.; Weyrauch, J. P.; Frey, W.; Bats, N. W. *Org. Lett.* **2004**, *6*, 4391–4394. (c) A. Fürstner, *Chem. Soc. Rev.* **2009**, 38, 3208–3221.
24. (a) Lavallo, V.; Frey, G. D.; Donnadieu, B.; Soleilhavoup, M.; Bertrand, G. *Angew. Chem. Int. Ed.* **2008**, *47*, 5224–5228. (b) Fructos, M. R.; Urbano, J.; Díaz-Requejo, M. M.; Pérez, P. J. *Beilstein J. Org. Chem.* **2015**, *11*, 2254–2260.

(hetero)arenes.[25] Subsequently, the resulting alkenyl gold(I) intermediates can undergo diverse pathways producing a variety of structural complex products.

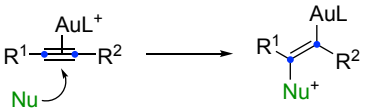

Scheme 4. Nucleophilic attack to (η^2-alkyne)-gold(I) complexes.

Gold-catalyzed transformations proceed *via* carbocation mechanisms in which gold plays a key role in stabilizing the intermediates and controlling their evolution through intricate cascades. The isolation of relevant intermediates was achieved in limited instances,[26] but labelling and kinetic experiments have provided evidences to understand the mechanistic scenarios. Moreover, computational chemistry has tremendously contributed to shed light on the intriguing pathways of gold-catalyzed reactions.[27]

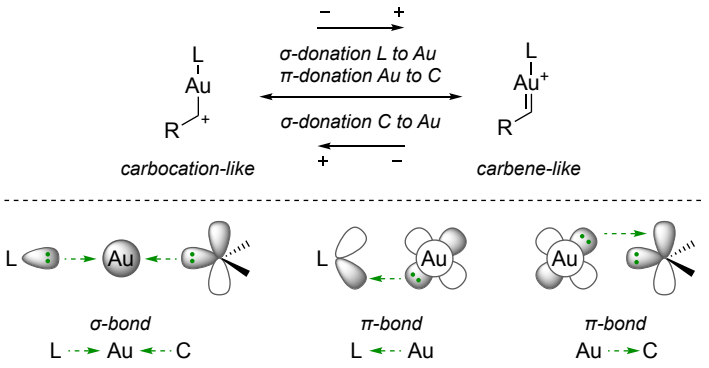

Scheme 5. Nature of gold carbenes.

25. (a) Echavarren, A. M.; Muratore, M. E.; López-Carrillo, V.; Escribano-Cuesta, A.; Huguet, N.; Obradors, C. *Org. React.* **2017**, *92*, 1−288. (b) Debrouwer, W.; Heugebaert, T. S. A.; Roman, B. I. A.; Stevens, C. V. *Adv. Synth. Catal.* **2015**, *357*, 2975–3006 (c) Dorel, R.; Echavarren, A. M. *Chem. Rev.* **2015**, *115*, 9028−9072.
26. (a) Ferrer, S.; Echavarren, A. M. *Organometallics* **2018**, *37*, 781–786. (b) Jones, A. C. *Top. Curr. Chem.* **2015**, *357*, 133–166. (c) Hashmi, A. S. K. *Angew. Chem. Int. Ed.* **2010**, *49*, 5232–5241. (d) Liu, L. P.; Hammond, G. B. *Chem. Soc. Rev.*, **2012**, *41*, 3129–3139.
27. (a) Thiel, W. *Angew. Chem. Int. Ed.* **2014**, *53*, 8605–8613. (b) Sameera, W. M. C.; Maseras, F. *WIREs Comput. Mol. Sci.* **2012**, *2*, 375–385. (c) Pyykkö, P. *Angew. Chem. Int. Ed.* **2004**, *43*, 4412–4456.

Gold carbenes have been proposed as crucial intermediates in multitudinous gold-mediated processes.[28] The bonding mode of these species has been described as a three-center four-electron σ-hyperbond (the ligand and the carbene donating electrons to gold) accompanied by two π-bonds (gold back-donating electrons from two filled 5*d* orbitals to the ligand and carbene) (Scheme 5).[29] Hence, the bonding and the reactivity of these intermediates depend on both the ligand and the carbon substituents. For instance, strongly σ-donating NHC ligands (*N*-heterocyclic carbenes) increase the electron density around gold and thus the gold-to-carbene π-donation, enhancing the carbene-like reactivity. Gold carbenes show very specific characteristics, albeit they could be considered Fischer carbenes due to the weak metal-to-carbene π-back-donation and their strongly electrophilic reactivity.[30]

Cycloisomerizations of 1,*n*-Enynes

Initially, the blooming of gold catalysis was linked to the cyclizations of 1,*n*-enynes, in which gold enables an outstanding increment of molecular complexity in one step. In particular, transformations of 1,6-enynes have been extensively explored (Scheme 6).[31] These reactions commence with the intramolecular nucleophilic attack of the alkene to the gold-activated alkyne to form cyclopropyl gold(I) carbenes **II** or **III** by *anti*-5-*exo*-dig or 6-*endo*-dig cyclization, respectively. The generation and evolution of these intermediates is determined by the substitution pattern of the enyne as well as the ligand of the gold complex.

Intermediates **II** can undergo the double-cleavage rearrangement that involves the insertion of the external carbon of the alkene into the alkyne, followed by α-proton elimination to afford 1,3-dienes **1**. In general, products with *Z* configuration are predominantly obtained. Alternatively, intermediates **II** evolve through the migration of the terminal alkene carbon

28. Harris, R. J.; Widenhoefer, R. A. *Chem. Soc. Rev.* **2016**, *45*, 4533–4551.
29. Benitez, D.; Shapiro, N. D.; Tkatchouk, E.; Wang, Y.; Goddard III, W. A.; Toste, F. D. *Nat. Chem.* **2009**, *1*, 482–486.
30. Wang, Y.; Michael E. Muratore, M. E.; Echavarren, A. M. *Chem. Eur. J.* **2015**, *21*, 7332–7339.
31. (a) Obradors, C; Echavarren, A. M. *Acc. Chem. Res*. **2014**, *47*, 902–912. (b) Jiménez-Núñez, E.; Echavarren, A. M. *Chem. Rev.* **2008**, *108*, 3326–3350. (c) Lee, Y. C; Kumar, K. *Isr. J. Chem.* **2018**, *58*, 531–556.

to the terminal carbon of the alkyne (single-cleavage rearrangement) to form intermediates **V**, ultimately giving 1,3-dienes **2**. Although the gold(I)-catalyzed single-cleavage rearrangement is normally stereospecific, some exceptions have been found.

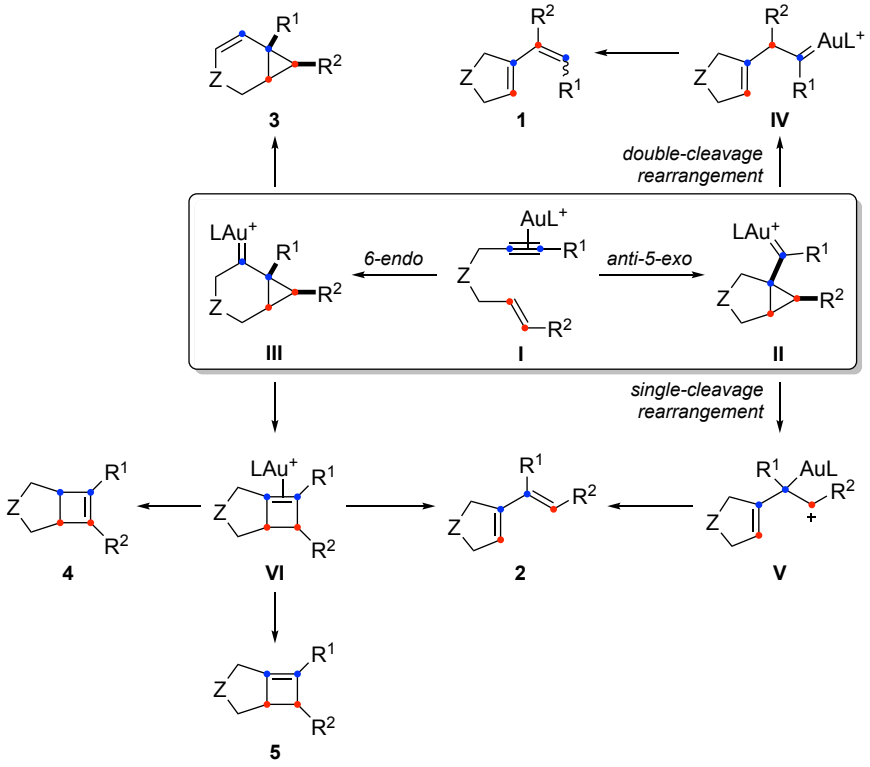

Scheme 6. Cycloisomerization of 1,6-enynes catalyzed by gold(I).

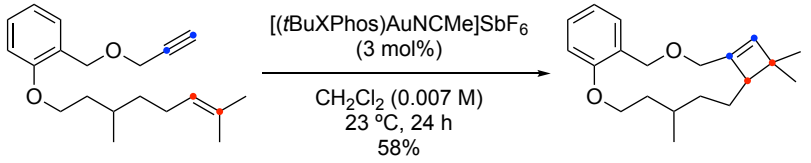

Scheme 7. Gold-catalyzed macrocyclization of a 1,14-enyne to form a 13-membered ring.

In contrast, intermediates **III** render **3** by α-proton elimination. Ring expansion of the cyclopropane in **III** gives rise to cyclobutene derivatives **VI** that either isomerize to afford **4** or undergo ring opening to produce 1,3-dienes **2**. Interestingly, only in few cases

cycloisomerizations of 1,6-enynes lead to cyclobutenes of type **5**,[32] whereas the macrocyclization of higher 1,*n*-enynes (*n* = 8-16) gives rise selectively to these cyclobutenes tethered to an up to 15-membered ring (Scheme 7).[33] The reactivity of 1,5-[34] and 1,7-enynes[35] is related to that found for 1,6-enynes.

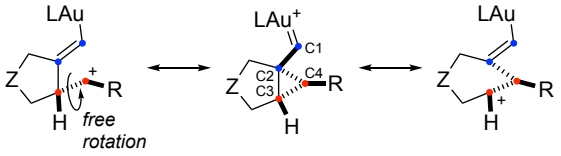

Scheme 8. Canonical structures of cyclopropyl gold(I) carbenes.

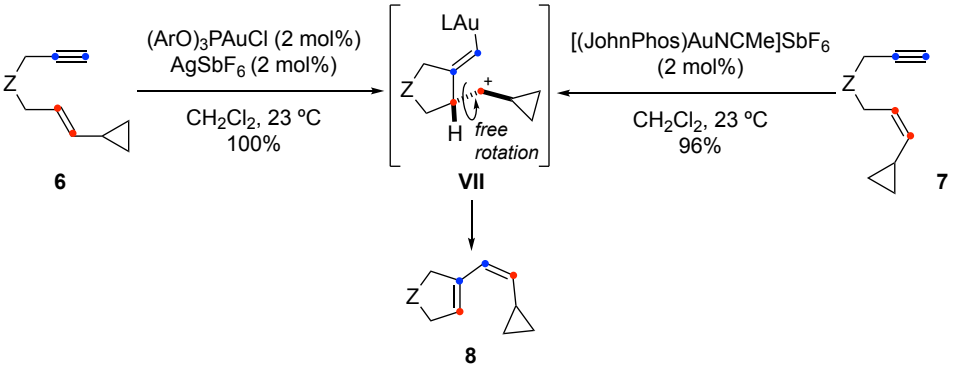

Scheme 9. *Cis*-selective single-cleavage rearrangement of 1,6-enynes (Z = $C(COOMe)_2$).

The proposed cyclopropyl gold carbenes intermediates are highly distorted species that are also represented as gold-stabilized homoallylic carbocations (Scheme 8).[36] The carbenic or

32. (a) Nieto-Oberhuber, C.; López, S.; Muñoz, M. P.; Cárdenas, D. J.; Buñuel, E.; Nevado, C.; Echavarren, A. M. *Angew. Chem. Int. Ed.* **2005**, *44*, 6146–6148. (b) Escribano-Cuesta, A.; Pérez-Galán, P.; Herrero-Gómez, E.; Sekine, M.; Braga, A. A. C.; Maseras, F.; Echavarren, A. M. *Org. Biomol. Chem.* **2012**, *10*, 6105–6111. (c) Brooner, R. E. M.; Brown, T. J.; Widenhoefer, R. A. *Angew. Chem. Int. Ed.* **2013**, *52*, 6259–6261.
33. (a) Odabachian, Y.; Gagosz, F. *Adv. Synth. Catal.* **2009**, *351*, 379–386. (b) Obradors, C.; Leboeuf, D.; Aydin, J.; Echavarren, A. M. *Org. Lett.* **2013**, *15*, 1576–1579.
34. (a) Sun, J.; Conley, M.; Zhang, L.; Kozmin, S. *J. Am. Chem. Soc*. **2006**, *128*, 9705–9710. (b) López-Carrillo, V.; Huguet, N.; Mosquera, Á.; Echavarren, A. M. *Chem. Eur. J.* **2011**, *17*, 10972–10978.
35. Cabello, N.; Rodríguez, C.; Echavarren, A. M. *Synlett*. **2007**, 1753–1758.
36. Jiménez-Núñez, E.; Claverie, C. K.; Bour, C.; Cárdenas, D. J.; Echavarren, A. M. *Angew. Chem., Int. Ed*. **2008**, *47*, 7892–7895.

cationic character is modulated by the substituents. According to DFT calculations, when the open carbocation is the enhanced canonical structure, rotation around the C3−C4 bond could occur, affecting the stereospecificity of the reaction. For instance, in the gold(I)-catalyzed reactions of enynes **6**,**7**, carbocation **VII** is favored because of the strongly electron-donating cyclopropyl substituent and C3−C4 bond rotation takes place prior to rearrangement, so the same *cis*-diene **8** is obtained in both cases (Scheme 9).[36]

The key cyclopropyl gold carbenes have never been isolated or fully characterized. However, their involvement in these transformations has been confirmed by trapping them intra- and intermolecularly with a series of carbo- and heteronucleophiles.[37]

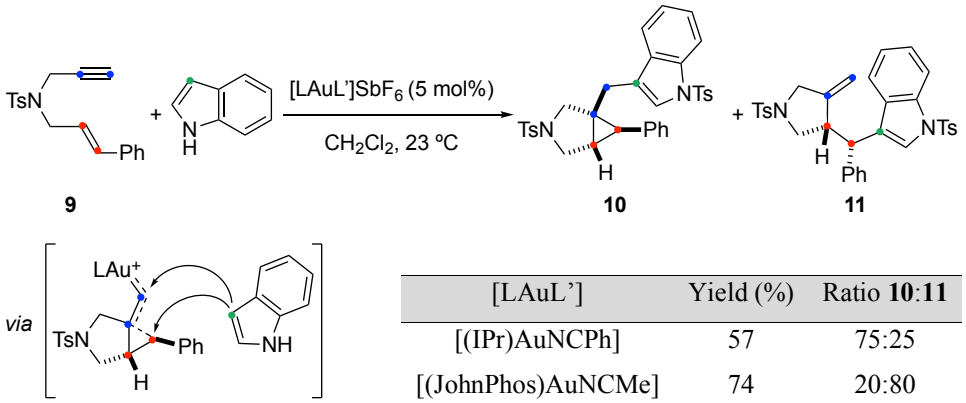

[LAuL']	Yield (%)	Ratio **10**:**11**
[(IPr)AuNCPh]	57	75:25
[(JohnPhos)AuNCMe]	74	20:80

Scheme 10. Intermolecular trapping of the cyclopropyl gold carbene by indole.

A representative example is the intermolecular trapping of the cyclopropyl gold carbene generated from 1,6-enyne **9** using indole (Scheme 10).[38] Depending on the ligand of the gold complex, the carbenic or carbocationic nature of the intermediate is stressed, and consequently, the ratio between the two plausible products **10** and **11** can be conveniently tuned.

37. Some examples: (a) Nieto-Oberhuber, C.; López, S.; Muñoz, M. P.; Jiménez-Núñez, E.; Buñuel, E.; Cárdenas, D. J.; Echavarren, A. M. *Chem. Eur. J.* **2006**, *12*, 1694–1702. (b) Pérez-Galán, P.; Herrero-Gómez, E.; Hog, D. T.; Martin, N. J. A.; Maseras, F.; Echavarren, A. M. *Chem. Sci.* **2011**, *2*, 141–149. (c) Calleja, P.; Pablo, O.; Ranieri, B.; Gaydou, M.; Pitaval, A.; Moreno, M.; Raducan, M.; Echavarren, A. M. *Chem. Eur. J.* **2016**, *22*, 13613–13618.
38. Amijs, C. H. M.; Lopez-Carrillo, V.; Raducan, M.; Pérez-Galán, P.; Ferrer, C.; Echavarren, A. M. *J. Org. Chem.* **2008**, *73*, 7721–7730.

The gold(I)-catalyzed reactions of 1,*n*-enynes have been broadly applied in organic chemistry due to the versatility of the intermediates. Numerous total syntheses have been completed taking advantage of the increase of molecular complexity in selective cascade cyclizations of enynes catalyzed by gold(I).[39] In the field of material science, the illustrative access to higher acenes was achieved by gold-catalyzed cycloisomerization of 1,7-enynes.[40]

Intermolecular Reactions of Alkynes with Alkenes by Gold(I)

In contrast with the advances in intramolecular gold(I)-catalyzed reactions of alkynes with alkenes, the parent intermolecular processes still remain challenging and scarce. The conceivable products are also alkenes that compete with the initial unsaturated substrates as potential ligands for gold, therefore hampering the formation of the active (η^2-alkyne)-gold(I) complex. Furthermore, the alkenyl products can act as nucleophiles and attack the gold intermediates, leading to higher adducts, oligomers or even polymers.[41]

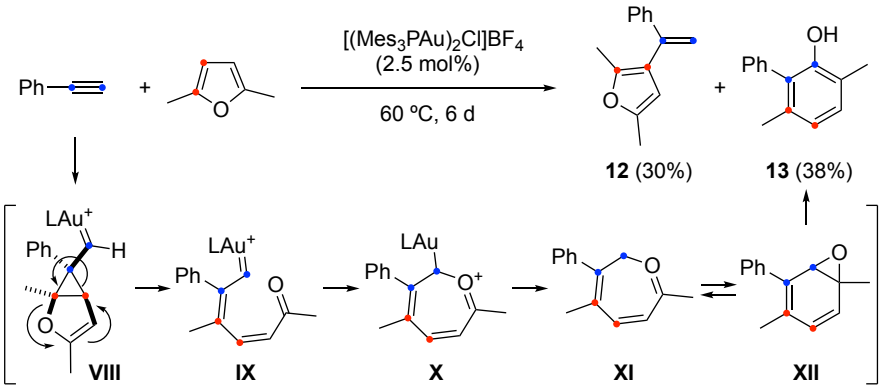

Scheme 11. First gold-catalyzed intermolecular reaction of alkynes with alkenes.

39. Pflästerer, D.; Hashmi, A. S. K. *Chem. Soc. Rev*. **2016**, *45*, 1331–1367.
40. Dorel, R.; McGonigal, P. R.; Echavarren, A. M. *Angew. Chem. Int. Ed.* **2016**, *55*, 11120–11123.
41. (a) Studies on (alkene)gold(I) complexes: Brown, T. J.; Dickens, M. G.; Widenhoefer, R. A. *Chem. Commun.* **2009**, 6451–6453. (b) Polymerization of alkenes catalyzed by gold: Urbano, J.; Hormigo, A. J.; de Frémont, P.; Nolan, S. P; Díaz-Requejo, M. M.; Pérez, P. J. *Chem. Commun.* **2008**, 759–761.

The first reported example was the intermolecular reaction of ethynylbenzene and 2,5-dimethylfuran to give rise to phenol **13** and a hydroarylated product **12** in poor yields (Scheme 11).[42] Later, this transformation was extended to different furans and terminal alkyl-, vinyl- and (hetero)arylalkynes to obtain a variety of phenols in good yields by using a different gold(I) catalyst.[43] According to experimental and theoretical studies, the mechanism involves the attack of the furan to the gold-activated alkyne to form the cyclopropyl gold carbene **VIII**, which rearranges to generate the oxepin **XI**. The oxepin is in equilibrium with epoxide **XII** that then leads to the phenol. The Introduction of **Chapter 3** includes a deeper discussion of other different hydroarylations of alkynes catalyzed by gold.

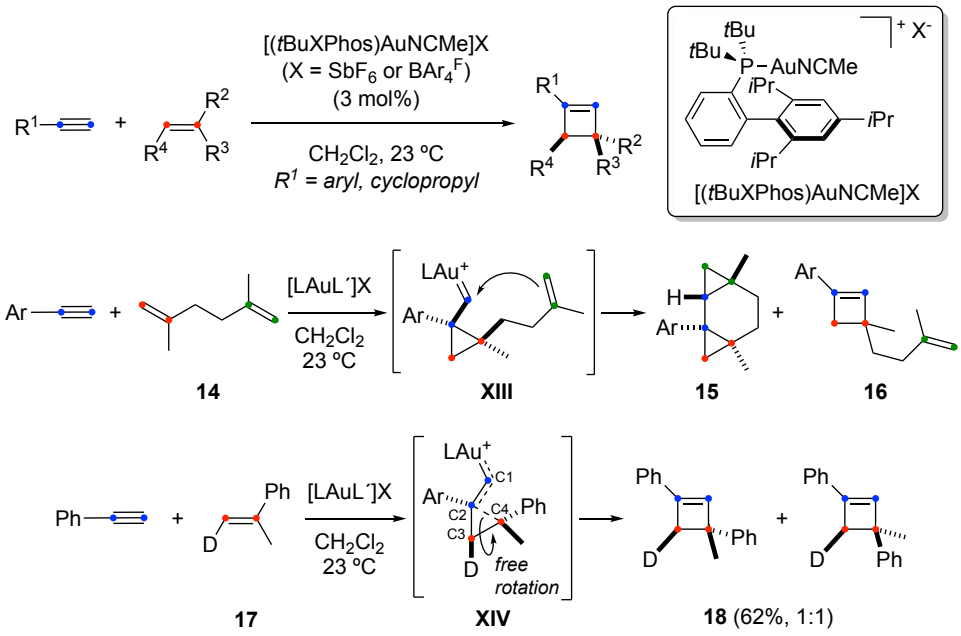

Scheme 12. Intermolecular [2+2] cycloaddition of arylalkynes with alkenes.

Our research group found that, under gold catalysis, terminal (hetero)aryl- and cyclopropylalkynes react with alkenes *via* intermolecular [2+2] cycloaddition to yield

42. Hashmi, A. S. K.; Blanco, M. C.; Kurpejović, E.; Frey, W.; Bat, J. W. *Adv. Synth. Catal.* **2006**, *348*, 709–713.
43. Huguet, N.; Leboeuf, D.; Echavarren, A. M. *Chem. Eur. J.* **2013**, *19*, 6581–6585.

regioselectively cyclobutenes (Scheme 12),[44] which are the same type of products obtained in the aforementioned cycloisomerizations of 1,*n*-enynes ($n > 7$). The key for the success of this transformation was the use of gold(I) catalysts bearing the sterically hindered *t*BuXPhos ligand, in which the counterion plays an important role. Changing the counterion SbF_6^- to the bulkier and less basic anion BAr_4^{F-}, higher yields were obtained by decreasing the generation of unproductive σ,π-(alkyne)digold(I) intermediates. Kinetic mechanistic studies showed that the rate-limiting step is the initial ligand exchange alkene-gold(I) complex to form the active alkyne-gold(I) complex, which highlights the existing competition of the unsaturated substrates to bind the gold catalyst.

Based on the cycloisomerizations of 1,*n*-enynes, the reaction was proposed to proceed through a cyclopropyl gold carbene that experiences ring opening to give the cyclobutene. In the reaction of arylalkynes with 1,5-diene **14**, the corresponding cyclopropyl gold carbenes **XIII** were trapped by the intramolecular attack of the pendant alkene to produce biscyclopropyl derivatives **15**. When performing the reaction between phenylacetylene and the deuterated alkene **17**, a 1:1 mixture of diastereomeric cyclobutenes **18** was obtained, which implies that in the corresponding cyclopropyl gold carbene **XIV** the free rotation around C3−C4 bond occurs prior to the ring expansion.

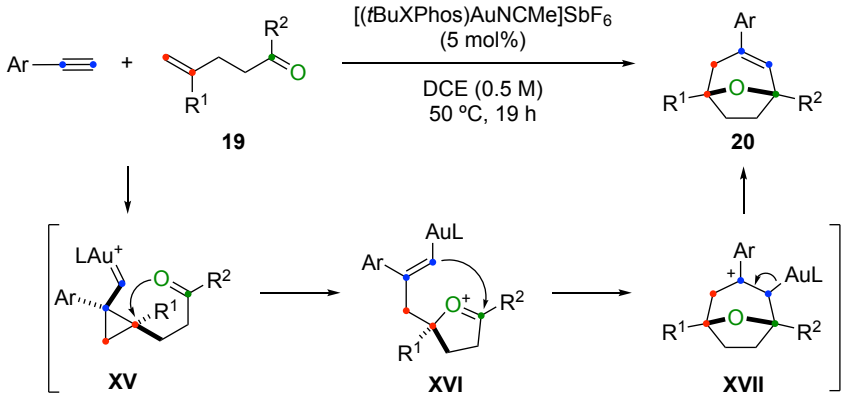

Scheme 13. Intermolecular [2+2+2] cycloaddition of arylalkynes with ketoalkenes.

44. (a) López-Carrillo, V.; Echavarren, A. M. *J. Am. Chem. Soc.* **2010**, *132*, 9292–9294. (b) Homs, A.; Obradors, C; Leboeuf, D.; Echavarren, A. M. *Adv. Synth. Catal.* **2014**, *356*, 221–228.

Our group also discovered the gold(I)-catalyzed [2+2+2] cycloaddition of terminal (hetero)arylalkynes with ketoalkenes **19** to afford regio- and stereoselectively 8-oxabicyclo[3.2.1]oct-3-enes **20** (Scheme 13).[45] In this case, after the attack of the alkene to the (η^2-alkyne)-gold(I) complex and generation of the cyclopropyl gold carbene **XV**, the carbonyl motif attacks the more substituted carbon of the alkene to build an oxonium cation **XVI**, which undergoes a Prins-type cyclization to give the bridged oxabicycles **20**.

Interestingly, the gold(I)-catalyzed intermolecular reaction of acceptor-substituted alkynes with alkenes leads to lactones **22** by [4+2] annulation or to 1,3-dienes **21** by stereospecific cross metathesis (Scheme 14).[46] Upon formation of the corresponding cyclopropyl gold carbenes, lactones arise from the intramolecular attack of the propiolate to the more substituted carbon of the alkene, while 1,3-dienes arise from a stepwise rearrangement.

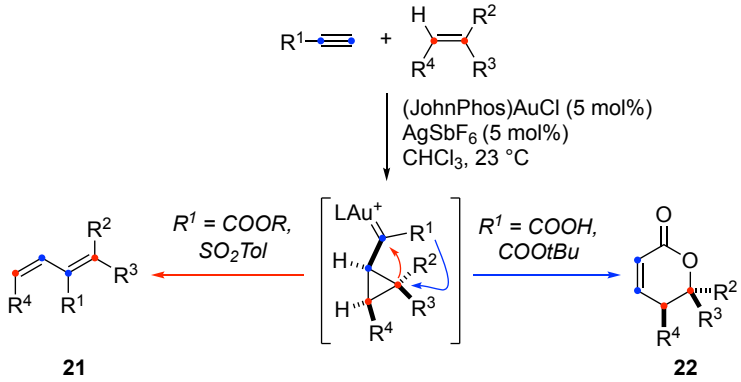

Scheme 14. Intermolecular reactions of acceptor-substituted alkynes with alkenes.

Other gold(I)-catalyzed [4+2] and [2+2+2] cycloadditions of alkynes with alkenes were developed using ynamides (Scheme 15).[47] When arylynamides react with alkenes, the resulting cyclopropyl gold carbenes evolve through intramolecular Friedel-Crafts-type reactions to furnish the [4+2] adducts **23**. However, when terminal ynamides react with enol ethers, the corresponding cyclopropyl gold carbenes are intermolecularly attacked by

45. Obradors, C; Echavarren, A. M. *Chem. Eur. J.* **2013**, *19*, 3547–3551.
46. Yeom, H.-S.; Koo, J.; Park, H.-S.; Wang, Y.; Liang, Y.; Yu, Z.-X.; Shin, S. *J. Am. Chem. Soc.* **2012**, *134*, 208–211.
47. Dateer, R. B.; Shaibu, B. S.; Liu, R.-S. *Angew. Chem. Int. Ed.* **2012**, *51*, 113–117.

another enol ether to construct stereoselectively 1,3,5-trisubstituted cyclohexenes **24** through the less hindered position.

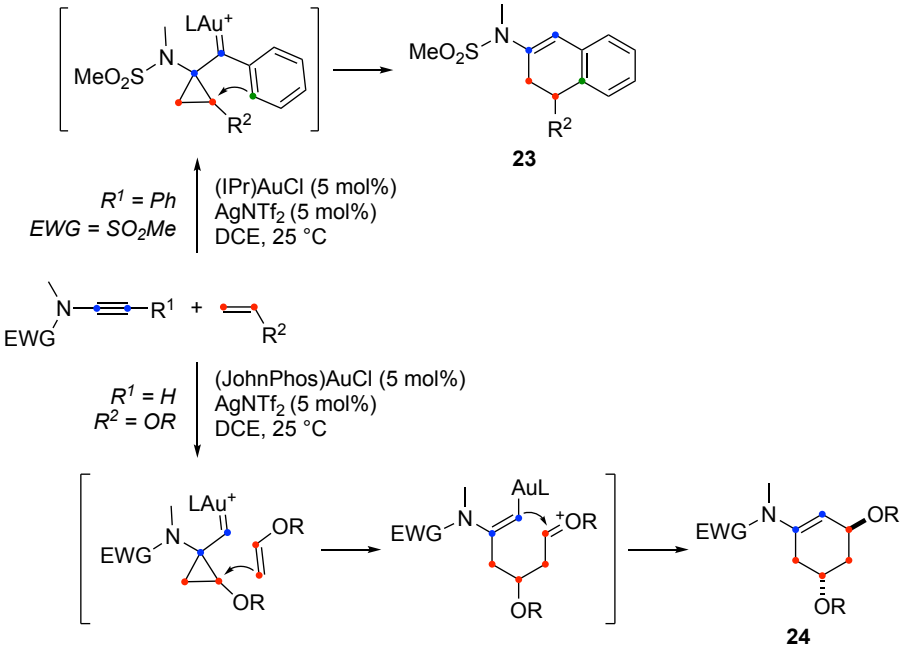

Scheme 15. Intermolecular [4+2] and [2+2+2] cycloadditions of ynamides and alkenes.

UNIVERSITAT ROVIRA I VIRGILI
GOLD-CATALYZED INTERMOLECULAR REACTIONS OF ALKYNES WITH ALKENES: NOVEL REACTIVITIES AND GLOBAL MECHANISTIC PICTURE
María Elena de Orbe Izquierdo

Chapter 1.

Cyclobutene *vs.* Diene Formation in Gold-Catalyzed Reactions of Alkynes with Alkenes

UNIVERSITAT ROVIRA I VIRGILI
GOLD-CATALYZED INTERMOLECULAR REACTIONS OF ALKYNES WITH ALKENES: NOVEL REACTIVITIES AND GLOBAL MECHANISTIC PICTURE
María Elena de Orbe Izquierdo

Introduction

Cyclobutenes are key features in natural products and pharmaceuticals, as well as highly valuable synthons to access a diversity of scaffolds (see **Chapter 2** for details). For this reason, they have inspired organic chemists to develop new methodologies for their synthesis. Among the strategies to prepare cyclobutenes, the [2+2] cycloaddition between alkynes and alkenes is a convenient straightforward route.

Besides photochemical processes,[48] different transition metals have been employed to promote [2+2] cycloadditions, which are however restricted to the use of specific alkenes.[49] Thus, under ruthenium,[50] rhodium,[51] iridium,[52] cobalt[53] and nickel[54] catalysis the [2+2] cycloaddition only proceeds with strained alkenes such as norbornene derivatives, in some cases in an enantioselective manner (Scheme 1.1).

Using rhodium catalysts, the [2+2] cycloaddition also takes place with β-nitrostyrene or electron-deficient alkenes as acrylates (Scheme 1.2).[55] In addition, different alkenes

48. (a) Yang, C.; Inoue, Y. *Chem. Soc. Rev.* **2014**, *43*, 4123−4143. (b) Brimioulle, R.; Lenhart, D.; Maturi, M. M.; Bach, T. *Angew. Chem., Int. Ed.* **2015**, *54*, 3872−3890. (c) Xu, Y.; Conner, M. L.; Brown, M. K. *Angew. Chem Int. Ed.* **2015**, *54*, 11918−11928. (d) Blum, T. R.; Miller, Z. D.; Bates, D. M.; Guzei, I. A.; Yoon, T. P. *Science* **2016**, *354*, 1391–1395. (e) Tröster, A.; Alonso, R.; Bauer, A.; Bach, T. *J. Am. Chem. Soc.* **2016**, *138*, 7808−7811. (f) Poplata, S.; Tröster, A.; Zou, Y.-Q.; Bach, T. *Chem. Rev.* **2016**, *116*, 9748–9815.
49. (a) Lautens, M.; Klute, W.; Tam, W. *Chem. Rev.* **1996**, *96*, 49–92. (b) Xu, Y.; Conner, M. L.; Brown, M. K. *Angew. Chem. Int. Ed.* **2015**, *54*, 11918–11928. (c) Fructos, M. R.; Prieto, A. *Tetrahedron* **2016**, *72*, 355–369.
50. (a) Jordan, R. W.; Tam, W. *Org. Lett.* **2000**, *2*, 3031–3034. (b) Alvarez, P.; Gimeno, J.; Lastra, E.; García-Granda, S.; Van der Maelen, J. F.; Bassetti, M. *Organometallics* **2001**, *20*, 3762–3771. c) Cockburn, N.; Karimi, E.; Tam, W. *J. Org. Chem.* **2009**, *74*, 5762–5765. (d) Enantioselective: Kossler, D.; Cramer, N. *Chem. Sci*. **2017**, 8, 1862–1866.
51. Enantioselective: Shibata, T.; Takami, K.; Kawachi, A. *Org. Lett.* **2006**, *8*, 1343–1345.
52. Enantioselective: Fan, B.-M.; Li, X.-J.; Peng, F.-Z.; Zhang, H.-B.; Chan, A. S. C.; Shao, Z.-H. *Org. Lett.* **2010**, *12*, 304–306.
53. (a) Chao, K. C.; Rayabarapu, D. K.; Wang, C.-C.; Cheng, C-H. *J. Org. Chem.* **2001**, *66*, 8804–8810. (b) Treutwein, J.; Hilt, G. *Angew. Chem. Int. Ed.* **2008**, *47*, 6811–6813. (c) Hilt, G.; Paul, A.; Treutwein, J. *Org. Lett.* **2010**, *12*, 1536–1539.
54. Huang, D.-J.; Rayabarapu, D. K.; Li, L.-P.; Sambaiah, T.; Cheng, C.-H. *Chem. Eur. J.* **2000**, *6*, 3706–3713.
55. (a) Motokura, K.; Nakayama, K.; Miyaji, A.; Baba, T. *ChemCatChem* **2011**, *3*, 1419–1421. (b) Smith, D. L.; Chidipudi, S. R.; Goundry, W. R.: Lam, H. W. *Org. Lett.* **2012**, *14*, 4934–4937. (c) Sakai, K.; Kochi, T.; Kakiuchi, F. *Org. Lett.* **2013**, *15*, 1024–1027.

undergo [2+2] cycloaddition with 1,3-enynes bearing an internal alkyne to give 1-vinylcyclobutenes by means of nickel[56] or cobalt[57] catalysis (Scheme 1.3). In the former case, carbonyl-substituted alkenes are required, whereas in the latter case a broad range of electron-donating alkenes is suitable.

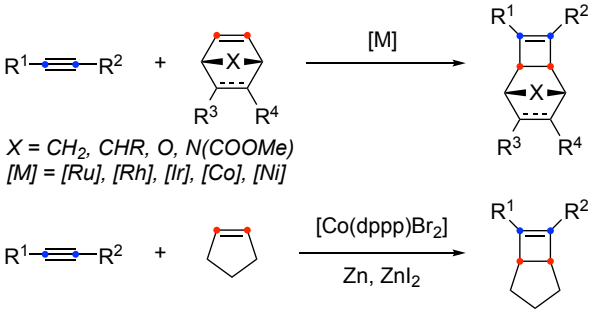

Scheme 1.1. Metal-catalyzed [2+2] cycloaddition of alkynes with strained alkenes.

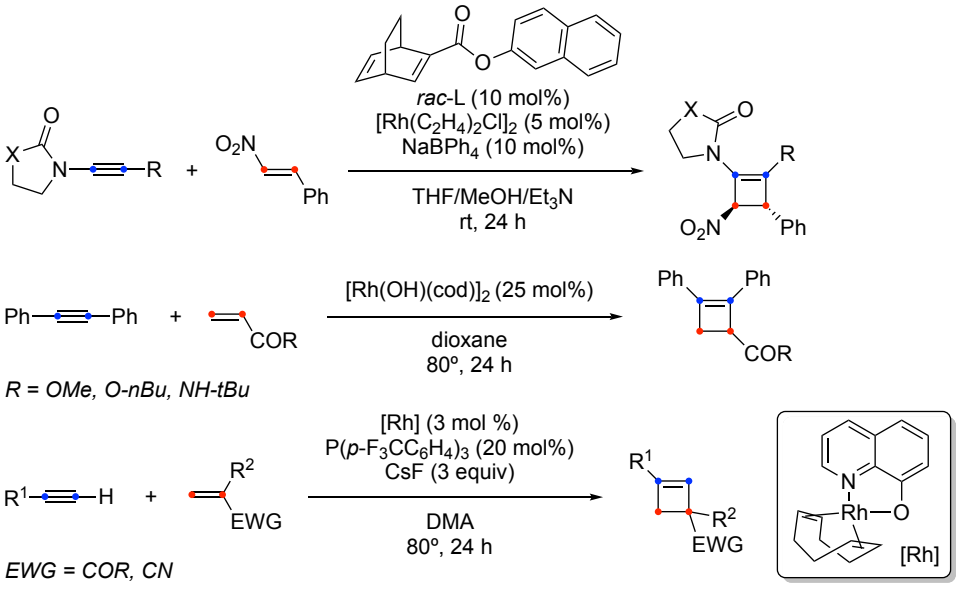

Scheme 1.2. Rhodium-catalyzed [2+2] cycloaddition with different alkenes.

56. Nishimura, A.; Ohashi, M.; Ogoshi, S. *J. Am. Chem. Soc.* **2012**, *134*, 15692–15695.
57. Nishimura, A.; Tamai, E.; Ohashi, M.; Ogoshi, S. *Chem. Eur. J.* **2014**, *20*, 6613–6617.

Noteworthy, the vast majority of these metal-catalyzed [2+2] cycloadditions have been proposed to proceed *via* coordination of both the alkyne and alkene to the metal center, followed by oxidative cyclization to form a metallacycle intermediate, which evolve through reductive elimination to construct the cyclobutene (Scheme 1.4).

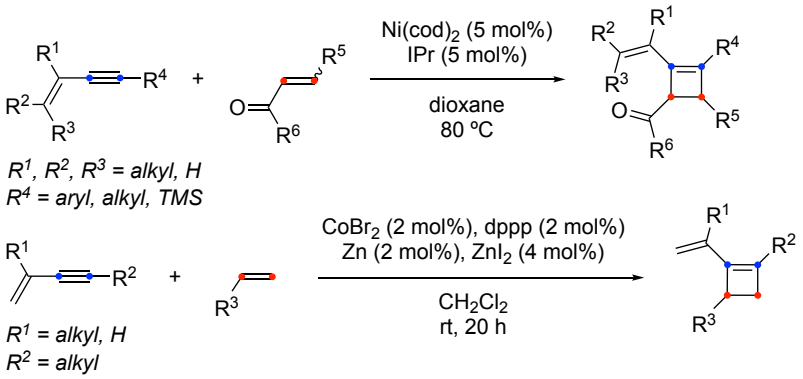

Scheme 1.3. [2+2] Cycloaddition of 1,3-enynes with alkenes to give 1-vinylcyclobutenes.

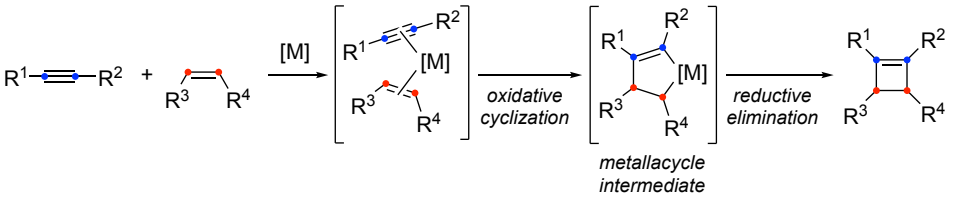

Scheme 1.4. Proposed mechanism for metal-catalyzed [2+2] cycloadditions.

In the presence of Lewis[58] or Brønsted acids,[59] the reaction between alkenes and acceptor-substituted alkynes like propiolates also leads to cyclobutenes. On the contrary, as mentioned in the **General Introduction**, in the presence of gold(I) this type of alkynes reacts with alkenes to give rise to lactones **2** or 1,3-dienes **3** (Scheme 1.5b).[46] Nevertheless, our group found that electron-rich aryl and cyclopropyl alkynes react with electron-rich alkenes by [2+2] cycloaddition to afford cyclobutenes **1** (Scheme 1.5a),[44] which show a

58. (a) Snider, B. B.; Rodini, D. J.; Conn, R. S. E.; Sealfon, S. *J. Am. Chem. Soc.* **1979**, *101*, 5283–5293. (b) Snider, B. B.; Roush, D. M.; Rodini, D. J.; Gonzalez, D.; Spindell, D. *J. Org. Chem.* **1980**, *45*, 2773–2785. (c) Snider, B. B. *Acc. Chem. Res.* **1980**, *13*, 426–432. (d) Okamoto, K.; Shimbayashi, T.; Tamura, E.; Ohe, K. *Org. Lett.* **2015**, *17*, 5843–5845 and references therein.
59. Inanaga, K.; Takasu, K.; Ihara, M. *J. Am. Chem. Soc.* **2005**, *127*, 3668–3669.

substitution pattern rather different than the cyclobutenes obtained by the aforementioned metal-catalyzed [2+2] cycloadditions. The divergent outcomes in the reactions of electron-deficient and electron-rich alkynes with alkenes are quite surprising, since even very similar gold(I)-catalysts bearing JohnPhos-based ligands are used in both cases.

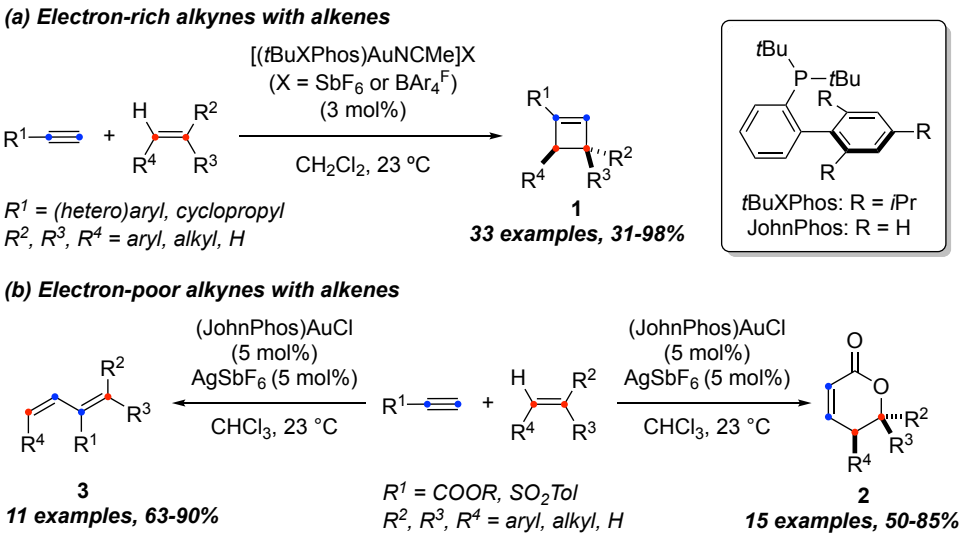

Scheme 1.5. Comparison of outcomes in gold-catalyzed reactions of terminal alkynes with alkenes.

In contrast with the mechanism of other metal-catalyzed transformations *via* metallacycle intermediates, gold(I)-catalyzed reactions of alkynes with alkenes presumably involve cyclopropyl gold carbenes intermediates (see **General Introduction** for details). Therefore, based on the mechanism of gold(I)-catalyzed cycloisomerizations of 1,*n*-enynes, our group hypothesized that alkenes attack at the internal carbon of the electron-rich alkynes to form cyclopropyl gold(I) carbenes of type **I**,[44] whereas electron-deficient alkynes were proposed to react at the terminal carbon leading to cyclopropyl gold carbenes of type **III** (Scheme 1.6).[46] These differences of the nucleophilic attack to electron-rich and electron-poor alkynes have been observed as well in hydroarylation reactions (see Introduction to **Chapter 3** for details).

Our group suggested that cyclopropyl gold(I) carbenes **I** evolve *via* ring expansion to give the benzylic carbocations **II** and, finally, cyclobutenes **1**.[44] Conversely, the groups of Shin and Yu proposed that intermediates **III** can experience intramolecular attack of the

carboxylic acid moiety to form lactones **2**, or undergo a formal 1,3-migration of C4 through intermediates **IV** to furnish 1,3-dienes **3**.[46] According to DFT calculations, the alternative migration of C3 *via* **V** to give dienes **4** is less kinetically favored due to the steric hindrance between the ester motif and the substituent in C3.

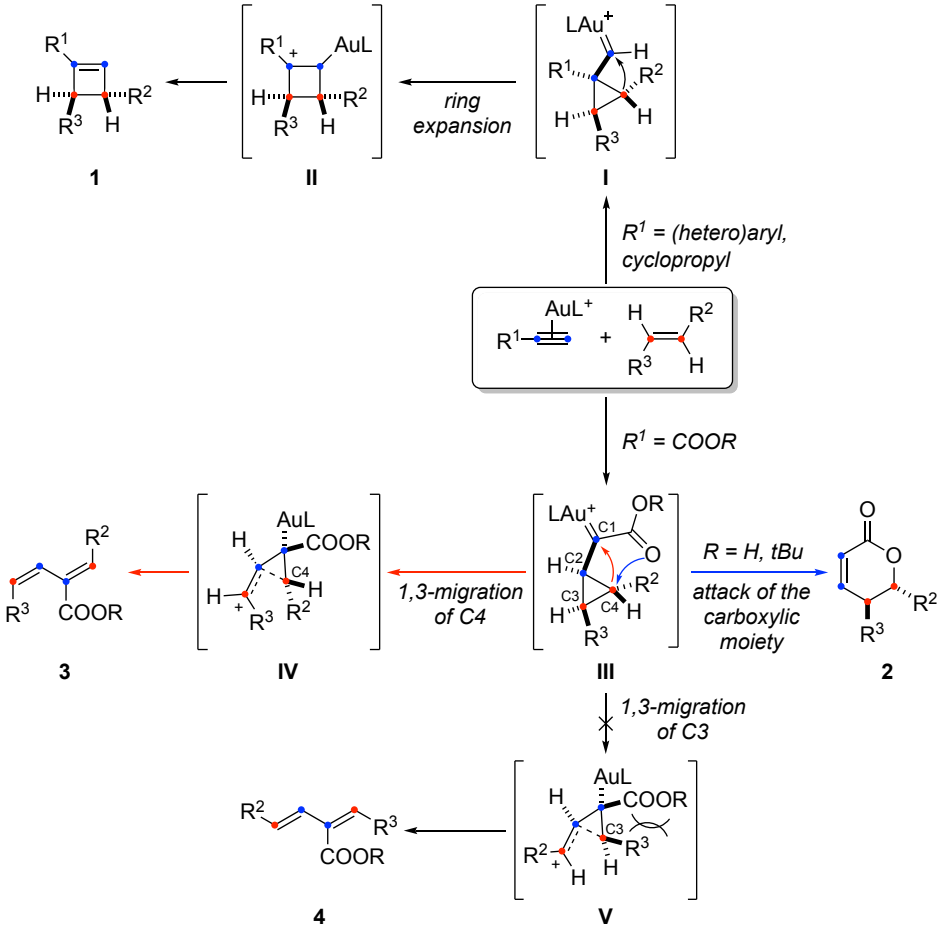

Scheme 1.6. Mechanism of intermolecular gold-catalyzed reactions of alkynes with alkenes.

Interestingly, the evolution of cyclopropylcarbenes to either cyclobutenes or 1,3-dienes has been observed in other systems. On one hand, cyclopropylcarbenes generated by diazo compounds **5**, **7** and **9** undergo ring expansion to afford the corresponding cyclobutenes (Scheme 1.7). Photolysis of *cis*- and *trans*-**5** gave *cis*- and *trans*-cyclobutenes **6**,

respectively, by a stereospecific ring expansion (Scheme 1.7a).[60] In these reactions, methyl propiolate and *cis*- or *trans*-2-butene were obtained as a result of a competitive fragmentation. Likewise, in the presence of AgOTf, *cis*- and *trans*-**7** undergo stereospecific ring expansion to *cis*- and *trans*-cyclobutenes **8**, respectively (Scheme 1.7b).[61,62] The thermal decomposition of the potassium salt of tosyl hydrazone **9** also led to the product of ring expansion **10**, together with the product of fragmentation **11** (Scheme 1.7c).[63]

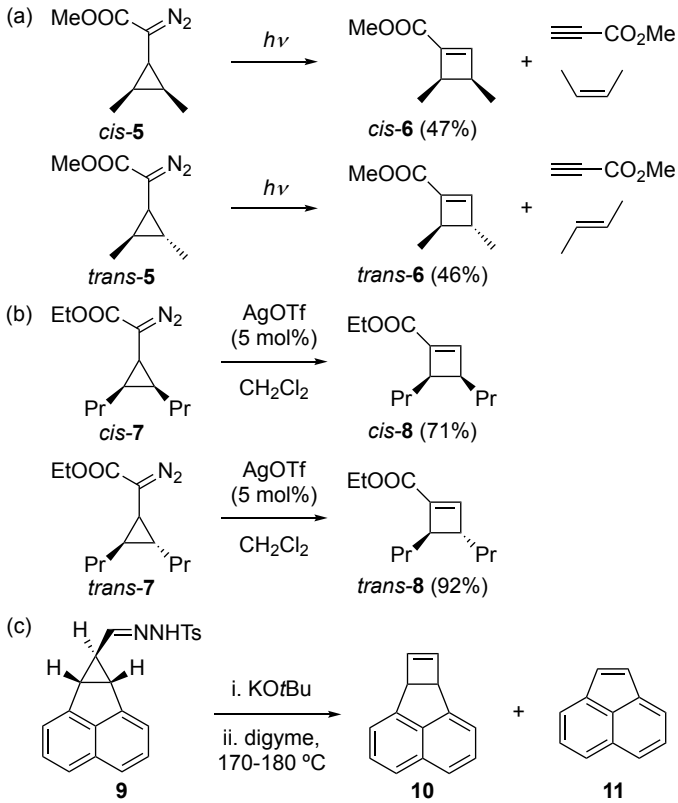

Scheme 1.7. Cyclopropyl carbenes by (a) photolysis, (b) metal-catalysis and (c) thermolysis.

60. Gallucci, R. R.; Jones, M. *J. Am. Chem. Soc.* **1976**, *98*, 7704–7711.
61. (a) Xu, H.; Zhang, W.; Shu, D.; Werness, J. B.; Tang, W. *Angew. Chem. Int. Ed.* **2008**, *47*, 8933–8936. (b) Similar transformation with cyclopropylphenyldiazomethane: Celebi, S.; Leyva, S.; Modarelli, D. A.; Platz, M. S. *J. Am. Chem. Soc.* **1993**, *115*, 8613–8620.
62. Cyclopropyl carbenes generated by Brook rearrangement also give cyclobutenes: Zhang, F.-G.; Marek, I. *J. Am. Chem. Soc.* **2017**, *139*, 8364–8370.
63. Meinwald, J.; Samuelson, G. E.; Ikeda, M. *J. Am. Chem. Soc.* **1970**, *92*, 7604–7606.

On the other hand, our group developed the generation of gold(I) carbenes by retro-Buchner reaction of 7-substituted 1,3,5-cyclohepatrienes **12** with gold(I) catalysts at high temperatures, which consists of a retro-cyclopropanation through norcaradienes **13**, followed by a formal decarbenation reaction with release of benzene (Scheme 1.8).[64] When this methodology was applied to derivative **14** to access cyclopropyl gold(I) carbene **15**, (*Z,Z*)-diene **16** was selectively delivered.[64b] Intermediate **15** could undergo ring expansion to form cyclobutene **17**, whose thermal conrotatory ring opening would lead to (*E,E*)-diene **16**. However, exclusively (*Z,Z*)-**16** was observed, which suggests that another mechanism operates in this transformation bypassing the formation of cyclobutene **17**.

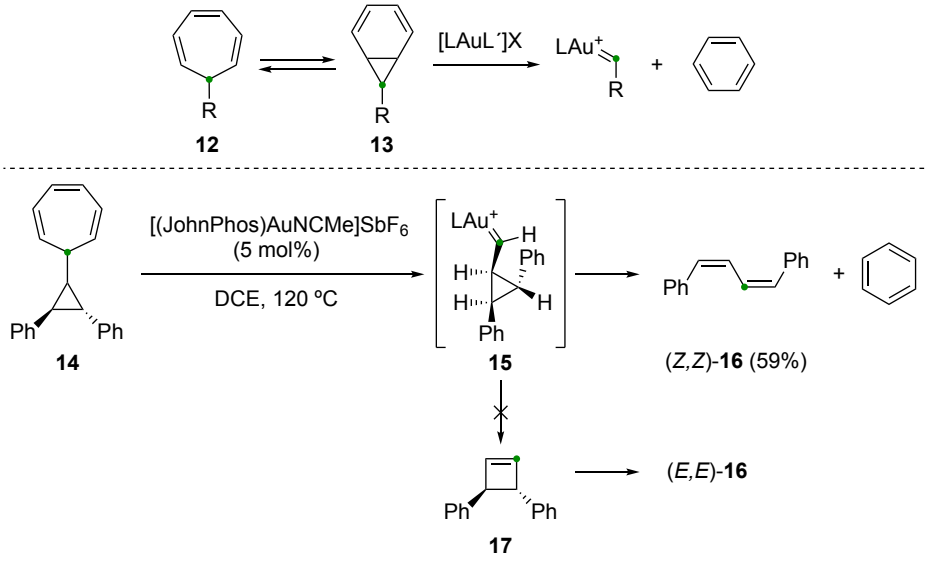

Scheme 1.8. Cyclopropyl gold(I) carbene generated by retro-Buchner reaction.

In principle, cyclopropyl gold(I) carbene **15** could be generated by gold(I) catalyzed intermolecular reaction of acetylene with *trans*-stilbene. However, the activation of acetylene by common gold catalysts has never been attained. Experimentation with acetylene involves high risks of flammability and explosion, difficulties of handle and the use of specific high-pressure equipment, especially when utilizing high pressure gas

64. (a) Solorio-Alvarado, C. R.; Echavarren, A. M. *J. Am. Chem. Soc.* **2010**, *132*, 11881–11883. (b) Solorio-Alvarado, C. R.; Wang, Y.; Echavarren, A. M. *J. Am. Chem. Soc.* **2011**, *133*, 11952–11955.

cylinders. Recently, safer and easy-to-handle calcium carbide[65] has been employed to produce acetylene *in situ* by treatment with water in one-[66] or two-chamber sealed reactors.[67] In the one-chamber reactor, the presence of calcium carbide and water in the reaction mixture is incompatible with base- or water-sensitive systems.

65. Rodygin, K. S.; Werner, G.; Kucherov, F. A.; Ananikov, V. P. *Chem. Asian J.* **2016**, *11*, 965–976.
66. Matake, R.; Niwa, y.; Matsubara, H. *Org. Lett.* **2015**, *17*, 2354–2357.
67. Voronin, V. V.; Ledovskaya, M. S.; Gordeev, E. G.; Rodygin, K. S.; Ananikov, V. P. *J. Org. Chem.* **2018**, *83*, 3819–3828, and references therein.

Objectives

Depending on the electronic nature of the alkyne, gold(I)-catalyzed intermolecular reactions of terminal alkynes with alkenes can lead to markedly different outcomes. In view of this striking difference, we decided to examine in further detail the reaction of a broader range of terminal alkynes, including acetylene itself, to get a clearer perspective of this fundamental reaction in gold(I) chemistry.

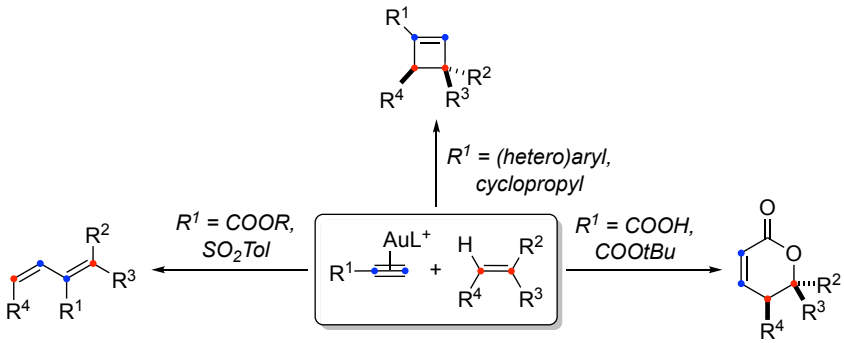

Scheme 1.9. Contrasting reactivity of alkynes in gold-catalyzed transformations with alkenes.

We aimed to gain a deeper understanding of how the divergent reaction pathways emerge by means of DFT calculations. The theoretical analysis of the mechanism leading to cyclobutenes could consolidate the one proposed based on the well-established cycloisomerizations of 1,*n*-enynes as well as kinetics and deuterium labelling experiments.

In order to support the initial involvement of cyclopropyl gold(I) carbenes in these transformations, we envisioned the independent generation of these intermediates by retro-Buchner reaction and study their reactivity.

These investigations would provide a comprehensive mechanistic picture of the gold(I)-catalyzed intermolecular reactions of alkynes with alkenes, which in turn could lead to the design of novel pathways to access new architectures. Moreover, the gold-catalyzed [2+2] cycloaddition could be further expanded to construct a variety of valuable cyclobutenes, overcoming the limitations imposed by the exclusive use of terminal (hetero)aryl- and cyclopropylalkynes.

Results and Discussion

On the Methods of Quenching the Gold-Catalyzed Reactions

Before exploring a wider range of alkynes in the gold(I)-catalyzed reactions with alkenes, we sought to develop a reproducible and unified procedure to perform these transformations. We realized that in the literature diverse methods have been used to quench the gold-catalyzed reactions, namely the simple addition of triethylamine, the use of Reaxa's QuadraPure™ MPA resin (Scheme 1.10)[68] and the filtration over silica gel or alumina oxide.

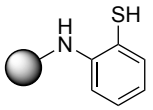

Scheme 1.10. Functionality of Reaxa's QuadraPure™ MPA scavenger resin.

In the former cases, the triethylamine and the resin bound scavenging agent QuadraPure™ MPA can bind irreversibly to gold by the amino or thiol groups, leading to the catalyst deactivation and, subsequently, the halt of the reaction. In the latter cases, the plug of silica gel and alumina oxide (neutral or basic) can retain the gold-catalyst and produce its conversion to much less active species such as aquo and hydroxy gold complexes.[69,70]

All these different methods of quenching gold-catalyzed reactions were evaluated in the same gold(I)-catalyzed [2+2] cycloaddition of phenylacetylene and α-methylstyrene (Scheme 1.11).

68. Biannic, B.; Ghebreghiorgis, T.; Aponick, A. *Beilstein J. Org. Chem*. **2011**, *7*, 802–807.
69. Examples of characterized aquo and hydroxy gold complexes: (a) Gaillard, S.; Bosson, J.; Ramon, R. S.; Nun, P.; Slawin, A. M. Z.; Nolan, S. P. *Chem. Eur. J.* **2010**, *16*, 13729–13740. (b) Tang, Y.; Yu, B. *RSC Adv.* **2012**, *2*, 12686–12689. (c) Zhdanko, A.; Ströbele, M.; Maier, M. E. *Chem. Eur. J.* **2012**, *18*, 14732–14744. (d) Adriaenssens, L.; Escribano-Cuesta, A.; Homs, A.; Echavarren, A. M.; Ballester, P. *Eur. J. Org. Chem.* **2013**, *8*, 1494–1500. See also ref. 10a.
70. (a) Hydroxy gold complexes proved to catalyze the hydration of alkynes: Gomez-Suarez, A.; Oonishi, Y.; Meiries, S.; Nolan, S. P. *Organometallics* **2013**, *32*, 1106–1111. (b) Studies on the catalytic activity of hydroxy gold complexes in cycloisomerizations of 1,6-enynes and [4+2] cycloaddition of arylenynes: Homs, A.; Echavarren, A. M. *Master Thesis, unpublished results.*

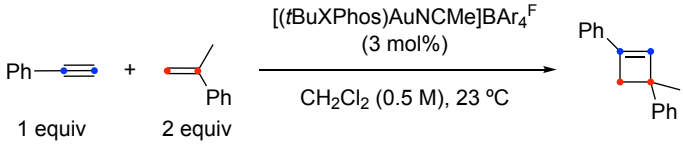

Scheme 1.11. Gold-catalyzed reaction used in the evaluation of the quenching methods.

Firstly, we attempted to test the addition of triethylamine as quenching agent. Two reactions in a 0.5 mmol scale were performed. Aliquots were taken from each reaction mixture and quenched by adding triethylamine. After removal of volatiles by rotatory evaporation, the resulting crudes were analyzed by quantitative ^{1}H NMR using 1,4-diacetylbenzene as internal standard. The curves in black and red in Figure 1.1 show the results of the aliquots quenched after 1 and 3 h, in which the reaction went to 47% and 57% yield, respectively. After 12 h, the reactions were otherwise completed obtaining more than 90% yield. ^{1}H NMR spectra of the aliquots were recorded again 4 and 7 h after the quenching, and during this period the reaction did not proceed further. This means that adding triethylamine to the reaction mixture is a valid method to quench gold(I)-catalyzed reactions.

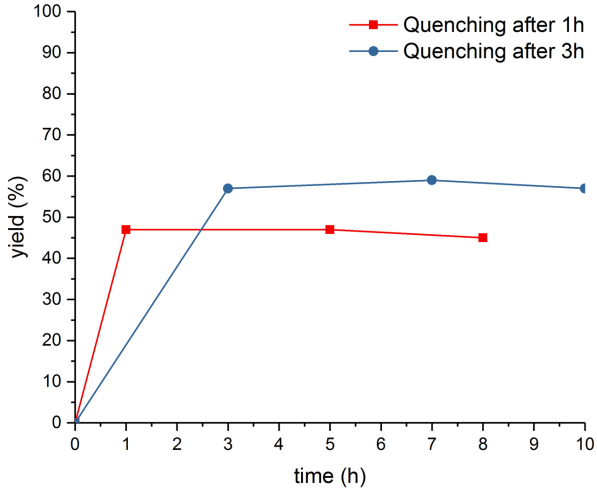

Figure 1.1. Quenching gold(I)-catalyzed reactions by addition of triethylamine.

The other methods of quenching gold(I)-catalyzed reactions were compared by analysis of gold traces in the reaction crudes (in the *Unitat d'Anàlisi de Metalls of the Centres Científics*

i Tecnològics (CCiTUB) at the *Universitat de Barcelona*). The same gold(I)-catalyzed [2+2] cycloaddition of phenylacetylene and α-methylstyrene was performed five times in 5 mmol scale. The reaction mixtures were quenched in different manners (Table 1.1) and divided in three replicas. After removal of the volatiles under vacuum, the resulting samples were subjected to analysis of gold traces. The results reveal that in every case only 1-2% (300 - 600 ppm) of all the gold loading used in the reaction remains in the crude after quenching. Consequently, all tested methods are equally effective to quench gold(I)-catalyzed reactions.

Table 1.1. Comparison of different methods to quench gold(I)-catalyzed reactions.

Sample	Replica	Method of quenching	% of Au in the sample[a]	% of Au in the crude[b]
1	1	Adding TEA and filtering through silica gel	1.45	1.65
	2		1.67	1.66
	3		1.36	1.99
2	1	Filtering through silica gel	1.58	1.65
	2		1.55	1.71
	3		1.73	1.46
3	1	Filtering through alumina oxide neutra	1.43	1.62
	2		1.64	1.52
	3		1.53	1.76
4	1	Filtering through alumina oxide basic	1.17	1.94
	2		1.40	1.74
	3		1.58	1.61
5	1	QuadraPure™ MPA[c] and filtering through Teflon	1.11	1.82
	2		1.38	1.58
	3		1.41	1.45

[a] % of Au in the sample reported by the CCiTUB.
[b] % of all the Au loading used in the reaction remaining in the crude after quenching.
[c] Following the procedure reported in ref. 68.

Arylalkynes Leading to Cyclobutenes and 1,3-Dienes

As explained in the **General Introduction**, the gold(I) catalyst **A** with a very bulky phosphine was key to succeed in the intermolecular [2+2] cycloaddition of arylalkynes with alkenes.[44a] Later, catalyst **B** with a softer BAr_4^{F-} counterion showed to provide even better yields (Scheme 1.12).[44b] These reactions proceed generally in good to excellent yields at 23 ºC with 3 mol% of gold(I) catalyst in CH_2Cl_2 as optimal solvent. Thus, under these conditions, reaction of phenylacetylene with α-methylstyrene (**19a**) affords regioselectively cyclobutene **20a** in 95% yield (Table 1.2, entry 1).

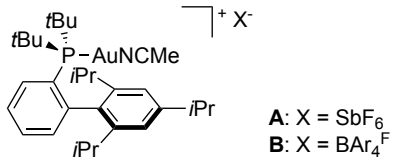

Scheme 1.12. Key gold(I) catalysts for the intermolecular reaction of arylalkynes with alkenes.

In the same manner, a series of cyclobutenes were obtained from *para*- and *meta*-substituted arylalkynes.[44] However, only one example using *ortho*-substituted arylalkynes was reported, namely the reaction of *o*-anisylacetylene (**18b**) with α-methylstyrene (**19a**) to form cyclobutene **20b** in a low 30% yield (Table 1.2, entry 2). For this reason, we focused on exploring the reactivity of differently *ortho*-substituted arylalkynes. In these cases, it was necessary to increase the catalyst loading up to 5 mol% and the temperature to 50 ºC to achieve good yields. Therefore, in the reaction between **18b** and **19a**, a higher 54% yield of cyclobutene **20b** was reached under the new conditions (Table 1.2, entry 3).

Surprisingly, not only did the reaction of *o*-tolylacetylene (**18c**) with **19a** lead to cyclobutene **20c**, but also the unexpected 1,3-diene **21c** (Table 1.2, entry 4), which were obtained in a 1.3:1 ratio in moderate yields. The stereoselective formation of such type of 1,3-butadienes **21** was never detected before in the gold(I)-catalyzed reactions of terminal cyclopropyl or (hetero)arylalkynes with alkenes. Likewise, the reaction of (*o*-fluorophenyl)acetylene (**18d**) with **19a** gave cyclobutene **20d** in good yield together with traces of 1,3-diene **21d** (Table 1.3, entry 5). In contrast, dienes **21e-g** were obtained as the major products in the reactions of *o*-chloro- and *o*-bromophenyl acetylenes (**18e,f**) with **19a**

(Table 1.2, entries 6-7).[71] Interestingly, arylalkyne **18g** with an *o*-CF_3 group only afforded 1,3-diene **21g** (Table 1.2, entry 8), whereas its analogous **18h** with CF_3 in the *para* position provided cyclobutene **20h** as the major product, restoring the usual reactivity (Table 1.2, entry 9).

Table 1.2. Gold(I)-catalyzed reaction of *o*-substituted arylalkynes with α-methylstyrene.[72,a]

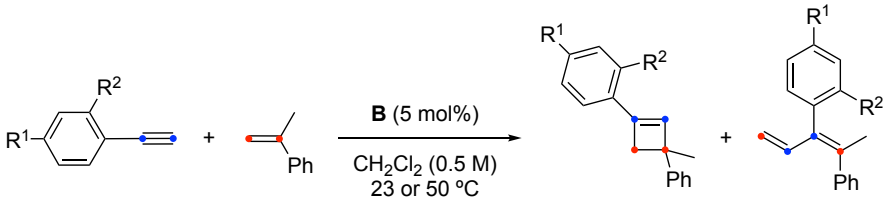

Entry	**18a-h**	R^1	R^2	T (ºC)	**B** (mol%)	**20** (%)[b]	**21** (%)[b]
1	**18a**	H	H	23	3	**20a** (95)[c]	-
2	**18b**	H	OMe	23	3	**20b** (30)[c]	-
3	**18b**	H	OMe	50	5	**20b** (54)	-
4[d,e]	**18c**	H	Me	50	5	**20c** (37)	**21c** (29)
5	**18d**	H	F	50	5	**20d** (64)	**21d** (3)
6[e-g]	**18e**	H	Cl	50	5	**20e** (9)	**21e** (48)
7[f]	**18f**	H	Br	50	5	**20f** (3)	**21f** (45)
8	**18g**	H	CF_3	50	5	-	**21g** (36)
9[e,h]	**18h**	CF_3	H	50	5	**20h** (75)	**21h** (5)

[a] Alkyne:alkene in a 1:2 ratio. [b] Yields determined by ^{1}H NMR using 1,4-diacetylbenzene as internal standard. See Experimental Part for isolated yields. [c] From ref. 44b.**Error! B ookmark not defined.** [d] Alkyne:alkene in a 1:4 ratio. [e] 4 mol% of catalyst. [f] Catalyst **A** instead of **B**. [g] Alkyne:alkene in a 1:3 ratio. [h] **B** prepared *in situ* from (*t*BuXPhos)AuCl and $NaBAr_4^F$.

1,3-Dienes **11c-h** were obtained as single *E*-stereoisomers as determined by nOe experiments. This assignment was confirmed in the case of **21f** (Table 1.2, entry 7) by X-ray diffraction of its crystalline derivative **21i** (Scheme 1.13). 1,3-Diene **21i** was synthesised *via* Suzuki coupling of **21f** with *p*-nitrophenylboronic acid.

71. In an independent study, the reactions of **18f** and *o*-iodophenylacetylene with 2,3-dimethyl-2-butene were shown to give only cyclobutenes as products: Hashmi, A. S. K.; Wieteck, M.; Braun, I.; Rudolph, M.; Rominger, F. *Angew. Chem. Int. Ed.* **2012**, *51*, 10633–10637.
72. This includes experiments performed initially by Laura Amenós and Verónica López-Carrillo.

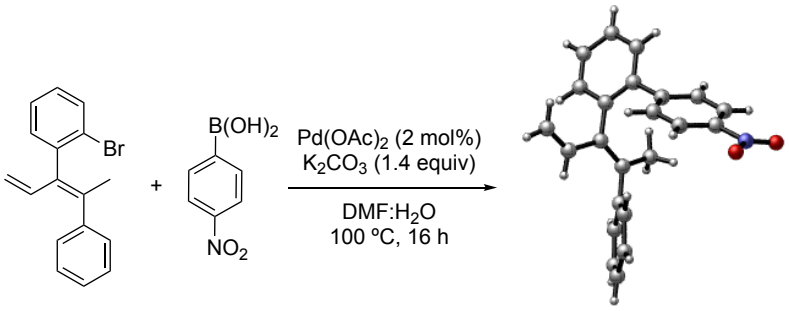

21f **21i**

Scheme 1.13. Derivatization of **21f** to form 1,3-diene **21i** (CYLview depiction of the X-ray crystal structure of **21i**).

Table 1.3. Gold(I)-catalyzed reaction of *o*-substituted arylalkynes with methylenecycloalkanes.[a]

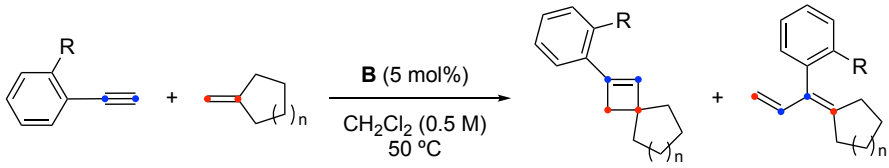

18b-f **19b-c** **20j-s** **21j-s**

Entry	**18b-f**	R^1	n	**20** (%)[b]	**21** (%)[b]
1	**18b**	OMe	2	**20j** (50)	**21j** (3)
2	**18c**	Me	2	**20k** (65)	**21k** (27)
3	**18d**	F	2	**20l** (50)	**21l** (25)
4	**18e**	Cl	2	**20m** (54)	**21m** (33)
5	**18f**	Br	2	**20n** (44)	**21n** (25)
6	**18b**	OMe	1	**20o** (58)	**21o** (24)
7	**18c**	Me	1	**20p** (61)	**21p** (38)
8	**18d**	F	1	**20q** (51)	**21q** (33)
9	**18e**	Cl	1	**20r** (25)	**21r** (43)
10	**18f**	Br	1	**20s** (24)	**21s** (42)

[a] Alkyne:alkene in a 1:2 ratio. [b] Yields determined by ^{1}H NMR using 1,4-diacetylbenzene as internal standard. See Experimental Part for isolated yields.

Reactions of *o*-substituted arylalkynes **18b-f** with methylenecyclohexane (**19b**) or methylenecyclopentane (**19c**) led to mixtures of cyclobutenes **20** and 1,3-dienes **21** (Table 1.3, entries 1-10). Noteworthy, in the reaction between *o*-anisylacetylene (**18b**) and **19b**,

cyclobutene **20j** was obtained as the major product (Table 1.3, entry 1). We did not find any clear correlation between the electronic character of the *ortho*-substituent in the arylalkyne and the ratio of the cyclobutene and diene products, as the same arylalkynes react with very similar methylenecycloalkanes **19b,c** giving different ratios of the products.

In the same manner, polyaromatic acetylenes such as 1-naphthylacetylene (**18i**) and 9-phenanthrylacetylene (**18j**) react with **19b** to give rise to cyclobutenes **20t,u** and 1,3-dienes **21t,u** (Scheme 1.14).

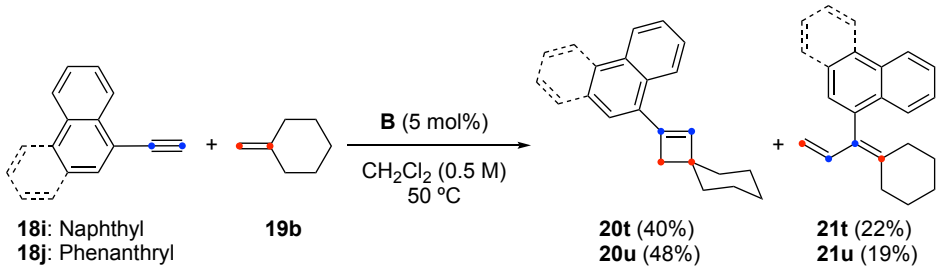

Scheme 1.14. Gold(I)-catalyzed reaction of polyaromatic-substituted alkynes with alkene **19b** (Alkyne:alkene in a 1:2 ratio. Yields determined by ^{1}H NMR using 1,4-diacetylbenzene as internal standard. See Experimental Part for isolated yields).

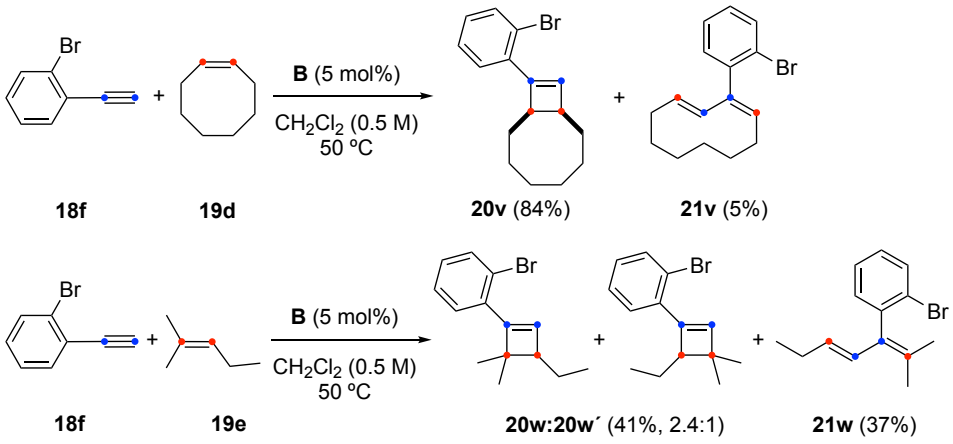

Scheme 1.15. Gold(I)-catalyzed reaction of arylalkyne **18f** with internal alkenes (Alkyne:alkene in a 1:2 ratio. Isolated yields).

Table 1.4. Reaction of arylalkynes **18a** and **18f** with **19a** using different catalysts.[a]

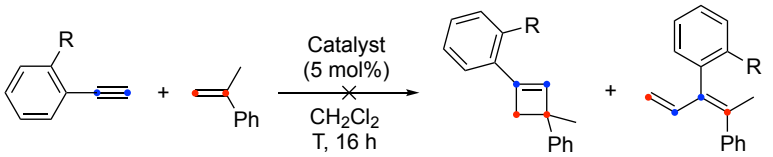

18a: R = H
18f: R = Br

19a

20a (0%)
20f (0%)

21a (0%)
21f (0%)

Entry	R	Catalyst	T (ºC)	Entry	R	Catalyst	T (ºC)
1	H	$PtCl_2$	23	16	Br	$GaCl_3$	50
2	H	$PtCl_2$	50	17	Br	$InCl_3$	23
3	H	$GaCl_3$	23	18	Br	$InCl_3$	50
4	H	$GaCl_3$	50	19	Br	CuCl	23
5	H	$InCl_3$	23	20	Br	CuCl	50
6	H	$InCl_3$	50	21	Br	AgCl	23
7	H	CuCl	23	22	Br	AgCl	50
8	H	AgCl	23	23	Br	AgOTf	23
9	H	AgOTf	23	24	Br	AgOTf	50
10	H	$AgNTf_2$	23	25	Br	$AgNTf_2$	23
11	H	$AgSbF_6$	23	26	Br	$AgNTf_2$	50
12	H	**C**	23	27	Br	$AgSbF_6$	23
13	Br	$PtCl_2$	23	28	Br	$AgSbF_6$	50
14	Br	$PtCl_2$	50	29	Br	**C**	23
15	Br	$GaCl_3$	23	30	Br	**C**	50

[a] Alkyne:alkene in a 1:2 ratio. The crude was analyzed by ^1H NMR.

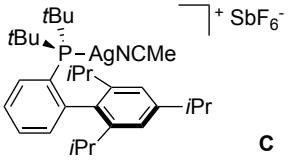

C

It is remarkable that in all these reactions with terminal alkenes, 1,3,3-trisubstituted cyclobutenes were formed by a regioselective [2+2] cycloaddition. The regioisomeric 1,4,4-trisubstituted cyclobutenes were not observed. The gold(I)-catalyzed reaction of (*o*-bromophenyl)acetylene (**18f**) with α-methylstyrene (**19a**) as well as the reaction (*o*-fluorophenyl)acetylene (**18d**) with methylenecyclohexane (**19b**) were performed on a 1 g

scale of the alkyne without significant change in the yield of the corresponding cyclobutenes and dienes.

In addition, internal alkenes were tested in this transformation (Scheme 1.15). In the reaction of **18f** with (*Z*)-cyclooctene (**19d**), cyclobutene **20v** was obtained as the major product in good yield together with butadiene **21v**. The structure of bicyclo[6.2.0]dec-9-ene **20v** was confirmed by X-ray diffraction, whereas the configuration of **21v** was determined by nOe experiments. However, reaction of **18f** with 2-methyl-2-pentene (**19e**) rendered a mixture of cyclobutenes **20w** and **20w´** in a 2.4:1 ratio, and 1,3-diene **21v**. These structures were assigned on basis of nOe experiments. Interestingly, in previously reported gold(I)-catalyzed [2+2] cycloaddition of alkynes with **19e** the major product was the 1,3,3,4-tetrasubstituted cyclobutene, which is the minor regioisomeric cyclobutene found in this case.[44]

Other metal catalysts known to promote cycloisomerization of 1,*n*-enynes such as $PtCl_2$, $GaCl_3$, $InCl_3$, fail to catalyze the reaction between alkynes **18a** or **18f** with α-methylstyrene (**19a**) at 23 °C or 50 °C (Table 1.4, entries 1-6 and 13-18). Similarly, neither cyclobutene nor 1,3-diene were observed in the presence of CuCl, AgCl, AgOTf, $AgNTf_2$, $AgSbF_6$ or silver complex **C** under these conditions (Table 1.4, entries 7-12 and 19-30).

1,3-Butadiynes Leading to Cyclobutenes

To delineate the importance of electronic and steric effects, we examined the gold(I)-catalyzed reaction of alkenes with aryl-1,3-butadiynes **22**,[73] ethynylogous to arylalkynes **18**. Reaction of the parent 1-phenyl-1,3-butadiyne (**22a**) with 2,3-dimethylbut-2-ene (**19f**) led selectively to cyclobutene **23a** by addition to the terminal triple bond with all the gold(I) catalysts tested (Table 1.5).[74] The transformation generally proceeds in good yields at 23

73. Other gold(I)-catalyzed reactions of 1,3-diynes: Asiri, A. M.; Hashmi, A. S. K. *Chem. Soc. Rev.* **2016**, *45*, 4471–4503.
74. Photochemical synthesis of 1-alkynylcyclobutenes from 1,3-diynes and alkenes: (a) Lee, T. S.; Lee, S. J.; Shim, S. C. *J. Org. Chem.* **1990**, *55*, 4544–4549. (b) Kwon, J. H.; Lee, S. J.; Shim, S. C. *Tetrahedron Lett.* **1991**, *32*, 6719–6722. (c) 1-Alkynylcyclobutenes from 1,3-diynes and alkenes by cobalt catalysis: ref. 53c.

ºC using phosphine-, phosphite- and NHC-based gold catalysts (Table 1.5, entries 1-6 and 8), although slightly better yields were reached employing NHC-gold(I) complex **F** (Table 1.5, entry 5). However, low conversion and yield were obtained with gold(I) complex **H** (Table 1.5, entry 7). In every case, the internal alkyne of **22a** remained unaltered.

Table 1.5. Gold(I)-catalyzed reaction of 1,3-butadiyne **22a** with alkene **19f**.[a]

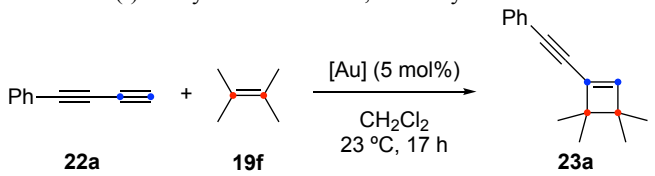

22a **19f** **23a**

Entry	[Au]	**23a** (%)[b]
1	**A**	70
2	**B**	70
3	**D**	70 (60)
4	**E**	69
5	**F**	78 (72)
6	**G**	74
7	**H**	16[c]
8	**I**	56

[a] 1,3-Diyne:alkene in a 1:2 ratio. [b] Yields determined by ^{1}H NMR using 1,4-diacetylbenzene as internal standard. Isolated yields in parentheses. [c] 45% conversion.

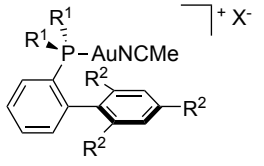

A: R^1 = *t*Bu; R^2 = *i*Pr; X = SbF_6
B: R^1 = *t*Bu; R^2 = *i*Pr; X = BAr_4^F
D: R^1 = *t*Bu; R^2 = H; X = SbF_6
E: R^1 = Cy; R^2 = *i*Pr; X = SbF_6

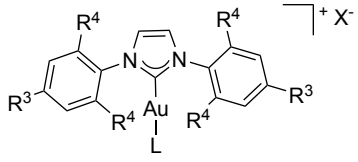

F: R^3 = H; R^4 = *i*Pr; L = NCMe; X = SbF_6
G: R^3 = H; R^4 = *i*Pr; L = NCPh; X = BAr_4^F
H: R^3 = Me; R^4 = Me; L = 2,4,6-$(OMe)_3C_6H_2CN$; X = SbF_6

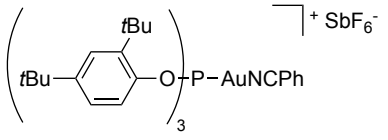

I

Differently substituted 1-aryl-1,3-diynes **22a-h** and 1-thienyl-1,3-diyne (**22i**) react with alkene **19f** to give 1-ethynyl-cyclobutenes **23a-i** in good to excellent yields (Table 1.6).

Alkyl substituted 1,3-diyne **22j** also provides the corresponding cyclobutene **23j**, which is remarkable, as alkynes with alkyl substituents are very poorly reactive with alkenes in the presence of gold(I) catalysts.[44] Likewise, other di-, tri-, and tetrasubstituted alkenes **19e-j** reacted with 1,3-diynes **22a**, **22c** and **22i** to give 1-alkynylcyclobutenes **23k-p**. Unsymmetrical alkenes such as 2-methylbut-2-ene and methylenecyclohexane produced a mixture of regioisomeric cyclobutenes **23m,n**, being the major the 1,4,4-substituted ones.

Table 1.6. Scope of the gold(I)-catalyzed reaction of 1,3-diynes with alkenes.

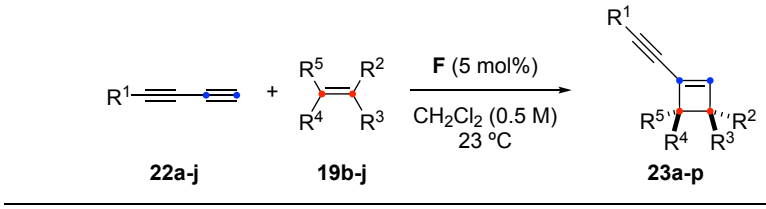

22a-j **19b-j** **23a-p**

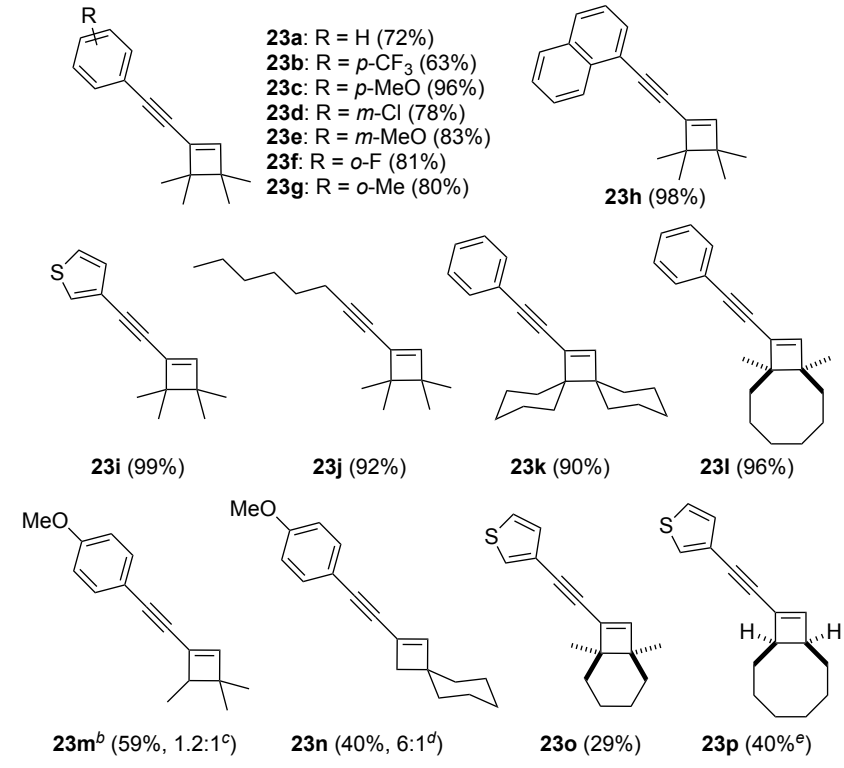

[a] 1,3-Diyne:alkene in a 1:2 ratio. Isolated yields. [b] Small amounts of 1,3-diene product was detected by ^{1}H NMR. [c] Minor regioisomer is the 1,3,4,4-tetrasubstituted cyclobutene. [d] Minor regioisomer is the 1,4,4-trisubstituted cyclobutene. Reaction at 40 °C. [e] Reaction at 50 °C.

Interestingly, the reaction of diyne **22a** with α-methylstyrene (**19a**) led to a mixture of regioisomeric cyclobutenes **23q**:**23q´** in a 5.5:1 ratio along with a mixture of diastereomeric cyclohexenes **24**:**24´** in a 4:1 ratio, which resulted from a [2+2+2] cycloaddition. The 1:2 adducts of type **24** were also formed in the reaction of ynamides with alkenes (see Scheme 15 of the **General Introduction**), although in those cases the *trans* stereoisomers were exclusively observed.

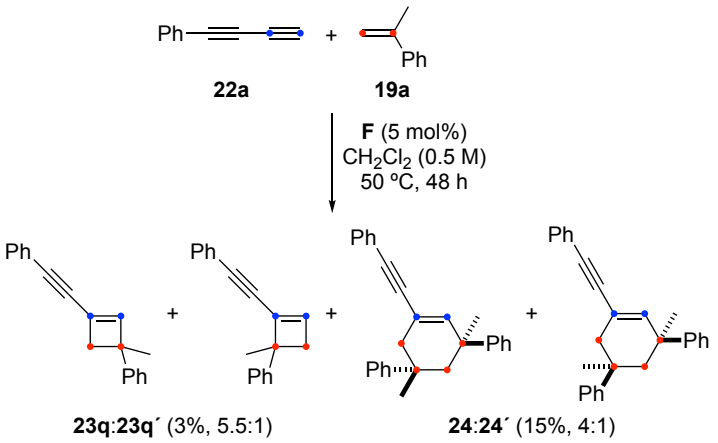

Scheme 1.16. Gold-catalyzed reaction of 1,3-diyne **22a** and **19a**.

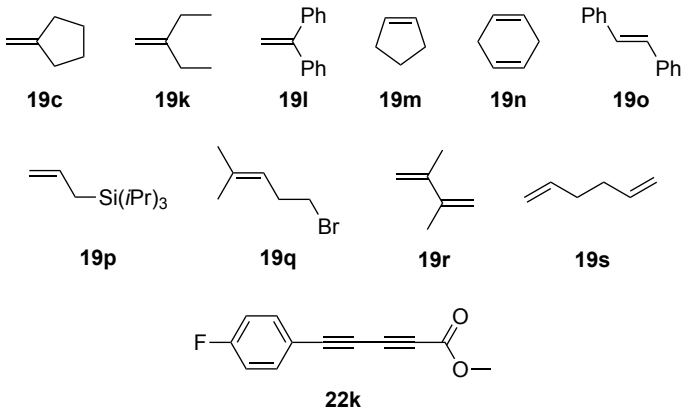

Scheme 1.17. Other substrates tested in the gold(I)-catalyzed reaction of 1,3-diynes with alkenes.

The reaction of various 1,3-diynes with terminal alkenes such as methylenecyclopentane (**19c**), 2-ethyl-1-butene (**19k**) or 1,1-diphenylethylene (**19l**) gave only traces of the corresponding cyclobutenes (Scheme 1.17). Disubstituted cyclic alkenes **19m** and **19n** also

provided traces of cyclobutenes. Similarly, 1,3-butadiynes were mainly recovered in the reaction with *trans*-stilbene (**19o**), monosubstituted alkene **19p** or trisubstituted alkene **19q**. In the case of dienes **19r** and **19s**, polymerization was observed. Finally, internal diyne **22k** did not undergo cycloaddition with different alkenes, using gold(I) catalysts **B**, **F** or **I**, neither at 23, 50 nor 80 ºC.

Mechanism for the Formation of Cyclobutenes and Dienes

Deuteration and Monitoring Experiments

To confirm the formal alkene fragmentation (metathesis-type) in the formation of 1,3-dienes in the intermolecular gold(I)-catalyzed reaction of *ortho*-substituted arylalkynes with alkenes, a simple experiment between terminally deuterated alkyne **18f-*d*1** and alkene **19a** with catalyst **A** was carried out (Scheme 1.18).[75] In this reaction, we obtained exclusively 1,3-diene **21f-*d*1**, revealing that a formal insertion of the alkyne into the alkene carbons takes place in this process, similar to the single-cleavage rearrangement in the cycloisomerizations of 1,*n*-enynes (see **General Introduction**). The alternative product **21f-*d*1'** was not observed, which would result from a formal cleavage of both the alkyne and the alkene, as the double-cleavage-type rearrangement in the cycloisomerizations of 1,*n*-enynes (see **General Introduction**).

Scheme 1.18. Reaction of arylalkyne **18f-*d*1** and alkene **19a** leading to diene **21f-*d*1**.

75. Experiment performed by Laura Amenós.

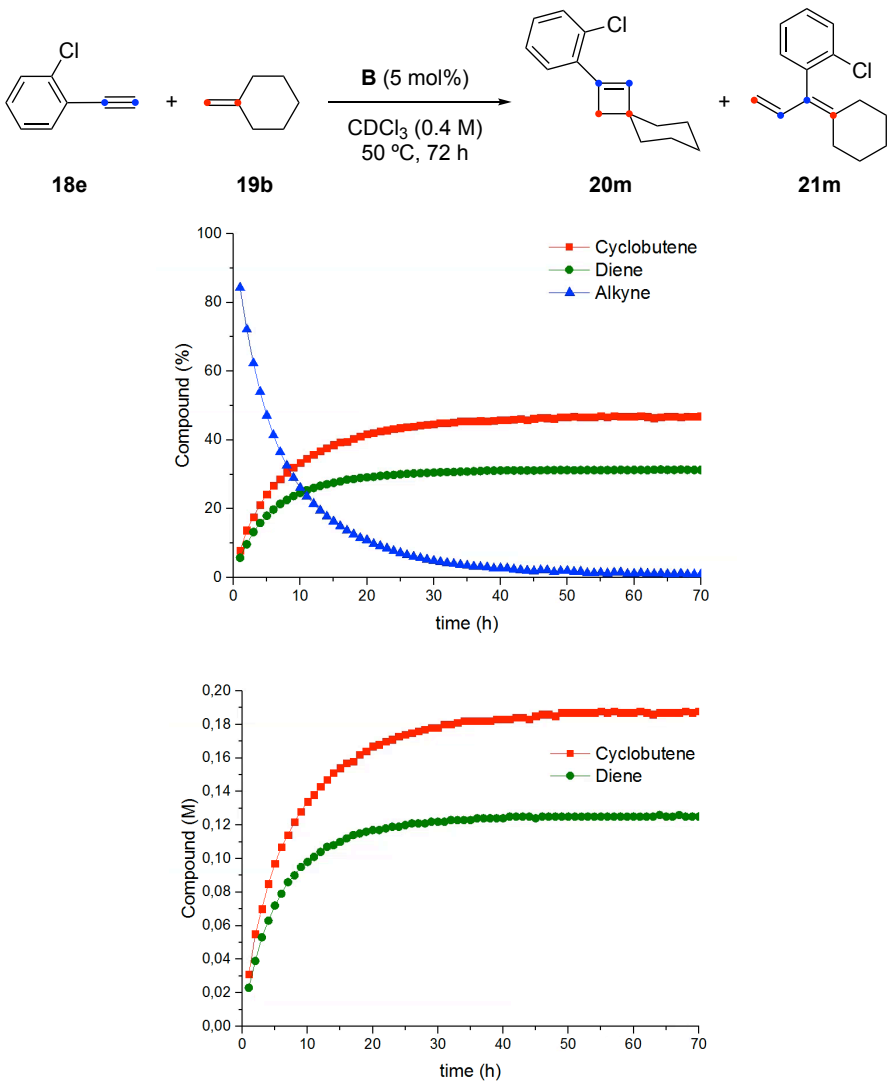

Scheme 1.19. Monitoring the reaction of arylalkyne **18e** with alkene **19b** by ^{1}H NMR using Ph_2CH_2 as internal standard (alkyne:alkene in a 1:2 ratio).

Monitoring the reaction of alkyne **18e** with alkene **19b** by ^{1}H NMR (Scheme 1.19) shows that the [2+2] cycloaddition leading to cyclobutene **20m** is *ca.* 1.4 times faster than the formation of 1,3-diene **21m**, as the initial rates resulted to be 8.7×10^{-6} M/s and 6.4×10^{-6} M/s, respectively (Table 1.7).

Table 1.7. Rates of the formation of **20m** and **21m**.[a]

$$\text{reaction rate} = \frac{d[\text{C}]}{d\text{t}}$$

$$\text{initial rate} = \frac{[\text{C}]_{\text{t1}} - [\text{C}]_{\text{t0}}}{\text{t}_1 - \text{t}_0} \qquad \text{overall rate} = \frac{[\text{C}]_{\text{f}} - [\text{C}]_{\text{t0}}}{\text{t}_{\text{f}} - \text{t}_0}$$

Parameter	20m	21m	Parameter	20m	21m
$[C]_{t1}$ (M)	0.031	0.023	$[C]_f$ (M)	0.19	0.12
t_1 (h)	1	1	t_f (h)	45	36
Initial rate (M/s)	**8.7×10^{-6}**	**6.4×10^{-6}**	**Overall rate (M/s)**	**1.1×10^{-6}**	**9.5×10^{-7}**

[a] [C] = concentration of the product. $[C]_f$ = maximum concentration of the product, at t_f. t_f = reaction time when the formation of the product is completed. $[C]_{t1}$ = concentration at t_1. $[C]_{t0}$ = initial concentration of the product = 0 M, at t_0 = 0 h.

Theoretical Studies

To get a deeper insight into the mechanism of the formation of cyclobutenes **20** and/or 1,3-dienes **21** as well as the influence of the substituents on the substrates in the reaction outcome, we performed DFT calculations[76] using PMe_3 as the ligand for gold(I).[77] We examined the reaction of phenylacetylene (**18a**) with α-methylstyrene (**19a**) to give cyclobutene **20a** as well as the reaction of (*o*-bromophenyl)acetylene (**18f**) with **19a** leading to 1,3-diene **21f** as the major product. For the sake of comparison, we also analyzed computationally the mechanism of the reaction between 1-phenyl-1,3-butadiyne (**22a**) and alkenes to generate cyclobutenes.

Reaction of Phenylacetylene with α-Methylstyrene

As commented in the **General Introduction**, electron-rich alkenes coordinate preferentially to gold(I) leading to (η^2-alkene)gold(I) complexes. According to the reported

76. (a) See the computational methods in the Experimental Part. (b) A data set collection of computational results is available in the ioChem-BD repository: Álvarez-Moreno, M.; de Graaf, C.; Lopez, N.; Maseras, F.; Poblet, J. M.; Bo, C. *J. Chem. Inf. Model.* **2015**, *55*, 95–103.
77. For a recent discussion on the coordination of phosphine ligands to gold(I), see: Ciancaleoni, G.; Scafuri, N.; Bistoni, G.; Macchioni, A.; Tarantelli, F.; Zuccaccia, D.; Belpassi, L. *Inorg. Chem.* **2014**, *53*, 9907–9916.

experimental evidences,[44b] the reaction begins with the associative ligand exchange of (η^2-alkene)gold(I) complex **Int1a** to generate the slightly less stable (η^2-alkyne)gold(I) complex **Int2a** (Scheme 1.20). The subsequent attack of the alkene to the activated alkyne **Int2a** can take place being the phenyl groups of the substrates in an *anti* (intermediates **a**) or *syn* (intermediates **b**) fashion. Moreover, the alkene can attack at the internal carbon of the alkyne to form intermediates **Int4a,b** or at the terminal carbon of the alkyne to form **Int3a,b**. Anyway, the generation of **Int4a,b** is kinetically more favored than the regioisomeric **Int3a,b** by at least 3.8 kcal/mol. Although formation of **Int4b** requires 0.9 kcal/mol lower energy than **Int4a**, further evolution of **Int4a** to other intermediates proceeds through lower energy barriers.

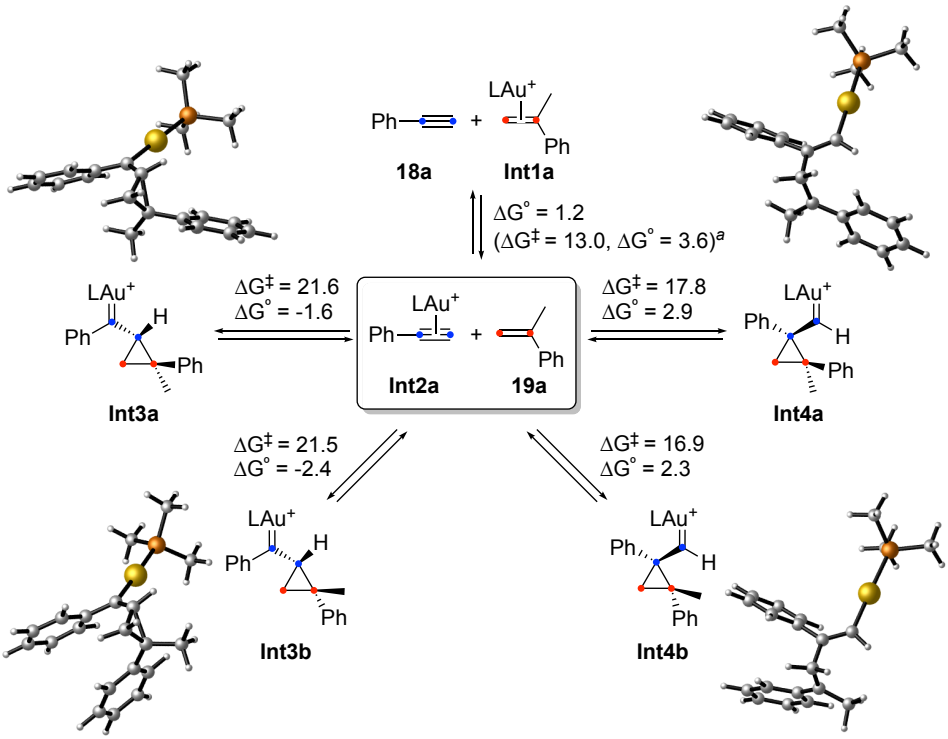

Scheme 1.20. Formation of cyclopropyl gold(I) carbenes **Int3a,b** and **Int4a,b** (L = PMe_3. Free energies in kcal/mol. [a] Calculations using 2-methylpropene instead of α-methylstyrene).

Interestingly, **Int4a** and **Int4b** are in equilibrium due to the C3−C4 bond rotation *via* ring opened intermediate **Int4ab** (Scheme 1.21), and they are also in equilibrium *via* C4 migration with the cyclopropyl-like intermediates **Int5a** and **Int5b** respectively (Scheme

1.22). In contrast, **Int5a** and **Int5b** cannot be converted by C2−C3 bond rotation since this process is more energetically costly ($\Delta G^{\ddagger}$ = 10.3, ΔG^{o} = -1.5 kcal/mol) than the transformation of **Int5a-b** into other intermediates.

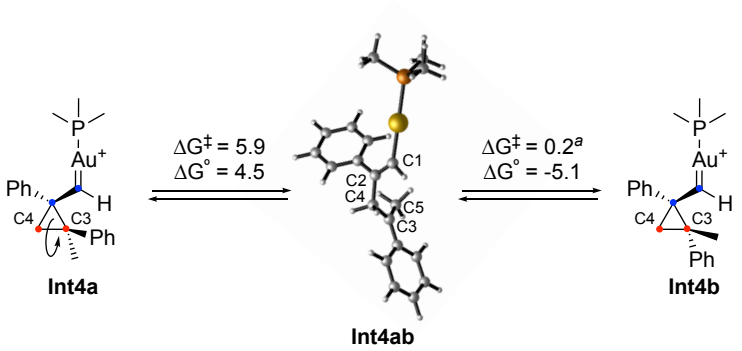

Scheme 1.21. Interconversion of **Int4a** and **Int4b** *via* C3−C4 bond rotation (Free energies in kcal/mol. [a] The energy of $\mathbf{TS_{4ab\text{-}4b}}$ was calculated freezing the dihedral angle (C5-C3-C4-C2). The value of this angle was taken from the previously optimized geometry of $\mathbf{TS_{4df\text{-}4f}}$, see Scheme 1.25).

The opening of the cyclopropyl motif of **Int5a,b** *via* $\mathbf{TS_{5\text{-}6}a,b}$ ($\Delta G^{\ddagger}$ = 10.7 (**a**), 14.7 (**b**) kcal/mol) to form the less stable intermediates **Int6a,b** followed by the highly exothermic 1,2-H shift affords the 1,3-diene-gold(I) complexes **Int9a,b**. These would be the dienes derived from a double-cleavage rearrangement that were not observed experimentally in any case (see Scheme 1.18). Alternatively, the cyclopropyl motif of **Int5a,b** undergoes ring opening through $\mathbf{TS_{5\text{-}8}a,b}$ ($\Delta G^{\ddagger}$ = 9.9 (**a**), 11.9 (**b**) kcal/mol) leading directly to 1,3-diene-gold(I) complexes **Int8a,b**, which correspond to the type of 1,3-dienes **21** obtained experimentally in certain cases. Noteworthy, intermediates similar to **Int5a,b** were proposed in the generation of 1,3-butadienes by reaction of electron-deficient alkynes with alkenes under gold(I) catalysis (see Scheme 1.6 of the Introduction to this **Chapter 1**). However, these rearrangements of **Int5a,b** to either **Int6a,b** or **Int8a,b** involve higher activation energies than the conversion of **Int5a,b** to the cyclopropyl gold(I) carbenes **Int4a,b** ($\Delta G^{\ddagger}$ = 5.7 (**a**), 11.1 (**b**) kcal/mol).

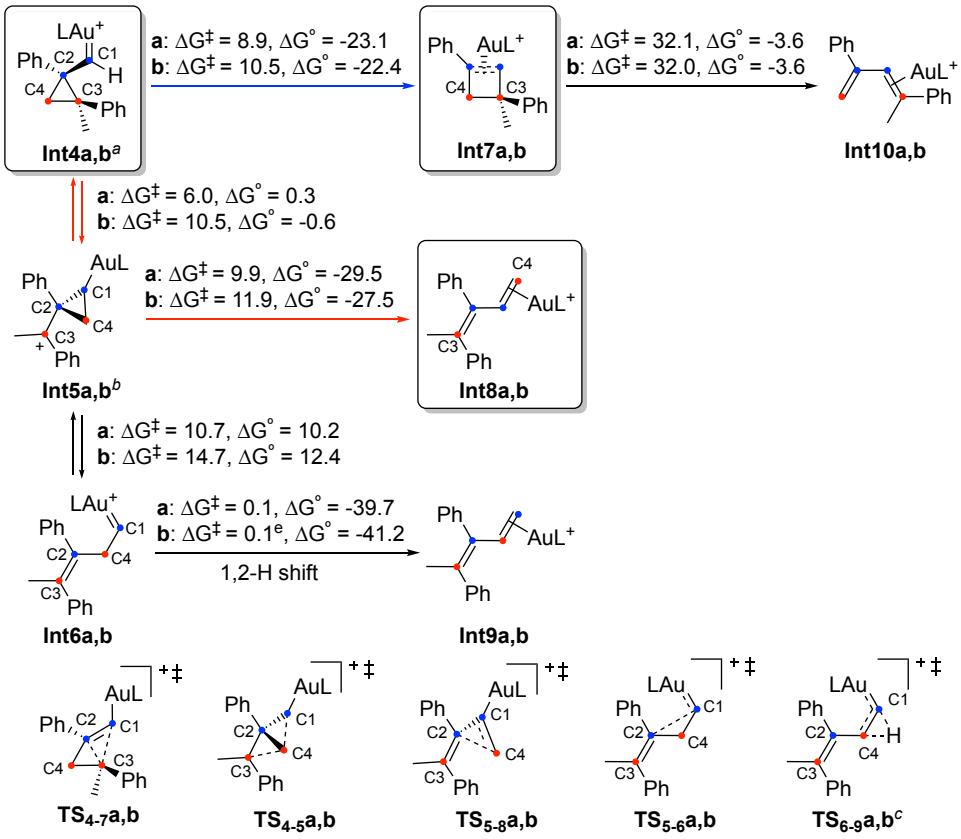

Scheme 1.22. Evolution of **Int4a,b** (L = PMe_3. Free energies in kcal/mol. Only pathway **a** is depicted. Pathway **b** leads to diastereomeric structures with the opposite configuration at C3. [a] Transformation of **Int4a** into **Int4b** *via* C3−C4 bond rotation: see Scheme 1.21. [b] Transformation of **Int5a** into **Int5b** *via* C2−C3 bond rotation: $\Delta G^{\ddagger}$ = 10.3, ΔG^{o} = -1.5. [c] The energy of **$TS_{6\text{-}9}$b** was calculated freezing the following distances: d(H−C1) and d(H−C4). The values of these distances were taken from the previously optimized geometry of **$TS_{6\text{-}9}$a**).

Comparing all the activation energies, the most favored reaction pathway is the straightforward ring expansion of **Int4a,b** to render (η^2-cyclobutene)gold(I) complexes **Int7a,b** ($\Delta G^{\ddagger}$ = 8.9 (**a**), 10.5 (**b**) kcal/mol). Interestingly, the transformation of the cyclopropyl gold(I) carbene to the cyclobutene had been previously proposed to proceed through a benzylic carbocation intermediate (see Scheme 1.6 of the Introduction to this **Chapter 1**), which was not found as stable specie by DFT calculations. Conrotatory ring opening of (η^2-cyclobutene)gold(I) complexes **Int7a,b** would require to overcome an excessively high energy barrier of 32 kcal/mol. Thus, after associative ligand exchange of

(η^2-cyclobutene)gold(I) complexes **Int7a,b** to regenerate the (η^2-alkene)gold(I) complex **Int1a**, cyclobutene **20a** would be the product of the reaction, which is consistent with the formation of **20a** in a 95% yield from **18a** and **19a** (Table 1.2, entry 1).

The possibility of a mechanism *via* an oxidative cyclometallation was also considered. However, neither the intermediate with the alkyne and the alkene coordinated simultaneously to gold(I) nor the gold(III) metallacyclopentene were found as stable species. Alternatively to the formation of cyclopropyl gold(I) carbenes **Int3a,b** or **Int4a,b** (Scheme 1.20), the generation of the metallacyclopentene-like intermediate **Int11** was computed (Scheme 1.23), in which the benzylic carbocation at C3 is stabilized by interacting with gold(I). This **Int11** could lead to (η^2-cyclobutene)gold(I) complexes **Int7** *via* **TS$_{11\text{-}7}$**. However, comparing the activation energies, the generation of **Int11** is less favored than the formation of **Int3a,b** or **Int4a,b**.

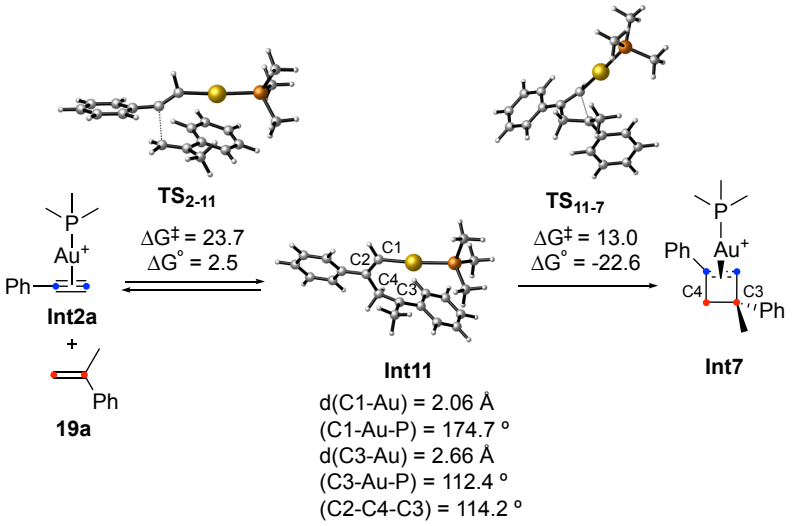

Scheme 1.23. Alternative pathway not *via* cyclopropyl gold carbene (Free energies in kcal/mol).

Reaction of (*o*-Bromophenyl)acetylene with α-Methylstyrene

The reaction of (*o*-bromophenyl)acetylene (**18f**) with α-methylstyrene (**19a**) is more complex since four different approaches of the alkene towards each carbon of the alkyne

could be conceived (Scheme 1.24), depending on the relative orientation of the phenyl groups of the substrates (*anti* or *syn*) and the position of the *ortho*-substituent in the alkyne respect to the carbons of the olefin (*ortho*-substituent closer to either the terminal or internal carbon of the alkene). Thus, four distinct reaction pathways were computed for this system (**c-f**). As in the case of the phenylacetylene (**18a**) with **19a**, the attack of the alkene to the internal carbon of the alkyne moiety of the *o*-bromophenyl derivative **Int2c** (**Int4c-f**, $\Delta G^{\ddagger}$ = 16.7-17.5 kcal/mol) is more favored than the attack to the terminal carbon of the alkyne (**Int3c-f**, $\Delta G^{\ddagger}$ = 18.8-20.1 kcal/mol).

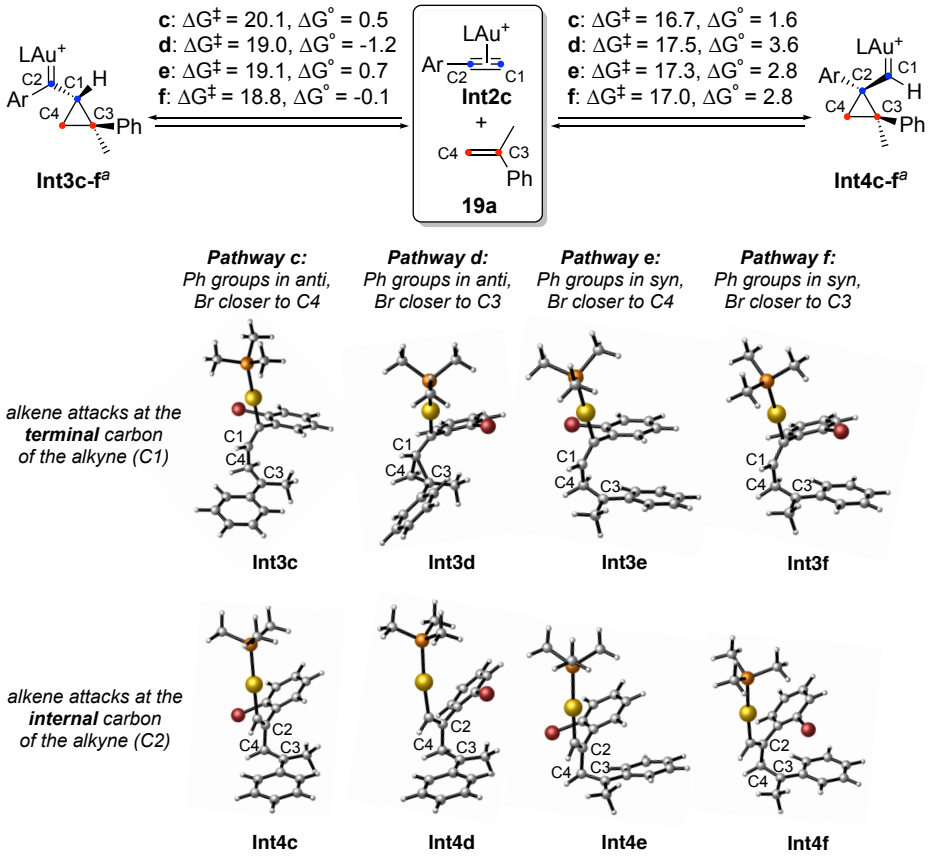

Scheme 1.24. Possible approaches of the alkene **19a** to **Int2c** leading to **Int3c-f** and **Int4c-f** (L = PMe_3. Ar = *o*-BrC_6H_4. Free energies in kcal/mol. [a] Depicted configuration of C3 for pathways **c** and **d**. Opposite configuration of C3 for pathways **e** and **f**).

Cyclopropyl gold(I) carbenes **Int4c** and **Int4e** as well as **Int4d** and **Int4f** are in equilibrium by C3−C4 bond rotation with low activation barriers (Scheme 1.25). However, the

equilibria between **Int4c** and **Int4d** as well as between **Int4e** and **Int4f** *via* C2−C6 bond rotations are more energetically costly (by at least 3.3 kcal/mol) than other rearrangements of **Int4c-f** (Scheme 1.26).

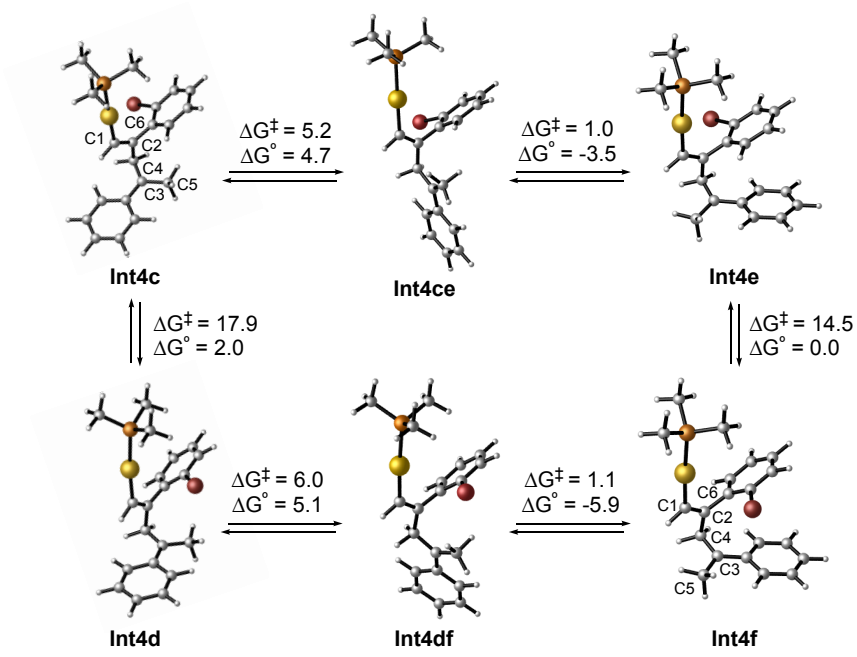

Scheme 1.25. Interconversions among **Int4c-f** *via* bond rotations (Free energies in kcal/mol).

Comparison of the activation energies of the transformations of **Int4c-f** into **Int7c-f** or **Int5c-f** (Scheme 1.26) suggests that the *o*-bromo substituent hampers the rearrangement of the near carbon of the alkene and favors the rearrangement of the further carbon of the alkene. Cyclopropyl gold(I) carbenes **Int4d** and **Int4f** bearing the bromo atom closer to C3 prefer to form the intermediates **Int5d** and **Int5f** *via* rearrangement of C4, which then lead to 1,3-diene-gold(I) complexes **Int8d** and **Int8f**, respectively. In contrast, cyclopropyl gold(I) carbene **Int4e** bearing the *o*-bromo substituent closer to C4 prefers to undergo ring expansion through C3 to give the (η^2-cyclobutene)gold(I) complex **Int7e**. Apart from that, the activation energies to transform **Int4c** into **Int5c** or **Int7c** are similar, therefore both pathways are possible. The alternative transformation of **Int5c-f** into **Int6c-f** is generally less favored than other competitive processes. **Int6c-f** would lead to **Int9c-f** by 1,2-H shift, which correspond to the experimentally undetected products of a double-cleavage-type

rearrangement (see Scheme 1.18). Again, **Int7c** and **Int7e** cannot evolve *via* electrocyclic ring opening to render the corresponding 1,3-diene-gold(I) complexes **Int10c** and **Int10e** as prohibitively high energy barriers of 37 kcal/mol are required.

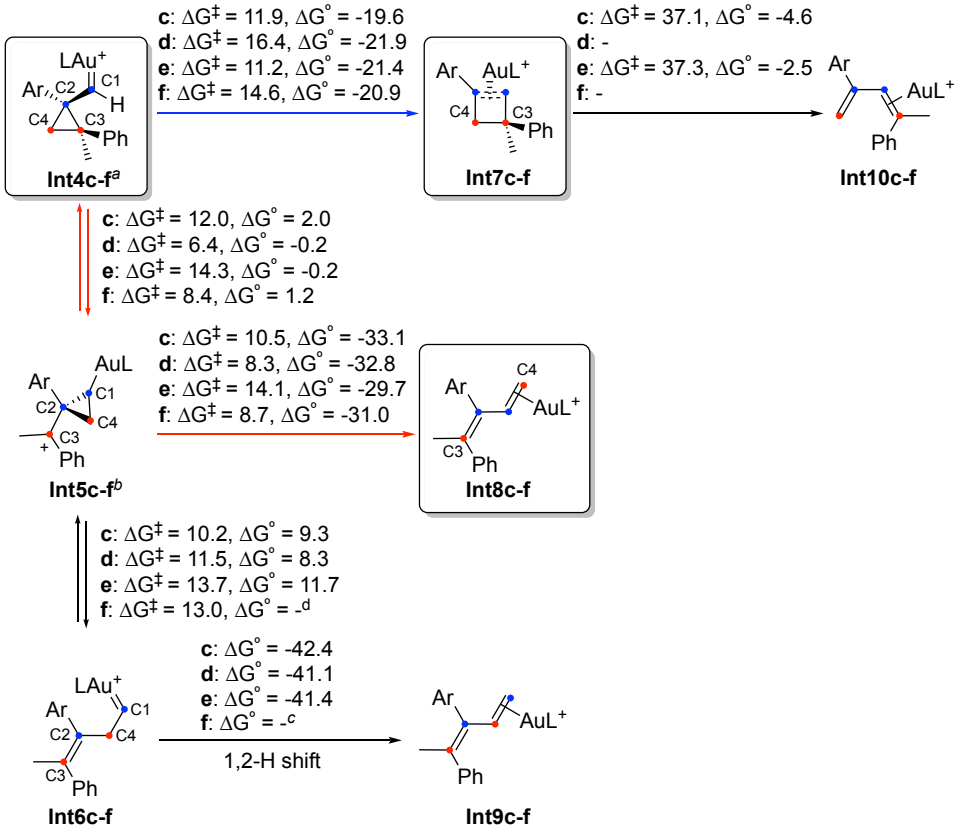

Scheme 1.26. Evolution of **Int4c-f** (L = PMe_3. Ar = *o*-BrC_6H_4. Free energies in kcal/mol. Depicted configuration of C3 for pathways **c** and **d**. Opposite configuration of C3 for pathways **e** and **f**. [a] Transformations among **Int4c-f** *via* bond rotations: see Scheme 1.25. [b] Transformation of **Int5f** into **Int5d** *via* C2−C3 bond rotation: $\Delta G^{\ddagger}$ = 14.0, ΔG^{o} = -0.6. [c] From **Int5f** to **Int9f**: ΔG^{o} = -31.0).

The structures of the transition states **TS$_{4\text{-}7}$c-f** and **TS$_{4\text{-}5}$c-f** leading to cyclobutene or 1,3-diene products evince an explanation for the difference in the energy barriers (Scheme 1.27). The distances among the substituents including the bromo atom in **TS$_{4\text{-}7}$d** and **TS$_{4\text{-}7}$f** ($\Delta G^{\ddagger}$ = 16.4 (**b**), 14.6 (**d**) kcal/mol) are shorter than in **TS$_{4\text{-}5}$d** and **TS$_{4\text{-}5}$f** ($\Delta G^{\ddagger}$ = 6.4 (**d**), 8.4 (**f**) kcal/mol) respectively. In consequence, the latter transition states, which show less steric hindrance, are favored. In addition, the unfavorable interaction between the gold(I) catalyst and the phenyl groups presumably also contributes to destabilize **TS$_{4\text{-}7}$d**. On the contrary,

in **TS$_{4\text{-}7}$c** and **TS$_{4\text{-}7}$e** ($\Delta G^{\ddagger}$ = 11.9 (**c**), 11.2 (**e**) kcal/mol) the bromo and the rest of substituents are further away than in **TS$_{4\text{-}5}$c** and **TS$_{4\text{-}5}$e** ($\Delta G^{\ddagger}$ = 12.0 (**c**), 14.3 (**e**) kcal/mol) respectively, therefore **TS$_{4\text{-}7}$c** and **TS$_{4\text{-}7}$e** are more prone to be formed. Thus, the cyclopropyl gold(I) carbene of type **Int4** evolve through the transition state involving less steric hindrance among the substituents, the *o*-substituent from the arylalkyne playing a crucial role.

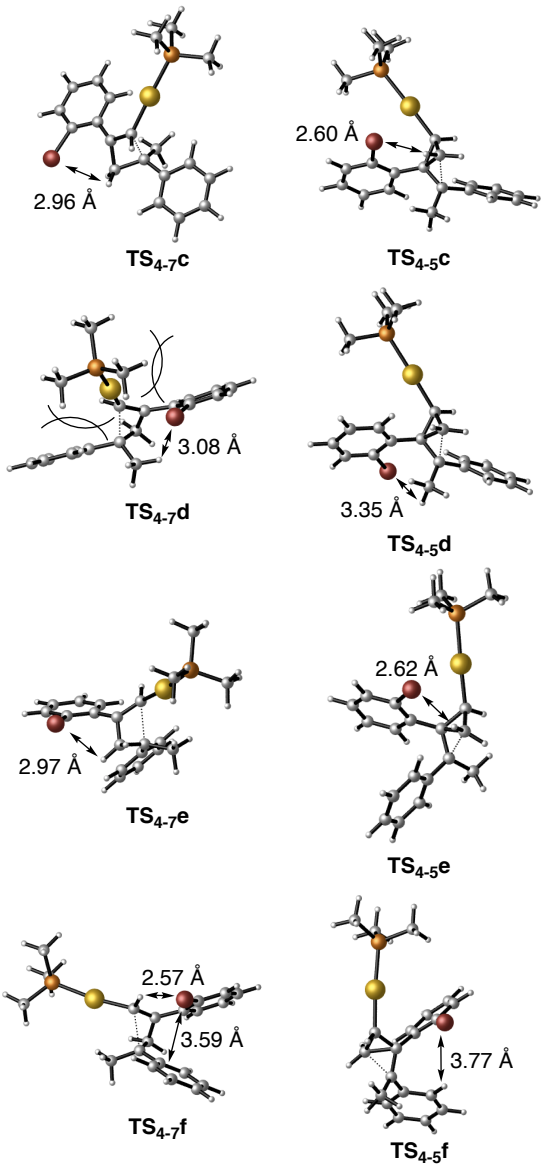

Scheme 1.27. Analysis of **TS$_{4\text{-}7}$c-f** and **TS$_{4\text{-}5}$c-f** leading to the cyclobutene or 1,3-diene.

Analyzing all the energy barriers (including bond rotations), the most favored pathway guide to 1,3-diene-gold(I) complex **Int8d**. This is in agreement with the experimental result, as 1,3-diene **21f** is obtained in a 45% yield and only traces of cyclobutene **20f** are detected (Table 1.2, entry 7). Nevertheless, the difference in the activation energies of the rearrangements of cyclopropyl gold(I) carbenes **Int4** are not large, so subtle changes in the substitution pattern of the substrates modify the steric interactions and, consequently, the reaction outcome. Hence, reasonably, different ratios of cyclobutene and 1,3-diene products were experimentally obtained depending on the differently substituted substrates.

Reaction of 1-Phenyl-1,3-butadiyne

In order to study the gold(I)-catalyzed intermolecular reaction of 1,3-butadienes and alkenes by means of computational techniques, we selected 1-phenyl-1,3-butadiyne (**22a**) and 2-methylpropene (**19t**) as model substrates. Notably, in this case two alkynes compete for the activation by gold(I) towards the nucleophilic attack of the alkene, although the experiments manifest that exclusively the terminal alkyne reacts to give the cycloadduct. To explain this observation, we first examined the activation of the diyne by gold(I) (Scheme 1.28).

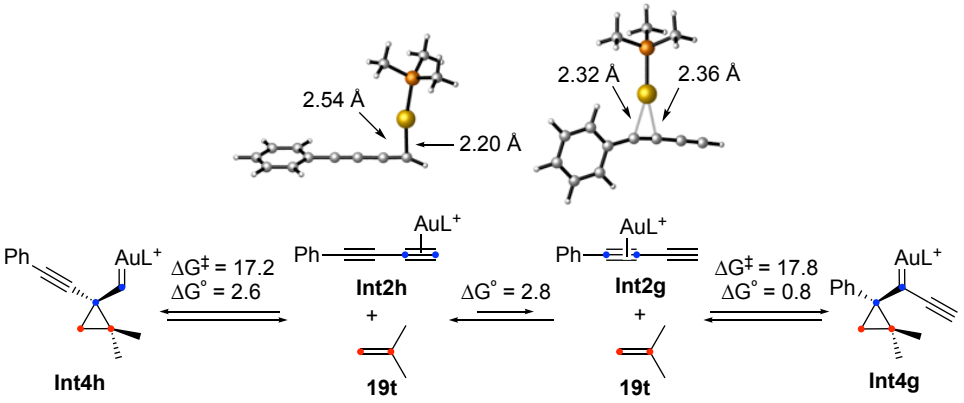

Scheme 1.28. Activation of the 1,3-butadiene **22a** by gold(I) towards the attack of the alkene **19t**.

Gold(I) complex **Int2h**, in which gold(I) binds the terminal alkyne, is 2.8 kcal/mol more stable than the complex **Int2g**, in which gold(I) binds the internal alkyne. The preferential coordination of gold(I) to the less substituted multiple bond has been experimentally

observed in the case of allenes, as displayed in the **General Introduction**. Alkyne gold(I) complex **Int2g** exhibits an almost symmetrical η^2-coordination with a significant bending back of the phenyl group, which is consistent with reported structures of related alkyne gold(I) complexes (see **General Introduction**). In contrast, in complex **Int2h**, the terminal alkyne binds unsymmetrically with gold(I), resulting in longer bonds with the substituted carbon atom, as observed in terminal alkene gold(I) complexes (see **General Introduction**). The subsequent activation barrier of the nucleophilic attack of the alkene **19t** to the terminal alkyne is 3.4 kcal/mol lower than the barrier corresponding to the attack at the internal alkyne. Consequently, in terms of both thermodynamics and kinetics, the alkene attacks selectively to complex **Int2h** at the terminal alkyne, forming distorted cyclopropyl gold(I) carbene **Int4h**.

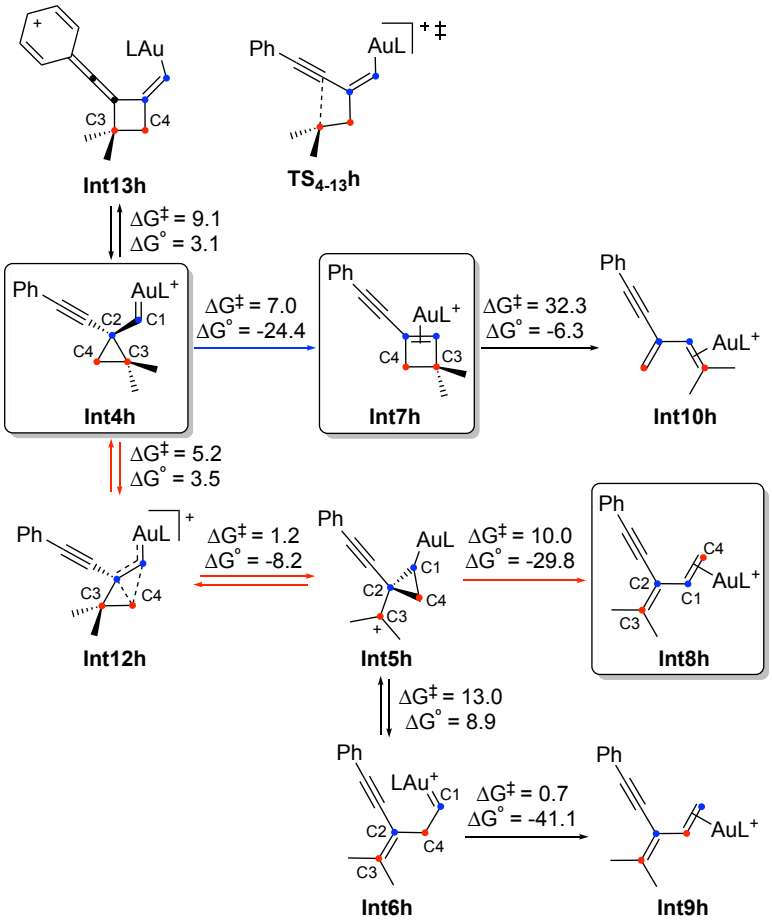

Scheme 1.29. Evolution of **Int4h** (L = PMe_3. Free energies in kcal/mol).

We then inspected the transformation of the resulting **Int4h** (Scheme 1.29). The ring expansion of **Int4h** through **TS$_{4\text{-}13}$h** leads to the less stable intermediate **Int13h**, which cannot evolve forward and is again converted into **Int4h**. Instead, other ring expansion of **Int4h** through C3 ($\Delta G^{\ddagger}$ = 7.0 kcal/mol) gives the much more stable (η^2-cyclobutene)gold(I) complex **Int7h**, which cannot undergo conrotatory ring opening to afford 1,3-diene-gold(I) complex **Int10h** due to the high energy barrier of this process ($\Delta G^{\ddagger}$ = 32.3 kcal/mol).

The alternative ring expansion of cyclopropyl gold(I) carbene **Int4h** *via* C4 to generate the distorted cyclobutene-gold(I) complex **Int12h** implies a low barrier of 5.2 kcal/mol. Interestingly, an intermediate similar to **Int12h** was not found in the reaction of phenylacetylene derivatives **18a** and **18f** with alkene **19a**, as previously discussed. Intermediate **Int12h** partakes in a formal insertion of the terminal carbon of the alkene C4 into the alkyne carbons to form a more stable cyclopropyl-like intermediate **Int5h**. On one hand, the cyclopropyl motif of **Int5h** can be opened through the C2−C4 bond ($\Delta G^{\ddagger}$ = 10.0 kcal/mol) to render 1,3-diene-gold(I) complex **Int8h**. On the other hand, the aperture of the cyclopropyl motif of **Int5h** through the C1−C2 bond leads to **Int6h** ($\Delta G^{\ddagger}$ = 13.0 kcal/mol), which affords the 1,3-diene-gold(I) complex **Int9h** by a highly exothermic 1,2-H shift.

Analyzing all the free energy reaction profile, although intermediates **Int4h**, **Int12h** and **Int5h** are in equilibrium through low barrier transformations, the opening of **Int5h** to either **Int6h** or **Int8h** is more energetically costly than the expansion of **Int4h** to (η^2-cyclobutene)gold(I) complex **Int7h** (13 and 10 *vs.* 7.0 kcal/mol). This is in accordance with the experimental results, since cyclobutenes **23** are the products obtained in the reaction of 1,3-butadienes **22** with alkenes (Table 1.6).

Key Cyclopropyl Gold(I) Carbenes: Generation and Reactivity

According to the obtained computational results, the cyclopropyl gold(I) carbenes are key intermediates in the gold(I)-catalyzed intermolecular reactions of electron-rich alkynes with alkenes to give cyclobutenes or 1,3-butadienes. In spite of many experimental efforts to isolate them, they are still elusive species. However, the formation of these intermediates

in the [2+2] cycloaddition of arylalkynes with alkenes was somehow proved by trapping them with another alkene, as indicated in the **General Introduction** (Scheme 12).

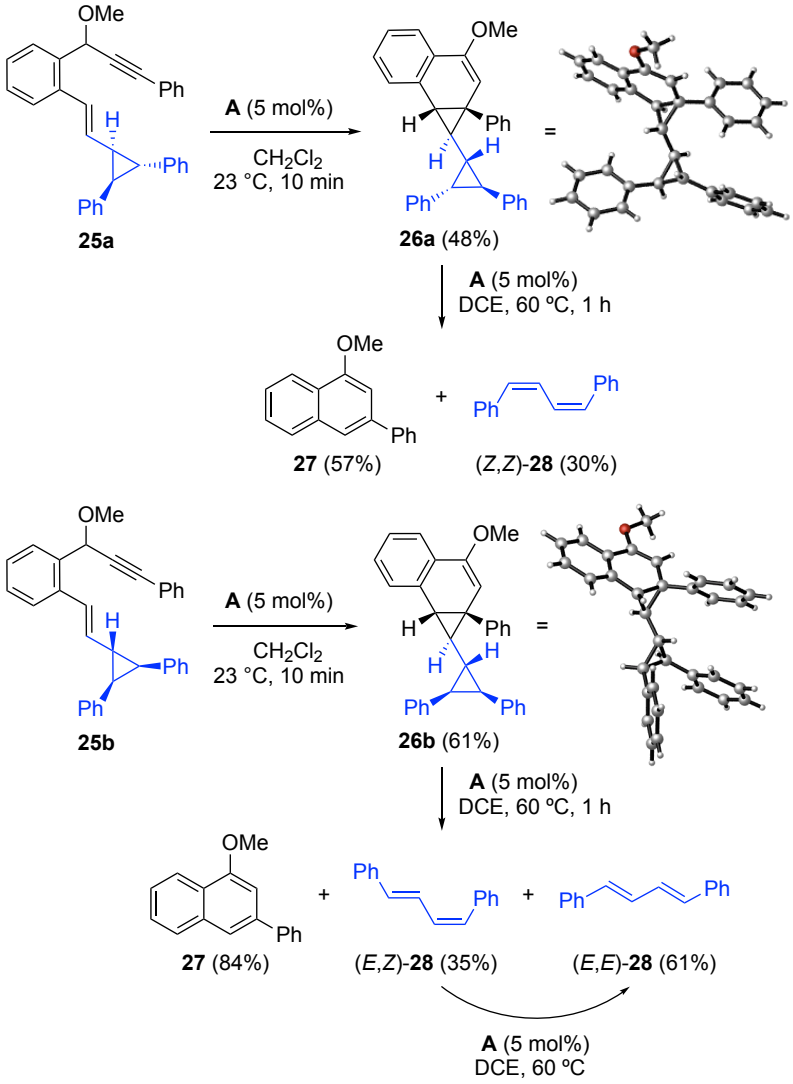

Scheme 1.30. Retro-Buchner reaction of **25a,b** to generate 1,3-dienes **28**.

To corroborate their involvement in the construction of 1,3-dienes, we recurred to the generation of gold(I) carbenes by retro-Buchner reaction, in particular the decarbenation of

1a,7b-dihydro-1*H*-cyclopropa[*a*]naphthalenes **26** (Scheme 1.30).[78] The reactivity of these compounds under gold catalysis should be equivalent to the rationalized for 7-cyclopropylcycloheptatriene **14**, although the *cis* isomer of **14** could not be prepared (see Scheme 1.8 in the Introduction to this **Chapter 1**).

1,6-Enynes **25a,b** were synthesized by olefination of the corresponding cyclopropyl carbaldehydes and obtained as a 1:1 mixture of epimers at the benzylic position. In presence of gold(I)-catalyst **A**, enynes **25a,b** undergo cycloisomerization under mild conditions to build enol ethers **26a,b** in 48% and 61% yields, respectively. The relative configurations of **26a,b** were confirmed by X-ray diffraction. To promote the decarbenation reaction, enol ethers **26a,b** were heated at 60 ºC with catalyst **A**. Apart from 1-methoxy-3-phenylnaphthalene **27**, in the case of **26a** we obtained (*Z*,*Z*)-**28**, while in the case of **26b** we obtained a mixture of (*E*,*Z*)- and (*E*,*E*)-**28**. Control experiments revealed that (*E*,*Z*)-**28** isomerizes to the more stable (*E*,*E*)-**28** under the reaction conditions.

Mechanistically, gold(I)-catalyzed retro-Buchner reaction of **26a** and **26b** would provide cyclopropyl gold(I) carbenes **Int4i** and **Int4j**, respectively, whose evolution was analyzed by DFT calculations[76] (Scheme 1.31). **Int4i** bearing the phenyl groups in *trans* position rearranges by 1,3-migration of C4 *via* **Int5i** to give (*Z*,*Z*)-diene complex **Int8i** and, ultimately, (*Z*,*Z*)-**28**. Conversely, **Int4j** bearing the phenyl groups in *cis* position undergoes 1,3-migration of C4 through **Int5j** to form (*E*,*Z*)-diene complex **Int8j**, which corresponds to (*E*,*Z*)-**28**. As experimentally observed, in the presence of gold(I) further isomerization of (*E*,*Z*)-**28** to the more stable (*E*,*E*)-**28** occurs under the reaction conditions. The alternative ring expansion of cyclopropyl gold(I) carbenes **Int4i,j** to deliver cyclobutenes **Int7i,j** is a much higher energy process.

Although both reaction pathways from **26a,b** could in principle be connected by the *trans*- to *cis*-isomerization of **Int4i** to **Int4j** *via* open carbocation **Int4ij**, the corresponding barriers are much higher in energy than those leading to C4 migration. Interestingly, this is in contrast to the energy barrier found in the equilibrium between **Int4a** and **Int4b** (Scheme

78. Experiments performed by Mariia S. Kirillova and Yahui Wang.

1.21). The higher energy barriers for the isomerization of **Int4i** to **Int4j** could be attributed to the steric hindrance between the phenyl groups.

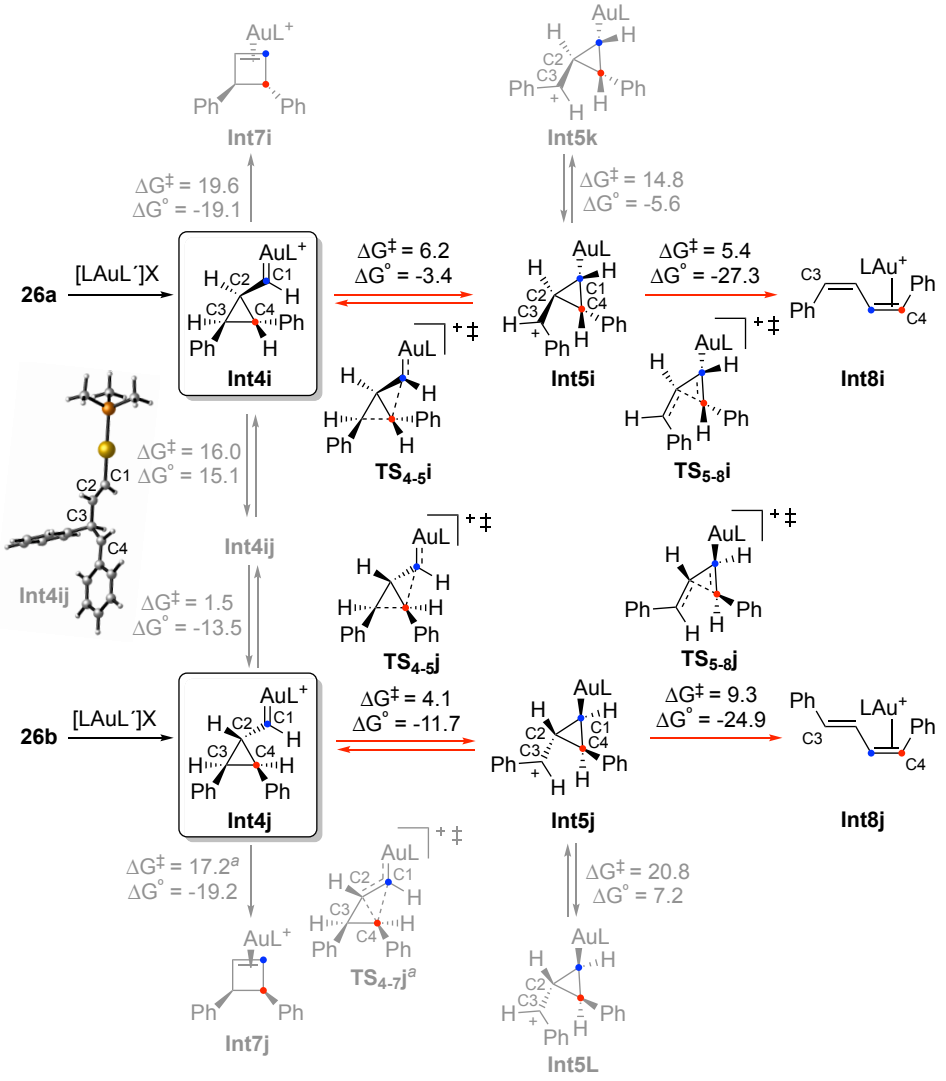

Scheme 1.31. Evolution of cyclopropyl gold(I) carbenes **Int4i,j** generated from **26a,b**. (L = PMe_3. Free energies in kcal/mol. [a] The energy of **TS_{4-7}j** was calculated freezing the following distances: d(C3−C1), d(C3−C2) and d(C3−C4). The values of these distances were taken from the previously optimized geometry of **TS_{4-7}i**).

Similarly, the reaction pathways from **Int5i,j** could be linked by C2−C3 bond rotation. This bond rotation in **Int5i** would generate **Int5k** (enantiomer of **Int5j**) that leads to (*E*,*Z*)-diene

complex **Int8j**, whereas the same bond rotation in **Int5j** would generate **Int5L** (enantiomer of **Int5i**) that leads to (*Z*,*Z*)-diene complex **Int8i** . However, rotational barriers around the C2−C3 bond in **Int5i,j** are higher (14.8 and 20.8 kcal/mol, respectively) than those required to straightforward give **Int8i,j**. As a consequence, the formation of dienes **28** results stereospecific.

Activation of Acetylene by Gold(I)

Intermediates **Int4i** and **Int4j** could be also formed by intermolecular gold(I)-catalyzed reaction of acetylene with *trans*- and *cis*-stilbene, respectively. However, the activation of acetylene by gold(I) has never been achieved so far, as mentioned in the Introduction to this **Chapter 1**. We ambitioned to generate *in situ* acetylene and make it react with alkenes under gold(I) catalysis.

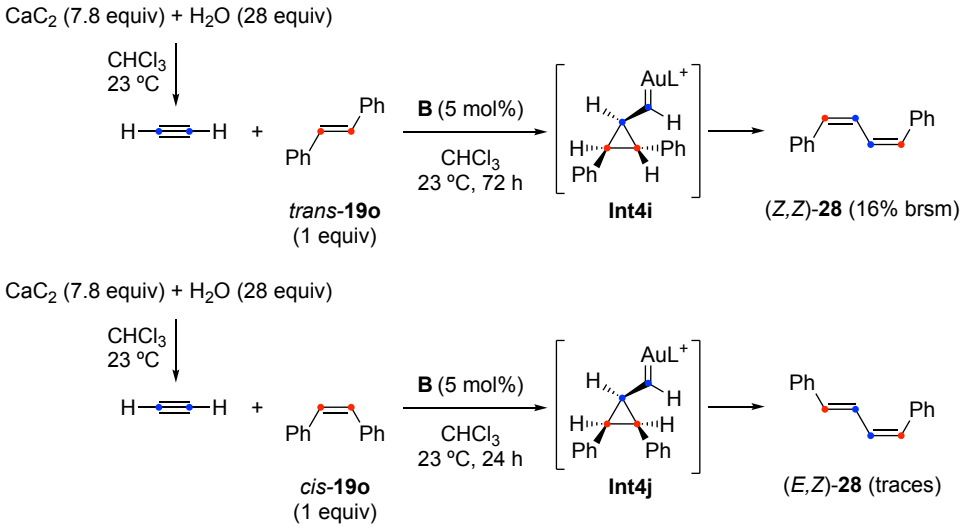

Scheme 1.32. Activation of acetylene by gold(I) in the reaction with stilbenes to form 1,3-dienes.

To perform these experiments, we used a two-chamber sealed reactor described recently in the literature.[67] In one chamber we mixed calcium carbide, chloroform and water to produce the acetylene gas, which passed to the other chamber containing a solution of the alkene and the gold(I) catalyst in chloroform. When carrying out the reaction with *trans*-stilbene

(*trans*-**19o**) in the presence of catalyst **B**, the expected 1,3-butadiene (*Z*,*Z*)-**28** was detected in the crude mixture in a 16% yield (brsm). Conversely, in the reaction with *cis*-stilbene (*cis*-**19o**), traces of 1,3-diene (*E*,*Z*)-**28** were found in the crude. These outcomes suggest that the gold(I) catalyst **B** did activate acetylene towards the nucleophilic attack of the *trans*- or *cis*-stilbene to form cyclopropyl gold(I) carbenes **Int4i** or **Int4j**, which rearrange to build 1,3-dienes (*Z*,*Z*)-**28** or (*E*,*Z*)-**28**, respectively, in agreement with the mechanistic studies displayed in Scheme 1.31.

Under the same conditions, the reaction of acetylene with α-methylstyrene led to polymerization, whereas according to GC-MS the reaction with (*Z*)-cyclooctene gave a mixture of adducts. Further optimization of these gold(I)-catalyzed transformations of acetylene are currently ongoing in our group.

Conclusions

Under gold(I) catalysis, terminal electron-rich alkynes have shown to react with alkenes by [2+2] cycloaddition to furnish cyclobutenes, while electron-deficient alkynes react with alkenes leading to 1,3-butadienes, in a metathesis-type process, or lactones. Now we found that 1,3-dienes can be formed by reaction of alkenes with electron-rich alkynes bearing *ortho*-substituted aryl groups. In contrast, we discovered that less sterically demanding 1,3-butadiynes react with alkenes to forge exclusively cyclobutenes.

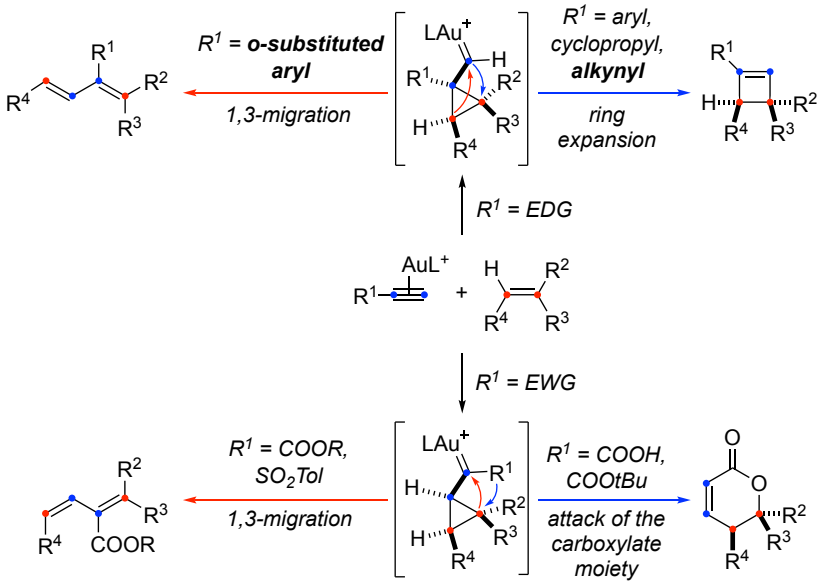

Scheme 1.33. Complete mechanistic picture of the gold(I)-catalyzed intermolecular reactions of alkynes with alkenes.

According to our detailed computational analysis of the reactions leading to cyclobutenes and 1,3-dienes, the key intermediates in these transformations are cyclopropyl gold(I) carbenes, whose electronic and steric properties govern their evolution through distinct reaction pathways close in energy. Firstly, the formation of regioisomeric cyclopropyl gold(I) carbenes depends on the electronic character of the initial alkyne: the gold carbene is generated at the terminal carbon of electron-rich alkynes, whilst at the internal carbon of electron-deficient alkynes. Secondly, steric differences among the substituents of the cyclopropyl gold(I) carbenes determine their rearrangement *via* ring expansion to construct

directly cyclobutenes or *via* a stepwise 1,3-migration of the less substituted carbon of the alkene to build 1,3-butadienes. Thus, the formation of 1,3-dienes implies the cleavage of the carbon–carbon double bond of the alkene in a two- or three-step process. These mechanisms leading to cyclobutenes or 1,3-dienes resemble the ones proposed for the intramolecular skeletal rearrangements of 1,*n*-enynes catalyzed by gold(I). The conrotatory opening of the cyclobutenes is not observed under the reaction conditions, which is consistent with the high energy barrier calculated for this transformation.

In order to experimentally support the involvement of the cyclopropyl gold(I) carbenes in these reactions, we generated these intermediates by the unrelated gold(I)-catalyzed retro-Buchner reaction, which give rise to 1,3-butadienes in a stereospecific manner. Furthermore, the activation of acetylene by gold(I) was achieved in the reaction with stilbenes to produce 1,3-butadienes.

By understanding the complete mechanistic landscape of the intermolecular reactions of alkynes with alkenes under gold(I) catalysis, it becomes possible to control the evolution of the reaction intermediates to access selectively a desired type of product (as in **Chapter 2**) and to design new routes towards a variety of skeletons (as in **Chapter 3**).

Experimental Part

General Information

Anhydrous reactions were performed under nitrogen or argon in solvents dried by passing through an activated alumina column on a PureSolv^{TM} solvent purification system (Innovative Technologies, Inc., MA). Analytical thin layer chromatography was carried out using TLC-aluminium sheets with 0.2 mm of silica gel (Merck GF_{234}) using UV light as the visualizing agent and an acidic solution of vanillin in ethanol as the developing agent. Purifications by chromatography were carried out using flash grade silica gel (SDS Chromatogel 60 ACC, 40-63 mm) or neutral aluminum oxide (SDS, 63-200 μm). Preparative TLC was performed on 20 cm × 20 cm silica gel plates (2.0 mm thick, catalogue number 02015, Analtech). If indicated, preparative TLC was performed on 20 cm x 20 cm aluminum oxide plates (0.25 mm thick, 90066, Fluka). Purifications by distillation were carried out in a Büchi glass oven B-585 Kugelrohr apparatus. Organic solutions were concentrated under reduced pressure on Büchi or IKA rotary evaporators.

NMR spectra were recorded at 298 K on a Bruker Avance 300, Bruker Avance 400 Ultrashield and Bruker Avance 500 Ultrashield apparatuses. The signals are given as δ / ppm (multiplicity, coupling constant (Hertz), number of protons) downfield from tetramethylsilane, with calibration on the residual protio-solvent used (δ_H = 7.26 ppm and δ_C = 77 ppm for $CDCl_3$). Mass spectra were recorded on a Waters UPLC-QqTOF (Maxis Impact, Bruker Daltonics) with ESI and APCI, or a Waters Alliance HPLC-TOF (MicroTOF Focus, Bruker Daltonics) with ESI and APCI. Melting points were determined using a Büchi melting point apparatus.

Crystal structure determinations were carried out using a Bruker-Nonius diffractomer equipped with an APEX II 4K CCD area detector, a FR591 rotating anode with Mo *K*α radiation, Montel mirrors as monochromator and a Kryoflex low temperature device (T = –173 ºC). Full-sphere data collection was used with w and j scans. Programs used: Data collection APEX-2, data reduction Bruker Saint V/.60A and absorption correction SADABS. Structure Solution and Refinement: Crystal structure solutions were achieved using direct methods as implemented in SHELXTL and visualized using the program XP. Missing atoms were subsequently located from difference Fourier synthesis and added to

the atom list. Least-squares refinement on F2 using all measured intensities was carried out using the program SHELXTL. All non-hydrogen atoms were refined including anisotropic displacement parameters.

All reagents were used as purchased, with no further purification, unless otherwise stated. (*Z*)-1,2-dimethyl-cyclohexene[79] and deuterated 1-bromo-2-ethynylbenzene[80] were synthesized according to the literature procedure. Complexes [(*t*BuXPhos)AuNCMe]BAr_4^F (**B**),[81] [(*t*BuXPhos)AgNCMe]SbF_6 (**C**),[82] [(IPr)AuNCMe]SbF_6 (**F**),[83] [(IPr)AuNCPh]BAr_4^F (**G**),[84] [(IMes)AuNCMe]SbF_6 (**H**)[85] and **I**[85] were also prepared following literature procedures. The NMR data were in agreement with the ones reported in the literature.

Synthetic Procedures and Characterization Data

General Procedure for the Reaction of Arylalkynes with Alkenes

The alkyne (1 equiv) was dissolved in CH_2Cl_2 (0.5 M, unless otherwise stated) in a vial. The alkene (2 equiv, unless otherwise stated) was added, followed by [(*t*BuXPhos)AuNCMe]X (X = SbF_6 or BAr_4^F) catalyst (3-5 mol%). The vial was sealed and the resulting mixture was stirred at 50 ºC until no alkyne was detected by GC-MS. Triethylamine (0.02 mL) was added to quench the reaction. The volatiles were removed under reduced pressure and the crude mixture was purified by silica gel preparative TLC or flash column chromatography (eluent = pentane or cyclohexane, unless otherwise stated).

Due to the similar polarity of the corresponding cyclobutene, 1,3-diene and oligomeric byproducts, isolated yields of the pure products may be lower than those reported in the table 1 of the manuscript, which were detected in the crude mixture by ^{1}H NMR (employing 1,2-diacetylbenzene as internal standard).

79. Waser, J.; Carreira, E. M. *Angew. Chem. Int. Ed.* **2004**, *43*, 4099–4102.
80. Bew, S. P.; Hiatt-Gipson, G. D.; Lovell, J. A.; Poullain, C. *Org. Lett*. **2012**, *14*, 456–459.
81. de Orbe, M. E.; Echavarren, A. M. *Org. Synth.* **2016**, *93*, 115–126. See also ref. 44.
82. Pérez-Galán, P.; Delpont, N.; Herrero-Gómez, E.; Maseras, F.; Echavarren, A. M. *Chem. Eur. J.* **2010**, *16*, 5324–5332.
83. de Frémont, P.; Marion, N.; Nolan, S. P. *J. Organomet. Chem.* **2009**, *694*, 551−560.
84. Huguet, N.; Leboeuf, D.; Echavarren, A. M. *Chem. Eur. J.* **2013**, *19*, 6581–6585.
85. Amijs, C. H. M.; López-Carrillo, V.; Raducan, M.; Pérez-Galán, P; Ferrer, C.; Echavarren, A. M. *J. Org. Chem.* **2008**, *73*, 7721−7730.

1-Methoxy-2-(3-methyl-3-phenylcyclobut-1-en-1-yl)benzene

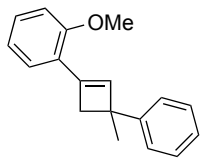

The title compound (pale yellow oil, 27 mg, 54%) was synthesized following the general procedure starting from 1-ethynyl-2-methoxybenzene (26 μL, 0.2 mmol) and α-methylstyrene (52 μL, 0.4 mmol) with [(*t*BuXPhos)AuNCMe]BAr_4^F (15 mg, 0.01 mmol, 5 mol%). The reaction time was 48 h.

^{1}H NMR (400 MHz, $CDCl_3$) δ 7.48 – 7.40 (m, 2H), 7.36 – 7.29 (m, 2H), 7.28 – 7.13 (m, 3H), 6.97 – 6.86 (m, 2H), 6.81 (s, 1H), 3.92 (s, 3H), 3.03 (d, *J* = 12.3 Hz, 1H), 2.95 (dd, *J* = 12.3, 0.7 Hz, 1H), 1.65 (s, 3H). **^{13}C NMR** (126 MHz, $CDCl_3$) δ 158.5, 148.1, 140.1, 138.5, 128.7, 128.0 (2C), 127.0, 125.9 (2C), 125.5, 123.4, 120.2, 110.3, 55.1, 46.7, 45.2, 27.7. **HRMS** (APCI) *m/z* calculated for $C_{18}H_{19}O^+$ $[M+H]^+$: 251.1430, found: 251.1422.

1-Methyl-2-(3-methyl-3-phenylcyclobut-1-en-1-yl)benzene (20c) and (*E*)-1-methyl-2-(4-phenylpenta-1,3-dien-3-yl)benzene (21c)

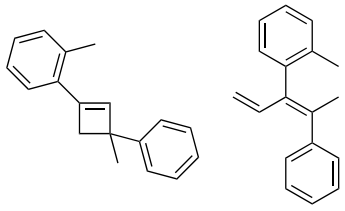

Cyclobutene **20c** and 1,3-diene **21c** were synthesized following the general procedure starting from 1-ethynyl-2-methylbenzene (22 μL, 0.17 mmol, 1 equiv) and α-methylstyrene (88 μL, 0.67 mmol, 4 equiv) in CH_2Cl_2 (0.8 mL, 0.2 M). [(*t*BuXPhos)AuNCMe]BAr_4^F (10 mg, 0.007 mmol, 4 mol%) was used as catalyst. The reaction time was 20 h. Both products were separated and isolated by chromatography.

Cyclobutene **20c** was obtained as a pale yellow oil (7 mg, 17%). **^{1}H NMR** (400 MHz, $CDCl_3$) δ 7.45 – 7.41 (m, 2H), 7.36 – 7.29 (m, 2H), 7.23 – 7.15 (m, 5H), 6.60 (s, 1H), 3.06 (d, *J* = 12.4 Hz, 1H), 3.00 (d, *J* = 12.4 Hz, 1H), 2.48 (s, 3H), 1.65 (s, 3H). **^{13}C NMR** (101 MHz, $CDCl_3$) δ 147.7, 143.7, 137.9, 137.0, 133.2, 130.6, 128.1 (2C), 127.6, 126.5, 125.8 (2C), 125.7, 125.6, 46.1, 46.0, 27.6, 21.9. **HRMS** (APCI) *m/z* calculated for $C_{18}H_{19}^+$ $[M+H]^+$: 235.1481, found: 235.1477.

1,3-Diene **21c** was obtained as a pale yellow oil (11 mg, 28%). **^{1}H NMR** (400 MHz, $CDCl_3$) δ 7.43 – 7.35 (m, 2H), 7.34 – 7.21 (m, 6H), 7.12 – 7.06 (m, 1H), 6.60 (dd, *J* = 17.2, 10.6 Hz, 1H), 4.87 (ddd, *J* = 11.2, 1.4, 0.7 Hz, 1H), 4.45 (ddd, *J* = 17.2, 1.6, 0.8 Hz, 1H), 2.23 (s, 3H), 1.79 (s, 3H). **^{13}C NMR** (101 MHz, $CDCl_3$) δ 143.0, 139.1, 137.7, 136.9, 136.4, 136.4, 129.8, 129.8, 128.7 (2C), 128.1 (2C), 126.9, 126.8, 125.7, 115.1, 22.6, 19.0. **HRMS** (APCI) *m/z* calculated for $C_{18}H_{19}^+$ $[M+H]^+$: 235.1481, found: 235.1474.

1-Fluoro-2-(3-methyl-3-phenylcyclobut-1-en-1-yl)benzene

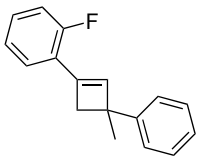

The title compound was synthesized following the general procedure starting from 1-ethynyl-2-fluorobenzene (23 μL, 0.2 mmol) and α-methylstyrene (52 μL, 0.4 mmol) with [(*t*BuXPhos)AuNCMe]BAr_4^F (15 mg, 0.01 mmol, 5 mol%). The reaction time was 20 h. In the first purification using pentane as eluent cyclobutene **3c** was isolated along with traces of the corresponding 1,3-diene (32 mg, 67%). However, the second purification using cyclohexane:EtOAc 9:1 as eluent afforded the pure cyclobutene **3c** as a pale yellow oil (27 mg, 57 % yield).

^{1}H NMR (400 MHz, $CDCl_3$) δ 7.43 – 7.38 (m, 2H), 7.37 – 7.29 (m, 2H), 7.25 – 7.17 (m, 3H), 7.13 – 7.01 (m, 2H), 6.82 (d, *J* = 3.3 Hz, 1H), 3.03 (d, *J* = 12.5 Hz, 1H), 2.96 (d, *J* = 12.5 Hz, 1H), 1.64 (s, 3H). **^{13}C NMR** (101 MHz, $CDCl_3$) δ 161.4 (d, *J* (^{13}C-^{19}F) = 251.9 Hz), 147.5, 139.4 (d, *J* (^{13}C-^{19}F) = 7.0 Hz), 138.3, 129.0 (d, *J* (^{13}C-^{19}F) = 8.2 Hz), 128.1 (2C), 127.2 (d, *J* (^{13}C-^{19}F) = 4.3 Hz), 125.8 (2C), 125.7, 123.8 (d, *J* (^{13}C-^{19}F) = 3.4 Hz), 122.6 (d, *J* (^{13}C-^{19}F) = 13.9 Hz), 115.5 (d, *J* (^{13}C-^{19}F) = 20.9 Hz), 47.5, 45.2, 27.6. **^{19}F NMR** (376 MHz, $CDCl_3$) δ –114.23. **HRMS** (APCI) *m/z* calculated for $C_{17}H_{16}F^+$ $[M+H]^+$: 239.1231, found: 239.1229.

(*E*)-1-Chloro-2-(4-phenylpenta-1,3-dien-3-yl)benzene

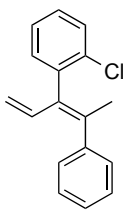

The title compound (colorless oil, 12 mg, 34%) was synthesized following the general procedure starting from 1-chloro-2-ethynylbenzene (18 μL, 0.14 mmol, 1 equiv) and α-methylstyrene (56 μL, 0.43 mmol, 3 equiv) in CH_2Cl_2 (0.7 mL, 0.2 M). [(*t*BuXPhos)AuNCMe]SbF_6 (5 mg, 0.006 mmol, 4 mol%) was used as catalyst. The reaction time was 20 h.

^{1}H NMR (400 MHz, $CDCl_3$) δ 7.50 – 7.45 (m, 1H), 7.43 – 7.36 (m, 2H), 7.36 – 7.24 (m, 5H), 7.21 (dd, *J* = 7.3, 2.0 Hz, 1H), 6.58 (dd, *J* = 17.3, 10.6 Hz, 1H), 4.90 (ddd, *J* = 10.6, 1.6, 0.8 Hz, 1H), 4.45 (ddd, *J* = 17.2, 1.6, 0.8 Hz, 1H), 1.82 (s, 3H). **^{13}C NMR** (126 MHz, $CDCl_3$) δ 142.6, 139.1, 138.3, 135.9, 134.9, 134.0, 131.5, 129.5, 128.7 (2C), 128.3, 128.1 (2C), 127.0, 126.7, 115.0, 22.7. **HRMS** (APCI) *m/z* calculated for $C_{17}H_{16}Cl^+$ $[M+H]^+$: 255.0935, found: 255.0927.

1-Bromo-2-(3-methyl-3-phenylcyclobut-1-en-1-yl)benzene (20f) and (*E*)-1-bromo-2-(4-phenylpenta-1,3-dien-3-yl)benzene (21f)

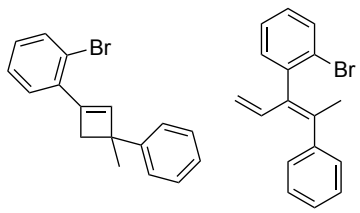

Cyclobutene **20f** and 1,3-diene **21f** were synthesized was synthesized following the general procedure starting from 1-bromo-2-ethynylbenzene (1 g, 0.69 mL, 5.52 mmol) and α-methylstyrene (1.44 mL, 11.0 mmol) with [(*t*BuXPhos)AuNCMe]SbF_6 (248 mg, 0.276 mmol, 5 mol%). The reaction time was 16 h.

Cyclobutene **20f** was obtained as a colorless oil (50 mg, 3%). **^{1}H NMR** (400 MHz, $CDCl_3$) δ 7.59 (dd, *J* = 7.9, 0.9 Hz, 1H), 7.46 – 7.41 (m, 2H), 7.38 – 7.31 (m, 2H), 7.31 – 7.27 (m, 2H), 7.25 – 7.16 (m, 1H), 7.18 (d, *J* = 1.2 Hz, 1H), 7.13 – 7.07 (m, 1H), 3.11 (d, *J* = 12.4 Hz, 1H), 3.04 (dd, *J* = 12.4, 1.0 Hz, 1H), 1.67 (s, 3H). **^{13}C NMR** (75 MHz, $CDCl_3$) δ 147.3, 142.0, 140.6, 133.8, 133.8, 128.6, 128.3, 128.2 (2C), 127.1, 125.8 (2C), 125.7, 121.8, 46.2, 45.8, 27.4. **HRMS** (APCI) *m/z* calculated for $C_{17}H_{16}Br^+$ $[M+H]^+$: 299.0430, found: 299.0420.

1,3-Diene **21f** was obtained as a colorless oil (712 mg, 43%). **^{1}H NMR** (400 MHz, $CDCl_3$) δ 7.66 (ddd, *J* = 7.9, 1.1, 0.4 Hz 1H), 7.42 – 7.27 (m, 6H), 7.24 – 7.15 (m, 2H), 6.57 (dd, *J* = 17.2, 10.6 Hz, 1H), 4.90 (ddd, *J* = 10.6, 1.6, 0.8 Hz, 1H), 4.45 (ddd, *J* = 17.3, 1.6, 0.8 Hz, 1H), 1.82 (s, 3H). **^{13}C NMR** (126 MHz, $CDCl_3$) δ 142.6, 140.4, 138.9, 136.7, 135.8, 132.8, 131.4, 128.6 (2C), 128.5, 128.1 (2C), 127.4, 127.0, 124.4, 115.1, 22.7. **HRMS** (APCI) *m/z* calculated for $C_{16}H_{12}Br^+$ $[M-CH_3]^+$: 283.0117, found: 283.0118.

(*E*)-1-(4-Phenylpenta-1,3-dien-3-yl)-2-(trifluoromethyl)benzene

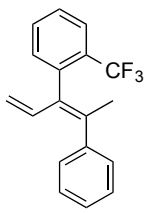

The title compound (colorless oil, 16 mg, 28%) was synthesized following the general procedure starting from 1-ethynyl-2-(trifluoromethyl)benzene (28 µL, 0.2 mmol) and α-methylstyrene (52 µL, 0.4 mmol) with [(*t*BuXPhos)AuNCMe]BAr_4^F (15 mg, 0.01 mmol, 5 mol%). The reaction time was 6 d.

The reaction was also performed on a larger scale (2 mmol of 1-ethynyl-2-(trifluoromethyl)benzene) and the same yield was obtained.

^{1}H NMR (400 MHz, $CDCl_3$) δ 7.76 (d, *J* = 7.9 Hz, 1H), 7.59 (tdd, *J* = 7.5, 1.4, 0.7 Hz, 1H), 7.48 – 7.36 (m, 3H), 7.34 – 7.28 (m, 3H), 7.27 – 7.22 (m, 1H), 6.60 (dd, *J* = 17.3, 10.7 Hz, 1H), 4.91 (ddd, *J* = 10.7, 1.5, 0.8 Hz, 1H), 4.31 (ddd, *J* = 17.3, 1.5, 0.8 Hz, 1H), 1.75 (s,

3H). **^{13}C NMR** (101 MHz, $CDCl_3$) δ 142.5, 139.2 (q, *J* (^{13}C-^{19}F) = 0.7 Hz), 138.7 (q, *J* (^{13}C-^{19}F) = 2.0 Hz), 137.2, 134.8, 132.0, 131.7, 129.4 (q, *J* (^{13}C-^{19}F) = 30.0 Hz), 128.5 (2C), 128.2 (2C), 127.2, 127.0, 126.3 (q, *J* (^{13}C-^{19}F) = 5.2 Hz), 124.2 (q, *J* (^{13}C-^{19}F) = 274.2 Hz), 115.7, 23.3. **^{19}F NMR** (376 MHz, $CDCl_3$) δ –60.69. **HRMS** (APCI) *m/z* calculated for $C_{18}H_{16}F_3^+$ $[M+H]^+$: 289.1199, found: 289.1195.

1-(3-Methyl-3-phenylcyclobut-1-en-1-yl)-4-(trifluoromethyl)benzene

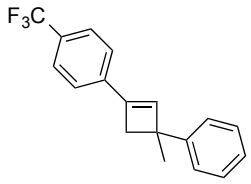

The title compound (colorless oil, 12 mg, 38%) was synthesized following the general procedure starting from 1-ethynyl-2-(trifluoromethyl)benzene (19 μL, 0.11 mmol) and α-methylstyrene (30 μL, 0.23 mmol) in CH_2Cl_2 (0.6 mL, 0.2 M). *t*BuXPhosAuCl (3 mg, 0.004 mmol, 4 mol%) and $NaBAr_4^F$ (4 mg, 0.004 mmol, 4 mol%) were added sequentially to form the [(*t*BuXPhos)AuNCMe]BAr_4^F catalyst *in situ*. The reaction time was 24 h.

^{1}H NMR (400 MHz, $CDCl_3$) δ 7.59 (d, *J* = 8.1 Hz, 2H), 7.47 (d, *J* = 8.1 Hz, 2H), 7.41 – 7.30 (m, 4H), 7.21 (tt, *J* = 1.3, 6.6 Hz, 1H), 6.87 (s, 1H), 3.00 (d, *J* = 12.5 Hz, 1H), 2.93 (d, *J* = 12.5 Hz, 1H), 1.64 (s, 3H). **^{13}C NMR** (101 MHz, $CDCl_3$) δ 147.1, 142.6, 137.9 (q, *J* (^{13}C-^{19}F) = 1.5 Hz), 136.7, 129.5 (q, *J* (^{13}C-^{19}F) = 32.4 Hz), 128.2 (2C), 125.9, 125.8 (2C), 125.3 (q, *J* (^{13}C-^{19}F) = 3.8 Hz, 2C), 124.8 (2C), 124.2 (q, *J* (^{13}C-^{19}F) = 271.4 Hz), 46.4, 44.1, 27.5. **^{19}F NMR** (376 MHz, $CDCl_3$) δ –62.61. **HRMS** (APCI) *m/z* calculated for $C_{18}H_{16}F_3^+$ $[M+H]^+$: 289.1199, found: 289.1206.

2-(2-Methoxyphenyl)spiro[3.5]non-1-ene

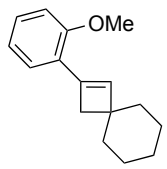

The title compound (pale yellow oil, 21 mg, 46%) was synthesized following the general procedure starting from 1-ethynyl-2-methoxybenzene (26 μL, 0.2 mmol) and methylenecyclohexane (48 μL, 0.4 mmol) with [(*t*BuXPhos)AuNCMe]BAr_4^F (15 mg, 0.01 mmol, 5 mol%). The reaction time was 72 h.

^{1}H NMR (500 MHz, $CDCl_3$) δ 7.21 (ddd, *J* = 8.2, 7.4, 1.8 Hz, 1H), 7.16 (dd, *J* = 7.5, 1.8 Hz, 1H), 6.92 (td, *J* = 7.5, 1.1 Hz, 1H), 6.87 (dd, *J* = 8.3, 1.0 Hz, 1H), 6.62 (s, 1H), 3.89 (s, 3H), 2.48 (s, 2H), 1.63 – 1.56 (m, 6H), 1.53 – 1.34 (m, 4H). **^{13}C NMR** (75 MHz, $CDCl_3$) δ 158.3, 140.5, 139.9, 128.3, 126.8, 123.9, 120.2, 110.2, 55.1, 45.0, 41.3, 36.6 (2C), 26.0,

24.5 (2C). **HRMS** (APCI) *m/z* calculated for $C_{16}H_{21}O^+$ $[M+H]^+$: 229.1587, found: 229.1593.

2-(2-Methylphenyl)spiro[3.5]non-1-ene (20k) and 1-(1-cyclohexylideneallyl)-2-methylbenzene (21k)

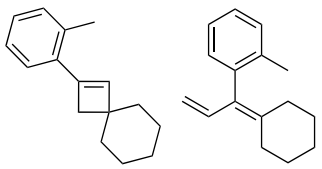

Cyclobutene **20k** and 1,3-diene **21k** were synthesized as a mixture in a 7:3 ratio (pale yellow oil, 37 mg, 87%) following the general procedure starting from 1-ethynyl-2-methylbenzene (25 μL, 0.2 mmol) and methylenecyclohexane (48 μL, 0.4 mmol) with [(*t*BuXPhos)AuNCMe]BAr_4^F (15 mg, 0.01 mmol, 5 mol%). The reaction time was 72 h.

Mixture of cyclobutene **20k** (*major*) and 1,3-diene **21k** (*minor*): **^{1}H NMR** (400 MHz, $CDCl_3$) δ 7.26 – 7.15 (m, 4H *major* and 3H *minor*), 7.04 (dd, *J* = 17.0, 10.6 Hz, 1H *minor*) 6.99 – 6.94 (m, 1H *minor*), 6.43 (s, 1H *mayor*), 4.98 (dd, *J* = 10.6, 2.1 Hz, 1H *minor*), 4.42 (dd, *J* = 17.0, 2.0 Hz, 1H *minor*), 2.55 (s, 2H *major*), 2.53 – 2.49 (m, 2H *minor*), 2.44 (s, 3H *major*), 2.14 (s, 3H *minor*), 1.90 – 1.84 (m, 2H *minor*), 1.74 – 1.36 (m, 10H *major* and 6H *minor*). **^{13}C NMR** (101 MHz, $CDCl_3$, *major*) δ 143.3, 139.9, 136.8, 133.7, 130.5, 127.1, 126.2, 125.7, 44.3, 42.0, 36.6 (2C), 26.0, 24.5 (2C), 21.9. **^{13}C NMR** (101 MHz, $CDCl_3$, *minor*) δ 140.9, 139.7, 136.6, 133.9, 130.1, 129.6, 126.5, 126.5, 125.4, 114.6, 32.9, 29.8, 28.3, 28.1, 26.9, 19.2.

After a second purification, pure cyclobutene **20k** was isolated as a pale yellow oil (11 mg, 26% yield). **^{1}H NMR** (400 MHz, $CDCl_3$) δ 7.24 – 7.13 (m, 4H), 6.41 (s, 1H), 2.53 (s, 2H), 2.42 (s, 3H), 1.67 – 1.31 (m, 10H). **^{13}C NMR** (126 MHz, $CDCl_3$) δ 143.3, 139.9, 136.8, 133.7, 130.5, 127.1, 126.2, 125.7, 44.4, 42.0, 36.6 (2C), 26.0, 24.5 (2C), 21.9. **HRMS** (APCI) *m/z* calculated for $C_{16}H_{21}^+$ $[M+H]^+$: 213.1638, found: 213.1637.

2-(2-Fluorophenyl)spiro[3.5]non-1-ene (20l) and 1-(1-cyclohexylideneallyl)-2-fluorobenzene (21l)

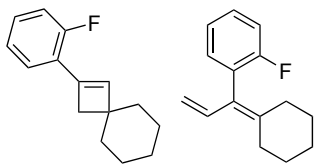

Cyclobutene **20l** and 1,3-diene **21l** were synthesized following the general procedure starting from 1-ethynyl-2-fluorobenzene (1 g, 0.943 mL, 8.32 mmol) and methylenecyclohexane (2 mL, 16.6 mmol) with

[(*t*BuXPhos)AuNCMe]BAr_4^F (635 mg, 0.4 mmol, 5 mol%). The reaction time was 72 h. Both products were separated and isolated by chromatography.

Cyclobutene **20l** was obtained as a colorless oil (874 mg, 49%). **^{1}H NMR** (400 MHz, $CDCl_3$) δ 7.24 – 7.15 (m, 2H), 7.08 (td, *J* = 7.5, 1.2 Hz, 1H), 7.02 (ddd, *J* = 10.8, 7.9, 1.2 Hz, 1H), 6.61 (d, *J* = 3.4 Hz, 1H), 2.48 (s, 2H), 1.69 – 1.32 (m, 10H). **^{13}C NMR** (101 MHz, $CDCl_3$) δ 161.3 (d, *J* (^{13}C-^{19}F) = 251.5 Hz), 141.4 (d, *J* (^{13}C-^{19}F) = 6.7 Hz), 137.9, 128.4 (d, *J* (^{13}C-^{19}F) = 8.2 Hz), 127.0 (d, *J* (^{13}C-^{19}F) = 4.5 Hz), 123.8 (d, *J* (^{13}C-^{19}F) = 3.5 Hz), 123.2 (d, *J* (^{13}C-^{19}F) = 14.0 Hz), 115.4 (d, *J* (^{13}C-^{19}F) = 21.1 Hz), 45.8, 41.3, 36.3 (2C), 25.9, 24.5 (2C). **^{19}F NMR** (376 MHz, $CDCl_3$) δ –114.65. **HRMS (**APCI) *m/z* calculated for $C_{15}H_{18}F^+$ $[M+H]^+$: 217.1387, found: 217.1388.

1,3-Diene **21l** was obtained as a colorless oil (354 mg, 20%). **^{1}H NMR** (400 MHz, $CDCl_3$) δ 7.30 – 7.23 (m, 1H), 7.12 (td, *J* = 7.4, 1.2 Hz, 1H), 7.09 – 6.98 (m, 3H), 5.01 (dd, *J* = 10.7, 1.7 Hz, 1H), 4.51 (d, *J* = 17.0 Hz, 1H), 2.50 (t, *J* = 6.0 Hz, 2H), 1.93 (t, *J* = 6.0 Hz, 2H), 1.76 – 1.55 (m, 4H), 1.53 – 1.38 (m, 2H). **^{13}C NMR** (101 MHz, $CDCl_3$) δ 160.1 (d, *J* (^{13}C-^{19}F) = 244.4 Hz), 143.3, 133.9, 132.3 (d, *J* (^{13}C-^{19}F) = 4.3 Hz), 128.4 (d, *J* (^{13}C-^{19}F) = 8.0 Hz), 127.3 (d, *J* (^{13}C-^{19}F) = 18.2 Hz), 126.1, 123.7 (d, *J* (^{13}C-^{19}F) = 3.6 Hz), 115.4 (d, *J* (^{13}C-^{19}F) = 22.8 Hz), 114.7, 33.3, 30.1, 28.2, 28.1, 26.8. **^{19}F NMR** (376 MHz, $CDCl_3$) δ –115.82. **HRMS** (APCI) *m/z* calculated for $C_{15}H_{18}F^+$ $[M+H]^+$: 217.1387, found: 217.1380.

2-(2-Chlorophenyl)spiro[3.5]non-1-ene (20m) and 1-chloro-2-(1-cyclohexylideneallyl)benzene (21m)

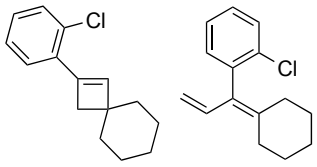

Cyclobutene **20m** and 1,3-diene **21m** were synthesized following the general procedure starting from 1-chloro-2-ethynylbenzene (24 μL, 0.2 mmol) and methylenecyclohexane (48 μL, 0.4 mmol) with [(*t*BuXPhos)AuNCMe]BAr_4^F (15 mg, 0.01 mmol, 5 mol%). The reaction time was 72 h. Both products were separated and isolated by chromatography.

Cyclobutene **20m** was obtained as a pale yellow oil (23 mg, 49%). **^{1}H NMR** (400 MHz, $CDCl_3$) δ 7.34 (dd, *J* = 7.9, 1.3 Hz, 1H), 7.30 – 7.18 (m, 2H), 7.14 (td, *J* = 7.5, 1.8 Hz, 1H), 6.85 (s, 1H), 2.54 (s, 2H), 1.67 – 1.34 (m, 10H). **^{13}C NMR** (101 MHz, $CDCl_3$) δ 142.9, 140.4, 132.8, 132.6, 130.2, 128.0, 127.7, 126.4, 44.7, 42.1, 36.3 (2C), 25.9, 24.5 (2C). **HRMS** (APCI) *m/z* calculated for $C_{15}H_{18}Cl^+$ $[M+H]^+$: 233.1092, found: 233.1082.

1,3-Diene **21m** was obtained as a pale yellow oil (13 mg, 28 %). **^{1}H NMR** (400 MHz, $CDCl_3$) δ 7.42 – 7.39 (m, 1H), 7.25 – 7.20 (m, 2H), 7.09 – 7.05 (m, 1H), 7.00 (dd, *J* = 17.1, 10.6 Hz, 1H), 4.99 (dd, *J* = 10.6, 1.7 Hz, 1H), 4.41 (dd, *J* = 17.1, 1.7 Hz, 1H), 2.58 – 2.40 (m, 2H), 1.88 – 1.83 (m, 2H), 1.72 – 1.64 (m, 2H), 1.62 – 1.37 (m, 4H). **^{13}C NMR** (101 MHz, $CDCl_3$) δ 142.4, 139.0, 134.1, 133.4, 131.8, 129.9, 129.3, 127.9 126.5, 114.6, 33.1, 29.9, 28.1, 27.9, 26.8. **HRMS** (APCI) *m/z* calculated for $C_{15}H_{16}Cl^+$ $[M-H]^+$: 231.0935, found: 231.0928.

2-(2-Bromophenyl)spiro[3.5]non-1-ene (20n) and 1-bromo-2-(1-cyclohexylideneallyl)benzene (21n)

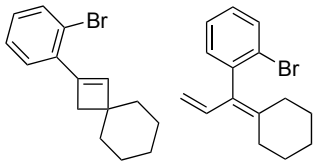

Cyclobutene **20n** and 1,3-diene **21n** were synthesized following the general procedure starting from 1-bromo-2-ethynylbenzene (25 μL, 0.2 mmol) and methylenecyclohexane (48 μL, 0.4 mmol) with [(*t*BuXPhos)AuNCMe]BAr_4^F (15 mg, 0.01 mmol, 5 mol%). The reaction time was 72 h. In the first purification using pentane as eluent a 2:1 mixture of cyclobutene and 1,3-diene (42 mg, 76%) was obtained. However, a second purification using cyclohexane as eluent allowed the separation and isolation of both products.

Cyclobutene **20n** was obtained as a pale yellow oil (17 mg, 31 % yield). **^{1}H NMR** (400 MHz, $CDCl_3$) δ 7.57 – 7.52 (m, 1H), 7.30 – 7.23 (m, 2H), 7.06 (ddd, *J* = 8.0, 5.8, 3.2 Hz, 1H), 6.96 (s, 1H), 2.55 (s, 2H), 1.66 – 1.31 (m, 10H). **^{13}C NMR** (101 MHz, $CDCl_3$) δ 142.7, 141.7, 134.3, 133.7, 128.2, 128.1, 127.0, 121.6, 44.2, 42.3, 36.2 (2C), 25.9, 24.5 (2C). **HRMS** (APCI) *m/z* calculated for $C_{15}H_{18}Br^+$ $[M+H]^+$: 277.0586, found: 277.0576.

1,3-Diene **21n** was obtained as a pale yellow oil (2 mg, 4%). **^{1}H NMR** (400 MHz, $CDCl_3$) δ 7.60 (dd, *J* = 8.0, 1.3 Hz, 1H), 7.29 (td, *J* = 7.5, 1.3 Hz, 1H), 7.13 (ddd, *J* = 7.9, 7.5, 1.8 Hz 1H), 7.07 (dd, *J* = 7.5, 1.8 Hz, 1H), 6.98 (dd, *J* = 17.1, 10.6 Hz, 1H), 5.00 (dd, *J* = 10.6, 1.7 Hz, 1H), 4.40 (dd, *J* = 17.1, 1.7 Hz, 1H), 2.59 – 2.37 (m, 2H), 1.91 – 1.77 (m, 2H), 1.74 – 1.56 (m, 5H), 1.48 – 1.37 (m, 1H). **^{13}C NMR** (101 MHz, $CDCl_3$) δ 142.1, 141.1, 133.3, 132.5, 131.7, 131.7, 128.1, 127.1, 124.7, 114.7, 33.1, 29.9, 28.0, 27.7, 26.8. **HRMS** (APCI) *m/z* calculated for $C_{15}H_{18}Br^+$ $[M+H]^+$: 277.0586, found: 277.0578.

2-(2-Methoxyphenyl)spiro[3.4]oct-1-ene (20o) and 1-(1-cyclopentylideneallyl)-2-methoxybenzene (21o)

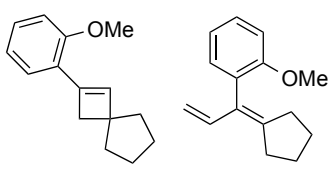

Cyclobutene **20o** and 1,3-diene **21o** were synthesized following the general procedure starting from 1-ethynyl-2-methoxybenzene (26 μL, 0.2 mmol) and methylenecyclopentane (42 μL, 0.4 mmol) with [(*t*BuXPhos)AuNCMe]BAr_4^F (15 mg, 0.01 mmol, 5 mol%). The reaction time was 72 h. Both products were separated and isolated by chromatography.

Cyclobutene **20o** was obtained as an orange oil (23 mg, 53%). **^{1}H NMR** (400 MHz, $CDCl_3$) δ 7.21 (ddd, *J* = 8.3, 7.4, 1.8 Hz, 1H), 7.15 (dd, *J* = 7.5, 1.8 Hz, 1H), 6.92 (td, *J* = 7.4, 1.1 Hz, 1H), 6.87 (dd, *J* = 8.2, 1.0 Hz, 1H), 6.48 (s, 1H), 3.89 (s, 3H), 2.65 (s, 2H), 1.80 – 1.67 (m, 8H). **^{13}C NMR** (126 MHz, $CDCl_3$) δ 158.3, 139.5, 138.6, 128.3, 126.8, 123.6, 120.2, 110.2, 55.1, 51.5, 43.6, 36.4 (2C), 24.5 (2C). **HRMS** (APCI) *m/z* calculated for $C_{15}H_{19}O^+$ $[M+H]^+$: 215.1430, found: 215.1440.

1,3-Diene **21o** was obtained as an orange oil (5 mg, 12%). **^{1}H NMR** (400 MHz, $CDCl_3$) δ 7.28 – 7.23 (m, 1H), 7.02 – 6.91 (m, 3H), 6.80 (dd, *J* = 17.2, 10.5 Hz, 1H), 4.91 (dq, *J* = 10.5, 0.9 Hz, 1H), 4.53 (dt, *J* = 17.1, 0.8 Hz, 1H), 3.77 (s, 3H), 2.57 (bs, 2H), 2.01 (t, *J* = 7.2 Hz, 2H), 1.74 (p, *J* = 7.2 Hz, 2H), 1.58 (p, *J* = 6.9 Hz, 2H). **^{13}C NMR** (75 MHz, $CDCl_3$) δ 156.9, 146.8, 136.2, 131.3, 129.1, 128.4, 127.9, 120.5, 112.2, 111.2, 55.7, 32.6, 30.3, 26.6, 26.2. **HRMS** (APCI) *m/z* calculated for $C_{15}H_{19}O^+$ $[M+H]^+$: 215.1430, found 215.1427.

2-(2-Methylphenyl)spiro[3.4]oct-1-ene (20p) and 1-(1-cyclopentylideneallyl)-2-methylbenzene (21p)

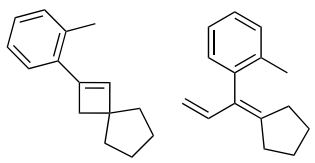

Cyclobutene **20p** and 1,3-diene **21p** were synthesized as a mixture in a 3:2 ratio (pale yellow oil, 30 mg, 75%) following the general procedure starting from 1-ethynyl-2-methylbenzene (25 μL, 0.2 mmol) and methylenecyclopentane (42 μL, 0.4 mmol) with [(*t*BuXPhos)AuNCMe]BAr_4^F (15 mg, 0.01 mmol, 5 mol%). The reaction time was 72 h.

Mixture of cyclobutene **20p** (*major*) and 1,3-diene **21p** (*minor*): **^{1}H NMR** (400 MHz, $CDCl_3$) δ 7.23 – 7.13 (m, 4H *major* and 3H *minor*), 6.99 – 6.97 (m, 1H *minor*), 6.78 (dd, *J* = 17.2, 10.5 Hz, 1H *minor*), 6.28 (d, *J* = 0.7 Hz, 1H *major*), 4.91 (dq, *J* = 10.5, 0.9 Hz, 1H

minor), 4.43 (dq, *J* = 17.1, 0.8 Hz, 1H *minor*), 2.71 (s, 2H *major*), 2.56 (t, *J* = 7.3 Hz, 2H *minor*), 2.43 (s, 3H *major*), 2.12 (s, 3H *minor*), 1.80 – 1.55 (m, 8H *major* and 6H *minor*). **^{13}C NMR** (126 MHz, $CDCl_3$) δ 145.6, 142.9, 139.9, 137.9, 136.8, 136.1, 136.0, 133.5, 131.7, 130.5, 129.8, 129.6, 127.2, 126.6, 126.3, 125.7, 125.7, 112.7, 50.9, 44.4, 36.4 (2C), 32.6, 30.1, 26.6, 26.3, 24.5 (2C), 21.9, 19.1. **HRMS** (APCI) *m/z* calculated for $C_{15}H_{19}^+$ $[M+H]^+$: 199.1481, found: 199.1481.

2-(2-Fluorophenyl)spiro[3.4]oct-1-ene (20q) and 1-(1-cyclopentylideneallyl)-2-fluorobenzene (21q)

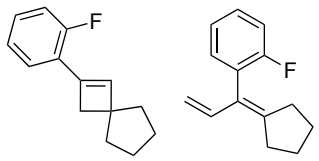

Cyclobutene **20q** and 1,3-diene **21q** were synthesized following the general procedure starting from 1-ethynyl-2-fluorobenzene (23 μL, 0.2 mmol) and methylenecyclopentane (42 μL, 0.4 mmol) with [(*t*BuXPhos)AuNCMe]BAr_4^F (15 mg, 0.01 mmol, 5 mol%). The reaction time was 72 h. Both products were separated and isolated by chromatography.

Cyclobutene **20q** was obtained as a pale yellow oil (18 mg, 44%). **^{1}H NMR** (400 MHz, $CDCl_3$) δ 7.23 – 7.14 (m, 2H), 7.12 – 6.98 (m, 2H), 6.48 (d, *J* = 3.4 Hz, 1H), 2.65 (s, 2H), 1.78 – 1.67 (m, 8H). **^{13}C NMR** (101 MHz, $CDCl_3$) δ 161.2 (d, *J* (^{13}C-^{19}F) = 251.1 Hz), 139.6 (d, *J* (^{13}C-^{19}F) = 7.0 Hz), 137.4, 128.4 (d, *J* (^{13}C-^{19}F) = 8.1 Hz), 127.0 (d, *J* (^{13}C-^{19}F) = 4.5 Hz), 123.8 (d, *J* (^{13}C-^{19}F) = 3.5 Hz), 123.0 (d, *J* (^{13}C-^{19}F) = 14.2 Hz), 115.4 (d, *J* (^{13}C-^{19}F) = 21.0 Hz), 52.2 (d, *J* (^{13}C-^{19}F) = 1.2 Hz), 43.6, 36.2 (2C), 24.5 (2C). **^{19}F NMR** (376 MHz, $CDCl_3$) δ –114.69. **HRMS** (APCI) *m/z* calculated for $C_{14}H_{16}F^+$ $[M+H]^+$: 203.1231, found: 203.1237.

1,3-Diene **21q** was obtained as a pale yellow oil (7 mg, 17%). **^{1}H NMR** (400 MHz, $CDCl_3$) δ 7.31 – 7.22 (m, 1H), 7.17 – 7.04 (m, 3H), 6.78 (dd, *J* = 17.1, 10.6 Hz, 1H), 4.96 (d, *J* = 10.9 Hz, 1H), 4.57 (d, *J* = 17.1 Hz, 1H), 2.57 (t, *J* = 7.3 Hz, 2H), 2.06 (t, *J* = 7.2 Hz, 2H), 1.77 (p, *J* = 6.8 Hz, 2H), 1.61 (p, *J* = 6.8 Hz, 2H). **^{13}C NMR** (101 MHz, $CDCl_3$) δ 159.9 (d, *J* (^{13}C-^{19}F) = 244.8 Hz), 148.1, 135.8, 131.9 (d, *J* (^{13}C-^{19}F) = 4.5 Hz), 128.4 (d, *J* (^{13}C-^{19}F) = 8.0 Hz), 127.4 (d, *J* (^{13}C-^{19}F) = 17.6 Hz), 126.0, 123.8 (d, *J* (^{13}C-^{19}F) = 3.5 Hz), 115.6 (d, *J* (^{13}C-^{19}F) = 22.7 Hz), 112.8, 32.7, 30.5, 26.5, 26.2. **^{19}F NMR** (376 MHz, $CDCl_3$) δ –115.83. **HRMS** (APCI) *m/z* calculated for $C_{14}H_{14}F^+$ $[M-H]^+$: 201.1074, found: 201.1068.

2-(2-Chlorophenyl)spiro[3.4]oct-1-ene (20r) and 1-chloro-2-(1-cyclopentylideneallyl)benzene (21r)

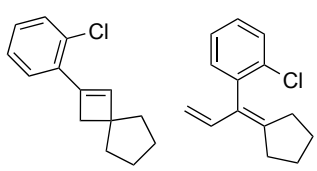

Cyclobutene **20r** and 1,3-diene **21r** were synthesized following the general procedure starting from 1-chloro-2-ethynylbenzene (24 μL, 0.2 mmol) and methylenecyclopentane (42 μL, 0.4 mmol) with [(*t*BuXPhos)AuNCMe]BAr_4^F (15 mg, 0.01 mmol, 5 mol%). The reaction time was 72 h. Both products were separated and isolated by chromatography.

Cyclobutene **20r** was obtained as a pale yellow oil (12 mg, 27%). **^{1}H NMR** (400 MHz, $CDCl_3$) δ 7.34 (dd, *J* = 7.8, 1.3 Hz, 1H), 7.24 (d, *J* = 2.1 Hz, 1H), 7.21 (td, *J* = 7.3, 1.3 Hz, 1H), 7.14 (ddd, *J* = 7.8, 7.0, 2.0 Hz, 1H), 6.72 (s, 1H), 2.71 (s, 2H), 1.80 – 1.36 (m, 8H). **^{13}C NMR** (101 MHz, $CDCl_3$) δ 141.0, 139.9, 132.8, 132.3, 130.2, 128.0, 127.7, 126.5, 51.1, 44.4, 36.2 (2C), 24.5 (2C). **HRMS** (APCI) *m/z* calculated for $C_{14}H_{16}Cl^+$ $[M+H]^+$: 219.0935, found: 219.0932.

1,3-Diene **21r** was obtained as a pale yellow oil (12 mg, 27%). **^{1}H NMR** (500 MHz, $CDCl_3$) δ 7.41 (dd, *J* = 7.7, 1.6 Hz, 1H), 7.27 – 7.19 (m, 2H), 7.10 (dd, *J* = 7.2, 2.0 Hz, 1H), 6.76 (dd, *J* = 17.2, 10.6 Hz, 1H), 4.94 (dt, *J* = 10.5, 0.9 Hz, 1H), 4.44 (dt, *J* = 17.3, 0.9 Hz, 1H), 2.64 – 2.49 (m, 2H), 1.97 (m, 2H), 1.76 (pd, *J* = 7.0, 3.3 Hz, 2H), 1.61 (pd, *J* = 6.9, 2.8 Hz, 2H). **^{13}C NMR** (75 MHz, $CDCl_3$) δ 147.4, 139.0, 135.4, 133.6, 131.4, 129.7, 129.5, 128.0, 126.7, 112.7, 32.5, 30.3, 26.5, 26.2. **HRMS** (APCI) *m/z* calculated for $C_{14}H_{16}Cl^+$ $[M+H]^+$: 219.0935, found: 219.0940.

1-Bromo-2-(1-cyclopentylideneallyl)benzene

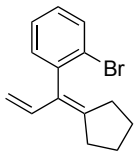

The title compound (pale yellow oil, 18 mg, 34%) was synthesized following the general procedure starting from 1-bromo-2-ethynylbenzene (25 μL, 0.2 mmol) and methylenecyclopentane (42 μL, 0.4 mmol) with [(*t*BuXPhos)AuNCMe]BAr_4^F (15 mg, 0.01 mmol, 5 mol%). The reaction time was 72 h.

^{1}H NMR (500 MHz, $CDCl_3$) δ 7.60 (dd, *J* = 8.0, 1.2 Hz, 1H), 7.30 (td, *J* = 7.4, 1.2 Hz, 1H), 7.13 (ddd, *J* = 7.9, 7.5, 1.8 Hz, 1H), 7.09 (dd, *J* = 7.5, 1.8 Hz, 1H), 6.75 (dd, *J* = 17.2, 10.6 Hz, 1H), 4.95 (dt, *J* = 10.7, 0.6 Hz, 1H), 4.43 (dt, *J* = 17.2, 0.7 Hz, 1H), 2.65 – 2.48 (m, 2H), 2.06 – 1.88 (m, 2H), 1.85 – 1.70 (m, 2H), 1.69 – 1.55 (m, 2H). **^{13}C NMR** (75 MHz, $CDCl_3$) δ 147.2, 141.1, 135.3, 132.7, 131.5, 131.3, 128.2, 127.4, 124.0, 112.8, 32.5, 30.2,

26.5, 26.2. **HRMS** (APCI) *m/z* calculated for $C_{12}H_{12}Br^+$ [M-C_2H_3]$^+$: 235.0117, found: 235.0111.

1-(Spiro[3.5]non-1-en-2-yl)naphthalene (20t) and 1-(1-cyclohexylideneallyl)naphthalene (21t)

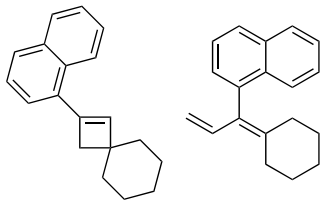

Cyclobutene **20t** and 1,3-diene **21t** were synthesized following the general procedure starting from 1-ethynylnaphthalene (28 μL, 0.2 mmol) and methylenecyclohexane (48 μL, 0.4 mmol) with [(*t*BuXPhos)AuNCMe]BAr_4^F (15 mg, 0.01 mmol, 5 mol%). The reaction time was 38 h. Both products were separated and isolated by chromatography.

Cyclobutene **20t** was obtained as a colorless oil (11 mg, 22%). Traces of the corresponding 1,4,4-trisubstituted cyclobutene were detected in the NMR spectra. **^{1}H NMR** (400 MHz, $CDCl_3$) δ 8.44 (d, *J* = 8.2 Hz, 1H), 7.89 – 7.81 (m, 1H), 7.75 (dd, *J* = 7.3, 2.0 Hz, 1H), 7.57 – 7.38 (m, 4H), 6.80 (s, 1H), 2.69 (s, 2H), 1.75 – 1.35 (m, 10H). **^{13}C NMR** (101 MHz, $CDCl_3$) δ 142.6, 140.1, 133.8, 132.1, 131.1, 128.6, 128.1, 126.3, 125.6, 125.3, 125.3, 124.5, 44.8, 42.7, 36.5 (2C), 26.0, 24.5 (2C). **HRMS** (APCI) *m/z* calculated for $C_{19}H_{21}^+$ [M+H]$^+$: 249.1638, found: 249.1636.

1,3-Diene **21t** was obtained as a colorless oil (5 mg, 10%). **^{1}H NMR** (400 MHz, $CDCl_3$) δ 7.84 (dd, *J* = 7.9, 1.6 Hz, 1H), 7.77 (d, *J* = 8.1 Hz, 2H), 7.49 – 7.36 (m, 3H), 7.21 – 7.11 (m, 2H), 4.94 (dd, *J* = 10.6, 1.9 Hz, 1H), 4.32 (dd, *J* = 17.1, 1.9 Hz, 1H), 2.70 – 2.53 (m, 2H), 1.86 – 1.68 (m, 4H), 1.62 – 1.55 (m, 2H), 1.44 – 1.31 (m, 2H). **^{13}C NMR** (126 MHz, $CDCl_3$) δ 142.8, 138.2, 134.5, 133.6, 132.5, 130.3, 128.1, 127.2, 126.7, 126.1, 125.6, 125.5, 125.5, 115.5, 33.3, 30.1, 28.5, 28.3, 26.9. **HRMS** (APCI) *m/z* calculated for $C_{19}H_{21}^+$ [M+H]$^+$: 249.1638, found: 249.1634.

9-(Spiro[3.5]non-1-en-2-yl)phenanthrene (20u) and 9-(1-cyclohexylideneallyl)phenanthrene (21u)

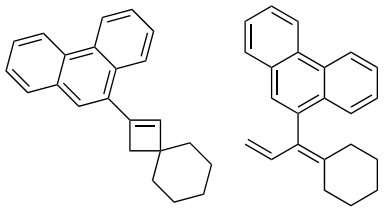

Cyclobutene **20u** and 1,3-diene **21u** were synthesized as a mixture in a 5:2 ratio (pale yellow oil, 40 mg, 67%) following the general procedure starting from 9-ethynylphenanthrene (40 mg, 0.2 mmol) and methylenecyclohexane (48 μL, 0.4 mmol) with [(*t*BuXPhos)AuNCMe]BAr_4^F (15 mg, 0.01 mmol, 5 mol%). The reaction time was 38 h.

Mixture of cyclobutene **20u** (*major*) and 1,3-diene **21u** (*minor*): traces of the corresponding 1,4,4-trisubstituted cyclobutene were detected in the NMR spectra. **^{1}H NMR** (400 MHz, $CDCl_3$) δ 8.77 – 8.70 (m, 1H *major* and 2H *minor*), 8.67 – 8.63 (m, 1H *major*), 8.59 – 8.54 (m, 1H *major*), 7.93 – 7.84 (m, 1H *major* and 2H *minor*), 7.74 – 7.49 (m, 5H *major* and 5H *minor*), 7.22 (dd, *J* = 17.1, 10.7 Hz, 1H *minor*), 6.87 (s, 1H *major*), 4.99 (dd, *J* = 10.7, 1.8 Hz, 1H *minor*), 4.51 (dd, *J* = 17.1, 1.8 Hz, 1H *minor*), 2.79 (s, 2H *major*), 2.74 – 2.59 (m, 2H *minor*), 1.99 – 1.36 (m, 10H *major* and 8H *minor*). **^{13}C NMR** (101 MHz, $CDCl_3$, *major*) δ 142.4, 140.5, 131.6, 130.6, 130.6, 130.4, 130.1, 128.7, 126.7 (2C), 126.7, 126.3, 126.0, 125.4, 123.0, 122.5, 44.6, 42.6, 36.6 (2C), 26.0, 24.6 (2C). **^{13}C NMR** (101 MHz, $CDCl_3$, *minor*) δ 143.1, 136.6, 134.3, 131.9, 131.7, 130.3, 129.8, 128.4, 127.6, 126.7 (2C), 126.5, 126.5, 126.3, 126.1, 122.7, 122.5, 115.6, 33.4, 30.2, 28.5, 28.3, 26.9.

After a second purification, cyclobutene **20u** was isolated as a colorless oil (7 mg, 12% yield). Traces of the corresponding 1,4,4-trisubstituted cyclobutene were detected in the NMR spectra. **^{1}H NMR** (400 MHz, $CDCl_3$) δ 8.77 – 8.69 (m, 1H), 8.67 – 8.61 (m, 1H), 8.57 – 8.51 (m, 1H), 7.86 (dd, *J* = 7.8, 1.6 Hz, 1H), 7.71 – 7.54 (m, 5H), 6.85 (s, 1H), 2.76 (s, 2H), 1.75 – 1.40 (m, 10H). **^{13}C NMR** (101 MHz, $CDCl_3$) δ 142.4, 140.5, 131.6, 130.6, 130.6, 130.4, 130.1, 128.7, 126.7 (2C), 126.7, 126.3, 126.0, 125.4, 123.0, 122.5, 44.6, 42.6, 36.6 (2C), 26.0, 24.6 (2C). **HRMS** (APCI) *m/z* calculated for $C_{23}H_{23}^+$ $[M+H]^+$: 299.1794, found: 299.1792.

(1*R,8*R**)-9-(2-Bromophenyl)bicyclo[6.2.0]dec-9-ene (20v) and (1*E*,3*E*)-2-(2-bromophenyl)cyclodeca-1,3-diene (21v)**

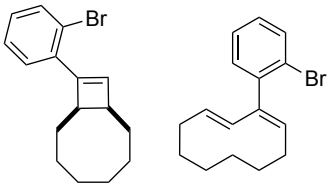

Cyclobutene **20v** and 1,3-diene **21v** were synthesized following the general procedure starting from 1-bromo-2-ethynylbenzene (38 µL, 0.3 mmol) and (*Z*)-cyclooctene (78 µL, 0.6 mmol) with [(*t*BuXPhos)AuNCMe]BAr_4^F (23 mg, 0.015 mmol, 5 mol%). The reaction time was 4 d. Both products were separated and isolated by chromatography (eluent = cyclohexane: CH_2Cl_2 95:5).

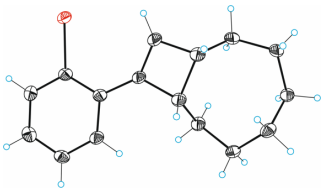

Cyclobutene **20v** was obtained as a white solid (73 mg, 84%). The structure was confirmed by single crystal X-ray diffraction. The crystals were obtained by evaporation of the solvents (cyclohexane: CH_2Cl_2 95:5). **M.p.** (cyclohexane/CH_2Cl_2) 60-62 ºC. **^{1}H NMR** (500 MHz, $CDCl_3$) δ 7.58 (dd, *J* = 8.0, 1.2 Hz, 1H), 7.31 – 7.22 (m, 2H), 7.07 (ddd, *J* = 8.0, 7.1, 1.9 Hz, 1H), 6.60 (d, *J* = 1.3 Hz, 1H), 3.32 – 3.24 (m, 1H), 2.79 (ddt, *J* = 12.0, 4.4, 1.7 Hz, 1H), 1.94 – 1.88 (m, 1H), 1.86 – 1.80 (m, 1H), 1.74 – 1.36 (m, 10H). **^{13}C NMR** (126 MHz, $CDCl_3$) δ 146.5, 137.4, 133.7, 133.6, 128.7, 127.9, 126.9, 121.8, 47.5, 44.9, 30.6, 30.3, 27.2, 26.3, 26.1, 25.3. **HRMS** (APCI) *m/z* calculated for $C_{16}H_{20}Br^+$ $[M+H]^+$: 291.0743, found: 291.0747.

1,3-Diene **21v** was obtained as a colorless oil (4 mg, 5%). **^{1}H NMR** (400 MHz, $CDCl_3$) δ 7.58 – 7.46 (m, 1H), 7.30 – 7.18 (m, 2H), 7.14 – 7.07 (m, 1H), 6.55 (d, *J* = 16.7 Hz, 1H), 5.59 (td, *J* = 8.3, 1.6 Hz, 1H), 5.16 (dt, *J* = 16.3, 7.7 Hz, 1H), 2.30 – 2.20 (m, 2H), 2.16 – 2.06 (m, 2H), 1.54 – 1.47 (m, 2H), 1.40 – 1.28 (m, 6H). **^{13}C NMR** (126 MHz, $CDCl_3$) δ 143.7, 142.9, 132.9, 132.7, 131.0, 130.9, 129.9, 128.2, 127.0, 122.7, 34.4, 29.3, 26.5, 26.4, 24.2, 23.3. **HRMS** (APCI) *m/z* calculated for $C_{16}H_{20}Br^+$ $[M+H]^+$: 291.0743, found 291.0732.

1-Bromo-2-(3-ethyl-4,4-dimethylcyclobut-1-en-1-yl)benzene (20w), 1-bromo-2-(4-ethyl-3,3-dimethylcyclobut-1-en-1-yl)benzene (20w´) and (*E*)-1-bromo-2-(2-methylhepta-2,4-dien-3-yl)benzene (21w)

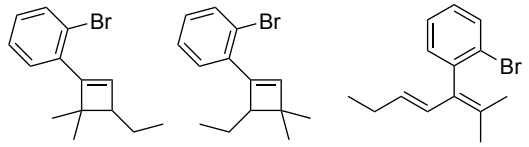

Cyclobutenes **20w** and **20w´** and 1,3-diene **21w** were synthesized following the general procedure starting from 1-bromo-2-ethynylbenzene (75 µL, 0.6 mmol) and 2-methylpent-2-ene (146 µL, 1.2 mmol) with [(*t*BuXPhos)AuNCMe]BAr_4^F (46 mg, 0.03 mmol, 5 mol%). The reaction time was 20 h. The products were separated and isolated by chromatography.

The mixture of cyclobutenes **20w** and **20w´** in a 2.4:1 ratio was obtained as a colorless oil (65 mg, 41%). **^{1}H NMR** (400 MHz, $CDCl_3$) δ 7.63 (dd, *J* = 8.0, 1.2 Hz, 1H *major*), 7.58 (dd, *J* = 8.0, 1.1 Hz, 1H *minor*), 7.38 – 7.21 (m, 2H *major* and 2H *minor*), 7.11 – 7.04 (m, 1H *major* and 1H *minor*), 6.90 (d, *J* = 1.4 Hz, 1H *major*), 6.64 (s, 1H *minor*), 2.85 (dd, *J* = 10.4, 4.3 Hz, 1H *minor*), 2.36 (ddd, *J* = 9.4, 6.3, 1.3 Hz, 1H *major*), 1.82 – 1.59 (m, 1H *major* and 1H *minor*), 1.50 – 1.39 (m, 4H *major* and 1H *minor*), 1.36 – 1.28 (m, 3H *major* and 3H *minor*), 1.24 (s, 3H *minor*), 1.04 (t, *J* = 7.4, 3H *major*), 0.98 (t, *J* = 7.4, 3H *minor*). **^{13}C NMR** (126 MHz, $CDCl_3$, *major*) δ 150.6, 136.5, 134.3, 133.5, 128.5, 127.7, 126.8, 122.8, 54.3, 47.3, 26.8, 22.7, 21.4, 12.7. **^{13}C NMR** (126 MHz, $CDCl_3$, *minor*) 144.7, 142.8, 134.6, 133.6, 128.9, 128.0, 126.9, 122.0, 55.3, 42.9, 27.8, 22.1, 21.5, 13.1. **HRMS** (APCI) *m/z* calculated for $C_{14}H_{16}Br^+$ $[M-H]^+$: 263.0430, found: 263.0432.

1,3-Diene **21w** was obtained as a colorless oil (58 mg, 37%). **^{1}H NMR** (300 MHz, $CDCl_3$) δ 7.58 (dd, *J* = 7.9, 1.3 Hz, 1H), 7.30 (td, *J* = 7.5, 1.3 Hz, 1H), 7.12 (td, *J* = 7.7, 1.8 Hz, 1H), 7.05 (dd, *J* = 7.5, 1.8 Hz, 1H), 6.55 (dt, *J* = 15.5, 1.6 Hz, 1H), 4.88 (dt, *J* = 15.4, 6.6 Hz, 1H), 2.14 – 2.00 (m, 2H), 1.95 (s, 3H), 1.47 (s, 3H), 0.94 (t, *J* = 7.4 Hz, 3H). **^{13}C NMR** (75 MHz, $CDCl_3$) δ 142.1, 134.1, 133.4, 132.5, 131.6, 131.0, 127.9, 127.1, 126.6, 124.5, 26.2, 22.5, 19.6, 13.8. **HRMS** (APCI) *m/z* calculated for $C_{13}H_{14}Br^+$ $[M-CH_3]^+$: 249.0273, found 249.0272.

Procedure for the Derivatization of 21f into 21i

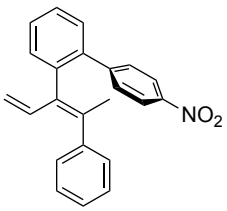

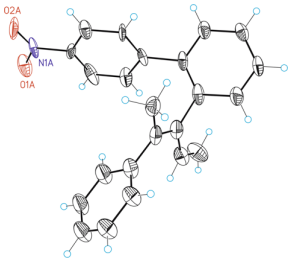

(*E*)-4'-Nitro-2-(4-phenylpenta-1,3-dien-3-yl)-1,1'-biphenyl was synthesized following a literature procedure for the preparation of related 1,1'-biphenyl derivatives.[86] (*E*)-1-Bromo-2-(4-phenylpenta-1,3-dien-3-yl)benzene (100 mg, 0.33 mmol, 1 equiv), (4-nitrophenyl)boronic acid (69 mg, 0.40 mmol, 1.2 equiv) and palladium(II) acetate (1.5 mg, 6.7 µmol, 2 mol%) under argon were dissolved in *N,N*-dimethylformamide (0.7 mL). Then, potassium carbonate (65 mg, 0.47 mmol, 1.4 equiv) in water (0.7 mL) was added. The resulting mixture was stirred at 100 °C for 16 h. The reaction was monitored by TLC (eluent = cyclohexane:EtOAc 10:1). The reaction mixture was allowed to cool to room temperature and CH_2Cl_2 (20 mL) was added. The mixture was then filtered through Celite™. The organic layer was washed with water (2 × 20 mL), dried over anhydrous Na_2SO_4, filtered and concentrated under reduced pressure. The crude was adsorbed on florisil and purified by silica gel column chromatography (eluent = cyclohexane:EtOAc from 1:0 to 10:1). 1,3-Diene **21i** (64 mg, 56%) was obtained as an orange solid. The product was crystallized by dissolving it in ethanol at 60 ºC and then cooling to room temperature. The structure was confirmed by single crystal X-ray diffraction.

M.p. (EtOH) 135-138 ºC. **^{1}H NMR** (400 MHz, $CDCl_3$) δ 8.25 – 8.19 (m, 2H), 7.62 – 7.56 (m, 2H), 7.51 – 7.41 (m, 3H), 7.35 – 7.22 (m, 4H), 7.02 – 6.96 (m, 2H), 6.52 (dd, *J* = 17.3, 10.6 Hz, 1H), 4.98 (ddd, *J* = 10.7, 1.6, 0.8 Hz, 1H), 4.67 (ddd, *J* = 17.3, 1.6, 0.8 Hz, 1H), 1.61 (s, 3H). **^{13}C NMR** (101 MHz, $CDCl_3$) δ 148.6, 146.9, 142.4, 139.8, 138.9, 137.8, 137.7, 135.9, 131.3, 129.6, 129.6 (2C), 128.5, 128.2 (2C), 128.1 (2C), 127.7, 127.0, 123.0 (2C), 116.3, 23.1. **HRMS** (APCI) *m/z* calculated for $C_{23}H_{20}NO_2^+$ $[M+H]^+$: 342.1489, found 342.1487.

Procedure for the Preparation of 1,3-Butadiynes

1,3-Diynes were synthesized following a slightly modified literature procedure.[87]

86. Lima, C. F. R. A. C.; Rodrigues, A. S. M. C.; Silva, V. L. M.; Silva, A. M. S.; Santos, L. M. N. B. F. *ChemCatChem* **2014**, *6*, 1291–1302.
87. Zatolochnaya, O. V.; Gevorgyan, V. *Org. Lett*. **2013**, *15*, 2562–2565.

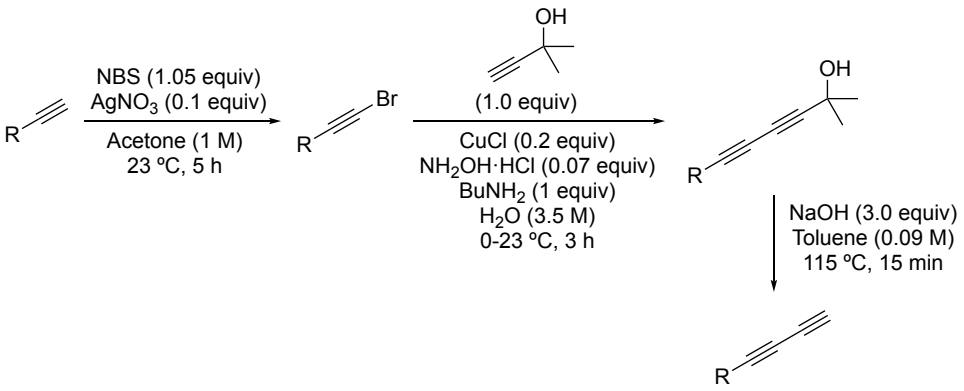

General procedure for the preparation of 6-substituted 2-methylhexa-3,5-diyn-2-ols

The alkyne (1 equiv) was dissolved in acetone (1 M). Silver nitrate (0.1 equiv) was added, followed by *N*-bromosuccinimide (1.05 equiv). The reaction mixture was stirred at 23 °C with exclusion of light for 5 h. Then, the reaction mixture was filtered through a Celite™ plug washing with CH_2Cl_2, the solvent was removed under reduced pressure and the crude containing the corresponding bromoalkyne was engaged in the next step without further purification.

Copper(I) chloride (0.2 equiv) was added to an aqueous solution of butan-1-amine (1 equiv) in water (3.5 M) at 0 ºC, which resulted in a blue solution. After stirring for 5 min, *N*-hydroxylamine hydrochloride (0.07 equiv) was added, which resulted in a colorless solution. 2-Methylbut-3-yn-2-ol (1 equiv) was then added and the resulting yellow solution was stirred for additional 10 min. A solution of freshly prepared bromoalkyne (1 equiv) in CH_2Cl_2 (2 M) was added dropwise, and the reaction mixture was allowed to warm to 23 °C and stirred for 3 h. Upon completion, water (5 mL) was added and the reaction mixture was extracted with CH_2Cl_2 (3 × 10 mL), dried over Na_2SO_4, filtered and concentrated under vacuum. The residue was adsorbed on silica gel and purified by silica gel flash column chromatography (eluent = cyclohexanes:EtOAc 4:1) to afford the corresponding 6-substituted 2-methylhexa-3,5-diyn-2-ol.

2-Methyl-6-phenylhexa-3,5-diyn-2-ol,[87] 6-(4-methoxyphenyl)-2-methylhexa-3,5-diyn-2-ol,[88] 6-(3-chlorophenyl)-2-methylhexa-3,5-diyn-2-ol,[89] 6-(3-methoxyphenyl)-2-

88. West, K.; Hayward, L. N.; Batsanov, A. S.; Bryce, M. R. *Eur. J. Org. Chem.* **2008**, 5093–5098.
89. Peng, H.; Xi, Y.; Ronaghi, N.; Dong, B.; Akhmedov, N. G.; Shi, X. *J. Am. Chem. Soc.* **2014**, *136*, 13174−13177.

methylhexa-3,5-diyn-2-ol,[88] 2-methyl-6-(2-methylphenyl)hexa-3,5-diyn-2-ol,[89] 2-methyl-6-(thiophen-3-yl)hexa-3,5-diyn-2-ol,[89] and 2-methyldodeca-3,5-diyn-2-ol[90] were reported in the literature. The NMR data obtained for those products are in agreement with the ones previously described in the literature.

2-Methyl-6-(4-(trifluoromethyl)phenyl)hexa-3,5-diyn-2-ol

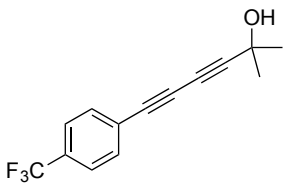

The title compound (white solid, 1.363 g, 61% yield) was synthesized according to the general procedure starting from 1-ethynyl-4-(trifluoromethyl)benzene (1.44 mL, 8.83 mmol) and 2-methylbut-3-yn-2-ol (0.86 mL, 8.83 mmol).

M.p. (CH_2Cl_2) 80-82 ºC. **^{1}H NMR** (300 MHz, $CDCl_3$) δ 7.58 (s, 4H), 1.99 (s, 1H), 1.59 (s, 6H). **^{13}C NMR** (126 MHz, $CDCl_3$) δ 132.7 (2C), 130.8 (q, *J* (^{13}C-^{19}F) = 32.7 Hz), 125.4 (q, *J* (^{13}C-^{19}F) = 1.3 Hz), 125.3 (q, *J* (^{13}C-^{19}F) = 3.7 Hz, 2C), 123.7 (q, *J* (^{13}C-^{19}F) = 272.1 Hz), 88.0, 77.1, 75.4, 66.6, 65.8, 31.0 (2C). **^{19}F NMR** (376 MHz, $CDCl_3$) δ –63.12. **HRMS** (APCI) *m/z* calculated for $C_{14}H_{11}F_3O^{+\square}$ $M^{+\square\cdot}$: 252.0757, found: 252.0747.

6-(2-Fluorophenyl)-2-methylhexa-3,5-diyn-2-ol

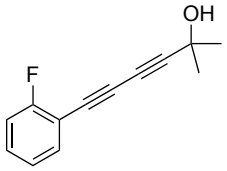

The title compound (orange solid, 1.213 g, 60% yield) was synthesized according to the general procedure starting from 1-ethynyl-2-fluorobenzene (1.13 mL, 10 mmol) and 2-methylbut-3-yn-2-ol (0.97 mL, 10 mmol).

M.p. (CH_2Cl_2) 40-43 ºC. **^{1}H NMR** (400 MHz, $CDCl_3$) δ 7.50 – 7.43 (m, 1H), 7.38 – 7.30 (m, 1H), 7.14 – 7.04 (m, 2H), 1.98 (s, 1H), 1.58 (s, 6H). **^{13}C NMR** (101 MHz, $CDCl_3$) δ 163.8 (d, *J* (^{13}C-^{19}F) = 253.1 Hz), 134.3, 131.0 (d, *J* (^{13}C-^{19}F) = 8.0 Hz), 124.0 (d, *J* (^{13}C-^{19}F) = 3.8 Hz), 115.6 (d, *J* (^{13}C-^{19}F) = 20.5 Hz), 110.4 (d, *J* (^{13}C-^{19}F) = 15.5 Hz), 87.7, 77.9 (d, *J* (^{13}C-^{19}F) = 3.1 Hz), 72.0, 66.8, 65.7, 31.0 (2C). **^{19}F NMR** (376 MHz, $CDCl_3$) δ –108.88. **HRMS** (APCI) *m/z* calculated for $C_{13}H_{10}F^+$ $[M\text{-}OH]^+$: 185.0761, found: 185.0763.

90. Jiang H.-F.; Wang, A.-Z. *Synthesis* **2007**, 1649–1654.

2-Methyl-6-(naphthalen-1-yl)hexa-3,5-diyn-2-ol

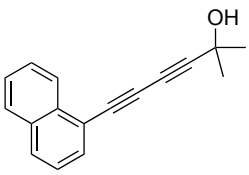

The title compound (orange solid, 0.460 g, 76% yield) was synthesized according to the general procedure starting from 1-ethynylnaphthalene (0.37 mL, 2.6 mmol) and 2-methylbut-3-yn-2-ol (0.25 mL, 2.6 mmol).

M.p. (CH_2Cl_2) 56-59 ºC. **^{1}H NMR** (400 MHz, $CDCl_3$) δ 8.36 – 8.24 (m, 1H), 7.88 – 7.83 (m, 2H), 7.74 (dd, *J* = 7.2, 1.2 Hz, 1H), 7.62 – 7.50 (m, 2H), 7.42 (dd, *J* = 8.3, 7.2 Hz, 1H), 2.03 (bs, 1H), 1.63 (s, 6H). **^{13}C NMR** (101 MHz, $CDCl_3$) δ 133.9, 133.1, 132.1, 129.7, 128.4, 127.2, 126.7, 126.0, 125.1, 119.2, 87.7, 77.7, 77.1, 67.3, 65.9, 31.2 (2C). **HRMS** (APCI) *m/z* calculated for $C_{17}H_{13}^+$ $[M\text{-}OH]^+$: 217.1012, found: 217.1014.

General procedure for the preparation of 1,3-diynes

A mixture of 6-substituted 2-methylhexa-3,5-diyn-2-ol (1 equiv) and finely powdered NaOH (3 equiv) under nitrogen was suspended in dry toluene (0.09 M). The resulting mixture was refluxed for 15 min at 115 °C. Upon completion of the reaction, the solvent was removed under reduced pressure at 23 ºC and the residue was purified by silica gel flash column chromatography (eluent = pentane). The obtained neat 1,3-diynes are unstable, therefore they were immediately subjected to the gold(I)-catalyzed reaction or stored as solutions in CH_2Cl_2 at –20 ºC.

Buta-1,3-diyn-1-ylbenzene,[87] 1-(buta-1,3-diyn-1-yl)-4-methoxybenzene,[88] 1-(buta-1,3-diyn-1-yl)-3-methoxybenzene,[88] 1-(buta-1,3-diyn-1-yl)-2-methylbenzene,[91] 1-(buta-1,3-diyn-1-yl)naphthalene,[92] 3-(buta-1,3-diyn-1-yl)thiophene[91] and deca-1,3-diyne[93] were reported in the literature. The NMR data obtained for those products were in agreement with the ones previously described in the literature.

1-(Buta-1,3-diyn-1-yl)-4-(trifluoromethyl)benzene

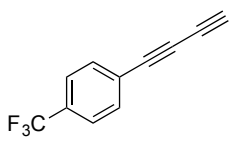

The title compound (brown solid, 0.195 g, 42% yield) was synthesized according to the general procedure starting from 2-methyl-6-(4-(trifluoromethyl)phenyl)hexa-3,5-diyn-2-ol (0.600 g, 2.38 mmol).

91. Aitken, R. A.; Seth, S. *J. Chem. Soc. Perkin Trans. 1* **1994**, *17*, 2461–2466.
92. Okamoto, Y.; Chellappa, K. L.; Kundu, S. K. *J. Org. Chem.* **1972**, 37, 3185–3187.
93. Nakamura, M.; Endo, K.; Nakamura, E. *Adv. Synth. Catal.* **2005**, *347*, 1681–1686.

M.p. (CH_2Cl_2) >250 ºC (dec.). **^{1}H NMR** (300 MHz, $CDCl_3$) δ 7.71 – 7.50 (m, 4H), 2.54 (s, 1H). **^{13}C NMR** (101 MHz, $CDCl_3$) δ 133.0 (2C), 131.2 (q, *J* (^{13}C-^{19}F) = 32.9 Hz), 125.4 (q, *J* (^{13}C-^{19}F) = 3.8 Hz, 2C), 124.9 (q, *J* (^{13}C-^{19}F) = 1.5 Hz), 123.6 (q, *J* (^{13}C-^{19}F) = 272.3 Hz), 75.7, 73.6, 72.5, 67.6. **^{19}F NMR** (376 MHz, $CDCl_3$) δ –63.17. **HRMS** (APCI) *m/z* calculated for $C_{11}H_6F_3^+$ $[M+H]^+$: 195.0416, found: 195.0407.

1-(Buta-1,3-diyn-1-yl)-3-chlorobenzene

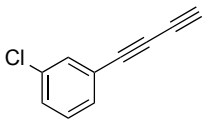

The title compound (brown solid, 0.141 g, 70% yield) was synthesized according to the general procedure starting from 6-(3-chlorophenyl)-2-methylhexa-3,5-diyn-2-ol (0.276 g, 1.26 mmol).

M.p. (CH_2Cl_2) >250 ºC (dec.). **^{1}H NMR** (300 MHz, $CDCl_3$) δ 7.49 (t, *J* = 1.7 Hz, 1H), 7.42 – 7.33 (m, 2H), 7.30 – 7.22 (m, 1H), 2.50 (s, 1H). **^{13}C NMR** (101 MHz, $CDCl_3$) δ 134.3, 132.5, 130.9, 129.9, 129.7, 122.8, 74.6, 73.7, 72.0, 67.7. **HRMS** (APCI) *m/z* calculated for $C_{10}H_6Cl^+$ $[M+H]^+$: 161.0153, found: 161.0159.

1-(Buta-1,3-diyn-1-yl)-2-fluorobenzene

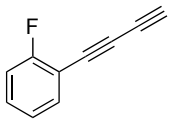

The title compound (brown solid, 0.262 g, 61% yield) was synthesized according to the general procedure starting from 6-(2-fluorophenyl)-2-methylhexa-3,5-diyn-2-ol (0.600 g, 2.97 mmol).

M.p. (CH_2Cl_2) >250 ºC (dec.). **^{1}H NMR** (400 MHz, $CDCl_3$) δ 7.53 – 7.47 (m, 1H), 7.40 – 7.32 (m, 1H), 7.15 – 7.05 (m, 2H), 2.54 (s, 1H). **^{13}C NMR** (126 MHz, $CDCl_3$) δ 164.1 (d, *J* (^{13}C-^{19}F) = 254.1 Hz), 134.5, 131.3 (d, *J* (^{13}C-^{19}F) = 8.0 Hz), 124.1 (d, *J* (^{13}C-^{19}F) = 3.8 Hz), 115.7 (d, *J* (^{13}C-^{19}F) = 20.6 Hz), 109.9 (d, *J* (^{13}C-^{19}F) = 15.7 Hz), 78.2, 72.4, 68.7, 67.8. **^{19}F NMR** (376 MHz, $CDCl_3$) δ –108.59. **HRMS** (APCI) *m/z* calculated for $C_{10}H_6F^+$ $[M+H]^+$: 145.0448, found: 145.0453.

Synthesis of 1,2-Dimethylcyclooct-1-ene

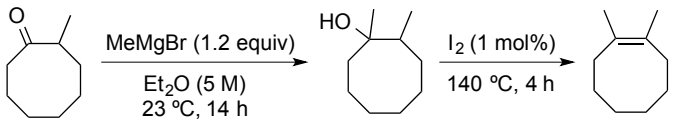

The synthesis of 1,2-dimethylcyclooct-1-ene was then accomplished following the reported procedure for similar 1,2-dimethylcycloalkenes.[79] 2-Methylcyclooctan-1-one[94] (3.5 g, 25 mmol) was diluted in dry diethyl ether (5 mL, 5 M) at 0 °C under argon and a 3 M solution of methylmagnesium bromide in diethyl ether (10 mL, 30 mmol) was added dropwise over 45 min. The resulting mixture was allowed to warm to 23 °C and stirred for 14 h. The reaction was quenched by addition of water (60 mL) at 0 ºC followed by a saturated aqueous solution of NH_4Cl until pH 8. The layers were separated and the organic layer was washed with brine, dried over Na_2SO_4 and filtered. The solvents were removed under reduced pressure (20 ºC, 400 mbar) and the crude product was purified by silica gel column chromatography (eluent = pentane:diethyl ether from 24:1 to 3:1). 1,2-Dimethylcyclooctan-1-ol was obtained as a colorless oil (3.019 g, 77%). The NMR data were in agreement with the ones reported in the literature.[95]

1,2-Dimethylcyclooctan-1-ol (1.140 g, 7.30 mmol) and iodine (0.023 g, 0.09 mmol) were mixed at 23 °C and the solution was heated to 140 °C and directly distilled under argon for 4 h. The collected fraction (containing water) was allowed to cool to room temperature, dried over Na_2SO_4, filtered washing with pentane and diethyl ether and concentrated under reduced pressure (20 ºC, 400 mbar). The crude material was purified by silica gel column chromatography (eluent = pentane) to afford (*Z*)-1,2-dimethylcyclooct-1-ene as a colorless oil (0.672 g, 67%). The NMR data were in agreement with the ones reported in the literature.[96]

General Procedure for the Reaction of 1,3-Butadiynes with Alkenes

The 1,3-diyne (1 equiv) was dissolved in CH_2Cl_2 (0.5 M). The alkene (2 equiv, unless otherwise stated) was added, followed by [(IPr)AuNCMe]SbF_6 catalyst (5 mol%). The resulting mixture was stirred at 23 ºC (unless otherwise stated) until no 1,3-diyne was detected by TLC or GC-MS. Triethylamine (0.02 mL) was added to quench the reaction. The volatiles were removed under reduced pressure and the crude was purified by silica gel flash column chromatography (eluent = pentane or cyclohexane, unless otherwise stated).

94. van Buijtenen, J.; van As, B. A. C.; Verbruggen, M.; Roumen, L.; Vekemans, J. A. J. M.; Pieterse, K.; Hilbers, P. A. J.; Hulshof, L. A.; Palmans, A. R. A.; Meijer, E. W. *J. Am. Chem. Soc.* **2007**, *129*, 7393–7398.
95. Molander, G. A.; McKie, J. A. *J. Org. Chem.* **1994**, *59*, 3186–3192.
96. Maercker, A.; Graule, T.; Girreser, U. *Angew Chem.* **1986**, *98*, 174–176.

((3,3,4,4-Tetramethylcyclobut-1-en-1-yl)ethynyl)benzene

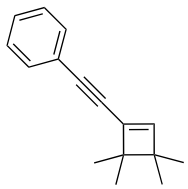

The title compound (colorless oil, 30 mg, 72%) was synthesized following the general procedure starting from buta-1,3-diyn-1-ylbenzene (25 mg, 0.2 mmol) and 2,3-dimethylbut-2-ene (48 μL, 0.4 mmol) with [(IPr)AuNCMe]SbF_6 (9 mg, 0.01 mmol). The reaction time was 17 h.

^{1}H NMR (400 MHz, $CDCl_3$) δ 7.49 – 7.42 (m, 2H), 7.35 – 7.27 (m, 3H), 6.25 (s, 1H), 1.17 (s, 6H), 1.12 (s, 6H). **^{13}C NMR** (101 MHz, $CDCl_3$) δ 145.9, 134.6, 131.6 (2C), 128.2 (2C), 128.1, 123.3, 92.5, 82.4, 50.5 46.8, 23.0 (2C), 22.3 (2C). **HRMS** (APCI) *m/z* calculated for $C_{16}H_{19}^+$ $[M+H]^+$: 211.1481, found: 211.1474.

1-((3,3,4,4-Tetramethylcyclobut-1-en-1-yl)ethynyl)-4-(trifluoromethyl)benzene

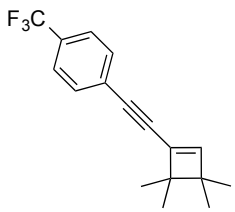

The title compound (pale yellow oil, 35 mg, 63%) was synthesized following the general procedure starting from 1-(buta-1,3-diyn-1-yl)-4-(trifluoromethyl)benzene (39 mg, 0.2 mmol) and 2,3-dimethylbut-2-ene (48 μL, 0.4 mmol) with [(IPr)AuNCMe]SbF_6 (9 mg, 0.01 mmol). The reaction time was 14 h.

^{1}H NMR (300 MHz, $CDCl_3$) δ 7.60 – 7.50 (m, 4H), 6.31 (s, 1H), 1.17 (s, 6H), 1.12 (s, 6H). **^{13}C NMR** (101 MHz, $CDCl_3$) δ 147.5, 134.1, 131.8 (2C), 129.8 (q, *J* (^{13}C-^{19}F) = 32.6 Hz), 127.1 (q, *J* (^{13}C-^{19}F) = 1.3 Hz), 125.2 (q, *J* (^{13}C-^{19}F) = 3.8 Hz, 2C), 123.9 (q, *J* (^{13}C-^{19}F) = 271.9 Hz), 91.1, 84.8, 50.7, 47.1, 22.9 (2C), 22.3 (2C). **^{19}F NMR** (376 MHz, $CDCl_3$) δ – 62.91. **HRMS (**APCI) *m/z* calculated for $C_{17}H_{18}F_3^+$ $[M+H]^+$: 279.1355, found: 279.1349.

1-Methoxy-4-((3,3,4,4-tetramethylcyclobut-1-en-1-yl)ethynyl)benzene

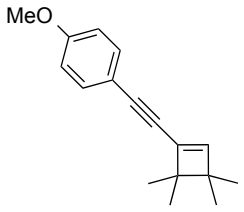

The title compound (yellow oil, 46 mg, 96%) was synthesized following the general procedure starting from 1-(buta-1,3-diyn-1-yl)-4-methoxybenzene (31 mg, 0.2 mmol) and 2,3-dimethylbut-2-ene (48 μL, 0.4 mmol) with [(IPr)AuNCMe]SbF_6 (9 mg, 0.01 mmol). The reaction time was 13 h.

^{1}H NMR (500 MHz, $CDCl_3$) δ 7.41 – 7.36 (m, 2H), 6.87 – 6.81 (m, 2H), 6.20 (s, 1H), 3.81 (s, 3H), 1.16 (s, 6H), 1.11 (s, 6H). **^{13}C NMR** (126 MHz, $CDCl_3$) δ 159.5, 145.1, 134.8, 133.1 (2C), 115.4, 113.9 (2C), 92.6, 81.1, 55.2, 50.4, 46.7, 23.0 (2C), 22.3 (2C). **HRMS (**APCI) *m/z* calculated for $C_{17}H_{21}O^+$ $[M+H]^+$: 241.1587, found: 241.1581.

1-Chloro-3-((3,3,4,4-tetramethylcyclobut-1-en-1-yl)ethynyl)benzene

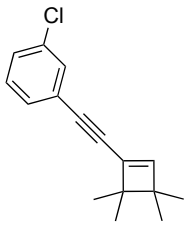

The title compound (yellow oil, 38 mg, 78%) was synthesized following the general procedure starting from 1-(buta-1,3-diyn-1-yl)-3-chlorobenzene (32 mg, 0.2 mmol) and 2,3-dimethylbut-2-ene (48 µL, 0.4 mmol) with [(IPr)AuNCMe]SbF_6 (9 mg, 0.01 mmol). The reaction time was 12 h.

^{1}H NMR (400 MHz, $CDCl_3$) δ 7.48 – 7.44 (m, 1H), 7.35 (dt, *J* = 7.2, 1.5 Hz, 1H), 7.32 – 7.22 (m, 2H), 6.30 (s, 1H), 1.18 (s, 6H), 1.14 (s, 6H). **^{13}C NMR** (101 MHz, $CDCl_3$) δ 146.9, 134.2, 134.1, 131.4, 129.7, 129.4, 128.4, 125.0, 91.0, 83.6, 50.6, 47.0, 22.9 (2C), 22.3 (2C). **HRMS (**APCI) *m/z* calculated for $C_{16}H_{18}Cl^+$ $[M+H]^+$: 245.1092, found: 245.1084.

1-Methoxy-3-((3,3,4,4-tetramethylcyclobut-1-en-1-yl)ethynyl)benzene

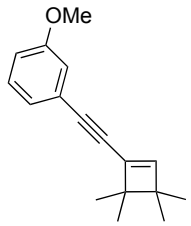

The title compound (pale yellow oil, 40 mg, 83%) was synthesized following the general procedure starting from 1-(buta-1,3-diyn-1-yl)-3-methoxybenzene (31 mg, 0.2 mmol) and 2,3-dimethylbut-2-ene (48 µL, 0.4 mmol) with [(IPr)AuNCMe]SbF_6 (9 mg, 0.01 mmol). The reaction time was 12 h.

^{1}H NMR (400 MHz, $CDCl_3$) δ 7.29 – 7.21 (m, 1H), 7.10 – 7.05 (m, 1H), 7.02 – 6.98 (m, 1H), 6.89 (ddd, *J* = 8.3, 2.7, 1.0 Hz, 1H), 6.28 (s, 1H), 3.83 (s, 3H), 1.19 (s, 6H), 1.14 (s, 6H). **^{13}C NMR** (101 MHz, $CDCl_3$) δ 159.3, 146.1, 134.6, 129.3, 124.2 (2C), 116.3, 114.9, 92.5, 82.2, 55.2, 50.5, 46.9, 23.0 (2C), 22.3 (2C). **HRMS (**APCI) *m/z* calculated for $C_{17}H_{21}O^+$ $[M+H]^+$: 241.1587, found: 241.1583.

1-Fluoro-2-((3,3,4,4-tetramethylcyclobut-1-en-1-yl)ethynyl)benzene

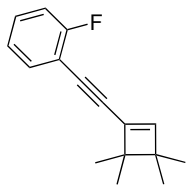

The title compound (pale yellow oil, 37 mg, 81%) was synthesized following the general procedure starting from 1-(buta-1,3-diyn-1-yl)-2-fluorobenzene (29 mg, 0.2 mmol) and 2,3-dimethylbut-2-ene (48 µL, 0.4 mmol) with [(IPr)AuNCMe]SbF_6 (9 mg, 0.01 mmol). The reaction time was 18 h.

^{1}H NMR (400 MHz, $CDCl_3$) δ 7.49 – 7.42 (m, 1H), 7.34 – 7.26 (m, 1H), 7.15 – 7.05 (m, 2H), 6.31 (s, 1H), 1.20 (s, 6H), 1.15 (s, 6H). **^{13}C NMR** (101 MHz, $CDCl_3$) δ 162.5 (d, *J* (^{13}C-^{19}F) = 251.7 Hz), 146.6, 134.3, 133.4 (d, *J* (^{13}C-^{19}F) = 1.1 Hz), 129.8 (d, *J* (^{13}C-^{19}F) =

7.9 Hz), 123.8 (d, J (^{13}C-^{19}F) = 3.7 Hz), 115.4 (d, J (^{13}C-^{19}F) = 20.9 Hz), 112.0 (d, J (^{13}C-^{19}F) = 15.8 Hz), 87.5 (d, J (^{13}C-^{19}F) = 3.3 Hz), 85.7, 50.6, 47.0, 22.9 (2C), 22.2 (2C). **^{19}F NMR** (376 MHz, $CDCl_3$) δ –109.85. **HRMS (**APCI) *m/z* calculated for $C_{16}H_{18}F^+$ $[M+H]^+$: 229.1387, found: 229.1381.

1-Methyl-2-((3,3,4,4-tetramethylcyclobut-1-en-1-yl)ethynyl)benzene

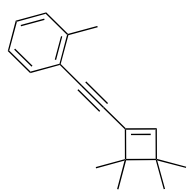

The title compound (pale yellow oil, 36 mg, 80%) was synthesized following the general procedure starting from 1-(buta-1,3-diyn-1-yl)-2-methylbenzene (28 mg, 0.2 mmol) and 2,3-dimethylbut-2-ene (48 µL, 0.4 mmol) with $[(IPr)AuNCMe]SbF_6$ (9 mg, 0.01 mmol). The reaction time was 15 h.

^{1}H NMR (500 MHz, $CDCl_3$) δ 7.42 (d, J = 7.4 Hz, 1H), 7.24 – 7.18 (m, 2H), 7.17 – 7.10 (m, 1H), 6.23 (s, 1H), 2.45 (s, 3H), 1.18 (s, 6H), 1.14 (s, 6H). **^{13}C NMR** (75 MHz, $CDCl_3$) δ 145.2, 140.0, 134.8, 131.8, 129.3, 128.2, 125.5, 123.1, 91.5, 86.4, 50.5, 46.8, 23.0 (2C), 22.3 (2C), 20.7. **HRMS (**APCI) *m/z* calculated for $C_{17}H_{21}^+$ $[M+H]^+$: 225.1638, found: 225.1629.

1-((3,3,4,4-Tetramethylcyclobut-1-en-1-yl)ethynyl)naphthalene

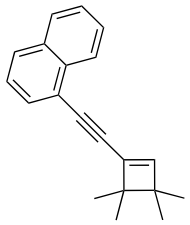

The title compound (colorless oil, 51 mg, 98%) was synthesized following the general procedure starting from 1-(buta-1,3-diyn-1-yl)naphthalene (35 mg, 0.2 mmol) and 2,3-dimethylbut-2-ene (48 µL, 0.4 mmol) with $[(IPr)AuNCMe]SbF_6$ (9 mg, 0.01 mmol). The reaction time was 18 h.

^{1}H NMR (300 MHz, $CDCl_3$) δ 8.35 (d, J = 8.7 Hz, 1H), 7.90 – 7.78 (m, 2H), 7.70 (dt, J = 7.1, 1.1 Hz, 1H), 7.60 (ddt, J = 8.3, 6.9, 1.5 Hz, 1H), 7.53 (ddt, J = 8.2, 6.9, 1.4 Hz, 1H), 7.48 – 7.39 (m, 1H), 6.35 (s, 1H), 1.27 (s, 6H), 1.18 (s, 6H). **^{13}C NMR** (101 MHz, $CDCl_3$) δ 145.9, 134.7, 133.2, 133.1, 130.4, 128.7, 128.2, 126.7, 126.3, 126.2, 125.2, 121.0, 90.6, 87.4, 50.7, 47.0, 23.0 (2C), 22.5 (2C). **HRMS (**APCI) *m/z* calculated for $C_{20}H_{21}^+$ $[M+H]^+$: 261.1638, found: 261.1649.

3-((3,3,4,4-Tetramethylcyclobut-1-en-1-yl)ethynyl)thiophene

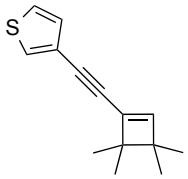

The title compound (brown oil, 43 mg, 99%) was synthesized following the general procedure starting from 3-(buta-1,3-diyn-1-yl)thiophene (26 mg, 0.2 mmol) and 2,3-dimethylbut-2-ene (48 µL, 0.4 mmol) with [(IPr)AuNCMe]SbF_6 (9 mg, 0.01 mmol). The reaction time was 18 h.

^{1}H NMR (400 MHz, $CDCl_3$) δ 7.47 (dd, *J* = 3.0, 1.2 Hz, 1H), 7.29 (dd, *J* = 5.0, 3.0 Hz, 1H), 7.15 (dd, *J* = 5.0, 1.2 Hz, 1H), 6.26 (s, 1H), 1.18 (s, 6H), 1.14 (s, 6H). **^{13}C NMR** (101 MHz, $CDCl_3$) δ 145.9, 134.5, 129.9, 128.6, 125.2, 122.3, 87.5, 82.0, 50.5, 46.8, 23.0 (2C), 22.3 (2C). **HRMS (**APCI) *m/z* calculated for $C_{14}H_{17}S^+$ $[M+H]^+$: 217.1045, found: 217.1042.

3,3,4,4-Tetramethyl-1-(oct-1-yn-1-yl)cyclobut-1-ene

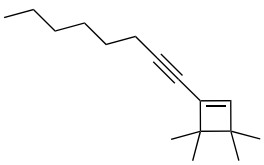

The title compound (colorless oil, 40 mg, 92%) was synthesized following the general procedure starting from deca-1,3-diyne (27 mg, 0.2 mmol) and 2,3-dimethylbut-2-ene (48 µL, 0.4 mmol) with [(IPr)AuNCMe]SbF_6 (9 mg, 0.01 mmol). The reaction time was 18 h.

^{1}H NMR (300 MHz, $CDCl_3$) δ 6.03 (s, 1H), 2.33 (t, *J* = 7.0 Hz, 2H), 1.60 – 1.46 (m, 2H), 1.46 – 1.22 (m, 6H), 1.07 (s, 6H), 1.05 (s, 6H), 0.88 (t, *J* = 7.0 Hz, 3H). **^{13}C NMR** (75 MHz, $CDCl_3$) δ 143.7, 135.3, 94.0, 73.7, 50.0, 46.2, 31.3, 28.7, 28.5, 23.0 (2C), 22.6, 22.2 (2C), 19.5, 14.0. **HRMS (**APCI) *m/z* calculated for $C_{16}H_{27}^+$ $[M+H]^+$: 219.2107, found: 219.2104.

13-(Phenylethynyl)dispiro[5.0.5.2]tetradec-13-ene

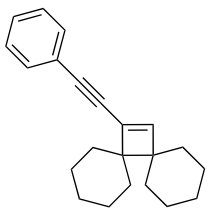

The title compound (yellow oil, 26 mg, 90%) was synthesized following the general procedure starting from buta-1,3-diyn-1-ylbenzene (13 mg, 0.1 mmol, 1 equiv) and 1,1'-bi(cyclohexylidene) (18 mg, 0.11 mmol, 1.1 equiv) with [(IPr)AuNCMe]SbF_6 (4 mg, 0.005 mmol). The reaction time was 48 h.

^{1}H NMR (300 MHz, $CDCl_3$) δ 7.47 – 7.39 (m, 2H), 7.36 – 7.28 (m, 3H), 6.64 (s, 1H), 1.97 – 1.09 (m, 20H). **^{13}C NMR** (75 MHz, $CDCl_3$) δ 145.0, 135.2, 131.3 (2C), 128.3 (2C), 128.1,

123.5, 93.0, 85.2, 55.0, 52.2, 32.1 (2C), 32.0 (2C), 26.5, 26.4, 24.1 (2C), 24.0 (2C). **HRMS (**APCI) *m/z* calculated for $C_{22}H_{27}^+$ $[M+H]^+$: 291.2107, found: 291.2110.

(1*R,8*R**)-1,8-Dimethyl-9-(phenylethynyl)bicyclo[6.2.0]dec-9-ene**

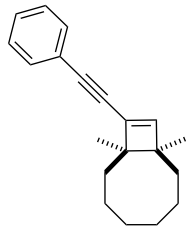

The title compound (colorless oil, 51 mg, 96%) was synthesized following the general procedure starting from buta-1,3-diyn-1-ylbenzene (25 mg, 0.2 mmol) and (*Z*)-1,2-dimethylcyclooct-1-ene (55 mg, 0.4 mmol) with [(IPr)AuNCMe]SbF_6 (9 mg, 0.01 mmol). The reaction time was 48 h.

^{1}H NMR (400 MHz, $CDCl_3$) δ 7.49 – 7.41 (m, 2H), 7.35 – 7.28 (m, 3H), 6.18 (s, 1H), 1.87 – 1.66 (m, 3H), 1.54 – 1.38 (m, 9H), 1.17 (s, 3H), 1.12 (s, 3H). **^{13}C NMR** (101 MHz, $CDCl_3$) δ 146.3, 134.9, 131.6 (2C), 128.2 (2C), 128.1, 123.3, 93.0, 82.4, 52.4, 49.2, 33.7, 32.9, 26.3, 26.1, 25.6, 25.5, 19.2, 18.6. **HRMS (**APCI) *m/z* calculated for $C_{20}H_{25}^+$ $[M+H]^+$: 265.1951, found: 265.1963.

Mixture of 1-Methoxy-4-((3,3,4-trimethylcyclobut-1-en-1-yl)ethynyl)benzene (23m, *major*) and 1-methoxy-4-((3,4,4-trimethylcyclobut-1-en-1-yl)ethynyl)benzene (23m´, *minor*)

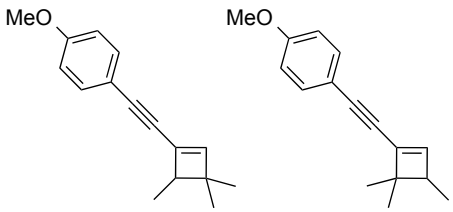

The mixture of cyclobutenes **23m** and **23m´** in a 1.2:1 ratio (orange oil, 20 mg, 59%) was synthesized following the general procedure starting from 1-(buta-1,3-diyn-1-yl)-4-methoxybenzene (23 mg, 0.15 mmol) and 2-methylbut-2-ene (32 µl, 0.3 mmol) with [(IPr)AuNCMe]SbF_6 (6 mg, 0.007 mmol). The reaction time was 18 h. The mixture of products was purified by preparative silica gel TLC (eluent = pentane:CH_2Cl_2 4:1).

^{1}H NMR (300 MHz, $CDCl_3$) δ 7.44 – 7.33 (m, 2H *major* and 2H *minor*), 6.88 – 6.78 (m, 2H *major* and 2H *minor*), 6.27 (s, 1H *major*), 6.19 (d, *J* = 1.3 Hz, 1H *minor*), 3.81 (s, 3H *major* and 3H *minor*), 2.62 (q, *J* = 7.2 Hz, 1H *major*), 2.50 (qd, *J* = 7.2, 1.4 Hz, 1H *minor*), 1.23 (s, 3H, *minor*), 1.19 (s, 3H, *major*), 1.13 (d, *J* = 7.1 Hz, 3H, *major*), 1.11 (s, 3H, *minor*), 1.07 (s, 3H, *major*), 1.05 (d, *J* = 7.2 Hz, 3H, *minor*). **^{13}C NMR** (75 MHz, $CDCl_3$) δ 159.5 (1C *major* and 1C *minor*), 147.3 (1C *major*), 140.4 (1C *minor*), 136.8 (1C *minor*), 133.1 (2C *minor*), 133.1 (2C *major*), 130.0 (1C *major*), 115.3 (1C *major*), 115.3 (1C *minor*),

113.9 (2C *major*), 113.9 (2C *minor*), 91.6 (1C *major* and 1C *minor*), 82.6 (1C *major* and 1C *minor*), 55.3 (1C *major* and 1C *minor*), 50.6 (1C *major*), 48.8 (1C *minor*), 46.7 (1C *minor*), 44.3 (1C *major)*, 26.6 (1C *major*), 25.8 (1C *minor*), 21.3 (1C *major*), 20.6 (1C *minor*), 14.1 (1C *minor*), 13.4 (1C *major*). **HRMS (**APCI) *m/z* calculated for $C_{16}H_{19}O^+$ $[M+H]^+$: 227.1430, found: 227.1427.

Mixture of 2-((4-Methoxyphenyl)ethynyl)spiro[3.5]non-1-ene (23n, *major*) and 1-((4-methoxyphenyl)ethynyl)spiro[3.5]non-1-ene (23n´, *minor*)

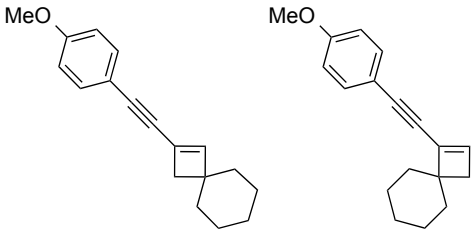

The mixture of cyclobutenes **23n** and **23n´** in a 6:1 ratio (yelow oil, 15 mg, 40%) was synthesized following the general procedure starting from 1-(buta-1,3-diyn-1-yl)-4-methoxybenzene (23 mg, 0.15 mmol) and methylenecyclohexane (36 µl, 0.3 mmol) with [(IPr)AuNCMe]SbF_6 (6 mg, 0.007 mmol). The reaction was stirred at 40 ºC for 24 h. The mixture of products was purified by preparative silica gel TLC (eluent = pentane:CH_2Cl_2 5:1).

^{1}H NMR (500 MHz, $CDCl_3$) δ 7.43 – 7.33 (m, 2H *major* and 2H *minor*), 6.87 – 6.78 (m, 2H *major* and 2H *minor*), 6.48 (s, 1H *major*), 6.26 (t, *J* = 1.4 Hz, 1H *minor*), 3.81 (s, 3H *major* and 3H *minor*), 2.39 (s, 2H *major*), 2.19 (d, *J* = 1.3 Hz, 2H *minor*), 1.81 – 1.30 (m, 10H *major* and 10H *minor*). **^{13}C NMR** (126 MHz, $CDCl_3$, *major*) δ 159.6, 148.4, 133.0 (2C), 125.9, 115.2, 113.9 (2C), 90.7, 84.0, 55.3, 47.0, 45.2, 35.7 (2C), 25.8, 24.4 (2C). **^{13}C NMR** (126 MHz, $CDCl_3$, *minor*, observable signals) δ 136.3, 133.0 (2C), 113.9 (2C), 51.9, 35.3 (2C), 25.7, 24.0 (2C). **HRMS (**APCI) *m/z* calculated for $C_{18}H_{21}O^+$ $[M+H]^+$: 253.1587, found: 253.1583.

3-(((1*R,6*R**)-1,6-Dimethylbicyclo[4.2.0]oct-7-en-7-yl)ethynyl)thiophene**

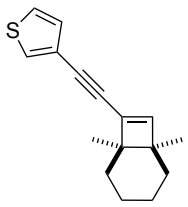

The title compound (colorless oil, 14 mg, 29%) was synthesized following the general procedure starting from 3-(buta-1,3-diyn-1-yl)thiophene (26 mg, 0.2 mmol) and (*Z*)-1,2-dimethylcyclohex-1-ene (53 µl, 0.4 mmol) with [(IPr)AuNCMe]SbF_6 (9 mg, 0.01 mmol). The reaction time was 5 d.

^{1}H NMR (500 MHz, $CDCl_3$) δ 7.44 (dd, *J* = 3.0, 1.2 Hz, 1H), 7.26 (dd, *J* = 5.0, 3.0 Hz, 1H), 7.12 (dd, *J* = 5.0, 1.2 Hz, 1H), 6.29 (s, 1H), 1.69 – 1.44 (m, 8H), 1.10 (s, 3H), 1.05 (s, 3H). **^{13}C NMR** (101 MHz, $CDCl_3$) δ 145.8, 133.9, 130.0, 128.6, 125.2, 122.4, 87.3, 82.4, 50.9, 47.2, 31.8, 31.2, 21.3, 20.4, 17.8, 17.5. **HRMS (**APCI) *m/z* calculated for $C_{16}H_{19}S^+$ $[M+H]^+$: 243.1202, found: 243.1195.

3-(((1*R,8*R**)-Bicyclo[6.2.0]dec-9-en-9-yl)ethynyl)thiophene**

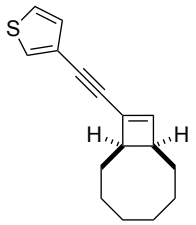

The title compound (yellow oil, 19 mg, 40%) was synthesized following the general procedure starting from 3-(buta-1,3-diyn-1-yl)thiophene (26 mg, 0.2 mmol) and (*Z*)-cyclooctene (52 μL, 0.4 mmol) with $[(IPr)AuNCMe]SbF_6$ (9 mg, 0.01 mmol). The reaction was stirred at 23 ºC for 24 h and then at 50 ºC for 24 h. The relative configuration of the product was determined by nOe experiments.

^{1}H NMR (300 MHz, $CDCl_3$) δ 7.45 (dd, *J* = 3.0, 1.2 Hz, 1H), 7.27 (dd, *J* = 5.2, 2.8 Hz, 1H), 7.13 (dd, *J* = 5.0, 1.2 Hz, 1H), 6.23 (d, *J* = 1.4 Hz, 1H), 2.90 (ddd, *J* = 12.0, 4.4, 2.0 Hz, 1H), 2.75 (ddt, *J* = 11.7, 4.3, 1.7 Hz, 1H), 2.00 – 1.89 (m, 1H), 1.79 – 1.29 (m, 11H). **^{13}C NMR** (75 MHz, $CDCl_3$) δ 143.0, 130.9, 129.9, 128.6, 125.2, 122.2, 86.6, 83.2, 50.4, 46.3, 30.3, 30.1, 26.6, 26.3, 26.1, 26.1. **HRMS (**APCI) *m/z* calculated for $C_{16}H_{19}S^+$ $[M+H]^+$: 243.1202, found: 243.1201.

The mixture of (1'*S,3'*R**)-1',3'-dimethyl-5'-(phenylethynyl)-1',2',3',4'-tetrahydro-1,1':3',1''-terphenyl (24, *major*) and (1'*S**,3'*S**)-1',3'-dimethyl-5'-(phenylethynyl)-1',2',3',4'-tetrahydro-1,1':3',1''-terphenyl (24´, *minor*)**

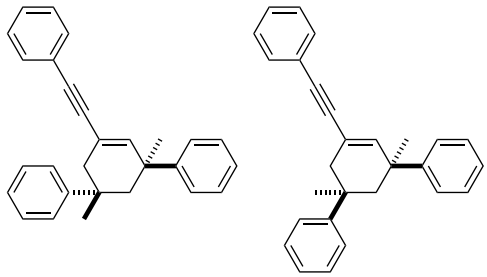

The mixture of the title compounds **24** and **24´** in a 4:1 ratio (yellow oil, 38 mg, 17%) was synthesized following the general procedure starting from buta-1,3-diyn-1-ylbenzene (76 mg, 0.6 mmol) and α-methylstyrene (156 μl, 1.2 mmol) with $[(IPr)AuNCMe]SbF_6$ (26 mg, 0.03 mmol). The reaction time was 48 h.

^{1}H NMR (500 MHz, $CDCl_3$) δ 7.61 – 6.86 (m, 15H *major* and 15H *minor*), 6.34 (s, 1H *major*), 6.30 (s, 1H *minor*), 2.95 – 2.84 (m, 1H *major* and 1H *minor*), 2.57 (d, *J* = 13.7 Hz,

1H *minor*), 2.50 – 2.40 (m, 1H *major* and 1H *minor*), 2.25 (s, 2H *major*), 2.02 (d, *J* = 13.7 Hz, 1H *minor*), 1.47 (s, 3H *minor*), 1.35 (s, 3H *minor*), 1.17 (s, 3H *major*), 0.99 (s, 3H *major*). **^{13}C NMR** (126 MHz, $CDCl_3$, *major)* δ 150.3,148.4, 141.2, 131.6, 128.3, 128.3, 128.2, 126.1, 125.8, 123.5, 118.8, 90.9, 87.8, 50.8, 41.2, 40.8, 37.9, 30.7, 29.1. **^{13}C NMR** (126 MHz, $CDCl_3$, *minor*) δ 148.2, 145.8, 141.4, 131.6, 128.0, 127.5, 126.3, 125.9, 125.2, 124.9, 123.6, 119.1, 90.9, 87.8, 50.9, 41.0, 40.4, 37.6, 32.0, 31.5. **HRMS** (APCI) *m/z* calculated for $C_{28}H_{27}^+$ $[M+H]^+$: 363.2107, found: 363.2105.

Procedure for the Preparation of 1,6-Enynes 25

Synthesis of ((1*S*,2*S*)-3-((*E*)-2-bromostyryl)cyclopropane-1,2-diyl)dibenzene

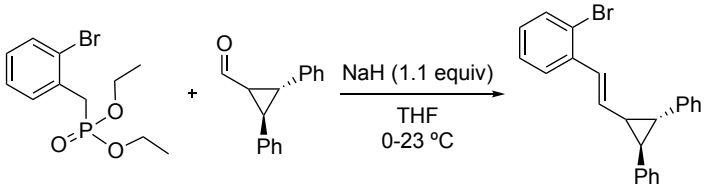

Diethyl 2-bromobenzylphosphonate (1.2 g, 3.69 mmol, 1.1 equiv) was slowly added to a suspension of NaH (60% in mineral oil, 160 mg, 3.96 mmol, 1.1 equiv) in dry THF (10 mL) at 0 ºC under argon. The resulting suspension was stirred for 1 h at 23 ºC. Then the reaction mixture was cooled to 0 ºC and a solution of *trans*-2,3-diphenylcyclopropan-1-carbaldehyde[97] (800 mg, 3.6 mmol, 1 equiv) in dry THF (2 mL) was added dropwise. The resulting mixture was slowly warmed to 23 ºC and stirred for 14 h. The reaction was quenched with ice water and the aqueous phase was extracted with Et_2O (3 × 30 mL). The combined organic layers were washed with brine (20 mL), dried over Na_2SO_4 and concentrated under reduced pressure. The residue was purified by silica gel flash column chromatography (eluent = cyclohexane) to give ((1*S*,2*S*)-3-((*E*)-2-bromostyryl)cyclopropane-1,2-diyl)dibenzene (colorless oil 1.12 g, 83% yield).

^{1}H NMR (400 MHz, $CDCl_3$) δ 7.50 (dt, *J* = 8.0, 1.5 Hz, 1H), 7.39 – 7.32 (m, 6H), 7.32 – 7.22 (m, 4H), 7.22 – 7.09 (m, 2H), 7.01 (td, *J* = 7.6, 2.0 Hz, 1H), 6.90 (dd, *J* = 15.6, 3.6 Hz, 1H), 5.66 (m, 1H), 2.90 (ddd, *J* = 8.8, 6.0, 2.2 Hz, 1H), 2.65 (dd, *J* = 6.5, 4.1 Hz, 1H), 2.43 (td, *J* = 9.3, 5.3 Hz, 1H). **^{13}C NMR** (101 MHz, $CDCl_3$) δ 141.2, 137.8, 137.2, 132.8, 132.1,

97. Komendatov, M. I.; Fomina, T. B.; Kuzina, N. A.; Domnin, I. N. *J. Org. Chem. USSR (English Translation)* **1974**, *10*, 219−221.

129.3, 128.8, 128.5, 128.3, 128.1, 127.3, 126.5, 126.5, 126.2, 126.1, 122.9, 34.0, 33.8, 31.2. **HRMS** (APCI) calculated for $C_{23}H_{20}Br^+$ $[M+H]^+$: 375.0743, found: 375.0747.

General procedure for the preparation of 1,6-enynes 25

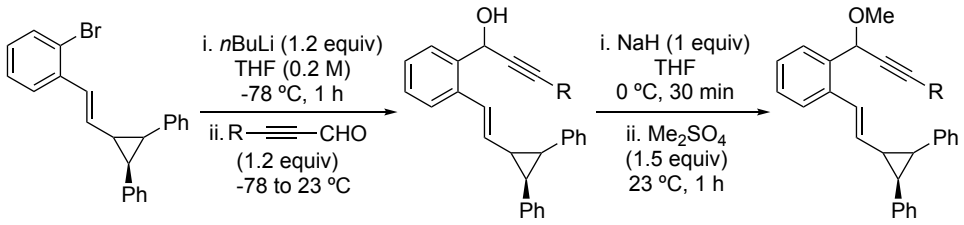

*n*BuLi (2.5 M in hexanes, 1.02 equiv) was added dropwise to a solution of aryl bromide (1 equiv) in dry THF (0.2 M) at –78 ºC under argon. The mixture was stirred for 1 h at –78 ºC and freshly purified 3-arylpropiolaldehyde (1.2 equiv) as a solution in dry THF (3.5 M) was added. After 20 min, the reaction was warmed to 23 ºC and stirred for 30 min. Then, the reaction was quenched with ice water (10 mL) and the aqueous phase was extracted with Et_2O (3 × 25 mL). The combined organic layers were washed with brine (20 mL), dried over Na_2SO_4 and concentrated under reduced pressure. The residue was filtered through a short pad of silica gel (eluent = cyclohexane:EtOAc 10:1) to give the corresponding crude 3-hydroxy-1,6-enyne, which was used in following step without further purification.

The 3-hydroxy-1,6-enyne was dissolved in dry THF (0.25 M) and added to the suspension of NaH (60% in mineral oil, 1 equiv) in dry THF (0.15 M) at 0 ºC. The resulting mixture was stirred at 0 °C for 30 min, then Me_2SO_4 (1.5 equiv) was added and stirring was continued at 23 ºC for 1 h. The reaction was quenched with brine (7 mL) and the aqueous phase was extracted with Et_2O (3 × 20 mL). The combined organic layers were washed with brine (10 mL), dried over Na_2SO_4 and concentrated under reduced pressure. The residue was purified by silica gel flash column chromatography (eluent = cyclohexane:EtOAc 80:1) to give the corresponding 3-methoxy-1,6-enyne.

((1*S*,2*S*)-3-((*E*)-2-(1-Methoxy-3-phenylprop-2-yn-1-yl)styryl)cyclopropane-1,2-diyl)dibenzene (25a)

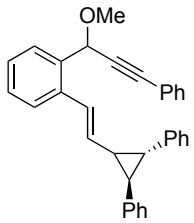

1,6-Enyne **25a** (mixture of diastereomers, colorless oil, 748 mg, 58% yield) was synthesized following the general procedure starting from ((1*S*,2*S*)-3-((*E*)-2-bromostyryl)cyclopropane-1,2-diyl)dibenzene (1.12 g, 2.93 mmol) and freshly purified 3-phenylpropiolaldehyde (455 mg, 3.52 mmol).

^{1}H NMR (500 MHz, $CDCl_3$) δ 7.64 – 7.59 (m, 2H), 7.48 – 7.41 (m, 4H), 7.36 – 7.29 (m, 16H), 7.27 – 7.17 (m, 16H), 7.01 (d, *J* = 12.5 Hz, 1H), 6.98 (d, *J* = 12.5 Hz, 1H), 5.65 (dd, *J* = 9.4, 2.6 Hz, 1H), 5.61 (dd, *J* = 9.4, 2.6 Hz, 1H), 5.41 (s, 1H), 5.37 (s, 1H), 3.45 (s, 3H), 3.43 (s, 3H), 2.87 (dd, *J* = 9.0, 6.2 Hz, 2H), 2.65 – 2.65 (m, 2H), 2.43 (qd, *J* = 9.2, 5.1 Hz, 2H). **^{13}C NMR** (126 MHz, $CDCl_3$) δ 141.4, 137.9, 137.9, 136.7, 136.6, 134.6, 134.5, 131.9, 131.8, 131.7, 131.7, 129.3, 129.2, 128.5, 128.5, 128.4, 128.4, 128.3, 128.2, 128.2, 127.9, 127.9, 127.2, 127.1, 126.9, 126.4, 126.4, 126.4, 126.3, 126.1, 126.0, 122.6, 122.6, 87.9, 87.8, 86.7, 86.7, 71.4, 71.2, 56.0, 55.9, 34.1, 34.1, 33.8, 33.7, 31.1, 31.1. **HRMS** (APCI) calculated for $C_{33}H_{29}O^+$ $[M+H]^+$: 441.2213, found: 441.2195.

((1*R*,2*S*,3*s*)-3-((*E*)-2-(1-Methoxy-3-phenylprop-2-yn-1-yl)styryl)cyclopropane-1,2-diyl)dibenzene (25b)

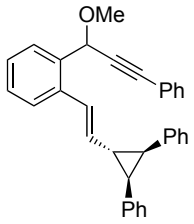

1,6-Enyne **25b** (colorless oil, 413 mg, 67% yield) was synthesized following the general procedure starting from ((1*R*,2*S*,3*s*)-3-((*E*)-2-bromostyryl)cyclopropane-1,2-diyl)dibenzene[98] (550 mg, 1.47 mmol) and freshly purified 3-phenylpropiolaldehyde (230 mg, 1.76 mmol).

^{1}H NMR (500 MHz, $CDCl_3$) δ 7.65 (dd, *J* = 7.5, 1.5 Hz, 1H), 7.53 (dd, *J* = 7.6, 1.4 Hz, 1H), 7.47 – 7.43 (m, 2H), 7.36 – 7.20 (m, 5H), 7.19 – 7.06 (m, 7H), 7.01 – 6.93 (m, 4H), 6.10 (dd, *J* = 15.6, 8.2 Hz, 1H), 5.51(s, 1H), 3.53 (s, 3H), 2.68 (d, *J* = 5.9 Hz, 2H), 2.56 (dt, *J* = 8.3, 5.6 Hz, 1H). **^{13}C NMR** (126 MHz, $CDCl_3$) δ 137.3, 136.6, 135.0, 134.7, 131.7, 128.9, 128.7, 128.4, 128.2, 128.2, 127.8, 127.0, 126.3, 125.9, 125.8,

98. Wang, Y.; McGonigal, P. R.; Herlé, B.; Besora, M.; Echavarren, A. M. *J. Am. Chem. Soc.* **2014**, *136*, 801–809.

122.6, 88.1, 86.7, 71.7, 56.1, 33.4, 30.1. **HRMS** (APCI) *m/z* calculated for $C_{33}H_{29}O^+$ $[M+H]^+$: 441.2213, found: 441.2207.

Procedure for the Gold(I)-Catalyzed Reaction of 1,6-Enynes 25

(1*S*,1a*S*,7b*R*)-1-((2*S*,3*S*)-2,3-Diphenylcyclopropyl)-3-methoxy-1a-phenyl-1a,7b-dihydro-1*H*-cyclopropa[*a*]naphthalene (26a)

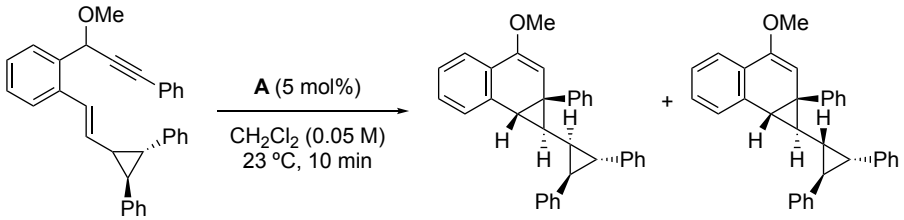

Catalyst **A** (10 mg, 0.0125 mmol, 0.05 equiv) was added to a solution of 1,6-enyne **25a** (110 mg, 0.25 mmol, 1 equiv) in dry CH_2Cl_2 (5 mL) at 23 ºC under argon atmosphere. The resulting red solution was stirred for 10 min, and then the reaction was quenched with a drop of triethylamine. The solvent was removed under reduced pressure and the residue was purified by preparative silica gel TLC (eluent = cyclohexane:EtOAc 80:1) to give **26a** (white solid, 53 mg, 48% yield). The structure was confirmed by X-ray diffraction. Crystals were obtained by slow concentration of the methanol–ether solution of the sample.

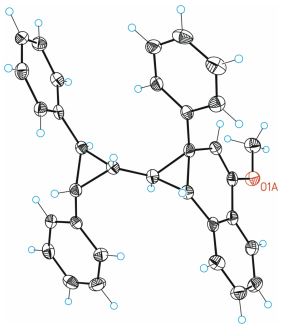

M.p. (MeOH/Et_2O) 161-163 ºC. NMR is given for the 2 rotamers. **^{1}H NMR** (500 MHz, $CDCl_3$) δ 7.62 – 7.57 (m, 1H *major*), 7.55 (dd, *J* = 7.6, 1.3 Hz, 1H *minor*), 7.40 – 7.35 (m, 2H *major* and 2H *minor*), 7.33 – 7.07 (m, 14H *major* and 14H *minor*), 7.01 (d, *J* = 7.4 Hz, 2H *minor*), 6.81 (d, *J* = 7.3 Hz, 2H *major*), 5.22 (d, *J* = 1.0 Hz, 1H *minor*), 5.17 (d, *J* = 1.0 Hz, 1H *major*), 3.61 (s, 3H *minor*), 3.58 (s, 3H *major*), 2.64 (d, *J* = 5.0 Hz, 1H *major*), 2.60 (d, *J* = 4.9 Hz, 1H *minor*), 2.47 (dd, *J* = 9.2, 5.7 Hz, 1H *major*), 2.41 (dd, *J* = 9.3, 5.6 Hz, 1H *minor*), 2.36 (t, *J* = 5.5 Hz, 1H *minor*), 2.25 (t, *J* = 5.6 Hz, 1H *major*), 1.24 (ddd, *J* = 9.2, 6.5, 5.6 Hz, 1H *major*), 0.92 (dt, *J* = 9.3, 5.4 Hz, 1H *minor*), 0.56 (dd, *J* = 6.4, 5.0 Hz, 1H *major*), 0.23 (dd, *J* = 9.3, 4.9 Hz, 1H *minor*). **^{13}C NMR** (126 MHz, $CDCl_3$) δ 148.6 (*minor* + *major*), 142.9 (*minor*), 142.7 (*major*), 142.1 (*minor*), 141.9 (*major*), 138.8 (*major*), 138.7 (*minor*), 135.8 (*minor*), 135.8 (*major*), 130.0 (*minor*), 129.7 (*major*), 129.4 (*minor*), 128.8 (*major*), 128.6 (*major*), 128.4

(*minor*), 128.2 (*major* + *minor*), 128.1 (*major*), 128.0 (*minor*), 127.9 (*major*), 127.8 (*minor*), 127.5 (*major*), 127.5 (*minor*), 126.6 (*minor*), 126.5 (*major*), 126.4 (*major*), 126.1 (*minor*), 126.0 (*minor*), 126.0 (*major*), 125.7 (*major*), 125.6 (*major*), 125.6 (*minor*), 125.5 (*minor*), 121.9 (*major*), 121.9 (*minor*), 103.3 (*major*), 103.0 (*minor*), 54.7 (*major*), 54.6 (*minor*), 36.1 (*minor*), 35.8 (*major*), 32.5 (*minor*), 31.9 (*major*), 31.7 (*minor*), 30.8 (*major*), 30.2 (*minor*), 29.8 (*major*), 29.4 (*minor*), 29.3 (*minor*). 28.8 (*major*), 28.7 (*major*). **HRMS** (APCI) calculated for $C_{33}H_{29}O^+$ $[M+H]^+$: 441.2213, found: 441.2213.

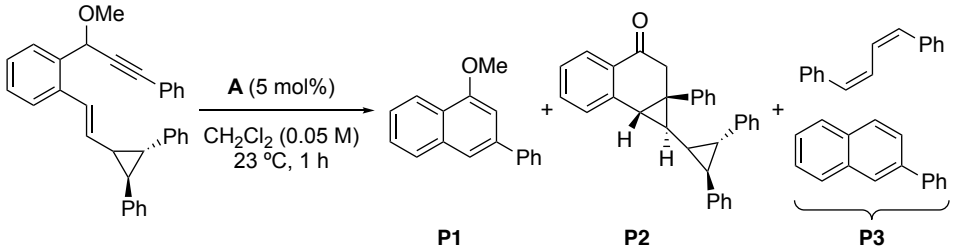

Catalyst **A** (4 mg, 0.005 mmol, 0.05 equiv) was added to a solution of 1,6-enyne **25a** (44 mg, 0.1 mmol, 1 equiv) in dry CH_2Cl_2 (2 mL) at 23 ºC under inert atmosphere. The resulting solution was stirred for 1 h at 23 ºC. The reaction was quenched with a drop of triethylamine and solvent was removed under reduced pressure. The residue was purified by preparative silica gel TLC (eluent = cyclohexane:EtOAc 80:1) to give **P1** (white solid, 5 mg, 21% yield), **P2** (mixture of 2 rotamers in a 1:35 ratio, yellow oil, 18 mg, 42% yield) and **P3** (mixture of (1*Z*,3*Z*)-1,4-diphenylbuta-1,3-diene and 2-phenylnaphthalene in a 3:4 ratio, 6 mg).

The spectroscopic data of **P1**[64a] and **P3**[99,64b] match with those reported in the literature.

Compound **P2**. NMR is given for the major rotamer. **^{1}H NMR** (500 MHz, $CDCl_3$) δ 7.80 (dd, *J* = 7.7, 1.4 Hz, 1H), 7.43 (dt, *J* = 7.5, 1.4 Hz 1H), 7.38 – 7.28 (m, 4H), 7.28 – 7.06 (m, 11H), 6.75 (d, *J* = 6.8 Hz, 2H), 3.12 (dd, *J* = 17.8 Hz, 1.3, 1H), 2.79 (d, *J* = 17.8 Hz, 1H), 2.49 (d, *J* = 4.3 Hz, 1H), 2.44 (dd, *J* = 9.2, 5.7 Hz, 1H), 2.21 (t, *J* = 5.7 Hz, 1H), 1.23 (dt, *J* = 9.2, 5.7 Hz, 1H), 0.72 (dd, *J* = 6.0, 4.5 Hz, 1H). **^{13}C NMR** (126 MHz, $CDCl_3$) δ 196.4, 145.0, 141.4, 141.0, 138.2, 133.3, 129.4, 129.1, 128.8, 128.6, 128.4, 128.3, 128.1, 127.0,

99. (a) Alacid, E.; Nájera, C. *J. Org. Chem.* **2008**, *73*, 2315-2322. (b) Alacid, E.; Nájera, C. *Adv. Synth. Catal.* **2006**, *348*, 2085-2091. (c) Wang, Z.-Y.; Chen, G.-Q.; Shao, L.-X. *J. Org. Chem.* **2012**, *77*, 6608−6614.

126.3, 126.3, 125.9, 125.8, 45.0, 39.3, 31.7, 31.0, 30.0, 28.8, 28.2. **HRMS** (APCI) calculated for $C_{32}H_{26}O^{+}$ $[M+Na]^{+}$: 449.1876, found: 449.1875.

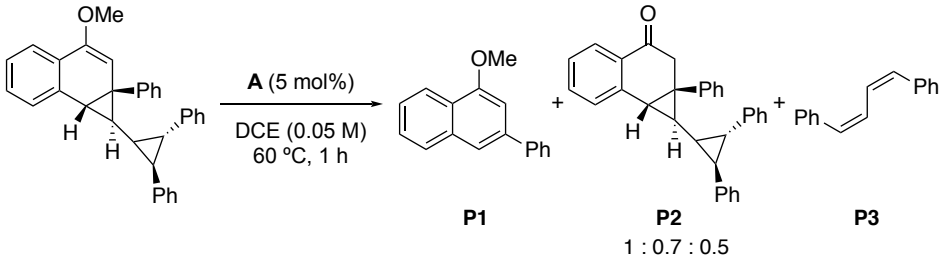

Catalyst **A** (2 mg, 0.0025 mmol, 0.05 equiv) was added to a solution of **26a** (22 mg, 0.05 mmol, 1 equiv) in dry dichloroethane (1 mL) at 23 ºC under inert atmosphere. The resulting solution was stirred for 1 h at 60 ºC. The reaction was quenched with a drop of triethylamine and solvent was removed under reduced pressure. The residue was filtered through a short pad of silica gel (eluent = cyclohexane:EtOAc 80:1) to give a **P1** (white solid, 6.7 mg, 57% yield), **P2** (yellow oil, 8.5 mg, 40% yield) and **P3** (3.3 mg, 30% yield). The spectroscopic data of **P1**[64a] and **P3**[64b] match with those reported in the literature.

(1*S*,1a*S*,7b*R*)-1-((1*s*,2*R*,3*S*)-2,3-Diphenylcyclopropyl)-3-methoxy-1a-phenyl-1a,7b-dihydro-1*H*-cyclopropa[*a*]naphthalene (26b)

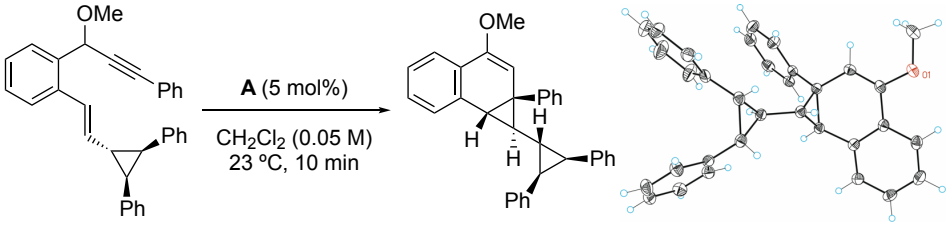

Catalyst **A** (4 mg, 0.005 mmol, 0.05 equiv) was added to a solution of 1,6-enyne **25b** (44 mg, 0.1 mmol, 1 equiv) in dry CH_2Cl_2 (2 mL) at 23 ºC under argon. The resulting red solution was stirred for 10 min, and then the reaction was quenched with a drop of triethylamine. The solvent was removed under reduced pressure and the residue was purified by preparative silica gel TLC (eluent = cyclohexane:EtOAc 80:1) to give **26b** (white solid, 27 mg, 61% yield). The structure was confirmed by X-ray diffraction. Crystals were obtained by slow concentration of the methanol–ether solution of the sample.

M.p. (MeOH/Et_2O) 159-162ºC. **^{1}H NMR** (500 MHz, $CDCl_3$) δ 7.70 (dd, *J* = 7.5, 1.6 Hz, 1H), 7.52 – 7.48 (m, 2H), 7.47 (dd, *J* = 7.3, 1.5 Hz, 1H), 7.35 – 7.23 (m, 5H), 7.04 – 6.94 (m, 6H), 6.65 – 6.60 (m, 2H), 6.59 – 6.54 (m, 2H), 5.39 (d, *J* = 0.9 Hz, 1H), 3.70 (s, 3H), 2.82 (d, *J* = 4.8 Hz, 1H), 2.46 (dd, *J* = 9.5, 5.8 Hz, 1H), 2.36 (dd, *J* = 9.5, 5.7 Hz, 1H), 1.30 (dt, *J* = 6.9, 5.8 Hz, 1H), 0.70 (dd, *J* = 6.9, 4.9 Hz, 1H). **^{13}C NMR** (126 MHz, $CDCl_3$) δ 148.6, 142.7, 137.7, 137.7, 136.1, 129.9, 128.8, 128.7, 128.7, 127.9, 127.8, 127.6, 127.5, 126.7, 125.8, 125.5, 125.4, 122.2, 103.4, 54.7, 36.3, 32.6, 31.7, 31.3, 30.6, 25.3. **HRMS** (APCI) *m/z* calculated for $C_{33}H_{29}O^+$ $[M+H]^+$: 441.2213, found: 441.2217.

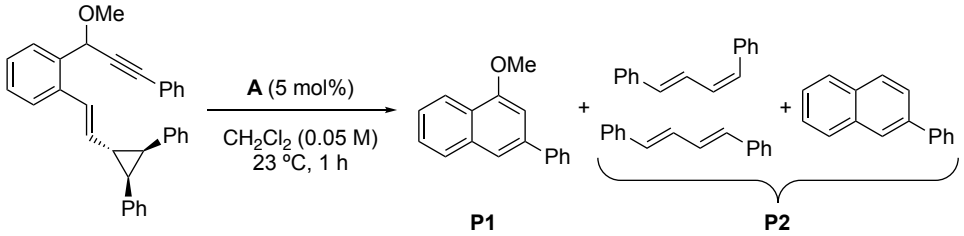

Catalyst **A** (4 mg, 0.005 mmol, 0.05 equiv) was added to a solution of 1,6-enyne **25b** (44 mg, 0.1 mmol, 1 equiv) in dry CH_2Cl_2 (2 mL) at 23 ºC under inert atmosphere. The resulting solution was stirred for 1 h at 23 ºC. The reaction was quenched with a drop of triethylamine and the solvent was removed under reduced pressure. The residue was purified by preparative silica gel TLC (eluent = cyclohexane:EtOAc 80:1) to give **P1** (white solid, 6 mg, 52% yield) and **P2** (mixture of (1*Z*,3*E*)-1,4-diphenylbuta-1,3-diene, (1*E*,3*E*)-1,4-diphenylbuta-1,3-diene and 2-phenylnaphthalene in a 2.2:1:4 ratio, 13.5 mg, 68% yield). The spectroscopic data of **P1**[64a] and **P2**[99] match with those reported in the literature.

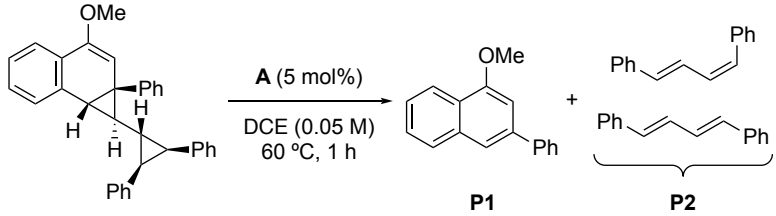

Catalyst **A** (2 mg, 0.0025 mmol, 0.05 equiv) was added to a solution of **26b** (22 mg, 0.05 mmol, 1 equiv) in dry dichloroethane (1 mL) at 23 ºC under inert atmosphere. The resulting solution was stirred for 1 h at 60 ºC. The reaction was quenched with a drop of triethylamine and solvent was removed under reduced pressure. The residue was filtered through a short

pad of silica gel (eluent = cyclohexane:EtOAc 80:1) to give a mixture of 1-methoxy-3-phenylnaphthalene, (1*Z*,3*E*)-1,4-diphenylbuta-1,3-diene and (1*E*,3*E*)-1,4-diphenylbuta-1,3-diene in a 1.4:0.6:1 ratio in 94% NMR yield (1,3,5-tribromobenzene was used as internal standard). The crude mixture was purified by preparative silica gel TLC (eluent = cyclohexane:EtOAc 80:1) to give **P1** (white solid, 9.7 mg, 84% yield) and **P2** (mixture of (1*Z*,3*E*)-1,4-diphenylbuta-1,3-diene and (1*E*,3*E*)-1,4-diphenylbuta-1,3-diene in a 1:2 ratio, 9.8 mg, 96% yield). The spectroscopic data of **P1**[64a] and **P2**[99] match with those reported in the literature.

Procedure for the Gold(I)-Catalyzed Reaction of Acetylene with Alkenes

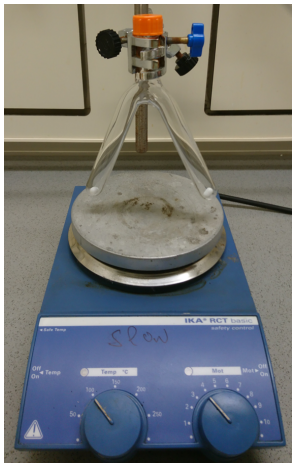

The reaction was performed in a two-chamber reactor (vessel A and B). The vessel A was loaded with calcium carbide (100 mg, 1.56 mmol, 7.8 equiv). Each vessel was loaded with a stirring bar. Then, a solution of [(*t*BuXPhos)AuNCMe]BAr_4^F (15 mg, 10 μmol) and the alkene (0.2 mmol) in chloroform (1 mL) was added to the vessel B. Chloroform (1 mL) was added to the vessel A, followed by water (0.1 mL). The reactor was immediately sealed, and the mixture was stirred at 23 ºC. The reaction mixture of the vessel B was taken with a syringe, the solvent was removed under vacuum at room temperature and the crude was analyzed by ^{1}H NMR.

Experimental Mechanistic Studies

Deuteration experiments with alkyne 18f-d_1

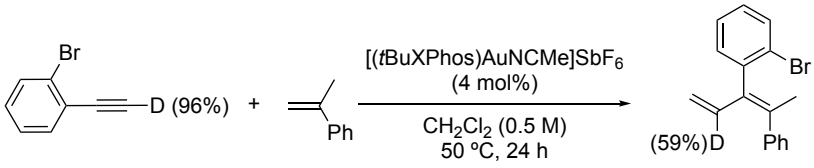

1-Bromo-2-(ethynyl-*d*)benzene (58 mg, 0.32 mmol, 1 equiv) was dissolved in dry CH_2Cl_2 (0.6 mL, 0.5 M). α-Methylstyrene (83 μL, 0.64 mmol, 2 equiv) was added, followed by [(*t*BuXPhos)AuNCMe]SbF_6 (11 mg, 0.013 mmol, 4 mol%). The resulting mixture was stirred at 50 ºC for 16 h. Triethylamine (0.02 mL) was added to quench the reaction. The

volatiles were removed under reduced pressure and the crude mixture was purified by silica gel flash column chromatography (eluent = pentane).

1-Bromo-2-(ethynyl-*d*)benzene (18f-d_1)

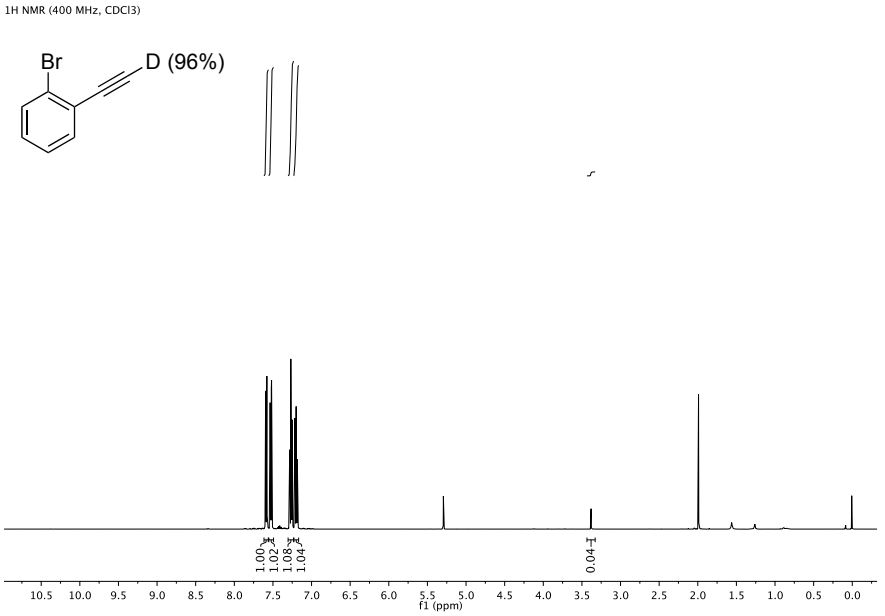

(*E*)-1-Bromo-2-(4-phenylpenta-1,3-dien-3-yl-2-*d*)benzene (21f-d_1)

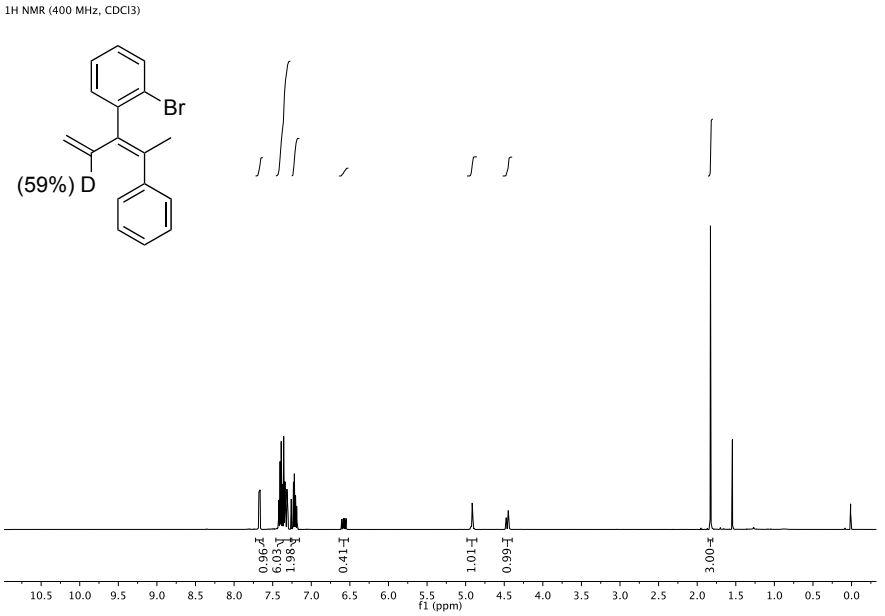

Monitoring the reaction of alkyne 18e with alkene 19b by ^{1}H NMR

1-Chloro-2-ethynylbenzene (24 μL, 0.2 mmol, 1 equiv) and methylenecyclohexane (48 μL, 0.4 mmol, 2 equiv) were dissolved in $CDCl_3$ (0.4 mL) in a Young NMR tube. Diphenylmethane (17 μL, 0.1 mmol, 0.5 equiv) was added as internal standard and the ^{1}H NMR spectrum was recorded (reaction time = 0 min). [(*t*BuXPhos)AuNCMe]BAr_4^F (15 mg, 0.01 mmol, 5 mol%) was added, followed by $CDCl_3$ (0.1 mL) rinsing the walls of the NMR tube. ^{1}H NMR spectra at 50 ºC were recorded every hour during 72 h.

Theoretical DFT Calculations

Computational methods

Calculations were performed by means of the Gaussian 09 suite of programs.[100] DFT was applied using M06.[101] The SDD basis set and ECP was utilized to describe Au[102] whereas the LANL2DZ basis set with additional polarization function (ζ_d = 0.428)[103] and ECP was used for Br. The 6-31G(d) basis set[104] was employed for all remaining atoms. Full geometry optimizations were carried out in CH_2Cl_2, through an implicit solvent SMD.[105] The stationary points were characterized by vibrational analysis. Transition states were identified by the presence of one imaginary frequency while minima by a full set of real

100. Gaussian 09, Revision B.1, Frisch, M. J.; Trucks, G. W.; Schlegel, H. B.; Scuseria, G. E.; Robb, M. A.; Cheeseman, J. R.; Scalmani, G.; Barone, V.; Mennucci, B.; Petersson, G. A.; Nakatsuji, H.; Caricato, M.; Li, X.; Hratchian, H. P.; Izmaylov, A. F.; Bloino, J.; Zheng, G.; Sonnenberg, J. L.; Hada, M.; Ehara, M.; Toyota, K.; Fukuda, R.; Hasegawa, J.; Ishida, M.; Nakajima, T.; Honda, Y.; Kitao, O.; Nakai, H.; Vreven, T.; Montgomery, J. A.; Peralta, Jr. J. E.; Ogliaro, F.; Bearpark, M.; Heyd, J. J.; Brothers, E.; Kudin, K. N.; Staroverov, V. N.; Kobayashi, R.; Normand, J.; Raghavachari, K.; Rendell, A.; Burant, J. C.; Iyengar, S. S.; Tomasi, J.; Cossi, M.; Rega, N.; Millam, J. M.; Klene, M.; Knox, J. E.; Cross, J. B.; Bakken, V.; Adamo, C.; Jaramillo, J.; Gomperts, R.; Stratmann, R. E.; Yazyev, O.; Austin, A. J.; Cammi, R.; Pomelli, C.; Ochterski, J. W.; Martin, R.L.; Morokuma, K.;, Zakrzewski, V. G.; Voth, G. A.; Salvador, P.; Dannenberg, J. J.; Dapprich, S.; Daniels, A. D.; Farkas, Ö.; Foresman, J. B.; Ortiz, J. V.; Cioslowski, J.; Fox, D. J. Gaussian, Inc., Wallingford CT **2009**.
101. Zhao, Y.; Truhlar, D. G. *Theor. Chem. Acc.* **2008**, *120*, 215–241.
102. Andrae, D.; Haussermann, U.; Dolg, M.; Stoll, H.; Preuss, H. *Theor. Chim. Acta* **1990**, *77*, 123–141.
103. Höllwarth, A.; Böhme, M.; Dapprich, S.; Ehlers, A. W.; Gobbi, A.; Jonas, V.; Köhler, K. F.; Stegmann, R.; Veldkamp, A.; Frenking, G. *Chem. Phys. Lett.* **1993**, *208*, 237–240.
104. Hehre, W. J.; Ditchfield, R.; Pople, J. A. *J. Chem. Phys.* **1972**, *56*, 2257–2261.
105. Marenich, A. V.; Cramer, C. J.; Truhlar, D. G. *J. Phys. Chem. B.* **2009**, *113*, 6378–6396.

frequencies. The connectivity of the transition states was confirmed by relaxing each transition state towards both the reactant and the product. The energy for the optimized geometry of some specific non-critical structures, that could not be located, was estimated through constrained optimizations with distances or angles frozen at reasonable values. These cases are indicated in the main schemes. Reported energies are potential energies (E) and free energies (G) in solution, computed at 298 K and 1 atm.

Computed Structures and Energies

Cartesian coordinates are provided in the supporting information of the corresponding published article.[106] A dataset collection of computational results is available in the ioChem-BD repository and can be accessed *via* DOI: 10.19061/iochembd-1-47.[76b]

Reaction of 18a with 19a

Ligand exchange

$AuPMe_3$

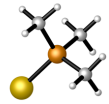

E = -596.603072 Hartrees
G = -596.523751 Hartrees

Phenylacetylene (18a)

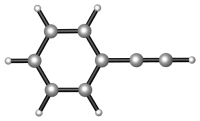

E = -308.146849 Hartrees
G = -308.067830 Hartrees

Int1a

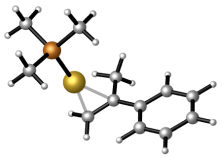

E = -945.326745 Hartrees
G = -945.094984 Hartrees

Int2a

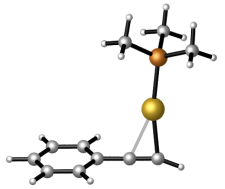

E = -904.790361 Hartrees
G = -904.611932 Hartrees

α-Methylstyrene (19a)

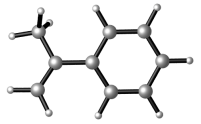

E = -348.677777 Hartrees
G = -348.548933 Hartrees

Int1b

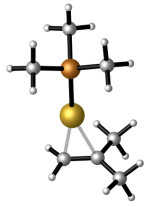

E = -753.736771 Hartrees
G = -753.556375 Hartrees

106. de Orbe, M. E.; Amenós, L.; Kirillova, M. S.; Wang, Y.; López-Carrillo, V.; Maseras, F.; Echavarren, A. M. *J. Am. Chem. Soc.* **2017**, *139*, 10302–10311.

2-Methylpropene (19t)

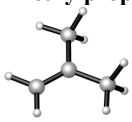

E = -157.086412 Hartrees
G = -157.006496 Hartrees

$TS_{1\text{-}2}$b

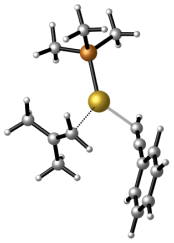

E = -1061.883339 Hartrees
G = -1061.603390 Hartrees

Pathway a

$TS_{2\text{-}3}$a

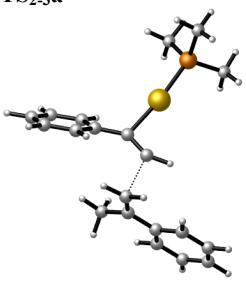

E = -1253.457190 Hartrees
G = -1253.126468 Hartrees

Int3a

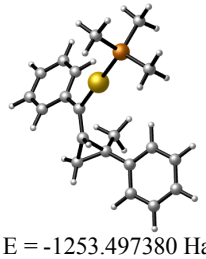

E = -1253.497380 Hartrees
G = -1253.163427 Hartrees

$TS_{2\text{-}4}$a

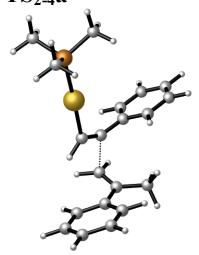

E = -1253.463187 Hartrees
G = -1253.132482 Hartrees

Int4a

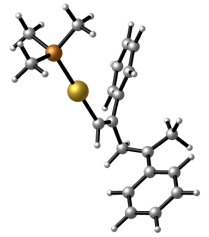

E = -1253.491128 Hartrees
G = -1253.156296 Hartrees

$TS_{4\text{-}5}$a

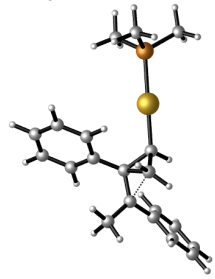

E = -1253.481201 Hartrees
G = -1253.146725 Hartrees

Int5a

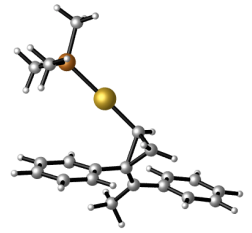

E = -1253.491038 Hartrees
G = -1253.155710 Hartrees

$TS_{5\text{-}6}a$

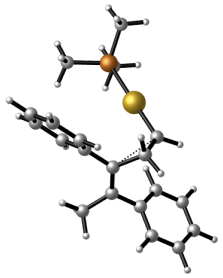

E = -1253.471915 Hartrees
G = -1253.138657 Hartrees

Int6a

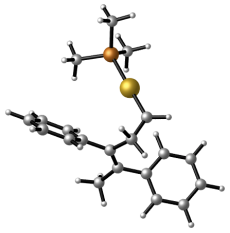

E = -1253.472327 Hartrees
G = -1253.139488 Hartrees

$TS_{4\text{-}7}a$

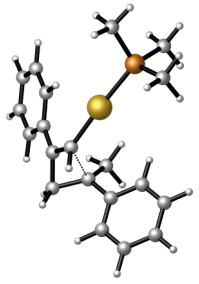

E = -1253.478980 Hartrees
G = -1253.142038 Hartrees

Int7a

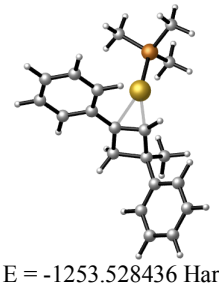

E = -1253.528436 Hartrees
G = -1253.193133 Hartrees

$TS_{5\text{-}8}a$

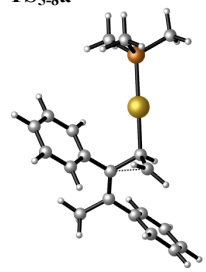

E = -1253.471961 Hartrees
G = -1253.139957 Hartrees

Int8a and Int9a

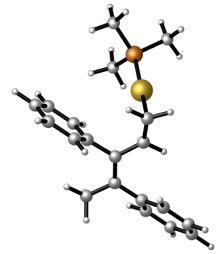

E = -1253.538031 Hartrees
G = -1253.202738 Hartrees

$TS_{6\text{-}9}a$

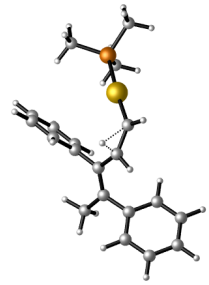

E = -1253.473202 Hartrees
G = -1253.139361 Hartrees

$TS_{7\text{-}10}a$

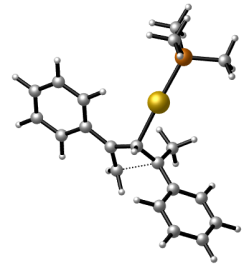

E = -1253.476209 Hartrees
G = -1253.141872 Hartrees

Int10a

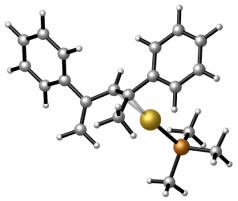

E = -1253.534638 Hartrees
G = -1253.198739 Hartrees

Pathway b

TS_{2-3}b

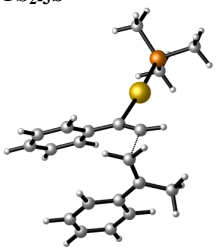

E = -1253.458921 Hartrees
G = -1253.126542 Hartrees

Int3b

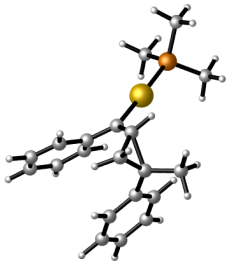

E = -1253.500255 Hartrees
G = -1253.164740 Hartrees

TS_{2-4}b

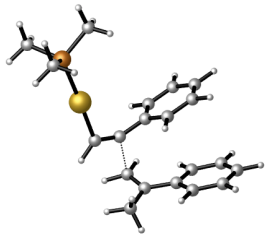

E = -1253.464913 Hartrees
G = -1253.133906 Hartrees

Int4b

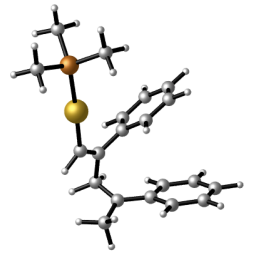

E = -1253.491805 Hartrees
G = -1253.157234 Hartrees

TS_{4-5}b

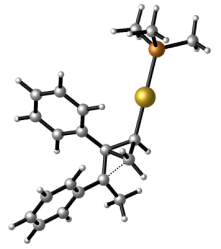

E = -1253.477808 Hartrees
G = -1253.140415 Hartrees

Int5b

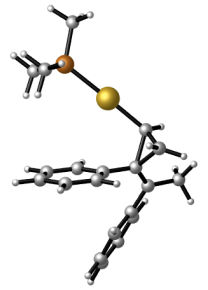

E = -1253.493756 Hartrees
G = -1253.158169 Hartrees

TS_{5-6}b

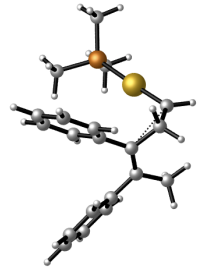

E = -1253.467951 Hartrees
G = -1253.134792 Hartrees

Int6b

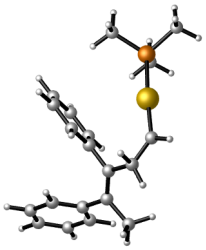

E = -1253.470864 Hartrees
G = -1253.138450 Hartrees

$TS_{4\text{-}7}$b

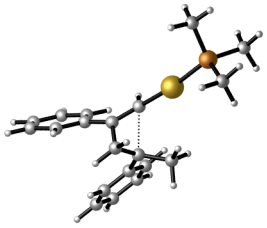

E = -1253.477154 Hartrees
G = -1253.140442 Hartrees

Int7b

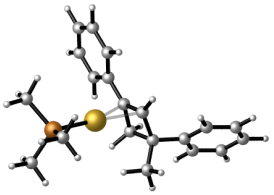

E = -1253.528490 Hartrees
G = -1253.192829 Hartrees

$TS_{5\text{-}8}$b

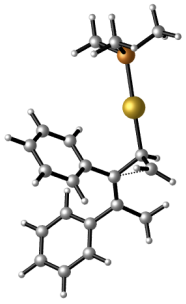

E = -1253.471787 Hartrees
G = -1253.139206 Hartrees

Int8b and Int9b

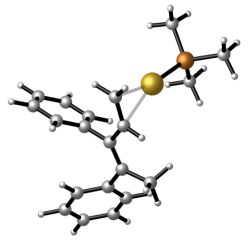

E = -1253.536297 Hartrees
G = -1253.201969 Hartrees

$TS_{6\text{-}9}$b

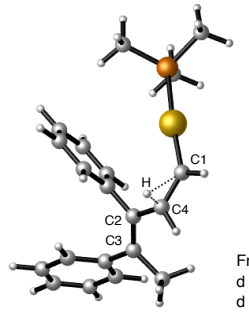

Frozen distances:
d (H-C1) = 1.70 Å
d (H-C4) = 1.16 Å

E = -1253.470784 Hartrees
G = -1253.138289 Hartrees

$TS_{7\text{-}10}$b

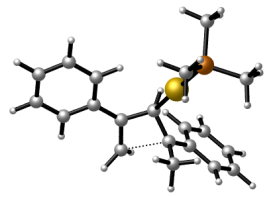

E = -1253.476209 Hartrees
G = -1253.141875 Hartrees

Int10b

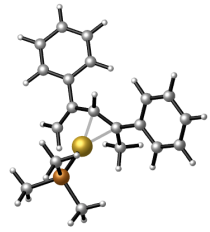

E = -1253.534776 Hartrees
G = -1253.198707 Hartrees

Bond rotations

TS_{4a-4ab}

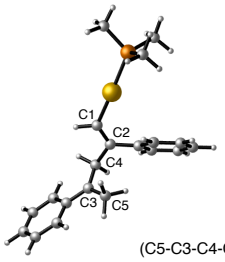

(C5-C3-C4-C2) = -28.7°

E = -1253.481914 Hartrees
G = -1253.146883 Hartrees

Int4ab

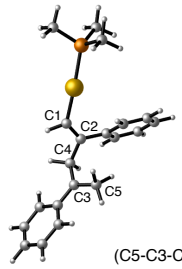

(C5-C3-C4-C2) = -27.0°

E = -1253.481926
G = -1253.149026

TS_{4ab-4b}

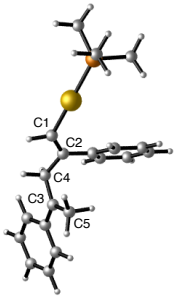

Frozen angle:
(C5-C3-C4-C2) = 24.4 °

E = -1253.483868 Hartrees
G = -1253.148698 Hartrees

TS_{5a-5b}

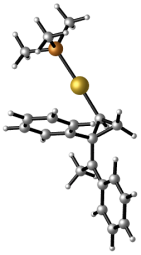

E = -1253.474829 Hartrees
G = -1253.139324 Hartrees

Pathway not *via* cyclopropyl gold(I) carbene

TS_{2-11}

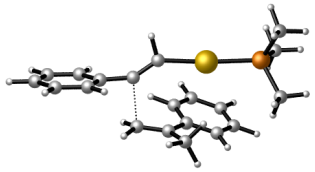

E = -1253.454636 Hartrees
G = -1253.123100 Hartrees

Int11

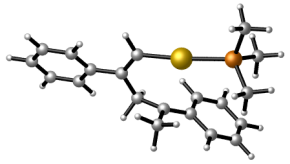

E = -1253.492210 Hartrees
G = -1253.156917 Hartrees

TS_{11-7}

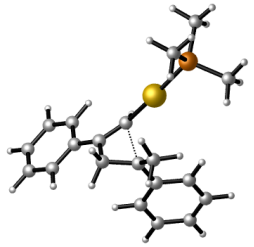

E = -1253.469938 Hartrees
G = -1253.136125 Hartrees

Reaction of 18f with 19a

(*o*-Bromophenyl)acetylene (18f)

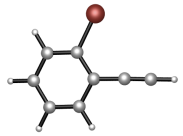

E = -320.694692 Hartrees
G = -320.629465 Hartrees

Int2c

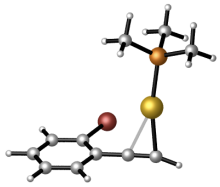

E = -917.337815 Hartrees
G = -917.172662 Hartrees

Pathway c

TS_{2-3}c

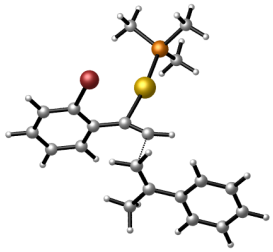

E = -1266.006286 Hartrees
G = -1265.689544 Hartrees

Int3c

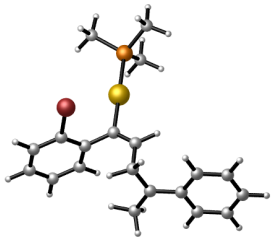

E = -1266.040695 Hartrees
G = -1265.720798 Hartrees

TS_{2-4}c

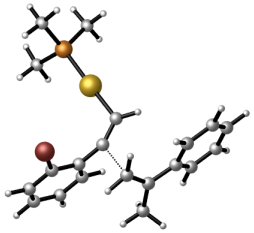

E = -1266.011299 Hartrees
G = -1265.695052 Hartrees

Int4c

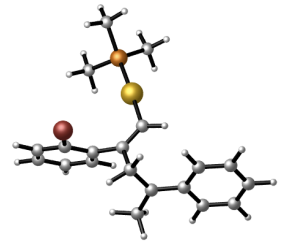

E = -1266.038840 Hartrees
G = -1265.719065 Hartrees

TS_{4-5}c

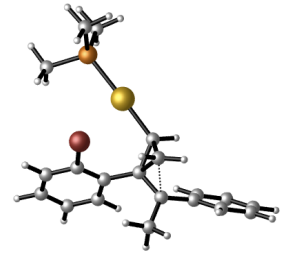

E = -1266.022151 Hartrees
G = -1265.699939 Hartrees

Int5c

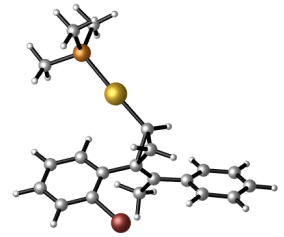

E = -1266.039899 Hartrees
G = -1265.715792 Hartrees

TS_{5-6}c

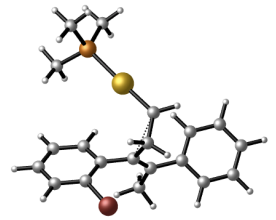

E = -1266.019856 Hartrees
G = -1265.699657 Hartrees

Int6c

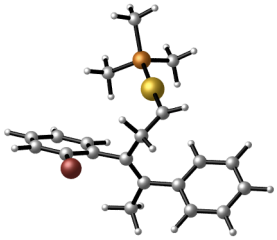

E = -1266.020503 Hartrees
G = -1265.701032 Hartrees

$TS_{4\text{-}7}$c

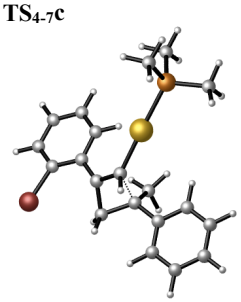

E = -1266.021362 Hartrees
G = -1265.700056 Hartrees

Int7c

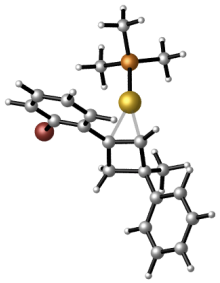

E = -1266.074214 Hartrees
G = -1265.750279 Hartrees

$TS_{5\text{-}8}$c

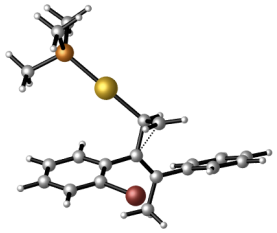

E = -1266.020228 Hartrees
G = -1265.699135 Hartrees

Int8c and Int9c

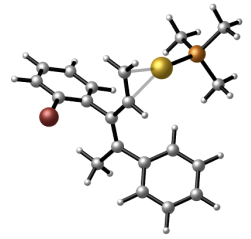

E = -1266.090346 Hartrees
G = -1265.768669 Hartrees

$TS_{7\text{-}10}$c

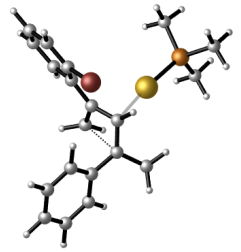

E = -1266.010163 Hartrees
G = -1265.691204 Hartrees

Int10c

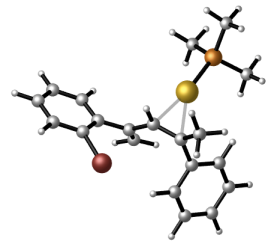

E = -1266.078839 Hartrees
G = -1265.757610 Hartrees

Pathway d

$TS_{2\text{-}3}$d

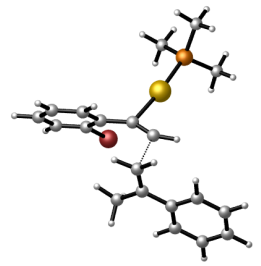

E = -1266.007481 Hartrees
G = -1265.691345 Hartrees

Int3d

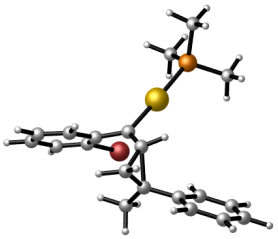

E = -1266.045114 Hartrees
G = -1265.723430 Hartrees

$TS_{2\text{-}4}$d

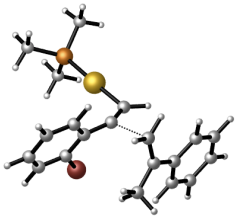

E = -1266.011249 Hartrees
G = -1265.693755 Hartrees

Int4d

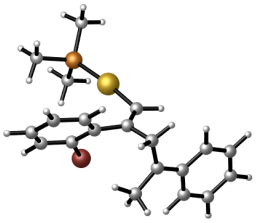

E = -1266.038301 Hartrees
G = -1265.715857 Hartrees

$TS_{4\text{-}5}$d

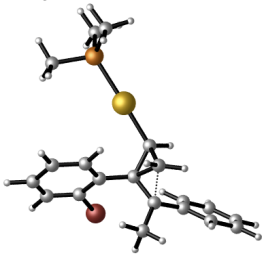

E = -1266.028038 Hartrees
G = -1265.705581 Hartrees

Int5d

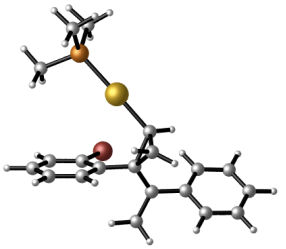

E = -1266.040665 Hartrees
G = -1265.716100 Hartrees

$TS_{5\text{-}6}$d

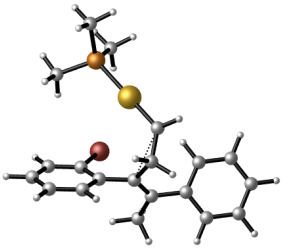

E = -1266.020905 Hartrees
G = -1265.697872 Hartrees

Int6d

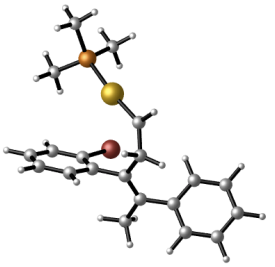

E = -1266.023662 Hartrees
G = -1265.702887 Hartrees

$TS_{4\text{-}7}$d

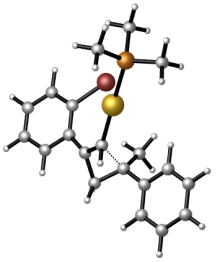

E = -1266.015382 Hartrees
G = -1265.689711 Hartrees

Int7d

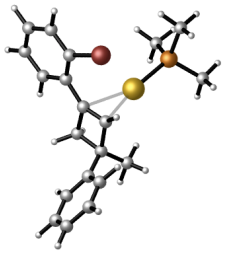

E = -1266.075155 Hartrees
G = -1265.750686 Hartrees

$TS_{5\text{-}8}$d

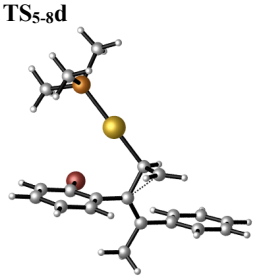

E = -1266.023897 Hartrees
G = -1265.702923 Hartrees

Int8d and Int9d

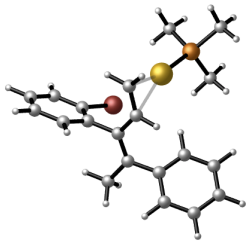

E = -1266.092424 Hartrees
G = -1265.768513 Hartrees

Pathway e

$TS_{2\text{-}3}$e

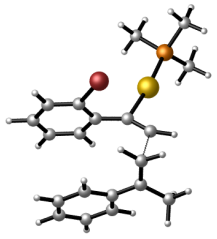

E = -1266.007712 Hartrees
G = -1265.691146 Hartrees

Int3e

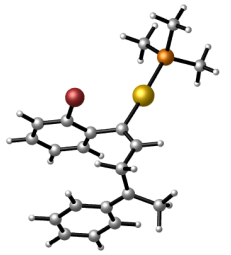

E = -1266.041551 Hartrees
G = -1265.720498 Hartrees

$TS_{2\text{-}4}$e

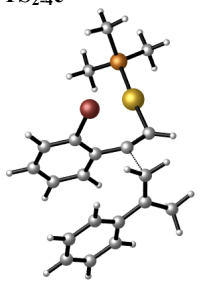

E = -1266.013421 Hartrees
G = -1265.694016 Hartrees

Int4e

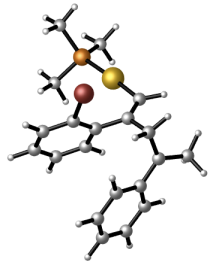

E = -1266.039959 Hartrees
G = -1265.717064 Hartrees

$TS_{4\text{-}5}$e

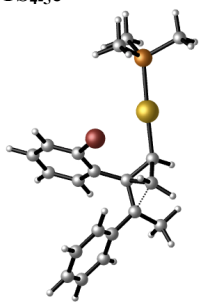

E = -1266.019065 Hartrees
G = -1265.694409 Hartrees

Int5e

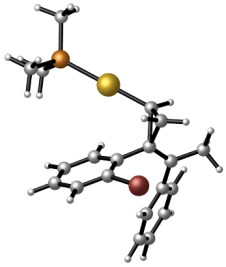

E = -1266.039746 Hartrees
G = -1265.717514 Hartrees

$TS_{5\text{-}6}$e

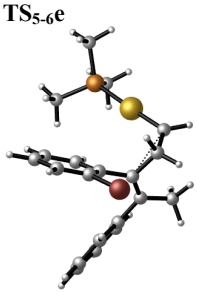

E = -1266.017101 Hartrees
G = -1265.695551 Hartrees

Int6e

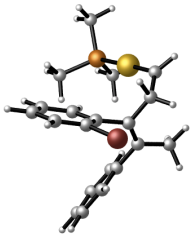

E = -1266.019794 Hartrees
G = -1265.698797 Hartrees

$TS_{4\text{-}7}$e

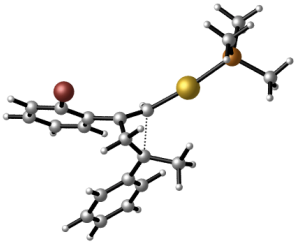

E = -1266.021282 Hartrees
G = -1265.699360 Hartrees

Int7e

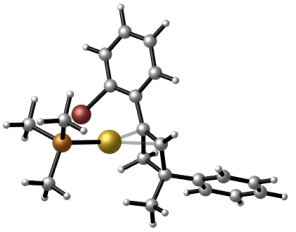

E = -1266.074298 Hartrees
G = -1265.751248 Hartrees

$TS_{5\text{-}8}$e

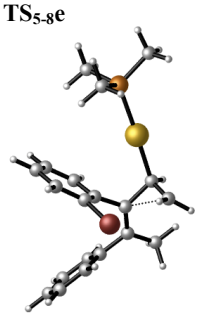

E = -1266.015496 Hartrees
G = -1265.694928 Hartrees

Int8e and Int9e

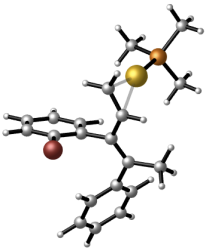

E = -1266.086025 Hartrees
G = -1265.764794 Hartrees

$TS_{7\text{-}10}$e

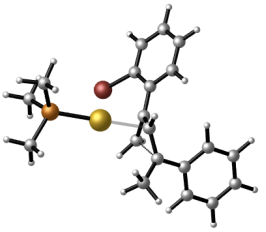

E = -1266.013264 Hartrees
G = -1265.691723 Hartrees

Int10e

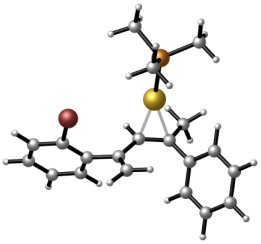

E = -1266.077714 Hartrees
G = -1265.755235 Hartrees

Pathway f

TS_{2-3}f

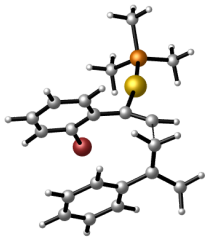

E = -1266.009440 Hartrees
G = -1265.691565 Hartrees

Int3f

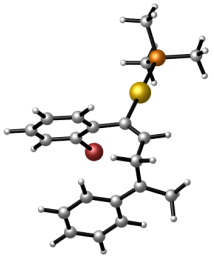

E = -1266.045055 Hartrees
G = -1265.721725 Hartrees

TS_{2-4}f

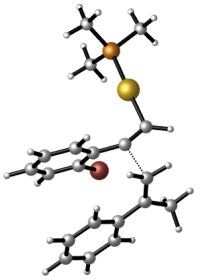

E = -1266.012893 Hartrees
G = -1265.694425 Hartrees

Int4f

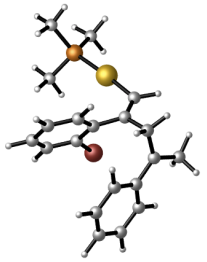

E = -1266.040890 Hartrees
G = -1265.717089 Hartrees

TS_{4-5}f

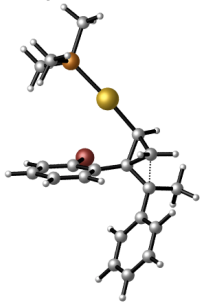

E = -1266.027104 Hartrees
G = -1265.703729 Hartrees

Int5f

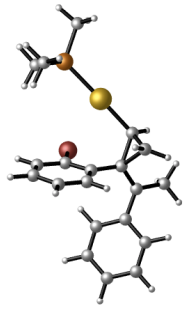

E = -1266.037603 Hartrees
G = -1265.715150 Hartrees

TS_{5-6}f

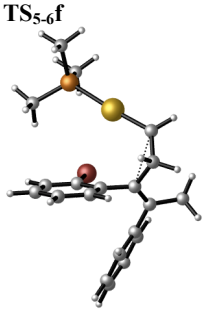

E = -1266.015912 Hartrees
G = -1265.694474 Hartrees

$TS_{4\text{-}7}f$

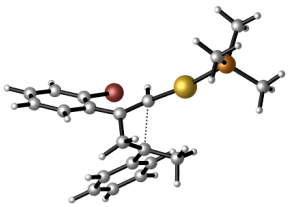

E = -1266.015281 Hartrees
G = -1265.693857 Hartrees

Int7f

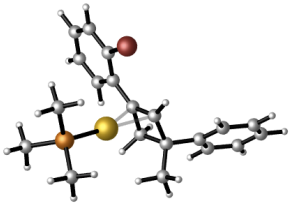

E = -1266.075113 Hartrees
G = -1265.750382 Hartrees

$TS_{5\text{-}8}f$

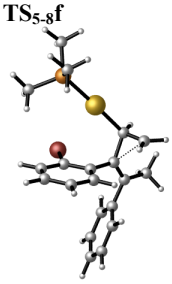

E = -1266.022216 Hartrees
G = -1265.701316 Hartrees

Int8f and Int9f

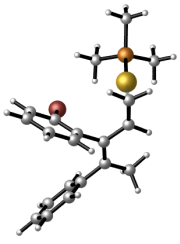

E = -1266.086543 Hartrees
G = -1265.764610 Hartrees

Bond rotations

$TS_{4c\text{-}4d}$

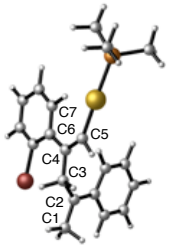

(C1-C2-C3-C4) = -171.8°
(C5-C4-C6-C7) = -0.1°

E = -1266.014108 Hartrees
G = -1265.690552 Hartrees

Int4ce

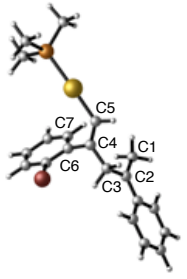

(C1-C2-C3-C4) = 16.3°
(C5-C4-C6-C7) = 66.5°

E = -1266.030845 Hartrees
G = -1265.711502 Hartrees

$TS_{4c\text{-}4ce}$

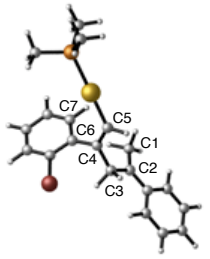

(C1-C2-C3-C4) = -16.2°
(C5-C4-C6-C7) = 61.6°

E = -1266.029940 Hartrees
G = -1265.710765 Hartrees

$TS_{4ce\text{-}4e}$

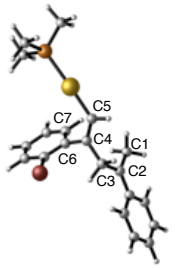

(C1-C2-C3-C4) = 19.3°
(C5-C4-C6-C7) = 67.0°

E = -1266.030831 Hartrees
G = -1265.710017 Hartrees

TS_{4d-4df}

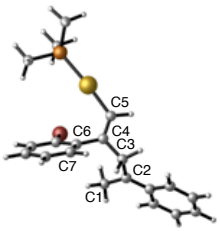

(C1-C2-C3-C4) = -32.9°
(C5-C4-C6-C7) = -116.2°

E = -1266.028193 Hartrees
G = -1265.706319 Hartrees

Int4df

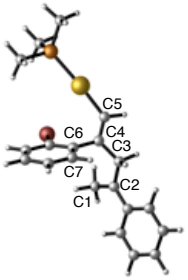

(C1-C2-C3-C4) = 21.8°
(C5-C4-C6-C7) = -118.7°

E = -1266.029032 Hartrees
G = -1265.707692 Hartrees

TS_{4df-4f}

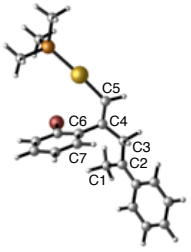

(C1-C2-C3-C4) = 24.4°
(C5-C4-C6-C7) = -118.8°

E = -1266.029018 Hartrees
G = -1265.705966 Hartrees

TS_{4e-4f}

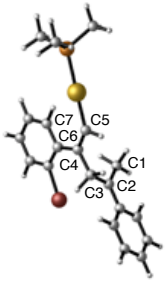

(C1-C2-C3-C4) = 13.0°
(C5-C4-C6-C7) = 2.6°

E = -1266.017740 Hartrees
G = -1265.694093 Hartrees

TS_{5f-5d}

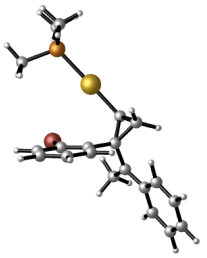

E = -1266.017881 Hartrees
G = -1265.692954 Hartrees

Reaction of 22a with 19t

1-Phenyl-1,3-butadiyne (22a)

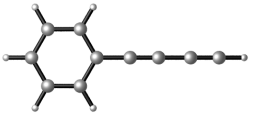

E = -384.247586 Hartrees
G = -384.160437 Hartrees

Int2g

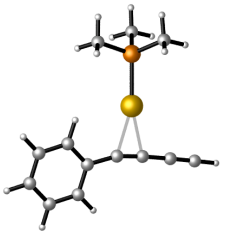

E = -980.882816 Hartrees
G = -980.696390 Hartrees

TS_{2-4g}

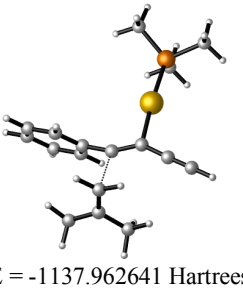

E = -1137.962641 Hartrees
G = -1137.674467 Hartrees

Int4g

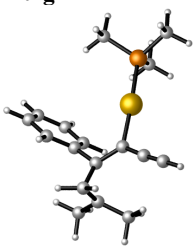

E = -1137.996472 Hartrees
G = -1137.701549 Hartrees

Int2h

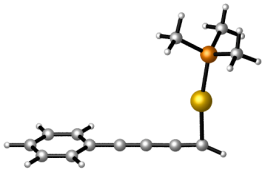

E = -980.886460 Hartrees
G = -980.700833 Hartrees

$TS_{2\text{-}4}$h

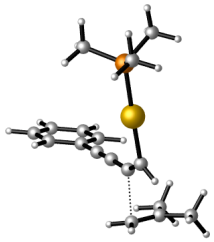

E = -1137.968646 Hartrees
G = -1137.679895 Hartrees

Int4h

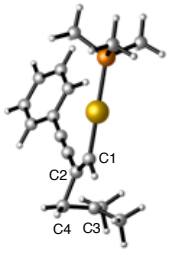

d (C1-C2) = 1.38 Å
d (C1-C4) = 2.57 Å
d (C2-C3) = 1.80 Å
d (C2-C4) = 1.58 Å
d (C3-C4) = 1.43 Å

E = -1137.996014 Hartrees
G = -1137.703224 Hartrees

$TS_{4\text{-}12}$h

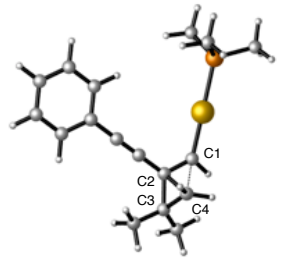

d (C1-C2) = 1.40 Å
d (C1-C4) = 2.09 Å
d (C2-C3) = 1.52 Å
d (C2-C4) = 1.65 Å
d (C3-C4) = 1.49 Å

E = -1137.990429 Hartrees
G = -1137.694961 Hartrees

Int12h

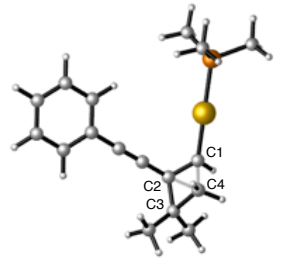

d (C1-C2) = 1.43 Å
d (C1-C4) = 1.69 Å
d (C2-C3) = 1.47 Å
d (C2-C4) = 1.69 Å
d (C3-C4) = 1.60 Å

E = -1137.992178 Hartrees
G = -1137.697663 Hartrees

$TS_{12\text{-}5}$h

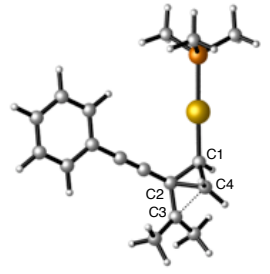

d (C1-C2) = 1.49 Å
d (C1-C4) = 1.53 Å
d (C2-C3) = 1.42 Å
d (C2-C4) = 1.64 Å
d (C3-C4) = 1.91 Å

E = -1137.990457 Hartrees
G = -1137.695770 Hartrees

Int5h

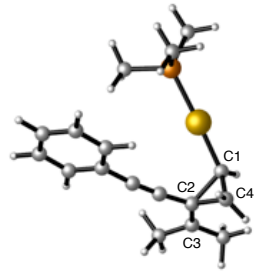

d (C1-C2) = 1.68 Å
d (C1-C4) = 1.44 Å
d (C2-C3) = 1.40 Å
d (C2-C4) = 1.57 Å
d (C3-C4) = 2.57 Å

E = -1138.004905 Hartrees
G = -1137.710694 Hartrees

$TS_{5\text{-}6}$h

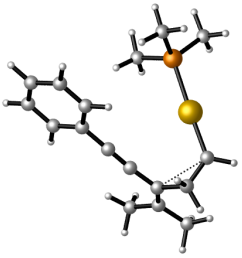

E = -1137.982166 Hartrees
G = -1137.689962 Hartrees

Int6h

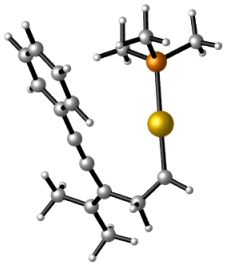

E = -1137.987005 Hartrees
G = -1137.696539 Hartrees

$TS_{4\text{-}7}$h

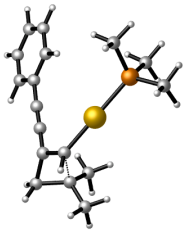

E = -1137.987748 Hartrees
G = -1137.692054 Hartrees

Int7h

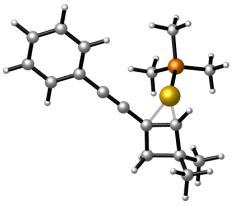

E = -1138.034292 Hartrees
G = -1137.742133 Hartrees

$TS_{5\text{-}8}$h

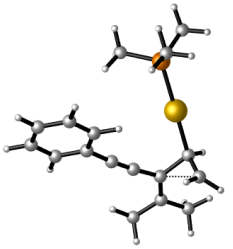

E = -1137.985605 Hartrees
G = -1137.694813 Hartrees

Int8h

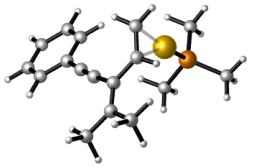

E = -1138.050613 Hartrees
G = -1137.757920 Hartrees

$TS_{6\text{-}9}$h

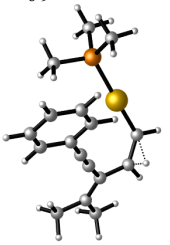

E = -1137.987659 Hartrees
G = -1137.695345 Hartrees

Int9h

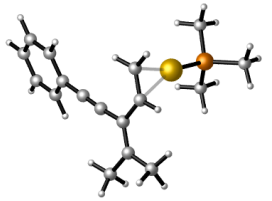

E = -1138.050353 Hartrees
G = -1137.761978 Hartrees

$TS_{7\text{-}10}$h

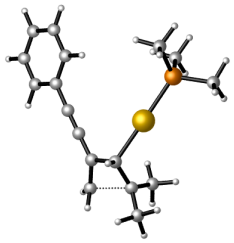

E = -1137.979657 Hartrees
G = -1137.690619 Hartrees

Int10h

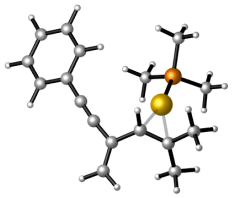

E = -1138.044854 Hartrees
G = -1137.752173 Hartrees

$TS_{4\text{-}13}$h

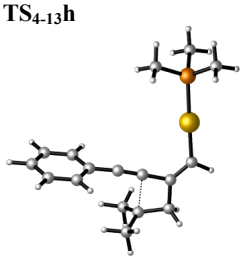

E = -1137.980731 Hartrees
G = -1137.688686 Hartrees

Int13h

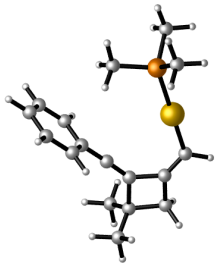

E = -1137.991105 Hartrees
G = -1137.698314 Hartrees

1,3-Dienes by retro-Buchner reaction

Substrate 26a

Int4i

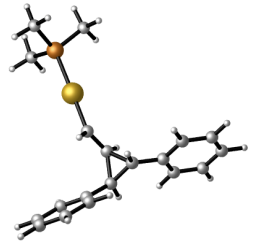

E = -1214.205830 Hartrees
G = -1213.896552 Hartrees

$TS_{4\text{-}5}$i

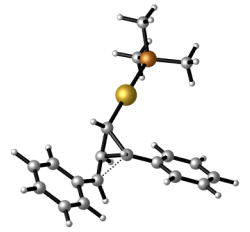

E = -1214.194566 Hartrees
G = -1213.886746 Hartrees

Int5i

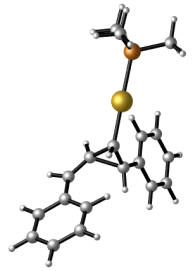

E = -1214.209385 Hartrees
G = -1213.902040 Hartrees

$TS_{4\text{-}7}$i

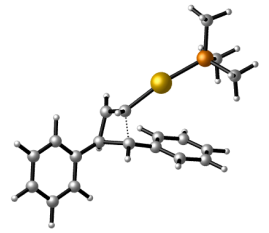

E = -1214.173391 Hartrees
G = -1213.865356 Hartrees

Int7i

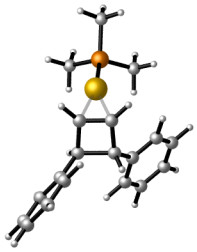

E = -1214.237337 Hartrees
G = -1213.926977 Hartrees

TS_{5-8}i

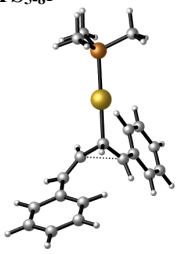

E = -1214.200713 Hartrees
G = -1213.893301 Hartrees

Int8i

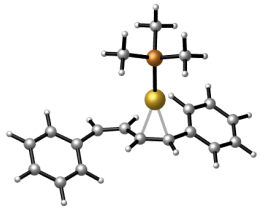

E = -1214.253635 Hartrees
G = -1213.945470 Hartrees

Substrate 26b

Int4j

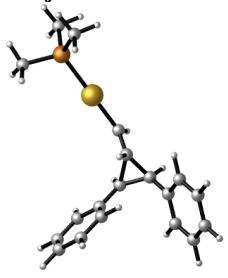

E = -1214.203021 Hartrees
G = -1213.893982 Hartrees

TS_{4-5}j

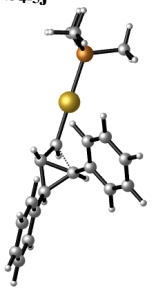

E = -1214.198754 Hartrees
G = -1213.887547 Hartrees

Int5j

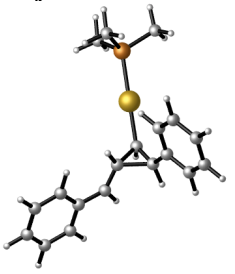

E = -1214.217092 Hartrees
G = -1213.912615 Hartrees

TS_{4-7}j

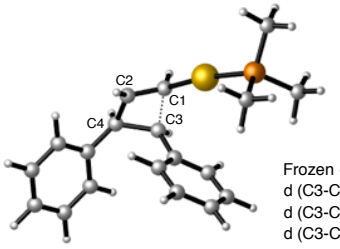

E = -1214.176363 Hartrees
G = -1213.866634 Hartrees

Int7j

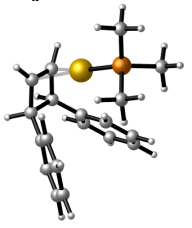

E = -1214.235832 Hartrees
G = -1213.924574 Hartrees

$TS_{5\text{-}8}$j

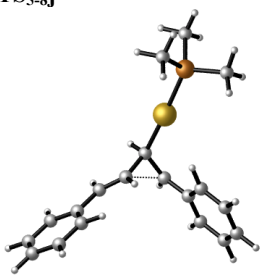

E = -1214.206849 Hartrees
G = -1213.897756 Hartrees

Int8j

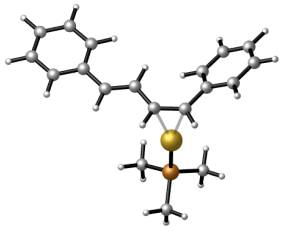

E = -1214.260475 Hartrees
G = -1213.952322 Hartrees

Bond rotations

$TS_{4i\text{-}4ij}$

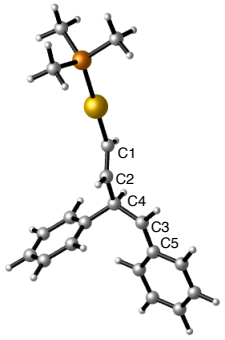

(C5-C3-C4-C2) = 166.5°

E = -1214.177985 Hartrees
G = -1213.870987 Hartrees

Int4ij

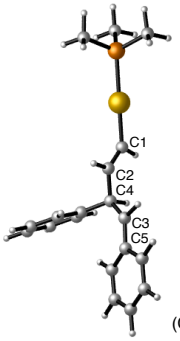

(C5-C3-C4-C2) = 164.8°

E = -1214.177987 Hartrees
G = -1213.872484 Hartrees

$TS_{4ij\text{-}4j}$

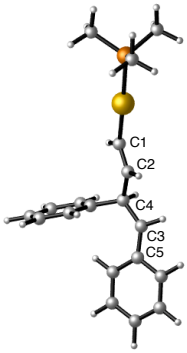

(C5-C3-C4-C2) = 152.9°

E = -1214.176780 Hartrees
G = -1213.870038 Hartrees

$TS_{5i\text{-}5k}$

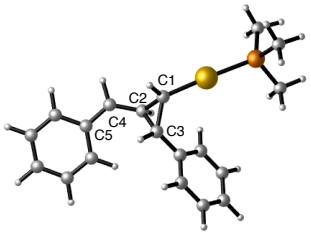

(C5-C4-C2-C1) = -127.4°

E = -1214.187446 Hartrees
G = -1213.878332 Hartrees

Int5k

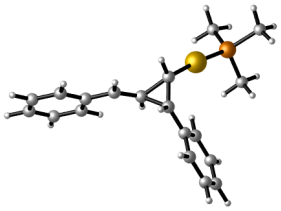

E = -1214.217406 Hartrees
G = -1213.910861 Hartrees

$TS_{5j\text{-}5L}$

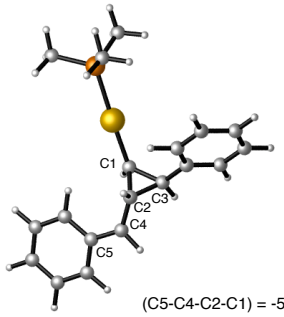

E = -1214.187677 Hartrees
G = -1213.879559 Hartrees

Int5L

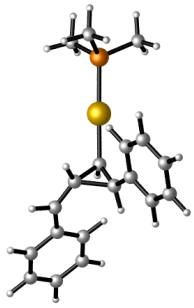

E = -1214.209441 Hartrees
G = -1213.901238 Hartrees

UNIVERSITAT ROVIRA I VIRGILI
GOLD-CATALYZED INTERMOLECULAR REACTIONS OF ALKYNES WITH ALKENES: NOVEL REACTIVITIES AND GLOBAL MECHANISTIC PICTURE
María Elena de Orbe Izquierdo

Chapter 2.

Cyclobutenes by Gold-Catalyzed [2+2] Cycloaddition: Extension and Further Transformations

UNIVERSITAT ROVIRA I VIRGILI
GOLD-CATALYZED INTERMOLECULAR REACTIONS OF ALKYNES WITH ALKENES: NOVEL REACTIVITIES AND GLOBAL MECHANISTIC PICTURE
María Elena de Orbe Izquierdo

Introduction

As mentioned in the Introduction to **Chapter 1**, cyclobutenes are important structural units in natural products and bioactive compounds (Scheme 2.1).[107] Due to the four-membered ring strain and the C–C double bond, cyclobutenes are especially reactive carbocyclic intermediates which have been exploited to construct a variety of frameworks *via* cycloaddition, fragmentation, ring contraction or expansion.[108] Moreover, the tethered double bond allows to apply the alkene chemistry into these small rings. Noteworthy, cyclobutenes provide access to cyclobutanes and cyclopropanes, which are also valuable compounds.[109]

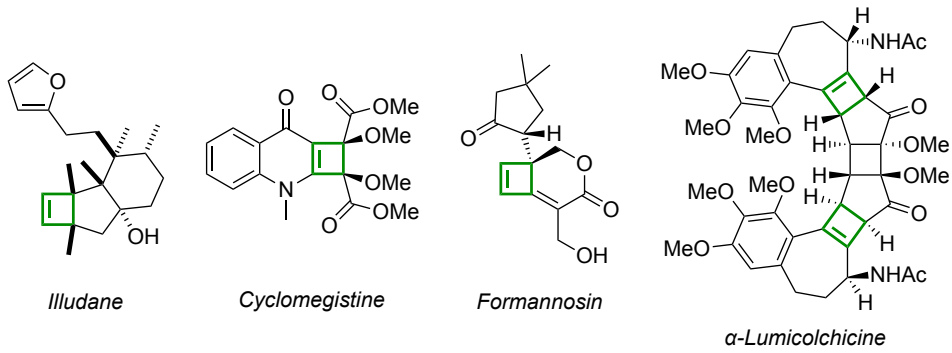

Scheme 2.1. Cyclobutenes exhibited in natural products.

107. (a) Chapman, O. L.; Smith, H. G.; King R. W. *J. Am. Chem. Soc.* **1963**, *85*, 803–806. (b) McMorris, T. C.; Nair, M. S. R.; Singh, P.; Anchel, M. *Phylochem.* **1971**, *10*, 1611–1615. (c) Bohlmann, F.; Grenz, M.; Wegner, P.; Jakupóvic, J. *Liebigs Ann. Chem.* **1983**, 2008–2020. (d) Fokialakis, N.; Magiatis, P.; Terzis, A.; Tillequin, F.; Skaltsounis, A.-L. *Tetrahedron Lett.* **2001**, *42*, 5323–5325. (e) Dembitsky, V. M. *J. Nat. Med.* **2008**, *62*, 1–33. (f) Sittiwong, W.; Zinniel, D. K.; Fenton, R. J.; Marshall, D. D.; Story, C. B.; Kim, B.; Lee, J.-Y.; Powers, R.; Barletta, R. G.; Dussault, P. H. *ChemMedChem* **2014**, *9*, 1838–1849.
108. (a) Luparia, M.; Audisio, D.; Maulide, N. *Synlett*. **2011**, 735–740. (b) Misale, A.; Niyomchon, S.; Maulide, N. *Acc. Chem. Res.* **2016**, *49*, 2444–2458. (c) Eisold, M.; Baumann, A. N.; Kiefl, G. M.; Emmerling, S. T.; Didier, D. *Chem. Eur. J.* **2017**, *23*, 1634–1644. (d) Eisold, E.; Didier, D. *Org. Lett.* **2017**, *19*, 4046−4049.
109. (a) Guisán-Ceinos, M.; Parra, A.; Martín-Heras, V.; Tortosa, M. *Angew. Chem. Int. Ed.* **2016**, *55*, 6969–6972. (b) Roy, S. R.; Eijsberg, H.; Bruffaerts, J.; Marek, I. *Chem. Sci.* **2017**, *8*, 334–339. (c) Namyslo, C. J.; Kaufmann, D. E. *Chem. Rev.* **2003**, *103*, 1485−1537. (d) Lee-Ruff, E.; Mladenova, G. *Chem. Rev.* **2003**, *103*, 1449−1483.

Different functionalities in the cyclobutenes broaden their potential synthetic versatility. In particular, 1-vinylcyclobutenes have been shown to be useful synthons to create structural complexity.[110] Diverse methods for the preparation of 1-alkenyl substituted cyclobutenes have been developed, although the intermolecular [2+2] cycloaddition of 1,3-enynes with alkenes results a more practical and direct strategy.[111] In the Introduction to **Chapter 1**, we examined the variety of metal-catalyzed synthesis of cyclobutenes by intermolecular [2+2] cycloaddition of alkynes with alkenes, including the nickel and cobalt approaches to construct 1-alkenylcyclobutenes (Scheme 1.3), and we concluded that they are generally limited to a narrow scope of substrates.

Regarding the gold(I)-catalyzed intermolecular [2+2] cycloaddition of alkynes with alkenes, initially it seemed restricted to the use of cyclopropyl and arylalkynes, as commented already in the **General Introduction**. Nevertheless, we could further expand this reaction to both aryl and alkyl 1,3-diynes to construct 1-alkynylcyclobutenes, as discussed along the **Chapter 1**. Simultaneously to these findings, our group developed the enantioselective synthesis of 1-arylcyclobutenes with alkenes using non C_2-chiral Josiphos digold(I) complexes as precatalysts, *via* the formation of the corresponding monocationic species (Scheme 2.2).[112] This methodology as well as the macrocyclization of 1,*n*-enynes (n = 10-16) leading to cyclobutenes[33b] were applied for the enantioselective total synthesis of rumphellaone A (Scheme 2.3).[113]

110. (a) Baumann, A. N.; Eisold, M.; Didier, D. *Org. Lett.* **2017**, *19*, 2114−2117. (b) Barluenga, J.; Aznar, F.; Palomero, M. A. *Angew. Chem. Int. Ed.* **2000**, *39*, 4346–4348. (c) Thummel, R. P.; Cravey, W. E.; Nutakul, W. *J. Org. Chem.* **1978**, *43*, 2473−2477. (d) Turnbull, P.; Heileman, M. J.; Moore, H. W. *J. Org. Chem.* **1996**, *61*, 2584−2585.
111. (a) By cyclobutenylmetal intermediates: Negishi, E.; Liu, F.; Choueiry, D.; Mohamud, M. M. *J. Org. Chem.* **1996**, *61*, 8325–8328. (b) By cycloisomerizations of allenynes: Matsuda, T.; Kadowaki, S.; Goya, T.; Murakami, M. *Synlett* **2006**, 575–578. (c) By 1,5-enyne metathesis: Debleds, O.; Campagne, J.-M. *J. Am. Chem. Soc.* **2008**, *130*, 1562–1563. (d) Other methods: Oishi, S; Shono, T.; Nagasawa, T.; Inoue, T.; Tsubouchi, A.; Takeda T. *Tetrahedron Lett.* **2008**, *49*, 6426–6428, and the references therein.
112. García-Morales, C.; Ranieri, B.; Escofet, I.; López-Suárez, L.; Obradors, C.; Konovalov, A. I.; Echavarren, A. M. *J. Am. Chem. Soc.* **2017**, *139*, 13628–13631.
113. Ranieri, B.; Obradors, C.; Mato, M.; Echavarren, A. M. *Org. Lett.* **2016**, *18*, 1614–1617.

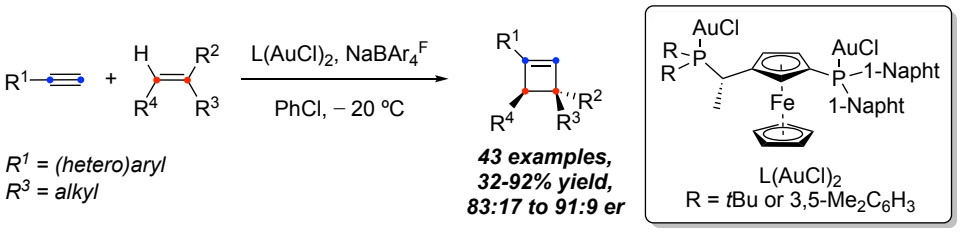

Scheme 2.2. Enantioselective gold(I)-catalyzed [2+2] cycloaddition leading to cyclobutenes.

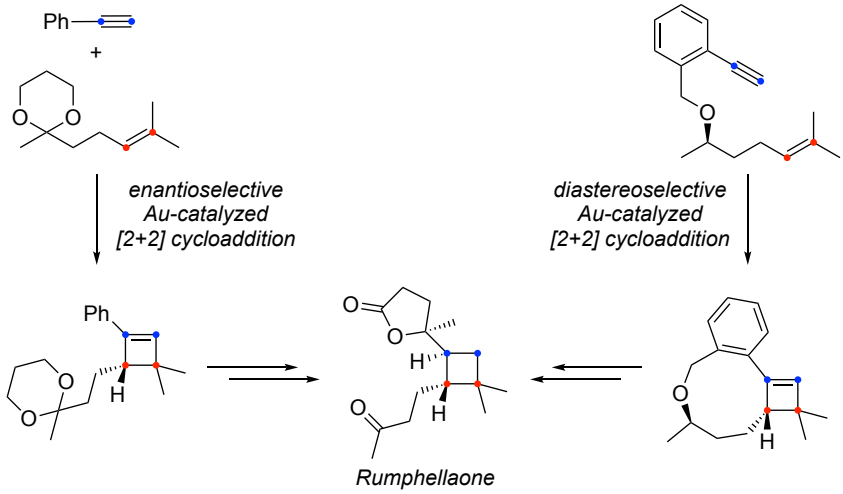

Scheme 2.3. Inter- and intramolecular gold-catalyzed [2+2] cycloaddition applied in total synthesis.

Apart from that, our group reported another relevant application of the cyclobutenes obtained by gold catalysis, namely the formal (4+1) cycloaddition of cyclobutenes **2** with gold(I) carbenes **I** generated by retro-Buchner reaction of cycloheptatrienes **1**[114] to build highly substituted cyclopentenes **3** (Scheme 2.4).[115] The reaction proceeds through bicyclo[2.1.0]pentane-gold(I) complexes **II** which undergo electrophilic cyclopropane opening to form tertiary carbocations **III** followed by 1,2-H shift to afford complexes **IV**. When utilizing other gold(I) carbene precursor such as phenyldiazomethane at 23 ºC, not only was cyclopentane **3a** obtained, but also bicyclo[2.1.0]pentane **5**. Derivative **5** could be

114. See details about the generation of gold(I) carbenes by retro-Buchner reaction of 7-substituted 1,3,5-cycloheptatrienes in the Introduction to **Chapter 1**.
115. Wang, Y.; Muratore, M. E.; Rong, Z.; Echavarren, A. M. *Angew. Chem. Int. Ed.* **2014**, *53*, 14022–14026.

converted into **3a** quantitatively by heating at 60 ºC under the same reaction conditions, which supports the involvement of intermediates **III** in the reaction mechanism.

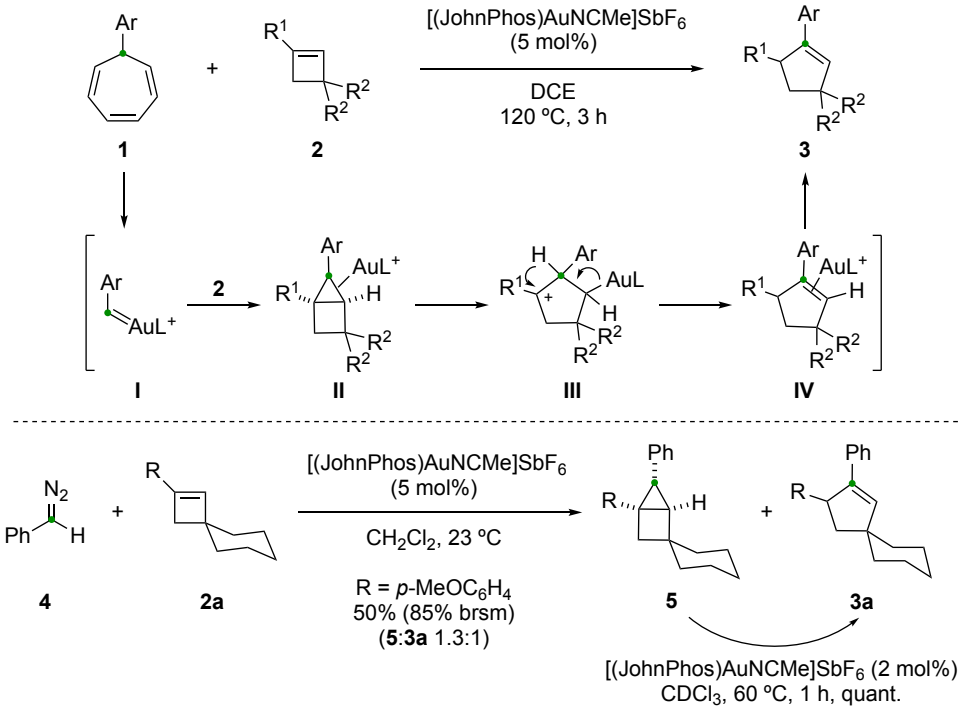

Scheme 2.4. Transformation of cyclobutenes into cyclopentenes by gold-catalysis.

In this context, it would be highly desirable to extend this gold(I)-catalyzed [2+2] cycloaddition to form a wider range of functionalized cyclobutenes. Due to the peculiarities of the gold-catalyzed reaction mechanism, electron-rich alkynes and electron-rich alkenes would be the substrates of choice (see **General Introduction**). However, in the presence of such competing unsaturations, it is remarkably challenging to selectively activate the alkyne with gold(I) catalysts towards the nucleophilic attack of a specific olefin avoiding side oligomerizations. Moreover, the installation of additional functional groups in the substrates could lead to new cyclization modes (see examples in the **General Introduction**), and even subtle changes in the substitution pattern of the initial cyclopropyl gold(I) carbenes intermediates could prompt different reaction pathways (see discussion in **Chapter 1**).

Objectives

Considering that the gold-catalyzed intermolecular [2+2] cycloaddition of alkynes with alkenes has shown to be a powerful strategy to access regioselectively to valuable cyclobutenes, we ambitioned to widen the scope of this transformation taking advantage of the key mechanistic details discovered in **Chapter 1**.

Firstly, we aimed to extend the reaction to 1,3-enynes bearing a terminal alkyne with electron-rich alkenes to forge synthetically useful 1-vinylcyclobutenes. Importantly, this gold-catalyzed approach to 1-vinylcyclobutenes would be complementary to the previously reported metal-catalyzed analogues, since the resulting 1-vinylcyclobutenes would show a different substitution pattern than in those cases.

Secondly, we envisioned to prepare selectively cyclobutenes by reaction of alkynes with polyunsaturated compounds, such as dienes. Notably, the larger the number of multiple bonds contained in both the substrates and products, the more challenging the selective [2+2] cycloaddition becomes.

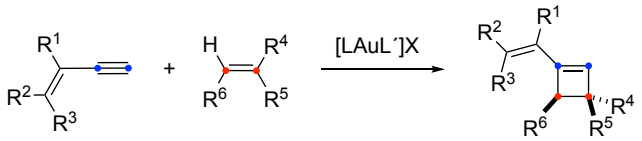

R^1, R^2, R^3 = aryl, alkyl, H
R^4, R^5, R^6 = vinyl, alkynyl, aryl, alkyl, H

Scheme 2.5. Expansion of the gold(I)-catalyzed [2+2] cycloaddition of alkynes with alkenes.

In addition, we sought to develop several one-pot transformations of cyclobutenes by cycloaddition, fragmentation, ring contraction or expansion in order to build distinct skeletons, highlighting the synthetic polyvalence of cyclobutenes.

Results and Discussion

Synthesis of Vinylcyclobutenes

Under the optimized conditions for the reported gold(I)-catalyzed [2+2] cycloaddition of arylalkynes with alkenes using gold catalysts **A** or **B**,[44] alkyl-substituted alkynes such as ethynylcyclohexane react very poorly with alkenes. However, we found that its unsaturated analogue 1-ethynylcyclohexene (**6a**), bearing a double bond conjugated to the alkynyl moiety, reacts with methylenecyclohexane (**7a**) to afford the desired 1-vinylcyclobutene **8a** in moderate yields (Table 2.1, entries 1 and 2).

As expected, a slightly better yield was achieved using catalyst **B** with BAr_4^{F-} as counterion (54%, Table 2.1, entry 2) than employing catalyst **A** with SbF_6^- (41%, Table 2.1, entry 1). Other related bulky phosphine gold(I) catalysts such as **C** or **D** (Table 2.1, entries 3 and 4 respectively) as well as gold(I) complexes with NHC ligands **E-G** (Table 2.1, entries 5-7) and phosphite ligand **H** (Table 2.1, entry 8) were tested, although lower yields were obtained in these cases. In contrast, NHC-based gold complex **E** provided the best yields in the intermolecular reactions of 1,3-butadiynes with alkenes (see **Chapter 1**). Variations in the temperature (Table 2.1, entries 9 and 10), stoichiometry of the substrates (Table 2.1, entries 11 and 12), catalyst loading (Table 2.1, entries 13 and 14) or concentration (Table 2.1, entries 15 and 16) did not improve the yield obtained with catalyst **B** (Table 2.1, entry 2).

With the best set of conditions in hand, we explored the reaction of a variety of 1,3-enynes with alkenes (Table 2.2). Enyne **6a** reacts with other terminal alkenes such as methylenecyclopentane (**7b**) and α-methylstyrenes **7c-e** to form 1-vinylcyclobutenes **8b-e** in moderate to good yields. Even 1,1-diphenylethylene (**7f**) reacts with **6a** providing **8f**, albeit in lower yield. The reaction of different aryl- and alkyl-substituted 1,3-enynes with terminal alkenes **7a** and **7c** gives rise to the corresponding vinylcyclobutenes **8g-s** in yields up to 98%. However, more electron-rich (*E*)-anisyl-1,3-enynes lead to cyclobutenes **8o-p** in poorer yields (31-36%, respectively). The structure of **8p** was confirmed by X-ray diffraction.

Table 2.1. Optimization of the gold(I)-catalyzed reaction between 1,3-enyne **6a** and alkene **7a**.

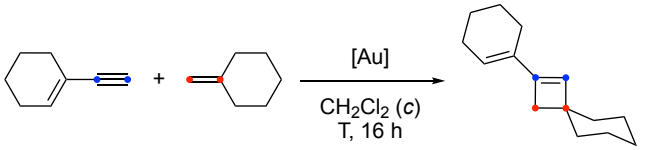

6a **7a** **8a**

Entry	[Au]	[Au] (mol%)	**6a**:**7a**	*c* (M)	T (ºC)	**8a** (%)[a]
1	**A**	5	1:2	0.5	23	41
2	**B**	5	1:2	0.5	23	54[b]
3	**C**	5	1:2	0.5	23	35
4	**D**	5	1:2	0.5	23	0
5	**E**	5	1:2	0.5	23	28
6	**F**	5	1:2	0.5	23	30
7	**G**	5	1:2	0.5	23	8
8	**H**	5	1:2	0.5	23	13
9	**B**	5	1:2	0.5	**40**	42
10	**B**	5	1:2	0.5	**80**	36
11	**B**	5	**2:1**	0.5	23	26
12	**B**	5	**1:3**	0.5	23	52[b]
13	**B**	**2**	1:2	0.5	23	27
14	**B**	**10**	1:2	0.5	23	46
15	**B**	5	1:2	**1.0**	23	43
16	**B**	5	1:2	**0.2**	23	34

[a] Yields determined by ^{1}H-NMR spectroscopy using 1,4-diacetylbenzene as internal standard. [b] Isolated yields.

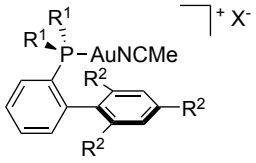

A: R^1 = *t*Bu; R^2 = *i*Pr; X = SbF_6
B: R^1 = *t*Bu; R^2 = *i*Pr; X = BAr_4^F
C: R^1 = *t*Bu; R^2 = H; X = SbF_6
D: R^1 = Cy; R^2 = *i*Pr; X = SbF_6

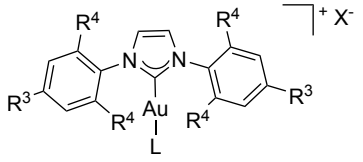

E: R^3 = H; R^4 = *i*Pr; L = NCMe; X = SbF_6
F: R^3 = H; R^4 = *i*Pr; L = NCPh; X = BAr_4^F
G: R^3 = Me; R^4 = Me; L = 2,4,6-$(OMe)_3C_6H_2CN$; X = SbF_6

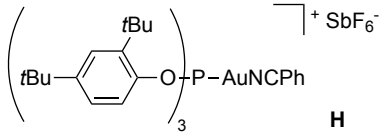

H

Table 2.2. Reaction of 1,3-enynes **6** with alkenes **7** leading to 1-vinylcyclobutenes **8**.[a]

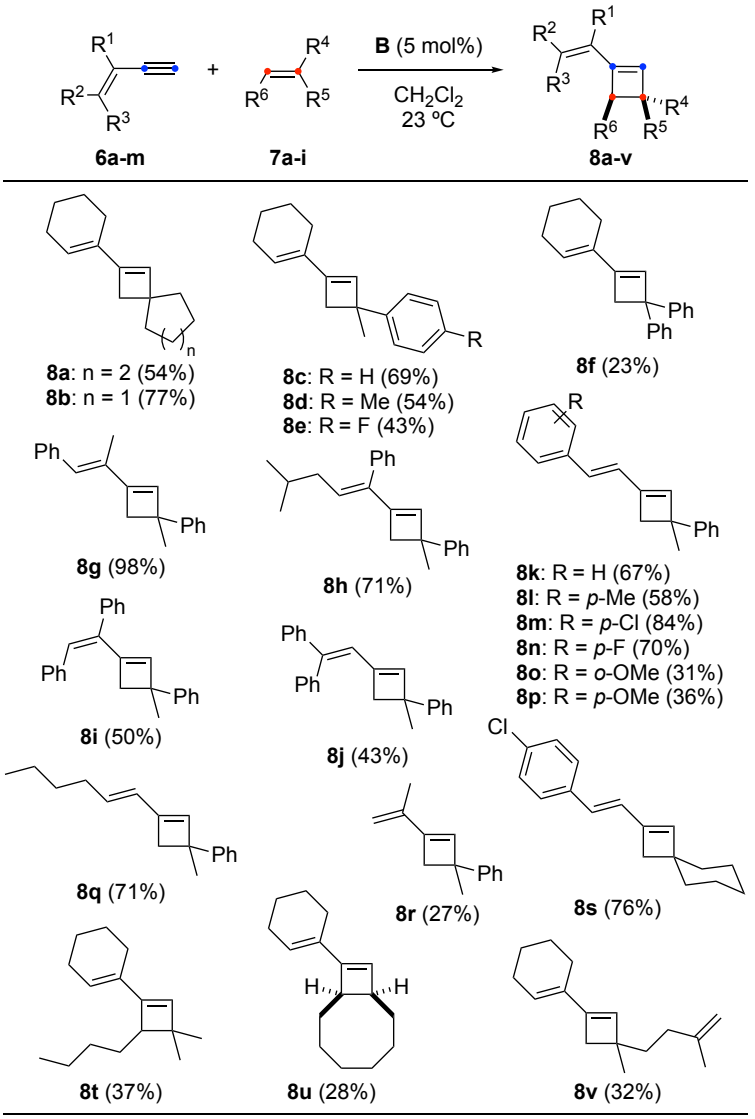

[a] 1,3-Enyne:alkene in a 1:2 ratio. Isolated yields.

Despite the facile dimerization of the starting 2-methyl-1-buten-3-yne under the reaction conditions, vinylcyclobutene **8r** could be also obtained. Internal di- and trisubstituted alkenes proved to react as well with 1,3-enyne **6a** to generate 1-vinylcyclobutenes **8t-u**. Moreover, 1:1 adduct **8v** was furnish in 32% yield in the reaction of enyne **6a** with 2,5-hexa-2,5-diene.

Since internal alkynes have been shown to be unreactive in the gold(I)-catalyzed [2+2] cycloaddition, we envisioned that 3-alkynylcyclobutenes could be delivered in the reaction of alkynes with 1,3-enynes containing a disubstituted alkyne moiety (Scheme 2.6). In fact, 1-vinyl-3-alkynylcyclobutenes **8w,x** were formed by reaction between two different 1,3-enynes **6a,b** and **6n**, in which the terminal alkyne of **6a,b** partakes in a [2+2] cycloaddition with the terminal alkene of **6n**. A better yield of cyclobutene **8y** was obtained in the reaction of phenylacetylene (**9a**) with 1,3-enyne **6n**.

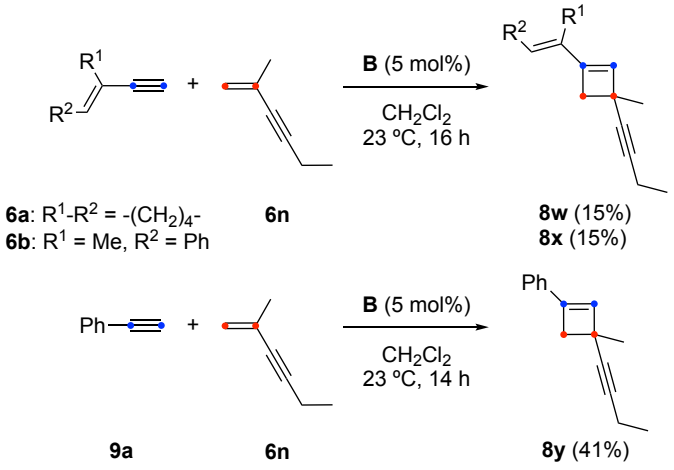

Scheme 2.6. Formation of 3-alkynylcyclobutenes by gold(I)-catalyzed [2+2] cycloaddition (Reacting alkyne:reacting alkene in a 1:2 ratio).

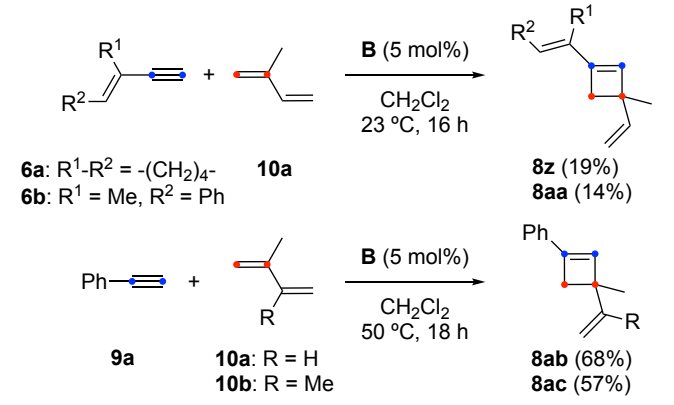

Scheme 2.7. Formation of 3-vinylcyclobutenes by gold(I)-catalyzed [2+2] cycloaddition (Reacting alkyne:diene in a 1:2 ratio).

We hypothesized that the gold(I)-catalyzed [2+2] cycloaddition of alkynes with 1,3-dienes could allow the access to 3-vinylcyclobutenes if the cycloaddition reaction takes place selectively with only one of the double bonds of the diene (Scheme 2.7). In the case of isoprene (**10a**), the cycloaddition with 1,3-enynes **6a-b** led to 1,3-divinylcyclobutenes **8z-aa** by the selective addition to the most substituted double bond of **10a**, although the isolated yields were low (14-19%). Better results were obtained in the reaction of phenylacetylene (**9a**) with 1,3-butadienes **10a-b** at 50 ºC to form the corresponding 3-vinylcyclobutenes **8ab-ac** in 57-68% yield.

Likewise, in the reaction of phenylacetylene (**9a**) with limonene (**10c**) and β-caryophyllene (**10d**), which are 1,5-dienes related to natural products, cyclobutenes **8ad** (1:1 dr) and **8ae** were isolated, respectively, as a result of the selective cycloaddition of only one alkene of the diene (Scheme 2.8). In the case of **10c**, the reaction occurred at the most accessible disubstituted terminal alkene, whereas for **10d**, the reaction took place at the most nucleophilic trisubstituted alkene.

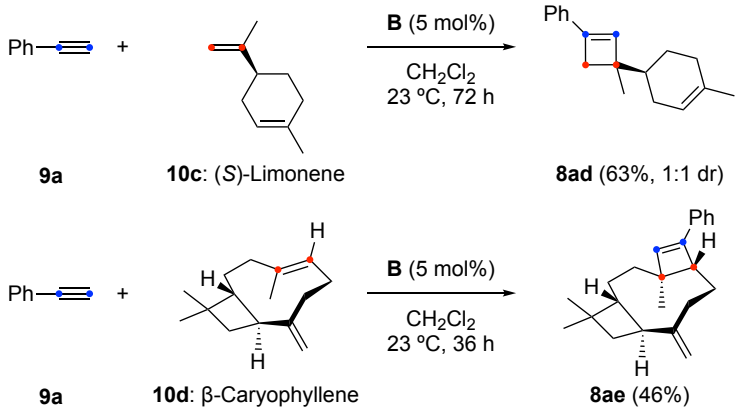

Scheme 2.8. Selective Gold(I)-Catalyzed [2+2] Cycloaddition Reaction of 1,5-Dienes **10c** and **10d** (Alkyne:diene in a 1:2 ratio).

Reaction of Alkynes with Cycloheptatriene

The gold(I)-catalyzed reaction of phenylacetylene (**9a**) with cycloheptatriene (**11a**) led to a totally different outcome. Instead of a [2+2] cycloaddition, a [6+2] cycloaddition was found to take place to give the bicyclic compound **12** (Table 2.3).

Table 2.3. Optimization of the reaction of **9a** with **11a** using different catalysts.

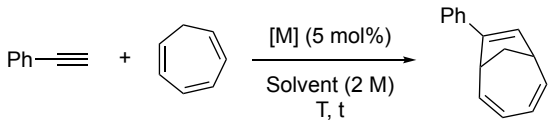

9a **11a** **12**

Entry	[M]	Solvent	T (ºC)	t (h)	**12** (%)[a]
1	**A**	CH_2Cl_2	50	16	4
2	**B**	CH_2Cl_2	50	16	2
3	**C**	CH_2Cl_2	50	16	13[b]
4	**D**	CH_2Cl_2	50	16	0
5	**E**	CH_2Cl_2	50	16	0
6	**F**	CH_2Cl_2	50	16	10
7	**H**	CH_2Cl_2	50	16	12
8	**A**	DCE	80	24	18
9	**B**	DCE	80	24	22
10	**C**	DCE	80	24	31[b]
11	**D**	DCE	80	24	0
12	**E**	DCE	80	24	16
13	**F**	DCE	80	24	17
14	**G**	DCE	80	24	traces
15	**H**	DCE	80	24	17
16	AuCl	DCE	80	24	0
17	$PtCl_2$	DCE	80	24	0

[a] Alkyne:Triene in a 1:5 ratio. Determined by ^1H NMR using 1,4-diacetylbenzene as internal standard. [b] Isolated yield.

Interestingly, this type of [6+2] cycloaddition reaction with cycloheptatriene (**11a**) had been reported before using cobalt, rhodium, titanium, molybdenum and platinum catalysis.[116] The cobalt-catalyzed strategy was recently applied to furnish the skeleton of the natural products echinopines.[117]

When we performed the reaction of **9a** with **11a** in a 1:5 ratio in the presence of gold(I)-catalysts **A-H** at 50 ºC (Table 2.3, entries 1-7), only traces or poor yields of the cycloadduct **12** could be observed. By heating at 80 ºC, the same catalysts provided slightly better yields (Table 2.3, entries 8-15), whereas AuCl and $PtCl_2$ did not promote the transformation (Table 2.3, entries 16-17). Among these results, the highest yield (31%) was obtained with catalyst **C** at 80 ºC (Table 2.3, entry 10).

Thus, we continued optimizing the conditions using phosphine-based catalyst **C** (Table 2.4). Decreasing the reaction temperature to 23 ºC (Table 2.4, entry 1-2) or increasing it up to 100 ºC (Table 2.4, entry 3) resulted in lower yields of the desired product. Whilst an excess of alkyne showed to be detrimental for the yield (Table 2.4, entry 4), higher excess of the cycloheptatriene gave the same 30% yield (Table 2.4, entry 5). Modifications in the concentration (Table 2.4, entries 8-13) and catalyst loading (Table 2.4, entries 14-15) did not affect significantly the yield. We tested neat (Table 2.4, entries 6-7) and anhydrous conditions (Table 2.4, entry 16), as well as the addition of 4 Å molecular sieves (Table 2.4, entry 17), although poorer yields were achieved in these cases.

116. Under cobalt catalysis: (a) Achard, M.; Tenaglia, A.; Buono, G. *Org. Lett.* **2005**, *7*, 2353–2356. (b) Toselli, N.; Martin, D.; Achard, M.; Tenaglia, A.; Bürgi, T.; Buono, G. *Adv. Synth. Catal.* **2008**, 350, 280–286. (c) Hilt, G.; Paul, A.; Hengst, C. *Synthesis* **2009**, 3305–3310. Under rhodium catalysis: (d) Zhang, X.; Wang, J.; Zhao, H.; Zhao, H.; Wang, J. *Organometallics* **2013**, *32*, 3529–3536. Under titanium catalysis: (e) D'yakonov, V. A.; Kadikova, G. N.; Kolokol'tsev, D. I.; Ramazanov, I. R.; Dzhemilev, U. M. *Eur. J. Org. Chem.* **2015**, 4464–4470. (f) Mach, K.; Antropiusová, H.; Petrusová, L.; Hanuš, V.; Tureček, F.; Sedmera, P. *Tetrahedron* **1984**, *40*, 3295–3302. Under molybdenum catalysis: (g) Bourner, D. G.; Brammer, L.; Green, M.; Moran, G.; Orpen, A. G.; Reeve, C.; Schaverien, C. J. *J. Chem. Soc., Chem. Commun.* **1985**, *20*, 1409–1411. Intramolecular version under platinum catalysis: (h) Tenaglia, A.; Gaillard, S. *Angew. Chem. Int. Ed.* **2008**, *47*, 2454–2457.
117. Dorel, R.; Echavarren, A. M. *J. Org. Chem.* **2016**, *81*, 8444−8454.

Table 2.4. Optimization of the reaction of **9a** with **11a** using catalyst **C**.

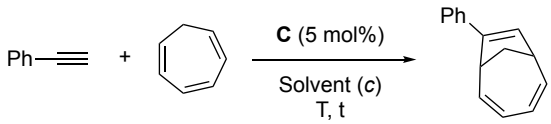

9a **11a** **12**

Entry	**C** (mol %)	**9a**:**11a**	Solvent	*c* (M)	T (ºC)	T	**12** (%)[a]
1	5	1:5	**CH_2Cl_2**	2.0	**23**	7 d	15
2	5	1:5	DCE	2.0	**50**	16 h	18
3	5	1:5	DCE	2.0	**100**	24 h	18
4	5	**5:1**	DCE	2.0	80	24 h	traces
5	5	**1:10**	DCE	2.0	80	24 h	30
6	**1**	**1:2**	**-**	**-**	80	24 h	traces
7	**1**	**2:1**	**-**	**-**	80	24 h	traces
8	5	**1:2**	DCE	**0.2**	80	24 h	18
9	5	**2:1**	DCE	**0.2**	80	24 h	17
10	5	1:5	DCE	**0.5**	80	24 h	26
11	5	1:5	DCE	**1.0**	80	24 h	27
12	5	1:5	DCE	**4.0**	80	24 h	27
13	5	1:5	DCE	**10**	80	24 h	22
14	**2**	1:5	DCE	2.0	80	24 h	22
15	**10**	1:5	DCE	2.0	80	24 h	26
16	5	1:5	DCE	2.0	80	24 h	20[b]
17	5	1:5	DCE	2.0	80	24 h	23[c]

[a] Determined by ^{1}H NMR using 1,4-diacetylbenzene as internal standard. [b] Using dry solvent, under argon. [c] Using 4 Å molecular sieves.

All in all, under the best conditions found, the reaction of alkyne **9a** and cycloheptatriene (**11a**) produced the cycloadduct **12** in a 31% isolated yield (Scheme 2.9). In contrast, under the same conditions, gold(I) promotes the overall *anti*-nucleophilic attack of cycloheptatriene (**11a**) to methyl propiolate (**9b**) to give *Z*-configured adduct **13** in a 57% yield.[118] These examples highlight the very different reactivity of alkynes bearing electron-

118. See Introduction to **Chapter 3** for comments on the hydroarylation of propiolates with arenes leading to the same *Z*-selectivity.

donating and electron-withdrawing groups in the presence of gold(I), which was also discussed in **Chapter 1**.[106,118]

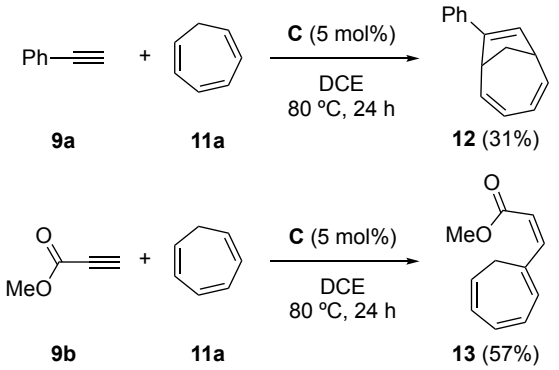

Scheme 2.9. Gold(I)-catalyzed reaction of alkynes **9a,b** with cycloheptatriene (**11a**) (Alkyne:triene in a 1:5 ratio).

Combining Cyclobutenes with Gold(I) Carbenes to Give Cyclopentenes

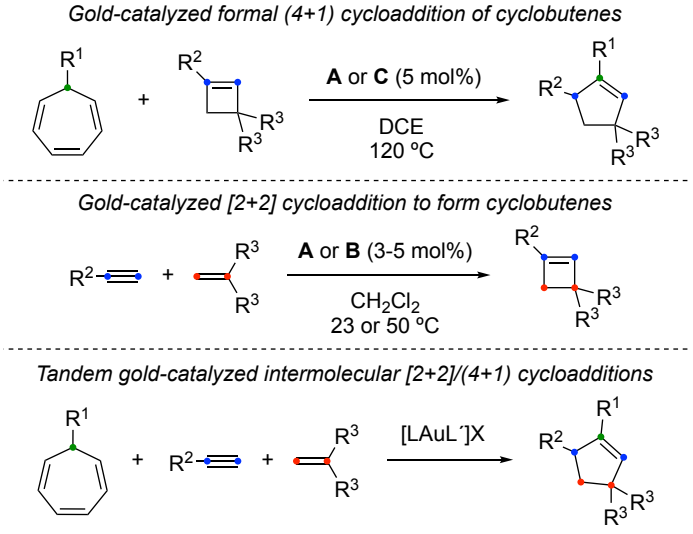

Scheme 2.10. Tandem gold-catalyzed [2+2]/(4+1) cycloadditions towards cyclopentenes.

Concerning cycloheptatrienes, our group previously reported the generation of gold(I) carbenes by retro-Buchner reaction of 7-substituted 1,3,7-cycloheptatrienes and their

application in a formal (4+1) cycloaddition with cyclobutenes to construct cyclopentenes (see Introduction to this **Chapter 2**). Gold(I)-catalysts **A** or **C** bearing a biphenylphosphine ligand were key for the success of this reaction, which is also generally the type of catalyst required for the intermolecular [2+2] cycloaddition of alkynes with alkenes to form cyclobutenes. Hence, we reasoned that both transformations could be combined for the development of the intermolecular [2+2]/(4+1) cycloadditions of alkynes, alkenes and cycloheptatrienes to give cyclopentenes in a one-pot manner (Scheme 2.10).

In gold(I)-catalyzed intermolecular reactions between alkynes and alkenes, an excess of alkene is often employed to favor the process. However, in this one-pot [2+2]/(4+1) cycloadditions, if an excess of alkyne or alkene is used for the initial [2+2] cycloaddition, the gold(I) complex could coordinate to the remaining starting material instead of catalyzing the subsequent (4+1) cycloaddition. In order to study the effect of the excess of the substrates in the (4+1) cycloaddition, the reaction of cycloheptatriene derivative **11b** with cyclobutene **8af** was performed in the presence of 0.5 equiv of alkyne **9a** or alkene **7a** (Scheme 2.11). The excess of alkyne proved to hamper the cycloaddition, whereas the excess of alkene did not prevent the reaction from occurring.

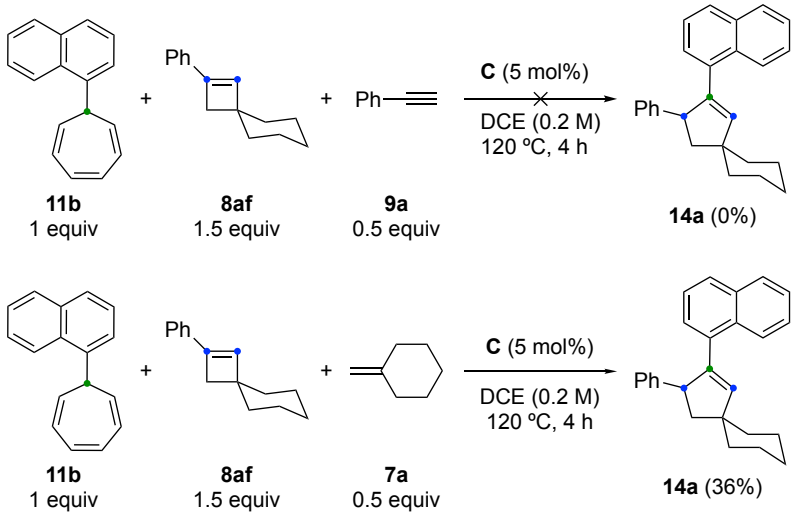

Scheme 2.11. Effect of the excess of alkyne or alkene in the (4+1) cycloaddition of **11b** with **8af**.

Regarding the reaction temperature, the gold(I)-catalyzed intermolecular [2+2] cycloaddition of alkynes with alkenes to give cyclobutenes occurs smoothly at 23 or 50 ºC, while the generation of gold(I)-cabenes from 7-substituted cycloheptatrienes requires normally 120 ºC.

Taking into account these details, we started to optimize the reaction conditions by testing different methods to set up the one-pot transformation (Table 2.5). For this, we employed the catalysts **A**, **C** and **E** that provided better yields in the [2+2] and formal (4+1) cycloaddition reactions separately.[64b,115]

- *Method I:* Cycloheptatriene **11b**, alkyne **9c** and alkene **7a** were dissolved in DCE in a vial. Catalyst was added, the vial was sealed and the resulting mixture was stirred at 50 ºC for 19 h and then, at 120 ºC for 3 h.
- *Method II:* Alkyne **9c** and alkene **7a** were dissolved in DCE in a vial. Catalyst was added, the vial was sealed and the resulting mixture was stirred at 50 ºC for 19 h. Cycloheptatriene **11b** was then added, the vial was sealed again and the mixture was stirred at 120 ºC for 3 h.
- *Method III:* Cycloheptatriene **11b**, alkyne **9c** and alkene **7a** were dissolved in DCE in a vial. Catalyst was added, the vial was sealed and the resulting mixture was stirred at 120 ºC for 4 h.
- *Method IV:* Alkyne **9c** and alkene **7a** were dissolved in DCE in a vial. Catalyst was added, the vial was sealed and the resulting mixture was stirred at 50 ºC for 14 h. The volatiles were removed under vacuum, DCE and cycloheptatriene **11b** were added, the vial was sealed again and the mixture was stirred at 120 ºC for 4 h.
- *Method V:* Cycloheptatriene **11b**, alkyne **9c** and alkene **7a** were dissolved in DCE in a vial. Catalyst was added, the vial was sealed and the resulting mixture was stirred at 50 ºC for 14 h. The volatiles were removed under vacuum, DCE was added, the vial was sealed again and the mixture was stirred at 120 ºC for 4 h.

Comparing the methods I and II with the different catalysts (Table 2.5, entries 1-6), complex **A** gave slightly higher yields of the desired cyclopentane **14b**, although still less than 20%. Using both catalysts **A** and **C** at the same time, the optimal for the [2+2] cycloaddition and for the formal (4+1) cycloaddition, respectively, the yield could not be improved (Table 2.5, entry 7). Among all the methods employing catalyst **A** (Table 2.5,

entries 3-4 and 8-10), the methods IV and V resulted in a better 36% yield of **14b** (Table 2.5, entries 9-10).

Table 2.5. Screening of methods and catalysts for the reaction between **11b**, **9c** and **7a**.[a]

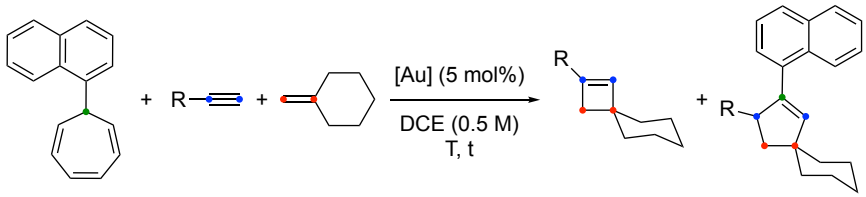

11b **9c** **7a** **8ag** **14b**

Entry	Method	[Au]	Recovered **11b** (%)[b]	**8ag** (%)[b]	**14b** (%)[b]
1	**I**	**C**	46	20	2
2	**II**	**C**	40	39	0
3	**I**	**A**	20	26	14
4	**II**	**A**	16	25	18
5	**I**	**E**	20	12	13
6	**II**	**E**	21	17	10
7	**I**	**C+A**[c]	24	16	18
8	**III**	**A**	10	12	18
9	**IV**	**A**	3	0	36
10	**V**	**A**	traces	traces	36

[a] R = *p*-*t*BuC_6H_4. Cyclohepatriene **11b**: Alkyne **9c**: Alkene **7a** in a 1:1:1 ratio. [b] Determined by ^{1}H NMR using diphenylmethane as internal standard. [c] 2.5 mol% of each catalyst.

Employing the method corresponding to the most convenient set-up (method III, Table 2.5, entry 8) and the method giving the highest yield of cyclopentene (method V, Table 2.5, entry 10), further screenings of the reaction conditions were performed (Tables 2.6 and 2.7).

In the case of method III, regardless the variations in the stoichiometry of the substrates (Table 2.6, entries 1-3), concentration (Table 2.6, entries 4-7), temperature (Table 2.6, entries 8-9) or catalyst loading (Table 2.6, entries 10-11), similar low yields of **14b** within the range from 13 to 29% were obtained.

Table 2.6. Screening of conditions for the reaction between **11b**, **9c** and **7a** using method III.

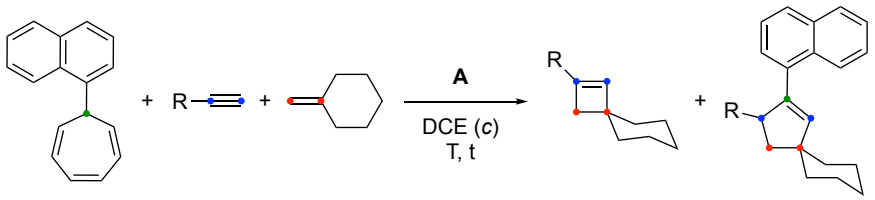

11b **9c** **7a** **8ag** **14b**

Entry	**11b**:**9c**:**7a**	**A** (mol%)	*c* (M)	T (ºC)	t (h)	Recovered **11b** (%)[a]	**8ag** (%)[a]	**14b** (%)[a]
1	**1:2:2**	5	0.5	120	6	18	51	16
2	**1:1.5:2**	5	0.5	120	6	14	41	14
3	**1:1:2**	5	0.5	120	6	14	30	13
4	1:1:1	5	**0.1**	120	6	6	12	20
5	1:1:1	5	**0.2**	120	6	5	11	23
6	1:1:1	5	**1.0**	120	6	3	7	26
7	1:1:1	5	**2.0**	120	6	6	5	24
8	1:1:1	5	0.5	**110**	8	17	17	22
9	1:1:1	5	0.5	**100**	13	22	20	17
10	1:1:1	**3**	**1.0**	120	6	13	11	20
11	1:1:1	**10**	**1.0**	120	6	0	traces	29

[a] R = *p*-*t*BuC_6H_4. Determined by ^{1}H NMR using diphenylmethane as internal standard.

In contrast, following the method V, the ratio of the substrates has an important impact on the yield of the desired cyclopentene **14b** (Table 2.7, entries 1-3), since adding 1.5 or 2 equiv of the alkyne and 2 equiv of the alkene provided a better 44% yield. Moreover, increasing the catalyst loading up to 10% (Table 2.7, entries 1-6), a 58% isolated yield of **14b** was achieved. Variations in the concentration or reaction times (Table 2.7, entries 7-11), did not lead to higher yields of **14b**.

Table 2.7. Screening of conditions for the reaction between **11b**, **9c** and **7a** using method V**.**

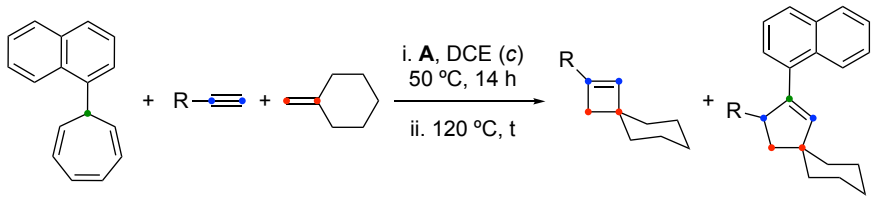

11b **9c** **7a** **8ag** **14b**

Entry	**11b**:**9c**:**7a**	**A** (mol%)	*c* (M)	t (h)	Recovered **11b** (%)[a]	**8ag** (%)[a]	**14b** (%)[a]
1	**1:3:3**	5	0.5	4	0	47	23
2	**1:2:2**	5	0.5	4	traces	22	44
3	**1:1.5:2**	5	0.5	4	traces	6	43
4	1:1.5:2	**10**	0.5	4	0	traces	58[b]
5	1:1.5:2	**7**	0.5	4	0	7	41
6	1:1.5:2	**3**	0.5	4	7	7	35
7	1:1.5:2	5	**M**[c]	4	9	28	36
8	1:1.5:2	5	0.5	**2.5**	3	20	44
9	1:1.5:2	5	0.5	**1**	17	44	39
10	1:1.5:2	**10**	0.5	**2.5**	0	traces	48
11	1:1.5:2	**10**	**1.0**	**2.5**	0	10	46

[a] R = *p*-*t*BuC$_6$H$_4$. Determined by ^{1}H NMR using diphenylmethane as internal standard. [b] Isolated yield. [c] Concentration at 50 ºC was 2.0 M and at 120 ºC, 0.2 M.

Thus, we concluded that the optimal conditions are obtained with method V, with 1:1.5:2 cycloheptatriene/alkyne/alkene ratio and catalyst **A** in a 10 mol%. In this manner, following method V, after performing the [2+2] cycloaddition of the alkynes **9a-d** with the alkene **7a** at 50 ºC to give rise the corresponding cyclobutenes, the temperature was raised to 120 ºC to allow the generation of the gold(I)-carbene from cycloheptatrienes **11b-c** to finally render the cyclopentene products **14a-c** in moderate yields in a one-pot process (Scheme 2.12). The reaction tolerated different substituents in the aryl groups of the cycloheptatriene derivative and the alkyne, whereas different alkenes such as α-methylstyrene or 2,3-dimethyl-2-butene led to complex mixtures of products.

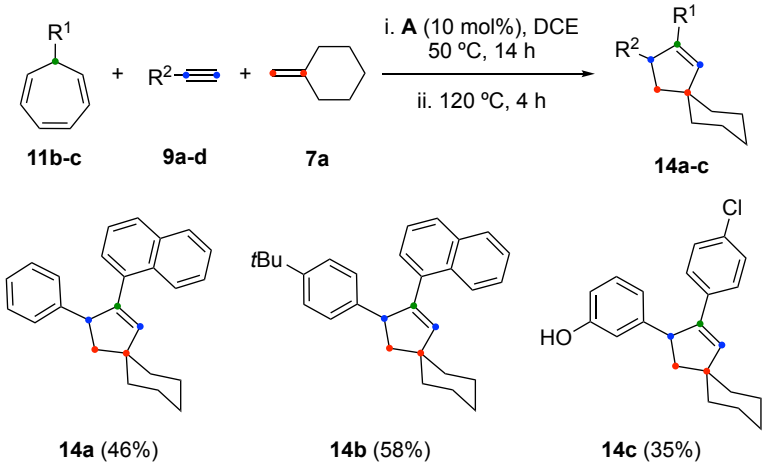

Scheme 2.12. One-pot gold(I)-Catalyzed [2+2]/(4+1) cycloadditions of alkynes, alkenes and cycloheptatrienes (Cycloheptatriene:alkyne:alkene in a 1:1.5:2 ratio).

Our group recently reported the generation of vinyl gold(I) carbenes from 7-vinyl substituted cycloheptatrienes at 75-100 ºC, and their application in the *cis*-vinylcyclopropanation of alkenes[119] or in the reaction with allenes to form cyclopentadienes.[120] We decided to explore the reaction of such vinyl gold(I) carbenes with the cyclobutenes. Surprisingly, when we performed the reaction of vinylcycloheptatriene **11d** with cyclobutene **8ag** under the usual conditions for these transformations, the expected cyclopentene **14d** was obtained together with another type of cyclopentene **15d** in 54% yield in a 1:1 ratio (Scheme 2.13). According to the mechanism of these transformations (see Introduction to this **Chapter 2**), after the cyclopropanation of the cyclobutene with the gold(I) carbene **Id** to form the bicyclic intermediate **IId**, gold(I)-promoted cyclopropane opening led to benzylic carbocation **IIId**. Thus, the formation of **14d** and **15d** could be rationalized by a 1,2-H or 1,2-vinyl shift, respectively, in the same tertiary carbocation intermediate **IIId**. The formal 1,2-vinyl shift could occur in a one-step (red pathway, Scheme 2.13) or in a stepwise manner through **Vd** (green pathway, Scheme 2.13).

119. Herlé, B.; Holstein, P. M.; Echavarren, A. M. *ACS Catal.* **2017**, *7*, 3668−3675.
120. Yin, X.; Mato, M.; Echavarren, A. M. *Angew. Chem. Int. Ed.* **2017**, *56*, 14591–14595.

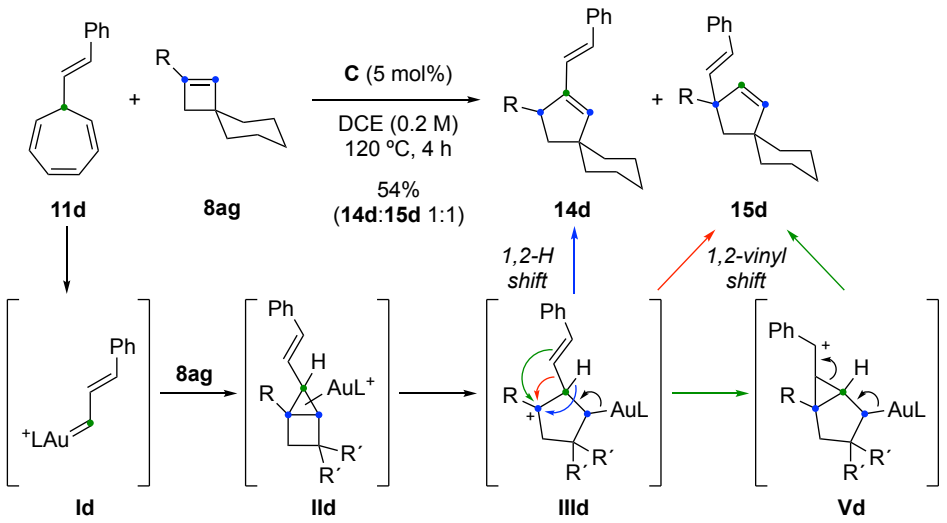

Scheme 2.13. Gold(I)-catalyzed reaction of **11d** and **8ag** to form cyclopentenes **14d** and **15d** (R = *p*-*t*BuC$_6$H$_4$. **11d**:**8ag** in a 1:2 ratio).

Interestingly, cyclopentenes of type **15d** had never been observed before in the reactions of gold(I)-carbenes with cyclobutenes. Hence, we became interested in optimizing the reaction conditions to obtain selectively each product **14** and **15** (Table 2.8). Neither the yield nor the ratio of the cyclopentane products were found to be influenced by a decrease in the reaction temperature (Table 2.8, entries 2-4). Although NHC-based catalyst **E** provided the same 1:1 ratio of products as **C** (Table 2.8, entries 5-6), catalyst **A** bearing a bulkier phosphine ligand generated cyclopentanes **14d**:**15d** in a 1:2.7 ratio. Therefore, we focused on using **A** in order to attain greater selectivity towards **15d**. Lower concentrations such as 0.05 or 0.1 M gave slightly better results than 0.5 or 1 M (Table 2.8, entries 8-11). Among the tested solvents, DCE proved to be the best choice (Table 2.8, entries 12-16). By modifying the catalyst loading (Table 2.8, entries 17-18), decreasing the temperature to 100 ºC (Table 2.8, entries 12-16) or reducing the reaction time (Table 2.8, entries 20-21), the yield and the ratio of the products remained unaltered. Finally, adding an excess of either vinylcycloheptatriene **11d** or cyclobutene **8ag**, using the optimal 0.1 M concentration, the inseparable mixture of cyclopentenes **14d** and **15d** was obtained in 56-58% yield in a 1:3.3-4 ratio.

Table 2.8. Optimization of the reaction between **11d** and **8ag** catalyzed by gold(I).

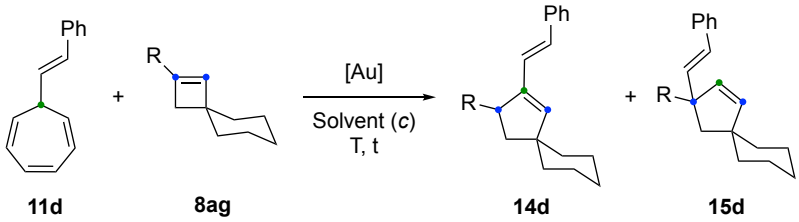

11d **8ag** **14d** **15d**

Entry	[Au]	[Au] (mol%)	**11d**:**8ag**	T (ºC)	t (h)	*c* (M)	Solvent	**14d** (%)[a]	**15d** (%)[a]
1	**C**	5	**1:2**	120	**4**	0.2	DCE	54 (1:1)[b]	
2	**C**	5	1:1	**100**	**4**	0.2	DCE	26	20
3	**C**	5	1:1	**80**	**24**	0.2	DCE	21	20
4	**C**	5	1:1	**60**	**24**	0.2	DCE	21	19
5	**C**	5	1:1	120	2	0.2	DCE	22	18
6	**E**	5	1:1	120	2	0.2	DCE	22	20
7	**A**	5	1:1	120	2	0.2	DCE	14	38
8	**A**	5	1:1	120	2	**0.05**	DCE	9	38
9	**A**	5	1:1	120	2	**0.1**	DCE	11	38
10	**A**	5	1:1	120	2	**0.5**	DCE	10	30
11	**A**	5	1:1	120	2	**1.0**	DCE	12	28
12	**A**	5	1:1	120	2	0.2	**PhMe**	13	19
13	**A**	5	1:1	120	2	0.2	**EtOAc**	17	20
14	**A**	5	1:1	120	2	0.2	**PhCl**	15	26
15	**A**	5	1:1	120	2	0.2	**TCA**[c]	10	26
16	**A**	5	1:1	120	2	0.2	**TeCA**[d]	-	-
17	**A**	**10**	1:1	120	2	0.2	DCE	11	37
18	**A**	**2**	1:1	120	2	0.2	DCE	10	31
19	**A**	5	1:1	**100**	**5.5**	0.2	DCE	12	38
20	**A**	5	1:1	120	**1**	0.2	DCE	12	38
21	**A**	5	1:1	120	**3**	0.2	DCE	11	32
22	**A**	5	**1:2**	120	2	**0.1**	DCE	56 (1:3.3)[b]	
23	**A**	5	**2:1**	120	2	**0.1**	DCE	58 (1:4)[b]	

[a] R = *p*-*t*BuC_6H_4. Determined by ^{1}H NMR using ethylene carbonate as internal standard. [b] Isolated yield. [c] TCA = 1,1,2-Trichloroethane. [d] TeCA = 1,1,2,2-Tetrachloroethane.

Table 2.9. Gold(I)-catalyzed reaction of cyclobutene **8ag** with vinylcycloheptatrienes **11d-f**.[a]

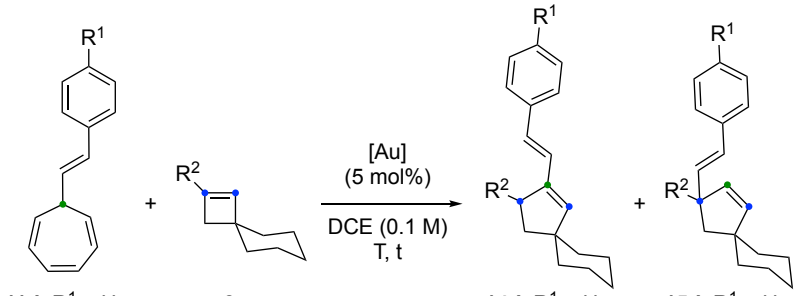

11d: R^1 = H
11e: R^1 = Br
11f: R^1 = OMe

8ag

14d: R^1 = H
14e: R^1 = Br
14f: R^1 = OMe

15d: R^1 = H
15e: R^1 = Br
15f: R^1 = OMe

Entry	R^1	[Au]	T (ºC)	T (h)	Yield (%)[b]	**14**:**15**[d]
1	Br	**A**	120	3	56	1:2
2	Br	**C**	120	3	56	2:1
3	H	**A**	120	3	55	1:3
4	H	**C**	120	3	54	3:2
5	OMe	**A**	120	3	37	1:9
6	OMe	**C**	120	3	35	1:2
7	OMe	**A**	23	72	traces[c]	-
8	OMe	**A**	50	18	12[c]	0:1
9	OMe	**A**	75	18	32	1:9

[a] R^2 = *p*-*t*BuC_6H_4. Cycloheptatriene:cyclobutene in a 1:2 ratio. [b] Isolated yields. [c] Determined by ^{1}H NMR using ethylene carbonate as internal standard. [d] **14**:**15** ratio determined by ^{1}H NMR.

We then studied the electronic effects of the styryl migrating group by performing the reaction of **8ag** with styrylcycloheptatrienes **11d-f** possessing different *p*-substituents under the same optimal conditions (Table 2.9). We observed that regardless the catalyst used, electron-rich substituents on the styryl moiety of **11d-f** favor the 1,2-styryl shift and, consequently, higher selectivity towards the cyclopentene **15d-f** are reached (Table 2.9, entries 1-6). Comparing the performance of catalysts **A** and **C**, we discovered that in all the cases **A** favors the formation of **15d-f** (Table 2.9, entries 1, 3 and 5), whereas the less sterically hindered complex **C** provokes the generation of **14d-f** in a greater extent (Table 2.9, entries 2, 4 and 6). Thus, the best selectivity for **15** was obtained in the reaction with *p*-methoxy derivative **11f** and catalyst **A**, in which the cyclopentenes **14** and **15** were formed

in a 1:9 ratio (Table 2.9, entry 5). The selectivity could not be further improved by diminishing the temperature to 75 ºC (Table 2.9, entries 7-9).

We also examined the reactivity of 1-vinylcylobutene **8s** with gold(I)-carbenes generated from styrylcycloheptatrienes **11d** and **11f** (Scheme 2.14). In both cases, a complex mixture of products was delivered. However, in the reaction of **8s** with arylcycloheptatriene **11b** we could isolate the corresponding cyclopentene **14g** in a 50% yield along with small amounts of an unidentified product (Scheme 2.14).

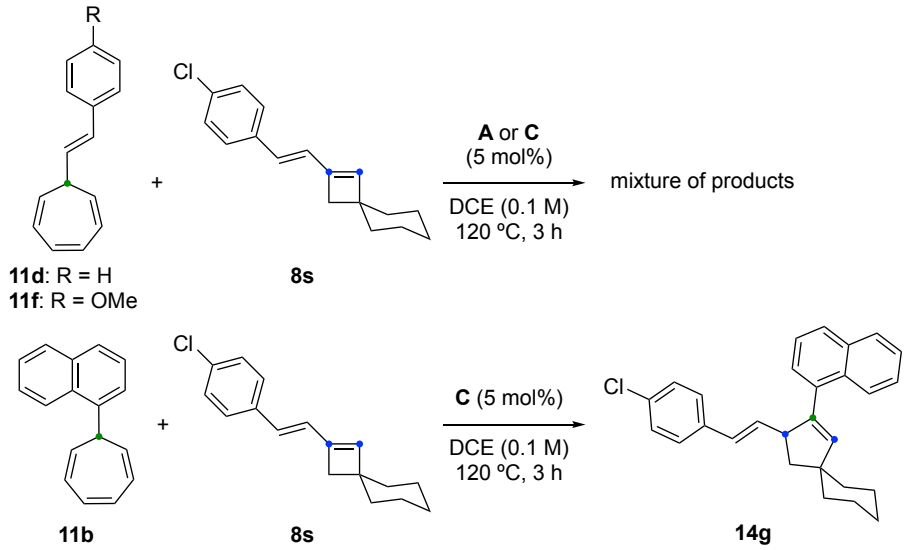

Scheme 2.14. Reaction of 1-vinylcyclobutene **8s** with gold(I)-carbenes generated from cycloheptatrienes (cycloheptatriene:cyclobutene 1:1.5).

Transformations of Cyclobutenes by Cycloaddition or Ring Opening

As expected, 1-vinylcyclobutenes **8a** and **8s** underwent Diels-Alder cycloaddition with maleic anhydride (**16**) to give penta- or tetracyclic compounds **17a** and **17b**, respectively, which contain a fused tricyclic core related to the protoilludane family of natural products (Scheme 2.15). Thus, complex architectures were obtained in two steps by [2+2]/Diels Alder cycloadditions from simple starting materials such as 1,3-enynes, alkenes and maleic anhydride. Similar transformations of 1-alkenylcyclobutenes into distinct protoilludane

skeleton derivatives have been previously reported, and some derivatives showed biological activity.[57,110a]

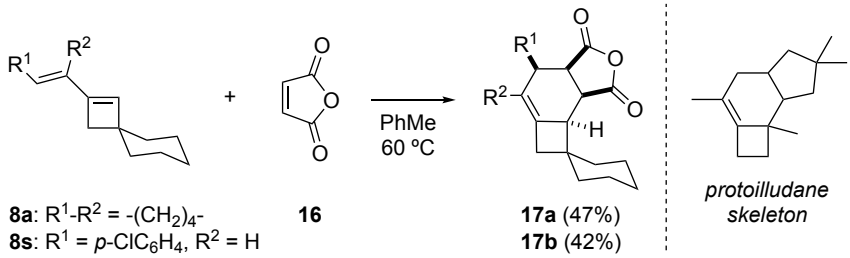

Scheme 2.15. Access to fused polycyclic skeletons **17** by Diels-Alder of vinylcyclobutenes (Cyclobutene:maleic anhydride in a 1:2 ratio).

Since this Diels-Alder cycloaddition proceeded slowly and in moderate yields at 60 ºC, we screened higher temperatures (75 and 90 ºC) in the reaction of **8s** with **16**. However, the yield slightly dropped under these conditions (Table 2.10).

Table 2.10. Screening of temperatures in the Diels-Alder reaction of **8s** with **16**.

T (ºC)	t (h)	**17b** (%)
60	7 d	42
75	3 d	39
90	48	31

Apart from that, cyclobutene **8ah** was subjected to different ring opening reactions. Thermal ring opening of **8ah** produced (*E*) and (*Z*)-1,3-dienes **18**, (*E*)-**18** being the major product (Table 2.11).[121] Among the tested solvents and temperatures (Table 2.11, entries 1-3), chlorobenzene at 140 ºC provided a higher 48% yield of a good 7:1 mixture of (*E*) and (*Z*)-**18** (Table 2.11, entry 2). By further decrease of the concentration (Table 2.11, entries 4-6), the (*E*) and (*Z*)-dienes **18** could be obtained in a better 9:1 ratio and 67% yield (Table 2.11, entry 6). No significant changes were observed in the reaction outcome when the thermolysis of cyclobutene **8ah** was performed in the presence of 5 mol% of gold(I)-

121. Recent discussions on the torquoselectivity in the ring opening of cyclobutenes: (a) Boon, B. A.; Green, A. G.; Liu, P.; Houk, K. N.; Merlic, C. A. *J. Org. Chem.* **2017**, *82*, 4613–4624. (b) Barquera-Lozada, J. E. *J. Phys. Chem. A* **2016**, 120, 8450−8460.

catalyst **A**, as the (*E*) and (*Z*)-1,3-dienes **18** were obtained in a 8:1 ratio and 68% yield (Table 2.11, entry 7). The high temperatures required for the thermal fragmentation of the cyclobutene **8ah** to give 1,3-dienes are consistent with the high activation energies computed for this transformation (see Scheme 1.21 in **Chapter 1**).

Table 2.11. Ring opening of cyclobutene **8ah** by thermolysis.

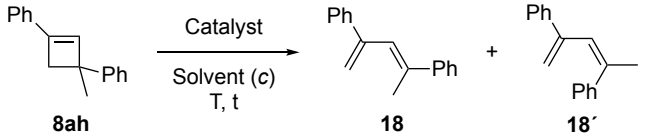

8ah **18** **18´**

Entry	Catalyst (mol%)	Solvent	*c* (M)	T (ºC)	t (h)	Yield (%) (**18:18´**)[a]
1	-	**PhMe**	0.2	**110**	72	40[b] (9:1)
2	-	**PhCl**	0.2	**140**	3	48 (7:1)
3	-	**Mesitylene**	0.2	**160**	3	39 (7:1)
4	-	PhCl	**0.4**	140	3	32 (7:1)
5	-	PhCl	**0.1**	140	3	67 (6:1)
6	-	PhCl	**0.05**	140	7	67[b] (9:1)
7	**A** (5)	PhCl	**0.05**	140	8	68[b] (8:1)

[a] Determined by ^{1}H NMR using diphenylmethane as internal standard. [b] Isolated yields.

Table 2.12. Ring opening of cyclobutene **8ah** by oxidative cleavage.

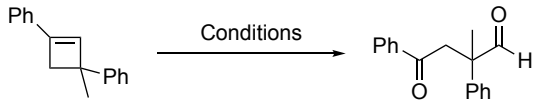

8ah **19**

Entry	Conditions	**19** (%)[a]
1	i. O_3, CH_2Cl_2, -23 ºC, 20 min. ii. Me_2S (3 equiv), CH_2Cl_2, 23 ºC, 22 h.	55
2	$RuO_2 \cdot H_2O$ (10 mol%), $NaIO_4$ (4 equiv), $CHCl_3/H_2O$, 23 ºC, 18 h.[122a]	37
3	i. OsO_4 (3 mol%), NMO (2.4 equiv), Acetone/H_2O, 23 ºC, 5 h. ii. $NaIO_4$ (4.4 equiv), Acetone/H_2O, 23 ºC, 2 h.	85

[a] Isolated yields.

In addition, the oxidative cleavage of the double bond of **8ah** delivered the corresponding dicarbonyl compound **19** (Table 2.12).[122] Ozonolysis or treatment with $RuO_2 \cdot H_2O/NaIO_4$ led to **19** in moderate yields (Table 2.12, entries 1-2). In contrast, using OsO_4 followed by $NaIO_4$, product **19** was generated in a 85% yield (Table 2.12, entry 3).

Turning Cyclobutenes into 2,3-Dihydrofurans

Cyclobutene **8ah** was successfully converted into 2,3-dihydrofuran **22a** *via* epoxidation to **20** and subsequent opening of the epoxide (Scheme 2.16). The epoxidation of the cyclobutene **8ah** was achieved in excellent yield with dimethyldioxirane either previously prepared (Conditions C in Scheme 2.16) or generated *in situ* (Conditions D in Scheme 2.16). In these cases, the corresponding diastereomeric epoxides were formed in a 1:3 ratio. In contrast, the epoxides **20** were obtained from **8ah** in low yields and in a 1:1 diastereomeric ratio by using H_2O_2 under the conditions reported for related transformations[123] (Conditions F in Scheme 2.16) or utilizing peroxyacetic acid in the presence of an excess of Na_2CO_3 (Conditions E in Scheme 2.16).

However, cyclopropanecarboxaldehyde **21** was produced in a 30% yield by treatment of **8ah** with more acidic conditions involving peroxyacetic acid in the presence of catalytic amounts of Na_2CO_3 (Conditions A in Scheme 2.16) or *m*CPBA (Conditions B in Scheme 2.16). By submitting the epoxides **20** to a 10% aqueous solution of HCl, cyclopropanecarboxaldehyde **21** was obtained in moderate yields, which was then transformed into 2,3-dihydrofuran **22a** in the presence of a Lewis acid (Conditions G in Scheme 2.16).[124] When **21** was heated at 80 ºC in $CDCl_3$, the formation of 2,3-dihydrofuran **22a** was also observed, but along with decomposition of the starting material (Conditions

122. Other examples of oxidative cleavage of related cyclobutenes: (a) Masarwa, A.; Fürstner, A.; Marek, I. *Chem. Commun.* **2009**, 5760–5762. (b) Atmaca, U.; Usanmaz, H. K.; Çelik, M. *Tetrahedron Lett.* **2014**, *55*, 2230–2232.
123. Lane, B. S.; Vogt, M.; DeRose, V. J.; Burgess, K. *J. Am. Chem. Soc.* **2002**, *124*, 11946–11954.
124. Selected examples of transformations of cyclopropyl carbonyl compounds into dihydrofurans: (a) Kurita, J.; Sakai, H.; Tsuchiya, T. *Chem. Pharm. Bull.* **1988**, 36, 2887–2896. (b) Honda, M.; Naitou, T.; Hoshino, H.; Takagi, S.; Segi, M.; Nakajima, T. *Tetrahedron Lett.* **2005**, *46*, 7345–7348. (c) Li, C.-W.; Lin, G.-Y.; Liu, R.-S. *Chem. Eur. J.* **2010**, *16*, 5803–5811. (d) Wang, H.; Denton, J. R.; Davies, H. M. L. *Org. Lett.* **2011**, *13*, 4316–4319.

H in Scheme 2.16). More importantly, Lewis acid-catalyzed opening of the epoxide **20** allows direct access to 2,3-dihydrofuran **22a**.

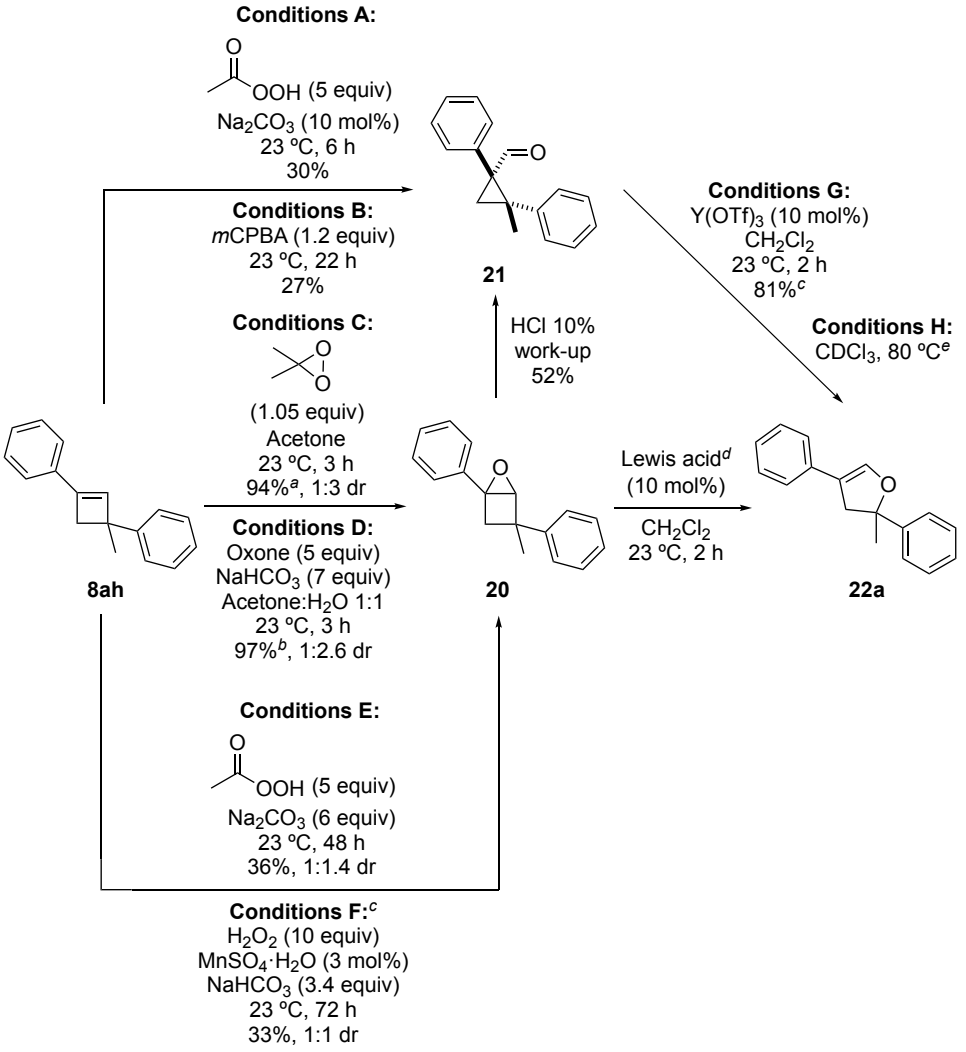

Scheme 2.16. Stepwise synthesis of 2,3-dihydrofuran **22a** from **8ah** (Yields determined by ^{1}H NMR using 1,3,5-trimethoxybenzene as internal standard. Diastereomeric ratio of epoxides (1*R**,3*S**,4*R**)- and (1*R**,3*R**,4*R**)-**20** is indicated. [a] Yield brsm. [b] Isolated yield. [c] Ref. 123. [d] See Table 2.13. [e] Decomposition of **21** was also observed by ^{1}H NMR).

Among all the Lewis acids tested to perform this transformation (Table 2.13), $Y(OTf)_3$ provided the best result (Table 2.13, entry 1), although $Tb(OTf)_3$, $La(OTf)_3$, $Fe(OTf)_3$, $Zn(OTf)_3$ and AuCl gave good yields as well (Table 2.13, entries 2-5 and 8, respectively).

The yield was 15% lower when the catalyst loading was decreased from 10 mol% to 5 or 3 mol% (Table 2.13, entries 19-20).

Table 2.13. Effect of the Lewis acid in the transformation of **8ah** into 2,3-dihydrofuran **22a**.

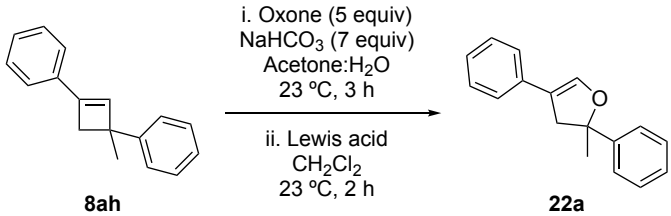

8ah **22a**

Entry	Lewis acid	Lewis acid (mol%)	**22a** (%)[a]
1	$Y(OTf)_3$	10	80[b]
2	$Tb(OTf)_3$	10	75[b]
3	$La(OTf)_3$	10	74[b]
4	$Fe(OTf)_3$	10	71
5	$Zn(OTf)_3$	10	70
6	ZnI_2	10	50
7	$ZnBr_2$	10	47
8	AuCl	10	69[b]
9	$AuCl_3$	10	26
10	Ag(OTf)	10	64
11	$Cu(OTf)_2$	10	55
12	$BiCl_3$	10	52
13	$Bi(OTf)_3$	10	23
14	$Sn(OTf)_2$	10	43
15	$Sc(OTf)_3$	10	31
16	$TiCl_4$	10	42
17	$BF_3 \cdot OEt_2$	10	42
18	*p*-TsOH	10	41
19	$Y(OTf)_3$	5	65
20	$Y(OTf)_3$	3	63

[a] Yields determined by ^{1}H-NMR spectroscopy using 1,3,5-trimethoxybenzene as internal standard. [b] Isolated yield.

Under the optimized conditions, 2,3-dihydrofurans **22a-h** were synthesized in good yields starting from cyclobutenes **8ah-ao** bearing *tert*-butyl, methyl, fluoro, chloro and bromo substituents in the aryl moieties (Table 2.14). Tetramethyl-substituted 2,3-dihydrofuran **22i** was obtained in lower yield.

Table 2.14. Synthesis of 2,3-dihydrofurans **22a-i** from cyclobutenes **8ah-ao**.[a]

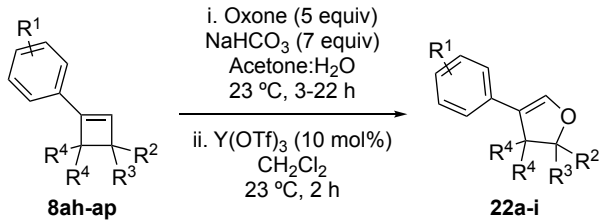

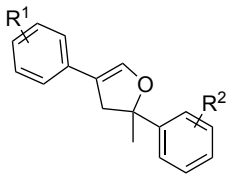

22a: $R^1 = R^2 = H$ (80%)
22b: R^1 = *p*-*t*Bu, $R^2 = H$ (85%)
22c: R^1 = *p*-Br, $R^2 = H$ (61%)
22d: R^1 = *p*-Cl, $R^2 = H$ (72%)
22e: R^1 = *m*-Me, $R^2 = H$ (86%)
22f: R^1 = *m*-Cl, $R^2 = H$ (85%)
22g: R^1 = *p*-*t*Bu, R^2 = *p*-*t*Bu (61%)
22h: $R^1 = H$, R^2 = *p*-F (60%)

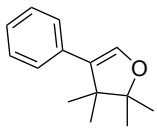

22i (37%)

[a] Isolated yields.

As mentioned in the Introduction to this **Chapter 2**, our group developed the enantioselective version of the intermolecular [2+2] cycloaddition between terminal arylalkynes and alkenes. Thus, we attempted to transform the enantioenriched cyclobutenes **8ah-ao**[125] into enantioenriched 2,3-dihydrofurans **22a-h** by the aforedescribed one-pot process (Table 2.15). Nevertheless, in every case we observed a loss of enantiopurity during the course of the reaction. When we started with cyclobutenes **8ah-ao** exhibiting enantiomeric ratios from 87:13 to 91:9, we obtained 2,3-dihydrofurans **22a-h** showing enantiomeric ratios in the range of 72:23 to 79:21.

We rationalized this reduction of enantiopurity by the mechanism of the Lewis acid-catalyzed conversion of the epoxide to the dihydrofuran (Scheme 2.17). Once the epoxide **VI** is opened, the resulting cyclopropanecarboxaldehyde **VII** is in equilibrium with its carbocationic tautomer **VIII**, in which the C3−C4 bond can rotate. This rotation has a rate

125. Enantioenriched cyclobutenes were provided by Cristina García-Morales and Imma Escofet.

comparable to the intramolecular attack of the oxygen to the stabilized benzylic carbocation, which leads to a diminution of enantiomeric ratio detected in the final 2,3-dihydrofurans.

Table 2.15. Synthesis of enantiomeric enriched 2,3-dihydrofurans **22a-h** from **8ah-ao**.

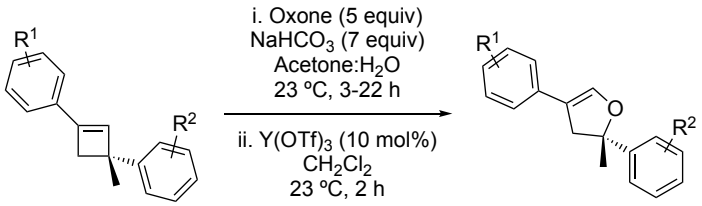

8ah-ao **22a-h**

Entry	R^1	R^2	**8** (er)	**22** (yield, er)[a]
1	H	H	**8ah** (90:10)	**22a** (60%, 72:23)
2	*p*-*t*Bu	H	**8ai** (87:13)	**22b** (71%, 72:28)
3	*p*-Br	H	**8aj** (93:7)	**22c** (61%, 79:21)
4	*p*-Cl	H	**8ak** (93:7)	**22d** (61%, 78:22)
5	*m*-Me	H	**8al** (90:10)	**22e** (64%, 77:23)
6	*p*-*t*Bu	*p*-*t*Bu	**8an** (89:11)	**22g** (44%, 78:22)
7	H	*p*-F	**8ao** (91:9)	**22h** (75%, 74:26)

[a] Isolated yields.

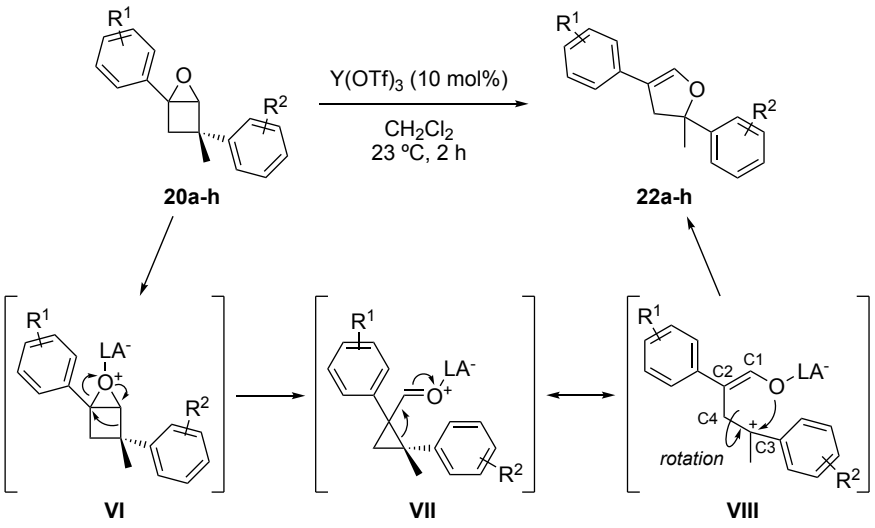

Scheme 2.17. Mechanism of the formation of 2,3-dihydrofurans **22** from epoxides **20**.

Conclusions

In summary, we have achieved the regioselective synthesis of 1-vinyl-3-substituted cyclobutenes by the intermolecular gold(I)-catalyzed [2+2] cycloaddition of 1,3-enynes with alkenes. Regarding the 1,3-enynes, a terminal alkyne is required whereas a variety of aryl or alkyl substituents are tolerated in their alkenyl moiety. The suitable reaction partners proved to be electron-rich di- or tri-substituted alkenes. Hence, this methodology is complementary to the previously reported metal-catalyzed [2+2] cycloadditions to form differently substituted 1-vinylcyclobutenes. Furthermore, selecting the appropriate pair of alkyne and alkene for the gold(I)-catalyzed [2+2] cycloaddition, 3-vinyl- and 3-alkynylcyclobutenes have also been accessed. All in all, the scope of the gold(I)-catalyzed [2+2] cycloaddition of alkynes with alkenes have been successfully broaden (Scheme 2.18).

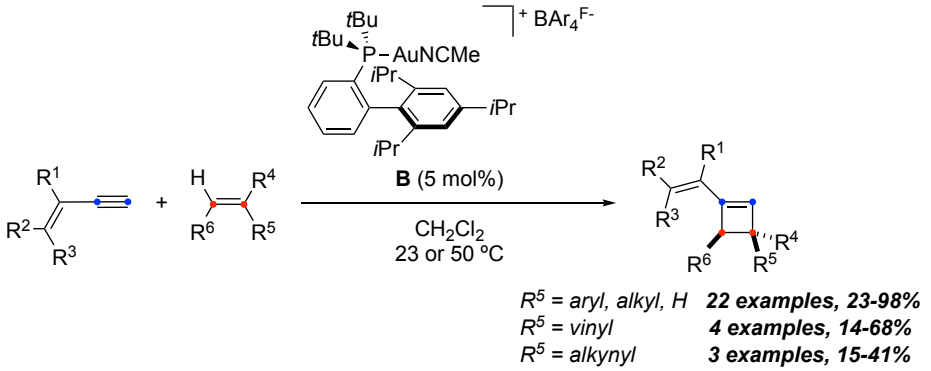

Scheme 2.18. Regioselective synthesis of 1-vinyl, 3-vinyl- and 3-alkynylcyclobutenes by gold(I)-catalyzed [2+2] cycloaddition of alkynes with alkenes.

In addition, we have developed relatively straightforward one-pot transformations of cyclobutenes to construct distinct skeletons such as 1,3-dienes, 1,4-dicarbonyl compounds, 2,3-dihydrofurans, highly substituted cyclopentenes and fused polycyclic structures which are analogous to protoilludane natural product (Scheme 2.19). These processes involved cycloadditions, ring expansions, contractions or scissions in the versatile cyclobutene core.

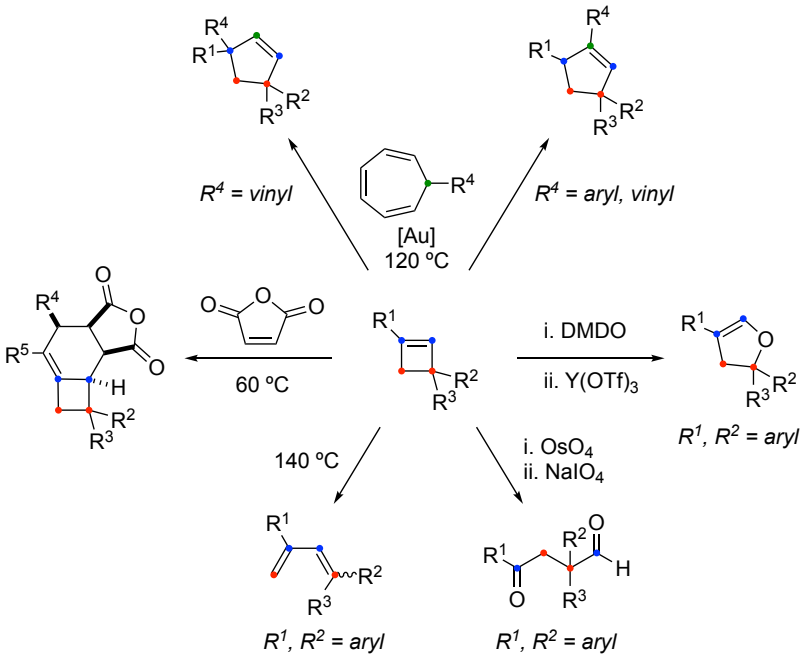

Scheme 2.19. One-pot transformations of cyclobutenes.

Recent Related Results by Other Groups

Very recently, the gold-catalyzed [2+2] cycloaddition to form cyclobutenes has also been extended to the use of chloroalkynes with mono- or 1,2-dialkyl substituted alkenes by the group of Liming Zhang (Scheme 2.20).[126] In contrast with the reactions of terminal alkynes, these reactions proceed at 40 or 60 ºC using a NHC-based gold catalyst, which was generated *in situ* from (IPr)AuCl and $NaBAr_4^F$. In these cases, functionalized 1-chlorocyclobutenes are generated, which have been transformed by cross-coupling reactions of the C(sp^2)−Cl bond to install various scaffolds.

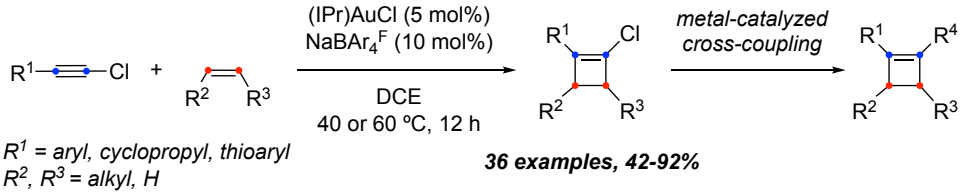

Scheme 2.20. Formation of 1-chlorocyclobutenes by gold-catalyzed [2+2] cycloaddition.

The oxidative ring contraction of cyclobutenes to give cyclopropylcarbonyl compounds has been recently accomplished by the group of Didier using air or *m*CPBA as oxidants (Scheme 2.21).[127] A series of cyclopropyl ketones and aldehydes have been prepared by this method. In addition, dicarbonyl compounds have been accessed by oxidative cleavage of 1-vinylcyclobutenes under O_2.

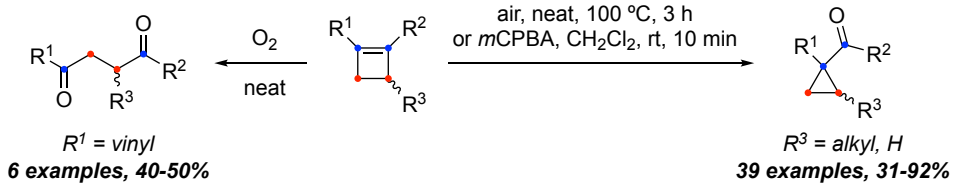

Scheme 2.21. Oxidative ring contraction and cleavage of cyclobutenes.

126. Bai, Y.-B.; Luo, Z.; Wang, Y.; Gao, J.-M.; Zhang, L. *J. Am. Chem.* **2018**, *140*, 5860–5865.
127. Baumann, A. N.; Schüppel, F.; Eisold, M; Kreppel, A.; de Vivie-Riedle, R.; Didier, D. *J. Org. Chem.* **2018**, *83*, 4905–4921.

Experimental Part

General Information

The general information is provided in the Experimental Part of the **Chapter 1**. Concerning the SFC analysis, it was carried out on a Waters Acquity UPC^2 instrument with PDA detector.

All reagents were used as purchased, with no further purification. 1,3-Enynes **6**,[128] 1-aryl cyclobutenes **8ah-ao**,[81,112] 7-substituted 1,3,7-cycloheptatrienes **11b-f**,[64b,129] were synthesized according to the literature procedures. The NMR data were in agreement with the ones reported in the literature.

Synthetic Procedures and Characterization Data

General Procedure for the Synthesis of Vinylcyclobutenes

The alkyne (1 equiv) was dissolved in CH_2Cl_2 (0.5 M). The alkene (2 equiv) was added, followed by [(*t*BuXPhos)AuNCMe]BAr_4^F (3 o 5 mol%). The resulting mixture was stirred at 23 ºC until no alkyne was detected by TLC or GC-MS. Triethylamine (0.02 mL) was added to quench the reaction. The volatiles were removed under reduced pressure and the crude product was purified by silica gel flash column chromatography.

2-(Cyclohex-1-en-1-yl)spiro[3.5]non-1-ene

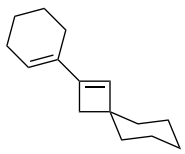

The title compound (colorless oil, 22 mg, 54%) was synthesized according to the general procedure starting from 1-ethynylcyclohex-1-ene (24 μL, 0.2 mmol), methylenecyclohexane (48 μL, 0.4 mmol) and [(*t*BuXPhos)AuNCMe]BAr_4^F (15 mg, 10 μmol, 5 mol%). The reaction time was 14 h. Pentane was used as eluent in the purification.

^{1}H NMR (500 MHz, $CDCl_3$) δ 6.02 (s, 1H), 5.69 – 5.63 (m, 1H), 2.19 (s, 2H), 2.15 – 2.08 (m, 4H), 1.71 – 1.24 (m, 14H). **^{13}C NMR** (126 MHz, $CDCl_3$) δ 145.6, 133.6, 133.0, 123.7,

128. Miwa, K.; Aoyama, T.; Shioiri, T. *Synlett* **1994**, 107–108.
129. Herlé, B.; Holstein, P. M.; Echavarren, A. M. *ACS Catal.* **2017**, *7*, 3668–3675.

43.7, 39.6, 36.7 (2C), 26.0, 25.3, 24.5 (2C), 23.8, 22.4, 22.3. **HRMS** (APCI) *m/z* calculated for $C_{15}H_{23}^+$ $[M+H]^+$: 203.1794, found: 203.1785.

2-(Cyclohex-1-en-1-yl)spiro[3.4]oct-1-ene

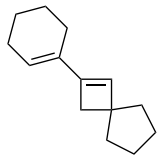

The title compound (colorless oil, 29 mg, 77%) was synthesized according to the general procedure starting from 1-ethynylcyclohex-1-ene (24 μL, 0.2 mmol), methylenecyclopentane (42 μL, 0.4 mmol) and [(*t*BuXPhos)AuNCMe]BAr_4^F (15 mg, 10 μmol, 5 mol%). The reaction time was 16 h. Pentane was used as eluent in the purification.

^{1}H NMR (400 MHz, $CDCl_3$) δ 5.88 (s, 1H), 5.68 – 5.62 (m, 1H), 2.36 (s, 2H), 2.17 – 2.06 (m, 4H), 1.73 – 1.54 (m, 12H). **^{13}C NMR** (101 MHz, $CDCl_3$) δ 145.3, 133.3, 131.0, 123.9, 50.2, 42.0, 36.4 (2C), 25.3, 24.4 (2C), 23.8, 22.4, 22.3. **HRMS** (APCI) *m/z* calculated for $C_{14}H_{21}^+$ $[M+H]^+$: 189.1638, found: 189.1635.

(3-(Cyclohex-1-en-1-yl)-1-methylcyclobut-2-en-1-yl)benzene

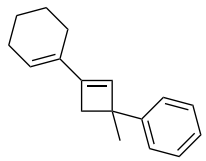

The title compound (colorless oil, 31 mg, 69%) was synthesized according to the general procedure starting from 1-ethynylcyclohex-1-ene (24 μL, 0.2 mmol), α-methylstyrene (52 μL, 0.4 mmol) and [(*t*BuXPhos)AuNCMe]BAr_4^F (15 mg, 10 μmol, 5 mol%). The reaction time was 14 h. Cyclohexane was used as eluent in the purification.

^{1}H NMR (500 MHz, $CDCl_3$) δ 7.39 – 7.34 (m, 2H), 7.34 – 7.29 (m, 2H), 7.22 – 7.15 (m, 1H), 6.24 (s, 1H), 5.73– 5.68 (m, 1H), 2.76 (d, J = 12.3 Hz, 1H), 2.70 (d, J = 12.3 Hz, 1H), 2.25 – 2.17 (m, 2H), 2.17 – 2.10 (m, 2H), 1.74 – 1.66 (m, 2H), 1.66 – 1.59 (m, 2H), 1.57 (s, 3H). **^{13}C NMR** (126 MHz, $CDCl_3$) δ 148.3, 145.9, 133.3, 131.1, 128.0 (2C), 125.9 (2C), 125.5, 124.9, 45.5, 43.7, 27.9, 25.4, 23.8, 22.3, 22.3. **HRMS** (APCI) *m/z* calculated for $C_{17}H_{21}^+$ $[M+H]^+$: 225.1638, found: 225.1638.

1-(3-(Cyclohex-1-en-1-yl)-1-methylcyclobut-2-en-1-yl)-4-methylbenzene

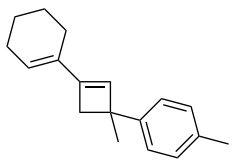

The title compound (colorless oil, 26 mg, 54%) was synthesized according to the general procedure starting from 1-ethynylcyclohex-1-ene (24 μL, 0.2 mmol), 1-methyl-4-(prop-1-en-2-yl)benzene (58 μL, 0.4 mmol) and

[(*t*BuXPhos)AuNCMe]BAr_4^F (15 mg, 10 μmol, 5 mol%). The reaction time was 14 h. Cyclohexane was used as eluent in the purification.

^{1}H NMR (400 MHz, $CDCl_3$) δ 7.24 (d, *J* = 7.8 Hz, 2H), 7.12 (d, *J* = 7.8 Hz, 2H), 6.20 (s, 1H), 5.72 – 5.65 (m, 1H), 2.72 (d, *J* = 12.2 Hz, 1H), 2.66 (d, *J* = 12.3, 1H), 2.33 (s, 3H), 2.24 – 2.07 (m, 4H), 1.74 – 1.57 (m, 4H), 1.54 (s, 3H). **^{13}C NMR** (101 MHz, $CDCl_3$) δ 145.8, 145.3, 134.9, 133.3, 131.3, 128.7 (2C), 125.8 (2C), 124.8, 45.2, 43.7, 27.9, 25.4, 23.8, 22.3, 22.3, 21.0. **HRMS** (APCI) *m/z* calculated for $C_{18}H_{23}^+$ $[M+H]^+$: 239.1794, found: 239.1792.

1-(3-(Cyclohex-1-en-1-yl)-1-methylcyclobut-2-en-1-yl)-4-fluorobenzene

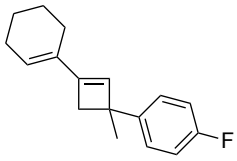

The title compound (colorless oil, 21 mg, 43%) was synthesized according to the general procedure starting from 1-ethynylcyclohex-1-ene (24 μL, 0.2 mmol), 1-fluoro-4-(prop-1-en-2-yl)benzene (54 μL, 0.4 mmol) and [(*t*BuXPhos)AuNCMe]BAr_4^F (15 mg, 10 μmol, 5 mol%). The reaction time was 14 h. Cyclohexane was used as eluent in the purification.

^{1}H NMR (400 MHz, $CDCl_3$) δ 7.35 – 7.26 (m, 2H), 7.04 – 6.94 (m, 2H), 6.20 (s, 1H), 5.74 – 5.68 (m, 1H), 2.70 (s, 2H), 2.25 – 2.09 (m, 4H), 1.76 – 1.58 (m, 4H), 1.55 (s, 3H). **^{13}C NMR** (101 MHz, $CDCl_3$) δ 161.0 (d, *J* (^{13}C-^{19}F) = 243.3 Hz), 145.9, 144.0 (d, *J* (^{13}C-^{19}F) = 3.1 Hz), 133.1, 130.9, 127.3 (d, *J* (^{13}C-^{19}F) = 7.8 Hz, 2C), 125.2, 114.6 (d, *J* (^{13}C-^{19}F) = 20.8 Hz, 2C), 45.0, 43.8, 27.9, 25.3, 23.8, 22.3, 22.2. **^{19}F NMR** (376 MHz, $CDCl_3$) δ -118.42. **HRMS** (APCI) *m/z* calculated for $C_{17}H_{20}F^+$ $[M+H]^+$: 243.1544, found: 243.1541.

(3-(Cyclohex-1-en-1-yl)cyclobut-2-ene-1,1-diyl)dibenzene

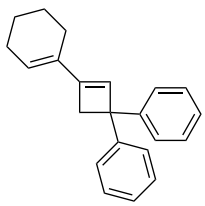

The title compound (pale yellow oil, 13 mg, 23%) was synthesized according to the general procedure starting from 1-ethynylcyclohex-1-ene (24 μL, 0.2 mmol), ethene-1,1-diyldibenzene (71 μL, 0.4 mmol) and [(*t*BuXPhos)AuNCMe]BAr_4^F (15 mg, 10 μmol, 5 mol%). The reaction time was 18 h. Pentane was used as eluent in the purification.

^{1}H NMR (400 MHz, $CDCl_3$) δ 7.36 – 7.27 (m, 8H), 7.23 – 7.16 (m, 2H), 6.51 (bs, 1H), 5.79 – 5.73 (m, 1H), 3.21 (s, 2H), 2.28 – 2.20 (m, 2H), 2.19 – 2.11 (m, 2H), 1.77 – 1.58 (m, 4H). **^{13}C NMR** (101 MHz, $CDCl_3$) δ 147.4, 146.7 (2C), 132.9, 129.2, 128.0 (4C), 127.1

(4C), 125.9, 125.7 (2C), 52.8, 44.5, 25.4, 23.8, 22.2, 22.2. **HRMS** (APCI) *m/z* calculated for $C_{22}H_{23}^+$ $[M+H]^+$: 287.1794, found: 287.1796.

(*E*)-(1-Methyl-3-(1-phenylprop-1-en-2-yl)cyclobut-2-en-1-yl)benzene

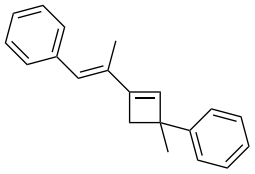

The title compound (yellow oil, 51 mg, 98%) was synthesized according to the general procedure starting from (*E*)-(2-methylbut-1-en-3-yn-1-yl)benzene (28 mg, 0.2 mmol), α-methylstyrene (52 μL, 0.4 mmol) and [(*t*BuXPhos)AuNCMe]BAr_4^F (15 mg, 10 μmol, 5 mol%). The reaction time was 14 h. In the purification, the eluent used was pentane and then, pentane:diethyl ether 95:5.

^{1}H NMR (300 MHz, $CDCl_3$) δ 7.50 – 7.16 (m, 10H), 6.54 (s, 1H), 6.45 (bs, 1H), 2.94 (d, *J* = 12.3, 1.6 Hz, 1H), 2.87 (d, *J* = 12.3, 1.6 Hz, 1H), 2.11 (s, 3H), 1.65 (s, 3H). **^{13}C NMR** (75 MHz, $CDCl_3$) δ 147.9, 147.5, 137.6, 134.6, 132.3, 129.1 (2C), 128.1 (2C), 128.1 (2C), 126.6, 126.6, 125.9 (2C), 125.6, 44.9, 43.7, 27.9, 13.4. **HRMS** (APCI) *m/z* calculated for $C_{20}H_{21}^+$ $[M+H]^+$: 261.1638, found: 261.1642.

(*Z*)-(4-Methyl-1-(3-methyl-3-phenylcyclobut-1-en-1-yl)pent-1-en-1-yl)benzene

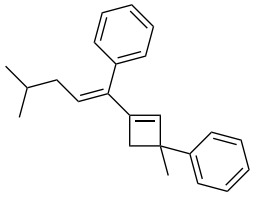

The title compound (colorless oil, 43 mg, 71%) was synthesized according to the general procedure starting from (*Z*)-(6-methylhept-3-en-1-yn-3-yl)benzene (37 mg, 0.2 mmol), α-methylstyrene (52 μL, 0.4 mmol) and [(*t*BuXPhos)AuNCMe]BAr_4^F (15 mg, 10 μmol, 5 mol%). The reaction time was 14 h. Pentane was used as eluent in the purification.

^{1}H NMR (400 MHz, $CDCl_3$) δ 7.46 – 7.31 (m, 7H), 7.30 – 7.25 (m, 2H), 7.22 (tt, *J* = 6.4, 2.0 Hz, 1H), 6.00 (s, 1H), 5.71 (t, *J* = 7.6 Hz, 1H), 2.92 (d, *J* = 12.3 Hz, 1H), 2.85 (d, *J* = 12.2 Hz, 1H), 2.00 (t, *J* = 7.3 Hz, 2H), 1.76 – 1.63 (m, 1H), 1.60 (s, 3H), 0.90 (t, *J* = 6.7 Hz, 6H). **^{13}C NMR** (101 MHz, $CDCl_3$) δ 148.3, 145.7, 138.0, 137.4, 133.8, 129.3 (2C), 128.8, 128.0 (2C), 127.9 (2C), 126.7, 125.9 (2C), 125.5, 45.2, 43.9, 37.7, 28.9, 28.1, 22.5, 22.4. **HRMS** (APCI) *m/z* calculated for $C_{23}H_{27}^+$ $[M+H]^+$: 303.2107, found: 303.2110.

(*E*)-(1-(3-Methyl-3-phenylcyclobut-1-en-1-yl)ethene-1,2-diyl)dibenzene

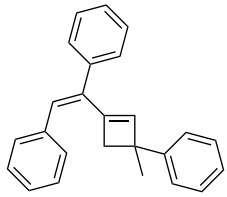

The title compound (yellow oil, 32 mg, 50%) was synthesized according to the general procedure starting from (*E*)-but-1-en-3-yne-1,2-diyldibenzene (41 mg, 0.2 mmol), α-methylstyrene (52 µL, 0.4 mmol) and [(*t*BuXPhos)AuNCMe]BAr_4^F (15 mg, 10 µmol, 5 mol%). The reaction time was 14 h. In the purification, the eluent used was pentane and then, pentane:diethyl ether 99:1.

^{1}H NMR (300 MHz, $CDCl_3$) δ 7.50 – 7.12 (m, 15H), 6.76 (s, 1H), 6.44 (s, 1H), 2.22 (d, *J* = 13.0 Hz, 1H), 2.12 (d, *J* = 13.0 Hz, 1H), 1.46 (s, 3H). **^{13}C NMR** (75 MHz, $CDCl_3$) δ 147.7, 143.3, 142.3, 141.8, 140.3, 139.3, 130.4 (2C), 128.2 (2C), 128.0 (2C), 127.8 (2C), 127.4, 127.3, 127.1 (2C), 125.7 (2C), 125.5, 122.1, 47.8, 46.8, 27.5. **HRMS** (APCI) *m/z* calculated for $C_{25}H_{23}^+$ $[M+H]^+$: 323.1794, found: 323.1795.

(2-(3-Methyl-3-phenylcyclobut-1-en-1-yl)ethene-1,1-diyl)dibenzene

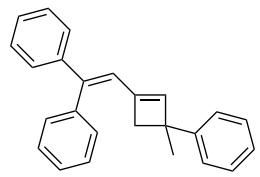

The title compound (pale yellow oil, 28 mg, 43%) was synthesized according to the general procedure starting from but-1-en-3-yne-1,1-diyldibenzene (41 mg, 0.2 mmol), α-methylstyrene (52 µL, 0.4 mmol) and [(*t*BuXPhos)AuNCMe]BAr_4^F (15 mg, 10 µmol, 5 mol%). The reaction time was 14 h. In the purification, the eluent used was pentane:CH_2Cl_2 100:0 (3 CV), 99:1 (3 CV) and then, 98:2.

^{1}H NMR (400 MHz, $CDCl_3$) δ 7.41 – 7.15 (m, 15H), 6.76 (s, 1H), 6.44 (s, 1H), 2.22 (d, *J* = 13.1 Hz, 1H), 2.12 (dm, *J* = 13.1 Hz, 1H), 1.46 (s, 3H). **^{13}C NMR** (126 MHz, $CDCl_3$) δ 147.7, 143.3, 142.4, 141.8, 140.3, 139.4, 130.4 (2C), 128.2 (2C), 128.0 (2C), 127.8 (2C), 127.4, 127.3, 127.1 (2C), 125.7 (2C), 125.5, 122.1, 47.8, 46.8, 27.5. **HRMS** (APCI) *m/z* calculated for $C_{25}H_{23}^+$ $[M+H]^+$: 323.1794, found: 323.1792.

(*E*)-(2-(3-Methyl-3-phenylcyclobut-1-en-1-yl)vinyl)benzene

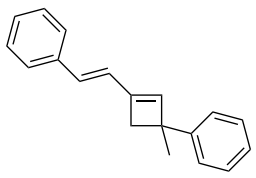

The title compound (yellow oil, 33 mg, 67%) was synthesized according to the general procedure starting from (*E*)-but-1-en-3-yn-1-ylbenzene (26 mg, 0.2 mmol), α-methylstyrene (52 µL, 0.4 mmol) and [(*t*BuXPhos)AuNCMe]BAr_4^F (15 mg, 10 µmol,

5 mol%). The reaction time was 14 h. In the purification, the eluent used was pentane and then, pentane:diethyl ether 9:1.

^{1}H NMR (400 MHz, $CDCl_3$) δ 7.51 – 7.21 (m, 10H), 6.89 (d, *J* = 15.9 Hz, 1H), 6.52 (d, *J* = 15.9 Hz, 1H), 6.50 (s, 1H), 2.92 (d, *J* = 12.4 Hz, 1H), 2.86 (dt, *J* = 12.3, 1.0 Hz, 1H), 1.65 (s, 3H). **^{13}C NMR** (101 MHz, $CDCl_3$) δ 147.8, 143.7, 137.5, 137.0, 130.6, 128.6 (2C), 128.1 (2C), 127.7, 126.6 (2C), 125.8 (2C), 125.7, 123.3, 47.1, 44.0, 27.7. **HRMS** (APCI) *m/z* calculated for $C_{19}H_{19}^+$ $[M+H]^+$: 247.1481, found: 247.1480.

(*E*)-1-Methyl-4-(2-(3-methyl-3-phenylcyclobut-1-en-1-yl)vinyl)benzene

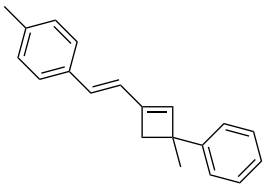

The title compound (colorless oil, 30 mg, 58%) was synthesized according to the general procedure starting from (*E*)-1-(but-1-en-3-yn-1-yl)-4-methylbenzene (28 mg, 0.2 mmol), α-methylstyrene (52 μL, 0.4 mmol) and [(*t*BuXPhos)AuNCMe]BAr_4^F (15 mg, 10 μmol, 5 mol%). The reaction time was 14 h. In the purification, the eluent used was pentane and then, pentane:CH_2Cl_2 8:2.

^{1}H NMR (500 MHz, $CDCl_3$) δ 7.44 – 7.36 (m, 2H), 7.36 – 7.30 (m, 4H), 7.24 – 7.18 (m, 1H), 7.17 – 7.11 (m, 2H), 6.81 (d, *J* = 16.0, 1H), 6.50 – 6.42 (m, 2H), 2.88 (d, *J* = 12.3 Hz, 1H), 2.82 (d, *J* = 12.3, 1H), 2.36 (s, 3H), 1.62 (s, 3H). **^{13}C NMR** (126 MHz, $CDCl_3$) δ 147.9, 143.7, 137.6, 136.9, 134.2, 130.5, 129.3 (2C), 128.1 (2C), 126.4 (2C), 125.8 (2C), 125.6, 122.4, 46.9, 43.9, 27.7, 21.2. **HRMS** (APCI) *m/z* calculated for $C_{20}H_{21}^+$ $[M+H]^+$: 261.1638, found: 261.1632.

(*E*)-1-Chloro-4-(2-(3-methyl-3-phenylcyclobut-1-en-1-yl)vinyl)benzene

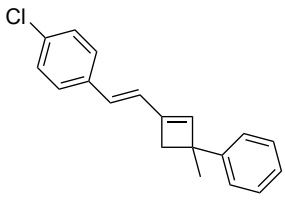

The title compound (white solid, 47 mg, 84%) was synthesized according to the general procedure starting from (*E*)-1-(but-1-en-3-yn-1-yl)-4-chlorobenzene (33 mg, 0.2 mmol), α-methylstyrene (52 μL, 0.4 mmol) and [(*t*BuXPhos)AuNCMe]BAr_4^F (15 mg, 10 μmol, 5 mol%). The reaction time was 14 h. Pentane was used as eluent in the purification.

M.p. 80-82 ºC. **^{1}H NMR** (400 MHz, $CDCl_3$) δ 7.42 – 7.27 (m, 8H), 7.26 – 7.19 (m, 1H), 6.83 (d, *J* = 16.0 Hz, 1H), 6.51 (s, 1H), 6.43 (d, *J* = 15.9 Hz, 1H), 2.89 (d, *J* = 12.4 Hz, 1H), 2.83 (d, *J* = 12.4 Hz, 1H), 1.63 (s, 3H). **^{13}C NMR** (101 MHz, $CDCl_3$) δ 147.6, 143.4, 138.2,

135.5, 133.3, 129.2, 128.8 (2C), 128.2 (2C), 127.7 (2C), 125.8 (2C), 125.7, 123.9, 47.1, 43.9, 27.7. **HRMS** (APCI) *m/z* calculated for $C_{19}H_{18}Cl^+$ $[M+H]^+$: 281.1092, found: 281.1090.

(*E*)-1-Fluoro-4-(2-(3-methyl-3-phenylcyclobut-1-en-1-yl)vinyl)benzene

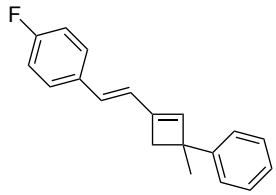

The title compound (white solid, 37 mg, 70%) was synthesized according to the general procedure starting from (*E*)-1-(but-1-en-3-yn-1-yl)-4-fluorobenzene (29 mg, 0.2 mmol), α-methylstyrene (52 μL, 0.4 mmol) and [(*t*BuXPhos)AuNCMe]BAr_4^F (15 mg, 10 μmol, 5 mol%). The reaction time was 14 h. Pentane was used as eluent in the purification.

M.p. 60-62 ºC. **^{1}H NMR** (500 MHz, $CDCl_3$) δ 7.42 – 7.31 (m, 6H), 7.24 – 7.18 (m, 1H), 7.05 – 6.99 (m, 2H), 6.76 (d, *J* = 15.8 Hz, 1H), 6.47 (s, 1H), 6.43 (d, *J* = 15.9 Hz, 1H), 2.87 (d, *J* = 12.3 Hz, 1H), 2.81 (d, *J* = 12.4, 1H), 1.61 (s, 3H). **^{13}C NMR** (126 MHz, $CDCl_3$) δ 162.4 (d, *J* (^{13}C-^{19}F) = 247.5 Hz), 147.7, 143.4, 137.5, 133.2 (d, *J* (^{13}C-^{19}F) = 3.3 Hz), 129.2, 128.1 (2C), 128.0 (d, *J* (^{13}C-^{19}F) = 7.9 Hz, 2C), 125.8 (2C), 125.7, 123.1 (d, *J* (^{13}C-^{19}F) = 2.4 Hz), 115.6 (d, *J* (^{13}C-^{19}F) = 21.7 Hz, 2C), 47.0, 43.9, 27.7. **^{19}F NMR** (376 MHz, $CDCl_3$) δ -114.12. **HRMS** (APCI) *m/z* calculated for $C_{19}H_{18}F^+$ $[M+H]^+$: 265.1387, found: 265.1384.

(*E*)-1-Methoxy-2-(2-(3-methyl-3-phenylcyclobut-1-en-1-yl)vinyl)benzene

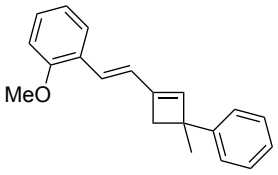

The title compound (pale yellow oil, 26 mg, 31%) was synthesized according to the general procedure starting from (*E*)-1-(but-1-en-3-yn-1-yl)-2-methoxybenzene (47 mg, 0.3 mmol), α-methylstyrene (78 μL, 0.6 mmol) and [(*t*BuXPhos)AuNCMe]BAr_4^F (23 mg, 15 μmol, 5 mol%). The reaction time was 14 h. In the purification, the eluent used was pentane and then, pentane:CH_2Cl_2 8:1.

^{1}H NMR (400 MHz, $CDCl_3$) δ 7.48 (dd, *J* = 7.7, 1.7 Hz, 1H), 7.40 – 7.34 (m, 2H), 7.34 – 7.28 (m, 2H), 7.25 – 7.15 (m, 2H), 6.97 – 6.76 (m, 4H), 6.42 (s, 1H), 3.86 (s, 3H), 2.89 (d, *J* = 12.4 Hz, 1H), 2.84 (d, *J* = 12.4 Hz, 1H), 1.60 (s, 3H). **^{13}C NMR** (126 MHz, $CDCl_3$) δ 156.9, 148.0, 144.3, 136.9, 128.7, 128.1 (2C), 126.8, 126.0, 125.8 (2C), 125.6, 125.3, 124.0, 120.7, 110.9, 55.5, 46.9, 44.0, 27.7. **HRMS** (APCI) *m/z* calculated for $C_{20}H_{21}O^+$ $[M+H]^+$: 277.1587, found: 277.1587.

(*E*)-1-Methoxy-4-(2-(3-methyl-3-phenylcyclobut-1-en-1-yl)vinyl)benzene

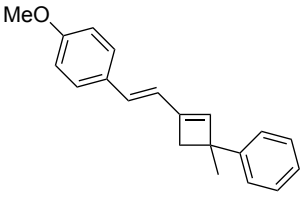

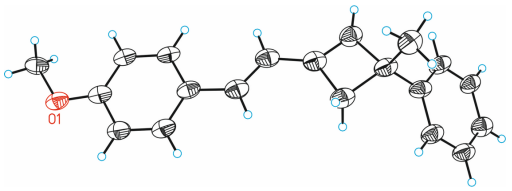

The title compound (white solid, 20 mg, 36%) was synthesized according to the general procedure starting from (*E*)-1-(but-1-en-3-yn-1-yl)-4-methoxybenzene (32 mg, 0.2 mmol), α-methylstyrene (52 µL, 0.4 mmol) and [(*t*BuXPhos)AuNCMe]BAr_4^F (15 mg, 10 µmol, 5 mol%). The reaction time was 4 h. In the purification, the eluent used was pentane and then, pentane:CH_2Cl_2 7:3. The product was crystallized by dissolving it in CH_2Cl_2, adding pentane, and subsequent slow evaporation of the solvents. The structure was confirmed by single crystal X-ray diffraction.

M.p. (CH_2Cl_2/pentane) 108-110 ºC. **^{1}H NMR** (300 MHz, $CDCl_3$) δ 7.43 – 7.27 (m, 6H), 7.23 – 7.15 (m, 1H), 6.91 – 6.82 (m, 2H), 6.72 (d, *J* = 16.0 Hz, 1H), 6.48 – 6.37 (m, 2H), 3.82 (s, 3H), 2.86 (d, *J* = 12.3 Hz, 1H), 2.80 (d, *J* = 12.3, 1H), 1.60 (s, 3H). **^{13}C NMR** (101 MHz, $CDCl_3$) δ 159.4, 147.9, 143.8, 136.3, 130.1, 129.8, 128.1 (2C), 127.8 (2C), 125.8 (2C), 125.6, 121.4, 114.1 (2C), 55.3, 46.9, 43.9, 27.7. **HRMS** (APCI) *m/z* calculated for $C_{20}H_{21}O^+$ $[M+H]^+$: 277.1587, found: 277.1585.

(*E*)-(3-(Hex-1-en-1-yl)-1-methylcyclobut-2-en-1-yl)benzene

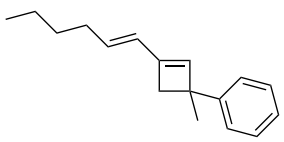

The title compound (colorless oil, 32 mg, 71%) was synthesized according to the general procedure starting from (*E*)-oct-3-en-1-yne (22 mg, 0.2 mmol), α-methylstyrene (52 µL, 0.4 mmol) and [(*t*BuXPhos)AuNCMe]BAr_4^F (15 mg, 10 µmol, 5 mol%). The reaction time was 14 h. Pentane was used as eluent in the purification. **^{1}H NMR** (300 MHz, $CDCl_3$) δ 7.39 – 7.27 (m, 4H), 7.23 – 7.14 (m, 1H), 6.21 (s, 1H), 6.13 (dm, *J* = 15.6 Hz, 1H), 5.66 (dt, *J* = 15.5, 7.0 Hz, 1H), 2.80 – 2.61 (m, 2H), 2.12 (q, *J* = 7.0 Hz, 2H), 1.56 (s, 3H), 1.47 – 1.24 (m, 4H), 1.01 – 0.81 (m, 3H). **^{13}C NMR** (75 MHz, $CDCl_3$) δ 148.2, 143.8, 133.8, 133.6, 128.0 (2C), 125.8 (2C), 125.5, 125.1, 46.6, 44.0, 32.2, 31.3, 27.8, 22.3, 13.9. **HRMS** (APCI) *m/z* calculated for $C_{17}H_{23}^+$ $[M+H]^+$: 227.1794, found: 227.1790.

(1-Methyl-3-(prop-1-en-2-yl)cyclobut-2-en-1-yl)benzene

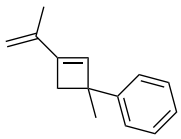

The title compound (colorless oil, 10 mg, 27%) was synthesized according to the general procedure starting from 2-methylbut-1-en-3-yne (19 μL, 0.2 mmol), α-methylstyrene (52 μL, 0.4 mmol) and [(*t*BuXPhos)AuNCMe]BAr_4^F (15 mg, 10 μmol, 5 mol%). The reaction time was 14 h. Pentane was used as eluent in the purification.

^{1}H NMR (400 MHz, $CDCl_3$) δ 7.38 – 7.28 (m, 4H), 7.22 – 7.15 (m, 1H), 6.36 (s, 1H), 4.89 (m, 2H), 2.78 (d, *J* = 12.4 Hz, 1H), 2.71 (d, *J* = 12.4 Hz, 1H), 1.92 – 1.86 (m, 3H), 1.56 (s, 3H). **^{13}C NMR** (101 MHz, $CDCl_3$) δ 147.9, 146.1, 139.1, 134.6, 128.1 (2C), 125.8 (2C), 125.6, 112.4, 45.2, 43.8, 27.8, 17.7. **HRMS** (APCI) *m/z* calculated for $C_{14}H_{17}^+$ $[M+H]^+$: 185.1325, found: 185.1329.

(*E*)-2-(4-Chlorostyryl)spiro[3.5]non-1-ene

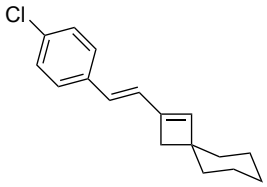

The title compound (white solid, 361 mg, 76%) was synthesized according to the general procedure starting from (*E*)-1-(but-1-en-3-yn-1-yl)-4-chlorobenzene (300 mg, 1.84 mmol), methylenecyclohexane (0.44 mL, 3.69 mmol) and [(*t*BuXPhos)AuNCMe]BAr_4^F (141 mg, 92 μmol, 5 mol%). The reaction time was 18 h. Pentane was used as eluent in the purification.

M.p. 75-78 ºC. **^{1}H NMR** (500 MHz, $CDCl_3$) δ 7.34 – 7.30 (m, 2H), 7.29 – 7.25 (m, 2H), 6.75 (dt, *J* = 15.9, 0.9 Hz, 1H), 6.38 (d, *J* = 15.9 Hz, 1H), 6.28 (s, 1H), 2.32 (d, *J* = 0.8 Hz, 2H), 1.60 – 1.31 (m, 10H). **^{13}C NMR** (101 MHz, $CDCl_3$) δ 143.2, 140.4, 135.8, 133.0, 128.7 (2C), 128.0, 127.6 (2C), 124.5, 45.5, 39.9, 36.4 (2C), 25.9, 24.4 (2C). **HRMS** (APCI) *m/z* calculated for $C_{17}H_{20}Cl^+$ $[M+H]^+$: 259.1248, found: 259.1248.

1-(4-Butyl-3,3-dimethylcyclobut-1-en-1-yl)cyclohex-1-ene

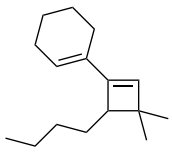

The title compound (colorless oil, 16 mg, 37%) was synthesized according to the general procedure starting from 1-ethynylcyclohex-1-ene (24 μL, 0.2 mmol), 2-methylhept-2-ene (62 μL, 0.4 mmol) and [(*t*BuXPhos)AuNCMe]BAr_4^F (15 mg, 10 μmol, 5 mol%). The reaction time was 16 h. Cyclohexane was used as eluent in the purification.

^{1}H NMR (400 MHz, $CDCl_3$) δ 5.79 (s, 1H), 5.69 – 5.63 (m, 1H), 2.47 (dd, *J* = 10.5, 3.4 Hz, 1H), 2.19 – 1.94 (m, 4H), 1.77 – 1.55 (m, 5H), 1.42 – 1.28 (m, 5H), 1.17 (s, 3H), 1.08

(s, 3H), 0.95 – 0.86 (m, 3H). **^{13}C NMR** (75 MHz, $CDCl_3$) δ 147.6, 133.6, 132.7, 124.1, 51.7, 42.4, 31.2, 29.2, 28.1, 25.3, 24.2, 23.1, 22.4, 22.3, 22.0, 14.2. Silicone grease was detected in the ^{13}C NMR spectrum. **HRMS** (APCI) *m/z* calculated for $C_{16}H_{27}^+$ $[M+H]^+$: 219.2107, found: 219.2107.

(1*R,8*R**)-9-(Cyclohex-1-en-1-yl)bicyclo[6.2.0]dec-9-ene**

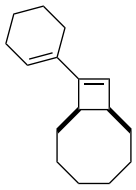

The title compound (colorless oil, 12 mg, 28%) was synthesized according to the general procedure starting from 1-ethynylcyclohex-1-ene (24 μL, 0.2 mmol), (*Z*)-cyclooctene (52 μL, 0.4 mmol) and [(*t*BuXPhos)AuNCMe]BAr_4^F (15 mg, 10 μmol, 5 mol%). The reaction time was 48 h. Pentane was used as eluent in the purification.

^{1}H NMR (400 MHz, $CDCl_3$) δ 5.71 (s, 1H), 5.68 – 5.63 (m, 1H), 2.85 (ddd, *J* = 11.3, 4.4, 1.8 Hz, 1H), 2.65 – 2.55 (m, 1H), 2.20 – 1.90 (m, 6H), 1.72 – 1.17 (m, 14H). **^{13}C NMR** (101 MHz, $CDCl_3$) δ 149.8, 132.0, 128.1, 124.2, 45.7, 44.4, 30.6, 30.5, 27.6, 26.4, 26.1, 25.8, 25.3, 24.1, 22.4, 22.3. **HRMS** (APCI) *m/z* calculated for $C_{16}H_{25}^+$ $[M+H]^+$: 217.1951, found: 217.1950.

1-(3-Methyl-3-(3-methylbut-3-en-1-yl)cyclobut-1-en-1-yl)cyclohex-1-ene

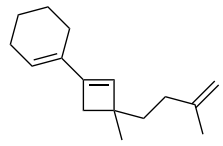

The title compound (colorless oil, 14 mg, 32%) was synthesized according to the general procedure starting from 1-ethynylcyclohex-1-ene (24 μL, 0.2 mmol), 2,5-dimethylhexa-1,5-diene (59 μL, 0.4 mmol) and [(*t*BuXPhos)AuNCMe]BAr_4^F (15 mg, 10 μmol, 5 mol%). The reaction time was 4 days. Pentane was used as eluent in the purification.

^{1}H NMR (400 MHz, $CDCl_3$) δ 5.91 (s, 1H), 5.69 – 5.58 (m, 1H), 4.67 (d, *J* = 1.2 Hz, 2H), 2.31 (d, *J* = 12.4 Hz, 1H), 2.20 (d, *J* = 12.4 Hz, 1H), 2.15 – 2.07 (m, 4H), 2.04 – 1.96 (m, 2H), 1.73 (t, *J* = 1.2 Hz, 3H), 1.69 – 1.54 (m, 6H), 1.17 (s, 3H). **^{13}C NMR** (101 MHz, $CDCl_3$) δ 146.8, 144.7, 133.5, 132.9, 123.9, 109.2, 42.0, 40.4, 38.5, 34.2, 25.3, 24.1, 23.8, 22.7, 22.3, 22.3. **HRMS** (APCI) *m/z* calculated for $C_{16}H_{25}^+$ $[M+H]^+$: 217.1951, found: 217.1950.

1-(3-(But-1-yn-1-yl)-3-methylcyclobut-1-en-1-yl)cyclohex-1-ene

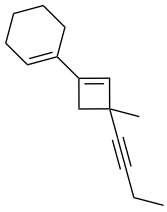

The title compound (yellow oil, 9 mg, 15%) was synthesized according to the general procedure starting from 1-ethynylcyclohex-1-ene (35 µL, 0.3 mmol) and 2-methylhex-1-en-3-yne (75 µL, 0.6 mmol) with [(*t*BuXPhos)AuNCMe]BAr_4^F (23 mg, 15 µmol, 5 mol%). The reaction time was 16 h. Pentane was used as eluent in the purification.

^{1}H and ^{13}C NMR spectra contained traces of grease. **^{1}H NMR** (400 MHz, $CDCl_3$) δ 5.86 (s, 1H), 5.70 – 5.64 (m, 1H), 2.78 (d, *J* = 12.4 Hz, 1H), 2.47 (d, *J* = 12.3 Hz, 1H), 2.19 (q, *J* = 7.5 Hz, 2H), 2.14 – 2.05 (m, 4H), 1.73 – 1.51 (m, 4H), 1.42 (s, 3H), 1.11 (t, *J* = 7.5 Hz, 3H). **^{13}C NMR** (101 MHz, $CDCl_3$) δ 146.2, 133.1, 130.4, 125.4, 84.4, 81.9, 43.5, 34.6, 27.0, 25.3, 23.7, 22.2, 22.2, 14.3, 12.6. **HRMS** (APCI) *m/z* calculated for $C_{15}H_{21}^+$ $[M+H]^+$: 201.1638, found: 201.1642.

(*E*)-(2-(3-(But-1-yn-1-yl)-3-methylcyclobut-1-en-1-yl)prop-1-en-1-yl)benzene

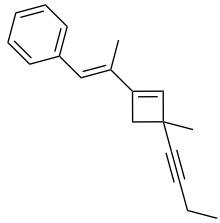

The title compound (yellow oil, 7 mg, 15%) was synthesized according to the general procedure starting from (*E*)-(2-methylbut-1-en-3-yn-1-yl)benzene (28 mg, 0.2 mmol) and 2-methylhex-1-en-3-yne (50 µL, 0.4 mmol) with [(*t*BuXPhos)AuNCMe]BAr_4^F (15 mg, 10 µmol, 5 mol%). The reaction time was 16 h. In the purification, the eluent used was pentane and then, pentane:CH_2Cl_2 95:5.

^{1}H NMR (400 MHz, $CDCl_3$) δ 7.41 – 7.13 (m, 5H), 6.37 (s, 1H), 6.13 (s, 1H), 2.92 (d, *J* = 12.3 Hz, 1H), 2.62 (d, *J* = 12.3 Hz, 1H), 2.21 (q, *J* = 7.5 Hz, 2H), 2.00 (d, *J* = 1.4 Hz, 3H), 1.48 (s, 3H), 1.13 (t, *J* = 7.5 Hz, 3H). **^{13}C NMR** (101 MHz, $CDCl_3$) δ 147.8, 137.4, 133.8, 132.2, 129.1 (2C), 128.2 (2C), 127.0, 126.7, 84.1, 82.1, 43.7, 34.1, 26.9, 14.3, 13.4, 12.6. **HRMS** (APCI) *m/z* calculated for $C_{18}H_{21}^+$ $[M+H]^+$: 237.1638, found: 237.1634.

(3-(But-1-yn-1-yl)-3-methylcyclobut-1-en-1-yl)benzene

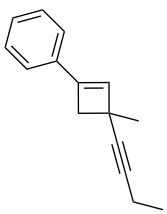

The title compound (light yellow oil, 16 mg, 41%) was synthesized according to the general procedure starting from ethynylbenzene (22 µL, 0.2 mmol) and 2-methylhex-1-en-3-yne (50 µL, 0.4 mmol) with [(*t*BuXPhos)AuNCMe]BAr_4^F (15 mg, 10 µmol, 5 mol%). The reaction time was 14 h. In the purification, the eluent used was pentane and then, pentane:CH_2Cl_2 1:1.

^{1}H NMR (400 MHz, $CDCl_3$) δ 7.40 – 7.32 (m, 4H), 7.30 – 7.25 (m, 1H), 6.40 (s, 1H), 3.06 (d, *J* = 12.5 Hz, 1H), 2.75 (d, *J* = 12.5 Hz, 1H), 2.23 (q, *J* = 7.5 Hz, 2H), 1.53 (s, 3H), 1.15 (t, *J* = 7.5 Hz, 3H). **^{13}C NMR** (126 MHz, $CDCl_3$) δ 144.1, 134.5, 133.0, 128.3 (2C), 128.0, 124.7 (2C), 83.8, 82.2, 44.0, 35.1, 26.8, 14.3, 12.6. **HRMS** (APCI) *m/z* calculated for $C_{15}H_{17}^{+}$ $[M+H]^{+}$: 197.1325, found: 197.1324.

1-(3-Methyl-3-vinylcyclobut-1-en-1-yl)cyclohex-1-ene

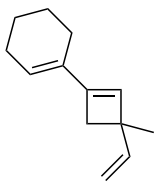

The title compound (colorless oil, 10 mg, 19%) was synthesized according to the general procedure starting from 1-ethynylcyclohex-1-ene (35 µL, 0.3 mmol) and isoprene (60 µL, 0.6 mmol) with [(*t*BuXPhos)AuNCMe]BAr_4^F (23 mg, 15 µmol, 5 mol%). The reaction time was 16 h. Pentane was used as eluent in the purification.

^{1}H and ^{13}C NMR spectra contained traces of pentane and grease. **^{1}H NMR** (400 MHz, $CDCl_3$) δ 6.03 (dd, *J* = 17.3, 10.4 Hz, 1H), 5.88 (bs, 1H), 5.70 – 5.64 (m, 1H), 5.00 (dd, *J* = 17.3, 1.7 Hz, 1H), 4.90 (dd, *J* = 10.4, 1.7 Hz, 1H), 2.45 (d, *J* = 12.4 Hz, 1H), 2.36 (d, *J* = 12.4 Hz, 1H), 2.16 – 2.08 (m, 4H), 1.70 – 1.56 (m, 4H), 1.29 (s, 3H). **^{13}C NMR** (101 MHz, $CDCl_3$) δ 145.80, 145.3, 133.3, 131.3, 124.7, 110.6, 44.1, 41.6, 25.3, 23.7, 23.6, 22.3, 22.2. **HRMS** (APCI) *m/z* calculated for $C_{13}H_{19}^{+}$ $[M+H]^{+}$: 175.1481, found: 175.1477.

(*E*)-(2-(3-Methyl-3-vinylcyclobut-1-en-1-yl)prop-1-en-1-yl)benzene

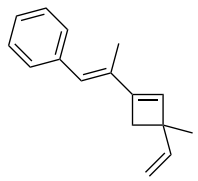

The title compound (colorless oil, 10 mg, 14%) was synthesized according to the general procedure starting from (*E*)-(2-methylbut-1-en-3-yn-1-yl)benzene (28 mg, 0.2 mmol) and isoprene (40 µL, 0.4 mmol) with [(*t*BuXPhos)AuNCMe]BAr_4^F (15 mg, 10 µmol, 5 mol%). The reaction time was 16 h. Pentane was used as eluent in the purification.

^{1}H NMR (400 MHz, $CDCl_3$) δ 7.37 – 7.31 (m, 4H), 7.25 – 7.18 (m, 1H), 6.38 (bs, 1H), 6.16 (s, 1H), 6.07 (dd, *J* = 17.3, 10.4 Hz, 1H), 5.05 (dd, *J* = 17.3, 1.7 Hz, 1H), 4.95 (dd, *J* = 10.4, 1.6 Hz, 1H), 2.59 (d, *J* = 12.3 Hz, 1H), 2.51 (d, *J* = 12.4 Hz, 1H), 2.02 (d, *J* = 1.4 Hz, 3H), 1.34 (s, 3H). **^{13}C NMR** (101 MHz, $CDCl_3$) δ 147.0, 145.4, 137.6, 134.8, 132.5, 129.1 (2C), 128.2 (2C), 126.6, 126.4, 111.0, 43.6, 41.8, 23.6, 13.4. **HRMS** (APCI) *m/z* calculated for $C_{16}H_{19}^{+}$ $[M+H]^{+}$: 211.1481, found: 211.1481.

(3-Methyl-3-vinylcyclobut-1-en-1-yl)benzene

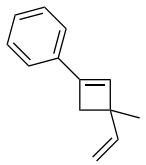

The title compound (colorless oil, 23 mg, 68%) was synthesized according to the general procedure starting from ethynylbenzene (22 μL, 0.2 mmol) and isoprene (40 μL, 0.4 mmol) with [(*t*BuXPhos)AuNCMe]BAr_4^F (9 mg, 6 μmol, 3 mol%). The reaction was performed at 50 ºC for 19 h. Pentane was used as eluent in the purification.

^{1}H NMR (300 MHz, $CDCl_3$) δ 7.42 – 7.31 (m, 4H), 7.30 – 7.23 (m, 1H), 6.43 (s, 1H), 6.11 (dd, *J* = 17.3, 10.4 Hz, 1H), 5.09 (dd, *J* = 17.3, 1.6 Hz, 1H), 4.98 (dd, *J* = 10.4, 1.6 Hz, 1H), 2.72 (d, *J* = 12.6 Hz, 1H), 2.63 (d, *J* = 12.6 Hz, 1H), 1.40 (s, 3H). **^{13}C NMR** (126 MHz, $CDCl_3$) δ 145.2, 143.2, 134.8, 133.9, 128.3 (2C), 127.7, 124.5 (2C), 111.1, 44.7, 42.2, 23.5. **HRMS** (APCI) *m/z* calculated for $C_{13}H_{15}^+$ $[M+H]^+$: 171.1168, found: 171.1165.

(3-Methyl-3-(prop-1-en-2-yl)cyclobut-1-en-1-yl)benzene

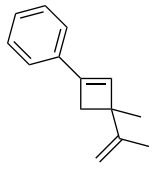

The title compound (colorless oil, 21 mg, 57%) was synthesized according to the general procedure starting from ethynylbenzene (22 μL, 0.2 mmol) and 2,3-dimethylbuta-1,3-diene (45 μL, 0.4 mmol) with [(*t*BuXPhos)AuNCMe]BAr_4^F (9 mg, 6 μmol, 3 mol%). The reaction was performed at 50 ºC for 22 h. Pentane was used as eluent in the purification.

^{1}H NMR (300 MHz, $CDCl_3$) δ 7.41 – 7.31 (m, 4H), 7.30 – 7.22 (m, 1H), 6.55 (s, 1H), 4.83 – 4.75 (m, 2H), 2.79 (d, *J* = 12.4 Hz, 1H), 2.57 (d, *J* = 12.5 Hz, 1H), 1.84 (dd, *J* = 1.4, 0.8 Hz, 3H), 1.42 (d, *J* = 0.6 Hz, 3H). **^{13}C NMR** (126 MHz, $CDCl_3$) δ 150.8, 143.2, 134.9, 134.3, 128.3 (2C), 127.6, 124.5 (2C), 109.0, 47.5, 41.3, 24.5, 19.3. **HRMS** (APCI) *m/z* calculated for $C_{14}H_{17}^+$ $[M+H]^+$: 185.1325, found: 185.1323.

3-Methyl-3-((*S*)-4-methylcyclohex-3-en-1-yl)cyclobut-1-en-1-yl)benzene

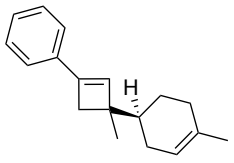

The title compound (yellow oil, 30 mg, 63%) was synthesized as a mixture of diastereomers in a 1:1 ratio according to the general procedure starting from ethynylbenzene (22 μL, 0.2 mmol) and (*S*)-(–)-limonene (65 μL, 0.4 mmol) with [(*t*BuXPhos)AuNCMe]BAr_4^F (15 mg, 10 μmol, 5 mol%). The reaction time was 72 h. Cyclohexane was used as eluent in the purification. The structure was confirmed by ^{1}H-^{1}H COSY, ^{1}H-^{13}C HMQC and ^{1}H-^{13}C HMBC experiments.

Mixture of diastereomers in a 1:1 ratio: **^{1}H NMR** (400 MHz, $CDCl_3$) δ 7.46 – 7.31 (m, 4H+4H), 7.30 – 7.21 (m, 1H+1H), 6.53 (s, 1H), 6.50 (s, 1H), 5.45 (bs, 1H+1H), 2.67 (d, *J* = 12.6, 1H), 2.65 (d, *J* = 12.6, 1H), 2.39 (d, *J* = 12.6, 1H), 2.36 (d, *J* = 12.6, 1H), 2.13 – 1.77 (m, 5H+5H), 1.69 (s, 3H+3H), 1.68 – 1.57 (m, 1H+1H), 1.42 – 1.27 (m, 1H+1H), 1.24 (s, 3H), 1.23 (s, 3H). **^{13}C NMR** (101 MHz, $CDCl_3$) δ 143.1, 142.9, 135.4, 135.3, 135.2, 135.1, 133.9 (1C+1C), 128.2 (2C+2C), 127.4 (1C+1C), 124.3 (2C+2C), 121.0, 120.9, 45.4, 45.3, 41.8, 41.4, 39.5, 39.0, 31.1, 31.0, 27.6, 27.3, 25.0, 24.9, 23.5, 23.5, 21.1, 20.7. **HRMS** (APCI) *m/z* calculated for $C_{18}H_{23}^+$ $[M+H]^+$: 239.1794, found: 239.1791.

(1*R*,4*S*,7*R*,11*S*)-4,13,13-Trimethyl-10-methylene-6-phenyltricyclo[9.2.0.0^{4,7}]tridec-5-ene

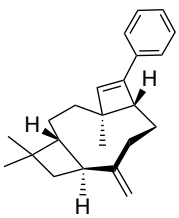

The title compound (dense colorless oil, 56 mg, 46%) was synthesized according to the general procedure starting from ethynylbenzene (44 μL, 0.4 mmol) and β-caryophyllene (181 μL, 0.8 mmol) with [(*t*BuXPhos)AuNCMe]BAr_4^F (31 mg, 20 μmol, 5 mol%). The reaction time was 36 h. Cyclohexane was used as eluent in the purification. The structure was confirmed by ^{1}H-^{1}H COSY, ^{1}H-^{13}C HMQC, ^{1}H-^{13}C HMBC and ^{1}H-^{1}H NOESY experiments.

^{1}H NMR (400 MHz, $CDCl_3$) δ 7.34 – 7.28 (m, 4H), 7.25 – 7.18 (m, 1H), 6.26 (s, 1H), 4.99 – 4.97 (m, 1H), 4.97 – 4.95 (m, 1H), 3.00 (dd, *J* = 13.0, 3.3 Hz, 1H), 2.52 – 2.42 (m, 1H), 2.15 – 2.04 (m, 1H), 1.94 – 1.72 (m, 3H), 1.68 – 1.33 (m, 6H), 1.17 (s, 3H), 1.02 (s, 3H), 0.99 (s, 3H). **^{13}C NMR** (101 MHz, $CDCl_3$) δ 153.1, 145.8, 136.5, 134.7, 128.3 (2C), 127.2, 125.0 (2C), 108.7, 55.2, 49.1, 46.3, 45.5, 42.0, 36.5, 33.7, 33.3, 30.4, 29.9, 26.5, 21.7, 18.2. **HRMS** (APCI) *m/z* calculated for $C_{23}H_{31}^+$ $[M+H]^+$: 307.2420, found: 307.2408.

(3,3,4,4-Tetramethylcyclobut-1-en-1-yl)benzene

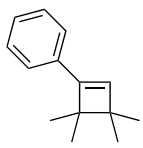

The title compound (colorless oil, 0.507 g, 91%) was synthesized according to the general procedure starting from ethynylbenzene (0.33 mL, 3 mmol) and 2,3-dimethylbut-2-ene (0.71 ml, 6 mmol) with [(*t*BuXPhos)AuNCMe]SbF_6 (81 mg, 0.09 mmol). The reaction time was 24 h. Triethylamine (0.1 mL) was added to quench the reaction before performing purification by chromatography.

^{1}H NMR (400 MHz, $CDCl_3$) δ 7.40 – 7.35 (m, 2H), 7.34 – 7.28 (m, 2H), 7.22 (tt, *J* = 7.3, 1.4 Hz, 1H), 6.30 (s, 1H), 1.31 (s, 6H), 1.13 (s, 6H). **^{13}C NMR** (101 MHz, $CDCl_3$) δ 150.9, 134.6, 134.3, 128.3 (2C), 127.1, 125.4 (2C), 47.1, 45.4, 23.3 (2C), 23.2 (2C). **HRMS** (APCI) *m/z* calculated for $C_{14}H_{19}^+$ $[M+H]^+$: 187.1481, found: 187.1481.

Procedure for the Reaction of Phenylacetylene with Cycloheptatriene

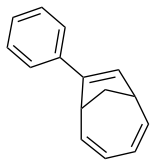

Ethynylbenzene (22 μL, 0.2 mmol, 1 equiv) was dissolved in DCE (0.1 mL, 2.0 M). Cycloheptatriene (0.104 mL, 1 mmol, 5 equiv) was added, followed by [(JohnPhos)AuNCMe]SbF_6 (8 mg, 0.01 mmol, 5 mol%). The resulting mixture was stirred at 80 ºC for 24 h. The reaction was followed by GC-MS. Triethylamine (0.02 mL) was added to quench the reaction. The volatiles were removed under reduced pressure and the product was isolated by preparative silica gel TLC (eluent = cyclohexane) to afford 7-phenylbicyclo[4.2.1]nona-2,4,7-triene (12 mg, 31%).

^{1}H NMR (300 MHz, $CDCl_3$) δ 7.53 – 7.47 (m, 2H), 7.34 – 7.26 (m, 2H), 7.24 – 7.16 (m, 1H), 6.39 – 6.16 (m, 2H), 5.94 – 5.84 (m, 2H), 5.83 (d, *J* = 2.8 Hz, 1H), 3.78 (t, *J* = 7.0 Hz, 1H), 3.24 (td, *J* = 7.0, 3.0 Hz, 1H), 2.37 (dtt, *J* = 11.4, 6.7, 1.1 Hz, 1H), 1.68 (d, *J* = 11.4 Hz, 1H). **^{13}C NMR** (75 MHz, $CDCl_3$) δ 139.2, 138.4, 137.7, 134.9, 128.3, 126.9, 126.8, 124.8, 124.1, 120.2, 44.6, 43.7, 31.2. The NMR data were in agreement with the ones reported in the literature.[130]

Procedure for the Reaction of Methyl Propiolate with Cycloheptatriene

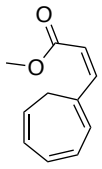

Methyl propiolate (18 μL, 0.2 mmol, 1 equiv) was dissolved in DCE (0.1 mL, 2.0 M). Cycloheptatriene (0.104 mL, 1 mmol, 5 equiv) was added, followed by [(JohnPhos)AuNCMe]SbF_6 (8 mg, 0.01 mmol, 5 mol%). The resulting mixture was stirred at 80 ºC for 24 h. The reaction was followed by TLC (eluent = cyclohexane:EtOAc 7:1) and GC-MS. Triethylamine (0.02 mL) was added to quench the reaction. The volatiles were removed under reduced pressure and the product was isolated by preparative silica gel TLC (eluent = cyclohexane:EtOAc 7:1) to afford (*Z*)-3-(cyclohepta-1,3,5-trien-1-yl)acrylate (yellow oil, 20 mg, 57%). The structure

130. Achard, M.; Tenaglia, A.; Buono, G. *Org. Lett.* **2005**, *7*, 2353–2356.

was confirmed by ^{1}H-^{1}H COSY, ^{1}H-^{13}C HMQC, ^{1}H-^{13}C HMBC and ^{1}H-^{1}H NOESY experiments.

^{1}H NMR (300 MHz, $CDCl_3$) δ 6.70 (dd, *J* = 11.1, 5.5 Hz, 1H), 6.64 – 6.55 (m, 2H), 6.43 (d, *J* = 6.1 Hz, 1H), 6.29 (dd, *J* = 9.4, 5.5 Hz, 1H), 5.78 – 5.69 (m, 1H), 5.66 (d, *J* = 12.8 Hz, 1H), 3.75 (s, 3H), 2.59 (d, *J* = 6.8 Hz, 2H). **^{13}C NMR** (75 MHz, $CDCl_3$) δ 166.6, 145.3, 133.2, 132.5, 129.2, 128.7, 126.5, 125.9, 116.7, 51.3, 30.8. **HRMS** (ESI+) *m/z* calculated for $C_{11}H_{12}O_2Na^+$ $[M+Na]^+$: 199.0730, found: 199.0732.

General Procedure for the One-pot Gold-Catalyzed [2+2]/(4+1) Cycloadditions

Cycloheptatriene (1 equiv) was dissolved in DCE (0.5 M) in a sealable vial. The alkyne (1.5 equiv) was added followed by the alkene (0.4 mmol, 2 equiv) and, finally, [*t*BuXPhos)AuNCMe]SbF_6 (0.1 equiv). The vial was sealed and the resulting mixture was stirred at 50 ºC for 14 h to form the corresponding cyclobutene. Then, the volatiles were removed under vacuum. DCE (0.5 M) was added, the vial was sealed again and the resulting mixture was stirred at 120 °C for 4 h. Triethylamine (0.02 mL) was added to quench the reaction and the volatiles were removed under vacuum. The crude was dissolved in the minimum CH_2Cl_2 and the product was isolated by preparative silica gel TLC (eluent = cyclohexane) to afford the corresponding cyclopentene.

2-(Naphthalen-1-yl)-3-phenylspiro[4.5]dec-1-ene

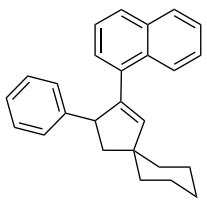

The title compound (31 mg, 46% yield) was synthesized according to the general procedure starting from 1-(cyclohepta-2,4,6-trien-1-yl)naphthalene (44 mg, 0.200 mmol), ethynylbenzene (33 µL, 0.3 mmol), methylenecyclohexane (48 µL, 0.4 mmol) and [(*t*BuXPhos)AuNCMe]SbF_6 (18 mg, 0.02 mmol).

^{1}H NMR (500 MHz, $CDCl_3$) δ 8.38 (d, *J* = 8.5 Hz, 1H), 7.80 (d, *J* = 8.1 Hz, 1H), 7.62 (d, *J* = 8.2 Hz, 1H), 7.53 (t, *J* = 7.8 Hz, 1H), 7.47 (t, *J* = 7.7 Hz, 1H), 7.27 (t, *J* = 7.5 Hz, 1H), 7.21 – 7.15 (m, 3H), 7.12 (t, *J* = 7.4 Hz, 2H), 7.07 – 7.00 (m, 1H), 6.14 (s, 1H), 4.65 (td, *J* = 8.2, 2.1 Hz, 1H), 2.64 (dd, *J* = 13.1, 8.6 Hz, 1H), 1.92 – 1.38 (m, 11H). **^{13}C NMR** (101 MHz, $CDCl_3$) δ 145.3, 142.7, 141.2, 135.4, 133.8, 131.8, 128.3, 128.1, 127.8, 126.7, 125.7, 125.6, 125.6, 125.3, 125.1, 125.0, 53.8, 49.4, 47.3, 39.3, 36.9, 26.1, 23.7, 23.5. The NMR data were in agreement with the literature.[115]

3-(4-(*tert*-Butyl)phenyl)-2-(naphthalen-1-yl)spiro[4.5]dec-1-ene

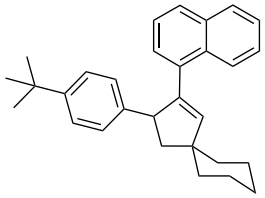

The title compound (46 mg, 58% yield) was synthesized according to the general procedure starting from 1-(cyclohepta-2,4,6-trien-1-yl)naphthalene (44 mg, 0.200 mmol), 1-(*tert*-butyl)-4-ethynylbenzene (54 µL, 0.3 mmol), methylenecyclohexane (48 µL, 0.4 mmol) and [(*t*BuXPhos)AuNCMe]SbF_6 (18 mg, 0.02 mmol).

^{1}H NMR (500 MHz, $CDCl_3$) δ 8.41 (d, *J* = 8.3 Hz, 1H), 7.84 – 7.78 (m, 1H), 7.63 (d, *J* = 8.3 Hz, 1H), 7.56 – 7.45 (m, 2H), 7.31 – 7.26 (m, 1H), 7.21 (dd, *J* = 7.2, 1.3 Hz, 1H), 7.18 – 7.13 (m, 2H), 7.12 – 7.07 (m, 2H), 6.13 (s, 1H), 4.64 (td, *J* = 8.4, 2.1 Hz, 1H), 2.62 (dd, *J* = 13.1, 8.7 Hz, 1H), 1.89 – 1.30 (m, 11H), 1.23 (s, 9H). **^{13}C NMR** (101 MHz, $CDCl_3$) δ 148.3, 142.8, 142.2, 141.2, 135.7, 133.8, 131.8, 129.1, 128.3, 127.3, 126.6, 125.7, 125.6, 125.3, 125.1, 125.0, 125.0, 53.1, 49.3, 47.4, 39.4, 36.9, 34.2, 31.3, 26.1, 23.7, 23.5. The NMR data were in agreement with the literature.[115]

3-(3-(4-Chlorophenyl)spiro[4.5]dec-3-en-2-yl)phenol

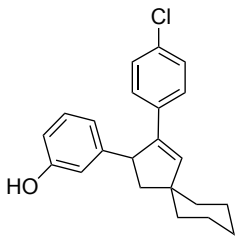

The title compound (18 mg, 35% yield) was synthesized according to the general procedure starting from 7-(4-chlorophenyl)cyclohepta-1,3,5-triene (30 mg, 0.15 mmol), 3-ethynylphenol (25 µL, 0.225 mmol), methylenecyclohexane (36 µL, 0.3 mmol) and [(*t*BuXPhos)AuNCMe]SbF_6 (13 mg, 0.015 mmol).

^{1}H NMR (500 MHz, $CDCl_3$) δ 7.20 (dt, *J* = 8.7, 2.4 Hz, 2H), 7.13 (dt, *J* = 8.7, 2.4 Hz, 2H), 7.11 – 7.06 (t, *J* = 7.7 Hz,1H), 6.74 (dt, *J* = 7.6, 1.3 Hz, 1H), 6.62 – 6.57 (m, 2H), 6.30 (s, 1H), 4.79 (m, 1H), 4.31 (ddd, *J* = 9.2, 6.2, 1.8 Hz, 1H), 2.46 (dd, *J* = 13.2, 9.2 Hz, 1H), 1.68 (dd, *J* = 13.2, 6.2 Hz, 2H), 1.65 – 1.32 (m, 10H). **^{13}C NMR** (75 MHz, $CDCl_3$) δ 155.6, 148.1, 140.1, 139.3, 134.6, 132.3, 129.6, 128.2, 127.7, 120.4, 114.4, 112.9, 50.6, 48.8, 47.3, 38.6, 37.6, 25.9, 23.5, 23.3. The NMR data were in agreement with the literature.[115]

General Procedure for the (4+1) Cycloaddition of Cyclobutenes with Cycloheptatrienes

Cyclobutene (0.2 mmol, 2 equiv) and cycloheptatriene (0.1 mmol, 1 equiv) were dissolved in DCE (1 mL, 0.1 M) in a sealable vial. [(*t*BuXPhos)AuNCMe]SbF_6 or

[(JohnPhos)AuNCMe]SbF_6 (5 μmol, 5 mol%) was added. The vial was sealed and the reaction mixture was stirred at 120 °C for 3 h. Triethylamine (2 drops) were added to quench the reaction and the volatiles were evaporated under reduced pressure. The crude was purified by silica gel flash column chromatography.

Mixture of (*E*)-3-(4-(*tert*-butyl)phenyl)-2-styrylspiro[4.5]dec-1-ene (14d, *minor*) and (*E*)-3-(4-(*tert*-butyl)phenyl)-3-styrylspiro[4.5]dec-1-ene (15d, *major*)

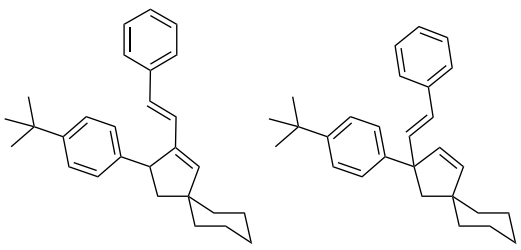

The title compounds **14d** and **15d** were synthesized as a mixture in a 1:3 ratio (colorless oil, 21 mg, 55% yield) following the general procedure starting from 2-(4-(tert-butyl)phenyl)spiro[3.5]non-1-ene (52 mg, 0.206 mmol), (*E*)-7-styrylcyclohepta-1,3,5-triene (20 mg, 0.103 mmol) and [(*t*BuXPhos)AuNCMe]SbF_6 (5 mg, 5 μmol). Pentane was used as eluent in the purification. The structures were confirmed by ^{1}H-^{1}H COSY, ^{1}H-^{13}C HMQC, ^{1}H-^{13}C HMBC and ^{1}H-^{1}H NOESY experiments.

^{1}H and ^{13}C NMR spectra contained traces of pentane. **^{1}H NMR** (400 MHz, $CDCl_3$) δ 7.41 – 7.10 (m, 9H *major* and 9H *minor*), 6.83 (d, *J* = 16.2, 1H *minor*), 6.58 (dd, *J* = 16.1, 1.2 Hz, 1H *major*), 6.31 (d, *J* = 16.1, 1H *major*), 6.11 (d, *J* = 16.3 Hz, 1H *minor*), 6.06 (s, 1H *minor*), 5.88 (s, 2H *major*), 4.19 – 4.12 (m, 1H *minor*), 2.42 (dd, *J* = 13.1, 9.3 Hz, 1H *minor*), 2.36 (d, *J* = 13.4, 1H *major*), 2.09 (dd, *J* = 13.4, 0.9 Hz, 1H *major*), 1.67 (ddd, *J* = 13.2, 6.2, 1.2 Hz, 1H *minor*), 1.64 – 1.22 (m, 19H *major* and 19H *minor*). **^{13}C NMR** (101 MHz, $CDCl_3$) δ 148.5, 148.4, 145.8, 143.2, 143.1, 141.3, 140.3, 139.3, 137.8, 137.8, 133.2, 130.2, 128.4, 128.4, 127.2, 126.9, 126.9, 126.7, 126.3, 126.2, 126.1, 125.2, 125.1, 125.0, 58.4, 50.4, 50.0, 49.5, 48.5, 38.8, 38.6, 37.8, 34.3, 34.3, 31.4, 31.4, 26.0, 26.0, 23.6, 23.5, 23.4. **HRMS** (APCI) *m/z* calculated for $C_{28}H_{35}^+$ $[M+H]^+$: 371.2733, found: 371.2725.

Mixture of (*E*)-2-(4-bromostyryl)-3-(4-(*tert*-butyl)phenyl)spiro[4.5]dec-1-ene (14e, *minor*) and (*E*)-3-(4-bromostyryl)-3-(4-(*tert*-butyl)phenyl)spiro[4.5]dec-1-ene (15e, *major*)

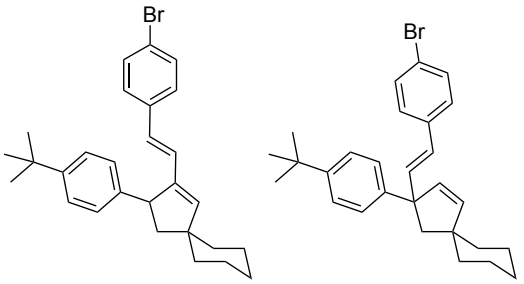

The title compounds **14e** and **15e** were synthesized as a mixture in a 1:2 ratio (white solid, 25 mg, 56% yield) following the general procedure starting from 2-(4-(*ter*t-butyl)phenyl)spiro[3.5]non-1-ene (51 mg, 0.2 mmol), (*E*)-7-(4-bromostyryl)cyclohepta-1,3,5-triene (27 mg, 0.1 mmol) and [(*t*BuXPhos)AuNCMe]SbF_6 (4.5 mg, 5 μmol). Cyclohexane was used as eluent in the purification. The structures were confirmed by ^{1}H-^{1}H COSY, ^{1}H-^{13}C HMQC, ^{1}H-^{13}C HMBC and ^{1}H-^{1}H NOESY experiments.

M.p. 43-46 ºC. **^{1}H NMR** (400 MHz, $CDCl_3$) δ 7.46 – 7.21 (m, 8H *major* and 4H *minor*), 7.18 – 7.13 (m, 2H *minor*), 7.10 – 7.04 (m, 2H *minor*), 6.83 (d, *J* = 16.2 Hz, 1H *minor*), 6.57 (d, *J* = 16.1 Hz, 1H *major*), 6.25 (d, *J* = 16.1 Hz, 1H *major*), 6.09 (s, 1H *minor*), 6.03 (d, *J* = 16.3 Hz, 1H *minor*), 5.91 (d, *J* = 10.7 Hz, 1H *major*), 5.88 (d, *J* = 10.7 Hz, 1H *major*), 4.19 – 4.12 (m, 1H *minor*), 2.43 (dd, *J* = 13.2, 9.2 Hz, 1H *minor*), 2.34 (d, *J* = 13.3 Hz, 1H *major*), 2.11 (d, *J* = 13.3 Hz, 1H *major*), 1.68 (dd, *J* = 13.2, 6.2 Hz, 1H *minor*), 1.64 – 1.25 (m, 19H *major* and 19H *minor*). **^{13}C NMR** (101 MHz, $CDCl_3$, *major*) δ 148.6, 145.5, 140.5, 140.3, 136.8, 132.9, 131.5 (2C), 127.7 (2C), 126.2 (2C), 125.6, 125.1 (2C), 120.5, 58.5, 50.4, 50.1, 38.7, 37.9, 34.3, 31.4 (3C), 25.9, 23.5, 23.4. **^{13}C NMR** (101 MHz, $CDCl_3$, *minor*) δ 148.6, 143.8, 143.0, 141.1, 136.8, 131.4 (2C), 128.8, 127.5 (2C), 127.1 (2C), 125.7, 125.3 (2C), 120.6, 49.4, 48.6, 47.9, 38.5, 37.7, 34.3, 31.4 (3C), 26.0, 23.5, 23.4. **HRMS** (APCI) *m/z* calculated for $C_{28}H_{34}Br^+$ $[M+H]^+$: 449.1838, found: 449.1822.

Mixture of (*E*)-3-(4-(*tert*-butyl)phenyl)-2-(4-methoxystyryl)spiro[4.5]dec-1-ene (14f, *minor*) and (*E*)-3-(4-(*tert*-butyl)phenyl)-3-(4-methoxystyryl)spiro[4.5]dec-1-ene (15f, *major*)

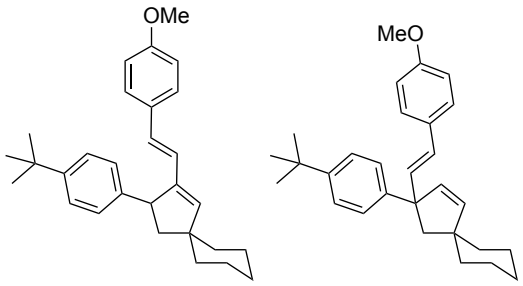

The title compounds **14f** and **15f** were synthesized as a mixture in a 1:9 ratio (colorless oil, 15 mg, 37% yield) following the general procedure starting from 2-(4-(tert-butyl)phenyl)spiro[3.5]non-1-ene (51 mg, 0.2 mmol), (*E*)-7-(4-methoxystyryl)cyclohepta-1,3,5-triene (22 mg, 0.1 mmol) and [(*t*BuXPhos)AuNCMe]SbF_6 (4.5 mg, 5 μmol). In the purification, the eluent used was pentane and then, pentane:CH_2Cl_2 7:1. The structures were confirmed by ^{1}H-^{1}H COSY, ^{1}H-^{13}C HMQC, ^{1}H-^{13}C HMBC and ^{1}H-^{1}H NOESY experiments.

^{1}H NMR (300 MHz, $CDCl_3$) δ 7.45 – 7.11 (m, 6H *major* and 6H *minor*), 6.90 – 6.81 (m, 2H *major*), 6.81 – 6.75 (m, 2H *minor*), 6.71 (d, *J* = 16.3 Hz, 1H *minor*), 6.44 (d, *J* = 16.1 Hz, 1H *major*), 6.25 (d, *J* = 16.1 Hz, 1H *major*), 6.06 (d, *J* = 16.4 Hz, 1H *minor*), 6.01 (s, 1H *minor*), 5.87 (s, 2H *major*), 4.19 – 4.10 (m, 1H *minor*), 3.81 (s, 3H *major*), 3.78 (s, 3H *minor*), 2.42 (dd, *J* = 13.2, 9.2 Hz, 1H *minor*), 2.35 (d, *J* = 13.3 Hz, 1H *major*), 2.08 (d, *J* = 13.3 Hz, 1H *major*), 1.66 (dd, *J* = 13.1, 6.1 Hz, 1H *minor*), 1.62 – 1.18 (m, 19H *major* and 19H *minor*). **^{13}C NMR** (101 MHz, $CDCl_3$, *major*) δ 158.7, 148.4, 146.0, 140.1, 137.3, 133.4, 130.7, 127.3 (2C), 126.3 (2C), 126.1, 125.1 (2C), 113.9 (2C), 58.4, 55.3, 50.0, 38.8, 37.9, 34.3, 31.4, 31.4 (3C), 26.0, 23.6, 23.5. **HRMS** (ESI+) *m/z* calculated for $C_{29}H_{37}O^+$ $[M+H]^+$: 401.2839, found: 401.2830.

(*E*)-3-(4-Chlorostyryl)-2-(naphthalen-1-yl)spiro[4.5]dec-1-ene

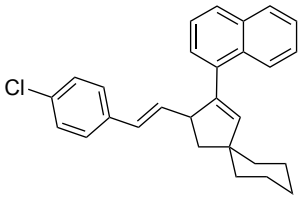

The title compound (colorless oil, 20 mg, 50% yield) was synthesized according to the general procedure starting from 1-(cyclohepta-2,4,6-trien-1-yl)naphthalene (22 mg, 0.1 mmol), (*E*)-2-(4-chlorostyryl)spiro[3.5]non-1-ene (39 mg, 0.15 mmol) and [(JohnPhos)AuNCMe]SbF_6 (4 mg, 5 μmol, 5 mol%). Cyclohexane was used as eluent in the purification.

^{1}H NMR (400 MHz, $CDCl_3$) δ 8.23 – 8.14 (m, 1H), 7.88 – 7.82 (m, 1H), 7.73 (d, *J* = 8.2 Hz, 1H), 7.54 – 7.47 (m, 2H), 7.44 – 7.38 (m, 1H), 7.31 (dm, *J* = 7.1, 1H), 7.18 – 7.13 (m, 2H), 7.10 – 7.05 (m, 2H), 6.19 (d, *J* = 15.8 Hz, 1H), 6.07 (dd, *J* = 15.8, 8.2 Hz, 1H), 5.97 (d, *J* = 2.0 Hz, 1H), 4.14 – 4.05 (m, 1H), 2.38 (dd, *J* = 13.0, 8.3 Hz, 1H), 1.84 (dd, *J* = 13.0, 6.6 Hz, 1H), 1.77 – 1.52 (m, 10H). **^{13}C NMR** (126 MHz, $CDCl_3$) δ 141.4, 136.0, 135.6, 134.6, 133.8, 132.3, 131.9, 128.5, 128.4 (2C), 128.3, 127.2 (2C), 127.0, 125.7, 125.6, 125.5, 125.5, 125.1, 51.7, 49.5, 39.3, 37.2, 26.1, 23.7, 23.5. **HRMS** (APCI) *m/z* calculated for $C_{28}H_{28}Cl^+$ $[M+H]^+$: 399.1874, found: 399.1867.

Diels-Alder Reaction of Vinylcyclobutenes with Maleic Anhydride

Cyclobutene (0.1 mmol, 1 equiv) and maleic anhydride (0.2 mmol, 2 equiv) were dissolved in toluene (1 mL, 0.1 M) in a sealable vial. The vial was sealed and the reaction mixture was stirred at 60 °C. The reaction was followed by TLC. Upon completion, the reaction mixture was concentrated under reduced pressure and the crude was purified by silica gel flash column chromatography.

(3a*S*,3b*S***,9a*S***,9b*R***)-3a,5,6,7,8,9,9a,9b-Octahydro-3*H*-spiro[cyclobuta[3,4]naphtho[1,2-*c*]furan-4,1'-cyclohexane]-1,3(3b*H*)-dione**

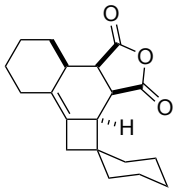

The title compound (yellow oil, 14 mg, 47%) was synthesized according to the general procedure starting from 2-(cyclohex-1-en-1-yl)spiro[3.5]non-1-ene (20 mg, 0.1 mmol) and maleic anhydride (20 mg, 0.2 mmol). The reaction time was 38 h. In the purification, the eluent used was cyclohexane:EtOAc 9:1 (4 CV), 7:1 (2 CV) and then, 5:1 (2 CV). The structure was confirmed by ^{1}H-^{1}H COSY, ^{1}H-^{13}C HSQC and ^{1}H-^{1}H NOESY experiments.

^{1}H NMR (500 MHz, $CDCl_3$) δ 3.41 (dd, *J* = 12.1, 8.6 Hz, 1H), 3.21 (dd, *J* = 8.7, 4.6 Hz, 1H), 2.83 – 2.75 (m, 1H), 2.44 – 2.34 (m, 3H), 2.30 – 2.13 (m, 2H), 1.98 – 1.79 (m, 2H), 1.77 – 1.05 (m, 14H). **^{13}C NMR** (126 MHz, $CDCl_3$) δ 172.1, 171.6, 129.8, 126.6, 48.1, 46.5, 46.4, 41.1, 40.0, 38.6, 32.2, 29.4, 26.4, 25.6, 25.4, 24.2, 23.7, 23.3, 23.1. **HRMS** (APCI) *m/z* calculated for $C_{19}H_{25}O_3^+$ $[M+H]^+$: 301.1798, found: 301.1793.

(3a*R,4*R**,7a*S**,7b*S**)-4-(4-Chlorophenyl)-4,6,7a,7b-tetrahydro-1*H*-spiro[cyclobuta[*e*]isobenzo-furan-7,1'-cyclohexane]-1,3(3a*H*)-dione**

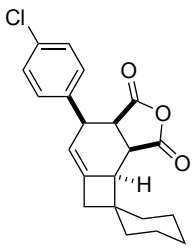

The title compound (yellow solid, 15 mg, 42%) was synthesized according to the general procedure starting from (*E*)-2-(4-chlorostyryl)spiro[3.5]non-1-ene (26 mg, 0.1 mmol) and maleic anhydride (20 mg, 0.2 mmol). The reaction time was 7 d. In the purification, the eluent used was cyclohexane:EtOAc 5:1. The structure was confirmed by ^{1}H-^{1}H COSY, ^{1}H-^{13}C HMQC, ^{1}H-^{13}C HMBC and nOe experiments.

M.p. 129-132 ºC. **^{1}H NMR** (400 MHz, $CDCl_3$) δ 7.34 (s, 4H), 5.92 – 5.88 (m, 1H), 3.64 (dd, *J* = 12.3, 8.9 Hz, 1H), 3.62 – 3.58 (m, 1H), 3.53 (dd, *J* = 8.9, 4.4 Hz, 1H), 2.98 (dm, *J* = 12.0 Hz, 1H), 2.52 (dm, *J* = 14.0 Hz, 1H), 2.40 (dm, *J* = 14.0 Hz, 1H), 1.81 – 1.41 (m, 8H), 1.32 – 1.05 (m, 2H). **^{13}C NMR** (101 MHz, $CDCl_3$) δ 170.9, 170.2, 141.6, 138.1, 133.0, 130.3, 128.4, 116.1, 49.5, 46.9, 46.4, 41.0, 40.4, 40.2, 37.3, 28.9, 25.4, 23.5, 23.1. **HRMS** (ESI+) *m/z* calculated for $C_{21}H_{21}ClO_3Na^+$ $[M+Na]^+$: 379.1071, found: 379.1074.

Ring Opening Reaction to Form 1,3-Dienes

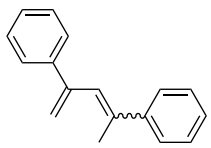

(3-Methylcyclobut-1-ene-1,3-diyl)dibenzene (33 mg, 0.15 mmol) was dissolved in chlorobenzene (3 mL, 0.05 M) in a sealable vial. The vial was sealed and the mixture was stirred at 140 °C for 7 h. The volatiles were removed under reduced pressure and the crude was purified by silica gel preparative chromatography (eluent = cyclohexane) to afford 1,3-dienes **18** and **18´** (colorless oil, 22 mg, 67%, *E*:*Z* in a 9:1 ratio). The configuration of each diene was confirmed by nOe experiments.

^{1}H NMR (400 MHz, $CDCl_3$) δ 7.61 – 7.10 (m, 10H *major* and 10H *minor*), 6.65 – 6.56 (m, 1H *major*), 6.31 – 6.28 (m, 1H *minor*), 5.75 – 5.70 (m, 1H *major*), 5.34 – 5.32 (m, 1H *minor*), 5.31 – 5.26 (m, 1H *major*), 4.94 – 4.91 (m, 1H *minor*), 2.27 – 2.23 (m, 3H *minor*), 2.19 – 2.14 (m, 3H *major*). **^{13}C NMR** (101 MHz, $CDCl_3$, *major*) δ 145.4, 143.4, 140.9, 138.8, 128.3 (2C), 128.3 (2C), 127.6, 127.5, 127.2, 126.6 (2C), 125.9 (2C), 115.4, 17.6. **^{13}C NMR** (101 MHz, $CDCl_3$, detected signals of the *minor*) δ 145.0, 140.2, 128.0, 127.8, 127.3, 126.8, 126.6, 116.2, 26.1. **HRMS** (APCI) *m/z* calculated for $C_{17}H_{17}^+$ $[M+H]^+$: 221.1325, found: 221.1317.

Oxidative Ring Opening Reaction to Form Dicarbonyl Compounds

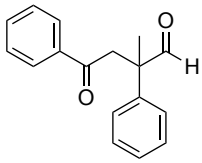

(3-Methylcyclobut-1-ene-1,3-diyl)dibenzene (44 mg, 0.2 mmol, 1 equiv) was dissolved in acetone (3 mL) and *N*-methylmorpholine-*N*-oxide (56 mg, 0.48 mmol, 2.4 equiv) was added followed by OsO_4 (0.3 mL of a previously prepared 5 mg/mL solution of OsO_4 in water, 6 μmol, 0.03 equiv). The vial was sealed and the black reaction mixture was stirred at 23 °C for 5 h to generate the corresponding 1,2-diol. The reaction was monitored by TLC (eluent = cyclohexane:EtOAc 5:1). Upon completion, the volatiles were removed under reduced pressure. The resulting residue was dissolved in acetone (1 mL) and water (1 mL) and $NaIO_4$ (188 mg, 0.88 mmol, 4.4 equiv) was added. The resulting light brown suspension was sonicated to dissolved the salt and stirred at 23 °C for 2 h to form the corresponding dicarbonyl compound. The reaction was monitored by TLC (eluent = cyclohexane:EtOAc 5:1). The reaction mixture became a white suspension. It was diluted with water (10 mL), extracted with diethyl ether (3 × 10 mL), dried over Na_2SO_4, filtered and concentrated under reduced pressure. The product was isolated by silica gel flash column chromatography (eluent = cyclohexane:EtOAc 14:1). The dicarbonyl product was obtained as a pale yellow oil (43 mg, 85% yield).

^{1}H NMR (400 MHz, $CDCl_3$) δ 9.74 (s, 1H), 7.96 – 7.91 (m, 2H), 7.56 (tt, *J* = 7.4, 1.2 Hz, 1H), 7.48 – 7.42 (m, 2H), 7.41 – 7.31 (m, 4H), 7.31 – 7.25 (m, 1H), 3.73 (app. d, *J* = 2.6 Hz, 2H), 1.69 (s, 3H). **^{13}C NMR** (101 MHz, $CDCl_3$) δ 201.4, 197.2, 139.7, 136.8, 133.3, 128.9 (2C), 128.6 (2C), 128.0 (2C), 127.3, 126.8 (2C), 51.8, 46.0, 20.7. **HRMS** (ESI+) *m/z* calculated for $C_{17}H_{16}O_2Na^+$ $[M+Na]^+$: 275.1043, found: 275.1043.

Procedure for the Epoxidation of Cyclobutenes

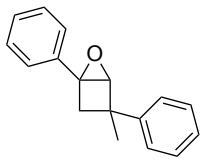

(3-Methylcyclobut-1-ene-1,3-diyl)dibenzene (44 mg, 0.2 mmol, 1 equiv) was dissolved in acetone (3 mL) in a flask, and water (3 mL) was added. $NaHCO_3$ (0.118 g, 1.4 mmol, 7 equiv) was added, followed by oxone (0.307 g, 1.0 mmol, 5 equiv).[131] ***Caution:***

131. The same reaction outcome is obtained when using previously prepared dimethyldioxirane (1.05 equiv) in acetone instead of generating it *in situ* with oxone (5 equiv) and $NaHCO_3$ (7 equiv) in acetone:H_2O (1:1). Dimethyldioxirane was synthesized following the literature procedure: Marron, T. G.; Pfeifer, L. A.; Roush, W. R. *Org. Synth.* **1997**, *74*, 91–100.

Dimethyldioxirane is produced. It is a volatile peroxide and should be treated as such.[132] The flask was capped with a stopper and the resulting mixture was stirred at 23 °C for 3 h. The reaction was monitored by TLC (eluent = cyclohexane). Upon completion, water (5 mL) was added and the product was extracted with CH_2Cl_2 (3 × 5 mL), dried over Na_2SO_4, filtered and concentrated under reduced pressure. The obtained crude was an analytically pure mixture of (1*R**,3*S**,4*R**)- and (1*R**,3*R**,4*R**)-3-methyl-1,3-diphenyl-5-oxabicyclo[2.1.0]pentane diastereoisomers in a 1:2.6 ratio (colorless oil, 46 mg, 97% yield) according to ^{1}H NMR. Both diastereoisomers were separated and isolated by preparative neutral aluminum oxide TLC (previously treated with a mixture of pentane:triethylamine 100:1, eluent = pentane:triethylamine 100:1). The relative configurations of the diastereoisomers were assigned on the basis of nOe experiments.

(1*R,3*R**,4*R**)-3-Methyl-1,3-diphenyl-5-oxabicyclo[2.1.0]pentane**

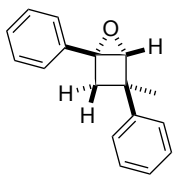

(1*R**,3*R**,4*R**)-3-Methyl-1,3-diphenyl-5-oxabicyclo[2.1.0]pentane was obtained as a colorless oil (Rf = 0.85 in neutral aluminum oxide TLC using pentane:triethylamine 100:1 as eluent, 33 mg, 70% yield). **^{1}H NMR** (400 MHz, $CDCl_3$) δ 7.33 – 7.14 (m, 10 H), 4.27 (d, *J* = 2.6 Hz, 1H), 2.71 (d, *J* = 11.5 Hz, 1H), 2.16 (dd, *J* = 11.5, 2.6 Hz, 1H), 1.38 (s, 3H). **^{13}C NMR** (101 MHz, $CDCl_3$) δ 146.3, 135.2, 128.6 (2C), 128.4 (2C), 127.8, 126.4, 125.9 (2C), 125.7 (2C), 67.8, 61.4, 46.5, 43.0, 21.5. **HRMS** (ESI+) *m/z* calculated for $C_{17}H_{17}O^+$ $[M+H]^+$: 237.1274, found: 237.1268.

132. ***Caution:*** *Reactions and subsequent operations involving peracids and peroxy compounds should be performed behind a safety shield. Peroxy compounds should be added to the organic material, never the other way around. For relatively fast reactions, the rate of addition of the peroxy compound should be slow enough so that it reacts rapidly and no significant unreacted excess is allowed to build up. The reaction mixture should be stirred efficiently while the peroxy compound is being added, and cooling should generally be provided since many reactions of peroxy compounds are exothermic. Reaction products should never be recovered from the final reaction mixture by distillation until all residual active oxygen compounds (including unreacted peroxy compounds) have been destroyed. Decomposition of active oxygen compounds may be accomplished by the procedure described in* Korach, M.; Nielsen, D. R.; Rideout, W. H. *Org. Synth.* **1962**, *42*, 50 (*Org. Synth.* **1973**, Coll. Vol. 5, 414).

(1*R,3*S**,4*R**)-3-Methyl-1,3-diphenyl-5-oxabicyclo[2.1.0]pentane**

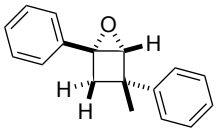

(1*R**,3*S**,4*R**)-3-Methyl-1,3-diphenyl-5-oxabicyclo[2.1.0]pentane was obtained as a colorless oil (Rf = 0.75 in neutral aluminum oxide TLC using pentane:triethylamine 100:1 as eluent, 13 mg, 27% yield).

^{1}H NMR (400 MHz, $CDCl_3$) δ 7.36 – 7.16 (m, 9H), 7.13 (tt, *J* = 7.0, 1.4 Hz, 1H), 4.30 (d, *J* = 2.3 Hz, 1H), 2.50 (d, *J* = 11.4 Hz, 1H), 2.41 (dd, *J* = 11.4, 2.3 Hz, 1H), 1.47 (s, 3H). **^{13}C NMR** (101 MHz, $CDCl_3$) δ 145.1, 135.5, 128.4 (4C), 127.8, 126.1 (2C), 125.9, 125.8 (2C), 68.1, 61.7, 47.4, 42.8, 26.9. **HRMS** (ESI+) *m/z* calculated for $C_{17}H_{17}O^+$ $[M+H]^+$: 237.1274, found: 237.1277.

Procedure for the Preparation of Cyclopropylaldehydes

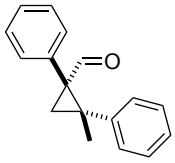

(3-Methylcyclobut-1-ene-1,3-diyl)dibenzene (44 mg, 0.2 mmol, 1 equiv) was dissolved in acetone (3 mL) in a flask, and water (3 mL) was added. $NaHCO_3$ (0.118 g, 1.4 mmol, 7 equiv) was added, followed by oxone (0.307 g, 1.0 mmol, 5 equiv).[131] ***Caution:*** *Dimethyldioxirane is produced. It is a volatile peroxide and should be treated as such.*[132] The flask was capped with a stopper and the resulting mixture was stirred at 23 °C for 3 h. The reaction was monitored by TLC (eluent = cyclohexane). Upon completion, water (5 mL) was added and the product was extracted with CH_2Cl_2 (2 × 5 mL). An aqueous solution of 10% HCl (10 mL) was added to the combined organic phase, the mixture was vigorously shaken and the layers were separated. The aqueous phase was extracted with CH_2Cl_2 (2 × 10 mL). The combined organic phases were dried over Na_2SO_4, filtered and concentrated under reduced pressure. The product was isolated by preparative silica gel TLC (eluent = cyclohexane:EtOAc 10:1) as a pale yellow solid (25 mg, 52% yield). The relative configuration of the cyclopropyl aldehyde was assigned on the basis of nOe experiments. The aldehyde converts into 2-methyl-2,4-diphenyl-2,3-dihydrofuran upon heating, thus its melting point could not be determined.

^{1}H NMR (400 MHz, $CDCl_3$) δ 8.77 (s, 1H), 7.47 – 7.32 (m, 9H), 7.29 – 7.23 (m, 1H), 2.39 (d, *J* = 5.3 Hz, 1H), 1.83 (d, *J* = 5.3 Hz, 1H), 1.15 (s, 3H). **^{13}C NMR** (75 MHz, $CDCl_3$) δ 200.0, 141.6, 134.7, 130.7 (2C), 128.8 (2C), 128.7 (2C), 128.5 (2C), 127.5, 127.1, 47.9,

38.5, 26.1, 23.9. **HRMS** (ESI+) *m/z* calculated for $C_{17}H_{16}ONa^+$ $[M+Na]^+$: 259.1093, found: 259.1095.

General Procedure for the Synthesis of 2,3-Dihydrofurans

The cyclobutene (0.2 mmol, 1 equiv) was dissolved in acetone (3 mL) in a flask, and water (3 mL) was added. $NaHCO_3$ (0.118 g, 1.4 mmol, 7 equiv) was added, followed by oxone (0.307 g, 1.0 mmol, 5 equiv). ***Caution:*** *Dimethyldioxirane is produced. It is a volatile peroxide and should be treated as such.*[132] The flask was capped with a stopper and the resulting mixture was stirred at 23 °C until no cyclobutene was detected (3-22 h) by TLC (eluent = cyclohexane). Then, water (5 mL) was added and the product was extracted with CH_2Cl_2 (3 × 5 mL), dried over Na_2SO_4, filtered and concentrated under reduced pressure. Without further purification, the crude containing the corresponding epoxide was dissolved in dry CH_2Cl_2 (0.4 mL) under nitrogen and yttrium (III) triflate (11 mg, 0.02 mmol, 0.1 equiv) was added. The resulting reaction mixture was stirred at 23 °C for 2 h. It was then diluted with water (5 mL), extracted with CH_2Cl_2 (3 × 5 mL), dried over Na_2SO_4, filtered and concentrated under reduced pressure. The product was isolated by preparative silica gel TLC (eluent = cyclohexane: EtOAc 10:1).

2-Methyl-2,4-diphenyl-2,3-dihydrofuran (22a)

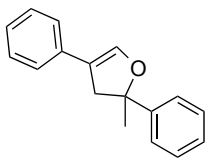

The title compound (colorless oil, 38 mg, 80% yield) was synthesized according to the general procedure starting from freshly prepared (3-methylcyclobut-1-ene-1,3-diyl)dibenzene (44 mg, 0.2 mmol).

^{1}H NMR (300 MHz, $CDCl_3$) δ 7.53 – 7.45 (m, 2H), 7.43 – 7.34 (m, 2H), 7.34 – 7.22 (m, 5H), 7.19 – 7.10 (m, 1H), 6.99 (t, *J* = 2.0 Hz, 1H), 3.23 (dd, *J* = 14.4, 2.1 Hz, 1H), 3.14 (dd, *J* = 14.4, 2.0 Hz, 1H), 1.78 (s, 3H). **^{13}C NMR** (101 MHz, $CDCl_3$) δ 147.3, 140.6, 134.3, 128.5 (2C), 128.4 (2C), 127.0, 125.6, 124.4 (2C), 124.0 (2C), 114.1, 88.5, 45.3, 29.4. **HRMS** (ESI+) *m/z* calculated for $C_{17}H_{16}ONa^+$ $[M+Na]^+$: 259.1093, found: 259.1094.

The title enantioenriched (*S*)-2,3-dihydrofuran (colorless oil, 18 mg, 53% yield, 77:23 *er*) was synthesized according to the general procedure starting from enantioenriched (*R*)-(3-methylcyclobut-1-ene-1,3-diyl)dibenzene (31 mg, 0.14 mmol, 90:10 *er*). **SFC** (Chiralpak

IA (100 mm × 4.6 mm, 3 µm), CO_2/isopropanol 90:10, 3 mL/min, 1500 psi of backpressure) t_R (*minor*) 2.0 min, t_R (*major*) 3.2 min. α_D^{589} ($CHCl_3$, *c* 0.01, 300 K) = 9.4 deg.cm^2.g^{-1}.

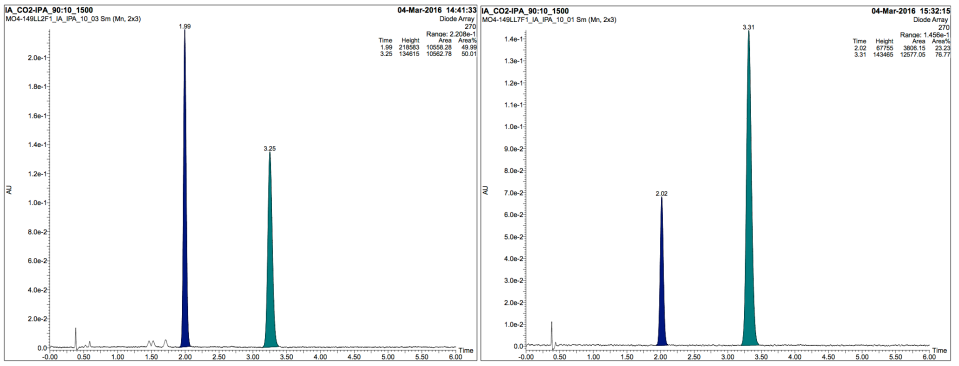

Time	Height	Area	Area%
1.99	218583	10558.28	49.99
3.25	134615	10562.78	50.01

Time	Height	Area	Area%
2.02	67755	3806.15	23.23
3.31	143465	12577.05	76.77

Figure S2.1. Chromatogram of the racemic (left) and enantioenriched (right) 2,3-dihydrofuran **22a**.

4-(4-(*tert*-Butyl)phenyl)-2-methyl-2-phenyl-2,3-dihydrofuran (22b)

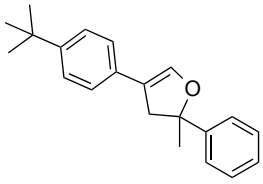

The title compound (yellow oil, 50 mg, 85 % yield) was synthesized according to the general procedure starting from freshly prepared 1-(*tert*-butyl)-4-(3-methyl-3-phenylcyclobut-1-en-1-yl)benzene (55 mg, 0.2 mmol).

^{1}H NMR (400 MHz, $CDCl_3$) δ 7.47 – 7.42 (m, 2H), 7.41 – 7.28 (m, 4H), 7.27 – 7.21 (m, 1H), 7.19 – 7.15 (m, 2H), 6.92 (t, *J* = 2.0 Hz, 1H), 3.19 (dd, *J* = 14.4, 2.0 Hz, 1H), 3.09 (dd, *J* = 14.4, 1.9 Hz, 1H), 1.73 (s, 3H), 1.30 (s, 9H). **^{13}C NMR** (101 MHz, $CDCl_3$) δ 148.7, 147.3, 140.0, 131.4, 128.3 (2C), 127.0, 125.4 (2C), 124.4 (2C), 123.7 (2C), 114.0, 88.4, 45.4, 34.4, 31.3 (3C), 29.3. **HRMS** (ESI+) *m/z* calculated for $C_{21}H_{24}ONa^+$ $[M+Na]^+$: 315.1719, found: 315.1712.

The title enantioenriched (*S*)-2,3-dihydrofuran (colorless oil, 19 mg, 71% yield, 72:28 *er*) was synthesized according to the general procedure starting from enantioenriched (*R*)-1-(*tert*-butyl)-4-(3-methyl-3-phenylcyclobut-1-en-1-yl)benzene (26 mg, 0.092 mmol, 87:13 *er*). **SFC** (Chiralpak IA (100 mm × 4.6 mm, 3 µm), CO_2/isopropanol 75:25, 3 mL/min, 1500 psi of backpressure) t_R (*minor*) 2.6 min, t_R (*major*) 3.6 min. α_D^{589} ($CHCl_3$, *c* 0.02, 299 K) = 16.2 deg.cm^2.g^{-1}.

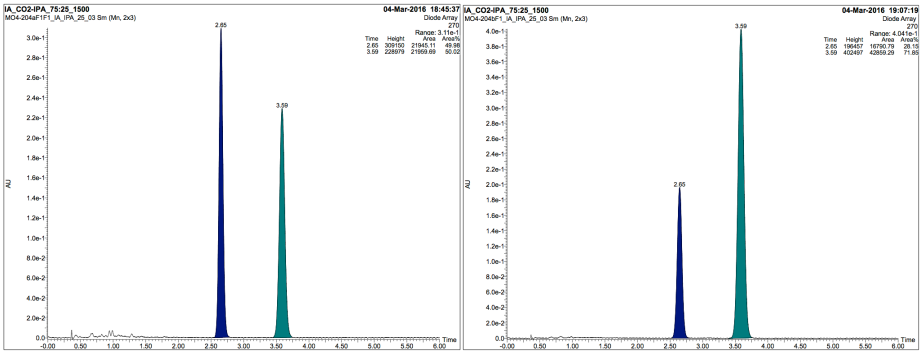

Time	Height	Area	Area%
2.65	309150	21945.11	49.98
3.59	228979	21959.69	50.02

Time	Height	Area	Area%
2.65	196457	16790.79	28.15
3.59	402497	42859.29	71.85

Figure S2.2. Chromatogram of the racemic (left) and enantioenriched (right) 2,3-dihydrofuran **22b**.

4-(4-Bromophenyl)-2-methyl-2-phenyl-2,3-dihydrofuran (22c)

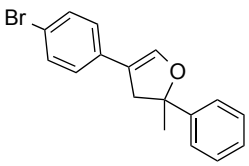

The title compound (white solid, 29 mg, 61% yield) was synthesized according to the general procedure starting from freshly prepared 1-bromo-4-(3-methyl-3-phenylcyclobut-1-en-1-yl)benzene (45 mg, 0.15 mmol). The reaction time was 8 h. **M.p.** 75-78 ºC. **^{1}H NMR** (400 MHz, $CDCl_3$) δ 7.47 – 7.42 (m, 2H), 7.40 – 7.34 (m, 4H), 7.30 – 7.24 (m, 1H), 7.08 (dt, *J* = 9.2, 2.6 Hz, 2H), 6.96 (t, *J* = 2.0 Hz, 1H), 3.17 (dd, *J* = 14.4, 2.1 Hz, 1H), 3.08 (dd, *J* = 14.4, 2.0 Hz, 1H), 1.75 (s, 3H). **^{13}C NMR** (101 MHz, $CDCl_3$) δ 147.0, 141.2, 133.3, 131.5 (2C), 128.4 (2C), 127.1, 125.5 (2C), 124.4 (2C), 118.9, 113.3, 88.8, 45.1, 29.5. **HRMS** (APCI) *m/z* calculated for $C_{17}H_{16}BrO^+$ $[M+H]^+$: 315.0379, found: 315.0367.

The title enantioenriched (*S*)-2,3-dihydrofuran (white solid, 20 mg, 66% yield, 79:21 *er*) was synthesized according to the general procedure starting from enantioenriched (*R*)-1-bromo-4-(3-methyl-3-phenylcyclobut-1-en-1-yl)benzene (29 mg, 0.096 mmol, 93:7 *er*). **M.p.** 72-74 ºC. **SFC** (Chiralpak IA (100 mm × 4.6 mm, 3 μm), CO_2/isopropanol 75:25, 3 mL/min, 1500 psi of backpressure) t_R (*minor*) 2.7 min, t_R (*major*) 3.6 min. $\boldsymbol{\alpha_D^{589}}$ ($CHCl_3$, *c* 0.02, 299 K) = 21.0 deg.cm^2.g^{-1}.

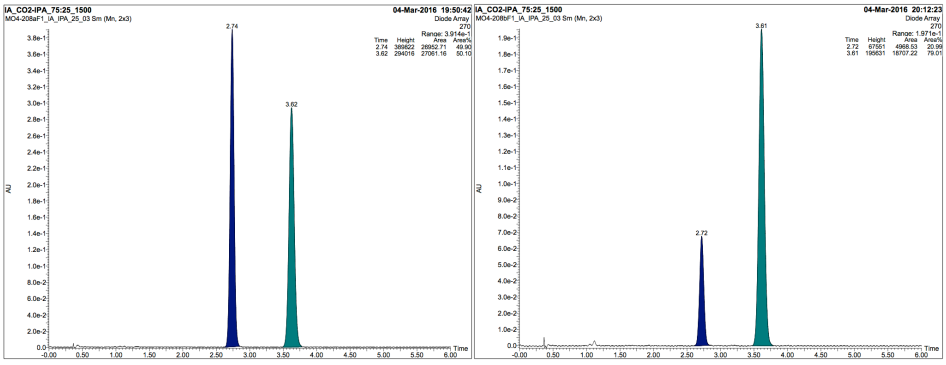

Time	Height	Area	Area%
2.74	389822	26952.71	49.90
3.62	294016	27061.16	50.10

Time	Height	Area	Area%
2.72	67551	4968.53	20.99
3.61	195631	18707.22	79.01

Figure S2.3. Chromatogram of the racemic (left) and enantioenriched (right) 2,3-dihydrofuran **22c**.

4-(4-Chlorophenyl)-2-methyl-2-phenyl-2,3-dihydrofuran (22d)

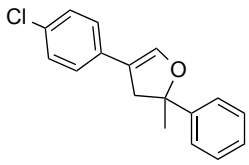

The title compound (yellow oil, 39 mg, 72% yield) was synthesized according to the general procedure starting from freshly prepared 1-chloro-4-(3-methyl-3-phenylcyclobut-1-en-1-yl)benzene (51 mg, 0.2 mmol).

^{1}H NMR (400 MHz, $CDCl_3$) δ 7.48 – 7.41 (m, 2H), 7.39 – 7.33 (m, 2H), 7.30 – 7.18 (m, 3H), 7.13 (dt, *J* = 9.1, 2.4 Hz, 2H), 6.94 (t, *J* = 2.0 Hz, 1H), 3.17 (dd, *J* = 14.4, 2.1 Hz, 1H), 3.08 (dd, *J* = 14.4, 2.0 Hz, 1H), 1.74 (s, 3H). **^{13}C NMR** (101 MHz, $CDCl_3$) δ 147.1, 141.1, 132.8, 130.9, 128.6 (2C), 128.4 (2C), 127.1, 125.1 (2C), 124.4 (2C), 113.2, 88.7, 45.2, 29.5. **HRMS** (ESI+) *m/z* calculated for $C_{17}H_{15}ClONa^+$ $[M+Na]^+$: 293.0704, found: 293.0703.

The title enantioenriched (*S*)-2,3-dihydrofuran (pale yellow solid, 17 mg, 61% yield, 78:22 *er*) was synthesized according to the general procedure starting from enantioenriched (*R*)-1-chloro-4-(3-methyl-3-phenylcyclobut-1-en-1-yl)benzene (27 mg, 0.11 mmol, 93:7 *er*). **M.p.** 50-53 ºC. **SFC** (Chiralpak IA (100 mm × 4.6 mm, 3 µm), CO_2/isopropanol 75:25, 3 mL/min, 1500 psi of backpressure) t_R (*minor*) 2.0 min, t_R (*major*) 2.8 min. $\boldsymbol{\alpha}_D^{589}$ ($CHCl_3$, *c* 0.02, 300 K) = 24.9 deg.cm^2.g^{-1}.

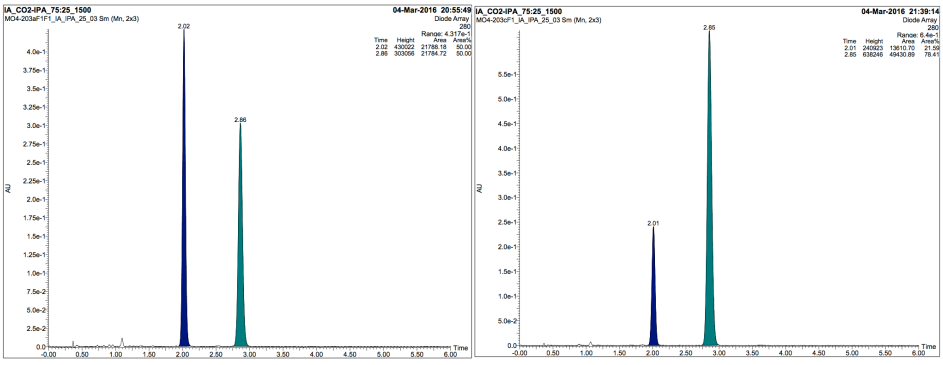

Time	Height	Area	Area%
2.02	430022	21788.18	50.00
2.86	303056	21784.72	50.00

Time	Height	Area	Area%
2.01	240923	13610.70	21.59
2.85	638246	49430.89	78.41

Figure S2.4. Chromatogram of the racemic (left) and enantioenriched (right) 2,3-dihydrofuran **22d**.

2-Methyl-2-phenyl-4-(3-methylphenyl)-2,3-dihydrofuran (22e)

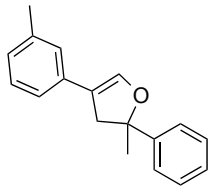

The title compound (colorless oil, 43 mg, 86% yield) was synthesized according to the general procedure starting from freshly prepared 1-methyl-3-(3-methyl-3-phenylcyclobut-1-en-1-yl)benzene (47 mg, 0.2 mmol).

^{1}H NMR (500 MHz, $CDCl_3$) δ 7.50 – 7.44 (m, 2H), 7.39 – 7.34 (m, 2H), 7.30 – 7.24 (m, 1H), 7.20 – 7.14 (m, 1H), 7.07 – 7.01 (m, 2H), 6.98 – 6.92 (m, 2H), 3.20 (dd, *J* = 14.4, 2.1 Hz, 1H), 3.12 (dd, *J* = 14.4, 2.0 Hz, 1H), 2.32 (s, 3H), 1.75 (s, 3H). **^{13}C NMR** (126 MHz, $CDCl_3$) δ 147.3, 140.5, 138.0, 134.2, 128.4, 128.3 (2C), 127.0, 126.5, 124.7, 124.4 (2C), 121.1, 114.2, 88.4, 45.4, 29.4, 21.5. **HRMS** (ESI+) *m/z* calculated for $C_{18}H_{18}ONa^+$ $[M+Na]^+$: 273.1250, found: 273.1249.

The title enantioenriched (*S*)-2,3-dihydrofuran (colorless oil, 10 mg, 64% yield, 77:23 *er*) was synthesized according to the general procedure starting from enantioenriched (*R*)-1-methyl-3-(3-methyl-3-phenylcyclobut-1-en-1-yl)benzene (14 mg, 0.06 mmol, 90:10 *er*). **SFC** (Chiralpak IA (100 mm × 4.6 mm, 3 μm), CO_2/isopropanol 90:10, 3 mL/min, 1500 psi of backpressure) t_R (*minor*) 1.5 min, t_R (*major*) 2.4 min. $\boldsymbol{\alpha_D}^{589}$ ($CHCl_3$, *c* 0.007, 299 K) = 23.0 deg.cm^2.g^{-1}.

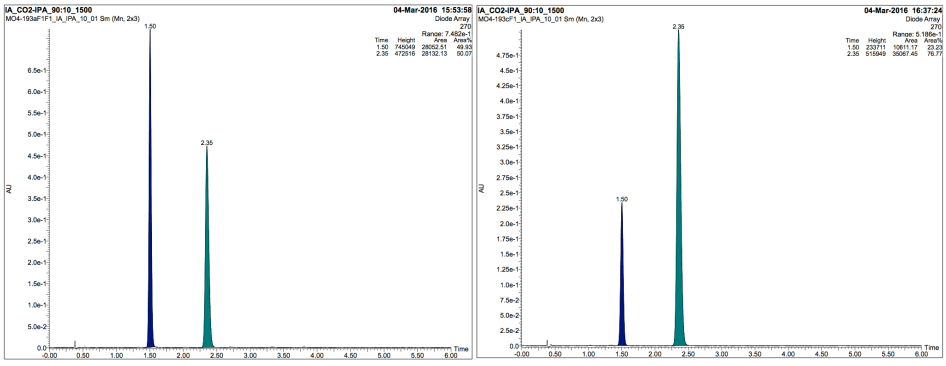

Time	Height	Area	Area%
1.50	745049	28052.51	49.93
2.35	472516	28132.13	50.07

Time	Height	Area	Area%
1.50	233711	10611.17	23.23
2.35	515949	35067.45	76.77

Figure S2.5. Chromatogram of the racemic (left) and enantioenriched (right) 2,3-dihydrofuran **22e**.

4-(3-Chlorophenyl)-2-methyl-2-phenyl-2,3-dihydrofuran (22f)

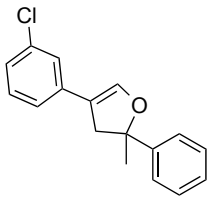

The title compound (colorless oil, 46 mg, 85% yield) was synthesized according to the general procedure starting from freshly prepared 1-chloro-3-(3-methyl-3-phenylcyclobut-1-en-1-yl)benzene (51 mg, 0.2 mmol).

^{1}H NMR (500 MHz, $CDCl_3$) δ 7.47 – 7.43 (m, 2H), 7.40 – 7.34 (m, 2H), 7.30 – 7.24 (m, 1H), 7.21 – 7.16 (m, 2H), 7.12 – 7.09 (m, 2H), 6.98 (t, *J* = 2.0 Hz, 1H), 3.18 (dd, *J* = 14.4, 2.1 Hz, 1H), 3.09 (dd, *J* = 14.4, 2.0 Hz, 1H), 1.75 (s, 3H). **^{13}C NMR** (126 MHz, $CDCl_3$) δ 146.9, 141.8, 136.2, 134.4, 129.6, 128.4 (2C), 127.1, 125.5, 124.3 (2C), 124.0, 122.0, 113.2, 88.9, 45.1, 29.5. **HRMS** (APCI) *m/z* calculated for $C_{17}H_{16}OCl^+$ $[M+H]^+$: 271.0884, found: 271.0875.

2,4-Bis(4-(*tert*-butyl)phenyl)-2-methyl-2,3-dihydrofuran (22g)

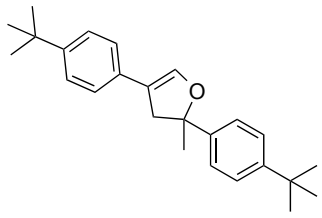

The title compound (white solid, 32 mg, 61% yield) was synthesized according to the general procedure starting from freshly prepared 4,4'-(3-methylcyclobut-1-ene-1,3-diyl)bis(*tert*-butylbenzene) (50 mg, 0.15 mmol).

M.p. 112-115 ºC. **^{1}H NMR** (400 MHz, $CDCl_3$) δ 7.38 (s, 4H), 7.33 – 7.28 (m, 2H), 7.22 – 7.15 (m, 2H), 6.92 (t, *J* = 2.0 Hz, 1H), 3.20 (dd, *J* = 14.4, 2.0 Hz, 1H), 3.07 (dd, *J* = 14.4, 2.0 Hz, 1H), 1.74 (s, 3H), 1.32 (s, 9H), 1.30 (s, 9H). **^{13}C NMR** (101 MHz, $CDCl_3$) δ 149.8, 148.6, 144.2, 140.1, 131.5, 125.4 (2C), 125.2 (2C), 124.2

(2C), 123.7 (2C), 114.0, 88.3, 45.3, 34.4 (2C), 31.4 (3C), 31.3 (3C), 29.2. **HRMS** (ESI+) *m/z* calculated for $C_{25}H_{32}ONa^+$ $[M+Na]^+$: 371.2345, found: 371.2337.

The title enantioenriched (*S*)-2,3-dihydrofuran (white solid, 29 mg, 44% yield, 78:22 *er*) was synthesized according to the general procedure starting from enantioenriched (*R*)-4,4'-(3-methylcyclobut-1-ene-1,3-diyl)bis(*tert*-butylbenzene) (63 mg, 0.19 mmol, 89:11 *er*). **M.p.** 104-107 ºC. **SFC** (Chiralpak IA (100 mm × 4.6 mm, 3 µm), CO_2/isopropanol 80:20, 3 mL/min, 1500 psi of backpressure) t_R (*minor*) 2.9 min, t_R (*major*) 4.9 min. $\boldsymbol{\alpha_D}^{589}$ ($CHCl_3$, *c* 0.02, 299 K) = 23.1 deg.cm^2.g^{-1}.

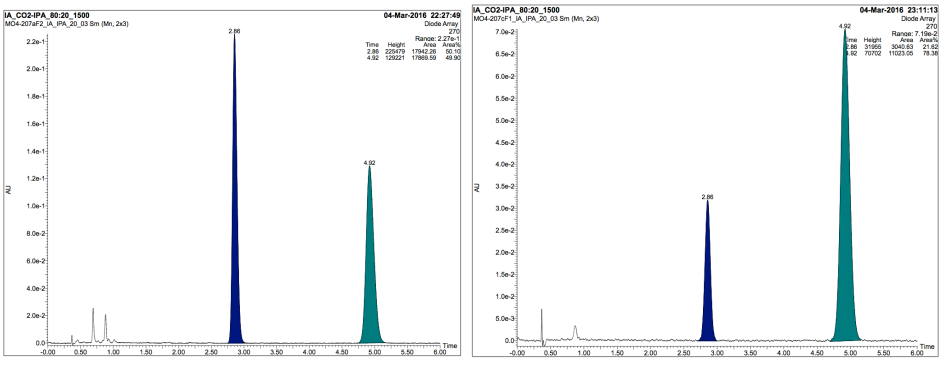

Figure S2.6. Chromatogram of the racemic (left) and enantioenriched (right) 2,3-dihydrofuran **22g**.

2-(4-Fluorophenyl)-2-methyl-4-phenyl-2,3-dihydrofuran (22h)

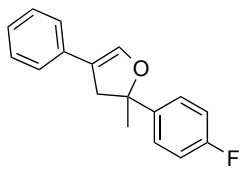

The title compound (colorless oil, 23 mg, 60% yield) was synthesized according to the general procedure starting from freshly prepared 1-fluoro-4-(1-methyl-3-phenylcyclobut-2-en-1-yl)benzene (36 mg, 0.15 mmol).

^{1}H NMR (400 MHz, $CDCl_3$) δ 7.45 – 7.38 (m, 2H), 7.30 – 7.19 (m, 4H), 7.16– 7.10 (m, 1H), 7.07 – 7.00 (m, 2H), 6.94 (t, *J* = 2.0 Hz, 1H), 3.16 (dd, *J* = 14.5, 2.1 Hz, 1H), 3.10 (dd, *J* = 14.4, 2.0 Hz, 1H), 1.73 (s, 3H). **^{13}C NMR** (101 MHz, $CDCl_3$) δ 161.8 (d, *J* (^{13}C-^{19}F) = 244.8 Hz), 143.0 (d, *J* (^{13}C-^{19}F) = 3.2 Hz), 140.5, 134.1, 128.5 (2C), 126.2 (d, *J* (^{13}C-^{19}F) = 8.0 Hz, 2C), 125.8, 124.0 (2C), 115.1 (d, *J* (^{13}C-^{19}F) = 21.4 Hz, 2C), 114.2, 88.1, 45.4, 29.4.

^{19}F NMR (376 MHz, $CDCl_3$) δ –116.22. **HRMS** (ESI+) *m/z* calculated for $C_{17}H_{15}FONa^+$ $[M+Na]^+$: 277.0999, found: 277.0995.

The title enantioenriched (*S*)-2,3-dihydrofuran (white solid, 16 mg, 75% yield, 74:26 *er*) was synthesized according to the general procedure starting from enantioenriched (*R*)-1-fluoro-4-(1-methyl-3-phenylcyclobut-2-en-1-yl)benzene (20 mg, 0.084 mmol, 91:9 *er*). **M.p.** 48-51 ºC. **SFC** (Chiralpak IA (100 mm × 4.6 mm, 3 μm), CO_2/isopropanol 90:10, 3 mL/min, 1500 psi of backpressure) t_R (*minor*) 1.8 min, t_R (*major*) 3.2 min. α_D^{589} ($CHCl_3$, *c* 0.04, 299 K) = 13.0 deg.cm^2.g^{-1}.

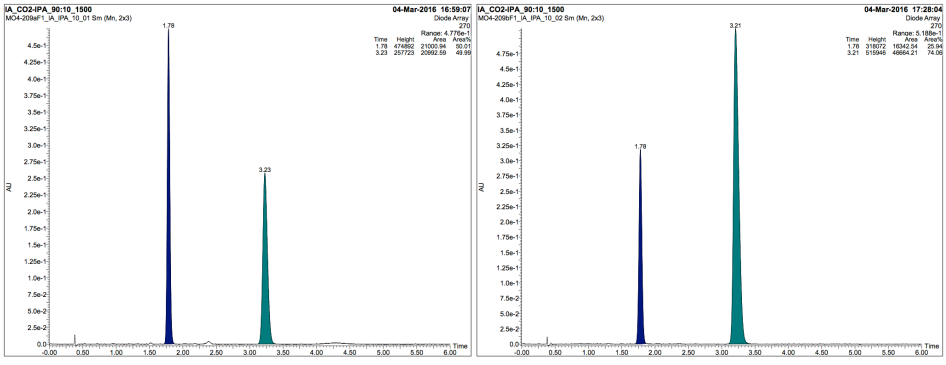

Time	Height	Area	Area%
1.78	474892	21000.94	50.01
3.23	257723	20992.59	49.99

Time	Height	Area	Area%
1.78	318072	16342.54	25.94
3.21	515946	46664.21	74.06

Figure S2.7. Chromatogram of the racemic (left) and enantioenriched (right) 2,3-dihydrofuran **22h**.

2,2,3,3-Tetramethyl-4-phenyl-2,3-dihydrofuran (22i)

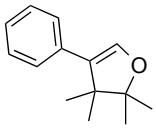

The title compound (white solid, 15 mg, 37% yield) was synthesized according to the general procedure starting from freshly prepared (3,3,4,4-tetramethylcyclobut-1-en-1-yl)benzene (37 mg , 0.2 mmol).

M.p. 37-40 ºC. **^{1}H NMR** (400 MHz, $CDCl_3$) δ 7.33 – 7.25 (m, 4H), 7.23 – 7.16 (m, 1H), 6.47 (s, 1H), 1.32 (s, 6H), 1.17 (s, 6H). **^{13}C NMR** (101 MHz, $CDCl_3$) δ 140.9, 134.7, 128.3 (2C), 126.4 (2C), 125.9, 124.9, 90.9, 47.8, 22.6 (2C), 22.4 (2C). **HRMS** (APCI) *m/z* calculated for $C_{14}H_{19}O^+$ $[M+H]^+$: 203.1430, found: 203.1422.

UNIVERSITAT ROVIRA I VIRGILI
GOLD-CATALYZED INTERMOLECULAR REACTIONS OF ALKYNES WITH ALKENES: NOVEL REACTIVITIES AND GLOBAL MECHANISTIC PICTURE
María Elena de Orbe Izquierdo

Chapter 3.

Novel Pathways

in Gold-Catalyzed Reactions of Bromoalkynes

UNIVERSITAT ROVIRA I VIRGILI
GOLD-CATALYZED INTERMOLECULAR REACTIONS OF ALKYNES WITH ALKENES: NOVEL REACTIVITIES AND GLOBAL MECHANISTIC PICTURE
María Elena de Orbe Izquierdo

Introduction

Hydroarylation of Alkynes

In addition to the gold(I)-catalyzed reactions of alkynes with alkenes thoroughly discussed in this manuscript, it is worth reviewing the hydroarylations of alkynes catalyzed by gold.[133] In these processes, the aryl moiety acts as nucleophile and attacks the gold-activated alkyne leading to a formal addition of the Ar−H across the triple bond.

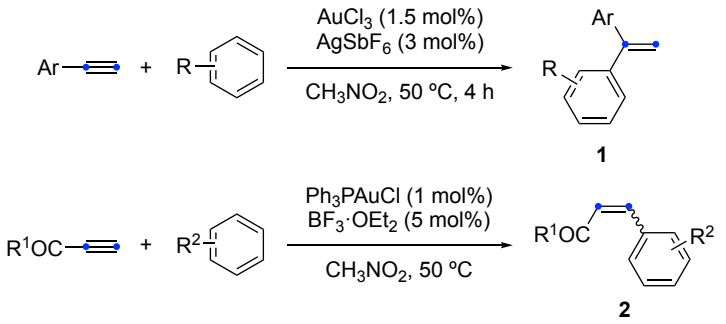

Scheme 3.1. Intermolecular hydroarylation of terminal alkynes catalyzed by gold.

Only few intermolecular reactions of this type have been disclosed. In these transformations, the nucleophilic attack of the aryl group takes place at the internal carbon with electron-rich alkynes, while it occurs at the terminal carbon with electron-deficient alkynes. The same regioselectivity has been observed in previously discussed intermolecular reactions of alkynes catalyzed by gold. Thus, in the hydroarylation of electron-rich arylalkynes with arenes, 1,1-disubstituted alkenes **1** are formed whereas in the hydroarylation of electron-deficient alkynes, *Z*- or *E*-alkenes **2** are obtained (Scheme 3.1).[134] Although different arenes react with ethyl propiolate leading to *Z*-configured olefins

133. Muratore, M. E.; Echavarren, A. M. *Gold-Catalyzed Hydroarylation of Alkynes*. In *The Chemistry of Organogold Compounds*; Rappoport, Z., Liebman, J. F., Marek, I., Eds.; John Wiley & Sons, Ltd.: Chichester, U.K., 2015; pp 805−900.
134. Pioneering work: (a) Reetz, M. T.; Sommer, K. *Eur. J. Org. Chem.* **2003**, *18*, 3485–3496. Further studies: (b) Shi, Z.; He, C. *J. Org. Chem.* **2004**, *69*, 3669–3671. (c) Tubaro, C.; Baron, M.; Biffis, A.; Basato, M. *Beilstein J. Org. Chem.* **2013**, *9*, 246–253.

with high selectivity, the reaction with acetylacetylene gives *E*-configured products presumably due to the isomerization of the *Z*-alkene products under the reaction conditions.

As explained in the **General Introduction**, the intermolecular reaction of 2,5-disubstituted furans with alkenes provides the C3 alkenylated furan together with the rearranged phenol.[135] However, furans unsubstituted at C2 react at that very C2 position with alkynes in a twofold hydroarylation *via* **3** to give **4** (Scheme 3.2).[136] Similarly, double hydroarylations of alkynes have been observed with either benzofurans, indoles or pyrroles (Scheme 3.2).[137]

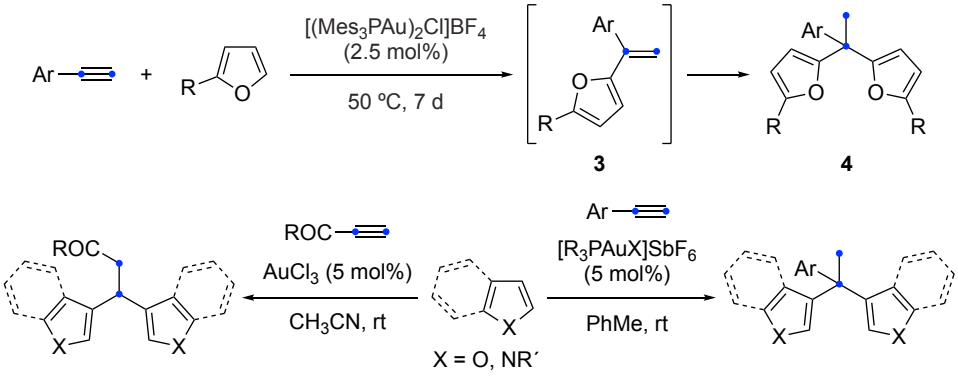

Scheme 3.2. Double hydroarylations of terminal alkynes catalyzed by gold.

In contrast with the gold-catalyzed intermolecular hydroarylation of alkynes, the analogous intramolecular transformation has been thoroughly explored and applied in several total syntheses.[138] Alkyne derivatives **5** typically undergo 6-*endo*-dig cyclization to afford

135. Other cascade reaction initiated by an intermolecular hydroarylation of alkynes: Samala, S.; Mandadapu, A. K.; Saifuddin, M.; Kundu, B. *J. Org. Chem.* **2013**, *78*, 6769−6774.
136. Hashmi, A. S. K.; Blanco, M. C. *Eur. J. Org. Chem.* **2006**, 4340–4342.
137. (a) Li, Z.; Shi, Z.; He, C. *J. Organomet. Chem.* **2005**, *690*, 5049–5054. (b) Ferrer, C.; Amijs, C. H. M.; Echavarren, A. M. *Chem. Eur. J.* **2007**, *13*, 1358–1373. (c) Schießl, J.; Rudolph, M.; Hashmi, A. S. K. *Adv. Synth. Catal.* **2017**, *359*, 639–653.
138. (a) Brimble, M. A.; Haym, I.; Sperry, J.; Furkert, D. P. *Org. Lett.* **2012**, *14*, 5820–5823. (b) Cervi, A.; Aillard, P.; Hazeri, N.; Petit, L.; Chai, C. L. L.; Willis, A. C.; Banwell, M. G. *J. Org. Chem.* **2013**, *78*, 9876−9882.

chromenes,[139] 1,2-dihydroquinolines[140] or phosphacoumarins[141] depending on the nature of the enyne tether (Scheme 3.3).[142] In the case of aryl propargyl ethers bearing electron-withdrawing groups on the arene, benzofurans **7** have also been obtained as a result of the fragmentation of the gold-alkenyl intermediates **I** to form allenes **II**, which evolve *via* 5-*exo*-dig cyclization.[143] Iodoalkynes derivatives produce iodoalkenes **8** and **9** in different ratios depending on the gold catalyst and the solvent used.[144]

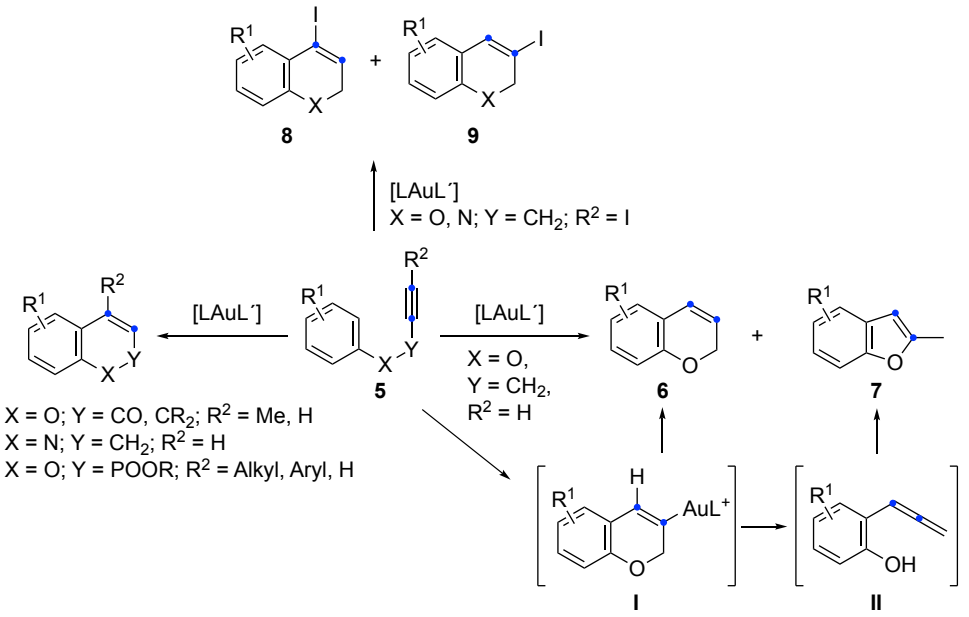

Scheme 3.3. Gold-catalyzed intramolecular hydroarylation of alkynes *via* 6-*endo*-dig pathway.

139. Curtis, N. R.; Prodger, J. C.; Rassias, G.; Walker, A. J. *Tetrahedron Lett.* **2008**, *49*, 6279–6281.
140. Nieto-Oberhuber, C.; Muñoz, M. P.; Buñuel, E.; Nevado, C.; Cárdenas, D. J.; Echavarren, A. M. *Angew. Chem. Int. Ed.* **2004**, *43*, 2402 –2406.
141. Kim, C.-E.; Ryu, T.; Kim, S.; Lee, K.; Lee, C.-H.; Lee, P. H. *Adv. Synth. Catal*. **2013**, *355*, 2873–2883.
142. Nevado, C.; Echavarren, A. M. *Chem. Eur. J.* **2005**, *11*, 3155–3164.
143. (a) Menon, R. S.; Findlay, A. D.; Bissember, A. C.; Banwell, M. G. *J. Org. Chem.* **2009**, *74*, 8901–8903. (b) Lykakis, I. N.; Efe, C.; Gryparis, C.; Stratakis, M. *Eur. J. Org. Chem.* **2011**, 2334–2338.
144. (a) Morán-Poladura, P.; Suárez-Pantiga, S.; Piedrafita, M.; Rubio, E.; González, J. M. *J. Organomet. Chem.* **2011**, *696*, 12–15. (b) Morán-Poladura, P.; Rubio, E.; González, J. M. *Beilstein J. Org. Chem.* **2013,** *9,* 2120–2128.

Similarly, homopropargylic anilines undergo a 6-*exo*-dig cyclization that produces dihydroquinolines containing an exocyclic alkene, which partially isomerizes to the more stable internal alkene under the reaction conditions (Scheme 3.4a).[145] In the same manner, *o*-alkynyldiarylmethanes have been employed to prepare anthracenes (Scheme 3.4b).[146]

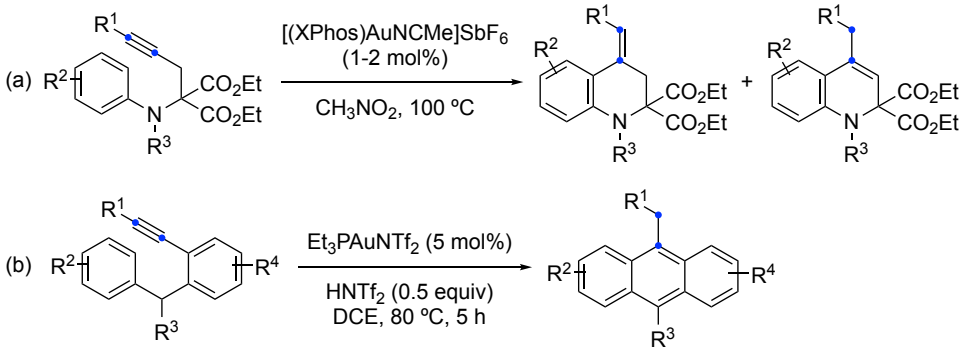

Scheme 3.4. Gold-catalyzed intramolecular hydroarylation of alkynes *via* 6-*exo*-dig pathway.

Gold-catalyzed hydroarylation of *ortho*-alkynylbiaryls **10** commonly leads to the formation of phenanthrenes, although 9-alkylidene fluorenes **13** are obtained by utilizing other metal catalysts (Table 3.1).[147] In the case of internal alkynes, two differently substituted phenanthrenes **11** and **12** can be generated, whose ratio is mostly influenced by the metal catalyst. Thus, indium(III) salts provide preferentially the non-rearranged hydroarylation product **11** (Table 3.1, entries 9 and 13), whereas gold salts give rise to **12** through the migration of the heteroatom from the terminal alkyne position to the internal position (Table 3.1, entries 10 and 14). Originally, it was proposed that phenanthrenes **12** were formed *via* gold–vinylidene intermediates of type **IV** that further partake in the hydroarylation (Scheme 3.5).[148] Nevertheless, theoretical calculations showed that the most favored pathway involves a 6-*endo*-dig hydroarylation of the alkyne, followed by a 1,2-H shift leading to a gold–carbene intermediate **VI**, and finally a 1,2-Br shift to give **VII**.[149]

145. Gronnier, C.; Odabachian, Y.; Gagosz, F. *Chem. Commun.* **2011**, *47*, 218–220.
146. Shu, C.; Chen, C.-B.; Chen, W.-X.; Ye, L.-W. *Org. Lett.* **2013**, *15*, 5542–5545.
147. (a) Fürstner, A.; Mamane, V. *J. Org. Chem.* **2002**, *67*, 6264–6267. (b) Mamane, V.;Hannen, P.; Fürstner, A. *Chem. Eur. J.* **2004**, *10*, 4556–4575. (c) Lim, W.; Rhee, Y. H. *Eur. J. Org. Chem.* **2013**, 460–464. (d) Carreras, J.; Gopakumar, G.; Gu, L.; Gimeno, A.; Linowski, P.; Petuškova, J.; Thiel, W.; Alcarazo, M. *J. Am. Chem. Soc.* **2013**, *135*, 18815−18823.
148. Soriano, E.; Marco-Contelles, J. *Organometallics* **2006,** *25,* 4542–4553.
149. Huang, G.; Cheng, B.; Xu, L.; Li, Y.; Xia, Y. *Chem. Eur. J.* **2012**, *18*, 5401–5415.

Table 3.1. Metal-catalyzed hydroarylation of *ortho*-alkynylbiaryls.

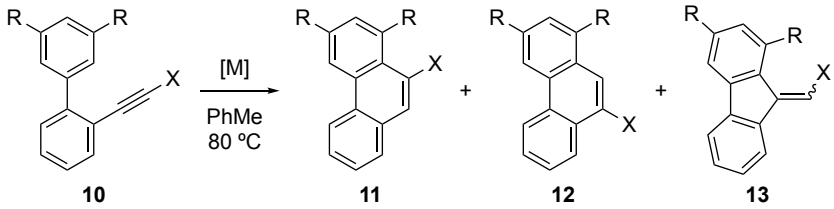

Entry	R	X	[M]	Ratio **11**:**12**:**13**
1	OMe	H	$GaCl_3$	96 : - : 4 [a]
2	OMe	H	$InCl_3$	44 : - : 56 [a]
3	OMe	H	$AuCl_3$	97 : - : 3 [a]
4	OMe	H	$[RuCl_2(CO)_3]_2$	67 : - : 33 [a]
5	OMe	H	$PtCl_2$	95 : - : 5 [a]
6	Me	H	$PtCl_2$	97 : - : 3 [a]
7	Me	Me	$PtCl_2$	100 : 0 : 0 [a]
8	Me	COOMe	$PtCl_2$	5 : 0 : 95 [a]
9	Me	SePh	$InCl_3$	65 : 9 : 0 [b]
10	Me	SePh	AuCl	0 : 94 : 0 [b]
11	Me	SePh	$PtCl_2$	4 : 64 : 0 [b]
12	Me	SePh	$RhCl_3$	0 : 23 : 0 [b]
13	Me	Br	$InCl_3$	7 : 0 : 0 [b]
14	Me	Br	AuCl	0 : 77 : 0 [b]

[a] Ratio of the products. When X = H, note that **11** = **12**. [b] Ratio determined by ^{1}H NMR in the crude.

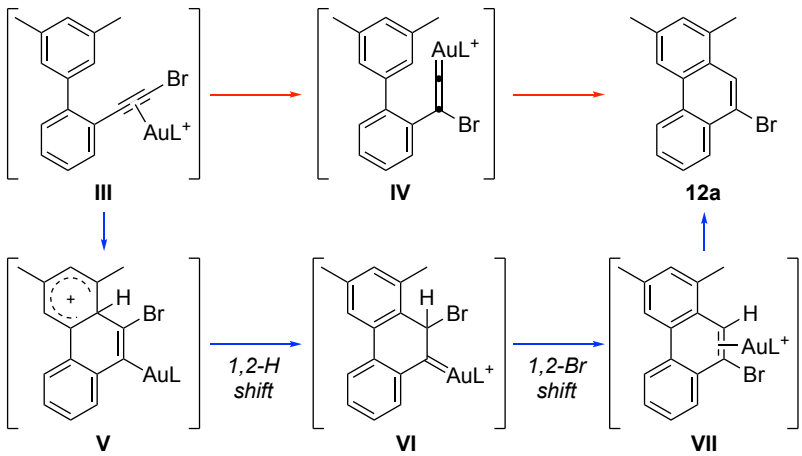

Scheme 3.5. Mechanism for the gold-catalyzed formation of phenanthrene **12a**.

Reactivity of Haloalkynes Under Gold Catalysis

Different gold-catalyzed intermolecular additions of nucleophiles to haloalkynes have been reported (Scheme 3.6). For instance, hydration of haloalkynes generates selectively α-halomethyl ketones **14**.[150] Similarly, the Markovnikov-type addition of hydrogen fluoride or carboxylic acids to iodoalkynes lead to (*Z*)-fluoroiodoalkenes **15** or (*Z*)-β-iodoenol esters **16**, respectively.[151] Interestingly, the stereoselective thioallylation of alkynes furnishing skipped dienes **17** has been recently developed.[152]

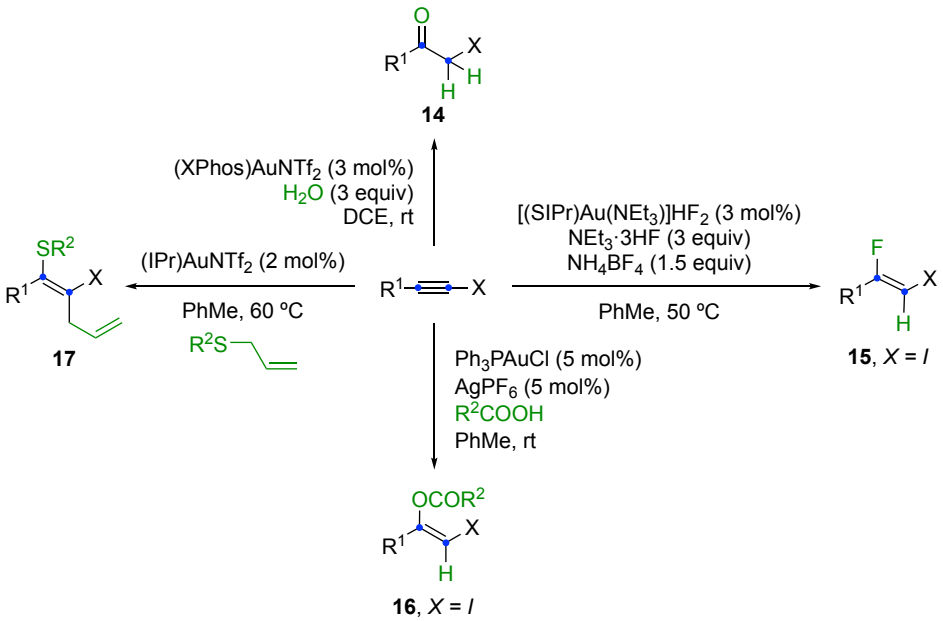

Scheme 3.6. Intermolecular additions of nucleophiles to haloalkynes catalyzed by gold.

In the presence of gold catalysts, the cycloisomerization of iodoalkyne derivatives **18** gives rise to indenes **19** (Scheme 3.7).[153] The reaction mechanism was proposed to involve the formation of gold iodovinylidenes **VIII** followed by a C(sp^3)–H insertion.

150. Xie, L.; Wu, Y.; Yi, W.; Zhu, L.; Xiang, J.; He, W. *J. Org. Chem.* **2013**, *78*, 9190−9195.
151. (a) Gómez-Herrera, A.; Nahra, F.; Brill, M.; Nolan, S. P.; Cazin, C. S. J. *ChemCatChem* **2016**, *8*, 3381–3388. (b) González-Liste, P. J.; Francos, J.; García-Garrido, S. E.; Cadierno, V. *J. Org. Chem.* **2017**, *82*, 1507−1516.
152. Wang, J.; Zhang, S.; Xu, C.; Wojtas, L.; Akhmedov, N. G.; Chen, H.; Shi, X. *Angew. Chem. Int. Ed.* **2018**, *57*, 6915–6920.
153. Morán-Poladura, P.; Rubio, E.; González, J. M. *Angew. Chem. Int. Ed.* **2015**, *54*, 3052–3055.

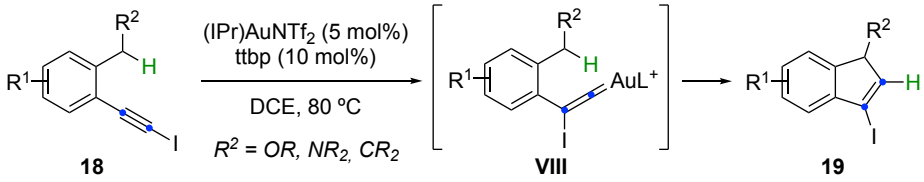

Scheme 3.7. Gold-catalyzed formation of indenes **19** from iodoalkynes **18**.

Additionally, head-to-tail dimerization of iodoalkynes has been described under dual gold catalysis (Scheme 3.8).[154] It was suggested that the reaction proceeds *via* gold acetylide **X**, which attacks on the activated (η^2-alkyne)gold(I) complex **IX** leading to vinyl gold species **XI**.

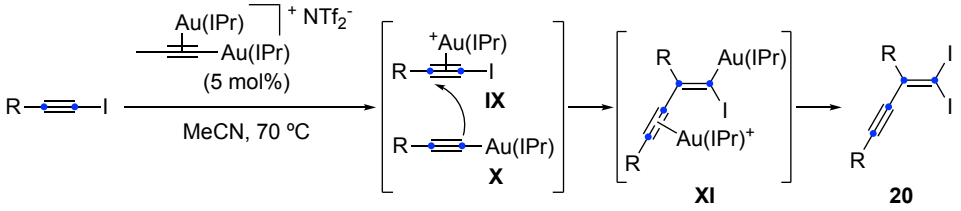

Scheme 3.8. Gold-catalyzed head-to-tail dimerization of iodoalkynes.

State-of-art on the Synthesis of Skipped Enynes

Skipped enynes are useful compounds in organic synthesis since they feature two proximal versatile motifs for further transformations.[155] Among the methods to prepare 1,4-enynes, several metal-catalyzed cross-coupling reactions of alkynylmetal species with allylic

154. Mader, S.; Molinari, L.; Rudolph, M.; Rominger, F.; Hashmi, A. S. K. *Chem. Eur. J.* **2015**, *21*, 3910–3913.
155. Selected applications of 1,4-enynes in synthesis: (a) Heffron, T. P.; Jamison, T. F. *Org. Lett.* **2003**, *5*, 2339–2342. (b) Buzas, A.; Gagosz, F. *J. Am. Chem. Soc.* **2006**, *128*, 12614–12615. (c) Hickmann, V.; Alcarazo, M.; Fürstner, A. *J. Am. Chem. Soc.* **2010**, *132*, 11042–11044.

halides[156] as well as decarboxylative couplings[157] have been disclosed. More importantly, copper-catalyzed asymmetric allylic alkylations of *E*-configured enyne chlorides[158] or phosphates[159] enable the formation of 1,4-enynes with excellent regio- and enantioselectivities (Scheme 3.9).[160]

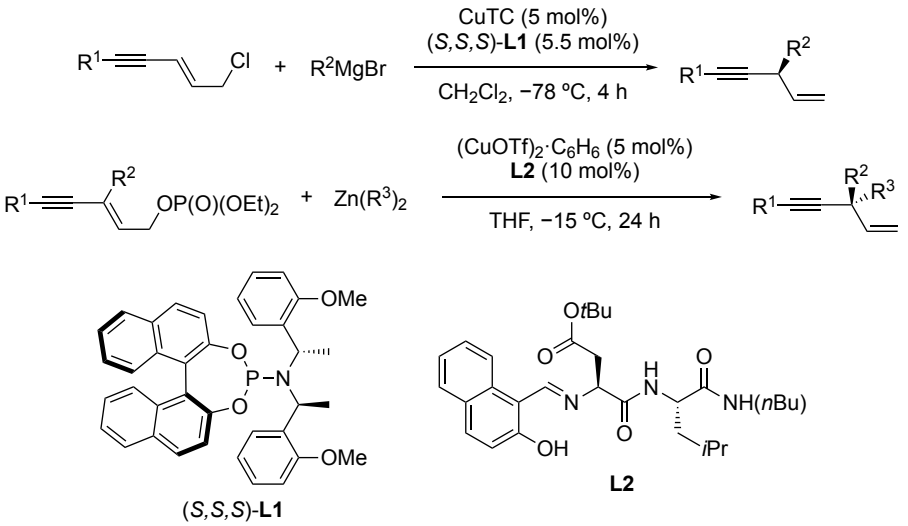

Scheme 3.9. Asymmetric synthesis of 1,4-enynes by metal-catalyzed allylic alkylation.

Another powerful strategy for the asymmetric synthesis of 1,4-enynes is the allylic alkynylation. For instance, alkynylaluminum[161] or alkynylcopper species[162] react with allylic phosphates in the presence of chiral copper catalysts to yield skipped enynes with high site- and enantioselectivity (Scheme 3.10a and 3.10b, respectively). Likewise, the

156. (a) Cui, D.-M.; Hashimoto, N.; Ikeda, S.; Sato, Y. *J. Org. Chem.* **1995**, *60*, 5752–5756. (b) Qian, M.; Negishi, E. *Synlett* **2005**, *11*, 1789–1793, and references therein.
157. (a) Rayabarapu, D. K.; Tunge, J. A. *J. Am. Chem. Soc.* **2005**, *127*, 13510–13511. (b) Choe, J.; Yang, Y.; Park, K.; Palani, T.; Lee, S. *Tetrahedron Lett.* **2012**, *53*, 6908–6912.
158. Li, H.; Alexakis, A. *Angew. Chem. Int. Ed.* **2012**, *51*, 1055–1058.
159. Kacprzynski, M. A.; Hoveyda, A. H. *J. Am. Chem. Soc.* **2004**, *126*, 10676–10681.
160. Other allylic alkylations with less selectivities: (a) Trost, B. M.; Hildbrand, S.; Dogra, K. *J. Am. Chem. Soc.* **1999**, *121*, 10416–10417. (b) Takeuchi, R.; Tanabe, K. *Angew. Chem. Int. Ed.* **2000**, *39*, 1975–1978.
161. (a) Dabrowski, J. A.; Gao, F.; Hoveyda, A. H. *J. Am. Chem. Soc.* **2011**, *133*, 4778−4781. (b) Dabrowski, J. A.; Haeffner, F.; Hoveyda, A. H. *Angew. Chem. Int. Ed.* **2013**, *52*, 7694−7699.
162. Harada, A.; Makida, Y.; Sato, T.; Ohmiya, H.; Sawamura, M. *J. Am. Chem. Soc.* **2014**, *136*, 13932−13939.

enantioselective substitution of allylic alcohols with potassium alkynyltrifluoroborates has been developed using chiral phosphoramidite-based iridium catalysts (Scheme 3.10c).[163]

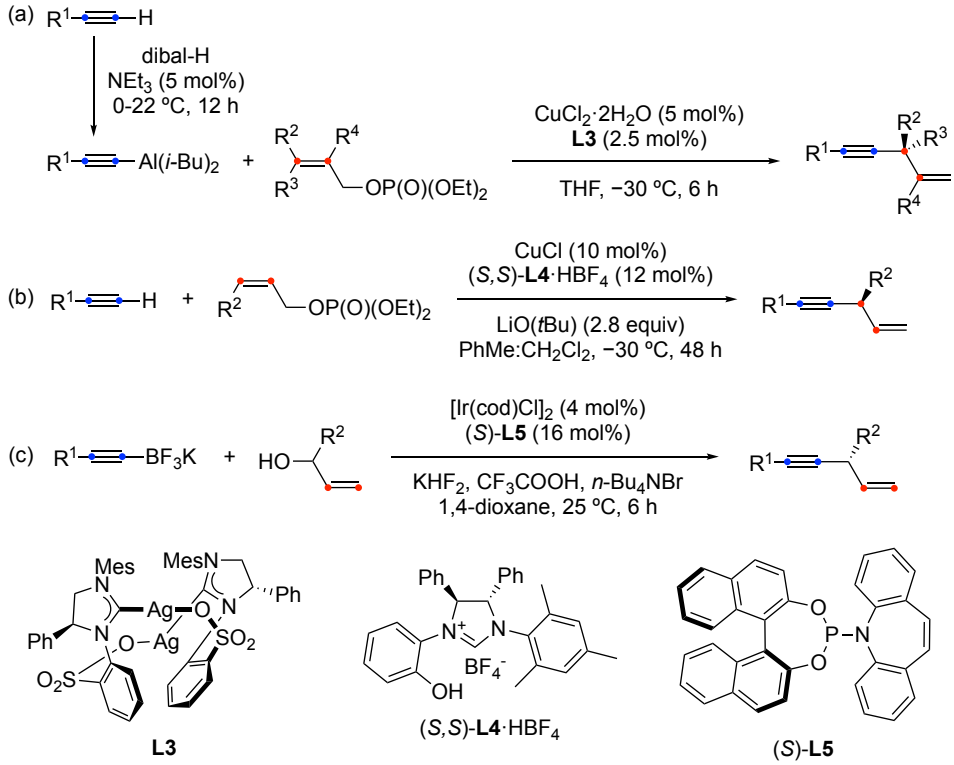

Scheme 3.10. Asymmetric synthesis of 1,4-enynes by metal-catalyzed allylic alkynylation.

163. Hamilton, J. Y.; Sarlah, D.; Carreira, E. M. *Angew. Chem. Int. Ed.* **2013**, *52*, 7532−7535.

Objectives

Gold-catalyzed intermolecular reactions of alkynes with alkenes are scarce owing to the challenge of controlling the selective progression towards a desired product over oligomerizations and other side reactions. As concluded in the **General Introduction** and in **Chapter 1**, these transformations commence with the formation of key cyclopropyl gold carbenes, in which the electronic and steric effects of the substituents determine their evolution through divergent reaction channels. In this chapter we aimed to discover novel pathways in the reaction of haloalkynes with allylsilanes catalyzed by Lewis acids such as gold complexes. Moreover, by installing aryl groups remotely from the haloalkyne motif, we envisioned to promote cascade reactions involving hydroarylations.

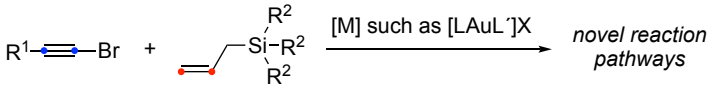

Scheme 3.11. Towards novel gold-catalyzed reactions of haloalkynes with allylsilanes.

Results and Discussion

Optimization of the Synthesis of Skipped Enynes

In order to evaluate the gold-catalyzed reaction of bromoalkynes with allylsilanes, we chose (bromoethynyl)benzene (**21a**) and simple allyltrimethylsilane (**22a**) as model substrates (Table 3.2). Unexpectedly, skipped enyne **23a** was formed in low yield in the presence of catalyst **A** as a result of a cross-coupling type process (Table 3.2, entry 1). Changing the counterion SbF_6 of **A** by BAr_4^F in **B**, a moderate yield (45%) was achieved (Table 3.2, entry 2). Not surprisingly, catalyst **B** outperforms **A**, as it has been observed before in other contexts. Nonetheless, other related phosphine-based catalysts **C** and **D** as well as NHC-based catalysts **E** and **F** also yielded enyne **23a** in low yields, comparable to that obtained with **A** (Table 3.2, entries 3-6). In contrast, complexes **G**, **I**, and more electrophilic complex **H** as well as gold salts AuCl and $AuCl_3$ failed to catalyze this transformation (Table 3.2, entries 7-11).

We then turned our attention to optimizing the solvent (Table 3.3) and other reaction conditions (Table 3.4) using catalyst **B**, which is the most efficient catalyst found for this transformation. Among the chlorinated (Table 3.3, entries 1-6), aromatic (Table 3.3, entries 7-10) and polar solvents tested (Table 3.3, entries 11-14), CH_2Cl_2, $PhCF_3$, CCl_4, THF and toluene provided similar results in terms of yield (*ca.* 40%, Table 3.3, entries 1, 6, 7, 9 and 13, respectively). We decided to continue employing CH_2Cl_2 since it is a common solvent in gold-catalyzed reactions of diverse substrates.

Regarding the catalyst loading, it could be decreased down to 3 mol% without substantial loss in yield (Table 3.4, entries 1-4). The stoichiometry of the substrates proved to have an important impact in this reaction (Table 3.4, entries 5-7), since an excess of allylsilane **22a** led to a significant increase of the yield up to 68%. Modifications of the concentration did not produce large changes in yield (Table 3.4, entries 8-10). In contrast, lower temperatures such as 0 ºC or higher temperatures such as 60 ºC had a detrimental effect on the reaction yield (Table 3.4, entries 11-13). By combining the best set of conditions, enyne **23a** was isolated in a 77% yield (Table 3.4, entry 14).

Table 3.2. Screening of gold catalysts in the reaction of bromoalkyne **21a** with allylsilane **22a**.[a]

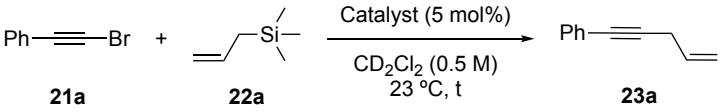

21a **22a** **23a**

Entry	Catalyst	t (h)	Yield (%)[b]
1	**A**	18	13 (7)
2	**B**	14	**45**
3	**C**	18	17
4	**D**	14	11
5	**E**	38	6
6	**F**	14	14
7	**G**	38	0
8	**H**	39	traces
9	**I**	39	traces
10	AuCl	40	0
11	$AuCl_3$	16	0

[a] Substrates **21a**:**22a** in a 1:1 ratio. [b] Yields determined by ^{1}H NMR using mesitylene as internal standard. Isolated yields in parentheses.

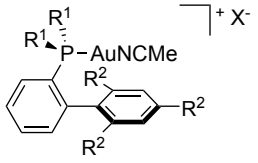

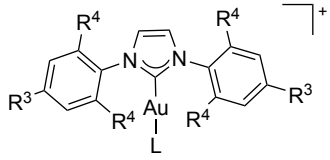

A: R^1 = *t*Bu; R^2 = *i*Pr; X = SbF_6
B: R^1 = *t*Bu; R^2 = *i*Pr; X = BAr_4^F
C: R^1 = *t*Bu; R^2 = H; X = SbF_6
D: R^1 = Cy; R^2 = *i*Pr; X = SbF_6

E: R^3 = H; R^4 = *i*Pr; L = NCMe; X = SbF_6
F: R^3 = H; R^4 = *i*Pr; L = NCPh; X = BAr_4^F
G: R^3 = Me; R^4 = Me; L = 2,4,6-$(OMe)_3C_6H_2CN$; X = SbF_6

I

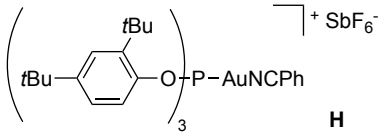

H

Table 3.3. Screening of solvents in the gold-catalyzed reaction of **21a** with **22a**.[a]

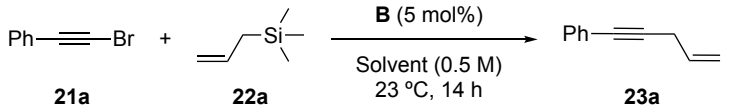

21a **22a** **23a**

Entry	Solvent	Yield (%)[b]	Entry	Solvent	Yield (%)[b]
1	**CH_2Cl_2**	**43**	8	Benzene	32
2	DCE	25	9	**$PhCF_3$**	**38**
3	$CHCl_3$	34	10	PhCl	37
4	$ClCH_2CHCl_2$	31	11	Et_2O	34
5	$Cl_2CHCHCl_2$	24	12	EtOAc	8
6	**CCl_4**	**39**	13	**THF**	**40**
7	**Toluene**	**40**	14	CH_3NO_2	26

[a] **21a**:**22a** in a 1:1 ratio. [b] Yields determined by ^{1}H NMR using mesitylene as internal standard.

Table 3.4. Optimization of conditions for the gold-catalyzed reaction of **21a** with **22a**.

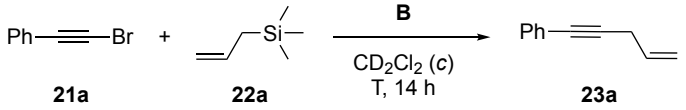

21a **22a** **23a**

Entry	**B** (mol%)	**21a**:**22a**	*c* (M)	T (ºC)	Yield (%)[a]
1	**1**	1:1	0.5	23	40
2	**3**	1:1	0.5	23	**50**
3	**5**	1:1	0.5	23	45
4	**10**	1:1	0.5	23	48
5	5	**2:1**	0.5	23	47
6	5	**1:2**	0.5	23	**64**
7	5	**1:3**	0.5	23	**68**
8	5	1:1	**0.2**	23	45
9	5	1:1	**1.0**	23	**52**
10	5	1:1	**2.0**	23	50
11	5	1:1	0.5	**0**	15
12	5	1:1	0.5	**40**	39
13	5	1:1	0.5	**60**	18
14	**3**	**1:2**	**1.0**	23	**77**[b]

[a] Yields determined by ^{1}H NMR using mesitylene as internal standard.
[b] Isolated yield.

With optimal conditions in hand, we explored the most suitable substitution pattern of the alkyne and the allyl derivative for this process (Table 3.5). (Chloroethynyl)benzene (**21b**) also reacted with allylsilane **22a** to build enyne **23a** in good yield (Table 3.5, entries 1-2). In contrast, (iodoethynyl)benzene (**21c**) provided **23a** in poor yield (Table 3.5, entry 3) together with a mixture of alkyne **21d** and allyliodide (**24a**) (Scheme 3.12). This reactivity of iodoalkyne **21c** was additionally evidenced by its reaction with phenyl substituted allylsilane **22h**, in which alkyne **21d** and iodoallyl derivative **24b** were isolated in *ca.* 77% and 64% yields, respectively (Scheme 3.12). The reaction of **21c** with **22a** did not take place in the absence of catalyst **B**. Based on the precedents of gold-catalyzed reactions of iodoalkynes, we hypothesized that these transformations of iodoalkyne **21c** proceeded through the formation of gold acetylide complexes.

Table 3.5. Screening of substrates for the formation of skipped enynes **23a**.[a]

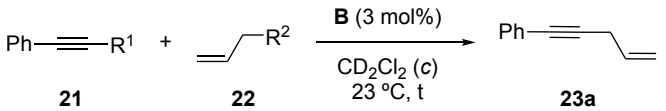

Entry	**21**	R^1	**22**	R^2	*c* (M)	t (h)	Yield (%)[b]
1	**21b**	**Cl**	**22a**	$Si(Me)_3$	0.5	14	45
2	**21b**	**Cl**	**22a**	$Si(Me)_3$	**1.0**	48	**68**
3	**21c**	**I**	**22a**	$Si(Me)_3$	0.5	14	9
4	**21a**	Br	**22b**	**$Si(OMe)_3$**	0.5	14	21
5	**21a**	Br	**22c**	**$Si(iPr)_3$**	0.5	14	23
6	**21a**	Br	**22d**	**$Si(Ph)_3$**	0.5	15	**66**
7	**21a**	Br	**22e**	**Bpin**	0.5	15	16
8	**21a**	Br	**22f**	**$Sn(Bu)_3$**	0.5	14	14
9	**21d**	**$Si(Me)_3$**	**22g**	**Br**	0.5	16	0[c]

[a] Substrates **21**:**22** in a 1:2 ratio. [b] Yields determined by ^1H NMR using mesitylene as internal standard. [c] No reaction.

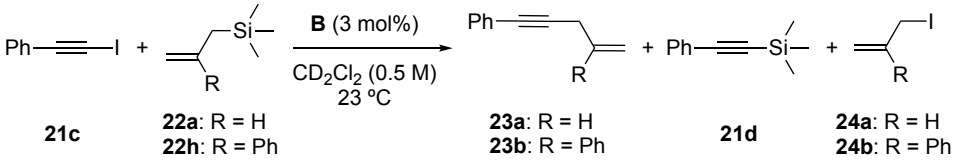

Scheme 3.12. Gold-catalyzed reaction of iodoalkyne **21c** with allylsilanes.

Triisopropyl- and trimethoxysilyl allyl derivatives **22b** and **22c** reacted poorly with bromoalkyne **21a** resulting in low yields of **23a** (Table 3.5, entries 4-5), whereas triphenylsilyl derivative **22d** gave the same product in 66% yield by reaction with **21a** (Table 3.5, entry 6). Alternative allylborane **22e** and allyltin **22f** reacted with **21a**, although low yields of **23a** were observed (Table 3.5, entries 7-8). The reversed reaction of alkynylsilane **21d** with allylbromide **22g** did not occur under these conditions (Table 3.5, entry 9). Thus, bromoalkynes and allyltrimethylsilanes are the substrates of choice (Table 3.4, entry 14), although chloroalkynes and allyltriphenylsilanes are also suitable reaction partners (Table 3.5, entries 2 and 6, respectively).

Table 3.6. Screening of Lewis acid catalysts in the reaction of **21a** with **22a**.[a]

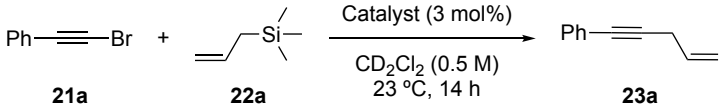

21a **22a** **23a**

Entry	Catalyst	Yield (%)[b]	Entry	Catalyst	Yield (%)[b]
1	$PtCl_2$	traces	14	$CoCl_2$	0
2	$GaCl_3$	28-45	15	WCl_6	0
3	$InCl_3$	27-58	16	$AlCl_3$	traces
4	InI_3	14-57	17	Tl(OAc)	0
5	$In(OTf)_3$	28-36	18	$Hg(OAc)_2$	0
6	**$InBr_3$**	**50-55**	19	$ZrCl_4$	0
7	$Cu(OAc)_2$	0	20	$ZnCl_2$	0
8	CuCl	0	21	TfOH	0
9	$CuCl_2$	0	22	TMSOTf	0
10	$Cu(OTf)_2$	0	23	$BiCl_3$	0
11	AgCl	0	24	$Bi(OTf)_3$	traces
12	Ag(OTf)	0	25	$Fe(OTf)_3$	0
13	$Pd(OAc)_2$	traces	26	**J**	traces

[a] Substrates **21a**:**22a** in a 1:1 ratio. [b] Yields determined by ^1H NMR using mesitylene as internal standard. Range of yields obtained in different runs.

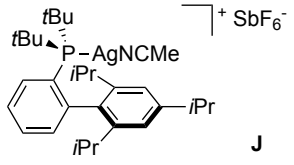

J

Table 3.7. Screening of solvents in the $InBr_3$-catalyzed reaction of **21a** with **22a**.[a]

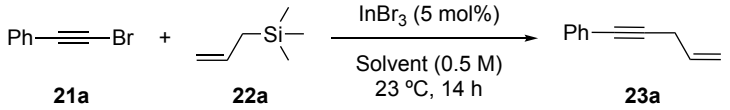

21a **22a** **23a**

Entry	Solvent	Yield (%)[b]	Entry	Solvent	Yield (%)[b]
1	**CH_2Cl_2**	**43**	8	Benzene	10
2	**DCE**	**40**	9	$PhCF_3$	8
3	$CHCl_3$	13	10	PhCl	18
4	$ClCH_2CHCl_2$	30	11	Et_2O	0
5	$Cl_2CHCHCl_2$	12	13	THF	0
6	CCl_4	3	14	CH_3NO_2	0
7	Toluene	6			

[a] Substrates **21a**:**22a** in a 1:1 ratio. [b] Yields determined by ^1H NMR using mesitylene as internal standard.

Table 3.8. Optimization of conditions for the $InBr_3$-catalyzed reaction of **21a** with **22a**.

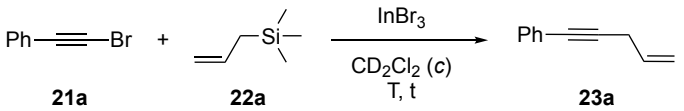

21a **22a** **23a**

Entry	$InBr_3$ (mol%)	**21a**:**22a**	*c* (M)	T (ºC)	Yield (%)[a]
1	**3**	1:1	0.5	23	48
2	**5**	1:1	0.5	23	53
3	**10**	1:1	0.5	23	32
4	5	**2:1**	0.5	23	47
5	5	**1:2**	0.5	23	76
6	5	**1:3**	0.5	23	81[b]
7	5	1:1	**0.2**	23	43
8	5	1:1	**1.0**	23	32
9	5	1:1	0.5	**0**	12
10	5	1:1	0.5	**40**	9
11	**3**	**1:2**	**0.5**	23	81[b]

[a] Yields determined by ^1H NMR using mesitylene as internal standard. [b] Isolated yields.

Moreover, we evaluated a variety of Lewis acids as catalysts for the reaction between **21a** and **22a** (Table 3.6). We first focused on platinum, gallium and indium salts that are known to catalyze cycloisomerizations of 1,*n*-enynes. In this case, $PtCl_2$ gave only traces of the enyne **23a** (Table 3.6, entry 1), while $GaCl_3$ as well as InX_3 were found to catalyze the reaction in moderate yields (Table 3.6, entries 2-6). Various copper and silver salts failed to catalyze the reaction (Table 3.6, entries 7-12), but traces of products were obtained using silver complex **J** (Table 3.6, entry 26), which bears the same phosphine ligand as the optimal gold complex **B**. Brønsted acid TfOH and the remaining Lewis acids surveyed in the screening were not catalytically active in this transformation (Table 3.6, entries 13-25), with the exception of $AlCl_3$, $Bi(OTf)_3$ and $Pd(OAc)_2$ that led to traces of the product (Table 3.6, entries 13, 16 and 24, respectively).

Among all the metal salts, $InBr_3$ provided the best performance. Thus, we optimized the conditions of the reaction of **21a** with **22a** using this catalyst in order to ascertain whether we could obtain yields of **23a** comparable to those observed with gold complex **B**. With regards to the solvent (Table 3.7), CH_2Cl_2 and DCE seemed to be the most suitable (Table 3.7, entries 1-2). The same trend was found for $InBr_3$ and for **B** in terms of yields when adjusting the catalyst loading, stoichiometry of substrates, concentration and temperature (Table 3.8). Therefore, 3 mol% of catalyst, an excess of alkene and 23 ºC were the optimal conditions for both catalysts, and similar 77-81% yields of **23a** were achieved (Table 3.4, entry 14 and Table 3.8, entry 11).

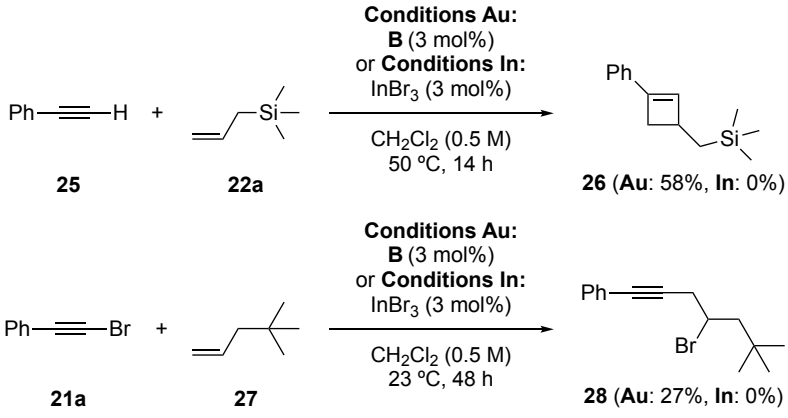

Scheme 3.13. Control experiments.

As control experiments, we carried out the reaction of phenylacetylene (**25**) with allylsilane **22a** under the optimized conditions (Scheme 3.13). In the presence of gold-catalyst **B**, cyclobutene **26** was formed as a result of the well-known [2+2] cycloaddition of alkynes with alkenes.[44,106] Conversely, in the presence of $InBr_3$, the reaction between **25** and **22a** did not take place. As already concluded in **Chapter 1**, this metal salt failed to catalyze the [2+2] cycloaddition of alkynes with alkenes.

Likewise, we performed the reaction of bromoalkyne **21a** and *tert*-butyl allyl derivative **27** (Scheme 3.13). Using gold complex **B** as catalyst, unexpected product **28** was isolated. Worthy of note is the recent report of a gold-catalyzed intermolecular [2+2] cycloaddition of chloroalkynes with alkenes that furnishes chloro-substituted cyclobutenes.[126] Product **28** provides information about the reaction mechanism, which is discussed later in this chapter.

Scope of the Synthesis of Skipped Enynes

With the two sets of conditions in hand utilizing either gold complex **B** or $InBr_3$ as catalyst, we began to explore the scope of the reaction between bromoalkynes **21** and allylsilanes **22** (Table 3.9). As observed in some other cases, in the reaction of mesityl substituted alkyne **21n** with **22a**, we obtained the skipped enyne **23l** together with its hydrobrominated derivative **29** (Scheme 3.14). The HBr responsible for the generation of byproduct **29** presumably arises from the hydrolysis of the TMSBr released in the course of the reaction. For this reason, we decided to routinely use anhydrous conditions.

Generally, comparable yields were achieved with both the gold and indium catalysts (Table 3.9). The reaction of allylsilane **22a** with bromoalkynes bearing differently substituted phenyl groups led to the corresponding 1,4-enynes **23a-l** in yields ranging from 43 to 96%. It was necessary to increase the reaction temperature to 50 ºC for electron-poor bromoalkynes such as *p*-bromo, *p*-trifluoromethyl or *m*-chloro substituted (bromoethynyl)benzenes, in order to favor the formation of the corresponding skipped enynes **23f**, **23g** and **23k**.

Table 3.8. Scope of the gold- or indium-catalyzed synthesis of skipped enynes **23a-y**.[a,164]

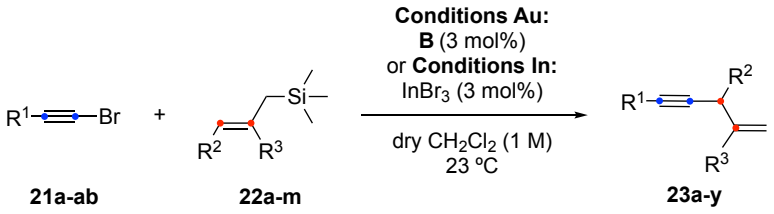

21a-ab **22a-m** **23a-y**

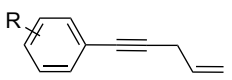

23a: R = H (**Au**: 77%, **In**: 81%)
23c: R = *p*-OMe (**Au**: 67%, **In**: 64%)
23d: R = *p*-Ph (**Au**: 62%, **In**: 80%)
23e: R = *p*-*t*Bu (**Au**: 71%, **In**: 53%)
23f: R = *p*-Br (**Au**[b]: 60%. **In**[b]: 73%)
23g: R = *p*-CF_3 (**Au**[b]: 62%, **In**[b]: 74%)
23h: R = *o*-Me (**Au**: 77%, **In**: 70%)
23i: R = *o*-F (**Au** : 50%, **In**: 78%)
23j: R = *m*-OH (**Au**[c]: 63%, **In**[c]: 56%)
23k: R = *m*-Cl (**Au**[b]: 45%, **In**[b]: 43%)

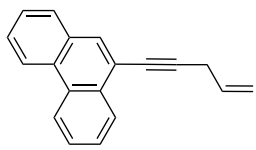

23n (**Au**: 61%, **In**: 55%)

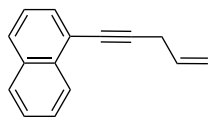

23o (**Au**: 55%, **In**: 65%)

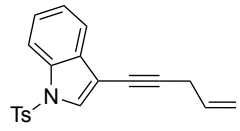

23s (**Au**: 87%, **In**: 19%)

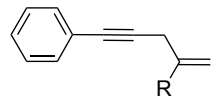

23t: R = Me (**Au**: 54%, **In**: 54%)
23u: R = Br (**Au**[b]: 64%, **In**: 0%)
23v: R = CH_2Cl (**Au**: 48%, **In**: 0%)

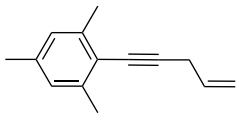

23l (**Au**: 96%, **In**: 92%)

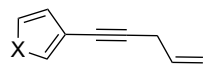

23p: X = S (**Au**: 48%, **In**: 44%)
23q: X = O (**Au**: 23 %, **In**: 20 %)

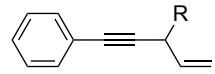

23w: R = Et (**Au**[b]: 47 %, **In**[b]: 73%)
23x: R = Ph (**Au**: 35 %, **In**: 55%)

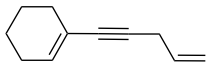

23m (**Au**: 31%, **In**: 21%)

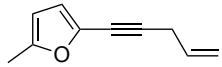

23r (**Au**: 31%, **In**: 22%)

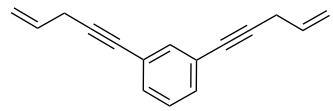

23y (**Au**: 44%, **In**: 63%)

[a] Isolated yields. [b] Reaction at 50 ºC. [c] Yields determined by ^{1}H NMR using mesitylene as internal standard.

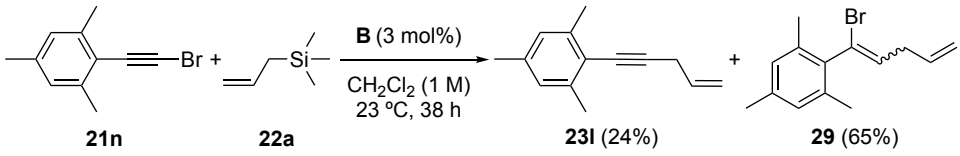

21n **22a** **23l** (24%) **29** (65%)

Scheme 3.14. Reaction of bromoalkyne **21n** with allylsilane **22a** under non-anhydrous conditions (Substrates **21n**:**22a** in a 1:2 ratio).

164. Experiments performed in collaboration with Dr. Ophélie Quinonero.

1-(Bromoethynyl)-1-cyclohexene reacted with **22a** to form 1,6-dien-3-yne **23m** in low yield. In contrast polyaromatic substituted bromoalkynes gave rise to enynes **23n,o** in good yields. By reaction with **22a**, 3-(bromoethynyl)thiophene provided enyne **23p** in moderate yield, whereas differently substituted (bromoethynyl)furans generated 1,4-enynes **23q,r** in low yields. We postulate this is due to decomposition of the sensitive furane moiety under the reaction conditions. Employing the gold catalyst, indole substituted 1,4-enyne **23s** was synthesized in 87% yield, whilst using $InBr_3$ a moderate 19% yield was obtained, to a large extent because of the formation of its hydrobrominated derivative.

Differently 2-substituted allylsilanes reacted with (bromoethynyl)benzene (**21a**) to afford skipped enynes **23t-v** in moderate to good yields in the presence of gold catalyst **B**. However, enynes **23u,v** could not be isolated using $InBr_3$ as catalyst presumably owing to the decomposition of haloalkyl intermediates under the reaction conditions. 3-Substituted 1,4-enynes **23w,x** arose from the reaction of 3-substituted allylsilanes with (bromoethynyl)benzene (**21a**), which indicate that the process comprises a 1,3-allylic substitution. Interestingly, higher yields of **23w,x** were isolated with $InBr_3$ than with catalyst **B**. Moreover, *m*-bis(bromoethynyl)benzene underwent a twofold reaction with allylsilane **22a** to construct bisallylated product **23y**.

In the gold-catalyzed reaction of (bromoethynyl)benzene (**21a**) with ester substituted allylsilane **22n**, bromo substituted enyne **23z** was isolated in a 17% yield (Scheme 3.15). This product most likely originates from the nucleophilic substitution (bromination) of the activated acetate moiety in **XII** assisted by the TMSBr that is formed in the reaction.

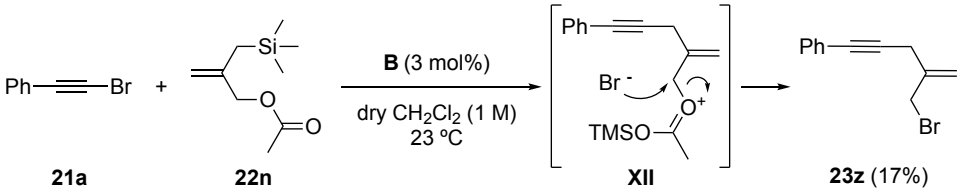

Scheme 3.15. Gold-catalyzed reaction of bromoalkyne **21a** with allylsilane **22n** (Substrates **21a**:**22n** in a 1:2 ratio).

Interestingly, when quenching the gold-catalyzed reaction of *o*-methyl substituted (bromoethynyl)benzene **21j** with allylsilane **22a** with triethylamine, not only was the 1,4-

enyne **23h** formed, but also the 3-allylindene **30a** (Scheme 3.16).[165] Control experiments showed that under the reaction conditions **23h** is not converted into **30a**. However, quenching in the same manner the corresponding $InBr_3$-catalyzed reaction, indene **30a** was never detected. Similarly, upon quenching with triethylamine, the gold-catalyzed reaction of *o*-ethyl substituted (bromoethynyl)benzene **21ac** with allylsilane **22a** produced 1,4-enyne **23aa** along with indene **30b** (Scheme 3.16).[165] This reactivity is reminiscent of the reported gold-catalyzed cyclization of *o*-substituted (iodoethynyl)benzenes to form 1-substituted 3-iodoindenes (see Scheme 3.7 in the Introduction to **Chapter 3**). Based on that precedent, we hypothesized that vinylidene gold species might be intermediates of the reaction and might undergo C−H insertion. Further studies on this reaction are currently ongoing in our group.

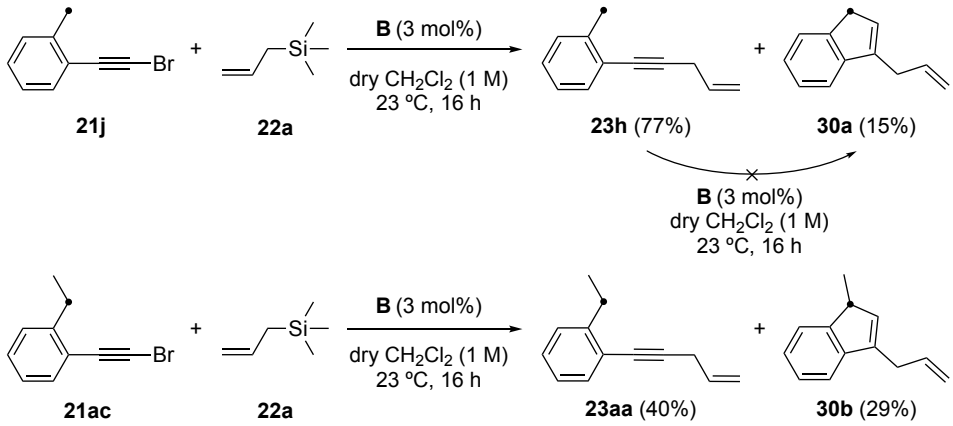

Scheme 3.16. Gold-catalyzed reaction of *o*-alkyl substituted bromoalkynes with allylsilane **22a** (Substrates **21**:**22a** in a 1:2 ratio).

Scheme 3.17[164] shows the bromoalkynes that failed to afford skipped enynes in the reaction with allylsilane **22a** in the presence of complex **B** or $InBr_3$ at 23 or 50 ºC. No reaction took place with pyridine substituted bromoalkyne **21ad**, presumably due to the strong binding of the Lewis-basic pyridine to the Lewis acid. In contrast, carbonyl substituted bromoalkynes **21ae,af** led to a complex mixture of products. Ferrocenyl, silyl and alkyl substituted derivatives **21ag-ai** were unreactive. As was commonly observed in the gold-catalyzed reactions of alkylalkynes with alkenes, bromoalkynes **21aj-al** were poorly

165. Experiments performed by Dr. Ophélie Quinonero.

reactive. In particular, hexyl substituted bromoalkyne **21am** provided a mixture of products, conceivably because of C−H insertion reactions analogous to the ones shown in Scheme 3.16.

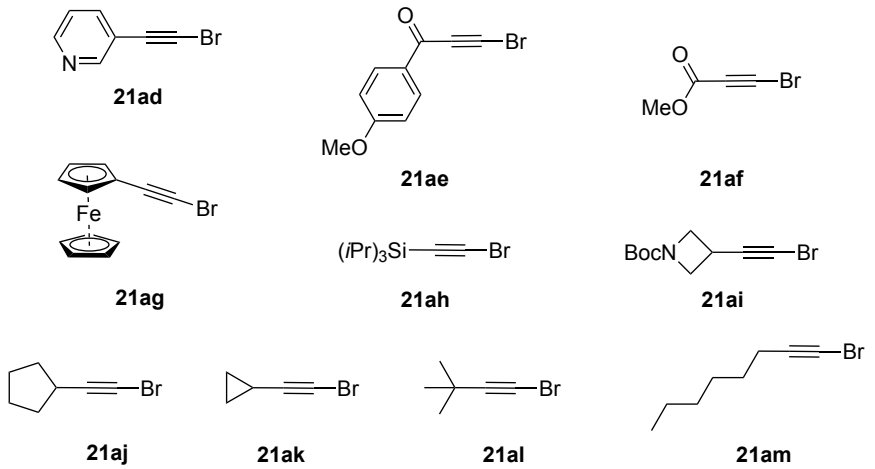

Scheme 3.17. Other bromoalkynes tested in the reaction with allylsilane **22a**.

Regarding the reactivity of the allylsilane counterparts (Scheme 3.18),[164] *tert*-butyl-substituted allylsilane **22o** reacted poorly with bromoalkyne **21a** to generate the corresponding skipped enyne, perhaps due to the steric bulk of the *tert*-butyl substituent. In the reaction with **21a**, allylsilanes **22p** and **22q** gave complex mixtures of products.

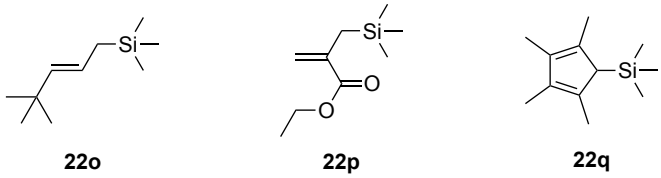

Scheme 3.18. Unsuccessful allylsilane partners in the reaction with bromoalkyne **21a**.

Reaction of Bromoalkynes with Allenylsilanes

As an extension, we investigated the gold- or indium-catalyzed intermolecular reaction of bromoalkynes **21a**, **21f** and **21h** with allenylsilane **31** under the previously optimized

conditions (Scheme 3.19). From the resulting complex mixture of products, we could isolate the highly substituted 1,3-enynes **32a-c** in low yields. The structure of **32c** was confirmed by X-ray crystallography. Moreover, vinyl bromide **32a** was subjected to a Suzuki cross-coupling reaction with *p*-nitrophenylboronic acid to form *p*-nitrophenyl derivative **33**, whose structure was also confirmed by single crystal X-ray diffraction.

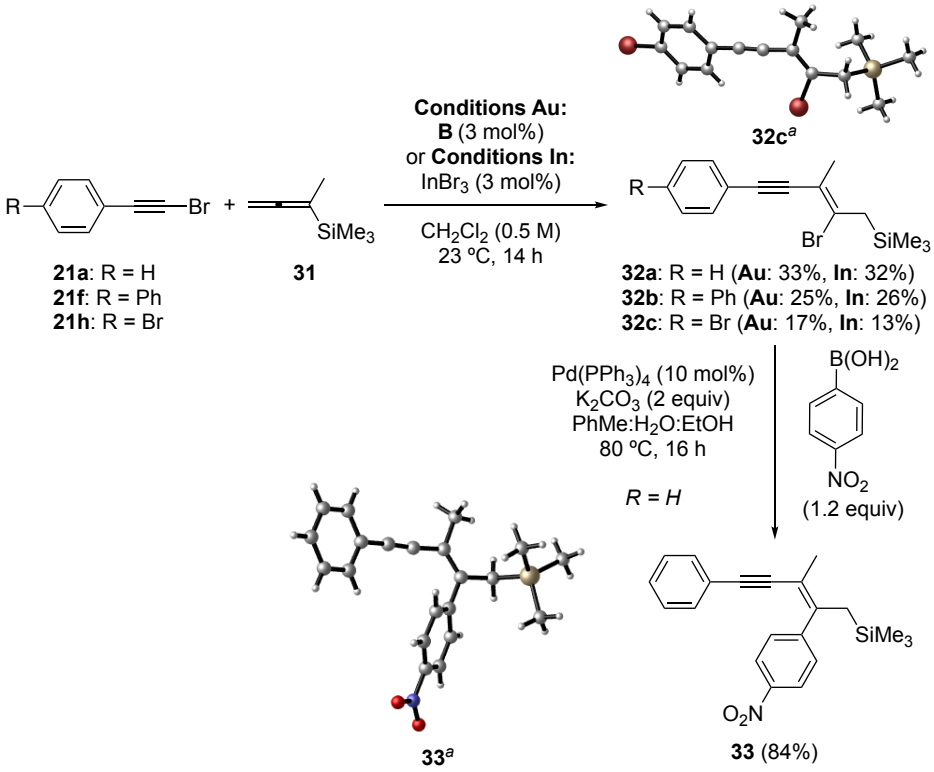

Scheme 3.19. Metal-catalyzed reaction of bromoalkynes with allenylsilanes and further derivatization ([a] CYLview depiction of the X-ray crystal structure).

The mechanism of this Lewis acid-catalyzed reaction of bromoalkynes with allenylsilane **31** providing 1,3-enynes **32** is discussed later in this chapter.

Allylation/Hydroarylation of Bromoalkynes

Considering the precedents on hydroarylation of alkynes (see Introduction to **Chapter 3**) and the observation of the C−H insertion in the reaction of *o*-alkyl substituted

(bromoethynyl)benzenes with allylsilanes (Scheme 3.16), we envisioned that the reaction of aryl substituted bromoalkynes with allylsilanes could trigger an allylation/hydroarylation cascade. In order for the hydroarylation reaction to occur, the aryl group should be linked to the alkyne through a spacer, such as in bromoalkyne **34a**.

When we performed the reaction of **34a** with allylsilane **22a** under the previously optimized conditions using catalyst **B**, we observed the formation of the cyclized product **35a** in 41% yield together with starting material **34a** (Table 3.9, entry 1). Compound **35a** arose from the desired allylation/hydroarylation of **34a**, in which the allyl group seemed to migrate from the C4 to the C3 position of the 1,2-dihydronaphthalene. The mechanism of this transformation is discussed later in this chapter.

Table 3.9. Optimization of the reaction of bromoalkyne **34a** with allylsilane **22a**.[a]

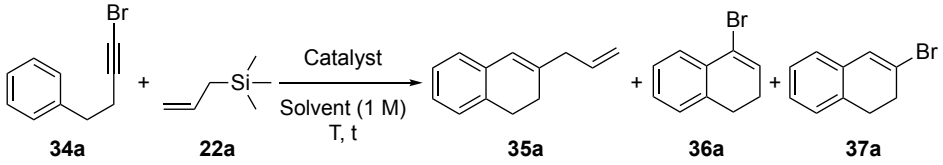

Entry	Catalyst (mol%)	Solvent	T (º C)	t	Recovered **34a** (%)[b]	**35a** (%)[b]
1	**B** (3 mol%)	CH_2Cl_2	23	10 d	19	41
2	**B** (3 mol%)	CH_2Cl_2	50	20 h	14	56
3	**B** (3 mol%)	CH_2Cl_2	50	3 d	-	62
4	**B** (5 mol%)	DCE	75	18 h	-	64[c]
5	$InBr_3$ (3 mol%)	CH_2Cl_2	50	24 h	61	4
6	$InBr_3$ (5 mol%)	DCE	75	18 h	85[d]	11[d]

[a] Substrates **21**:**22** in a 1:2 ratio. [b] Isolated yields. [c] A mixture of **36a**:**37a** was also isolated in a 15% yield and 6:1 ratio. [d] Yields determined by ^1H NMR using mesitylene as internal standard.

Increasing the temperature up to 50 ºC, full conversion and 62% yield of **35a** were achieved after 3 days of reaction (Table 3.9, entries 2-3). Moreover, the same results were obtained at 75 ºC in DCE after 18 h of reaction (Table 3.9, entry 4). In this case, a mixture of hydroarylated compounds **36a** and **37a** was also isolated in a 15% yield and 6:1 ratio. However, using $InBr_3$ as catalyst, bromoalkyne **34a** was mainly recovered and **35a** was produced in low 4-11% yield (Table 3.9, entries 5-6).

Similarly, $InBr_3$ failed to catalyze the reaction of bromoalkynes **34b** and **34a** with allylsilanes **22a** and **22i**, respectively (Table 3.10, entries 2 and 4). Employing gold catalyst **B**, bromoalkyne **34b** react with allylsilane **22a** leading to skipped diene **35b** in 42% yield and a 5:1 mixture of **36b**:**37b** in 36% yield (Table 3.10, entry 1). In the gold-catalyzed reaction of bromoalkyne **34a** with 2-substituted allylsilane **22i**, the corresponding skipped diene **35c** was obtained in low yield together with a 3:1 mixture of hydroarylated products **36b**:**37b** (61%) (Table 3.10, entry 3). Notably, non-rearranged **36a,b** were always obtained as major regioisomers of the intramolecular hydroarylation reaction of **34a,b**.

Table 3.10. Reaction of bromoalkynes **34a,b** with allylsilanes **22a,i**.[a]

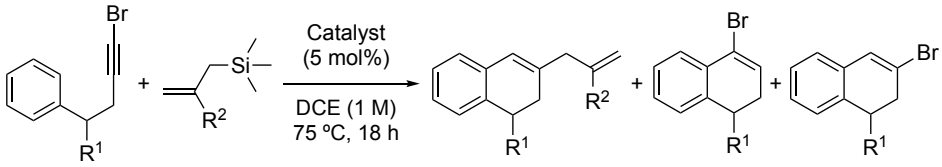

34a,b **22a,i** **35b-c** **36a,b** **37a,b**

Entry	**34**	R^1	**22**	R^2	Catalyst	**35** (%)[b]	**36:37** (%, ratio)[b]
1	**34b**	Me	**22a**	H	**B**	**35b** (42)	**36b:37b** (36, 5:1)
2	**34b**	Me	**22a**	H	$InBr_3$	**35b** (traces)[c]	**36b:37b** (traces)[c]
3	**34a**	H	**22i**	CH_2Cl	**B**	**35c** (13)	**36a:37a** (61, 3:1)
4	**34a**	H	**22i**	CH_2Cl	$InBr_3$	**35c** (0)[c]	**36a:37a** (0)[c]

[a] Substrates **34**:**22** in a 1:2 ratio. [b] Isolated yields. Ratio determined by ^1H NMR.
[c] Determined by ^1H NMR.

In this context, we evaluated the reaction of allylsilane **22a** with *o*-alkynylbiaryls **34d-f** (Table 3.11).[164] Utilizing catalyst **B**, bromoalkyne **34d**—without substituents on the aryl moieties—provided skipped enyne **38d** and allylphenanthrene **35d** in a 53 and 23% yield, respectively (Table 3.11, entry 1). Using $InBr_3$, both products are obtained in similar ratio but lower yield (Table 3.11, entry 2). In the case of methyl substituted derivative **34e**, gold catalysis led to the enyne **38e** and the cyclized product **35e** in 41 and 26% yield, respectively, whereas $InBr_3$ only gives **38e** in low yield (Table 3.11, entries 3-4). Importantly, the structure of **35e** was determined by nOe experiments. In contrast, gold- and indium-catalyzed reactions of trifluoromethyl substituted derivative **34f** with **22a** produced exclusively the 1,4-enyne **38f** in excellent yields (Table 3.11, entries 5-6). This

suggests that the hydroarylation reaction is considerably influenced by the electronic properties of the aryl moiety involved in the hydroarylation.

Table 3.11. Reaction of bromoalkynes **34d-f** with allylsilane **22a**.

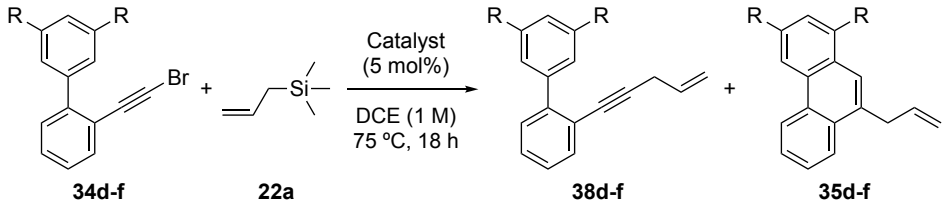

Entry	**34**	R	Catalyst	**38** (%)[b]	**35** (%)[b]
1	**34d**	H	**B**	**38d** (53)	**35d** (23)
2	**34d**	H	$InBr_3$	**38d** (32)	**35d** (17)
3	**34e**	Me	**B**	**38e** (41)	**35e** (26)
4	**34e**	Me	$InBr_3$	**38e** (21)	**35e** (0)
5	**34f**	CF_3	**B**	**38f** (85)	**35f** (0)
6	**34f**	CF_3	$InBr_3$	**38f** (90)	**35f** (0)

[a] Substrates **34**:**22** in a 1:2 ratio. [b] Isolated yields.

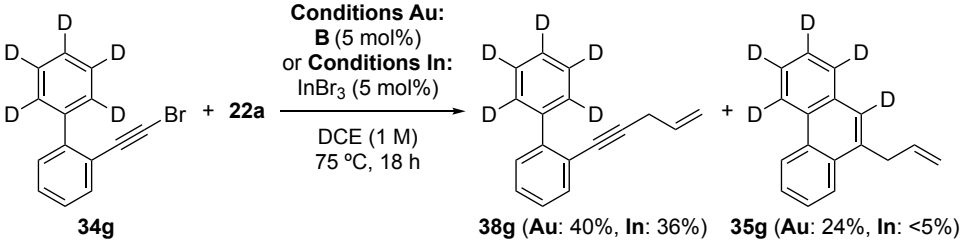

Scheme 3.20. Reaction of deuterated bromoalkyne **34g** with allylsilane **22a**.

As expected, a similar reaction outcome was obtained in the reaction of allylsilane **22a** with deuterated bromoalkyne **34g** (Scheme 3.20)[165] and non-deuterated analogue **34d** (Table 3.11, entries 1-2) in terms of yields of the corresponding products. The experiment with the deuterated substrate indicated that in the hydroarylation reaction, the deuterium remains on the carbon contiguous to the reacting aryl group.

Table 3.12. Generation of allylphenanthrenes **39d-f** from enynes **38d-f**.

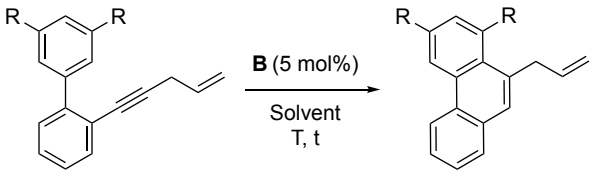

38d-f **39d-f**

Entry	**38**	R	Catalyst	Solvent	T (ºC)	T (h)	**38:39**[a]
1	**38d**	H	-	DCE	75	18	1:0 (no reaction)
2	**38d**	H	**B**	DCE	75	18	2.5:1
3	**38d**	H	**B**	DCE	100	18	1:1.7
4	**38d**	H	**B**	DCE	100	72	1:2.7
5	**38d**	H	**B**	DCE	120	18	1:1.7
6	**38d**	H	**B**	PhCl	120	18	3.5:1 and decomposition
7	**38d**	H	**B**	PhCl	140	18	2:1 and decomposition
8	**38e**	Me	**B**	DCE	100	18	0:1 (quant. yield)[b]
9	**38f**	CF_3	**B**	DCE	100	18	1:0 (no reaction)

[a] Determined by ^{1}H NMR. Note that allylphenanthrene **39d** = **35d** since R = H. [b] Isolated yield.

We next investigated the possible the intermediacy of enynes **38** in the formation of cyclized products **35**. By heating enyne **38d** at 75 ºC in DCE in the absence of a Lewis acid, no reaction took place (Table 3.12, entry 1). Nevertheless, in the presence of catalyst **B**, phenanthrene **39d** was generated, although starting material **38d** was recovered to a large extent (Table 3.12, entry 2). Furthermore, an increase of the reaction temperature up to 120 ºC favored the cyclization (Table 3.12, entries 3-5). When chlorobenzene was used as solvent instead of DCE, phenanthrene **39d** was observed to a small extent and decomposition was detected either at 120 or 140 ºC (Table 3.12, entries 6-7). Interestingly, by heating at 100 ºC with gold complex **B**, the methyl substituted derivative **38e** led to **39e** in quantitative yield (Table 3.12, entry 8), while trifluoromethyl substituted analogue **38f** remained unreacted (Table 3.12, entry 9).[165] The experiment with **38e** showed that the allyl substituent does not migrate in this transformation. Cyclized compounds of type **39** differ from the previously obtained allylphenanthrenes **35** in the position of the allyl substituent. This demonstrates that enynes **38** are not reaction intermediates in the generation of phenanthrenes **35.**

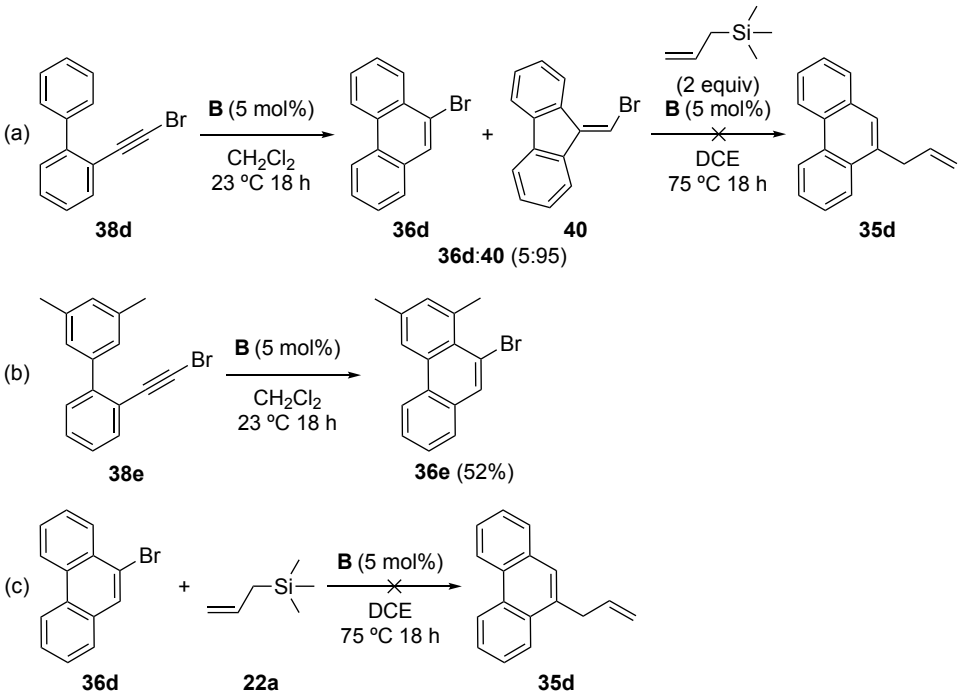

Scheme 3.21. Studies on the formation of allylphenanthrenes **35**.

In addition, we investigated if the intramolecular hydroarylation of the aryl substituted bromoalkynes occurs prior to the intermolecular reaction with the allylsilane in the construction of allylphenantrenes **35** (Scheme 3.21). Thus, when we treated **38d** with gold catalyst **B**, a 95:5 mixture of fluorene **40** and phenanthrene **36d** was formed as a result of a 5-*exo* or 6-*endo* pathway, respectively (Scheme 3.21a). This mixture was subjected to the reaction with allylsilane **22a** under the optimized conditions, however the generation of **35d** did not take place. Interestingly, using catalyst **B** in the hydroarylation of methyl substituted derivative **38e**, phenanthrene **36e** was exclusively isolated, whereas the corresponding fluorene was not detected (Scheme 3.21b).[165] Commercially available phenanthrene **36d** did not reacted either with allylsilane **22a**, to give **35d**, under the optimized conditions (Scheme 3.21c).

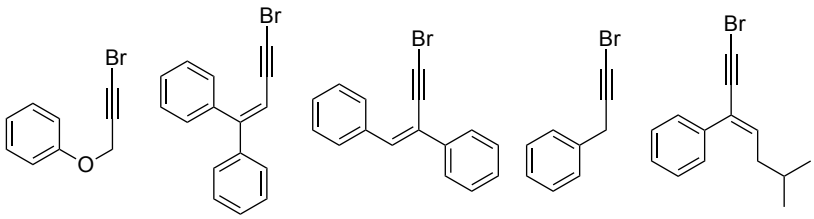

34h **34i** **34j** **34k** **34l**

Scheme 3.22. Unsuccessful aryl substituted bromoalkynes in the allylation/hydroarylation cascade.

The allylation/hydroarylation cascade could not be extended to bromoalkyne **34h**, since undesired 4-bromo-2*H*-chromene was obtained along with decomposition. Other aryl substituted bromoalkynes **34i-l** gave rise to complex mixtures of products.

Mechanistic Insight into Gold-Catalyzed Reactions of Bromoalkynes

Experiments with σ-Gold and σ,π-Digold Alkyne Complexes

Gold-catalyzed reactions of haloalkynes have been proposed to proceed *via* gold acetylide and/or σ,π-digold(I) alkyne intermediates,[166] hence we first investigated if this was the case in the reaction of bromoalkynes **21** with allylsilanes **22** to form skipped enynes **23**. According to literature procedures, we prepared gold acetylide complex **K1** and σ,π-digold(I) alkyne complex **K2** bearing the same ligand as the optimal gold catalyst for the reaction developed herein. Then, we conducted stoichiometric reactions of allylsilane **22a** with complexes **K1** or **K2** in the presence and absence of gold catalyst **B** and we observed that no reaction took place (Scheme 3.23). The reaction did not occur either with complexes **K1** or **K2** in the presence of bromide sources such as LiBr or $(n\text{Bu})_4\text{NBr}$ (Scheme 3.24).[167] This demonstrates that even if **K1** and **K2** are formed during the reaction, they are not intermediates leading to the final 1,4-enynes **23a** under these reaction conditions.

166. (a) Nösel, P.; Lauterbach, T.; Rudolph, M.; Rominger, F.; Hashmi, A. S. K. *Chem. Eur. J.* **2013**, *19*, 8634–864. (b) See also references 26a and 154.
167. Experiments performed by Margherita Zanini.

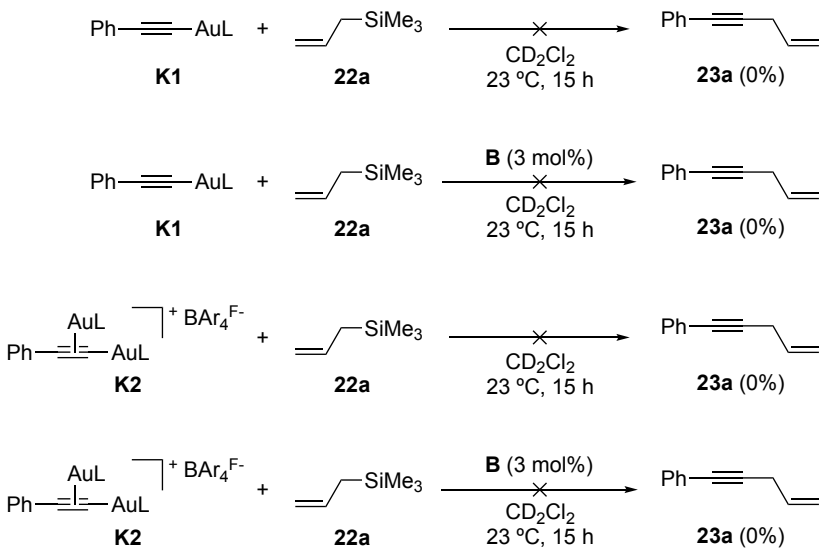

Scheme 3.23. Stoichiometric experiments with gold acetylide and σ,π-digold(I) alkyne complexes in the presence or absence of catalyst **B** (L = *t*BuXPhos).

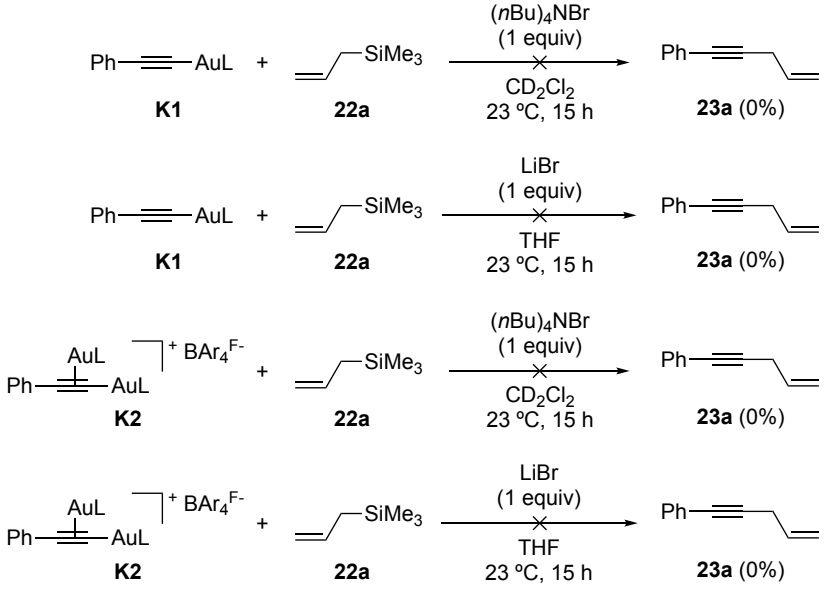

Scheme 3.24. Stoichiometric experiments with gold acetylide and σ,π-digold(I) alkyne complexes in the presence of bromide sources (L = *t*BuXPhos).

We also performed the reaction of bromoalkyne **21a** with **22a** under catalytic amounts of complexes **K1** or **K2** (Scheme 3.25). Complex **K1** was not catalytically active, since enyne product **23a** was not detected. Nonetheless, the reaction was effective using complex **K2**,

presumably because a ligand exchange between gold acetylide **K2** and bromoalkyne **21a** could initiate the catalytic cycle to generate enyne **23a**.

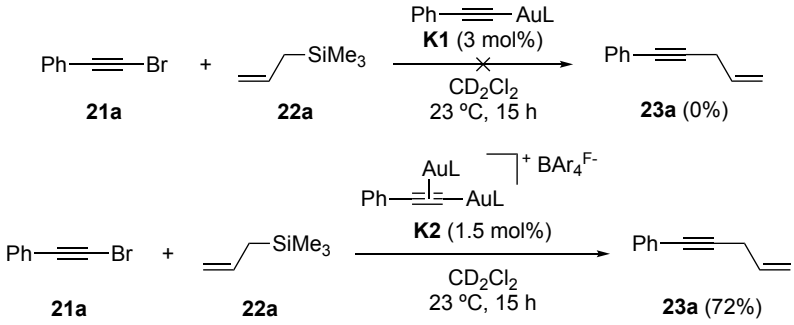

Scheme 3.25. Experiments with gold acetylide and σ,π-digold(I) alkyne complexes as catalysts (L = *t*BuXPhos).

Mechanism of the Formation of Skipped Enynes

In order to gain a deeper understanding of the mechanism of the reaction of bromoalkynes **21** with allylsilanes **22** to form skipped enynes **23**, we carried out DFT calculations.[168] We selected substrates **21a** and **22a** as model system, and the gold(I) catalyst bearing PMe_3 as ligand.[77]

As already mentioned in the **General Introduction**, gold preferentially coordinates to alkenes leading to (η^2-alkene)gold(I) complexes such as **Int1** (Scheme 3.26). We considered that the straightforward reaction of **Int1** with **21a** *via* **TS1-4a** could give 1,4-enyne **In4a**. However, the extremely high energy barrier indicates that this process is unlikely to happen. Based on the previously studied gold-catalyzed intermolecular reactions of alkynes with alkenes (see **Chapter 1**), we reasoned that the reaction commences with the associative ligand exchange of **Int1** to generate the less stable (η^2-alkyne)gold(I) complex **Int2a**. The alternative complex **Int3a**, in which gold is bound to the bromine atom of the bromoalkyne, is 12.9 kcal/mol less stable than **Int2a**.

168. See the computational methods in the Experimental Part.

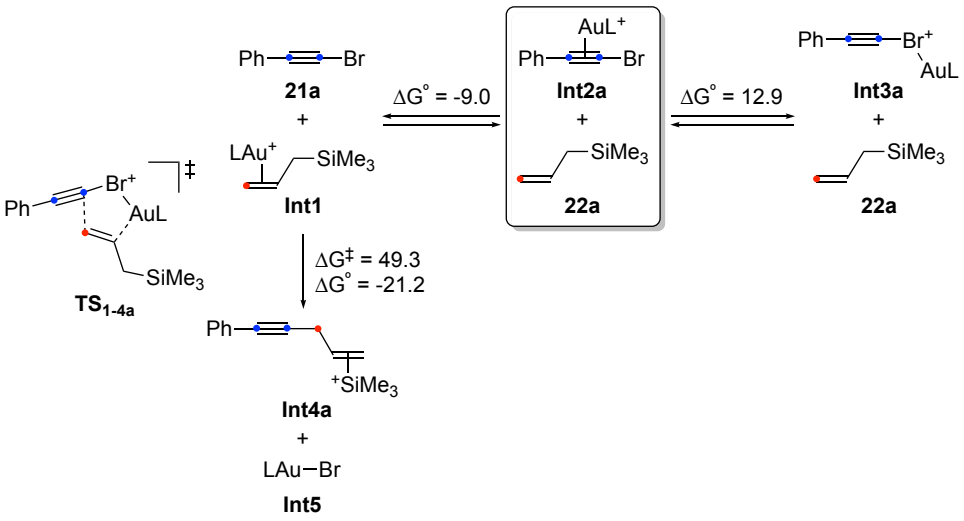

Scheme 3.26. Initial gold intermediates in the gold-catalyzed reaction of **21a** and **22a** (L = PMe_3. Free energies in kcal/mol).

Then, the gold-activated bromoalkyne **Int2a** can undergo different reaction pathways (Scheme 3.27). On one hand, alkyne **Int2a** can rearrange to form gold vinylidene **Int6a** ($\Delta G^{‡}$ = 20.3, ΔG^{o} = 18.4 kcal/mol), as proposed in several gold-catalyzed transformations of alkynes.[169] On the other hand, the double bond of the allylsilane **22a** may attack on activated alkyne **Int2a** to forge regioisomeric cyclopropyl gold(I) carbenes **Int7a-c** or **Int8a-c**. Thus, the gold carbene can be generated at the C2 carbon connected to the more electron-donating phenyl group (**Int7a-c**) or at the C1 carbon attached to the more electron-withdrawing bromine atom (**Int8a-c**). Various conformers (**a-c**) were evaluated for each case. Those are in equilibrium through their corresponding bond rotations (calculated bond rotation barriers: $\Delta G^{‡}$ = 5.1-8.7 kcal/mol). Analyzing the energy barriers, the formation of cyclopropyl gold(I) carbenes **Int8a-c** ($\Delta G^{‡}$ = 12.7-15.9 kcal/mol) is more favorable than the generation of **Int7a-c** ($\Delta G^{‡}$ = 17.9-20.7 kcal/mol). This is consistent with the conclusions of **Chapter 1** on the origin of regioisometic cyclopropyl gold(I) carbenes in intermolecular reactions of alkynes with alkenes: the carbene is preferentially formed at the alkyne carbon bound to electron-withdrawing groups, and at the alkyne carbon which is in

169. (a) Ye, L.; Wang, Y.; Aue, D. H.; Zhang, L. *J. Am. Chem. Soc.* **2012**, *134*, 31−34. (b) Hashmi, A. S. K.; Wieteck, M.; Braun, I.; Nösel, P.; Jongbloed, L.; Rudolph, M.; Rominger, F. *Adv. Synth. Catal.* **2012**, *354*, 555–562. (c) Debrouwer, W.; Fürstner, A. *Chem. Eur. J.* **2017**, *23*, 4271–4275.

β-position to electron-donating groups. Since the generation of **Int8a-c** is also more favorable than the formation of **Int6a**, we continued exploring the evolution of **Int8a-c**.

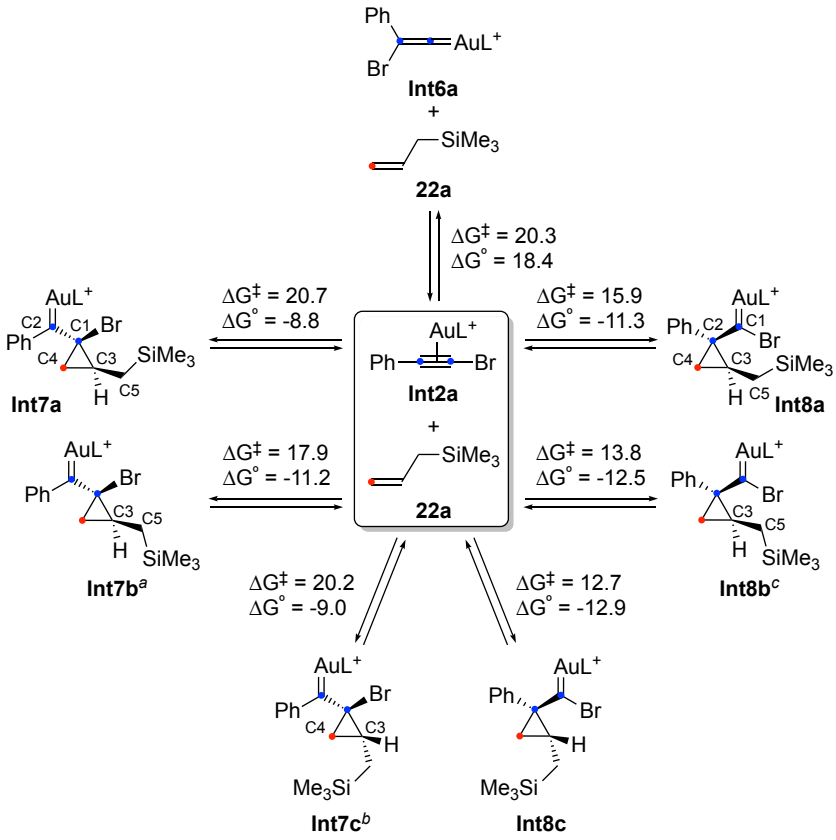

Scheme 3.27. Evolution of (η^2-alkyne)gold(I) complex **Int2a** (L = PMe_3. Free energies in kcal/mol. [a] Transformation of **Int7b** into **Int7a** *via* C3−C5 bond rotation: $\Delta G^{\ddagger}$ = 5.1, ΔG^{o} = 2.4. [b] Transformation of **Int7c** into **Int7a** *via* C3−C4 bond rotation: $\Delta G^{\ddagger}$ = 6.2, ΔG^{o} = 0.2. [c] Transformation of **Int8b** into **Int8a** *via* C3−C5 bond rotation: $\Delta G^{\ddagger}$ = 8.7, ΔG^{o} = 1.2).

In particular, we focused on comparing the possible reaction pathways of **Int8a** (Scheme 3.28 and 3.29), which exhibits the conformation required for the bromide-assisted migration of the silyl group to give **Int9a** (Scheme 3.28). The low energy release of TMSBr in **Int9a** would afford gold vinylidene **Int10a**, which could undergo an exothermic 1,2-migration of either the phenyl ($\Delta G^{\ddagger}$ = 4.0 kcal/mol) or allyl group ($\Delta G^{\ddagger}$ = 10.2 kcal/mol) to render the final skipped enynes **Int11a** or **Int12a**, respectively. Therefore, **Int11a** and **Int12a** only differ in the location of the carbons C1 and C2 in the final alkyne. Based on

the activation energies, the phenyl migration is preferred over the allyl migration and that would lead to the predominant formation of **Int11a**.

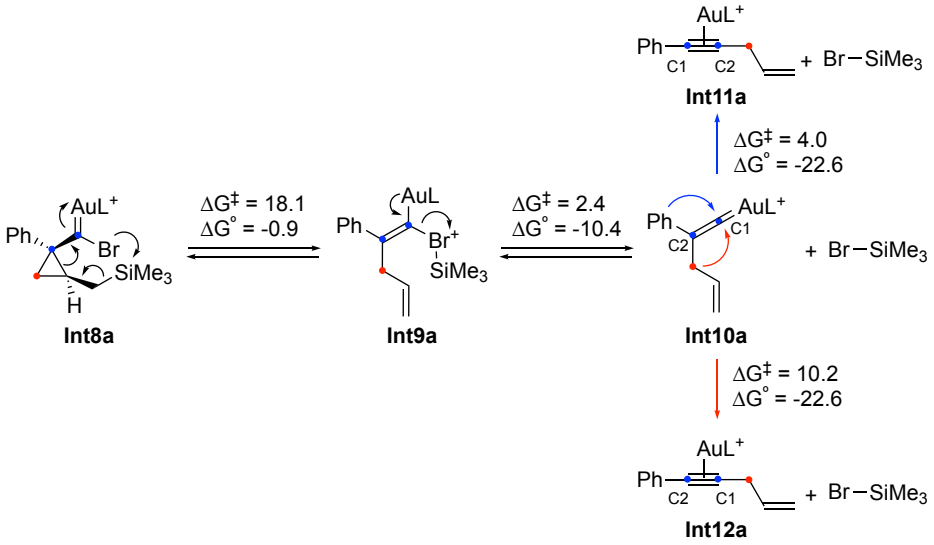

Scheme 3.28. Evolution of **Int8a** *via* migration of the silyl group (L = PMe_3. Free energies in kcal/mol).

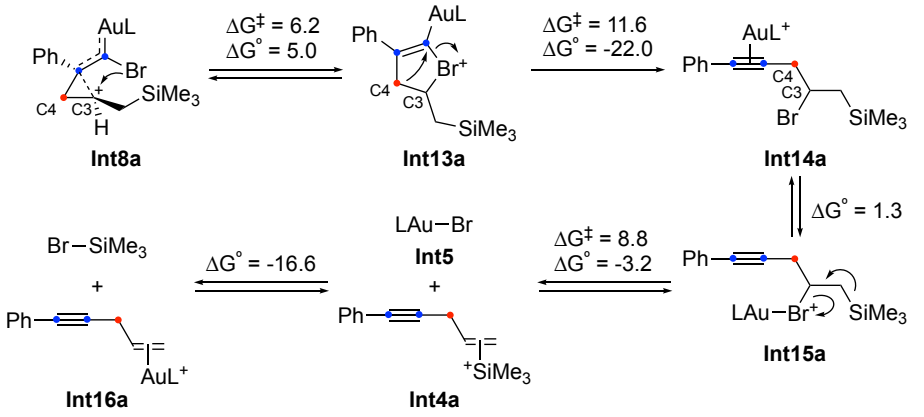

Scheme 3.29. Evolution of **Int8a** *via* bromonium cyclopentene **Int13a** (L = PMe_3. Free energies in kcal/mol).

Alternatively, the C3 carbocation of **Int8a**, which is stabilized by the silyl group in β-position, could experience nucleophilic attack by the bromide to generate the less stable bromonium **Int13a** (Scheme 3.29). This cyclic intermediate **Int13a** could then ring-open *via* an exothermic rearrangement of the C4 carbon to furnish (η^2-alkyne)gold(I) complex

Int14a. Subsequently, the gold-promoted elimination of the bromide *via* **Int15a** could lead to bromide gold complex **Int5** and skipped enyne **Int4a**, in which the trimethylsilyl group is still bound to the alkene. Finally, the activation of the gold complex **Int5** with the trimethylsilyl derivative **Int4a** could generate TMSBr along with (η^2-alkene)gold(I) complex **Int16a**, which can turn over the catalytic cycle by ligand exchange to form **Int2a**.

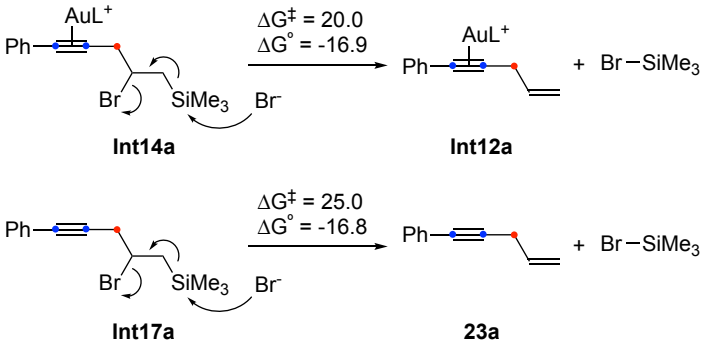

Scheme 3.30. Alternative eliminations of TMSBr (L = PMe_3. Free energies in kcal/mol).

We also considered that the release of TMSBr from **Int14a** or **Int17a** could be assisted by an external bromide (Scheme 3.30). However, the activation energies of such processes are much higher than the gold-promoted route.

Analyzing all the energy barriers, the evolution of **Int8a** *via* migration of the bromide (Scheme 3.29) is kinetically favored over the migration of the silyl group (Scheme 3.28). Moreover, the proposed intermediates **Int14a** resembles the brominated product **28**, which was obtained in the control reaction of (bromoethynyl)benzene (**21a**) with 4,4-dimethylpent-1-ene (**27**) (Scheme 3.13). In that transformation, the presence of the *tert*-butyl group instead of the trimethylsilyl group would prevent the elimination of the bromide and the generation of the alkene.

To further discard the reaction pathway leading to **Int11a**, we performed ^{13}C-labeling experiments (Scheme 3.31). We prepared ^{13}C-labeled bromoalkyne **^{13}C-21a** and we subjected it to the reaction with allylsilane **22a** in the presence of gold complex **B** or $InBr_3$. In both cases, we obtained skipped enyne **^{13}C-23a** as exclusive product, in which the carbons of the alkyne remained at their initial position. The alternative **^{13}C-23a´**, which

would correspond to a mechanism involving **Int11a**, was not detected. Therefore, we concluded that **Int11a** is not an intermediate of the reaction.

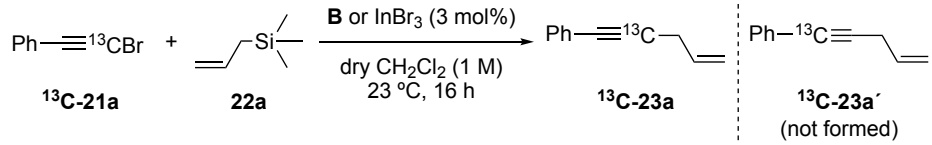

Scheme 3.31. ^{13}C-Labeling experiments.

In order to evaluate the regeneration of the active gold species from bromide gold complex **Int5** and trimethylsilyl derivative **Int4a**, we conducted experiments with chloride gold complex **K3** (Scheme 3.32). Complex **K3** failed to catalyze the reaction of bromoalkyne **21a** with allylsilane **22a** in the presence of TMSCl, which was added to mimic the byproduct that is released in the reaction. In contrast, upon addition of TMSOTf[170] as a trimethylsilyl source, the 1,4-enyne **23a** was formed in a 19% yield as a result of the activation of gold complex **K3**. As previously demonstrated in the optimization of the reaction conditions, the reaction between **21a** and **22a** did not take place using TMSOTf as sole catalytic additive (Table 3.6, entry 22). In view of this experiments, the activation of halide gold complexes such as **Int5** with a trimethylsilylium source such as intermediate **Int4a** seems feasible and is conceivably the key catalytic turnover step.

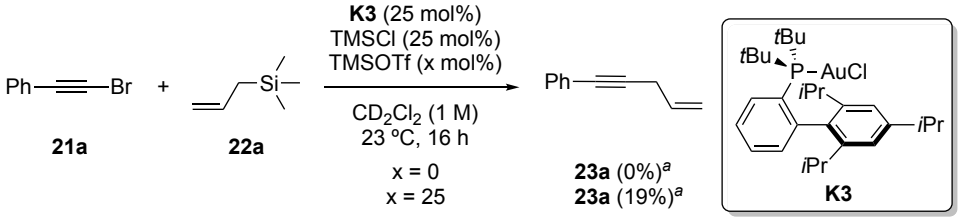

Scheme 3.32. Activation of chloride gold complex **K3** with TMSOTf (Substrates **21a**:**22a** in a 1:2 ratio. [a] Yields determined by ^{1}H NMR using mesitylene as internal standard).

Based on our experimental and computational data, we propose that the gold-catalyzed reaction of bromoalkyne **21a** with allylsilane **22a** proceeds through cyclopropyl gold(I)

170. TMSOTf has previously been used to activate gold complexes. See for instance: Sarria Toro, J. M.; García-Morales, C.; Raducan, M.; Smirnova, E. S.; Echavarren, A. M. *Angew. Chem. Int. Ed.* **2017**, *56*, 1859–1863.

carbene **Int8a** and subsequent cyclic bromonium intermediate **Int13a**, which rearranges to form 2-bromo-1-silyl intermediate **Int14a** as depicted in Scheme 3.28. We postulate that the indium-catalyzed transformation follows a similar mechanism to that of the gold-catalyzed reactions.[171] It is worth mentioning that the rearrangements of cyclopropyl gold(I) carbenes to intermediates of type **Int13a** and **Int14a** had never been proposed before.

Mechanism of the Reaction of Bromoalkynes with Allenylsilanes

It is known that allenylsilanes undergo isomerization to propargylsilanes in the presence of Lewis acids (Scheme 3.33).[172] Hence, we reasoned that allenylsilane **31** may undergo this isomerization in the presence of the gold complex **B** or $InBr_3$ to form the corresponding propargylsilane **41**, which then reacts with the bromoalkynes to generate products **32a-c**. We postulated that the mechanism of this reaction operates in a manner homologous to that of the previously discussed reaction of bromoalkynes **21** with allylsilanes **22**.

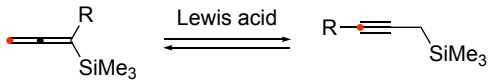

Scheme 3.33. Isomerization of allenylsilanes to propargylsilanes catalyzed by Lewis acids.

According to DFT calculations[168] (Scheme 3.34), the nucleophilic attack of propargylsilane **41** onto the gold-activated alkyne **Int2a** leads to the formation of cyclopropenyl gold(I) carbene **Int8d**, which rearranges to give cyclic bromonium intermediate **Int13d**. Subsequent 1,2-migration of the C4 carbon in **Int13d** can generate another type of cyclopropenyl intermediate **Int18**, which was not one of the located stable intermediates in the reaction of bromoalkyne **21a** with allylsilane **22a**. Finally, opening of the cyclopropenyl ring of **Int18** affords the gold complex **Int14d**, which corresponds to the isolated products **32a**. The energy barriers for this process are comparable to those calculated for the reaction of bromoalkyne **21a** with allylsilane **22a**.

171. (a) Zhuo, L.-G.; Zhang, J.-J.; Yu, Z.-X. *J. Org. Chem.* **2014**, *79*, 3809–3820. (b) Zhuo, L.-G.; Zhang, J.-J.; Yu, Z.-X. *J. Org. Chem.* **2012**, *77*, 8527–8540. (c) Zhuo, L.-G.; Shi, Y.-C.; Yu, Z.-X. *Asian J. Org. Chem.* **2014**, *3*, 842–846.
172. Yoshikawa, E.; Kasahara, M.; Asao, N.; Yamamoto, Y. *Tetrahedron Lett.* **2000**, *41*, 4499–4502.

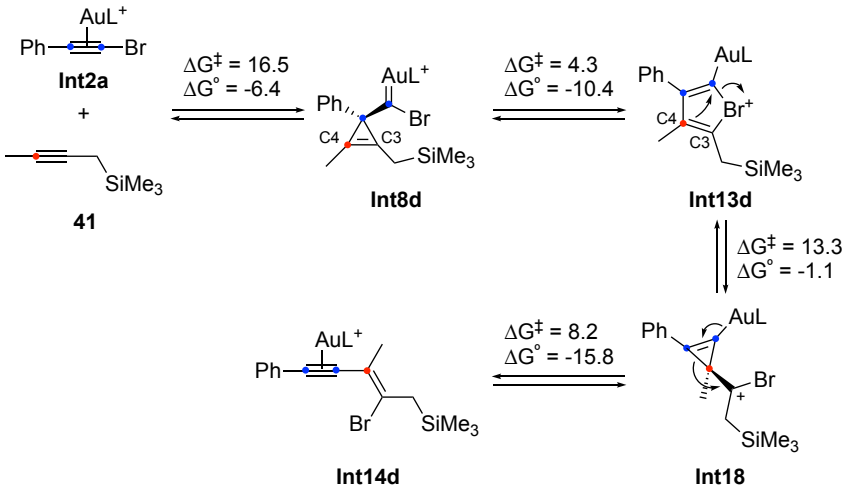

Scheme 3.34. Proposed mechanism for the formation of complexes **Int14d** (L = PMe_3. Free energies in kcal/mol).

Mechanism of the Allylation/Cyclization Cascade

In order to shed light on the mechanism for the allylation/cyclization of bromoalkynes **34** yielding skipped dienes or enynes, we carried out DFT calculations.[168] In particular, we examined the reaction of simple bromoalkyne **34a** with allylsilane **22a** producing skipped diene **35a** (Table 3.9).

We firstly studied the evolution of the corresponding (η^2-alkyne)gold(I) complex **Int2e** (Scheme 3.35). Both the rearrangement of **Int2e** that generates gold vinylidene intermediate **Int6e** ($\Delta G^{\ddagger}$ = 20.0, ΔG^{o} = 17.2 kcal/mol) and the formation of cyclopropyl gold(I) carbene **Int7e** ($\Delta G^{\ddagger}$ = 19.2, ΔG^{o} = -9.4 kcal/mol) are processes less favorable than the formation of cyclopropyl gold(I) carbene **Int8e** ($\Delta G^{\ddagger}$ = 14.2, ΔG^{o} = -14.2 kcal/mol), in which the gold carbene is α to the bromine and β to the electron-donating substituent. This follows the same trend as the one that was found in the gold-catalyzed reaction of (bromoethynyl)benzene (**21a**) with allylsilane **22a**. We also computed the alternative cyclization of **Int2e** *via* 5-*exo* pathway leading to **Int19** and ultimately to **40e**, or *via* 6-*endo* pathway leading to **Int20** and finally **36a**. Due to the high activation energy ($\Delta G^{\ddagger}$ =

18.0 kcal/mol), **Int19** is unlikely to be produced. However, the energy barrier for the generation of **Int20** is only 2.5 kcal/mol higher than that for formation of cyclopropyl gold(I) carbene **Int8e**. Thus, it is reasonable that we experimentally isolated byproducts of type **36a** in these transformations.

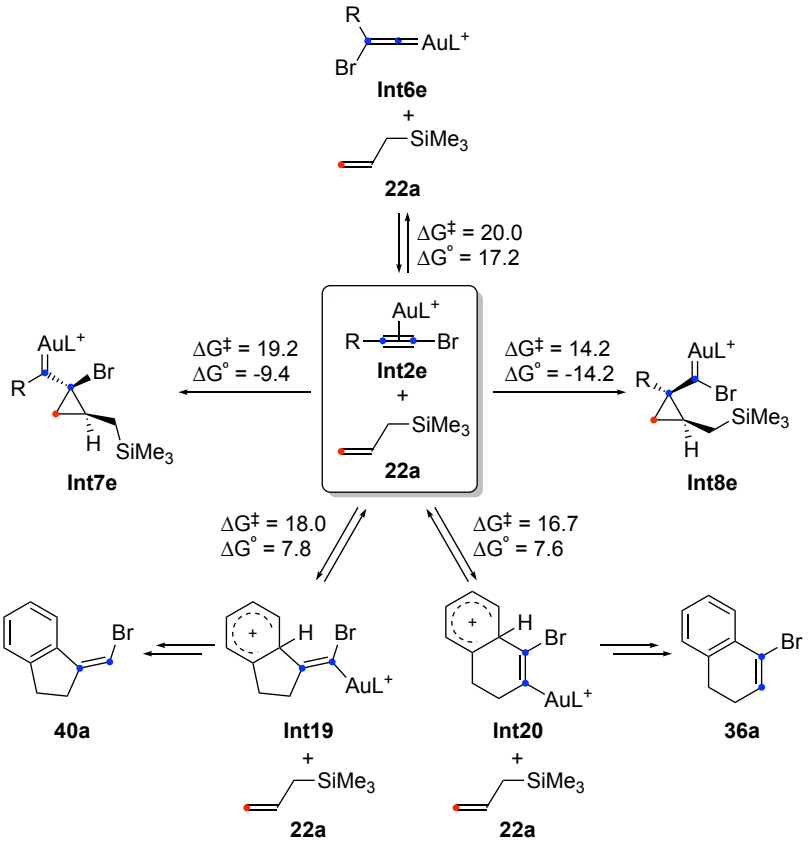

Scheme 3.35. Evolution of (η^2-alkyne)gold(I) complex **Int2e** (R = $(CH_2)_2$Ph. L = PMe_3. Free energies in kcal/mol).

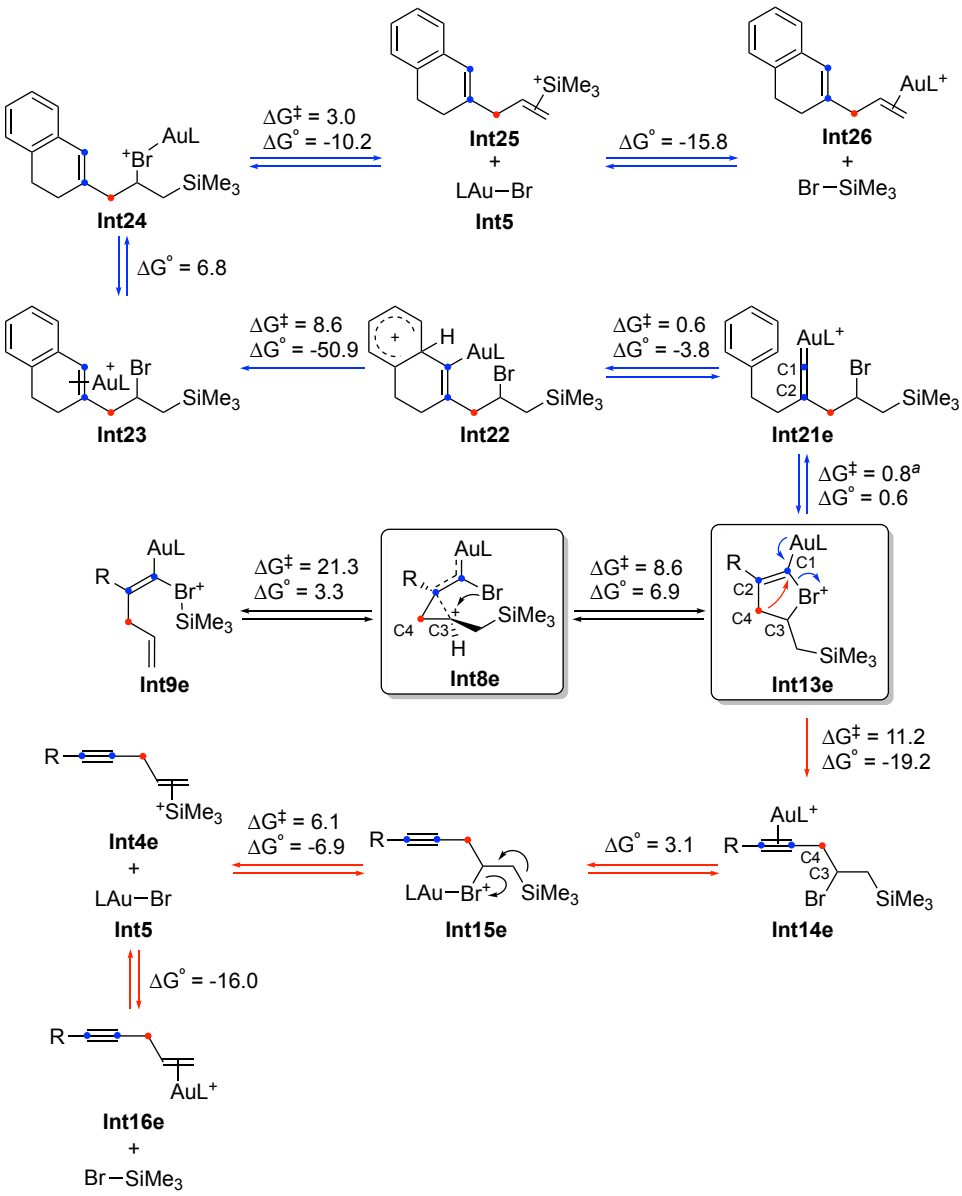

Scheme 3.36. Evolution of cyclopropyl gold(I) carbene **Int8e** (R = $(CH_2)_2$Ph. L = PMe_3. Free energies in kcal/mol. [a] The energy of this TS was calculated by freezing the distance of the bond C–Br which is cleaved in this step. The value of the distance was taken from the previously optimized geometry of the corresponding TS with R = *o*-MeC_6H_4).

Since cyclopropyl gold(I) carbene **Int8e** is preferentially formed on both thermodynamic and kinetic grounds, we then focused on investigating the evolution of this intermediate (Scheme 3.36). As in the case of the analogous reaction of (bromoethynyl)benzene (**21a**)

with allylsilane **22a**, the migration of the trimethylsilyl group to give **Int9e** is kinetically disfavored compared to the construction of the bridged bromonium intermediate **Int13e** ($\Delta G^{\ddagger}$ = 21.3 *vs.* 8.6 kcal/mol). This cyclic intermediate can then undergo 1,2-migration of the C4 carbon to give rise to (η^2-alkyne)gold(I) complex **Int14e**, which partakes in a gold-mediated TMSBr elimination *via* **Int15e** to deliver the skipped enyne **Int4e** and, finally, **Int16e**. Alternatively, **Int13e** can easily rearrange to produce gold vinylidene **Int21e**. Low energy cyclization of **Int21e** generates the Wheland-type intermediate **Int22**, which leads to dihydronaphthalene **Int23** upon highly exothermic 1,2-H shift. Subsequently, **Int23** undergoes a gold-promoted elimination of TMSBr *via* **Int24** to give **Int25**, and then **Int26**.

Analyzing the energy barriers, the rearrangement of **Int13e** into **Int14e** is more energetically costly than the formation of **Int23e** ($\Delta G^{\ddagger}$ = 11.2 *vs.* 8.6 kcal/mol). Hence, in agreement with the experimental result, skipped diene **35a** is obtained in this reaction, while the corresponding skipped enyne was not observed. Nevertheless, the difference in the activation energies of the reaction pathways of **Int13e** are not large, so reasonably modifications in the substitution pattern of the substrates can lead to different ratios of skipped dienes **35** and skipped enynes **38** (Tables 3.9-3.11).

In addition, we studied the mechanism of the hydroarylation of 1,4-enynes **38d-f** to form allylphenanthrenes **39d-f** (Table 3.12). In order to do so, we performed DFT calculations[168] on the hydroarylation of the simple substrate **Int12e** (Scheme 3.37). Based on precedents on the hydroarylation of related alkynes (see Introduction to **Chapter 3**), two possible mechanistic routes were considered. On one hand, alkyne **Int12e** could undergo a straightforward 6-*endo*-dig hydroarylation to give **Int27**, followed by 1,2-H shift to generate gold carbene **Int28**. Another exothermic 1,2-H shift could then provide allyl dihydronaphthalene **Int29**, which upon deauration would deliver products of type **39**. The alternative allyl migration from **Int28** to **Int32** is kinetically less favored than the formation of **Int29**.

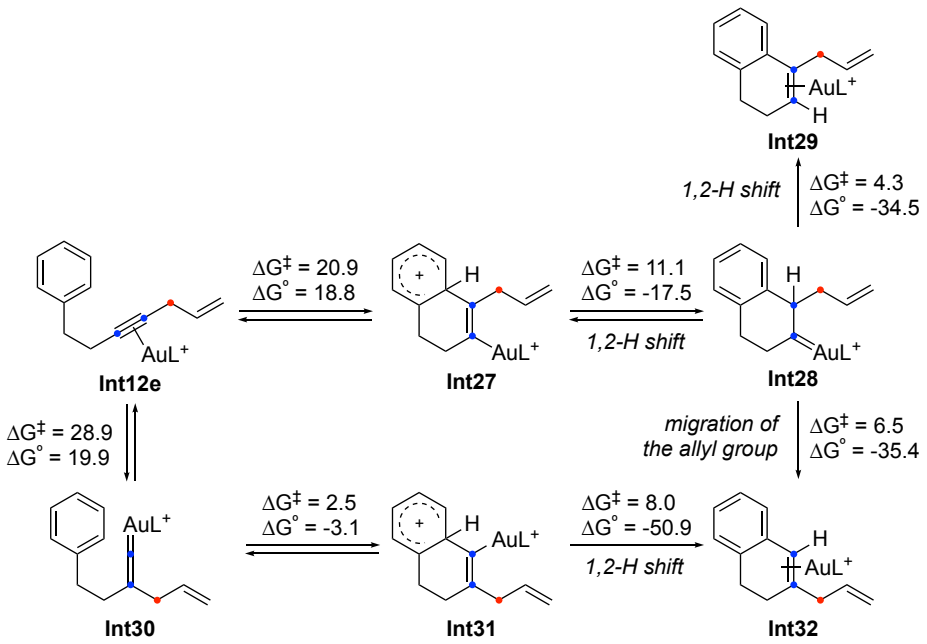

Scheme 3.37. Hydroarylation of alkyne **Int12e** (L = PMe_3. Free energies in kcal/mol).

On the other hand, **Int12e** could undergo allyl migration leading to gold vinylidene **Int30**, which cyclizes to give rise to **Int31**. Subsequently, highly exothermic rearomatization *via* 1,2-H shift would afford allyl dihydronaphthalene **Int32**, which upon deauration would deliver products of type **35**. It is worth noting that **Int29** and **Int32** are regioisomers that cannot be interconverted by allyl migration *via* **Int28**. Consequently, the hydroarylation of **Int12e** (corresponding to **38d-f**) to form **Int29** (corresponding to **39d-f**) most likely proceeds through the corresponding intermediates of type **Int27** and **Int28**.

Extension to the Intramolecular Reaction of 1-Bromo-1,6-enynes

We envisioned that the gold-catalyzed intermolecular reactions of bromoalkynes *via* bridged bromonium intermediates could be extended to the intramolecular cyclization of 1-bromo-1,6-enynes.

According to DFT computational studies[168] (Scheme 3.38), in the (η^2-alkyne)gold(I) complex **Int2f**, the activated alkyne could undergo the exothermic nucleophilic attack of

the alkene to form cyclopropyl gold(I) carbene **Int8f**. The subsequent attack of the bromide onto the stabilized benzylic carbocation C3 would generate the less stable bridged bromonium intermediate **Int13f**, which could undergo a low energy ring opening to give gold vinylidene species **Int21f.** The aryl moiety of **Int21f** could then trigger a low barrier Friedel-Crafts type reaction through **Int33**, which rearomatizes *via* highly exothermic 1,2-H shift to afford **Int34**. Although these calculations have been performed on the model system **Int2f**, our group recently evaluated the reactivity of related 1-bromo-1,6-enynes experimentally and polyaromatic products of type **42** were obtained.[167] Indeed, these products could arise from a straightforward aromatization by HBr elimination from **Int34**. Studies on these transformations are currently ongoing in our research group.

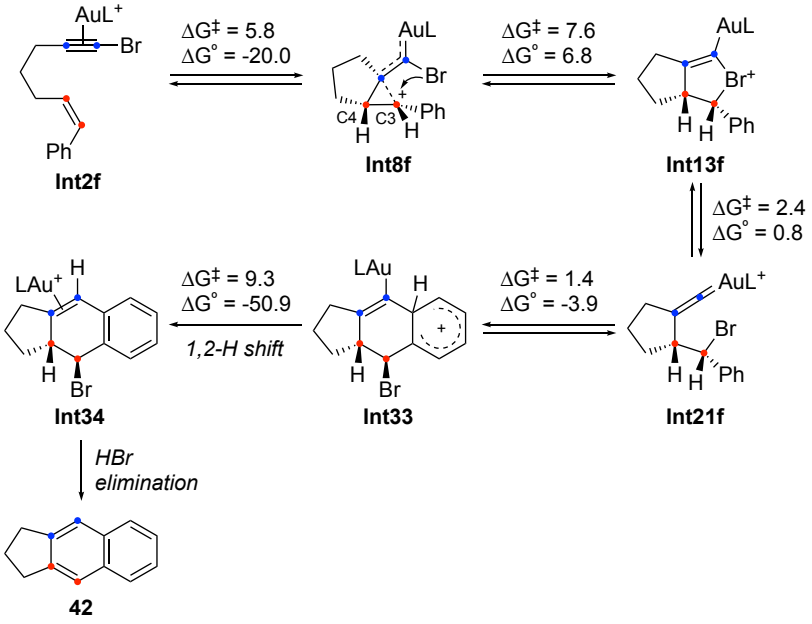

Scheme 3.38. Proposed mechanism for the cyclization of 1-bromo-1,6-enyne **Int2f** (L = PMe_3. Free energies in kcal/mol).

Towards the Enantioselective Synthesis of Skipped Enynes

The gold- or indium-catalyzed reaction of bromoalkynes with 3-substituted allylsilanes gives rise to 3-substituted 1,4-enynes containing a stereogenic center. Thus, we decided to

investigate the feasibility of an enantioselective version of this transformation. Gold complex **B** showed to be a more efficient catalyst than $InBr_3$ for the reaction of a broader range of substrates. Therefore, we first focused on the use of chiral gold complexes to mediate the enantioselective allylation.

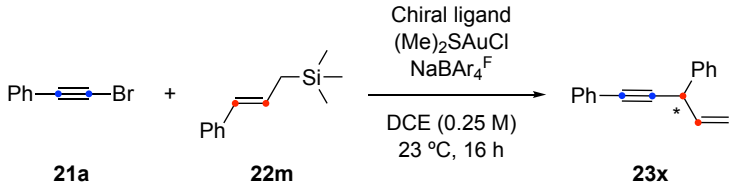

21a **22m** **23x**

Scheme 3.39. Towards the gold-catalyzed enantioselective reaction of **21a** with **22m**.

By means of high-throughput experimentation (HTE) techniques, we performed the screening of *ca.* 100 chiral ligands (Schemes 3.38-3.47) for the gold-catalyzed reaction of (bromoethynyl)benzene (**21a**) and cinnamyltrimethylsilane (**22m**) (Scheme 3.39). In this study, we prepared *in situ* the chiral gold complexes. Firstly, we dissolved the chiral ligand and (dimethylsulfide)gold(I) chloride in DCE to form the corresponding chiral gold chloride complex. After evaporation of the generated dimethyl sulfide, we added a solution of the substrates and the chloride abstractor to form the cationic gold complex, which can then initiate the catalytic cycle. In our initial screening, we employed $NaBAr_4^F$ as chloride abstractor, since the optimal gold catalyst **B** for the non-stereoselective reaction contained BAr_4^{F-} as counterion. When bidentate ligands were tested, the addition of 1 and 2 equivalents of $NaBAr_4^F$ with regards to the ligand were evaluated to abstract 1 and 2 chlorides anions from the digold dichloride complexes, respectively.

Schemes 3.40-3.49 show the enantioselectivities provided by each ligand, which were measured on the crude mixtures by chiral SFC. We examined the use of chiral biphenyl- and binaphthyl-based bisphosphine ligands (Scheme 3.40), bisphosphite ligands (Scheme 3.41), phosphoramidite ligands (Scheme 3.42), monophosphine ligands (Scheme 3.43), 1,1´-spirobiindane-based ligands (Scheme 3.44), other bisphosphine ligands (Scheme 3.45) and ferrocenyl based ligands (MandyPhos, Scheme 3.46; Walphos, Scheme 3.47; Josiphos, Scheme 3.48; others, Scheme 3.49). Unfortunately, the reaction did not proceed in various cases and we obtained maximum enantioselectivities of 26%. Only in the case of the spiro

bisphosphine ligand (*R*,*R*,*R*)-Tol-SKP (Scheme 3.45) we achieved a 37% ee. Moreover, low conversions were generally reached and the desired product was formed in up to 15% yield. Yields were determined by UPLC using 4,4′-dimethylbiphenyl as internal standard.

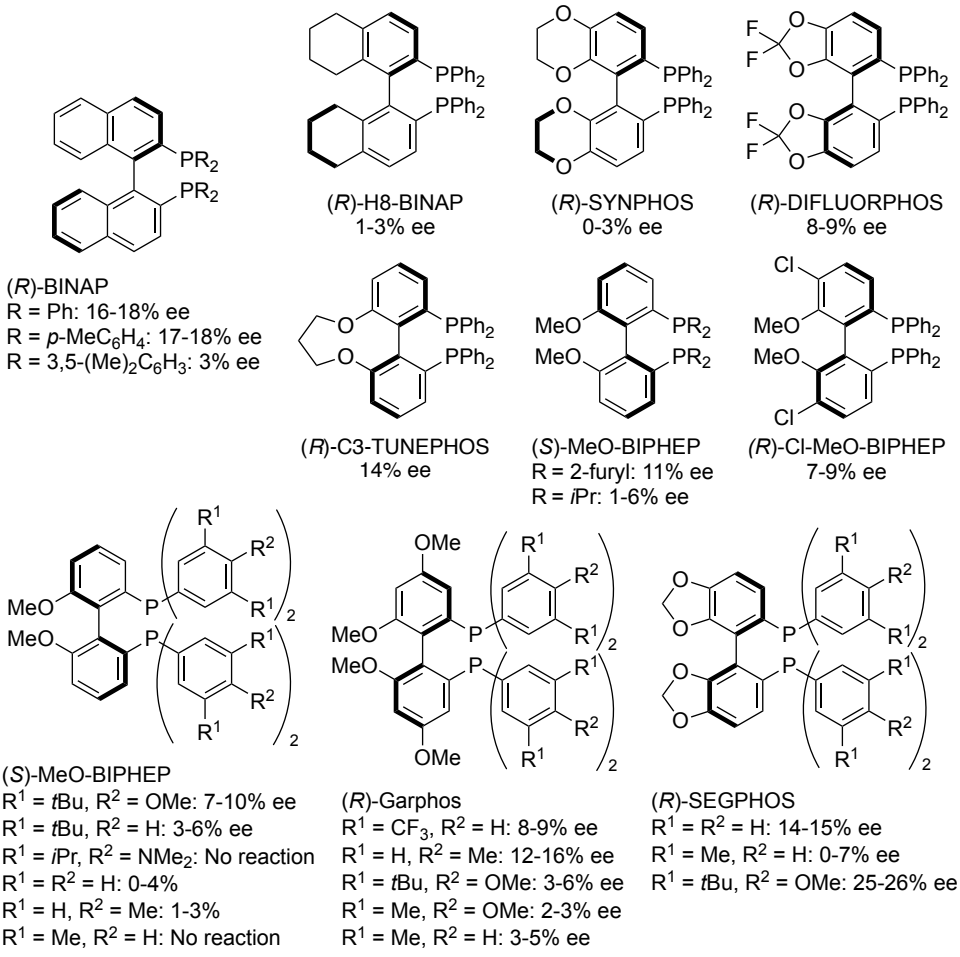

Scheme 3.40. Chiral biphenyl- and binaphthyl-based bisphosphine ligands tested.

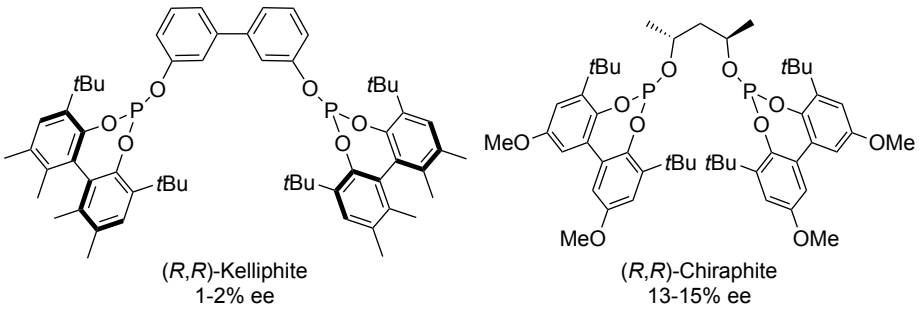

Scheme 3.41. Chiral bisphosphite ligands tested.

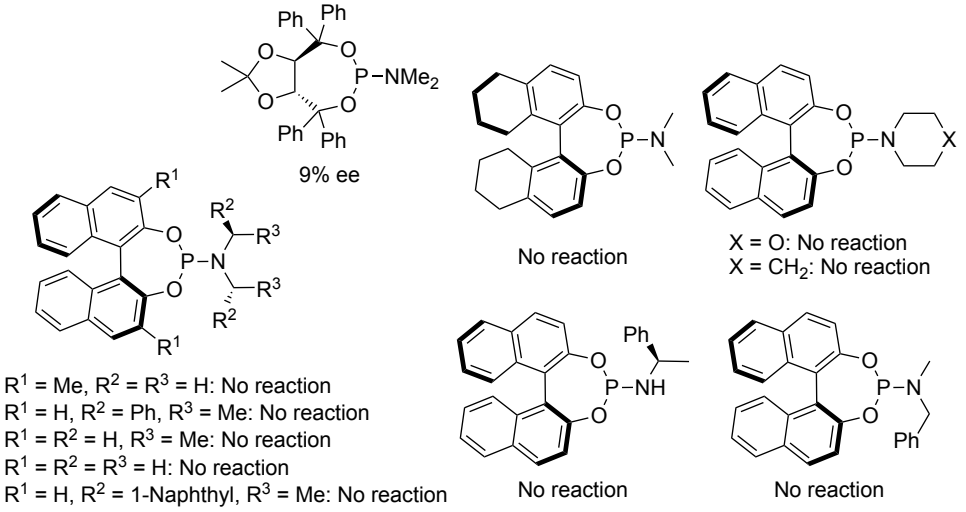

Scheme 3.42. Chiral phosphoramidite ligands tested (MonoPhos).

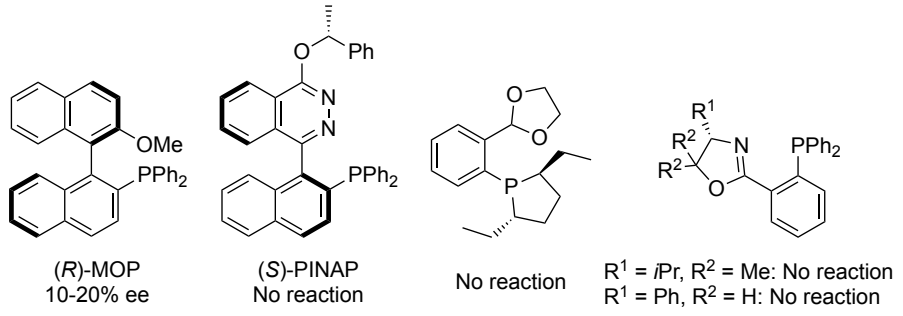

Scheme 3.43. Chiral monophosphine ligands tested.

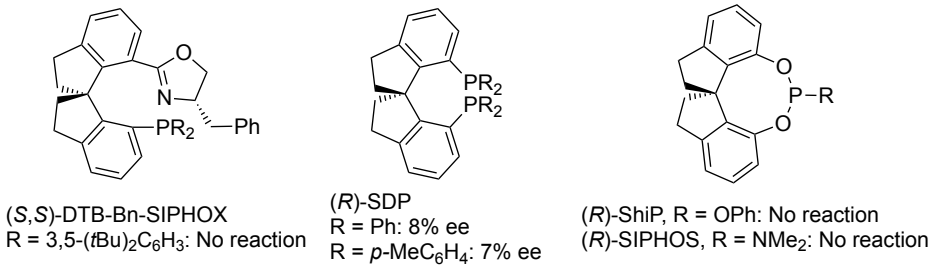

Scheme 3.44. Chiral 1,1´-spirobiindane based ligands tested.

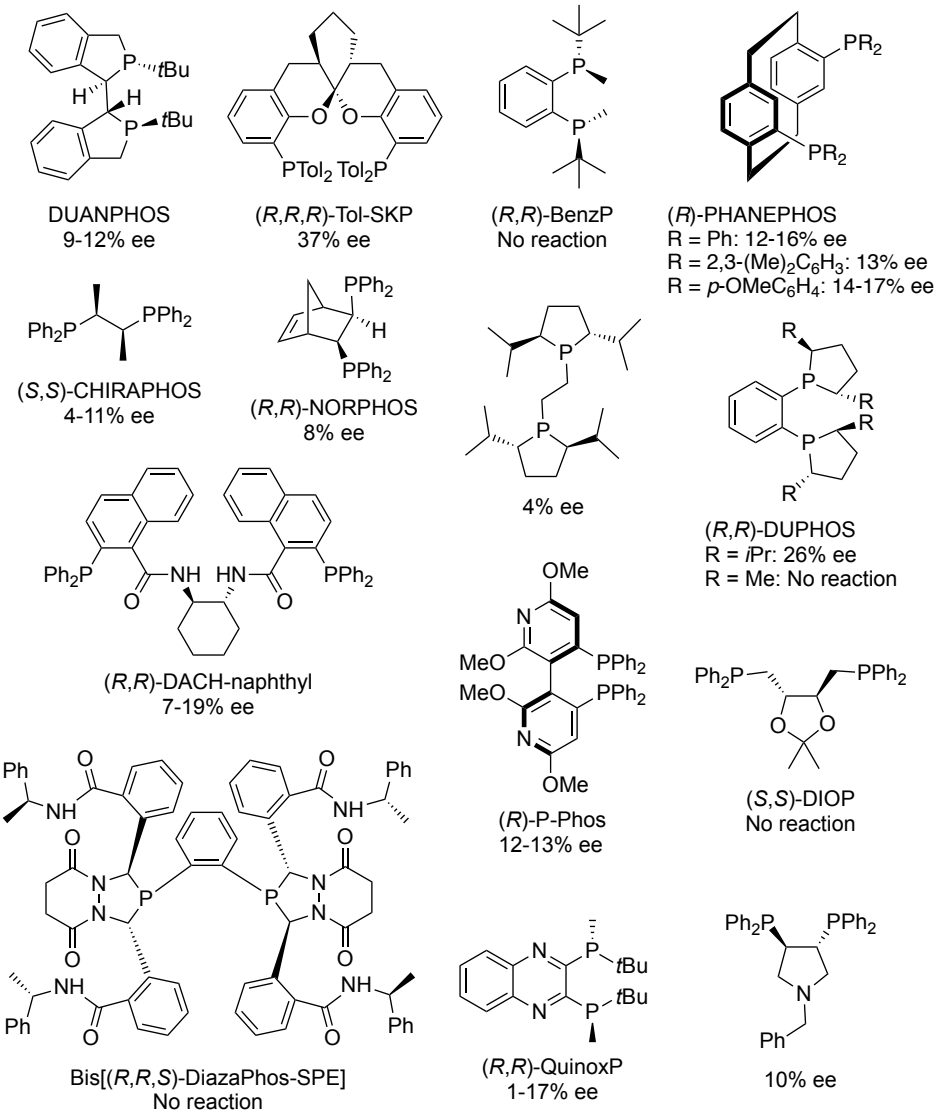

Scheme 3.45. Other chiral bisphosphine ligands tested.

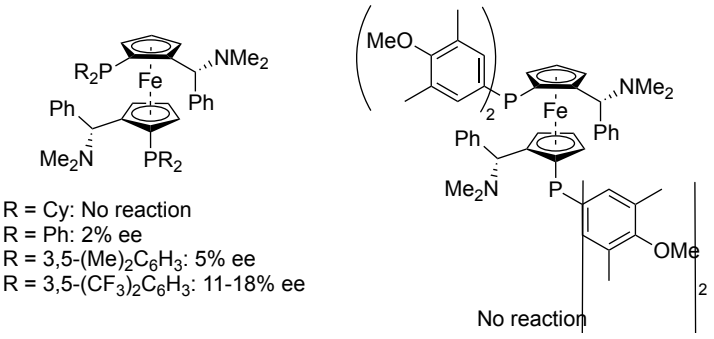

Scheme 3.46. Chiral ferrocenyl based ligands tested (MandyPhos).

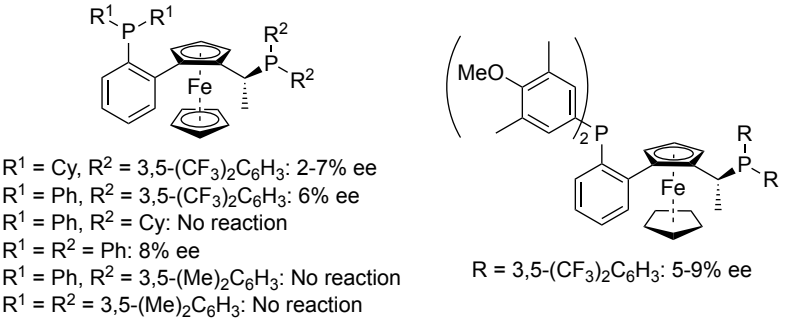

Scheme 3.47. Chiral ferrocenyl based ligands tested (Walphos).

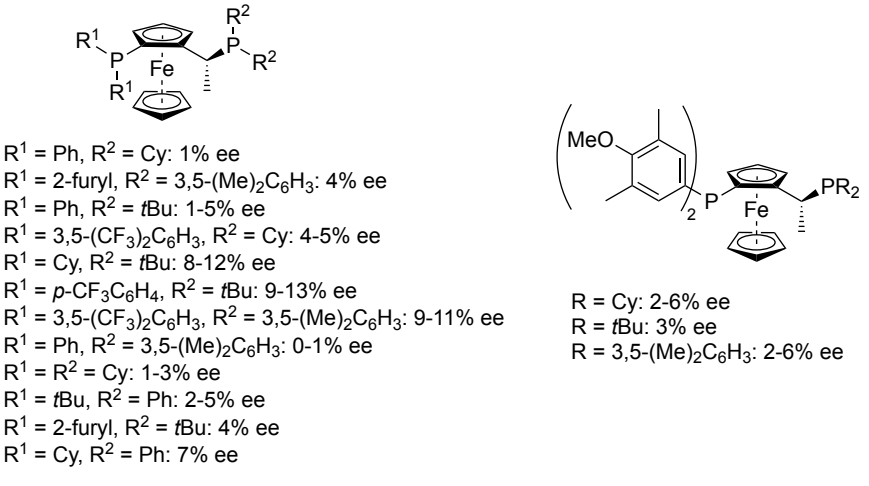

Scheme 3.48. Chiral ferrocenyl based ligands tested (Josiphos).

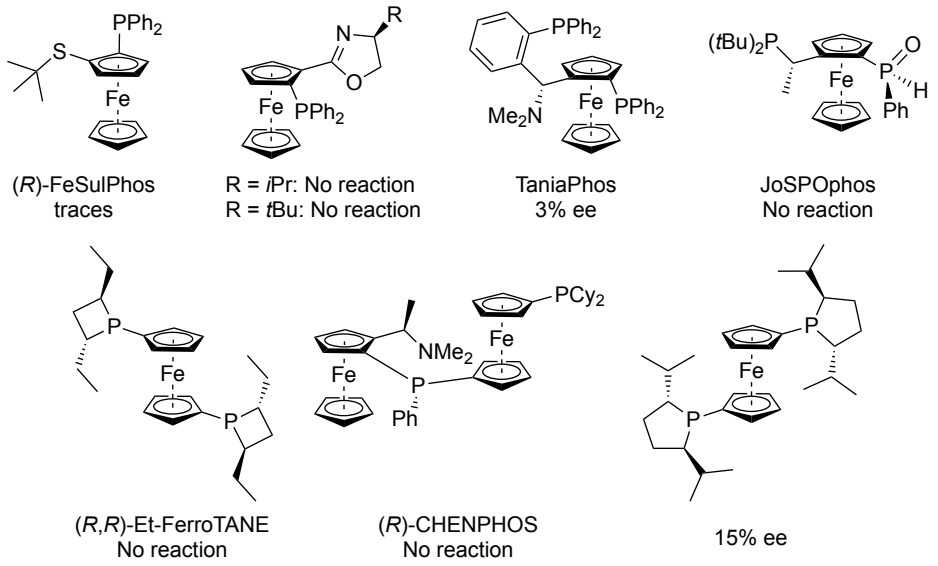

Scheme 3.49. Other chiral ferrocenyl based ligands tested.

In order to further optimize the reaction conditions, we selected the chiral ligands providing the highest enantioselectivities and we prepared the corresponding gold chloride complexes following the literature procedures (Scheme 3.50). As the (*R*,*R*,*R*)-Tol-SKP ligand seemed to be superior in terms of enantioselectivity, we also prepared the gold chloride complexes with the related (*R*,*R*,*R*)-Ph-SKP and (*R*,*R*,*R*)-Xyl-SKP ligands (Scheme 3.50). With this set of gold chloride complexes in hand, we screened different halide abstractors (Table 3.13)[164] and solvents (Table 3.14). However, only yields up to 10% and enantioselectivities up to 25% were obtained.

We repeated the reactions using the selected chiral (di)gold (di)chloride complexes and $NaBAr_4^F$ as halide scavenger at larger scale in order to isolate the desired product and measure the ee of the pure compound. We found that the yields remained lower than 10% and we obtained enantioselectivities similar to those obtained through HTE methods. Although only low yields and selectivities were achieved, this study on larger scale validated the HTE approach as a tool to identify the optimal chiral catalyst in this transformation.

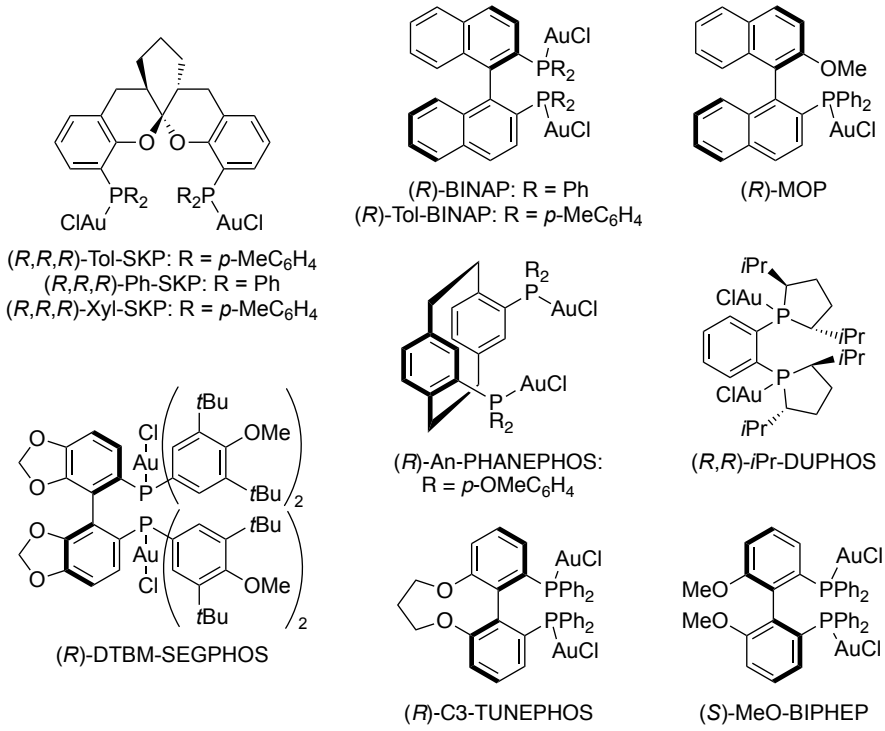

Scheme 3.50. Chiral (di)gold (di)chloride complexes selected for further optimization.

Table 3.13. Screening of chloride abstractors for the enantioselective reaction of **21a** with **22m**.[a]

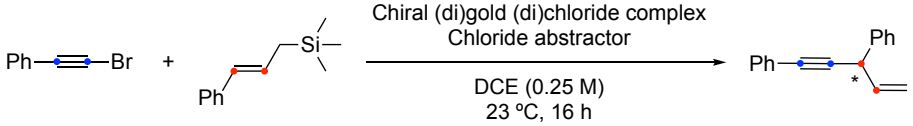

21a **22m** **23x**

Chloride abstractor	Chloride abstractor
Lithium tetrakis(pentafluorophenyl)borate	$Cu(OTf)_2$
$AgNTf_2$	$Cu(NCMe)_4BF_4$
$AgBF_4$	$Cu(NCMe)_4PF_6$
$AgSbF_6$	$NaSbF_6$
$AgPF_6$	$NaBF_4$
AgOTf	$NaPF_6$

[a] See the chiral (di)gold (di)chloride complexes tested in Scheme 3.50.

Table 3.14. Screening of solvents for the enantioselective reaction **21a** with **22m**. [a]

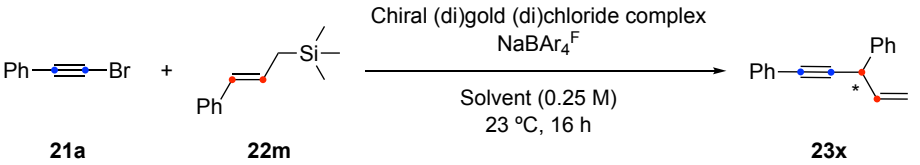

21a **22m** **23x**

Solvents	Solvents	Solvents
CH_2Cl_2	PhCl	Pentane
$CHCl_3$	$PhCF_3$	Diglyme
Toluene	Xylene	Butanone
THF	Et_2O	Perfluorohexane

[a] See the chiral (di)gold (di)chloride complexes tested in Scheme 3.50.

In addition, we evaluated the generation of the cationic gold complexes by mixing the chiral ligands **L*** with the previously prepared gold sources **M1-3** (Scheme 3.51).[164] Nevertheless, the reaction did not take place in most of the cases, and very poor yields and enantioselectivities were achieved otherwise.

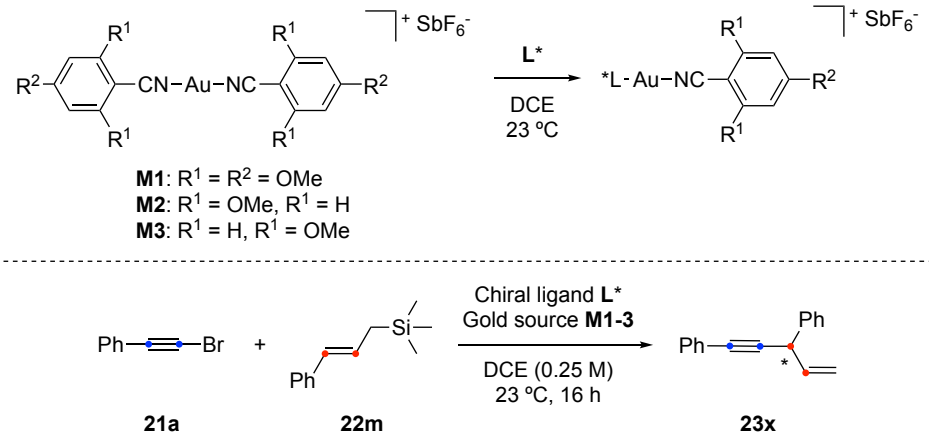

Scheme 3.51. Generation of chiral gold complexes using gold sources **M1-3.**

In view of the unpromising results in the gold-catalyzed enantioselective transformation, we decided to turn our attention to the use of chiral indium catalysts. Following literature

procedures to prepare indium complexes *in situ*,[173] we carried out a screening of *ca.* 60 chiral ligands (Scheme 3.52),[164] including chiral phosphoric acids, mono and bisphosphines (also ferrocenyl based ligands: JosiPhos, MandyPhos and Walphos), phosphoramidites, diols, diamines, aminols, and oxazolines (such as Pybox ligands). In the vast majority of the cases, the reaction did not take place. The desired product was only formed as a racemic mixture using few chiral diol ligands. By adding halide scavengers ($AgNTf_2$, $AgBF_4$, $AgSbF_6$, $AgPF_6$, AgOTf, $Cu(OTf)_2$, $Cu(NCMe)_4BF_4$ or $Cu(NCMe)_4BF_4$) or changing the indium(III) salt (InI_3 or $In(OTf)_3$), neither the conversion nor the enantioselectivity improved.

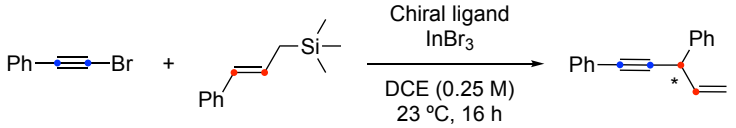

21a **22m** **23x**

Scheme 3.52. Towards the indium-catalyzed enantioselective reaction of **21a** and **22m**.

Overall, chiral gold catalysts shown in Scheme 3.50 provided better enantioselectivities than chiral indium catalysts. In order to increase the yield and induce higher enantioselectivity, the ligands of those gold complexes could be modified electronically and sterically. Moreover, the corresponding cationic gold complexes could be prepared and tested to ensure that the otherwise used chloride abstractor has not a detrimental effect on the reaction. Furthermore, 3-substituted allylsilanes different from **22m** should be evaluated in the asymmetric reaction with bromoalkynes.

173. (a) Michelet, B.; Colard-Itté, J.-R.; Thiery, G.; Guillot, R.; Bour, C.; Gandon, V. *Chem. Commun.* **2015**, *51*, 7401−7404. (b) Surendra, K.; Corey, E. J. *J. Am. Chem. Soc.* **2014**, *136*, 10918−10920. (c) Lv, J.; Zhang, L.; Hu, S.; Cheng, J.-P.; Luo, S. *Chem. Eur. J.* **2011**, *18*, 799−803. (d) Lu, J.; Ji, S.-J.; Teo, Y.-C.; Loh, T.-P. *Org. Lett.* **2005**, 7, 159–161.

Conclusions

We discovered that the gold-catalyzed intermolecular reactions of bromoalkynes with allylsilanes give rise to skipped enynes *via* a formal cross-coupling process or skipped dienes *via* allylation/cyclization cascade (Scheme 3.53). In addition, we found that the reaction of bromoalkynes with allenylsilanes yields highly substituted 1,3-enynes. Interestingly, simple $InBr_3$ is also an efficient catalyst for some of these transformations.

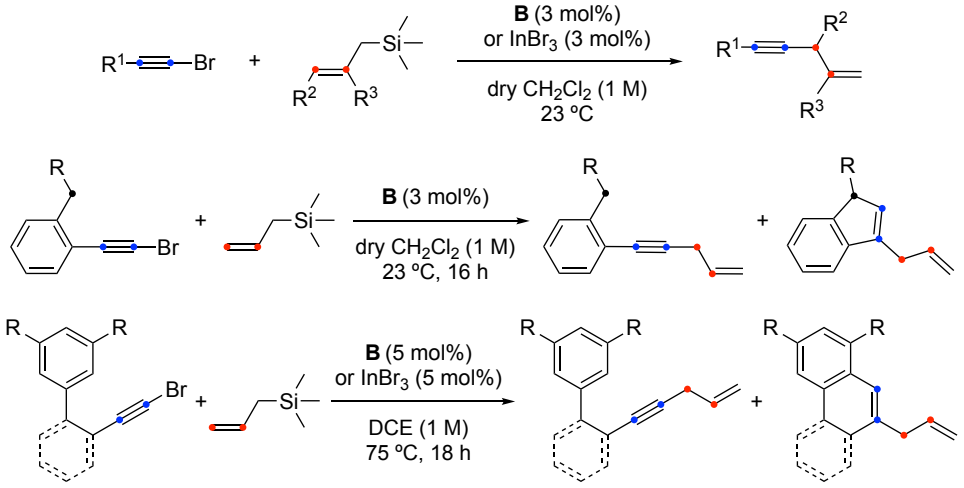

Scheme 3.53. Gold- and indium-catalyzed reactions of bromoalkynes with allylsilanes to form skipped enynes and dienes.

Based on experimental mechanistic studies and DFT calculations, we proposed that the key intermediates are the cyclopropyl gold(I) carbenes and unprecedented bridged bromonium intermediates (Scheme 3.54). In accordance with the conclusions of **Chapter 1**, in these transformations the gold carbene moiety is formed preferentially α to the electron-withdrawing bromine and β to the electron-donating substituent of the initial alkyne. The cyclopropyl gold(I) carbenes evolve through bromide migration to form cyclic bromonium intermediates, which undergo ring opening to afford either gold-alkyne π-complexes leading to 1,4-enynes or gold vinylidenes. Depending on the substituents of the gold vinylidenes, these intermediates may take part in a hydroarylation reaction to deliver skipped dienes. Moreover, in the reaction of *o*-alkyl substituted (bromoethynyl)benzenes, a cyclization takes place presumably *via* a C(sp^3)–H insertion into the gold vinylidene intermediate leading to allyl indenes.

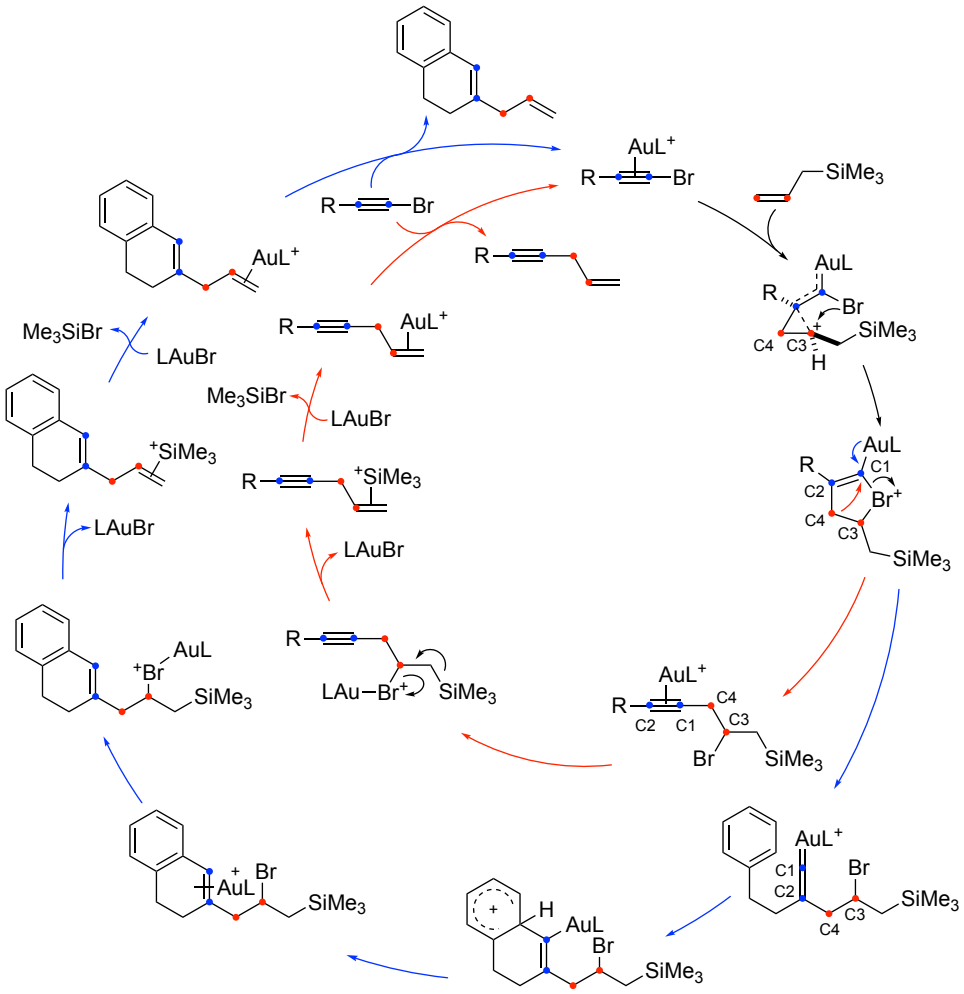

Scheme 3.54. Catalytic cycle of the gold(I)-catalyzed reaction of bromoalkynes with allylsilanes.

As an extension, we envision that the bromide migration *via* bridged bromonium intermediates might occur as well in intramolecular reactions of 1-bromo-1,6-enynes, thus providing new modes of cyclizations and rapid access to complex polycycles.

Finally, our preliminary studies towards developing a gold- or indium-catalyzed asymmetric synthesis of skipped enynes resulted in generally poor reaction yields. However, enantiomeric excesses of up to 37% ee were measured and current efforts aim at improving these selectivities.

Experimental Part

General Information

The general information is provided in the Experimental Part of the **Chapter 1**. All reagents were used as purchased, with no further purification. The terminal alkynes,[128] cinnamyltrimethylsilane,[174] (*E*)-trimethyl(pent-2-en-1-yl)silane[175] and complexes **K1,2**[44b] were synthesized according to the literature procedure. The NMR data were in agreement with the ones reported in the literature.

Synthetic Procedures and Characterization Data

General Procedure for the Preparation of Bromoalkynes

Bromoalkynes were synthesized following the literature procedure.[87]

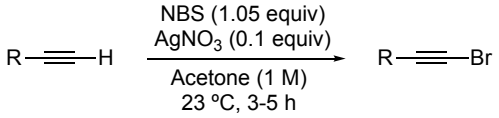

The alkyne (1 equiv) was dissolved in acetone (1 M). Silver nitrate (0.1 equiv) was added, followed by *N*-bromosuccinimide (1.05 equiv). The reaction mixture was stirred at 23 °C with exclusion of light for 3-5 h. Then, the reaction mixture was filtered through a Celite™ plug washing with CH_2Cl_2, concentrated under reduced pressure at room temperature and adsorbed on silica gel. The residue was purified by silica gel column chromatography (eluent = pentane) to afford the corresponding bromoalkyne.

9-(Bromoethynyl)phenanthrene

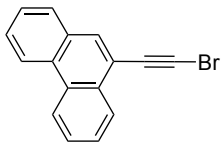

The title compound (154 mg, 46%) was synthesized according to the general procedure starting from 9-ethynylphenanthrene (0.225 mL, 1.19 mmol).

174. Selander, N.; Paasch, J. R.; Szabó K. *J. Am. Chem. Soc.* **2011**, *133*, 409–411.
175. Terwilliger, D. W.; Trauner, D. *J. Am. Chem. Soc.* **2018**, *140*, 2748–2751.

^{1}H NMR (400 MHz, $CDCl_3$) δ 8.72 – 8.61 (m, 2H), 8.44 – 8.37 (m, 1H), 8.02 (s, 1H), 7.85 (dd, *J* = 7.9, 1.5 Hz, 1H), 7.73 – 7.64 (m, 3H), 7.60 (ddd, *J* = 8.1, 7.0, 1.2 Hz, 1H). **^{13}C NMR** (101 MHz, $CDCl_3$) δ 132.8, 131.2, 131.0, 130.4, 130.0, 128.5, 127.7, 127.2, 127.2, 127.0, 126.7, 122.8, 122.6, 119.1, 78.6, 53.6. **HRMS** (APCI) *m/z* calculated for $C_{16}H_{10}Br^+$ $[M+H]^+$: 280.9960, found: 280.9960.

2-(Bromoethynyl)-1,1'-biphenyl

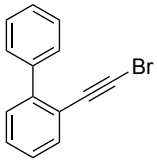

The title compound (yellow oil, 346 mg, 86%) was synthesized according to the general procedure starting from 2-ethynyl-1,1'-biphenyl (278 mg, 1.56 mmol).

^{1}H NMR (400 MHz, $CDCl_3$) δ 7.60 – 7.54 (m, 3H), 7.47 – 7.35 (m, 5H), 7.29 (ddd, *J* = 7.7, 6.3, 2.5 Hz, 1H). **^{13}C NMR** (101 MHz, $CDCl_3$) δ 144.4, 140.1, 133.7, 129.5, 129.1 (2C), 128.9, 128.0 (2C), 127.5, 127.0, 121.0, 79.6, 52.2. **HRMS** (APCI) *m/z* calculated for $C_{14}H_{10}Br^+$ $[M+H]^+$: 256.9960, found: 256.9951.

(5-Bromopent-4-yn-2-yl)benzene

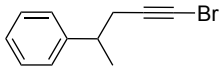

The title compound (colorless oil, 570 mg, 71%) was synthesized according to the general procedure starting from pent-4-yn-2-ylbenzene (518 mg, 3.59 mmol).

^{1}H NMR (400 MHz, $CDCl_3$) δ 7.35 – 7.29 (m, 2H), 7.25 – 7.16 (m, 3H), 2.98 (h, *J* = 7.0 Hz, 1H), 2.51 (dd, *J* = 16.6, 6.0 Hz, 1H), 2.41 (dd, *J* = 16.6, 8.0 Hz, 1H), 1.37 (d, *J* = 7.0 Hz, 3H). **^{13}C NMR** (101 MHz, $CDCl_3$) δ 145.4, 128.4 (2C), 126.8 (2C), 126.5, 79.0, 39.0, 38.8, 28.8, 20.7. **HRMS** (APCI) *m/z* calculated for $C_{11}H_{12}Br^+$ $[M+H]^+$: 223.0117, found: 223.0116.

2-(Bromoethynyl)-3',5'-bis(trifluoromethyl)-1,1'-biphenyl

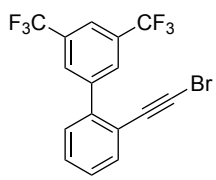

The title compound (white solid, 1 g) was synthesized according to the general procedure starting from 2-ethynyl-3',5'-bis(trifluoromethyl)-1,1'-biphenyl.

M.p. 56-61 ºC. **^{1}H NMR** (400 MHz, $CDCl_3$) δ 8.07 (s, 2H), 7.90 (s, 1H), 7.62 (ddd, *J* = 7.6, 1.5, 0.6 Hz, 1H), 7.52 – 7.36 (m, 3H). **^{13}C NMR** (101 MHz, $CDCl_3$) δ 142.0, 141.3, 134.0, 131.6 (q, *J* = 33.3 Hz, 2C), 129.6 (2C), 129.5, 129.4, 128.7, 123.5 (q, *J* = 272.6 Hz, 2C), 121.6 – 121.2 (m), 121.4, 78.7, 54.5. **^{19}F**

NMR (376 MHz, $CDCl_3$) δ -62.88. **HRMS** (APCI) *m/z* calculated for $C_{16}H_7BrF_6^{+\cdot}$ $[M]^{+\cdot}$: 391.9630, found: 391.9631.

2-(Bromoethynyl)-1,1'-biphenyl-2',3',4',5',6'-d$_5$

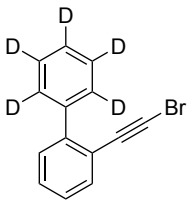

The title compound (yellow oil, 800 mg) was synthesized according to the general procedure starting from 2-(bromoethynyl)-1,1'-biphenyl-2',3',4',5',6'-*d*$_5$.

^{1}H NMR (400 MHz, $CDCl_3$) δ 7.59 (ddd, *J* = 7.7, 1.6, 0.9 Hz, 1H), 7.51 – 7.38 (m, 2H), 7.31 (ddd, *J* = 7.7, 5.8, 3.0 Hz, 1H). **^{13}C NMR** (101 MHz, $CDCl_3$) δ 144.5, 140.1, 133.8, 129.7, 129.3 (2C), 129.0, 128.2 (2C), 127.7, 127.1, 121.1, 79.8, 52.3. **HRMS** (APCI) *m/z* calculated for $C_{14}H_4BrD_5^+$ $[M]^{+\cdot}$: 261.0196, found: 261.0189.

General Procedure for the Synthesis of 1,4-Enynes 23

The bromoalkyne (0.2 mmol, 1 equiv) was dissolved in dry CH_2Cl_2 (0.2 mL, 1 M). The allylsilane (0.4 mmol, 2 equiv) was added, followed by the catalyst (3 mol%, **method A**: 9 mg of [(*t*BuXPhos)AuNCMe]BAr_4^F or **method B**: 2 mg of $InBr_3$). The resulting mixture was stirred at 23 ºC for 18 h (otherwise stated). The reaction was monitored by TLC or GC-MS. The crude was directly subjected to silica gel column chromatography (eluent = pentane, otherwise stated) to obtain the pure 1,4-enyne.

Pent-4-en-1-yn-1-ylbenzene

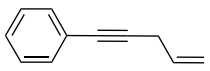

The title compound (colorless oil, method A: 22 mg, 77%; method B: 23 mg, 81%) was synthesized according to the general procedure starting from (bromoethynyl)benzene (36 mg, 0.2 mmol) and allyltrimethylsilane (64 µL, 0.4 mmol).

^{1}H NMR (500 MHz, $CDCl_3$) δ 7.47 – 7.38 (m, 2H), 7.32 – 7.23 (m, 3H), 5.98 – 5.81 (m, 1H), 5.46 – 5.35 (m, 1H), 5.22 – 5.12 (m, 1H), 3.24 – 3.15 (m, 1H). **^{13}C NMR** (101 MHz, $CDCl_3$) δ 132.4, 131.6 (2C), 128.2 (2C), 127.7, 123.7, 116.2, 86.5, 82.9, 23.7. The NMR data match with those reported in the literature.[157b]

1-Methoxy-4-(pent-4-en-1-yn-1-yl)benzene

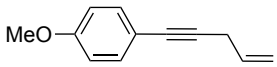

The title compound (yellow oil, method A: 23 mg, 67%; method B: 22 mg, 64%) was synthesized according to the general procedure starting from 1-(bromoethynyl)-4-methoxybenzene (42 mg, 0.2 mmol) and allyltrimethylsilane (64 μL, 0.4 mmol).

^{1}H NMR (500 MHz, $CDCl_3$) δ 7.40 – 7.33 (m, 2H), 6.87 – 6.79 (m, 2H), 5.95 – 5.85 (m, 1H), 5.40 (dq, *J* = 16.9, 1.8 Hz, 1H), 5.16 (dq, *J* = 10.0, 1.7 Hz, 1H), 3.80 (s, 3H), 3.18 (dt, *J* = 5.3, 1.8 Hz, 2H). **^{13}C NMR** (126 MHz, $CDCl_3$) δ 159.2, 132.9 (2C), 132.7, 116.1, 115.8, 113.8 (2C), 84.9, 82.6, 55.2, 23.7. The NMR data match with those reported in the literature.[157b]

4-(Pent-4-en-1-yn-1-yl)-1,1'-biphenyl

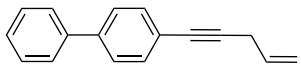

The title compound (sticky yellow oil, method A: 27 mg, 62%; method B: 35 mg, 80%) was synthesized according to the general procedure starting from 4-(bromoethynyl)-1,1'-biphenyl (51 mg, 0.2 mmol) and allyltrimethylsilane (64 μL, 0.4 mmol).

^{1}H NMR (300 MHz, $CDCl_3$) δ 7.66 – 7.31 (m, 9H), 6.04 – 5.84 (m, 1H), 5.52 – 5.38 (m, 1H), 5.26 – 5.15 (m, 1H), 3.28 – 3.19 (m, 2H). ^{13}C NMR (75 MHz, $CDCl_3$) δ 140.5, 140.4, 132.4, 132.0 (2C), 128.8 (2C), 127.5, 127.0 (2C), 126.9 (2C), 122.6, 116.3, 87.2, 82.7, 23.8. **HRMS** (APCI) *m/z* calculated for $C_{17}H_{15}^+$ $[M+H]^+$: 219.1168, found: 219.1160.

1-(*tert*-Butyl)-4-(pent-4-en-1-yn-1-yl)benzene

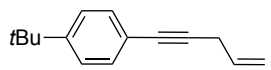

The title compound (yellow oil, method A: 28 mg, 71%; method B: 21 mg, 53%) was synthesized according to the general procedure starting from 1-(bromoethynyl)-4-(*tert*-butyl)benzene (47 mg, 0.2 mmol) and allyltrimethylsilane (64 μL, 0.4 mmol).

^{1}H NMR (400 MHz, $CDCl_3$) δ 7.40 – 7.35 (m, 2H), 7.34 – 7.29 (m, 2H), 5.97 – 5.85 (m, 1H), 5.42 (dq, *J* = 17.0, 1.7 Hz, 1H), 5.17 (dq, *J* = 10.0, 1.7 Hz, 1H), 3.20 (dt, *J* = 5.2, 1.9 Hz, 2H), 1.32 (s, 9H). **^{13}C NMR** (75 MHz, $CDCl_3$) δ 150.9, 132.6, 131.3 (2C), 125.2 (2C), 120.7, 116.1, 85.7, 82.9, 34.7, 31.2 (3C), 23.7. The NMR data match with those reported in the literature.[157b]

1-Bromo-4-(pent-4-en-1-yn-1-yl)benzene

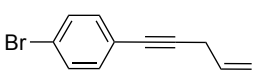

The title compound (yellow oil, method A: 27 mg, 60%; method B: 32 mg, 73%) was synthesized according to the general procedure starting from 1-bromo-4-(bromoethynyl)benzene (52 mg, 0.2 mmol) and allyltrimethylsilane (64 µL, 0.4 mmol). The reaction was carried out at 50 ºC for 16 h in a sealed vial.

^{1}H NMR (500 MHz, $CDCl_3$) δ 7.45 – 7.39 (m, 2H), 7.31 – 7.25 (m, 2H), 5.89 (ddt, *J* = 17.0, 10.0, 5.3 Hz, 1H), 5.39 (dq, *J* = 17.0, 1.8 Hz, 1H), 5.17 (dq, *J* = 10.0, 1.7 Hz, 1H), 3.18 (dt, *J* = 5.3, 1.8 Hz, 2H). **^{13}C NMR** (126 MHz, $CDCl_3$) δ 133.2 (2C), 132.3, 131.6 (2C), 122.8, 122.0, 116.6 (2C), 88.0, 82.0, 23.9. The NMR data match with those reported in the literature.[176]

1-(Pent-4-en-1-yn-1-yl)-4-(trifluoromethyl)benzene

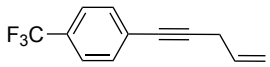

The title compound (yellow oil, method A: 26 mg, 62%; method B: 31 mg, 74%) was synthesized according to the general procedure starting from 1-(bromoethynyl)-4-(trifluoromethyl)benzene (49.8 mg, 0.2 mmol) and allyltrimethylsilane (64 µL, 0.4 mmol). The reaction was carried out at at 50 ºC for 40 h.

^{1}H NMR (500 MHz, $CDCl_3$) δ 7.55 (d, *J* = 8.5 Hz, 2H), 7.52 (d, *J* = 8.5 Hz, 2H), 5.90 (ddt, *J* = 17.0, 10.3, 5.3 Hz, 1H), 5.40 (dd, *J* = 17.0, 1.7 Hz, 1H), 5.19 (dq, *J* = 10.0, 1.6 Hz, 1H), 3.22 (dt, *J* = 5.3, 1.8 Hz, 2H). **^{13}C NMR** (126 MHz, $CDCl_3$) δ 132.1, 132.0, 129.7 (q, *J* = 32.6 Hz), 127.7, 125.3 (q, *J* = 3.8 Hz), 124.1 (q, *J* = 272 Hz) 116.7, 89.6, 81.8, 23.9. **^{19}F NMR** (376 MHz, $CDCl_3$) δ -62.88. **HRMS** (APCI) *m/z* calculated for $C_{12}H_{10}F_3^+$ $[M+H]^+$: 211.0729, found: 211.0724.

1-Methyl-2-(pent-4-en-1-yn-1-yl)benzene and 3-allyl-1H-indene

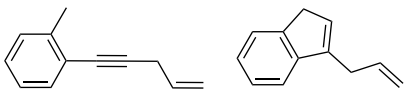

The title compounds were synthesized according to the general procedure (methods A and B) starting from 1-(bromoethynyl)-2-methylbenzene (39 mg, 0.2 mmol) and allyltrimethylsilane (64 µL, 0.4 mmol).

176. Katritzky, A. R.; Abdel-Fattah, A. A. A.; Wang, M. *J. Org. Chem.* **2002**, *67*, 7526–7529.

1-Methyl-2-(pent-4-en-1-yn-1-yl)benzene was obtained as a yellow oil (method A: 24 mg, 77%; method B: 22 mg, 70%). **^{1}H NMR** (500 MHz, $CDCl_3$) δ 7.40 (dt, *J* = 7.4, 1.1 Hz, 1H), 7.23 – 7.16 (m, 2H), 7.15 – 7.08 (m, 1H), 5.93 (ddt, *J* = 16.9, 10.2, 5.2 Hz, 1H), 5.45 (dq, *J* = 17.0, 1.8 Hz, 1H), 5.18 (dq, *J* = 10.0, 1.7 Hz, 1H), 3.25 (dt, *J* = 5.2, 1.8 Hz, 2H), 2.44 (s, 3H). **^{13}C NMR** (126 MHz, $CDCl_3$) δ 140.1, 132.8, 132.1, 129.5, 127.9, 125.6, 123.6, 116.3, 90.6, 82.0, 24.0, 20.9. The NMR data match with those reported in the literature.[157b]

3-Allyl-1H-indene was obtained by method A upon quenching the reaction with triethylamine. This product was isolated as a colorless oil in mixture 1:0.10 with 1-methyl-2-(pent-4-en-1-yn-1-yl)benzene (method A: 7.5 mg, 24% isolated yield, 20% yield according to ^{1}H NMR using 2-bromomesitylene as internal standard). **^{1}H NMR** (500 MHz, Chloroform-d) δ 7.46 (dt, J = 7.3, 1.0 Hz, 1H), 7.37 (dt, J = 7.5, 1.0 Hz, 1H), 7.29 (tdd, J = 7.5, 1.2, 0.6 Hz, 1H), 7.20 (td, J = 7.4, 1.2 Hz, 1H), 6.25 (t, J = 1.6 Hz, 1H), 6.05 (ddt, J = 16.6, 10.1, 6.5 Hz, 1H), 5.19 (dq, J = 17.1, 1.6 Hz, 1H), 5.14 – 5.09 (m, 1H), 3.38 – 3.30 (m, 4H). **^{13}C NMR** (126 MHz, Chloroform-d) δ 144.6, 142.6, 139.7, 135.8, 129.1, 126.1, 124.7, 123.9, 119.3, 116.4, 37.9, 32.6. The NMR data match with those reported in the literature.[177]

1-Fluoro-2-(pent-4-en-1-yn-1-yl)benzene

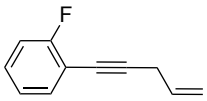

The title compound (colorless oil, method A: 16 mg, 50%; method B: 25 mg, 78%) was synthesized according to the general procedure starting from 1-(bromoethynyl)-2-fluorobenzene (40 mg, 0.2 mmol) and allyltrimethylsilane (64 μL, 0.4 mmol). The reaction time was 72 h.

^{1}H NMR (400 MHz, $CDCl_3$) δ 7.46 – 7.38 (m, 1H), 7.33 – 7.20 (m, 1H), 7.11 – 6.99 (m, 2H), 5.91 (ddt, *J* = 17.0, 10.2, 5.2 Hz, 1H), 5.44 (dq, *J* = 17.0, 1.8 Hz, 1H), 5.19 (dq, *J* = 10.0, 1.7 Hz, 1H), 3.24 (dt, *J* = 5.1, 1.7 Hz, 2H). **^{13}C NMR** (75 MHz, $CDCl_3$) δ 164.3 (d, *J* (^{13}C-^{19}F) = 250.6 Hz), 133.5 (d, *J* (^{13}C-^{19}F) = 1.6 Hz), 132.0, 129.3 (d, *J* (^{13}C-^{19}F) = 7.9 Hz), 123.8 (d, *J* (^{13}C-^{19}F) = 3.7 Hz), 116.4, 115.4 (d, *J* (^{13}C-^{19}F) = 21.0 Hz), 112.15 (d, *J* (^{13}C-^{19}F) = 15.8 Hz), 92.0 (d, *J* (^{13}C-^{19}F) = 3.3 Hz), 76.2, 23.8. **^{19}F NMR** (376 MHz, $CDCl_3$) δ -110.93. **HRMS** (APCI) *m/z* calculated for $C_{11}H_{10}F^+$ $[M+H]^+$: 161.0761, found: 161.0755.

177. Silver, S.; Leppänen, A.-S.; Sjöholm, R.; Penninkangas, A.; Leino, R. *Eur. J. Org. Chem.* **2005**, 1058–1081.

3-(Pent-4-en-1-yn-1-yl)phenol

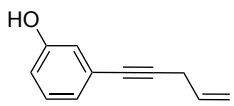

The title compound (yellow oil, method A: 63%; method B: 56%) was synthesized according to the general procedure starting from 1-(bromoethynyl)-3-chlorobenzene (43 mg, 0.2 mmol) and allyltrimethylsilane (64 µL, 0.4 mmol). The reaction time was 72 h. The eluent used in the purification was pentane, and then pentane:DCM 1:1. The desired product and a byproduct showed almost the same polarity, so only 13 mg of the pure product (42% yield) was isolated.

^{1}H NMR (400 MHz, $CDCl_3$) δ 7.16 (t, *J* = 7.9 Hz, 1H), 7.01 (dt, *J* = 7.6, 1.2 Hz, 1H), 6.89 (dd, *J* = 2.6, 1.4 Hz, 1H), 6.77 (ddd, *J* = 8.2, 2.6, 1.0 Hz, 1H), 5.89 (ddt, *J* = 17.0, 10.0, 5.3 Hz, 1H), 5.40 (dq, *J* = 17.0, 1.8 Hz, 1H), 5.17 (dq, *J* = 10.0, 1.7 Hz, 1H), 4.86 – 4.73 (m, 1H), 3.19 (dt, *J* = 5.3, 1.8 Hz, 2H). **^{13}C NMR** (75 MHz, $CDCl_3$) δ 155.2, 132.3, 129.5, 124.9, 124.3, 118.3, 116.3, 115.2, 86.7, 82.4, 23.7. **HRMS** (ESI-) *m/z* calculated for $C_{11}H_9O^-$ [M-H]$^-$: 157.0659, found: 157.0659.

1-Chloro-3-(pent-4-en-1-yn-1-yl)benzene

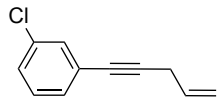

The title compound (yellow oil, method A: 16 mg, 45%; method B: 15 mg, 43%) was synthesized according to the general procedure starting from 1-(bromoethynyl)-3-chlorobenzene (43 mg, 0.2 mmol) and allyltrimethylsilane (64 µL, 0.4 mmol). The reaction was carried out at 50 ºC in a sealed vial.

^{1}H NMR (400 MHz, $CDCl_3$) δ 7.41 – 7.45 (m, 1H), 7.35 – 7.20 (m, 3H), 5.91 (ddt, *J* = 16.9, 10.3, 5.3 Hz, 1H), 5.41 (dq, *J* = 17.0, 1.8 Hz, 1H), 5.20 (dq, *J* = 10.0, 1.7 Hz, 1H), 3.21 (dt, *J* = 5.3, 1.8 Hz, 2H). **^{13}C NMR** (126 MHz, $CDCl_3$) δ 134.0, 132.1, 131.5, 129.7, 129.4, 128.0, 125.4, 116.4, 88.0, 81.5, 23.6. **HRMS** (APCI) *m/z* calculated for $C_{11}H_8Cl^+$ [M-H]$^+$: 175.0309, found: 175.0309.

1,3,5-Trimethyl-2-(pent-4-en-1-yn-1-yl)benzene

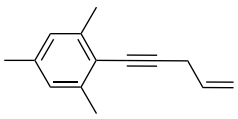

The title compound (yellow oil, method A: 36 mg, 98%; method B: 34 mg, 92%) was synthesized according to the general procedure starting from 2-(bromoethynyl)-1,3,5-trimethylbenzene (45 mg, 0.2 mmol) and allyltrimethylsilane (64 µL, 0.4 mmol). In the purification, a mixture of cyclohexane:triethylamine 99:1 was used as eluent.

^{1}H NMR (300 MHz, $CDCl_3$) δ 6.93 – 6.79 (m, 2H), 6.04 – 5.85 (m, 1H), 5.46 (dq, *J* = 17.0, 1.9 Hz, 1H), 5.17 (dq, *J* = 10.0, 1.7 Hz, 1H), 3.29 (dt, *J* = 5.1, 1.9 Hz, 2H), 2.40 (s, 6H), 2.27 (s, 3H). **^{13}C NMR** (75 MHz, $CDCl_3$) δ 140.0 (2C), 136.9, 132.9, 127.4 (2C), 120.4, 115.9, 93.9, 80.6, 24.0, 21.2, 21.0 (2C). **HRMS** (APCI) *m/z* calculated for $C_{14}H_{17}^+$ $[M+H]^+$: 185.1325, found: 185.1217.

1-(Pent-4-en-1-yn-1-yl)cyclohex-1-ene

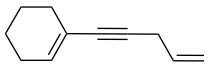

The title compound (colorless oil, method A: 9 mg, 31%; method B: 6 mg, 21%) was synthesized according to the general procedure starting from 1-(bromoethynyl)cyclohex-1-ene (37 mg, 0.2 mmol) and allyltrimethylsilane (64 µL, 0.40 mmol).

^{1}H NMR (500 MHz, $CDCl_3$) δ 6.08 – 6.02 (m, 1H), 5.84 (ddt, *J* = 17.0, 10.2, 5.3 Hz, 1H), 5.32 (dq, *J* = 16.9, 1.8 Hz, 1H), 5.11 (dq, *J* = 10.0, 1.7 Hz, 1H), 3.14 – 3.02 (m, 2H), 2.19 – 2.01 (m, 4H), 1.72 – 1.48 (m, 4H). **^{13}C NMR** (126 MHz, $CDCl_3$) δ 133.7, 132.9, 120.8, 115.9, 84.7, 83.5, 29.5, 25.6, 23.6, 22.4, 21.6. **HRMS** (APCI) *m/z* calculated for $C_{11}H_{15}^+$ $[M+H]^+$: 147.1168, found: 141.1166.

9-(Pent-4-en-1-yn-1-yl)phenanthrene

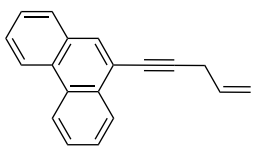

The title compound (sticky yellow oil, method A: 22 mg, 61%; method B: 20 mg, 55%) was synthesized according to the general procedure starting from 9-(bromoethynyl)phenanthrene (42 mg, 0.15 mmol) and allyltrimethylsilane (48 µL, 0.30 mmol). The eluent used in the purification was pentane, and then pentane:DCM 5:1.

^{1}H NMR (400 MHz, $CDCl_3$) δ 8.72 – 8.62 (m, 2H), 8.57 – 8.42 (m, 1H), 7.99 (s, 1H), 7.90 – 7.78 (m, 1H), 7.74 – 7.51 (m, 4H), 6.03 (ddt, *J* = 17.0, 10.2, 5.3 Hz, 1H), 5.55 (dq, *J* = 17.0, 1.8 Hz, 1H), 5.27 (dq, *J* = 10.0, 1.7 Hz, 1H), 3.41 (dt, *J* = 5.4, 1.8 Hz, 2H). **^{13}C NMR** (126 MHz, $CDCl_3$) δ 132.5, 131.5, 131.4, 131.3, 130.1, 130.0, 128.4, 127.2, 127.0, 126.9, 126.9, 126.8, 122.7, 122.5, 120.1, 116.5, 91.2, 81.0, 24.1. **HRMS** (APCI) *m/z* calculated for $C_{19}H_{15}^+$ $[M+H]^+$: 243.1168, found: 243.1167.

1-(Pent-4-en-1-yn-1-yl)naphthalene

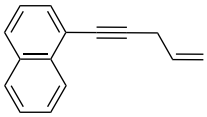

The title compound (yellow oil, method A: 21 mg, 55%; method B: 25 mg, 65%) was synthesized according to the general procedure starting from 1-(bromoethynyl)naphthalene (46 mg, 0.2 mmol) and allyltrimethylsilane (64 µL, 0.4 mmol). The eluent used in the purification was pentane, and then pentane:DCM 5:1.

^{1}H NMR (400 MHz, $CDCl_3$) δ 8.42 – 8.36 (m, 1H), 7.90 – 7.77 (m, 2H), 7.68 (dd, *J* = 7.2, 1.2 Hz, 1H), 7.55 (dddd, *J* = 22.9, 8.1, 6.8, 1.4 Hz, 2H), 7.43 (dd, *J* = 8.3, 7.1 Hz, 1H), 6.02 (ddt, *J* = 17.0, 10.2, 5.2 Hz, 1H), 5.54 (dq, *J* = 17.0, 1.8 Hz, 1H), 5.25 (dq, *J* = 10.0, 1.7 Hz, 1H), 3.39 (dt, *J* = 5.3, 1.8 Hz, 2H). **^{13}C NMR** (101 MHz, $CDCl_3$) δ 133.5, 133.2, 132.5, 130.2, 128.2, 128.2, 126.5, 126.2 (2C), 125.2, 121.4, 116.4, 91.5, 80.9, 24.0. **HRMS** (APCI) *m/z* calculated for $C_{15}H_{13}^{+}$ $[M+H]^{+}$: 193.1012, found: 193.1012.

3-(Pent-4-en-1-yn-1-yl)thiophene

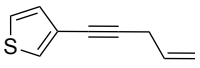

The title compound (yellow oil, method A: 14 mg, 48%; method B: 13 mg, 44%) was synthesized according to the general procedure starting from 3-(bromoethynyl)thiophene (37.4 mg, 0.2 mmol) and allyltrimethylsilane (64 µL, 0.4 mmol).

^{1}H NMR (300 MHz, $CDCl_3$) δ 7.39 (dd, *J* = 3.0, 1.2 Hz, 1H), 7.24 (dd, *J* = 5.0, 3.0 Hz, 1H), 7.10 (dd, *J* = 5.0, 1.2 Hz, 1H), 5.90 (ddt, *J* = 17.0, 9.9, 5.3 Hz, 1H), 5.39 (dq, *J* = 17.0, 1.8 Hz, 1H), 5.17 (dq, *J* = 10.0, 1.7 Hz, 1H), 3.18 (dt, *J* = 5.3, 1.8 Hz, 2H). **^{13}C NMR** (126 MHz, $CDCl_3$) δ 132.5, 130.1, 128.0, 125.2, 122.8, 116.4, 86.2, 78.0, 23.9. **HRMS** (APCI) *m/z* calculated for $C_9H_9S^{+}$ $[M+H]^{+}$: 149.0419, found: 149.0419.

3-(Pent-4-en-1-yn-1-yl)furan

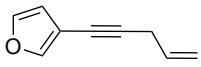

The title compound (yellow oil, method A: 6 mg, 23%; method B: 4 mg, 20%) was synthesized according to the general procedure starting from 3-(bromoethynyl)furan (25.6 mg, 0.15 mmol) and allyltrimethylsilane (48 µL, 0.3 mmol).

^{1}H NMR (400 MHz, $CDCl_3$) δ 7.62 – 7.57 (m, 1H), 7.37 (t, *J* = 1.7 Hz, 1H), 6.45 (dd, *J* = 1.9, 0.8 Hz, 1H), 5.90 (ddt, *J* = 16.9, 9.9, 5.4 Hz, 1H), 5.39 (dq, *J* = 16.9, 1.8 Hz, 1H), 5.18 (dq, *J* = 10.0, 1.7 Hz, 1H), 3.18 (dt, *J* = 5.4, 1.8 Hz, 2H). **^{13}C NMR** (126 MHz, $CDCl_3$) δ

145.2, 142.6, 132.4, 116.29, 112.7, 107.8, 88.3, 73.7, 23.8. **HRMS** (APCI) *m/z* calculated for $C_9H_9O^+$ $[M+H]^+$: 133.0648, found: 133.0649.

2-Methyl-5-(pent-4-en-1-yn-1-yl)furan

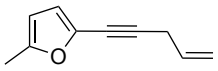

The title compound (yellow oil, method A: 9 mg, 31%; method B: 7 mg, 22%) was synthesized according to the general procedure starting from 2-(bromoethynyl)-5-methylfuran[178] (61.7 mg, 0.2 mmol) and allyltrimethylsilane (64 µL, 0.4 mmol).

^{1}H NMR (500 MHz, Chloroform-d) δ 6.40 (d, J = 3.2 Hz, 1H), 5.94 (dq, J = 3.1, 1.0 Hz, 1H), 5.86 (ddt, J = 17.0, 10.0, 5.4 Hz, 1H), 5.37 (dq, J = 17.0, 1.7 Hz, 1H), 5.16 (dq, J = 10.0, 1.6 Hz, 1H), 3.21 (dt, J = 5.4, 1.8 Hz, 2H), 2.28 (t, J = 0.7 Hz, 3H). **^{13}C NMR** (126 MHz, Chloroform-d) δ 153.3, 135.9, 132.1, 117.0, 115.6, 107.1, 90.9, 73.8, 24.2, 14.1. **HRMS** (APCI) *m/z* calculated for $C_{10}H_{11}O^+$ $[M+H]^+$: 147.0804, found: 147.0804.

3-(Pent-4-en-1-yn-1-yl)-1-tosyl-1H-indole

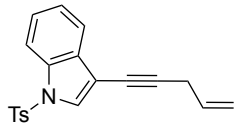

The title compound (yellow oil, method A: 58 mg, 87%; method B: 13 mg, 19%) was synthesized according to the general procedure starting from 3-(bromoethynyl)-1-tosyl-1H-indole[179] (75 mg, 0.2 mmol) and allyltrimethylsilane (64 µL, 0.4 mmol).

^{1}H NMR (500 MHz, $CDCl_3$) δ 8.00 – 7.94 (m, 1H), 7.80 – 7.73 (m, 2H), 7.69 (s, 1H), 7.63 (dt, *J* = 7.7, 0.9 Hz, 1H), 7.34 (ddd, *J* = 8.4, 7.2, 1.3 Hz, 1H), 7.28 (td, *J* = 7.9, 1.3 Hz, 1H), 7.21 (d, *J* = 8.2 Hz, 2H), 5.92 (ddt, *J* = 17.0, 10.3, 5.3 Hz, 1H), 5.44 (dq, *J* = 16.9, 1.8 Hz, 1H), 5.19 (dq, *J* = 10.0, 1.7 Hz, 1H), 3.26 (dt, *J* = 5.3, 1.8 Hz, 2H), 2.33 (s, 3H). **^{13}C NMR** (126 MHz, $CDCl_3$) δ 145.3, 135.1, 134.3, 132.4, 131.2, 130.1 (2C), 128.5, 127.0 (2C), 125.5, 123.8, 120.6, 116.6, 113.7, 105.8, 91.1, 73.8, 24.1, 21.7. **HRMS** (APCI) *m/z* calculated for $C_{20}H_{18}NO_2S^+$ $[M+H]^+$: 336.1053, found: 336.1065; *m/z* calculated for $C_{20}H_{17}NNaO_2S^+$ $[M+Na]^+$: 358.0872, found: 358.0887.

178. Moodapelly, S. K.; Sharma, G. V. M.; Doddi, V. K. *Adv. Synth. Catal*. **2017**, *359*, 1535–1540.
179. Campbell, C. D.; Greenaway, R. L.; Holton, O. T.; Walker, P. R.; Chapman, H. A.; Russell, C. A.; Carr, G.; Thomson, A. L.; Anderson, E. A. *Chem. Eur. J.* **2015**, *21*, 12627–12639.

(4-Methylpent-4-en-1-yn-1-yl)benzene

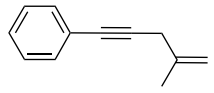

The title compound (colorless oil, method A and B: 17 mg, 54%) was synthesized according to the general procedure starting from (bromoethynyl)benzene (36 mg, 0.2 mmol) and trimethyl(2-methylallyl)silane (70 μL, 0.4 mmol). The reaction time was 72 h.

^{1}H NMR (300 MHz, $CDCl_3$) δ 7.47 – 7.39 (m, 2H), 7.34 – 7.25 (m, 3H), 5.14 – 5.06 (m, 1H), 4.94 – 4.85 (m, 1H), 3.14 (bs, 2H), 1.91 – 1.82 (m, 3H). **^{13}C NMR** (75 MHz, $CDCl_3$) δ 140.5, 131.6 (2C), 128.2 (2C), 127.7, 123.8, 111.8, 87.1, 82.8, 28.1, 22.1. The NMR data match with those reported in the literature.[156a]

(4-Bromopent-4-en-1-yn-1-yl)benzene

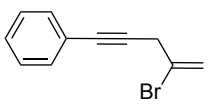

The title compound (yellow oil, method A: 28 mg, 64%) was synthesized according to the general procedure starting from (bromoethynyl)benzene (36 mg, 0.2 mmol) and (2-bromoallyl)trimethylsilane (69 μL, 0.4 mmol). The reaction was carried out at 50 ºC for 72 h in a sealed vial.

^{1}H NMR (500 MHz, $CDCl_3$) δ 7.48 – 7.41 (m, 2H), 7.35 – 7.28 (m, 3H), 6.10 – 6.05 (m, 1H), 5.62 – 5.58 (m, 1H), 3.58 (t, J = 1.5 Hz, 2H). **^{13}C NMR** (126 MHz, $CDCl_3$) δ 131.6 (2C), 128.3 (2C), 128.2, 127.1, 123.0, 118.0, 84.6, 84.0, 32.4. **HRMS** (APCI) *m/z* calculated for $C_{11}H_{10}Br^+$ $[M+H]^+$: 220.9960, found: 220.9952.

(4-(Chloromethyl)pent-4-en-1-yn-1-yl)benzene

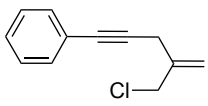

The title compound (green oil, method A: 18 mg, 48%) was synthesized according to the general procedure starting from (bromoethynyl)benzene (36 mg, 0.2 mmol) and (2-(chloromethyl)allyl)trimethylsilane (72 μL, 0.4 mmol). The reaction time was 48 h.

^{1}H NMR (400 MHz, $CDCl_3$) δ 7.46 – 7.39 (m, 2H), 7.33 – 7.27 (m, 3H), 5.41 – 5.36 (m, 1H), 5.32 – 5.26 (m, 1H), 4.18 (bs, 2H), 3.34 (bs, 2H). **^{13}C NMR** (101 MHz, $CDCl_3$) δ 140.3, 131.6 (2C), 128.2 (2C), 127.9, 123.4, 116.4, 85.6, 83.5, 47.4, 24.2. **HRMS** (APCI) *m/z* calculated for $C_{12}H_{12}Cl^+$ $[M+H]^+$: 191.0622, found: 191.0619.

(3-Ethylpent-4-en-1-yn-1-yl)benzene

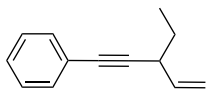

The title compound (yellow oil, method A (50ºC, 64 h): 16 mg, 47%; method B (50ºC, 16 h): 25 mg, 73%) was synthesized according to the general procedure starting from (bromoethynyl)benzene (36 mg, 0.2 mmol) and (*E*)-trimethyl(pent-2-en-1-yl)silane (40% solution in pentane, 157 mg, 0.44 mmol).

^{1}H NMR (400 MHz, $CDCl_3$) δ 7.47 – 7.39 (m, 2H), 7.33 – 7.25 (m, 3H), 5.85 (ddd, *J* = 17.0, 10.0, 6.1 Hz, 1H), 5.38 (dt, *J* = 17.0, 1.6 Hz, 1H), 5.14 (dt, *J* = 10.1, 1.5 Hz, 1H), 3.23 (dtt, *J* = 7.5, 6.0, 1.5 Hz, 1H), 1.77 – 1.56 (m, 2H), 1.06 (t, *J* = 7.4 Hz, 3H). **^{13}C NMR** (126 MHz, $CDCl_3$) δ 138.0, 131.8 (2C), 128.3 (2C), 127.8, 124.0, 115.3, 90.5, 83.8, 37.8, 28.6, 11.6. The NMR data match with those reported in the literature.[180]

Pent-4-en-1-yne-1,3-diyldibenzene

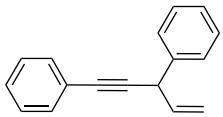

The title compound (yellow oil, method A (20ºC, 5 days): 15 mg, 35%; method B (20ºC, 20 h): 24 mg, 55%) was synthesized according to the general procedure starting from (bromoethynyl)benzene (36 mg, 0.2 mmol) and cinnamyltrimethylsilane (76 mg, 0.4 mmol).

^{1}H NMR (300 MHz, $CDCl_3$) δ 7.54 – 7.44 (m, 4H), 7.40 – 7.20 (m, 6H), 6.03 (ddd, *J* = 16.9, 9.9, 6.1 Hz, 1H), 5.48 (dt, *J* = 16.9, 1.5 Hz, 1H), 5.22 (dt, *J* = 9.9, 1.4 Hz, 1H), 4.61 (d, *J* = 6.1, 1H). **^{13}C NMR** (75 MHz, $CDCl_3$) δ 140.1, 137.9, 131.7 (2C), 128.6 (2C), 128.2 (2C), 128.0, 127.7 (2C), 127.0, 123.5, 115.2, 88.6, 85.3, 42.0. The NMR data match with those reported in the literature.[181]

1,3-Di(pent-4-en-1-yn-1-yl)benzene

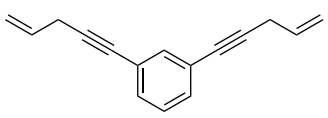

The title compound (colorless oil, method A: 18 mg, 44%; method B: 26 mg, 63%) was synthesized according to the general procedure starting from 1,3-bis(bromoethynyl)benzene (56.8 mg, 0.2 mmol) and allyltrimethylsilane (175 µL, 1.1 mmol).

180. Li, H.; Alexakis, A. *Angew. Chem. Int. Ed*, **2012**, 51, 1055–1058.
181. Hamilton, J. Y.; Sarlah, D.; Carreira, E. M. *Angew. Chem. Int. Ed.* **2013**, *52*, 7532–7535.

^{1}H NMR (500 MHz, $CDCl_3$) δ 7.50 (t, *J* = 1.7 Hz, 1H), 7.34 (dd, *J* = 7.7, 1.6 Hz, 2H), 7.22 (t, *J* = 7.7 Hz, 1H), 5.89 (ddt, *J* = 17.0, 10.3, 5.3 Hz, 2H), 5.40 (dq, *J* = 17.0, 1.7 Hz, 3H), 5.17 (dq, *J* = 10.0, 1.6 Hz, 3H), 3.19 (dt, *J* = 5.3, 1.9 Hz, 4H). **^{13}C NMR** (126 MHz, $CDCl_3$) δ 134.8, 132.4 (2C), 131.0 (2C), 128.3, 124.0 (2C), 116.5 (2C), 87.2 (2C), 82.3 (2C), 23.8 (2C). **HRMS** (APCI) *m/z* calculated for $C_6H_{15}^+$ $[M+H]^+$: 207.1168, found: 207.1160.

(4-(Bromomethyl)pent-4-en-1-yn-1-yl)benzene

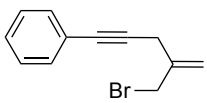

The title compound (yellow oil, method A: 8 mg, 17%) was synthesized according to the general procedure starting from (bromoethynyl)benzene (36 mg, 0.2 mmol) and 2-((trimethylsilyl)methyl)allyl acetate (85 μL, 0.4 mmol). The reaction time was 7 d.

^{1}H NMR (300 MHz, $CDCl_3$) δ 7.47 – 7.38 (m, 2H), 7.33 – 7.27 (m, 3H), 5.38 (q, *J* = 1.6 Hz, 1H), 5.34 (q, *J* = 1.0 Hz, 1H), 4.10 (bs, 2H), 3.38 (t, *J* = 1.4 Hz, 2H). **^{13}C NMR** (101 MHz, $CDCl_3$) δ 140.6, 131.6 (2C), 128.2 (2C), 128.0, 123.4, 116.8, 85.6, 83.6, 35.5, 24.6. **HRMS** (APCI) *m/z* calculated for $C_{12}H_{12}Br^+$ $[M+H]^+$: 235.0117, found: 235.0114.

Mixture of 1-ethyl-2-(pent-4-en-1-yn-1-yl)benzene and 3-allyl-1-methyl-1H-indene (1.5:1)

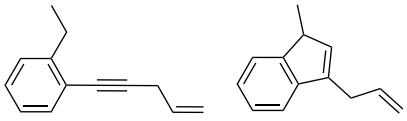

The title compounds were synthesized according to the general procedure (method A) starting from 1-(bromoethynyl)-2-ethylbenzene (23 mg, 0.1 mmol) and allyltrimethylsilane (64 μL, 0.4 mmol). The cyclized product was only observed with method A upon quenching the reaction with triethylamine and both products were obtained as a mixture after purification. ^{1}H NMR yields were determined using 2-bromomesitylene as internal standard.

1-Ethyl-2-(pent-4-en-1-yn-1-yl)benzene was obtained as a yellow oil (method A: 40% yield according to ^{1}H NMR) **^{1}H NMR** (500 MHz, $CDCl_3$) δ 7.43 – 7.37 (m, 1H), 7.26 – 7.20 (m, 1H), 7.23 – 7.17 (m, 1H), 7.12 (td, *J* = 7.3, 1.9 Hz, 1H), 5.92 (ddt, *J* = 17.0, 10.2, 5.2 Hz, 1H), 5.43 (dq, *J* = 17.0, 1.8 Hz, 1H), 5.21 – 5.14 (m, 1H), 3.24 (dt, *J* = 5.2, 1.9 Hz, 2H), 2.82 (q, *J* = 7.6 Hz, 2H), 1.25 (t, *J* = 7.6 Hz, 3H).**^{13}C NMR** (126 MHz, $CDCl_3$) δ 146.4, 136.0, 133.0, 132.6, 128.3, 128.2, 125.9, 123.2, 116.5, 90.3, 81.9, 24.2, 15.2.

3-Allyl-1-methyl-1H-indene was obtained as a yellow oil (method A: 29% yield according to ^{1}H NMR). **^{1}H NMR** (500 MHz, $CDCl_3$) δ 7.43 – 7.37 (m, 1H), 7.32 (dt, *J* = 7.3, 1.1 Hz,

1H), 7.29 – 7.25 (m, 2H), 6.17 (q, *J* = 1.7 Hz, 1H), 6.04 (ddt, *J* = 16.8, 10.1, 6.6 Hz, 1H), 5.19 (dq, *J* = 7.8, 1.7 Hz, 1H), 5.12 (dq, *J* = 10.1, 1.5 Hz, 1H), 3.44 (qd, *J* = 7.5, 2.0 Hz, 1H), 3.29 (dp, *J* = 6.6, 1.6 Hz, 2H), 1.30 (d, *J* = 7.6 Hz, 3H). **^{13}C NMR** (126 MHz, $CDCl_3$) δ 150.3, 144.6, 141.0, 136.6 (2C), 126.5, 125.2, 122.9, 119.6, 116.6, 44.0, 32.6, 16.6.

Synthesis of Cyclobutene 26

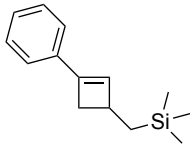

Ethynylbenzene (22 μL, 0.2 mmol, 1 equiv) was dissolved in dry CH_2Cl_2 (0.4 mL, 0.5 M). Allyltrimethylsilane (64 μL, 0.4 mmol, 2 equiv) was added, followed by [(*t*BuXPhos)AuNCMe]BAr_4^F (9 mg, 3 mol%). The resulting mixture was stirred at 50 ºC for 14 h in a sealed vial. The crude was directly subjected to silica gel column chromatography (eluent = pentane) to obtain the pure trimethyl((3-phenylcyclobut-2-en-1-yl)methyl)silane (colorless oil, 25 mg, 58%).

^{1}H NMR (500 MHz, $CDCl_3$) δ 7.43 – 7.31 (m, 4H), 7.29 – 7.24 (m, 1H), 6.41 (d, *J* = 1.2 Hz, 1H), 3.05 (dd, *J* = 12.6, 4.4 Hz, 1H), 3.00 – 2.86 (m, 1H), 2.33 (dd, *J* = 12.6, 1.7 Hz, 1H), 0.97 – 0.84 (m, 2H), 0.09 (s, 9H). **^{13}C NMR** (75 MHz, $CDCl_3$) δ 143.7, 135.1, 133.5, 128.2 (2C), 127.4, 124.3 (2C), 37.8, 35.3, 22.4, -1.0 (3C). **HRMS** (APCI) *m/z* calculated for $C_{14}H_{21}Si^+$ $[M+H]^+$: 217.1407, found: 217.1406.

Synthesis of Homopropargyl Bromide 28

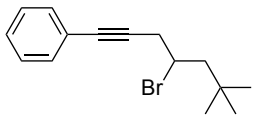

(Bromoethynyl)benzene (36 mg, 0.2 mmol, 1 equiv) was dissolved in dry CH_2Cl_2 (0.4 mL, 0.5 M). 4,4-Dimethylpent-1-ene (58 μL, 0.4 mmol, 2 equiv) was added, followed by [(*t*BuXPhos)AuNCMe]BAr_4^F (9 mg, 3 mol%). The resulting mixture was stirred at 23 ºC for 48 h. The crude was directly subjected to preparative silica gel TLC (eluent = pentane) to obtain the pure (4-bromo-6,6-dimethylhept-1-yn-1-yl)benzene (colorless oil, 15 mg, 27%).

^{1}H NMR (400 MHz, $CDCl_3$) δ 7.47 – 7.40 (m, 2H), 7.35 – 7.30 (m, 3H), 4.20 (tdd, *J* = 7.3, 5.6, 3.6 Hz, 1H), 3.07 (dd, *J* = 17.1, 5.7 Hz, 1H), 2.99 (dd, *J* = 17.1, 7.3 Hz, 1H), 2.14 (dd, *J* = 15.5, 3.6 Hz, 1H), 2.06 (dd, *J* = 15.5, 7.4 Hz, 1H), 1.05 (s, 9H). **^{13}C NMR** (101 MHz, $CDCl_3$) δ 131.6 (2C), 128.3 (2C), 128.0, 123.3, 86.6, 82.9, 51.6, 48.0, 32.4, 31.1, 29.7 (3C). **HRMS** (APCI) *m/z* calculated for $C_{15}H_{20}Br^+$ $[M+H]^+$: 279.0743, found: 279.0740.

Synthesis of Hydrobrominated Product 29

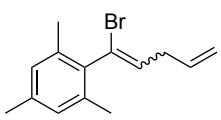

2-(Bromoethynyl)-1,3,5-trimethylbenzene (45 mg, 0.2 mmol, 1 equiv) was dissolved in CH_2Cl_2 (0.2 mL, 1 M). Allyltrimethylsilane (64 µL, 0.4 mmol, 2 equiv) was added, followed by [(*t*BuXPhos)AuNCMe]BAr_4^F (9 mg, 3 mol%). The resulting mixture was stirred at 23 ºC for 38 h. The crude was directly subjected to preparative silica gel TLC (eluent = cyclohexane) to obtain 2-(1-bromopenta-1,4-dien-1-yl)-1,3,5-trimethylbenzene (yellow oil, 24 mg, 45%).

^{1}H NMR (300 MHz, $CDCl_3$) δ 6.88 (s, 2H), 6.27 (td, *J* = 7.6, 0.9 Hz, 1H), 5.82 – 5.63 (m, 1H), 5.06 – 4.99 (m, 1H), 4.99 – 4.95 (m, 1H), 2.49 (tm, *J* = 7.7, 2H), 2.29 (s, 3H), 2.26 (s, 6H). **^{13}C NMR** (75 MHz, $CDCl_3$) δ 138.3, 136.1, 134.7, 134.3, 132.2, 128.3 (2C), 128.2, 120.2, 115.8, 34.6, 21.1, 19.4 (2C). **HRMS** (APCI) m/z calculated for $C_{14}H_{18}Br^+$ $[M+H]^+$: 265.0586, found: 265.0584.

General Procedure for the Synthesis of 1,3-Enynes 32

The bromoalkyne (0.2 mmol, 1 equiv) was dissolved in dry CH_2Cl_2 (0.4 mL, 0.5 M). Buta-2,3-dien-2-yltrimethylsilane (67 µL, 0.4 mmol, 2 equiv) was added, followed by the catalyst (3 mol%, **method A**: 9 mg of [(*t*BuXPhos)AuNCMe]BAr_4^F or **method B**: 2 mg of $InBr_3$). The resulting mixture was stirred at 23 ºC for 14 h. The reaction was monitored by TLC or GC-MS. The crude was directly subjected to preparative neutral aluminum oxide TLC (eluent = pentane) to obtain the pure 1,3-enyne.

(*Z*)-(2-Bromo-3-methyl-5-phenylpent-2-en-4-yn-1-yl)trimethylsilane

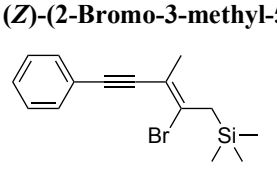

The title compound (yellow oil, method A: 20 mg, 33%; method B: 20 mg, 32%) was synthesized according to the general procedure starting from (bromoethynyl)benzene (36 mg, 0.2 mmol).

^{1}H NMR (400 MHz, $CDCl_3$) δ 7.54 – 7.41 (m, 2H), 7.37 – 7.26 (m, 3H), 2.32 (q, *J* = 0.8 Hz, 2H), 1.92 (t, *J* = 0.8 Hz, 3H), 0.16 (s, 9H). **^{13}C NMR** (101 MHz, $CDCl_3$) δ 131.4 (2C), 129.5, 128.2 (2C), 127.9, 123.7, 114.9, 91.8, 91.7, 30.8, 19.9, -0.8 (3C). **HRMS** (APCI) *m/z* calculated for $C_{15}H_{20}BrSi^+$ $[M+H]^+$: 307.0512, found: 307.0513.

(*Z*)-(5-([1,1'-Biphenyl]-4-yl)-2-bromo-3-methylpent-2-en-4-yn-1-yl)trimethylsilane

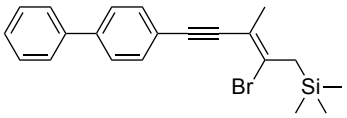

The title compound (pale yellow solid, method A: 19 mg, 25%; method B: 21 mg, 26%) was synthesized according to the general procedure starting from 4-(bromoethynyl)-1,1'-biphenyl (51 mg, 0.2 mmol).

M.p. (pentane/CH_2Cl_2) 63-66 ºC. **^{1}H NMR** (500 MHz, $CDCl_3$) δ 7.62 – 7.58 (m, 2H), 7.55 (s, 4H), 7.48 – 7.41 (m, 2H), 7.36 (tt, *J* = 7.3, 1.3 Hz, 1H), 2.33 (s, 2H), 1.94 (s, 3H), 0.17 (s, 9H). **^{13}C NMR** (126 MHz, $CDCl_3$) δ 140.6, 140.4, 131.8 (2C), 129.6, 128.8 (2C), 127.5, 127.0 (2C), 126.9 (2C), 122.6, 114.9, 92.5, 91.7, 30.8, 19.9, -0.8 (3C). **HRMS** (APCI) *m/z* calculated for $C_{21}H_{24}BrSi^+$ $[M+H]^+$: 383.0825, found: 383.0815.

(*Z*)-(2-Bromo-5-(4-bromophenyl)-3-methylpent-2-en-4-yn-1-yl)trimethylsilane

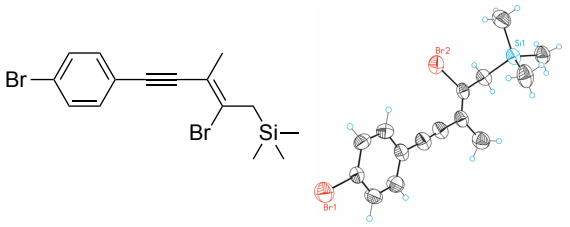

The title compound (brown solid, method A: 13 mg, 17%; method B: 10 mg, 13%) was synthesized according to the general procedure starting from 1-bromo-4-(bromoethynyl)benzene (52 mg, 0.2 mmol). The product was crystallized by dissolving it in ethanol and subsequent slow evaporation of the solvent. The structure was confirmed by single crystal X-ray diffraction.

M.p. (pentane/CH_2Cl_2) 39-42 ºC. **^{1}H NMR** (500 MHz, $CDCl_3$) δ 7.46 – 7.41 (m, 2H), 7.35 – 7.29 (m, 2H), 2.31 (s, 2H), 1.90 (s, 3H), 0.15 (s, 9H). **^{13}C NMR** (126 MHz, $CDCl_3$) δ 132.8 (2C), 131.5 (2C), 130.2, 122.6, 122.1, 114.6, 92.9, 90.6, 30.9, 19.8, -0.9 (3C). **HRMS** (APCI) *m/z* calculated for $C_{15}H_{19}Br_2Si^+$ $[M+H]^+$: 384.9617, found: 384.9608.

Synthesis of Derivatized 1,3-Enyne 33

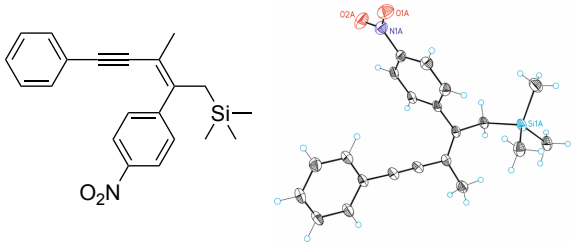

The title compound was synthesized following a literature procedure for the preparation of related compounds.[182] (*Z*)-(2-Bromo-3-methyl-5-phenylpent-2-

182. Zhou, H.; Moberg, C. *J. Am. Chem. Soc.* **2012**, *134*, 15992–15999.

en-4-yn-1-yl)trimethylsilane (81 mg, 0.26 mmol, 1 equiv), (4-nitrophenyl)boronic acid (55 mg, 0.32 mmol, 1.2 equiv) and $Pd(PPh_3)_4$ (31 mg, 26 μmol, 10 mol%) under argon were dissolved in toluene (3.2 mL). Then, K_2CO_3 (73 mg, 0.53 mmol, 2 equiv) in water (1 mL) was added. The mixture was stirred at 80 °C for 16 h. The reaction was monitored by TLC (eluent: cyclohexane:EtOAc 10:1). The reaction mixture was allowed to cool to room temperature and CH_2Cl_2 (20 mL) was added. The mixture was filtered through Celite™, washing with CH_2Cl_2. The filtrate was dried over anhydrous Na_2SO_4, filtered and concentrated under reduced pressure. The crude was adsorbed in florisil and purified by silica gel column chromatography (eluent: cyclohexane:EtOAc from 1:0 to 10:1). The product (78 mg, 84%) was obtained as an orange solid. The product was crystallized by dissolving it in ethanol at 50 ºC, allowing to cool to room temperature, and subsequent slow evaporation of the solvent. The structure was confirmed by single crystal X-ray diffraction. **M.p.** (cyclohexane/EtOAc) 69-71 ºC.**^{1}H NMR** (500 MHz, $CDCl_3$) δ 8.23 – 8.18 (m, 2H), 7.67 – 7.62 (m, 2H), 7.25 – 7.19 (m, 3H), 7.16 – 7.10 (m, 2H), 2.13 (d, *J* = 0.8 Hz, 2H), 2.06 (t, *J* = 0.8 Hz, 3H), -0.10 (s, 9H). **^{13}C NMR** (126 MHz, $CDCl_3$) δ 150.8, 146.6, 144.5, 131.0 (2C), 129.9 (2C), 128.3 (2C), 127.8, 123.5, 122.9 (2C), 113.4, 91.8, 90.8, 26.3, 20.5, -0.9 (3C). **HRMS** (APCI) *m/z* calculated for $C_{21}H_{24}NO_2Si^+$ $[M+H]^+$: 350.1571, found: 350.1571.

General Procedure for the Synthesis of 1,4-Enynes 35 and 1,4-Dienes 38

The bromoalkyne (0.2 mmol, 1 equiv) was dissolved in DCE (0.2 mL, 1 M). The allylsilane (0.4 mmol, 2 equiv) was added, followed by the catalyst (5 mol%; **method C**: 15 mg of [(*t*BuXPhos)AuNCMe]BAr_4^F or **method D**: 3.5 mg of $InBr_3$). The resulting mixture was stirred at 75 ºC for 18 h (otherwise stated). The reaction was monitored by TLC or GC-MS. The crude was directly subjected to silica gel column chromatography (eluent = pentane, otherwise stated) to obtain the pure 1,4-enyne and 1,4-diene.

3-Allyl-1,2-dihydronaphthalene

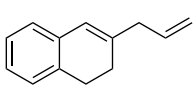

The title compound (colorless oil, method C: 22 mg, 64%) was synthesized according to the general procedure starting from (4-bromobut-3-yn-1-yl)benzene (42 mg, 0.2 mmol) and allyltrimethylsilane (64 μL, 0.40 mmol). The structure was assigned on basis of nOe experiments.

^{1}H NMR (400 MHz, $CDCl_3$*d*) δ 7.17 – 7.06 (m, 3H), 7.03 – 6.95 (m, 1H), 6.25 (bs, 1H), 5.89 (ddtd, *J* = 16.8, 10.0, 6.8, 0.9 Hz, 1H), 5.41 – 4.95 (m, 2H), 2.94 (bd, *J* = 6.7, 2H), 2.82 (t, *J* = 8.2 Hz, 2H), 2.26 (bt, *J* = 8.9, 2H). **^{13}C NMR** (126 MHz, $CDCl_3$) δ 140.1, 135.8, 134.8, 134.4, 127.2, 126.4, 126.2, 125.5, 123.1, 116.4, 41.8, 28.1, 27.2. **HRMS** (APCI) *m/z* calculated for $C_{13}H_{15}^+$ $[M+H]^+$: 171.1168, found: 171.1167.

3-Allyl-1-methyl-1,2-dihydronaphthalene

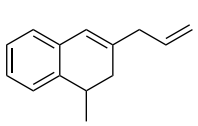

The title compound (colorless oil, method C: 15 mg, 42%) was synthesized according to the general procedure starting from (5-bromopent-4-yn-2-yl)benzene (45 mg, 0.2 mmol) and allyltrimethylsilane (64 µL, 0.40 mmol).

^{1}H NMR (400 MHz, $CDCl_3$) δ 7.18 – 7.09 (m, 3H), 7.04 – 6.94 (m, 1H), 6.23 (p, *J* = 1.4 Hz, 1H), 5.87 (ddt, *J* = 16.9, 10.0, 6.8 Hz, 1H), 5.42 – 4.98 (m, 2H), 3.01 – 2.86 (m, 3H), 2.40 (dddt, *J* = 16.6, 6.7, 1.9, 1.0 Hz, 1H), 2.03 (ddq, *J* = 16.7, 7.5, 1.0 Hz, 1H), 1.22 (d, *J* = 7.0 Hz, 3H). **^{13}C NMR** (101 MHz, $CDCl_3$) δ 139.4, 138.4, 135.7, 134.0, 126.5, 126.3, 125.8, 125.7, 122.5, 116.5, 41.9, 35.2, 32.3, 20.1. **HRMS** (APCI) m/z calculated for $C_{14}H_{17}^+$ $[M+H]^+$: 185.1325, found: 185.1323.

3-(2-(Chloromethyl)allyl)-1,2-dihydronaphthalene

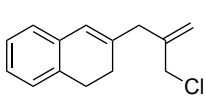

The title compound (colorless oil, method C: 6 mg, 13%) was synthesized according to the general procedure starting from (4-bromobut-3-yn-1-yl)benzene (42 mg, 0.2 mmol) and (2-(chloromethyl)allyl)trimethylsilane (72 µL, 0.40 mmol).

It was isolated together with traces of an inseparable impurity which is shown in the ^{1}H NMR spectrum. **^{1}H NMR** (500 MHz, $CDCl_3$) δ 7.17 – 7.11 (m, 1H), 7.11 – 7.08 (m, 2H), 7.04 – 6.99 (m, 1H), 6.33 (bs, 1H), 5.25 (bs, 1H), 5.10 (q, *J* = 1.3 Hz, 1H), 4.05 (d, *J* = 0.9 Hz, 1H), 3.07 (s, 1H), 2.81 (t, *J* = 8.2 Hz, 1H), 2.22 (t, *J* = 7.9 Hz, 2H). **^{13}C NMR** (101 MHz, $CDCl_3$) δ 142.8, 138.0, 134.5, 134.5, 127.2, 126.6, 126.5, 125.7, 125.1, 116.6, 47.5, 41.5, 28.2, 26.7. **HRMS** (APCI) m/z calculated for $C_{14}H_{16}Cl^+$ $[M+H]^+$: 219.0935, found: 219.0935.

2-(Pent-4-en-1-yn-1-yl)-1,1'-biphenyl and 9-allylphenanthrene

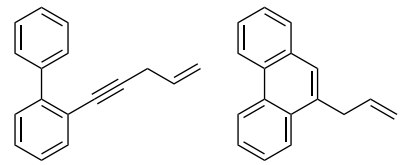

The title compounds were synthesized according to the general procedure (methods C and D) starting from 2-(bromoethynyl)-1,1'-biphenyl (51 mg, 0.2 mmol) and allyltrimethylsilane (64 μL, 0.40 mmol). The final products were separated and isolated by chromatography using as eluent pentane and then, pentane:DCM 9:1.

2-(Pent-4-en-1-yn-1-yl)-1,1'-biphenyl was obtained as a colorless oil (method C: 23 mg, 53%, method D: 14 mg, 32%). **^{1}H NMR** (400 MHz, $CDCl_3$) δ 7.64 – 7.58 (m, 2H), 7.58 – 7.53 (m, 1H), 7.46 – 7.32 (m, 5H), 7.31 – 7.25 (m, 1H), 5.78 (ddtd, *J* = 16.6, 10.2, 5.2, 1.3 Hz, 1H), 5.20 (dp, *J* = 17.0, 1.6 Hz, 1H), 5.06 (dp, *J* = 9.9, 1.6 Hz, 1H), 3.09 (dq, *J* = 5.1, 1.6 Hz, 2H). **^{13}C NMR** (101 MHz, $CDCl_3$) δ 143.7, 140.7, 133.1, 132.1, 129.4, 129.3 (2C), 127.9, 127.8 (2C), 127.2, 126.9, 122.0, 116.1, 89.5, 82.4, 23.8. **HRMS** (APCI) *m/z* calculated for $C_{17}H_{15}^+$ $[M+H]^+$: 219.1168, found: 219.1168.

9-Allylphenanthrene was obtained as a colorless oil (method C: 10 mg, 23%, method D: 7 mg, 17%). **^{1}H NMR** (500 MHz, $CDCl_3$) δ 8.74 (dd, *J* = 7.9, 1.6 Hz, 1H), 8.67 (d, *J* = 8.1 Hz, 1H), 8.10 (dd, *J* = 7.8, 1.7 Hz, 1H), 7.85 (dd, *J* = 7.7, 1.6 Hz, 1H), 7.74 – 7.54 (m, 5H), 6.20 (ddt, *J* = 15.7, 11.2, 6.2 Hz, 1H), 5.19 (bs, 1H), 5.16 (dm, *J* = 7.1, 1H), 3.90 (bd, *J* = 6.3, 2H). **^{13}C NMR** (126 MHz, $CDCl_3$) δ 136.7, 134.4, 131.9, 131.3, 130.7, 129.8, 128.1, 126.7, 126.6, 126.5, 126.2, 126.1, 124.7, 123.1, 122.5, 116.6, 37.6. The NMR data match with those reported in the literature.[183]

3',5'-Dimethyl-2-(pent-4-en-1-yn-1-yl)-1,1'-biphenyl and 9-allyl-1,3-dimethylphenanthrene

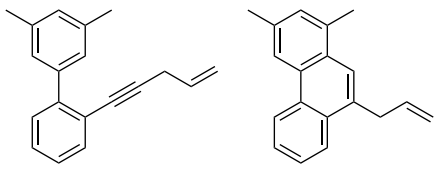

The title compounds were synthesized according to the general procedure (methods C and D) starting from 2-(bromoethynyl)-3',5'-dimethyl-1,1'-biphenyl (57 mg, 0.2 mmol) and allyltrimethylsilane (64 μL, 0.40 mmol). The final products were separated and isolated by chromatography.

183. Li, M.-B.; Wang, Y.; Tian, S.-K. *Angew. Chem. Int. Ed.* **2012**, *51*, 2968–2971.

3',5'-Dimethyl-2-(pent-4-en-1-yn-1-yl)-1,1'-biphenyl was obtained as a colorless oil (method C: 20 mg, 41%, method D: 11 mg, 21%). **^{1}H NMR** (500 MHz, $CDCl_3$) δ 7.54 (dd, *J* = 7.7, 1.4 Hz, 1H), 7.40 – 7.30 (m, 2H), 7.29 – 7.24 (m, 1H), 7.24 (s, 2H), 7.00 (s, 1H), 5.80 (ddt, *J* = 17.0, 10.2, 5.2 Hz, 1H), 5.24 (dq, *J* = 17.0, 1.8 Hz, 1H), 5.08 (dq, *J* = 10.0, 1.7 Hz, 1H), 3.11 (dt, *J* = 5.3, 1.9 Hz, 2H), 2.37 (s, 6H). **^{13}C NMR** (126 MHz, $CDCl_3$) δ 144.2, 140.9, 137.7 (2C), 133.5, 132.7, 129.78, 129.3, 128.3, 127.5 (2C), 127.1, 122.3, 116.5, 89.8, 82.9, 24.3, 21.7 (2C). **HRMS** (MALDI) m/z calculated for $C_{19}H_{18}^{+\cdot}$ $[M]^{+\cdot}$: 246.1403, found: 246.1415.

9-Allyl-1,3-dimethylphenanthrene was obtained as a colorless oil (method C: 13 mg, 26%). **^{1}H NMR** (500 MHz, $CDCl_3$) δ 8.73 (dd, *J* = 7.9, 1.8 Hz, 1H), 8.34 (s, 1H), 8.07 (dd, *J* = 7.5, 2.1 Hz, 1H), 7.76 (s, 1H), 7.65 – 7.55 (m, 2H), 7.27 (s, 1H), 6.24 – 6.08 (m, 1H), 5.15 (t, *J* = 1.6 Hz, 1H), 5.12 (dq, *J* = 7.7, 1.7 Hz, 1H), 3.89 (dd, *J* = 6.2, 1.2 Hz, 2H), 2.70 (s, 3H), 2.56 (s, 3H). **^{13}C NMR** (126 MHz, $CDCl_3$) δ 137.4, 135.6, 134.6, 133.4, 131.4, 131.2, 130.4, 130.0, 128.9, 126.6, 126.3, 125.0, 123.8, 123.1, 120.7, 116.8, 38.4, 22.4, 20.1. **HRMS** (APCI) m/z calculated for $C_{19}H_{19}^{+}$ $[M+H]^{+}$: 247.1481, found: 247.1477.

2-(Pent-4-en-1-yn-1-yl)-3',5'-bis(trifluoromethyl)-1,1'-biphenyl

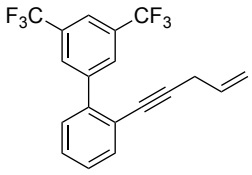

The title compound (yellow oil, method C: 60 mg, 85%; method D: 64 mg, 90%) was synthesized according to the general procedure starting from 2-(bromoethynyl)-3',5'-bis(trifluoromethyl)-1,1'-biphenyl (79 mg, 0.2 mmol) and allyltrimethylsilane (64 µL, 0.4 mmol).

^{1}H NMR (400 MHz, $CDCl_3$) δ 8.10 (dd, *J* = 1.7, 0.9 Hz, 2H), 7.96 – 7.81 (m, 1H), 7.60 (dt, *J* = 7.1, 1.3 Hz, 1H), 7.45 – 7.32 (m, 3H), 5.76 (ddt, *J* = 17.0, 10.0, 5.4 Hz, 1H), 5.17 (dq, *J* = 17.0, 1.8 Hz, 1H), 5.07 (dq, *J* = 10.0, 1.6 Hz, 1H), 3.08 (dt, *J* = 5.5, 1.8 Hz, 2H). **^{13}C NMR** (101 MHz, $CDCl_3$) δ 142.5, 140.5, 133.4, 131.7, 131.2 (q, *J* = 33.2 Hz, 2C), 129.6 (d, *J* = 3.0 Hz, 2C), 129.1, 128.4 (2C), 123.5 (q, *J* = 272.6 Hz, 2C), 122.2, 121.0 (p, *J* = 3.8 Hz), 116.4, 91.3, 81.1, 23.6. **^{19}F NMR** (376 MHz, $CDCl_3$) δ -62.88. **HRMS** (APCI) m/z calculated for $C_{19}H_{11}F_6$+ $[M-H]^{+}$: 353.0759, found: 353.0759.

2-(Pent-4-en-1-yn-1-yl)-1,1'-biphenyl-2',3',4',5',6'-*d*$_5$ and 9-allylphenanthrene-1,2,3,4,10-*d*$_5$

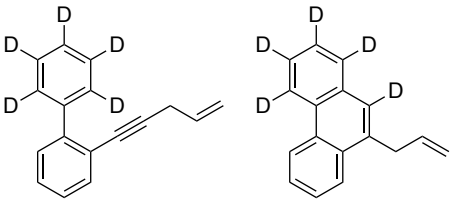

The title compounds were synthesized according to the general procedure (methods C and D) starting from 2-(bromoethynyl)-1,1'-biphenyl-2',3',4',5',6'-*d*$_5$ (53 mg, 0.2 mmol) and allyltrimethylsilane (64 μL, 0.40 mmol). The final products were separated and isolated by chromatography.

2-(Pent-4-en-1-yn-1-yl)-1,1'-biphenyl-2',3',4',5',6'-*d*$_5$ (65% deuterated) was obtained as a colorless oil (method C: 18 mg, 40%, method D: 16 mg, 36%). **^{1}H NMR** (400 MHz, $CDCl_3$) δ 7.64 – 7.52 (m, 1H), 7.45 – 7.26 (m, 3H), 5.78 (ddt, J = 17.0, 10.2, 5.2 Hz, 1H), 5.20 (dq, J = 17.0, 1.8 Hz, 1H), 5.06 (dq, J = 10.0, 1.7 Hz, 1H), 3.09 (dt, J = 5.2, 1.8 Hz, 2H). **^{13}C NMR** (101 MHz, $CDCl_3$) δ 143.70 (d, J = 4.8 Hz), 140.65 (d, J = 19.3 Hz), 133.2, 132.2, 129.5, 129.3 (2C), 128.0, 127.9 (2C), 127.3, 126.9, 122.1, 116.2, 89.5, 82.4, 23.8. **HRMS** (APCI) m/z calculated for $C_{17}H_{10}D_5^+$ $[M+H]^+$: 224.1482, found: 224.1471.

9-Allylphenanthrene-1,2,3,4,10-*d*$_5$ (65% deuterated) was obtained as a colorless oil (method C: 11 mg, 24%). The structure was assigned on basis of nOe experiments. **^{1}H NMR** (400 MHz, $CDCl_3$) δ 8.77 – 8.71 (m, 1H), 8.13 – 8.08 (m, 1H), 7.71 – 7.57 (m, 2H), 6.29 – 6.12 (m, 1H), 5.20 (t, J = 1.5 Hz, 1H), 5.16 (dt, J = 6.5, 1.6 Hz, 1H), 3.90 (dt, J = 6.2, 1.5 Hz, 2H). **^{13}C NMR** (126 MHz, $CDCl_3$) δ 136.8, 134.4, 131.9, 131.4, 130.8, 129.9, 128.3, 126.8, 126.8, 126.6, 126.4, 126.3, 124.9, 123.3, 122.6, 116.8, 37.7. **HRMS** (APCI) m/z calculated for $C_{17}H_9D_5^{+\cdot}$ $[M]^{+\cdot}$: 223.1404, found: 223.1414.

Synthesis of Allylphenanthrene 38e

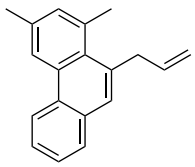

The title compound (colorless oil, 6 mg, quant.) was synthesized by mixing (3',5'-dimethyl-2-(pent-4-en-1-yn-1-yl)-1,1'-biphenyl) (5.7 mg, 0.023 mmol) with [(*t*BuXPhos)AuNCMe]BAr_4^F (5 mol%, 1.8 mg) in DCE (0.46 mL, 0.05 M). The resulting mixture was stirred at 100 ºC for 18 h under argon. After this time, TLC indicated completion of the reaction and the crude was directly subjected to silica gel column chromatography (eluent = pentane) to obtain 10-allyl-1,3-dimethylphenanthrene (90% pure). The structure was assigned on basis of nOe experiments. **^{1}H NMR** (400 MHz, $CDCl_3$) δ 8.64 (dd, *J* = 7.6, 1.7 Hz, 1H), 8.46 (s, 1H), 7.77 (dd, *J* = 7.6, 1.7 Hz, 1H), 7.60 – 7.52 (m, 2H), 7.51 (s, 1H), 7.25 (s, 1H), 6.18

(ddt, J = 17.2, 10.5, 5.4 Hz, 1H), 5.12 (dq, J = 10.3, 1.8 Hz, 1H), 4.89 (dq, J = 17.2, 1.9 Hz, 1H), 4.05 (d, J = 5.3 Hz, 2H), 2.92 (s, 3H), 2.56 (s, 3H). **^{13}C NMR** (101 MHz, $CDCl_3$) δ 138.6, 135.3, 135.2, 134.9, 133.1, 132.6, 131.7, 130.2, 129.6, 129.1, 127.7, 126.5, 126.1, 123.1, 121.8, 116.2, 41.4, 25.6, 21.7. **HRMS** (APCI) m/z calculated for $C_{19}H_{19}^+$ $[M+H]^+$: 247.1481, found: 247.1474.

Experimental Mechanistic Studies

Studies on the Formation of Allylphenanthrenes 35

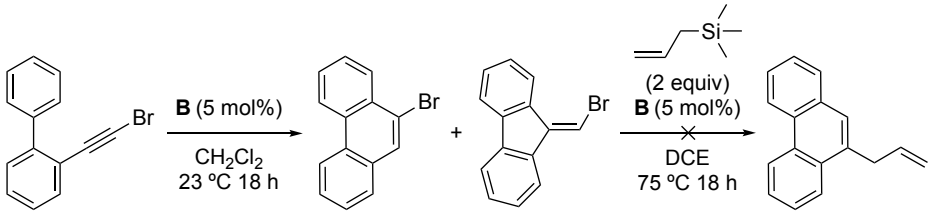

2-(Bromoethynyl)-1,1'-biphenyl (5 mg, 20 µmol, 1 equiv) was dissolved in CH_2Cl_2 (40 µL). [(*t*BuXPhos)AuNCMe]BAr_4^F (1.5 mg, 1 µmol, 5 mol%) was added. The resulting mixture was stirred at 23 °C for 18 h. The crude was analyzed by NMR. A mixture of 9-(bromomethylene)-9H-fluorene and 9-bromophenanthrene was detected in a 95:5 ratio. The crude was filtered through a small plug of silica gel, concentrated under reduced pressure and subjected to the next reaction without further purification.

The crude was dissolved in DCE (0.1 mL). Allyltrimethylsilane (6.2 µL, 40 µmol, 2 equiv) was added, followed by [(*t*BuXPhos)AuNCMe]BAr_4^F (1.5 mg, 1 µmol, 5 mol%). The reaction was stirred at 75 °C for 18 h. The crude was analyzed by NMR. No reaction was detected.

9-(Bromomethylene)-9H-fluorene: **^{1}H NMR** (300 MHz, $CDCl_3$) δ 8.60 (dt, J = 7.6, 0.9 Hz, 1H), 7.73 (ddd, J = 7.5, 1.3, 0.6 Hz, 1H), 7.69 (ddd, J = 7.6, 1.3, 0.7 Hz, 1H), 7.59 (dt, J = 7.5, 0.9 Hz, 1H), 7.46 (td, J = 7.5, 1.2 Hz, 1H), 7.41 (s, 1H), 7.42 – 7.34 (m, 2H), 7.33 – 7.26 (m, 1H). **^{13}C NMR** (101 MHz, $CDCl_3$) δ 141.4, 139.1, 138.8, 138.4, 136.6, 129.4, 128.6, 127.3, 127.2, 125.7, 120.1, 119.8, 119.8, 105.8. The NMR data were in agreement with the ones previously reported in the literature.[184]

184. Paul, G. C.; Gajewski, J. J. *Synthesis* **1997**, *5*, 524–526.

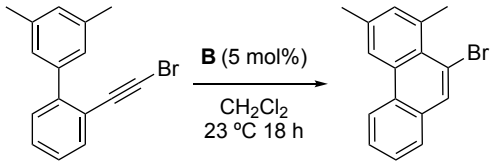

2-(Bromoethynyl)-3',5'-dimethyl-1,1'-biphenyl (57 mg, 0.2 mmol) was dissolved in CH_2Cl_2 (0.2 mL). [(*t*BuXPhos)AuNCMe]BAr_4^F (15 mg, 10 μmol, 5 mol%) was added. The resulting mixture was stirred at 23 °C for 14 h. The product was isolated by silica gel column chromatography (eluent = pentane). The NMR data were in agreement with the ones previously reported in the literature.[147a]

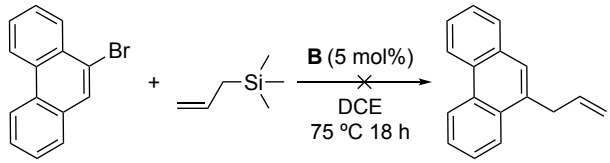

9-Bromophenanthrene (26 mg, 0.1 mmol, 1 equiv) was dissolved in DCE (0.1 mL). Allyltrimethylsilane (32 μL, 0.2 mmol, 2 equiv) was added, followed by [(*t*BuXPhos)AuNCMe]BAr_4^F (7.6 mg, 5 μmol, 5 mol%). The reaction was stirred at 75 °C for 18 h. The crude was allowed to cool to room temperature and analyzed by ^{1}H NMR. No reaction was detected.

Mechanistic Studies with Gold Complexes K1-3 (L = *t*BuXPhos)

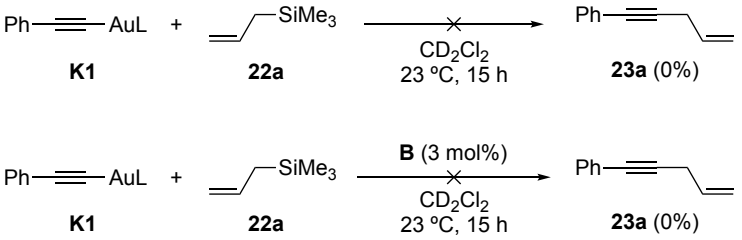

σ-(Phenylacetylene)gold(I) complex **K1** (30 mg, 42 μmol, 1 equiv) was dissolved in CD_2Cl_2 (0.1 mL). Allyltrimethylsilane (13 μL, 83 μmol, 2 equiv) was added, followed (or not) by [(*t*BuXPhos)AuNCMe]BAr_4^F (1.9 mg, 1.2 μmol, 3 mol%). The mixture was stirred at 23 °C for 15 h. Mesitylene (5 μL) was added as internal standard and the crude was analyzed by ^{1}H and ^{31}P NMR. No reaction was detected.

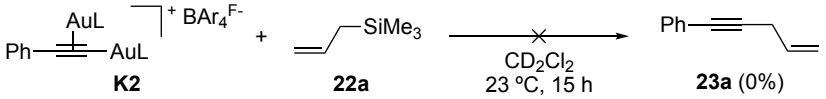

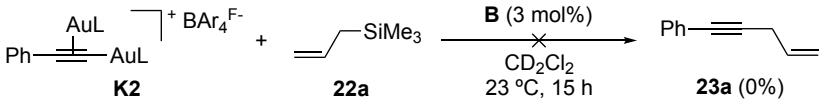

σ,π-(Phenylacetylene)digold(I) complex **K2** (30 mg, 13 μmol, 1 equiv) was dissolved in CD_2Cl_2 (0.1 mL). Allyltrimethylsilane (4.3 μL, 27 μmol, 2 equiv) was added, followed (or not) by [(*t*BuXPhos)AuNCMe]BAr_4^F (0.6 mg, 0.4 μmol, 3 mol%). The mixture was stirred at 23 ºC for 15 h. Mesitylene (5 microL) was added as internal standard and the crude was analyzed by ^1H and ^{31}P NMR. No reaction was detected.

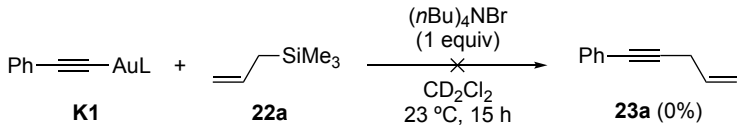

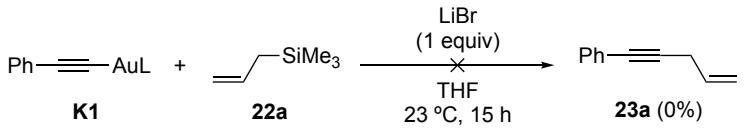

σ-(Phenylacetylene)gold(I) complex **K1** (6 mg, 8.3 μmol, 1 equiv), allyltrimethylsilane (4 μL, 25 μmol, 3 equiv) and tetra-*n*-butylammonium bromide (3 mg, 8.3 μmol, 1 equiv) or LiBr (0.7 mg, 8.3 μmol, 1 equiv) were dissolved in CD_2Cl_2 or THF (5 μL), respectively. The mixture was stirred at 23 °C for 16 h. The crude was analyzed by NMR. No reaction was detected.

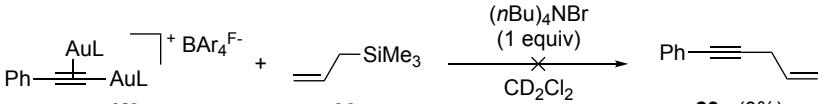

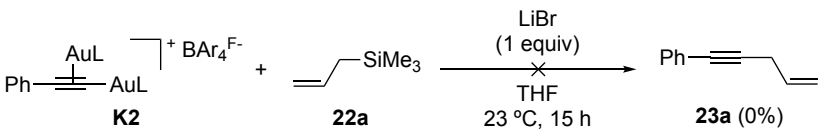

σ,π-(Phenylacetylene)digold(I) complex **K2** (6 mg, 2.7 μmol, 1 equiv), allyltrimethylsilane (1.3 μL, 8.1 μmol, 3 equiv) and tetra-*n*-butylammonium bromide (1 mg, 2.7 μmol, 1 equiv)

or LiBr (0.2 mg, 2.7 μmol, 1 equiv) were dissolved in CD_2Cl_2 or THF (5 μL), respectively. The mixture was stirred at 23 °C for 16 h. The crude was analyzed by NMR. No reaction was detected.

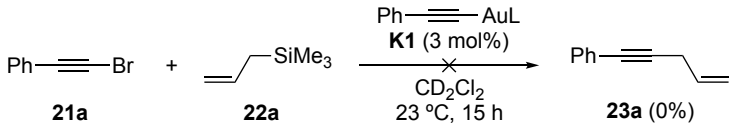

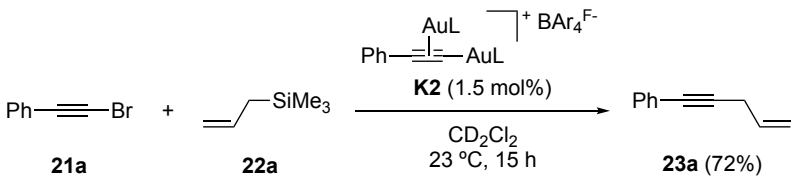

(Bromoethynyl)benzene (36 mg, 0.2 mmol, 1 equiv) was dissolved in CD_2Cl_2 (0.2 mL). Allyltrimethylsilane (64 μL, 0.4 mmol, 2 equiv) was added, followed by *σ*-(phenylacetylene)gold(I) complex **K1** (4.34 mg, 6 μmol, 3 mol%) or *σ,π*-(phenylacetylene)digold(I) complex **K2 (**6.7 mg, 3 μmol, 1.5 mol%). The mixture was stirred at 23 °C for 15 h. Mesitylene (10 μL) was added as internal standard and the crude was analyzed by ^{1}H and ^{31}P NMR. Reaction was detected only in the case of using *σ,π*-(phenylacetylene)digold(I) complex **K2**, in which the 1,4-enyne **23a** was formed in 72% yield.

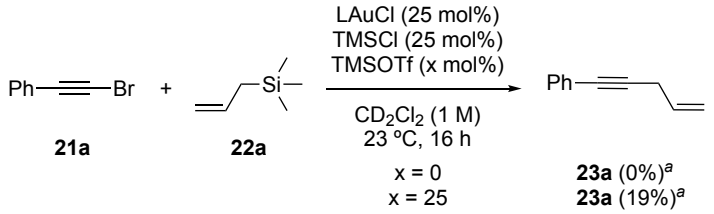

(Bromoethynyl)benzene (36 mg, 0.2 mmol, 1 equiv) was dissolved in dry CD_2Cl_2 (0.2 mL). Allyltrimethylsilane (64 μL, 0.4 mmol, 2 equiv) was added followed by LAuCl complex **K3** (33 mg, 0.05 mmol, 25 mol%) and chlorotrimethylsilane (6.4 μL, 0.05 mmol, 25 mol%). The resulting mixture was stirred at 23 °C for 16 h. No reaction was detected by NMR. Trimethylsilyl trifluoromethanesulfonate (9 μL, 0.05 mmol, 25 mol%) was added and the reaction mixture was stirred 18 h. Mesitylene (10 microL) was added as internal standard

and the crude was analyzed by NMR. The product was formed in 19% yield according to ^{1}H NMR.

^{13}C Labeling Experiments

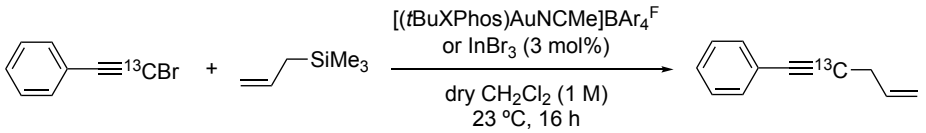

^{13}C-Labeled (bromoethynyl)benzene (36 mg, 0.2 mmol, 1 equiv) was dissolved in dry CH_2Cl_2 (0.2 mL, 1 M). Allyltrimethylsilane (64 μL, 0.4 mmol, 2 equiv) was added, followed by the catalyst (3 mol%, method A: 9 mg of [(*t*BuXPhos)AuNCMe]BAr_4^F or method B: 2 mg of $InBr_3$). The resulting mixture was stirred at 23 ºC for 16 h. The crude was directly subjected to silica gel column chromatography (eluent = pentane) to obtain the pure ^{13}C-labeled 1,4-enyne (colorless oil, method A: 20 mg, 71%; method B: 19 mg, 68%). **^{13}C-Labeled (bromoethynyl)benzene: ^{13}C NMR** (101 MHz, $CDCl_3$) δ 132.0 (d, *J* = 3.5 Hz, 2C), 128.7 (d, *J* = 1.3 Hz), 128.3 (2C), 122.7 (d, *J* = 13.7 Hz), 80.1 (d, *J* = 203.0 Hz), 49.7. **^{13}C-Labeled pent-4-en-1-yn-1-ylbenzene: ^{13}C NMR** (101 MHz, $CDCl_3$) δ 132.4 (d, *J* = 2.1 Hz), 131.6 (d, *J* = 1.8 Hz, 2C), 128.2 (d, *J* = 5.5 Hz, 2C), 127.7 (d, *J* = 1.7 Hz), 123.7 (d, *J* = 90.7 Hz), 116.2, 86.2 (d, *J* = 71.7 Hz), 82.9, 23.7 (d, *J* = 11.2 Hz). The signal at 127.0 in the ^{13}C NMR spectrum corresponds to a ^{13}C-labeled impurity.

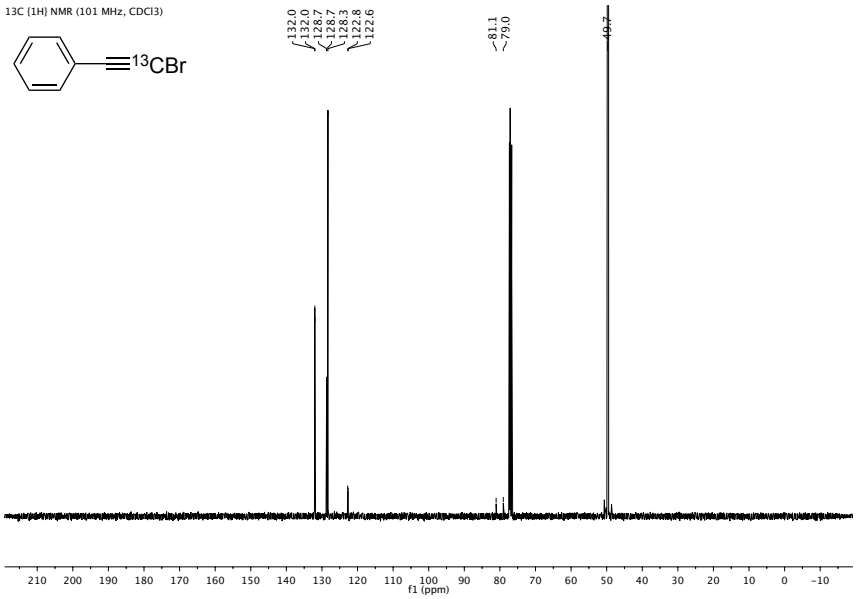

1D INADEQUATE (SELINQUATE) experiment

We performed a 1D INADEQUATE (SELINQUATE) experiment, irradiating the C(sp^3), to assign each alkynyl signal.

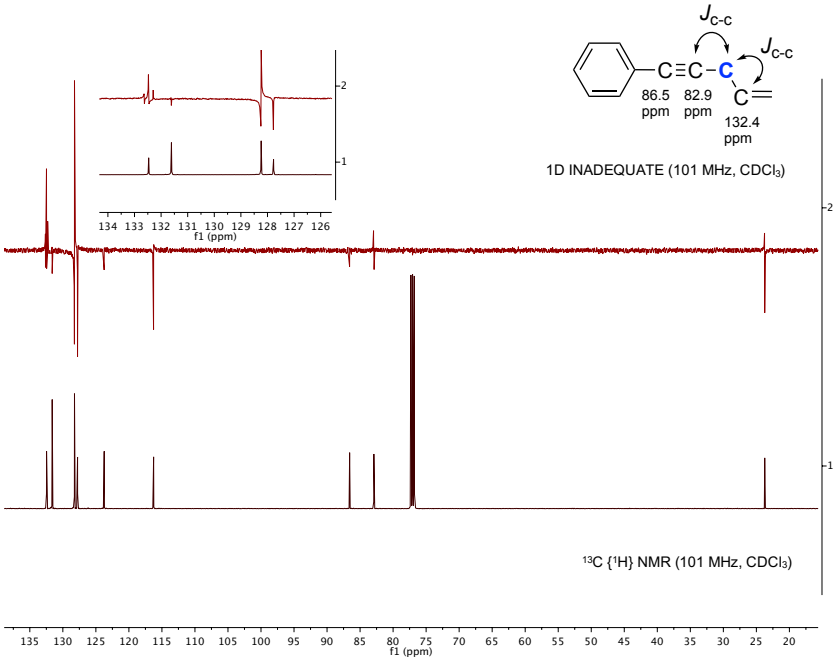

1D INADEQUATE (101 MHz, $CDCl_3$)

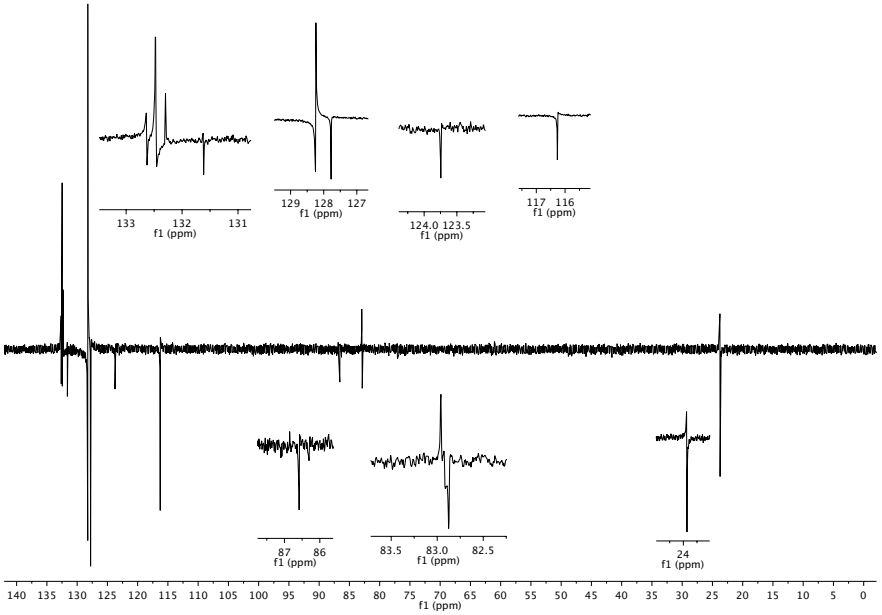

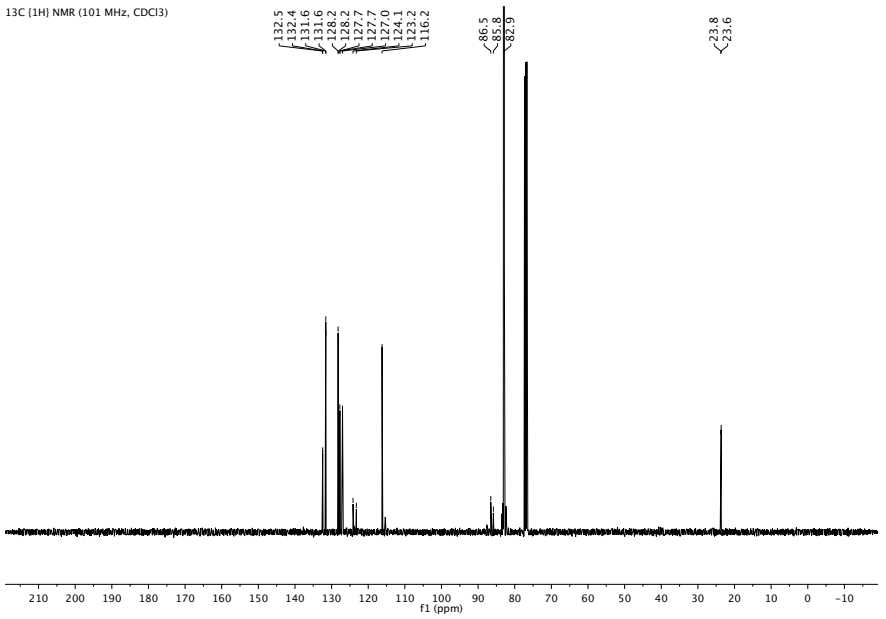

General HTE Procedure for the Enantioselective Reactions

Experiments were set inside a glovebox under a nitrogen atmosphere. Screening reaction was carried out in 0.75 mL glass vials (8x30mm) in 24- or a 96-well aluminum block (equipment available from Analytical Sales and Services). Chemicals were dosed using multi-channel or single-channel pipettors as a solution.

Previously to the experiment a library of predosed chiral ligands was prepared (each vial containing 2 μmol for monodentate ligands or 1 μmol for bidentate ligands). The ligands were added to the reaction vials as a solution in dry and degassed THF or DCE using multichannel pippetors. The solvent was removed to dryness using a GeneVac.

The glass vials (0.75 mL, 8x30mm) with the predosed chiral ligands were charged into a 96-well aluminum block. Then (dimethylsulfide)gold(I) chloride (1.95 μmol/reaction) was dosed in DCE (50 μL). After 30 min the solvent was removed to dryness using a GeneVac and a parylene coated stir bar was then added to each reaction vial.

(Bromoethynyl)benzene (25 μmol/reaction) and cinnamyltrimethylsilane (50 μmol/reaction) were then dosed together into each reaction vial as a solution in DCE (50 μL). $NaBAr_4^F$ (2 μmol for monodentate ligands, 1 or 2 μmol for bidentate ligands) were

then dosed to the corresponding vial as a solution in DCE (50 μL). The reaction volume is 100 μL. The 96-well plate was then sealed and stirred at 23 ºC for 16 h.

Upon opening the plate to air, a solution of 4,4′-dimethylbiphenyl as internal standard (30 μmol/reaction) in acetonitrile (400 μL) was added into each vial to measure UPLC yields. The plate was covered again and the vials stirred to ensure good homogenization. After stirring, the plate was centrifuged for 20 min in order that all the insoluble will settle to the bottom of the vial. Into a separate 96-well LC block was added 500 μL of acetonitrile, followed by 10 μL of the diluted reaction mixtures. The LC block was then sealed with a silicon-rubber storage mat and mounted on an automated UPLC instrument for analysis. The reactions that gave some desired product were analyzed by UPC^2 in order to determine the ee.

Based on this general procedure, different reaction conditions were screened by changing the metal source ((dimethylsulfide)gold(I) chloride or indium(III) source), the solvent (instead of DCE) and the chloride abstractor (instead of $NaBAr_4^F$, if required).

Theoretical DFT Calculations

Computational Methods

The computational methods used in the studies of this **Chapter 3** are identical than the ones explained in the Experimental Part of the **Chapter 1**, except from the basis set for Au. In this case, Au was described by ECP with the LANL2DZ basis set with an additional polarization function ($\zeta_f = 1.050$).[185]

Computed Structures and Energies

Reaction of 21a with 22a

$AuPMe_3$

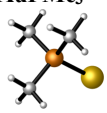

E = -596.285531 Hartrees
G = -596.206222 Hartrees

21a

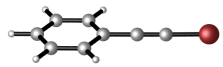

E = -320.690177 Hartrees
G = -320.624009 Hartrees

185. Ehlers, A.; Böhme, M.; Dapprich, S.; Gobbi, A.; Höllwarth, A.; Jonas, V.; Köhler,K.; Stegmann, R.; Veldkamp, A.; Frenking, G. *Chem. Phys. Lett.* **1993**, *208*, 111−114.

22a

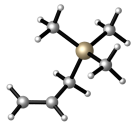

E = -526.337057 Hartrees
G = -526.192697 Hartrees

Int1

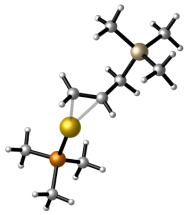

E = -1122.666956 Hartrees
G = -1122.422385 Hartrees

Int2a

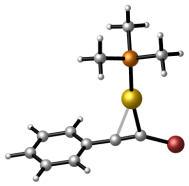

E = -917.005188 Hartrees
G = -916.839399 Hartrees

Int3a

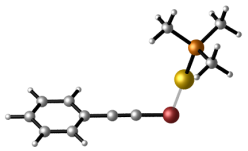

E = -916.983388 Hartrees
G = -916.818782 Hartrees

$TS_{1\text{-}4a}$

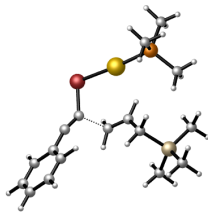

E = -1443.302569 Hartrees
G = -1442.967944 Hartrees

Int4a

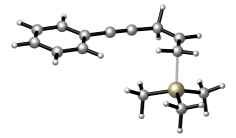

E = -833.734326 Hartrees
G = -833.495116 Hartrees

Int5

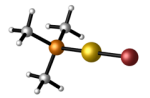

E = -609.661436 Hartrees
G = -609.585184 Hartrees

$TS_{2a\text{-}6a}$

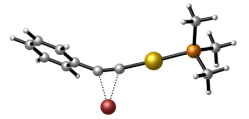

E = -916.972001 Hartrees
G = -916.807066 Hartrees

Int6a

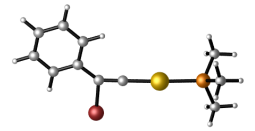

E = -916.974224 Hartrees
G = -916.810155 Hartrees

$TS_{2a\text{-}7a}$

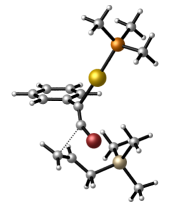

E = -1443.332051 Hartrees
G = -1442.999147 Hartrees

Int7a

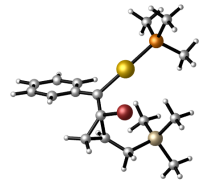

E = -1443.388523 Hartrees
G = -1443.046143 Hartrees

TS_{2a-7b}

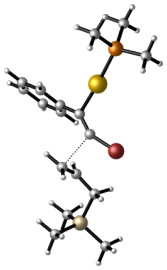

E = -1443.332906 Hartrees
G = -1443.003499 Hartrees

Int7b

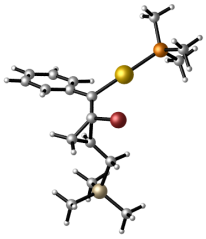

E = -1443.385638 Hartrees
G = -1443.050019 Hartrees

TS_{2a-7c}

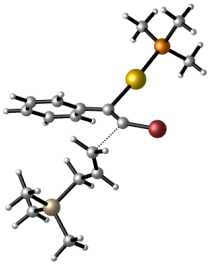

E = -1443.332322 Hartrees
G = -1442.999974 Hartrees

Int7c

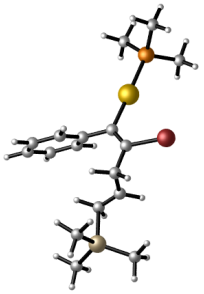

E = -1443.383649 Hartrees
G = -1443.046384 Hartrees

TS_{7b-7a}

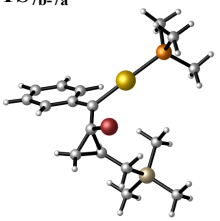

E = -1443.381372 Hartrees
G = -1443.041744 Hartrees

TS_{7c-7a}

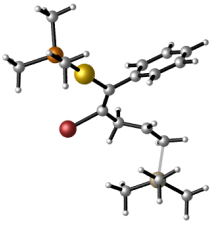

E = -1443.377199 Hartrees
G = -1443.036555 Hartrees

TS_{2a-8a}

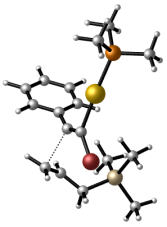

E = -1443.341615 Hartrees
G = -1443.006714 Hartrees

Int8a

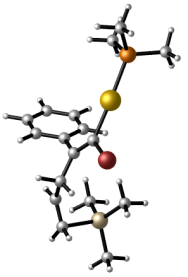

E = -1443.388423 Hartrees
G = -1443.050093 Hartrees

TS_{2a-8b}

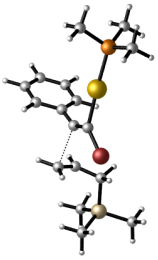

E = -1443.341355 Hartrees
G = -1443.010038 Hartrees

Int8b

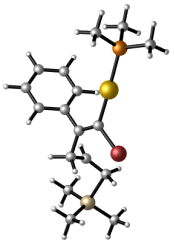

E = -1443.389057 Hartrees
G = -1443.051952 Hartrees

TS_{2a-8c}

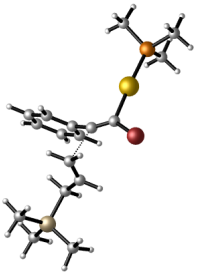

E = -1443.345029 Hartrees
G = -1443.011914 Hartrees

Int8c

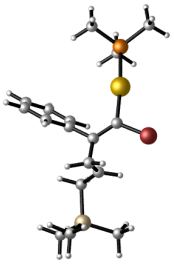

E = -1443.392267 Hartrees
G = -1443.052591 Hartrees

TS_{8b-8a}

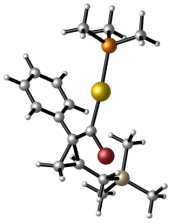

E = -1443.378962 Hartrees
G = -1443.038141 Hartrees

TS_{8a-9a}

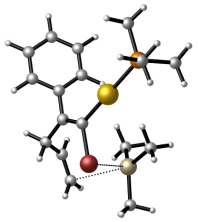

E = -1443.360667 Hartrees
G = -1443.021300 Hartrees

Int9a

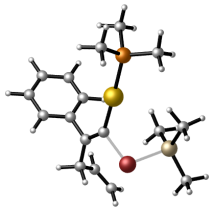

E = -1443.387853 Hartrees
G = -1443.051538 Hartrees

TS_{9a-10a}

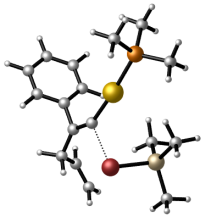

E = -1443.386079 Hartrees
G = -1443.047769 Hartrees

Int10a

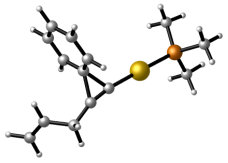

E = -1021.052307 Hartrees
G = -1020.818080 Hartrees

$TS_{10a-11a}$

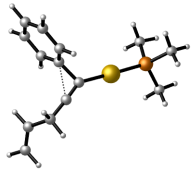

E = -1021.044896 Hartrees
G = -1020.811813 Hartrees

$TS_{10a-12a}$

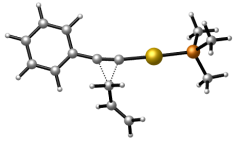

E = -1021.038332 Hartrees
G = -1020.801922 Hartrees

Int11a and Int12a

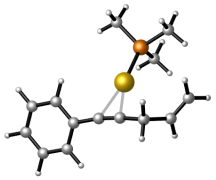

E = -1021.088724 Hartrees
G = -1020.854108 Hartrees

TS_{8a-13a}

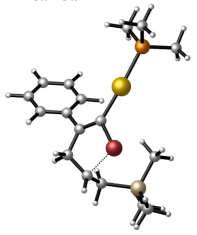

E = -1443.380179 Hartrees
G = -1443.040235 Hartrees

Int13a

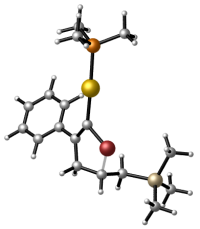

E = -1443.383549 Hartrees
G = -1443.042177 Hartrees

$TS_{13a-14a}$

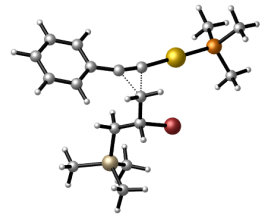

E = -1443.360906 Hartrees
G = -1443.023592 Hartrees

Int14a

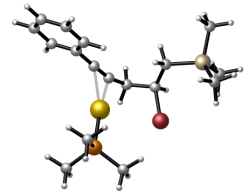

E = -1443.414971 Hartrees
G = -1443.077192 Hartrees

Int15a

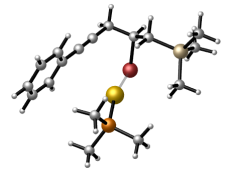

E = -1443.414110 Hartrees
G = -1443.075077 Hartrees

TS_{15a-4a}

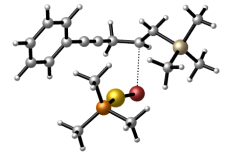

E = -1443.400975 Hartrees
G = -1443.061044 Hartrees

Int16a

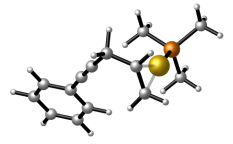

E = -1021.094438 Hartrees
G = -1020.856693 Hartrees

TMSBr

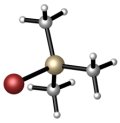

E = -422.327535 Hartrees
G = -422.249984 Hartrees

Br^-
E = -13.283606 Hartrees
G = -13.299781 Hartrees

$TS_{14a-12a}$

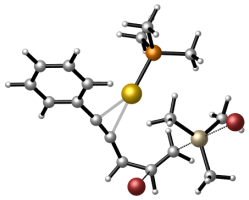

E = -1456.682609 Hartrees
G = -1456.345086 Hartrees

Int17a

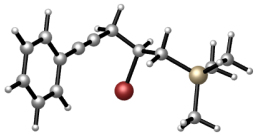

E = -847.091351 Hartrees
G = -846.855114 Hartrees

$TS_{17a-23a}$

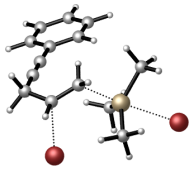

E = -860.349334 Hartrees
G = -860.115123 Hartrees

23a

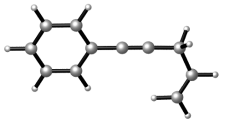

E = -424.766500 Hartrees
G = -424.631895 Hartrees

Reaction of 21a with 41

41

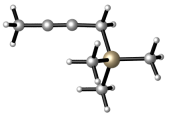

E = -564.387032 Hartrees
G = -564.241172 Hartrees

TS_{2a-8d}

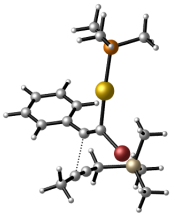

E = -1481.391748 Hartrees
G = -1481.054316 Hartrees

Int8d

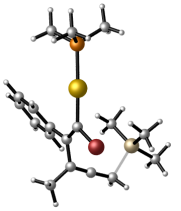

E = -1481.432528 Hartrees
G = -1481.090734 Hartrees

TS_{8d-13d}

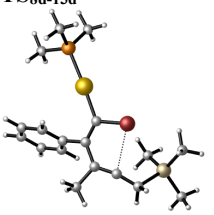

E = -1481.427478 Hartrees
G = -1481.083937 Hartrees

Int13d

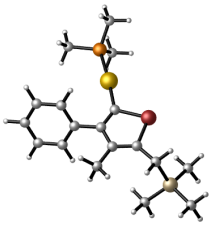

E = -1481.449902 Hartrees
G = -1481.107361 Hartrees

TS_{13d-18}

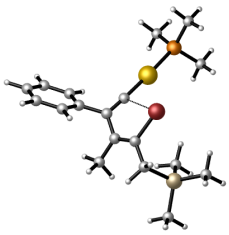

E = -1481.427435 Hartrees
G = -1481.086205 Hartrees

Int18

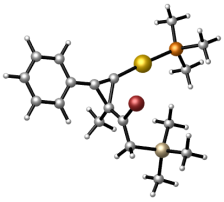

E = -1481.452853 Hartrees
G = -1481.109156 Hartrees

TS_{18-14d}

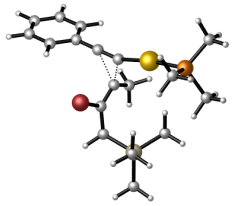

E = -1481.442452 Hartrees
G = -1481.095966 Hartrees

Int14d

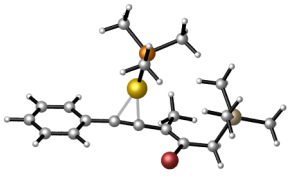

E = -1481.479477 Hartrees
G = -1481.134288 Hartrees

Reaction of 34a with 22a

Int2e

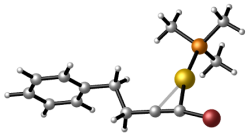

E = -995.565187 Hartrees
G = -995.347107 Hartrees

TS_{2e-6e}

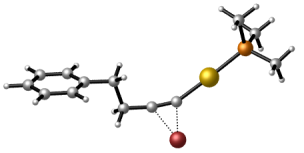

E = -995.532868 Hartrees
G = -995.315255 Hartrees

Int6e

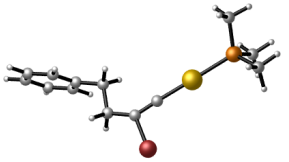

E = -995.536834 Hartrees
G = -995.319683 Hartrees

TS_{2e-7e}

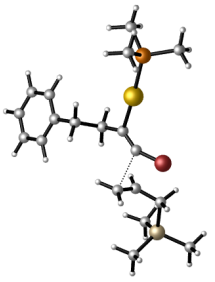

E = -1521.894316 Hartrees
G = -1521.509162 Hartrees

Int7e

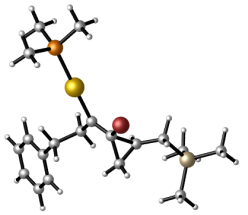

E = -1521.946050 Hartrees
G = -1521.554744 Hartrees

TS_{2e-8e}

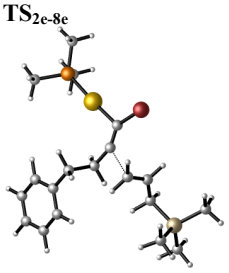

E = -1521.902552 Hartrees
G = -1521.517107 Hartrees

Int8e

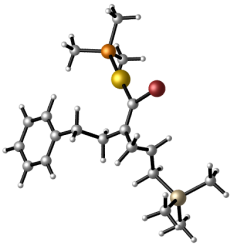

E = -1521.954258 Hartrees
G = -1521.562363 Hartrees

TS_{2e-19}

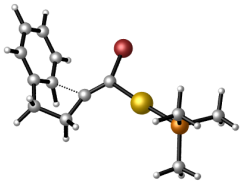

E = -995.538878 Hartrees
G = -995.318382 Hartrees

Int19

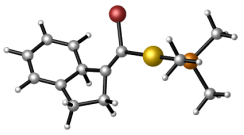

E = -995.557427 Hartrees
G = -995.334676 Hartrees

TS_{2e-20}

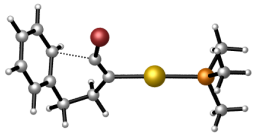

E = -995.542198 Hartrees
G = -995.320466 Hartrees

Int20

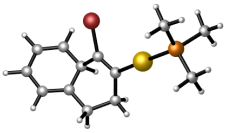

E = -995.557517 Hartrees
G = -995.335046 Hartrees

TS_{8e-13e}

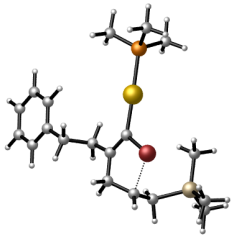

E = -1521.941067 Hartrees
G = -1521.548723 Hartrees

Int13e

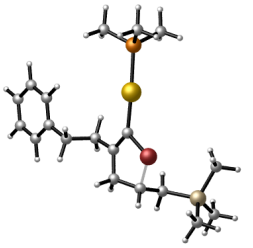

E = -1521.944641 Hartrees
G = -1521.551452 Hartrees

$TS_{13e-14e}$

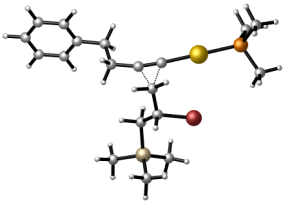

E = -1521.922887 Hartrees
G = -1521.533559 Hartrees

Int14e

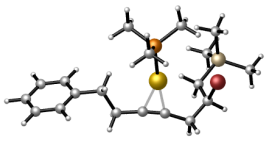

E = -1521.976039 Hartrees
G = -1521.582068 Hartrees

Int15e

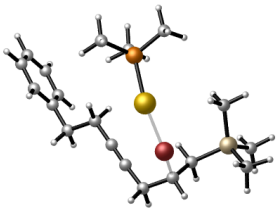

E = -1521.970376 Hartrees
G = -1521.577136 Hartrees

TS_{15e-4e}

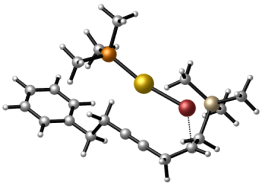

E = -1521.958979 Hartrees
G = -1521.567320 Hartrees

Int4e

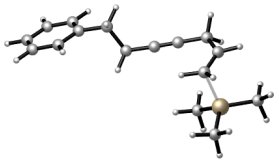

E = -912.293076 Hartrees
G = -912.002835 Hartrees

Int16e

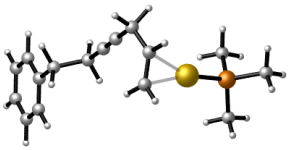

E = -1099.651987 Hartrees
G = -1099.363607 Hartrees

$TS_{13e-21e}$

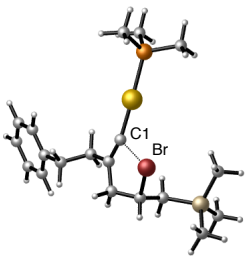

Frozen distance: d(C1−Br) = 2.56 Å.

E = -1521.940598 Hartrees
G = -1521.550227 Hartrees

Int21e

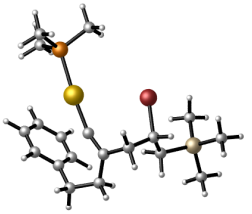

E = -1521.943863 Hartrees
G = -1521.550433 Hartrees

TS_{21e-22}

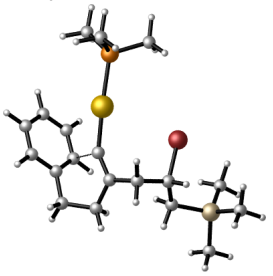

E = -1521.942163 Hartrees
G = -1521.549526 Hartrees

Int22

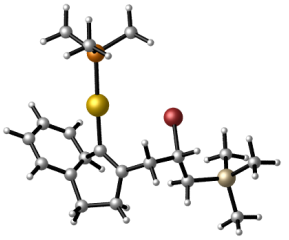

E = -1521.951195 Hartrees
G = -1521.556609 Hartrees

TS_{22-23}

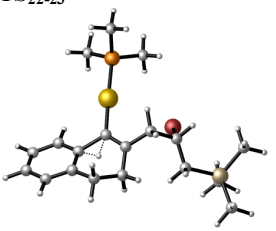

E = -1521.936015 Hartrees
G = -1521.542864 Hartrees

Int23

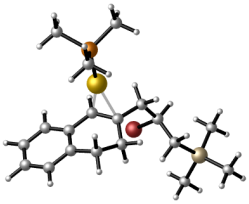

E = -1522.034490 Hartrees
G = -1521.637645 Hartrees

Int24

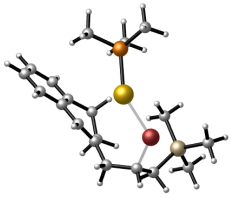

E = -1522.029035 Hartrees
G = -1521.626855 Hartrees

TS_{24-25}

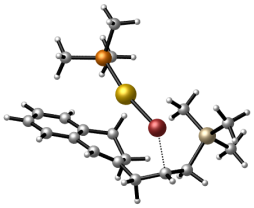

E = -1522.022227 Hartrees
G = -1521.621962 Hartrees

Int25

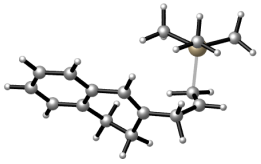

E = -912.356970 Hartrees
G = -912.057942 Hartrees

Int26

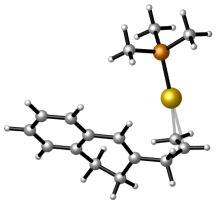

E = -1099.715837 Hartrees
G = -1099.418224 Hartrees

Int12e

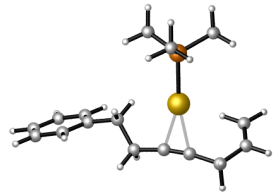

E = -1099.649521 Hartrees
G = -1099.362657 Hartrees

TS_{12e-27}

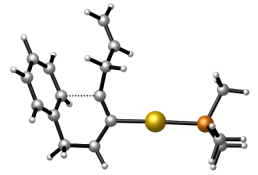

E = -1099.619856 Hartrees
G = -1099.329415 Hartrees

Int27

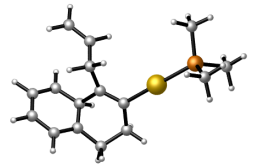

E = -1099.624288 Hartrees
G = -1099.332671 Hartrees

TS_{27-28}

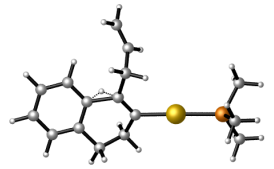

E = -1099.604921 Hartrees
G = -1099.314990 Hartrees

Int28

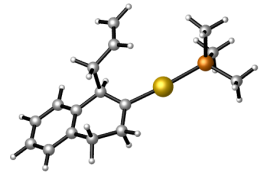

E = -1099.653817 Hartrees
G = -1099.360521 Hartrees

TS_{28-29}

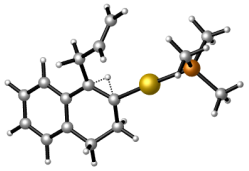

E = -1099.644620 Hartrees
G = -1099.353660 Hartrees

Int29

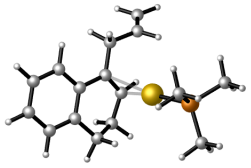

E = -1099.710922 Hartrees
G = -1099.415583 Hartrees

TS_{28-32}

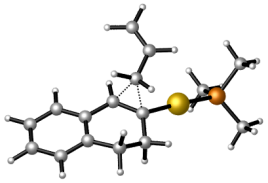

E = -1099.644054 Hartrees
G = -1099.350297 Hartrees

TS_{12e-30}

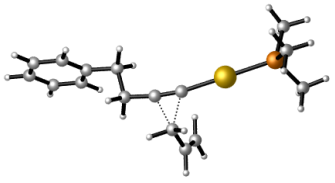

E = -1099.600881 Hartrees
G = -1099.316590 Hartrees

Int30

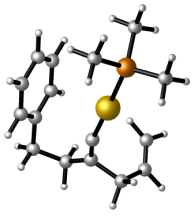

E = -1099.619867 Hartrees
G = -1099.330879 Hartrees

TS_{30-31}

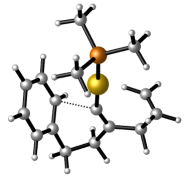

E = -1099.617033 Hartrees
G = -1099.326884 Hartrees

Int31

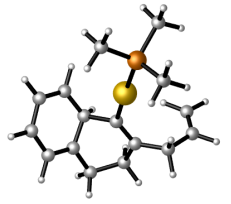

E = -1099.626658 Hartrees
G = -1099.335942 Hartrees

TS_{31-32}

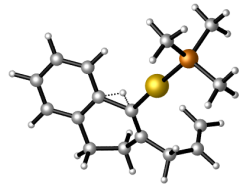

E = -1099.612118 Hartrees
G = -1099.323074 Hartrees

Int32

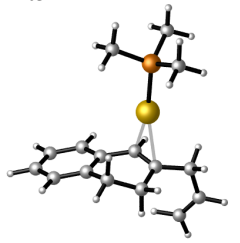

E = -1099.711919 Hartrees
G = -1099.416980 Hartrees

Cyclization of 1-Bromo-1,6-enynes

Int2f

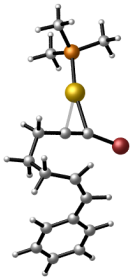

E = -1112.178583 Hartrees
G = -1111.900253 Hartrees

TS_{2f-8f}

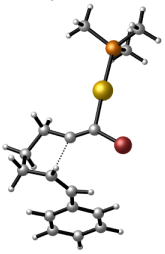

E = -1112.169439 Hartrees
G = -1111.890997 Hartrees

Int8f

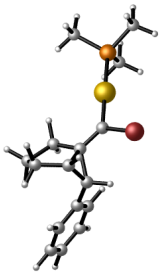

E = -1112.214437 Hartrees
G = -1111.932123 Hartrees

TS_{8f-13f}

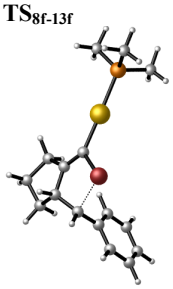

E = -1112.203238 Hartrees
G = -1111.919938 Hartrees

Int13f

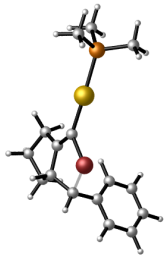

E = -1112.203418 Hartrees
G = -1111.921250 Hartrees

$TS_{13f-21f}$

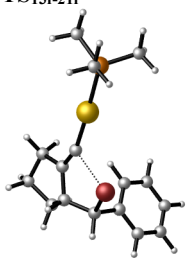

E = -1112.200428 Hartrees
G = -1111.917490 Hartrees

Int21f

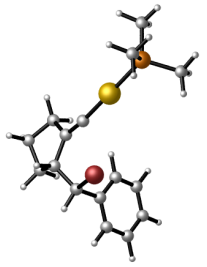

E = -1112.201022 Hartrees
G = -1111.920020 Hartrees

TS_{21f-33}

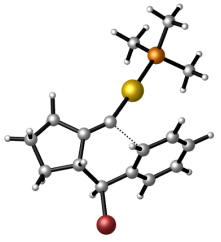

E = -1112.200078 Hartrees
G = -1111.917848 Hartrees

Int33

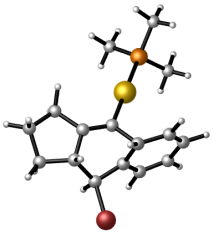

E = -1112.210068 Hartrees
G = -1111.926307 Hartrees

TS_{33-34}

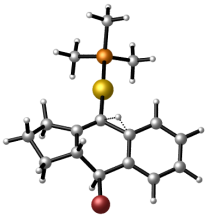

E = -1112.193675 Hartrees
G = -1111.911351 Hartrees

Int34

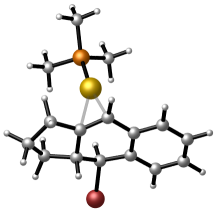

E = -1112.293826 Hartrees
G = -1112.007327 Hartrees

UNIVERSITAT ROVIRA I VIRGILI
GOLD-CATALYZED INTERMOLECULAR REACTIONS OF ALKYNES WITH ALKENES: NOVEL REACTIVITIES AND GLOBAL MECHANISTIC PICTURE
María Elena de Orbe Izquierdo

General Conclusions

In this Doctoral Thesis, the gold(I)-catalyzed intermolecular reactions of diverse alkynes with alkenes were studied experimentally and computationally.

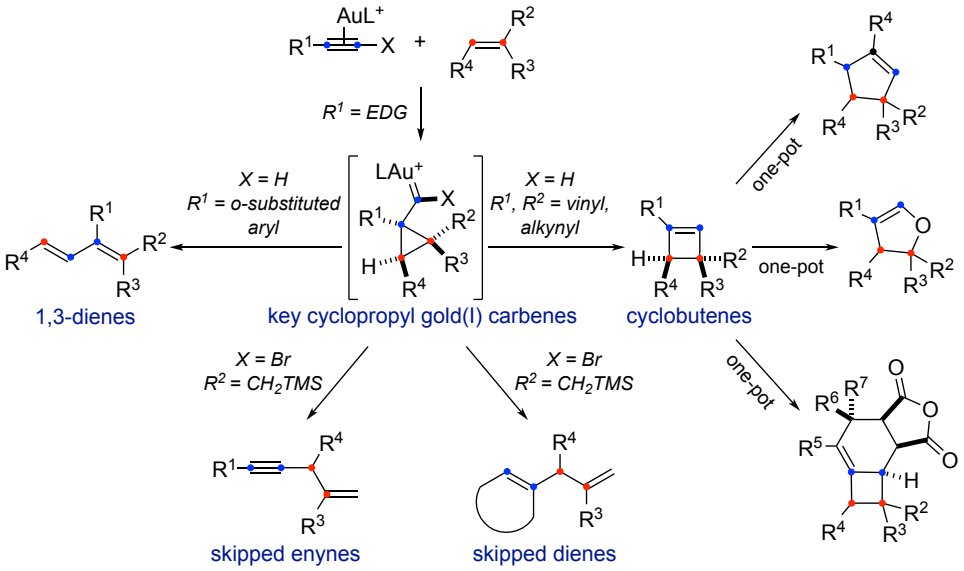

The main conclusions of this work are as follows:

- The *o*-substituted arylalkynes react with alkenes leading to 1,3-dienes in a metathesis-type process, whereas less sterically hindered 1,3-butadiynes undergo [2+2] cycloaddition with alkenes to give rise exclusively to cyclobutenes. DFT calculations showed that the key intermediates of these transformations are cyclopropyl gold(I) carbenes, in which steric and electronic effects determine their evolution *via* divergent pathways close in energy. From this common intermediate, 1,3-dienes are generated by a stepwise 1,3-migration of the less substituted carbon of the alkene, while cyclobutenes are formed by ring expansion through the more substituted carbon of the alkene. The involvement of the cyclopropyl gold(I) carbenes was demonstrated by their independent generation by the gold(I)-catalyzed retro-Buchner reaction. Moreover, we have accomplished the first intermolecular reaction of acetylene with an alkene catalyzed by gold(I).

- The scope of the gold(I)-catalyzed [2+2] cycloaddition of alkynes with alkenes was extended to 1-vinyl-, 3-vinyl-, and 3-alkynylcyclobutenes. This methodology is complementary to the other previously reported metal-catalyzed [2+2] cycloadditions to form 1-vinylcyclobutenes. Furthermore, one-pot processes have been developed to convert cyclobutenes into distinct frameworks such as highly substituted cyclopentenes, 2,3-dihydrofurans, and more complex polycyclic structures.
- The gold(I)-catalyzed intermolecular reactions of bromoalkynes with allylsilanes gives rise to skipped enynes *via* a cross-coupling type process or skipped dienes *via* allylation/cyclization cascade. Based on experimental mechanistic studies and DFT calculations, an unprecedented rearrangement was proposed to be responsible of these novel reactivities. Simple indium salts were also found to be efficient catalysts for some of these transformations.

Appendix

UNIVERSITAT ROVIRA I VIRGILI
GOLD-CATALYZED INTERMOLECULAR REACTIONS OF ALKYNES WITH ALKENES: NOVEL REACTIVITIES AND GLOBAL MECHANISTIC PICTURE
María Elena de Orbe Izquierdo

ACS Catalysis

Research Article

Cite This: ACS Catal. 2018, 8, 2166−2172

pubs.acs.org/acscatalysis

Broad-Scope Rh-Catalyzed Inverse-Sonogashira Reaction Directed by Weakly Coordinating Groups

Eric Tan,[†,§] Ophélie Quinonero,[†,§] M. Elena de Orbe,[†] and Antonio M. Echavarren*[,†,‡]

[†]Institute of Chemical Research of Catalonia (ICIQ), Barcelona Institute of Science and Technology, Av. Països Catalans 16, 43007 Tarragona, Spain

[‡]Departament de Química Orgànica i Analítica, Universitat Rovira i Virgili, C/Marcel·lí Domingo s/n, 43007 Tarragona, Spain

Supporting Information

ABSTRACT: We report the alkynylation of C(sp^2)−H bonds with bromoalkynes (inverse-Sonogashira reaction) directed by synthetically useful ester, ketone, and ether groups under rhodium catalysis. Other less common directing groups such as amine, thioether, sulfoxide, sulfone, phenol ester, and carbamate are also suitable directing groups. Mechanistic studies indicate that the reaction proceeds by a turnover-limiting C−H activation step via an electrophilic-type substitution.

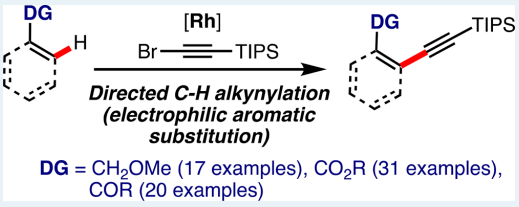

KEYWORDS: *alkynylation, rhodium catalysis, C−H functionalization, inverse Sonogashira, metallacycle, Hammett correlation, DFT*

INTRODUCTION

Alkynes are among the most versatile functional groups[1] and are widely present in natural products,[2] drugs,[3] and organic materials.[4] The chemistry of alkynes has gained particular momentum in recent years by the discovery of a wide variety of catalytic transformations triggered by gold(I), platinum(II), and other alkynophilic Lewis acids.[5] Therefore, the development of methods for the introduction of alkyne groups onto organic molecules is of high importance. To this end, the Sonogashira coupling reaction is the most general method for the formation of C(sp)−C(sp^2) bonds from aryl or alkenyl (pseudo)halides and terminal alkynes.[6]

The main limitation of the Sonogashira coupling reaction resides in the synthetic availability of the required (pseudo)-halides. An alternative approach that is better suited for the late-stage functionalization of complex molecules involves the alkynylation of C(sp^2)−H bonds with terminal alkynes or activated acetylenes such as ethynylbenziodoxolone (EBX) reagents or haloalkynes using transition-metal catalysts.[7] Often named inverse-Sonogashira coupling, this methodology relies on the reactivity of electronically activated (hetero)arenes[8] or on a chelating group to assist a C−H activation process.[9] The former strategy is restricted to aromatic C(sp^2)−H bonds, which need in addition to be acidic or electron-rich enough to undergo deprotonation or a Friedel−Crafts type reaction. The latter has been achieved for both arenes and alkenes[9b] with a variety of directing groups, typically amides or nitrogen coordinating groups such as heterocycles or imine derivatives (oxime, nitrone, azomethine).[9c] The applicability of this strategy in multistep synthesis is however limited, as in most cases the directing groups need to be installed and/or removed. Therefore, to render this approach useful, the development of new protocols using instead widely used functional groups serving as synthetic handles is highly desirable.[10]

Toward this goal, we recently reported a general peri-alkynylation of naphthols using ruthenium catalysis.[11] Benzoic acids can also be alkynylated at the ortho position,[11,12] although the use of other versatile O functionalities[13,14] as directing groups is still limited, mainly due to the challenging formation of a weakly coordinated metallacyclic intermediate.[15] In particular, despite intense efforts in the field of catalytic C(sp^2)−H functionalization, only two examples of the use of benzyl ether as a directing group have been reported in the context of C−H borylation.[16]

Here, we report the use of synthetically useful ether, ester, and ketone as directing groups for the direct alkynylation of C(sp^2)−H bonds with bromoalkynes under rhodium catalysis (Scheme 1).[17] We also demonstrate for the first time that amine,[18] thioether,[19] sulfoxide,[20] sulfone,[21] carbamate,[22] and phenol esters[23] are suitable directing groups in this transformation. Furthermore, our experimental and theoretical mechanistic study shows that this Rh-catalyzed alkynylation occurs by a turnover-determining C−H activation in which a five-membered ring metallacycle is formed by an electrophilic aromatic substitution type process.

RESULTS AND DISCUSSION

Reaction Scope. Our studies began by evaluating the reactions of TIPS-protected bromoacetylene (**1**) with ethyl benzoate (**2a**) and benzyl methyl ether (**4a**). We discovered that a combination of [Cp*RhCl$_2$]$_2$ (2.5 mol %), AgSbF$_6$ (20

Received: December 20, 2017
Revised: January 23, 2018
Published: January 29, 2018

DOI: 10.1021/acscatal.7b04395
ACS Catal. 2018, 8, 2166−2172

Scheme 1. C(sp²)−H Alkynylation with Bromoalkynes Directed by a Broad Range of Coordinating Groups under Rhodium Catalysis

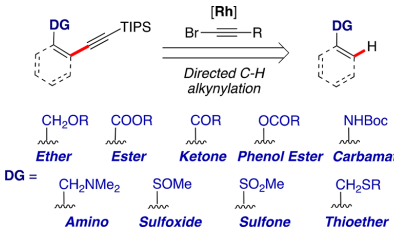

mol %), Ag_2CO_3 (1 equiv), and LiOAc (20 mol %) in 1,2-dichloroethane (DCE) at 45 °C provided **3a** in 69% yield (Table 1, entry 1). Control experiments showed the essential role of all reaction components (Table 1, entries 2−11). Thus, lower yields of **3a** were obtained at temperatures lower or higher than 45 °C (Table 1, entries 2 and 3). Similar results were obtained by decreasing the amount of Ag_2CO_3 to 0.5 equiv or replacing this silver salt by K_2CO_3 (Table 1, entries 4 and 5). Solvents different from DCE led to poor results (Table 1, entries 6−11). The use of other bromoalkynes, such as (bromoethynyl)benzene and 1-bromooctyne, led to no conversion.[24]

Although treatment of benzyl methyl ether (**4a**) with bromoacetylene **1** under essentially the same conditions did not lead to the product of alkynylation (Table 1, entry 12), simply increasing the temperature to 100 °C led to **5a** in 64% yield (Table 1, entry 13). Using ethynyltriisopropylsilane instead of **1** did not afford **5a** (Table 1, entry 23). Replacing $[Cp^*RhCl_2]_2$ with other metal catalysts typically used in C−H functionalization did not lead to alkynylated product (Table 1, entries 24−26). The alternative hydroxy-directed alkynylation of primary, secondary, or tertiary benzyl alcohol led to oxidation, decomposition, or unproductive reaction.

Different alkyl benzoates **2a−d** could be ortho-alkynylated, with ethyl benzoate **2a** giving the highest yield (Scheme 2). Electron-donating alkyl or methoxy groups and electron-withdrawing substituents such as NO_2, CF_3, and different

Table 1. Rh-Catalyzed *o*-C−H Alkynylation of Ethyl Benzoate and Benzyl Methyl Ether: Optimization Conditions[24]

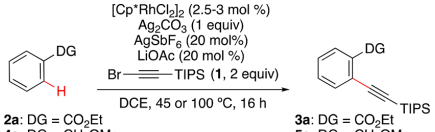

entry	DG	variation from the "standard conditions"[a]	yield (%)[b]
1	ester	none	58−69
2	ester	at 25 °C[c]	35
3	ester	at 65 °C[c]	16
4	ester	with Ag_2CO_3 (0.5 equiv)[d]	41
5	ester	with K_2CO_3 (1 equiv)[d]	5
6	ester	in dichloromethane[e]	8−14
7	ester	in toluene[e]	0
8	ester	in *t*-AmOH[e]	0
9	ester	in Et_2O[e]	4
10	ester	in EtOAc[e]	18
11	ester	in MeOH[e]	0
12	ether	none	0
13	ether	at 100 °C[c]	50−64
14	ether	without $[Cp^*RhCl_2]_2$	0
15	ether	without Ag_2CO_3	0
16	ether	without LiOAc	0
17	ether	without $AgSbF_6$	0
18	ether	with AgOAc (1.2 equiv)[f]	<1.5
19	ether	AgOAc (1 equiv) + Ag_2CO_3 (0.2 equiv)[g]	12
20	ether	in toluene[e]	0
21	ether	in *tert*-amOH[e]	0
22	ether	in 1,4-dioxane[e]	0
23	ether	with TIPS-acetylene[h]	0
24	ether	with $[Cp^*IrCl_2]_2$[i]	0
25	ether	with $Pd(OAc)_2$[i]	0
26	ether	with $[RuCl_2(p\text{-cymene})]_2$[i]	<3

[a]Standard reaction conditions: **2a** or **4a** (0.2 mmol), **1** (2 equiv), $[Cp^*RhCl_2]_2$ (2.5 mol % for DG = ester, 3 mol % for DG = ether), Ag_2CO_3 (1 equiv), $AgSbF_6$ (0.2 equiv), LiOAc (0.2 equiv), DCE, 16 h, 45 °C. [b]Yield of the monoalkynylated product determined by ^1H NMR using bromomesitylene as internal standard. [c]Instead of 45 °C. [d]Instead of Ag_2CO_3 (1 equiv). [e]Instead of DCE. [f]Instead of Ag_2CO_3 and LiOAc. [g]Without LiOAc. [h]Instead of **1**. [i]Instead of $[Cp^*RhCl_2]_2$.

Scheme 2. Rh-Catalyzed *o*-C−H Alkynylation of Alkyl Benzoates[a]

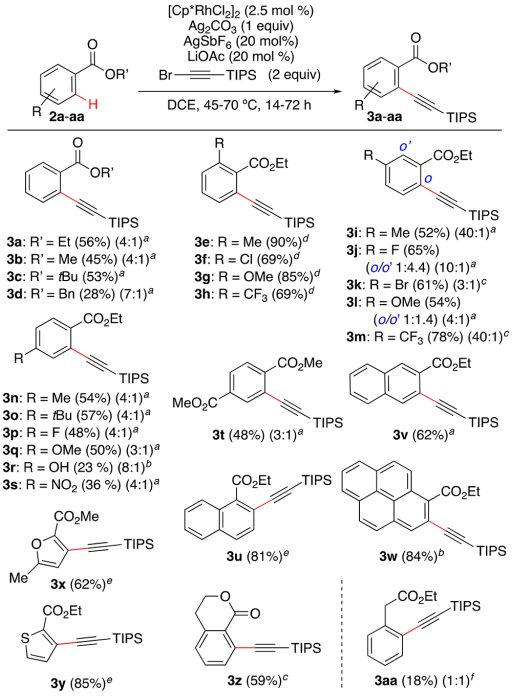

[a]Legend to conditions: (a) 45 °C, 16−24 h; (b) 45 °C, 48 h; (c) 45 °C, 72 h; (d) 60 °C, 48 h; (e) 70 °C, 24−72 h; (f) 90 °C, 72 h (0.2 mmol scale). Yields of isolated monoalkynylated products are shown. In cases in which diakynylated products were also formed, mono- vs dialkynylation selectivity is shown in parentheses.

DOI: 10.1021/acscatal.7b04395
ACS Catal. 2018, 8, 2166−2172

halides at the ortho, meta, and para positions were well tolerated, affording alkynylated products **3e−w** in 23−90% yield. In the case of meta-substituted substrates **2i,k,m**, the alkynylation occurred at the least sterically hindered site. However, fluoro and methoxy derivatives **2j,l** favor formation of the 1,2,3-trisubstituted compounds **3j,l**, respectively.

The alkynylation of ethyl 1-naphthoate (**2u**) and ethyl pyrene-1-carboxylate (**2w**) does not take place at the peri position, leading instead to ortho-fuctionalized products **3u,w**, respectively. Reaction of ethyl 2-naphthoate (**2v**) afforded exclusively the product of alkynylation at C-3 (**3v**). Furan and thiophene esters were also alkynylated to give **3x** (62%) and **3y** (85%), respectively. The carbonyl group of isochroman-1-one is also an effective directing group, affording **3z** in 59% yield. On the other hand, the alkynylation of ethyl phenylacetate required heating at 90 °C and was less efficient, leading to **3aa** in 18% yield along with an equivalent amount of the dialkynylated product.

Whereas the alkynylation of **4a** leads to **5a** in 64% yield, substrates **4b−d** with bulkier alkyl or silyl groups failed to give the expected products (Scheme 3). Similarly, MOM-protected

Scheme 3. Rh-Catalyzed *o*-C−H Alkynylation of Benzyl Ethers[a]

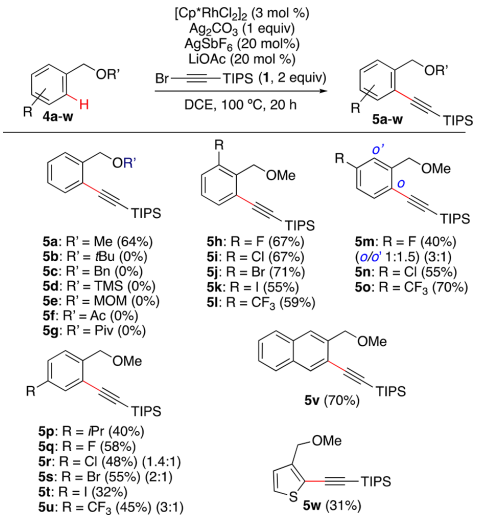

[a]Yields of isolated monoalkynylated products are shown. In cases in which diakynylated products were also formed, mono- vs dialkynylation selectivity is shown in parentheses.

benzyl alcohol **4e** and esters **4f,g** were unreactive substrates. On the other hand, methyl benzyl ethers bearing diverse substituents at the ortho, meta, or para positions such as *i*-Pr, CF_3, fluoro, chloro, bromo, and iodo led to *o*-alkynylated products **5h−u** in 32−71% yields. As observed for the benzoates, the alkynylation of meta-substituted substrates **4n,o** occurred at the least sterically hindered site, whereas fluoro derivative **4m** led to a mixture of ortho-alkynylated derivatives **5m**, favoring the formation of the 1,2,3-trisubstituted product. Again, the alkynylation of naphthyl derivative **4v** takes place at C-3 to form **5v** in 70% yield. The reaction of thiophene **4w** provided **5w**, the product of C-2 alkynylation, which was isolated in 31% yield.

Under conditions similar to those used for the reaction of the ester derivatives, a wide variety of aryl ketones **6a−p** could be alkynylated in a general manner to give **7a−p** in good to excellent yield (Scheme 4). Bis(alkynylated)acetophenone **7k**

Scheme 4. Rh-Catalyzed *o*-C−H Alkynylation of Aryl Ketones[a]

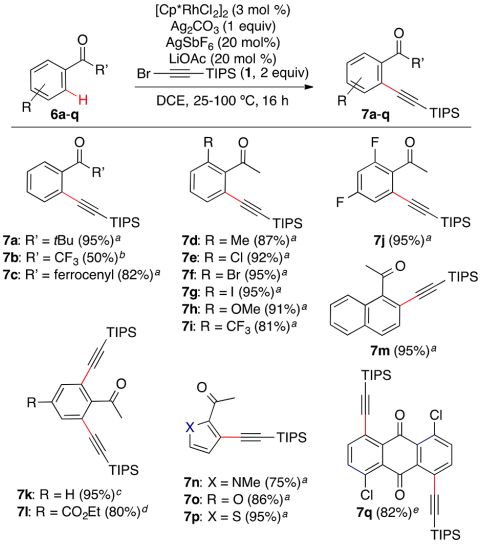

[a]Legend to conditions: (a) 45 °C, (1 equiv **1**); (b) 90 °C, (1 equiv **1**); (c) 25 °C, (2 equiv **1**); (d) 45 °C, (2 equiv **1**); (e) 100 °C, (2 equiv **1**).

was obtained in quantitative yield from acetophenone at room temperature, while bulkier alkyl substituents allowed a monoselective alkynylation, affording products **7a−c** in 50−95% yield. Diverse substituents at the ortho position of acetophenone were well tolerated to give products **7d−i** in 81−95% yield. 2-Acetyl derivatives *N*-methylpyrrole (**6n**), furan (**6o**), and thiophene (**6p**) were alkynylated at C-3 in 75−95% yield. The double alkynylation of 1,5-dichloroanthraquinone (**6q**) proceeded at 100 °C to give dialkynylated product **7q** in 82% yield.

As an example of late-stage functionalization of a pharmaceutical compound, fenofibrate (**6r**) was alkynylated in 35% yield for the major product (Scheme 5).

Scheme 5. Late-Stage Alkynylation of Fenofibrate[a]

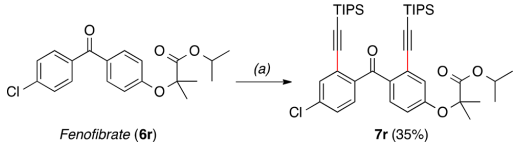

[a]Standard conditions for the Rh-catalyzed reaction using 2 equiv of bromoalkyne, at 50 °C, 14 h.

DOI: 10.1021/acscatal.7b04395
ACS Catal. 2018, 8, 2166−2172

Stereocontrolled synthesis of conjugated enynes or acyclic tri- and tetrasubstituted alkenes is a longstanding challenge in organic chemistry.[25] We were pleased to find that the alkynylation of vinyl C−H bonds of α,β-unsaturated esters **8a−e** and ketones **8f,g** proceeded under the standard conditions at 45−85 °C to afford a series of *Z*-configured 1,3-enynes **9a−g** in 44−84% yield, with total control of the stereoselectivity (Scheme 6).

Scheme 6. Alkynylation of Vinyl C−H Bonds[a]

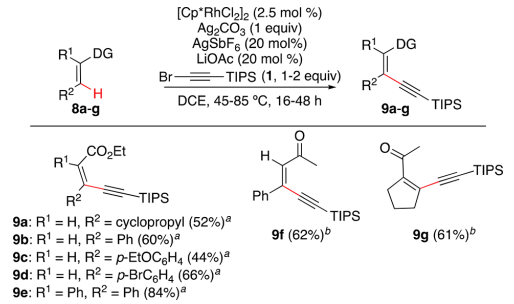

[a]Legend to conditions: (a) 85 °C 48 h, (2 equiv **1**); (b) 45 °C, 16 h (1 equiv **1**).

Other Directing Groups. With slight modification of the reaction conditions, we discovered that other functional groups are viable chelating groups (Scheme 7). As rare examples of the use of a simple phenol ester as a directing group,[23] the ortho alkynylation of phenol pivalate (**10a**) and 1-naphthol acetate (**10b**) led to **11a,b** in moderate yields. Although they are considered to bind too tightly to metals to be involved in catalytic processes, strongly coordinating groups could also be used under similar conditions. Thus, the reaction proceeds on substrates bearing sulfoxide, thioether, thioacetal, sulfone, and tertiary amine functional groups, giving products **11c−h** in 53−75% yield. Boc-protected pyrrole **10i** could also be dialkynylated to give product **11i** in 66% yield.

Scheme 7. Rhodium-Catalyzed C(sp²)−H Alkynylation with Other Directing Groups[a]

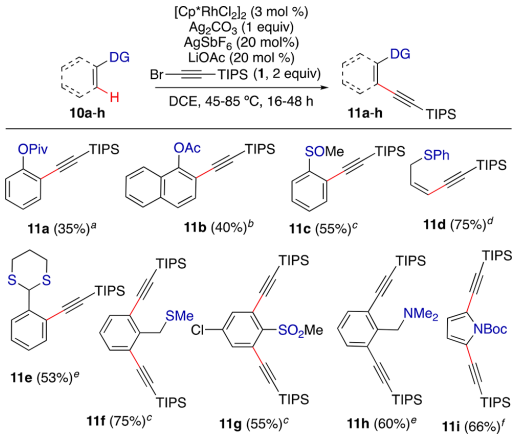

[a]Legend to conditions: (a) 90 °C, 72 h; (b) 70 °C, 24 h; (c) 100 °C, 16 h; (d) 50 °C, (1 equiv **1**), 16 h; (e) 90 °C, 16 h; (f) 45 °C, 16 h.

Mechanistic Studies. Several experiments were carried out in order to shed light on the reaction mechanism. First, the C−H functionalization step was found to be irreversible according to the reaction of **2a**-d_5 in the presence of water and in the absence of bromoalkyne **1** (Scheme 8i). The intermolecular and parallel competition experiments between deuterated and hydrogenated labeled substrates (Scheme 8ii) showed the same kinetic isotope effect (KIE = 3.1) in both cases, indicating that the C−H bond cleavage probably occurs in the rate-determining step of the catalytic cycle,[26] which is consistent with related rhodium-catalyzed C−H functionalizations.[27] Finally, the intermolecular competition between electron-rich and electron-poor substrates (Scheme 8iii) suggests that substrates bearing electron-donating groups (Me or MeO) at the meta position of the C−H functionalization site are more reactive. This result indicates that the C−H functionalization step might occur through an electrophilic aromatic substitution type mechanism.[12b,28]

Scheme 8. D/H Exchange, Kinetic, and Competition Experiments[a,24]

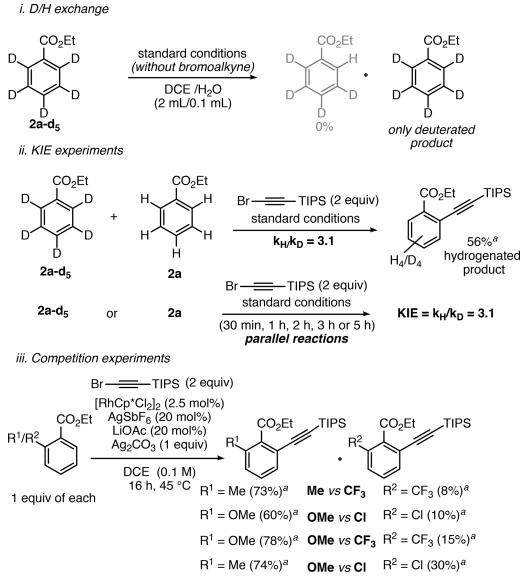

[a]Yield of the monoalkynylated product determined by ^{1}H NMR using bromomesitylene as internal standard.

A Hammett correlation was found (R^2 = 0.99 using σ_p^+) for meta-substituted substrates (Figure 1).[29] A negative ρ value also suggests that electron density decreases at the aryl ring in the product-determining step, which is in accordance with a C−H functionalization step occurring through an electrophilic aromatic substitution type mechanism.

To get a deeper insight into the reaction mechanism, we performed DFT calculations (Scheme 9).[30,31] According to our studies, the C−H functionalization of methyl benzoate (**2b**) proceeds from **Int1a** by the intramolecular assistance of the

DOI: 10.1021/acscatal.7b04395
ACS Catal. 2018, 8, 2166−2172

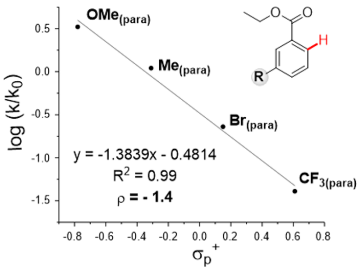

Figure 1. Hammett plot for the reaction of meta-substituted benzoates.[24]

Scheme 9. Proposed Mechanism of the Rh-Catalyzed C(sp²)−H Alkynylation on the Basis of DFT Calculations[a]

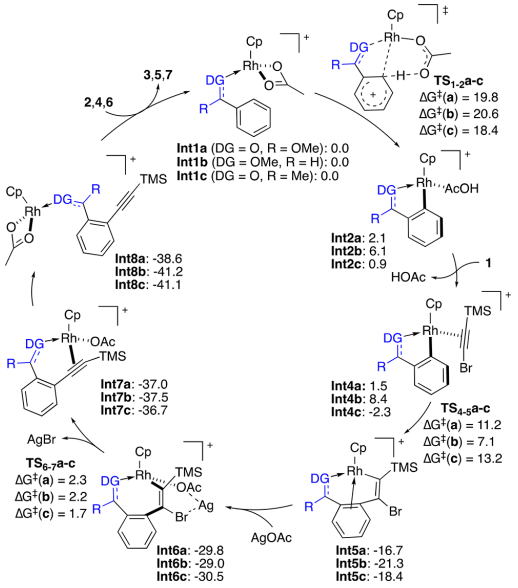

[a]Free energies in kcal/mol.

acetate ligand through the six-membered cyclic transition state $\mathbf{TS_{1-2}a}$ ($\Delta G^{\ddagger}$ = 19.8 kcal/mol). The alternative four-membered cyclic transition state ($\Delta G^{\ddagger}$ = 34.6 kcal/mol) or the intermolecular acetate-assisted C−H activation ($\Delta G^{\ddagger}$ = 51.2 kcal/mol) would require much higher energy barriers.[24,32] The resulting **Int2a** undergoes dissociative ligand exchange with bromoacetylene **1b** through **Int3a** (not shown)[24] to form the (η^2-alkyne)rhodium complex **Int4a**. Subsequent alkyne insertion ($\Delta G^{\ddagger}$ = 11.2 kcal/mol) to give **Int5a**, followed by AgOAc-assisted bromide elimination ($\Delta G^{\ddagger}$ = 2.3 kcal/mol) leads to **Int7a** and then **Int8a**. The catalytic cycle restarts upon ligand exchange, delivering the final alkynylated product **3ab** and regenerating **Int1a**.

Analysis of the Mulliken atomic charges in **Int1a**, $\mathbf{TS_{1-2}a}$, and **Int2a**[24] shows that the process involves an ambiphilic metal ligand activation.[32e] Both an electrophilic metal center and an intramolecular basic ligand are key for the heterolytic scission of the C−H bond and formation of the C−Rh bond (Figure 2). In

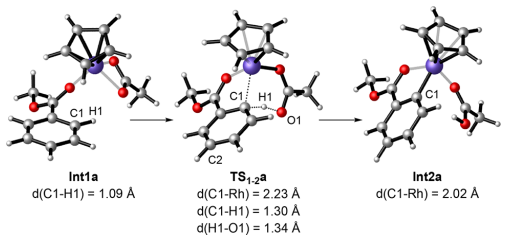

Figure 2. Calculated structures for the C−H activation via $\mathbf{TS_{1-2}a}$.[24]

$\mathbf{TS_{1-2}a}$, the carbon involved in the C−H activation shows a certain sp^3 character (the Rh−C−H angle is 73.8°).[24] The C−Rh distance (2.23 Å) in $\mathbf{TS_{1-2}a}$ is slightly longer than that of the metallacycle **Int2a** (2.02 Å), whereas the C−H distance is lengthened from 1.09 Å in **Int1a** to 1.30 Å in $\mathbf{TS_{12}a}$, which suggests that the formation of the Rh−C bond preceeds the cleavage of the C−H bond in a concerted, but asynchronous, process.

Table 2. Substituent Effect in the Activation Energy of the C−H Activation of Benzoates[a]

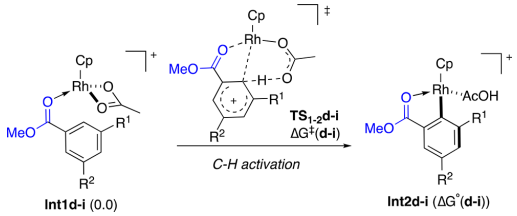

entry	R^1	R^2	$\mathbf{TS_{1-2}d-i}$	$\Delta G^{\ddagger}$(d−i)	Int2d−i	ΔG°(d−i)
1	H	OMe	$\mathbf{TS_{1-2}d}$	17.2	**Int2d**	2.9
2	H	Me	$\mathbf{TS_{1-2}e}$	18.9	**Int2e**	3.3
3	H	Br	$\mathbf{TS_{1-2}f}$	20.8	**Int2f**	3.1
4	H	CF_3	$\mathbf{TS_{1-2}g}$	21.5	**Int2g**	3.4
5	H	F	$\mathbf{TS_{1-2}h}$	19.5	**Int2h**	2.5
6	F	H	$\mathbf{TS_{1-2}i}$	17.8	**Int2i**	2.7

[a]Free energies in kcal/mol.

Alternative alkynylation pathways were also considered, although they proved to be less favored.[24] For instance, the oxidative addition of the C(sp)−Br bond to the metal center in **Int4a** to form a Rh(V) intermediate[33] demands a highly unlikely activation energy of 41.6 kcal/mol. On the basis of the computed energies, the C−H metalation is the rate-determining step, which is in agreement with the experimental results. Similar energy profiles were found in the case of methyl benzyl ether **4a** (Scheme 9, pathway **b**) and acetophenone **6k** (Scheme 9, pathway **c**), which means that the same reaction mechanism presumably operates for them.[24] Consistent with the experimental results, among the different substrates, the C−H functionalization of the ketones is the most energetically favored ($\Delta G^{\ddagger}$ = 18.4 kcal/mol), whereas the corresponding to the benzyl ethers is the most energetically costly ($\Delta G^{\ddagger}$ = 20.6 kcal/mol).

In addition, the C−H activation step was computed for differently meta-substituted methyl benzoates to study the influence of the electronic effects on the energy barrier. Calculations showed that the more electron-rich the sub-

DOI: 10.1021/acscatal.7b04395
ACS Catal. 2018, 8, 2166−2172

stituent, the lower the activation energy results (Table 2, entries 1−4). This is in total agreement with the experimental results observed for meta-substituted ethyl benzoates (Figure 1) and supports an electrophilic substitution type mechanism for the formation of the five-membered-ring rhodacycle.

In the case of *m*-fluorobenzoate, the C−H activation preferentially occurs at the ortho ($\Delta G^{\ddagger}$ = 17.8 kcal/mol, Table 2, entry 6) rather than the para position ($\Delta G^{\ddagger}$ = 19.5 kcal/mol, Table 2, entry 5) respect to the fluoro substituent. This *o*-fluorine effect has been experimentally observed with *m*-fluoro-substituted benzoate **3j** (Scheme 2) or benzyl ether compound **5m** (Scheme 3), as the metal−carbon bond strength would be increased at this position.[34]

CONCLUSIONS

In summary, we have found that the alkynylation of benzyl methyl ethers, aryl esters, and aryl ketones can be carried out using rhodium catalysis in a general manner. This is the first report of a broad-range *o*-C−H functionalization of weakly coordinating benzyl ethers. The Rh-catalyzed alkynylation of aryl esters and aryl ketones takes place under milder conditions (45−70 °C for esters and 25−90 °C for ketones) in comparison to those recently reported using Ir catalysis (120 °C). The alkynylation of vinyl C−H bonds of α,β-unsaturated esters and ketones is also possible using rhodium catalysis. Furthermore, other uncommon functional groups such as amine, thioether, thioacetal, sulfoxide, sulfone, phenol ester, and carbamate can also be used as directing groups for the alkynylation. Our mechanistic study shows that the alkynylation reaction proceeds by a turnover-limiting C−H activation step via an electrophilic-type substitution, followed by insertion of the bromoalkyne and bromide elimination.

ASSOCIATED CONTENT

Supporting Information

The Supporting Information is available free of charge on the ACS Publications website at DOI: 10.1021/acscatal.7b04395.

Additional details, experimental procedures, characterization data for compounds, and computational results (PDF)

AUTHOR INFORMATION

Corresponding Author

*E-mail for A.M.E.: aechavarren@iciq.es.

ORCID

Ophélie Quinonero: 0000-0003-4561-8763
M. Elena de Orbe: 0000-0001-9603-3699
Antonio M. Echavarren: 0000-0001-6808-3007

Author Contributions

§E.T. and O.Q. contributed equally.

Notes

The authors declare no competing financial interest.

ACKNOWLEDGMENTS

We thank the Agencia Estatal de Investigación (CTQ2016-75960-P MINECO/AEI/FEDER, UE), Severo Ochoa Excellence Acreditation 2014-2018 (SEV-2013-0319 and Severo Ochoa predoctoral fellowship to M.E.d.O.), Juan de la Cierva postdoctoral fellowship (O.Q.), the European Research Council (Advanced Grant No. 321066), the AGAUR (2014 SGR 818), and the CERCA Program/Generalitat de Catalunya for financial support. We also thank CELLEX-ICIQ HTE laboratory.

REFERENCES

(1) (a) *Acetylene Chemistry: Chemistry, Biology and Material Science*; Diederich, F., Stang, P. J., Tykwinski, R. R., Eds.; Wiley-VCH: Weinheim, Germany, 2005. (b) Boyd, G. V. *The Chemistry of Triple Bonded Functional Groups*; Patai, S., Ed.; Wiley: Hoboken, NJ, 1994; Chapter 5.
(2) (a) Zhou, Z.-F.; Menna, M.; Cai, Y. S.; Guo, Y. W. *Chem. Rev.* **2015**, *115*, 1543−1596. (b) Chai, Q.-Y.; Yang, Z.; Lin, H. W.; Han, B. N. *Mar. Drugs* **2016**, *14*, 216.
(3) Lamberth. *Bioorg. Med. Chem.* **2009**, *17*, 4047−4063.
(4) Broggi, A.; Tomasi, I.; Bianchi, L.; Marrocchi, A.; Vaccaro, L. *ChemPlusChem* **2014**, *79*, 486−507.
(5) (a) Fürstner, A. *Chem. Soc. Rev.* **2009**, *38*, 3208−3221. (b) Shapiro, N. D.; Toste, F. D. *Synlett* **2010**, *2010*, 675−691. (c) Obradors, C.; Echavarren, A. M. *Acc. Chem. Res.* **2014**, *47*, 902−912. (d) Fensterbank, L.; Malacria, M. *Acc. Chem. Res.* **2014**, *47*, 953−965. (e) Dorel, R.; Echavarren, A. M. *Chem. Rev.* **2015**, *115*, 9028−9072. (f) Pflästerer, D.; Hashmi, A. S. K. *Chem. Soc. Rev.* **2016**, *45*, 1331−1367. (g) Echavarren, A. M.; Muratore, M. N.; López-Carrillo, V.; Escribano-Cuesta, A.; Huguet, A.; Obradors, C. *Org. React.* **2017**, *92*, 1.
(6) (a) Negishi, E.; Anastasia, L. *Chem. Rev.* **2003**, *103*, 1979−2018. (b) Doucet, H.; Hierso, J.-C. *Angew. Chem., Int. Ed.* **2007**, *46*, 834−871. (c) Chinchilla, R.; Nájera, C. *Chem. Soc. Rev.* **2011**, *40*, 5084−5121. (d) Chinchilla, R.; Nájera, C. *Chem. Rev.* **2014**, *114*, 1783−1826. (e) Wang, D.; Gao, S. *Org. Chem. Front.* **2014**, *1*, 556−566.
(7) For reviews on C(sp^2)−H alkynylation, see: (a) Colby, D. A.; Bergman, R. G.; Ellman, J. A. *Chem. Rev.* **2010**, *110*, 624−655. (b) Dudnik, A. S.; Gevorgyan, V. *Angew. Chem., Int. Ed.* **2010**, *49*, 2096−2098. (c) Chen, Z.; Wang, B.; Zhang, J.; Yu, W.; Liu, Z.; Zhang, Y. *Org. Chem. Front.* **2015**, *2*, 1107−1295. For a review on EBX, see: (d) Waser, J. *Synlett* **2016**, *27*, 2761−2773. For more works in the field of C(sp^2)−H alkynylation, see: (e) Kim, S. H.; Yoon, J.; Chang, S. *Org. Lett.* **2011**, *13*, 1474−1477. (f) Feng, C.; Feng, D.; Luo, Y.; Loh, T.-P. *Org. Lett.* **2014**, *16*, 5956−5959. (g) Feng, C.; Loh, T.-P. *Angew. Chem., Int. Ed.* **2014**, *53*, 2722−2726. (h) Feng, C.; Feng, D.; Loh, T.-P. *Chem. Commun.* **2014**, *50*, 9865−9868. (i) Zhang, X.; Qi, Z.; Gao, J.; Li, X. *Org. Biomol. Chem.* **2014**, *12*, 9329−9332. (j) Zhang, Z.-Z.; Liu, B.; Wang, C.-Y.; Shi, B.-F. *Org. Lett.* **2015**, *17*, 4094−4097. (k) Sauermann, N.; González, M. J.; Ackermann, L. *Org. Lett.* **2015**, *17*, 5316−531. (l) Landge, V. G.; Midya, S. P.; Rana, J.; Shinde, D. R.; Balaraman, E. *Org. Lett.* **2016**, *18*, 5252−5255. (m) Ye, X.; Xu, C.; Wojtas, L.; Akhmedov, N. G.; Chen, H.; Shi, X. *Org. Lett.* **2016**, *18*, 2970−2973. (n) Boobalan, R.; Gandeepan, P.; Cheng, C.-H. *Org. Lett.* **2016**, *18*, 3314−3317. (o) Tang, G.-D.; Pan, C.-L.; Xie, F. *Org. Biomol. Chem.* **2016**, *14*, 2898−2904. (p) Liu, B.; Wang, X.; Ge, Z.; Li, R. *Org. Biomol. Chem.* **2016**, *14*, 2944−2949. (q) Landge, V. G.; Jaiswal, G.; Balaraman, E. *Org. Lett.* **2016**, *18*, 812−815. (r) Wang, S.-B.; Gu, Q.; You, S.-L. J. *J. Org. Chem.* **2017**, *82*, 11829−11835. (s) Székely, A.; Péter, Á.; Aradi, K.; Tolnai, G. L.; Novák, Z. *Org. Lett.* **2017**, *19*, 954−957. (t) Hu, S.; Lu, L.; Zhu, T.; Wu, Q.; Chen, Y.; Li, J. J.; Zhao, J. *Org. Biomol. Chem.* **2018**, *16*, 43−47.
(8) (a) Seregin, I. V.; Ryabova, V.; Gevorgyan, V. *J. Am. Chem. Soc.* **2007**, *129*, 7742−7743. (b) Matsuyama, N.; Hirano, K.; Satoh, T.; Miura, M. *Org. Lett.* **2009**, *11*, 4156−4159. (c) Besselievre, F.; Piguel, S. *Angew. Chem., Int. Ed.* **2009**, *48*, 9553−9556. (d) Wei, Y.; Zhao, H.; Kan, J.; Su, W.; Hong, M. *J. Am. Chem. Soc.* **2010**, *132*, 2522−2523. (e) Brand, J. P.; Charpentier, J.; Waser, J. *Angew. Chem., Int. Ed.* **2009**, *48*, 9346−9349.
(9) (a) Tobisu, M.; Ano, Y.; Chatani, N. *Org. Lett.* **2009**, *11*, 3250−3252. (b) Collins, K. D.; Lied, F.; Glorius, F. *Chem. Commun.* **2014**, *50*, 4459−4461. (c) Xie, F.; Qi, Z.; Yu, S.; Li, X. *J. Am. Chem. Soc.* **2014**, *136*, 4780−4787. (d) Ruan, Z.; Sauermann, N.; Manoni, E.; Ackermann, L. *Angew. Chem., Int. Ed.* **2017**, *56*, 3172−3176.
(10) Gensch, T.; James, M.; Dalton, T.; Glorius, F. *Angew. Chem., Int. Ed.* **2017**, DOI: 10.1002/anie.201710377.

(11) Tan, E.; Konovalov, A. I.; Fernández, G. A.; Dorel, R.; Echavarren, A. M. *Org. Lett.* **2017**, *19*, 5561−5564.
(12) (a) Chen, C.; Liu, P.; Tang, J.; Deng, G.; Zeng, X. *Org. Lett.* **2017**, *19*, 2474−2477. (b) Mei, R.; Zhang, S.-K.; Ackermann, L. *Org. Lett.* **2017**, *19*, 3171−3174. (c) Chen, C.; Zeng, X. *Eur. J. Org. Chem.* **2017**, *2017*, 4749−4752.
(13) For examples of ester-directed C(sp^2)−H functionnalization, see: (a) Sonoda, M.; Kakiuchi, F.; Kamatani, A.; Chatani, N.; Murai, S. *Chem. Lett.* **1996**, *25*, 109−110. (b) Kawamorita, S.; Ohmiya, H.; Hara, K.; Fukuoka, A.; Sawamura, M. *J. Am. Chem. Soc.* **2009**, *131*, 5058−5059. (c) Kim, J.; Chang, S. *Angew. Chem.* **2014**, *126*, 2235−2239. (d) Yang, Y.; Lin, Y.; Rao, Y. *Org. Lett.* **2012**, *14*, 2874−2877. (e) Yu, W.; Zhang, W.; Liu, Z.; Zhang, Y. *Chem. Commun.* **2016**, *52*, 6837−6840. (f) Coxon, T. J.; Fernandez, M.; Barwick-Silk, J.; McKay, A. I.; Britton, L. E.; Weller, A.; Willis, M. C. *J. Am. Chem. Soc.* **2017**, *139*, 10142−10149.
(14) For examples of ketone-directed C(sp^2)−H functionnalization, see: (a) Murai, S.; Kakiuchi, F.; Sekine, S.; Tanaka, Y.; Kamatani, A.; Sonoda, M.; Chatani, N. *Nature* **1993**, *366*, 529−531. For a review, see: (b) Huang, Z.; Lim, H. N.; Mo, F.; Young, M. C.; Dong, G. *Chem. Soc. Rev.* **2015**, *44*, 7764−7786. (c) Shang, R.; Ilies, L.; Nakamura, E. *J. Am. Chem. Soc.* **2016**, *138*, 10132−10135. (d) Zhao, Y.; Li, S.; Zheng, X.; Tang, J.; She, Z.; Gao, G.; You, J. *Angew. Chem., Int. Ed.* **2017**, *56*, 4286−4289. (e) Zhang, B.; Wang, H.-W.; Kang, Y.-S.; Zhang, P.; Xu, H.-J.; Lu, Y.; Sun, W.-Y. *Org. Lett.* **2017**, *19*, 5940−5943.
(15) Engle, K. M.; Mei, T. S.; Wasa, M.; Yu, J.-Q. *Acc. Chem. Res.* **2012**, *45*, 788−802.
(16) For examples of ether-directed C−H functionalization, see: (a) Kawamorita, S.; Ohmiya, H.; Hara, K.; Fukuoka, A.; Sawamura, M. *J. Am. Chem. Soc.* **2009**, *131*, 5058−5059. (b) Liskey, C. W.; Hartwig, J. F. *J. Am. Chem. Soc.* **2012**, *134*, 12422−12425. (c) Li, G.; Leow, D.; Wan, L.; Yu, J.-Q. *Angew. Chem., Int. Ed.* **2013**, *52*, 1245−1247.
(17) During the preparation of this paper, the ortho alkynylation of aryl ketones was reported using $[IrCp^*Cl_2]_2$ (4 mol %), $AgNTf_2$ (16 mol %), NaOAc (30 mol %), and AgOAc (2 equiv) in DCE at 120 °C: Li, X.; Wu, G.; Liu, X.; Zhu, Z.; Huo, Y.; Jiang, H. *J. Org. Chem.* **2017**, *82*, 13003−13011. The alkynylation of esters (six examples) and one example of alkynylation of an α,β-unsaturated ketone were also reported in this study.
(18) For *N*,*N*-dimethylamino-directed C(sp^2)−-H functionalization, see: (a) Kakiuchi, F.; Igi, K.; Matsumoto, M.; Hayamizu, T.; Chatani, N.; Murai, S. *Chem. Lett.* **2002**, *31*, 396−397. (b) Cai, G.; Fu, Y.; Li, Y.; Wan, X.; Shi, Z. *J. Am. Chem. Soc.* **2007**, *129*, 7666−7673. (c) Gao, D.-W.; Shi, Y.-C.; Gu, Q.; Zhao, Z.- L.; You, S.-L. *J. Am. Chem. Soc.* **2013**, *135*, 86−89.
(19) For thioether-directed C(sp^2)−H functionalization, see: (a) Yu, M.; Xie, Y.; Xie, C.; Zhang, Y. *Org. Lett.* **2012**, *14*, 2164−2167. (b) Yao, J.; Yu, M.; Zhang, Y. *Adv. Synth. Catal.* **2012**, *354*, 3205−3210. (c) Xu, B.; Liu, W.; Kuang, C. *Eur. J. Org. Chem.* **2014**, *2014*, 2576−2583. (d) Villuendas, P.; Urriolabeitia, E. P. *Org. Lett.* **2015**, *17*, 3178−3181. (e) Zhang, X.-S.; Zhang, Y.-F.; Li, Z.-W.; Luo, F.-X.; Shi, Z.-J. *Angew. Chem., Int. Ed.* **2015**, *54*, 1−6.
(20) For sulfoxide-directed C(sp^2)−H functionalization, see: (a) Samanta, R.; Antonchick, A. P. *Angew. Chem., Int. Ed.* **2011**, *50*, 5217−5220. (b) Hazra, C. K.; Dherbassy, Q.; Wencel-Delord, J.; Colobert, F. *Angew. Chem., Int. Ed.* **2014**, *53*, 13871−13875. (c) Nobushige, K.; Hirano, K.; Satoh, T.; Miura, M. *Org. Lett.* **2014**, *16*, 46−49. (d) For a review, see: Pulis, A. P.; Procter, D. J. *Angew. Chem., Int. Ed.* **2016**, *55*, 9842.
(21) For an example of sulfone-directed C(sp^2)−H functionalization, see: Nobushige, K.; Hirano, K.; Satoh, T.; Miura, M. *Tetrahedron* **2015**, *71*, 6506−6512.
(22) For examples of carbamate-directed C(sp^2)−H functionalization, see: (a) Hoshino, Y.; Shibata, Y.; Tanaka, K. *Adv. Synth. Catal.* **2014**, *356*, 1577−1585. (b) Zhang, X.; Si, W.; Bao, M.; Asao, N.; Yamamoto, Y.; Jin, T. *Org. Lett.* **2014**, *16*, 4830−4833. (c) Morita, T.; Satoh, T.; Miura, M. *Org. Lett.* **2017**, *19*, 1800−1803.
(23) For an example of phenol ester directed C(sp^2)-H functionalization, see: Xiao, B.; Fu, Y.; Xu, J.; Gong, T.-J.; Dai, J.-J.; Yi, J.; Liu, L. *J. Am. Chem. Soc.* **2010**, *132*, 468−469.
(24) See the Supporting Information for additional details.
(25) Wang, J. *Stereoselective Alkene Synthesis*; Springer-Verlag: Berlin, Heidelberg, 2012.
(26) Simmons, E. M.; Hartwig, J. F. *Angew. Chem., Int. Ed.* **2012**, *51*, 3066−3072.
(27) Stuart, D. R.; Alsabeh, P.; Kuhn, M.; Fagnou, K. *J. Am. Chem. Soc.* **2010**, *132*, 18326−18339.
(28) Ma, W.; Mei, R.; Tenti, G.; Ackermann, L. *Chem. - Eur. J.* **2014**, *20*, 15248−15251.
(29) Hansch, C.; Leo, A.; Taft, R. W. *Chem. Rev.* **1991**, *91*, 165−195.
(30) DFT calculations were performed using the Gaussian 09 suite of programs, using wB97XD. Rh, Ag, and Br atoms were described by ECP with the LANL2DZ basis set. Polarization functions were added for Rh (ζ_f = 1.35), Ag (ζ_f = 1.611) and Br (ζ_d = 0.428). The 6-31G(d) basis set was employed for all remaining atoms. Full geometry optimizations were carried out in 1,2-dichloroethane, through an implicit solvent SMD.[24]
(31) Sperger, T.; Sanhueza, I. A.; Kalvet, I.; Schoenebeck, F. *Chem. Rev.* **2015**, *115*, 9532−9586.
(32) Selected discussions of C−H activation mechanisms: (a) Qi, X.; Li, Y.; Bai, R.; Lan, Y. *Acc. Chem. Res.* **2017**, *50*, 2799−2808. (b) Roudesly, F.; Oble, J.; Poli, G. *J. Mol. Catal. A: Chem.* **2017**, *426*, 275−296. (c) Ackermann, L. *Chem. Rev.* **2011**, *111*, 1315−1345. (d) Lapointe, D.; Fagnou, K. *Chem. Lett.* **2010**, *39*, 1118−1126. (e) Boutadla, Y.; Davies, D. L.; Macgregor, S. A.; Poblador-Bahamonde, A. I. *Dalton Trans.* **2009**, 5820−5831. (f) Gorelsky, S. I.; Lapointe, D.; Fagnou, K. *J. Am. Chem. Soc.* **2008**, *130*, 10848−10849. (g) Oxgaard, J.; Tenn, W. J., III; Nielsen, R. J.; Periana, R. A.; Goddard, W. A., III *Organometallics* **2007**, *26*, 1565−1567. (h) García-Cuadrado, D.; de Mendoza, P.; Braga, A. A. C.; Maseras, F.; Echavarren, A. M. *J. Am. Chem. Soc.* **2007**, *129*, 6880−6886. (i) Li, L.; Brennessel, W. W.; Jones, W. D. *Organometallics* **2009**, *28*, 3492−3500.
(33) Vásquez-Céspedes, S.; Wang, X.; Glorius, F. *ACS Catal.* **2018**, *8*, 242−257.
(34) (a) Clot, E.; Mégret, C.; Eisenstein, O.; Perutz, R. N. *J. Am. Chem. Soc.* **2009**, *131*, 7817−7827. (b) Evans, M. E.; Burke, C. L.; Yaibuathes, S.; Clot, E.; Eisenstein, O.; Jones, W. D. *J. Am. Chem. Soc.* **2009**, *131*, 13464−13473. (c) Clot, E.; Besora, M.; Maseras, F.; Mégret, C.; Eisenstein, O.; Oelckers, B.; Perutz, R. B. *Chem. Commun.* **2003**, 490−491.

DOI: 10.1021/acscatal.7b04395
ACS Catal. 2018, 8, 2166−2172

UNIVERSITAT ROVIRA I VIRGILI
GOLD-CATALYZED INTERMOLECULAR REACTIONS OF ALKYNES WITH ALKENES: NOVEL REACTIVITIES AND GLOBAL MECHANISTIC PICTURE
María Elena de Orbe Izquierdo

Bioorganic & Medicinal Chemistry xxx (xxxx) xxx–xxx

Contents lists available at ScienceDirect

Bioorganic & Medicinal Chemistry

journal homepage: www.elsevier.com/locate/bmc

Synthetic molecules for disruption of the MYC protein-protein interface

Nicholas T. Jacob, Pedro O. Miranda[a], Ryan J. Shirey, Ritika Gautam, Bin Zhou, M. Elena de Orbe Izquierdo, Mark S. Hixon[b], Jonathan R. Hart, Lynn Ueno, Peter K. Vogt, Kim D. Janda*

Department of Chemistry, BCC-582, 10550 N Torrey Pines Road, The Scripps Research Institute, La Jolla, CA 92037, United States

A B S T R A C T

MYC is a key transcriptional regulator involved in cellular proliferation and has established roles in transcriptional elongation and initiation, microRNA regulation, apoptosis, and pluripotency. Despite this prevalence, functional chemical probes of MYC function at the protein level have been limited. Previously, we discovered **5a**, that binds to MYC with potency and specificity, downregulates the transcriptional activities of MYC and shows efficacy *in vivo*. However, this scaffold posed intrinsic pharmacokinetic liabilities, namely, poor solubility that precluded biophysical interrogation. Here, we developed a screening platform based on field-effect transistor analysis (Bio-FET), surface plasmon resonance (SPR), and a microtumor formation assay to analyze a series of new compounds aimed at improving these properties. This blind SAR campaign has produced a new lead compound of significantly increased *in vivo* stability and solubility for a 40-fold increase in exposure. This probe represents a significant advancement that will not only enable biophysical characterization of this interaction and further SAR, but also contribute to advances in understanding of MYC biology.

1. Introduction

The v-myc myeleocytomatosis viral oncogene homolog (MYC) protein is an essential regulator of cell-cycle progression occupying and apical space in the trasncriptome.[1] Importantly, MYC has been directly implicated in most human cancers and its role recognized as a hallmark of cancer initiation and maintenance.[2–6] In general, MYC expression has a strong correlation to dramatic effects on cellular proliferation and function, but the molecular determinants responsible for these effects remain controversial.[7] Part of the difficulty in studying MYC is its frenetic mode of action: although having an ephemeral existence, it is able to seemingly affect transcription in both a local and global manner. Moreover, MYC exists as an intrinsically disordered protein (IDP), taking on structure only in the presence of other basic helix-loop-helix leucine zipper (bHLH-LZ) transcription factors of the MAX network.[8,9] This lack of structure and instability greatly impairs the ability to structurally or biophysically characterize MYC interactions. In all, these attributes have worked to make MYC an attractive, but elusive target in drug discovery.

Previously, we described an inhibitory scaffold of the MYC-MAX-DNA complex, KJ-Pyr-9, **5a**.[10] This compound exhibited potent inhibition of the transforming capabilities of an oncogenic ATG-MYC virus in chicken embryo fibroblasts (CEF); importantly, it also demonstrated a higher specificity of inhibition for MYC than other oncogenes. However, the scaffold presents intrinsic liabilities: namely, a very modest solubility (~8 μM), compounding the difficulty in characterizing this interaction, as well as several undesirable moieties, namely the nitro group. To overcome these obstacles, we developed a multifaceted screening platform combining *in vitro* biophysical characterization with *in vivo* methods.

2. Results and discussion

With no structural characterization of the interaction between **5a** and MYC, a blind SAR campaign was undertaken primarily directed at accessing a more soluble scaffold to enable formal characterization. A series of compounds with bioisosteric replacements of the undesirable moieties and aimed at increased solubility were produced via the Kröhnke pyridine synthesis. Thus, a family of α,β-unsaturated ketones **2** were synthesized using two pathways (Scheme 1): (a) Reaction of a methyl ketone bearing variety of different five-membered heterocycles such as thiazole, imidazole and triazole (b) an oxazole reaction with the corresponding acylchloride, which allowed for introduction of the oxazole moiety. A second reaction between **2** and pyridinium salts **1** (obtained from the corresponding phenacyl bromide derivative) using ammonium acetate at 100 °C gave the corresponding 2,4,6-trisubstituted pyridines **3**. Compounds **5i–k** were obtained at this point, while all others contained a *p*-methylester group in the R^3 position. The

* Corresponding author.
E-mail address: kdjanda@scripps.edu (K.D. Janda).
[a] Present address: Instituto de Productos Naturales y Agrobiología, CSIC, Avda. Franscisco Sánchez 3, 38206 La Laguna, Tenerife, Spain.
[b] Present address: Mark S. Hixon Consulting LLC, 11273 Spitfire Road, San Diego, CA 92126, United States.

https://doi.org/10.1016/j.bmc.2018.07.019
Received 1 June 2018; Received in revised form 3 July 2018; Accepted 10 July 2018

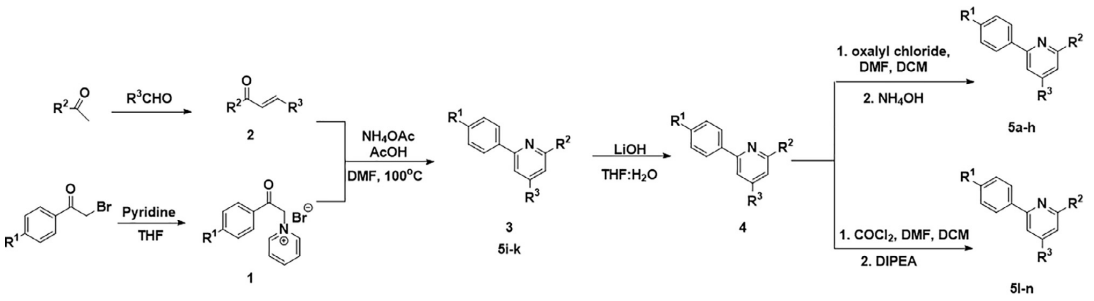

5a: R^1= NO_2; R^2= 2-furanyl; R^3 = *p*-C_6H_4-$CONH_2$
5b: R^1= CN; R^2= 2-furanyl; R^3 = *p*-C_6H_4-$CONH_2$
5c: R^1= CN; R^2= 2-thiazolyl; R^3 = *p*-C_6H_4-$CONH_2$
5d: R^1= CN; R^2= 2-oxazolyl; R^3 = *p*-C_6H_4-$CONH_2$
5e: R^1= CN; R^2= N-methyl-2-imidazolyl; R^3 = *p*-C_6H_4-$CONH_2$
5f: R^1= CN; R^2= 1-methy-1*H*-1,2,3-triazol-5-yl; R^3 = *p*-C_6H_4-$CONH_2$
5g: R^1= 2-thiazolyl; R^2= 2-furanyl; R^3 = *p*-C_6H_4-$CONH_2$
5h: R^1= 5-oxazolyl; R^2= 2-furanyl; R^3 = *p*-C_6H_4-$CONH_2$
5i: R^1= CN; R^2= 2-furanyl; R^3 = C_6H_5
5j: R^1= 2-thiazolyl; R^2= 2-furanyl; R^3 = 2-thiazolyl
5k: R^1= CN; R^2= 2-furanyl; R^3 = *p*-C_6H_4-CN_4H
5l: R^1= CN; R^2= 2-furanyl; R^3 = *p*-C_6H_4-CONHMe
5m: R^1= CN; R^2= 2-furanyl; R^3 = *p*-C_6H_4-$CONHSO_2Me$
5n: R^1= CN; R^2= 2-furanyl; R^3 = *p*-C_6H_4-$CONHNH_2$
5o: R^1= CN; R^2= *m*-C_6H_4F; R^3 = *p*-C_6H_4-$CONH_2$

Scheme 1. Synthesis of pyridine scaffolds **5a–5o**.

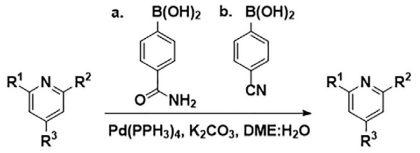

6a: R^1= *p*-CNPh, R^2= H, R^3= Br
6b: R^1= Br, R^2= 2-furanyl, R^3= H

7a: R^1= CN; R^2= H; R^3 = *p*-C_6H_4-$CONH_2$
7b: R^1= CN; R^2= 2-furanyl; R^3 =H

Scheme 2. Synthesis of pyridine scaffolds **7a** and **7b**.

methylester group of **3** was hydrolyzed to obtain carboxylic acid **4**. The carboxylic acid was reacted with oxalyl chloride and *N,N*-dimethylformamide in order to obtain the corresponding acyl chlorides, which were then reacted with different nucleophiles to form compounds **5**. In order to access truncated pyridine scaffolds, such as **7a** and **7b**, a palladium-catalyzed Suzuki cross-coupling strategy was used as shown in Scheme 2. After the preparation of these compounds, the next step was to examine their activity relative to **5a**.

Initially, compound solubilities were measured by dynamic light scattering (Table 1). In order to screen new compounds for MYC binding, a field-effect transistor (Bio-FET) was used. Bio-FET offers several advantages for characterizing this interaction[11,12]: 1. A much lower limit of detection as compared with SPR or isothermal calorimetry. 2. Detection being conducted on a graphene surface, which reduces the interaction of the disordered protein with the chip surface. 3. Site-specific functionalization, which reduces the amount of noise caused from aggregates on the chip surface. The basic-helix-loop-helix (bHLH) motif of MYC has been established a solvent-accessible region critical for MYC function.[10,13] A His-tagged bHLH construct was immobilized on the chip (see Materials and Methods) and compounds screened for interaction. We were able to observe saturation of surface-bound MYC across chips at 10 μM **5a** in 3% DMSO in MES buffer to give a maximal response signal. This was used as the control on each chip screened and gave a benchmark in terms of both solubility and affinity for the protein (Fig. 1a, Table 1). Compounds were screened by measuring the chip response at 10 μM and normalized to the response found for **5a** in that run. All compounds were also screened against a monomeric form of MAX (mMAX), as well as MYC-MAX and MAX-MAX dimers (see Supplemental Material). The lack of observed binding to mMAX, MAX-MAX and the unbound control surface, as well as the general ability to regenerate the chip surface, indicates that there is a specificity in the observed binding interactions.

Table 1
Activity summary.

ID	MW	Solubility (μM)[a]	FET R_{eq} (%)[b]	CEF IC_{50} (μM)[c]
5a	385.4	8	100	1
5b	365.4	10	106	3
5c	382.4	64	79	30
5d	299.3	250	0	> 100
5e	379.4	8	41	40
5f	380.4	32	55	40
5g	423.5	125	97	5
5h	407.4	15	154	2.5
5i	366.4	2	72	5
5j	387.5	< 1	188	> 100
5k	390.4	18	92	2
5l	379.4	25	3.2	NT
5m	443.5	32	76	10
5n	380.4	500	0	> 100
5o	393.4	2	0	> 100
7a	322.4	32	0	10[d]
7b	246.3	10	0	NT
10a	366.4	8	66	7
10b	381.4	< 1	0	> 100
10c	393.4	25	0	> 100

NT – not tested.
[a] Measured by DLS in MES (pH 6.0) with < 0.1% DMSO.
[b] Relative to **5a** R_{eq}.
[c] Measured in CEF transfected with ATG-MYC.
[d] Inhibited all cell growth.

The affinity of the MYC-MAX interaction is relatively weak (K_d = 176 nM[14]), making measurement of the perturbation in this interaction difficult. However, positive results have been obtained

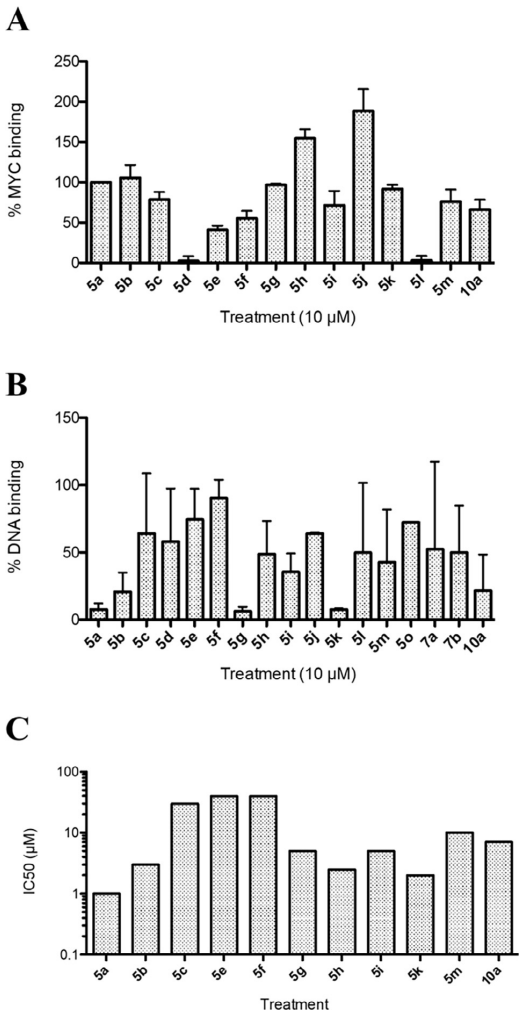

Fig. 1. Activity screening of test compounds. a) Relative binding to MYC compared with **5a**. b) Inhibition of MYC-MAX binding to DNA measured by SPR. c) IC_{50} of optimized compounds in CEF assay. Error bars are SEM, n = 3.

measuring the binding affinity for DNA using a stabilized MYC-MAX complex.[10] Using surface plasmon resonance (SPR), we established a characteristic binding response of stabilized MYC-MAX dimers to immobilized E-BOX oligonucleotides on the chip surface. Heterodimers were stabilized through disulfide formation through a C-terminal cystine residue introduced to the MYC bHLH and MAX constructs. This stabilization was found necessary to prevent aggregation of MYC monomer on the chip surface during runs. Incubation of dimer with treatment compound prior to flowing over the chip surface showed a perturbation in the sensogram when compared to the vehicle control. Compounds were incubated with dimer at 10 μM and their ability to prevent interaction with DNA measured (Fig. 1b). Importantly, compounds observed to have no interaction with MYC were also found to have no effect in preventing dimer binding to DNA, and no interaction was observed between the DNA and compounds alone.

The ultimate assessment of anti-MYC activity was done through a well-established focus assay examining the ability of an ATG-MYC expressing vector to establish microtumors in CEF.[15] Compelling compounds from binding studies were examined for inhibition of microtumor formation in this assay (Fig. 1c). Several derivatives were found to inhibit microtumor formation with similar efficacy to **5a** (Table 1). Overall, the CEF and FET data correlated well (Supplemental Fig. 1), apart from **5j**, which was of much poorer solubility than **5a**. This was opposed to the SPR data, which did not correlate well with either the FET or CEF data. We reason that this discrepancy is due to the covalent linkage of the MYC-MAX dimers, which alters the affinity necessary to perturb the complex greatly. Additionally, the MYC-MAX-DNA complex is far more stable than the heterodimer itself[16], and thus shifts the equilibrium of MYC-MAX heterodimerization. We also note that while the FET and CEF data correlate very well, there is a discrepancy between the affinity for MYC and the potency in cells. This is a common pharmacodynamic phenomenon when targeting protein-protein interactions. *MYC* is pleiotropic, the MYC-MAX complex coordinates and controls the expression of thousands of other genes, and thus the precise molecular determinants responsible for any observed phenotype related to a change in MYC concentration are unknown. The intervening factors will be illuminated by further studies of MYC biology with an effective inhibitor.

The results of these experiments provide the beginnings of a structure-activity map for MYC inhibition. In general, the whole framework of **5a** appears necessary as compounds **7a** and **7b** lost all activity when entire substituents of the central pyridine were eliminated. This may indicate the "Y-shape" of the scaffold is a necessary pharmacophore. Critically, the most prominent liability, the p-nitro moiety in R^1, was found dispensable, able to be effectively replaced with a cyano (**5b**) or thiazole heterocycle (**5g**). This also assuaged concerns that inhibition proceeds through a covalent mechanism.

By contrast, it was found there was little plasticity in the chemical space of the furan substituent at the R^2 position. Elimination of the furan ablated activity (**7a**) and replacement with another heterocycle resulted in a loss or significant attenuation of activity (**5d**, **5f**, and **5o**). In general, there are concerns that furan functionality is prone to oxidation and the formation of reactive metabolites,[17] however, it was not known the degree to which this moiety presented a pharmacokinetic liability in these particular scaffolds. We reasoned that the π-conjugation throughout the scaffold would impart increased stability to the furan from oxidation. To test this, we examined the stability of several compounds incubated with rat liver microsomes (Fig. 2). We found that while the nitro group of **5a** was readily eliminated, the furan was exceedingly recalcitrant to oxidation in these conditions. Importantly, the mass of oxidized furan ion was not detected.

Ablation of the *p*-benzylamide lost all activity (**7b**), but complete replacement of the *p*-benzylamide in **5j** was the only compound found to have significantly greater binding to MYC than **5a**, indicating a pliability. However, the solubility was reduced and it was not found to have any activity in the CEF assay. We reason that the lack of aqueous solubility even at low doses completely precludes cell penetration. In a

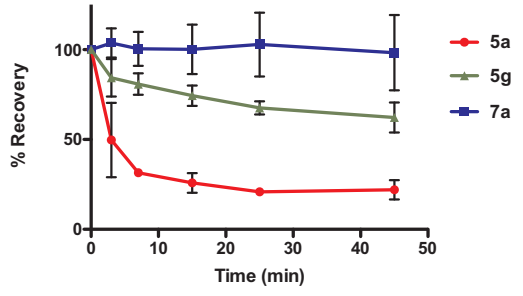

Fig. 2. Oxidation susceptibility by rat liver microsomes by mass analysis. Compounds were incubated with microsomes at 37 °C for indicated time. Recovery calculated from AUC of extracted ion.

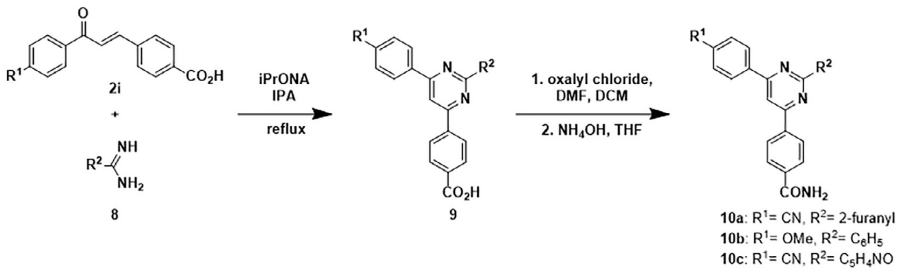

Scheme 3. Pyrimidine synthesis.

similar vein, carboxylic acids of **4** were also found inactive in both the Bio-FET and CEF assays. However, it was found there was significant plasticity in the space around the amide substituent. The use of a *N*-methylsulfonyl benzamide in **5m** had a modest improvement in solubility, but it was found lesseffective in binding MYC and had a 10-fold loss of potency compared to **5a**. Similar results were obtained with **5k**, containing a tetrazole in place of the amide, indicating an advanced plasticity in this region.

Importantly, it was also found that changes to the core heterocycle were tolerated. Diversity was introduced into the core heterocycle with the formation of a pyrimidine ring in an attempt to optimize solubility. An α,β-unsaturated ketone **2i** was refluxed with furancarboximidine **8** in the presence of excess sodium methoxide in ethanol to produce carboxylic acid **9**, which was converted to the corresponding amide via the same strategy of forming acylchloride and reacting it with NH_4OH to give pyrimidine **10** (Scheme 3). **10a** has an activity profile comparable to **5a**. Further diversification of the scaffold using a pyrimidine core presents an opportunity to produce more soluble derivatives.

Overall, **5g** is ideal in that it is readily accessed, has greatly increased solubility, lacks the labile nitro group, and demonstrates similar binding and efficacy to **5a**. The affinity of **5g** is 12.5 ± 4.1 nM, comparable to the affinity measured for **5a** of 6.5 ± 2.6 nM (Supplementary Fig. 4). A 10 mg/kg i.v. PK study was conducted in mouse to determine if these favored properties translated into improved PK. Non-compartmental analysis of the mouse PK followed by allometric scaling to the rat afforded a comparison to the rat PK study conducted previously[10] on **5a** and is shown in Table 2. This relatively simple substitution has significantly increased the mean residence time from 1 h to 4.8 producing a 30-fold improvement in exposure (AUC) (Supplementary Fig. 6). Replacement of the nitro group, along with the increased solubility, stability and concomitant increase in PK, make **5g** a significant improvement on this scaffold, with little cost to ligand efficiency (LE). The LE of **5a** and **5g** was found to be 0.40 and 0.36, respectively (Supplementary Table 1). This demonstrates that there is sufficient plasticity in the chemical space discovered through **5a** to improve the physiochemical properties without compromising efficacy.

Table 2
PK comparison of **5a** and **5g**.

	5a[a]	5a[b]	5g[c]
MW (g/mol)	385.3	385.3	423.5
Half-life (h)	1.6	1.0	4.8
AUC (ng*h/mL)	258	1450	44,000
MRT (h)	1.7	0.94	4.3
Vss (L)	6.44	6.44	0.97
Cl (mL/min/kg)	65	115	3.8

[a] Values determined in Sprague Dawley rat.
[b] Values are allometrically scaled from those determined in rat.[10]
[c] Values determined in C57Bl6 mice.

3. Conclusion

Through analysis of a blind SAR campaign, we developed a new series of compounds that retain the efficacy of **5a**, but with improved *in vivo* stability and solubility. We hypothesize there is a goldilocks effect, whereby the hydrophobicity imparted by the conjugation of the scaffold is intrinsically necessary for binding to MYC, but this hydrophobicity negatively affects the pharmacokinetic properties of such a molecule. Thus, the slight activity compromise of **5g** for the sake of solubility may represent an optimally balanced scaffold for targeting MYC. The necessary potency of a MYC inhibitor for *in vivo* efficacy remains to be delineated. **5g** provides new opportunities assessing the balance between retaining target level potency while optimizing drug-like properties. This information will help to open access to thorough biophysical characterization of this inhibition interaction to allow for a structure-based SAR campaign to be undertaken.

4. Experimental section

All solvents and chemicals were acquired from Thermo-Fisher or Millipore Sigma unless otherwise specified. Solvent was anhydrous unless otherwise specified. Purification of compounds was carried out by prep TLC on 1 mm PLC silica gel 60 F_{254} plates and by flash chromatography on a Teledyne ISCO Combiflash Rf + Lumen. Compounds and intermediates were characterized by NMR on a Bruker DPX-400 or NEO-500 instrument in indicated solvent, and high-resolution mass-spectrometry on an Agilent ESI-TOF. Purity of > 95% was determined by HPLC analysis on an Agilent 1260 Infinity (see Supplement). Compounds were screened for known PAINS compounds through 2 database searches (ZINC Patterns, FAF-Drugs4).

4.1. General procedure for compounds *5a–o*

Chalcone **2** (1 g, 4 mmol.), and NH_4OAc (9.2 g, 120 mmol) were dissolved in a mixture of acetic acid (20 mL) and DMF (30 mL). To it, pyridinium salt **1** (1.2 g. 4 mmol) was added and the reaction mixture was heated at 100 °C overnight. Solvent was evaporated under vacuum and the remaining brown oil was dissolved in DCM (100 mL) and solid $NaHCO_3$ was added until the gas release ceased. The organic phase was dried over $MgSO_4$ and evaporated under reduced pressure. The product **3** is crashed out using Et_2O-MeOH as a brown solid. This material was carried on without further purification. LiOH (2.5 g, 104 mmol) was added to a solution of **3** in THF:H_2O (9:1) and stirred overnight. The reaction mixture was filtered through a pad of silica gel and evaporated to dryness to afford carboxylic acid **4**. **4** (3 g, 8.2 mmol.) was dissolved in dry DCM (100 mL) and oxalyl chloride (0.7 mL, 8.2 mmol) followed by 1 drop of DMF. The reaction was stirred at room temperature overnight, then the solvent was removed in vacuo and the remaining solid was redissolved in dry DCM (100 mL). The solution was poured onto a NH_4OH solution (50 mL) and the reaction mixture was stirred for 30 min. The organic layer was separated, dried and evaporated under

vacuo to afford a brown oil which was purified to obtain pyridine **5**.

5b: ^{1}H NMR (600 MHz, DMSO-d_6): δ= 8.54 (d, J = 12 Hz, 2H), 8.35 (s, 1H), 8.12 (m, 3H), 8.08 (d, J = 6 Hz, 2H), 8.04 (d, J = 12 Hz, 2H), 7.94 (s, 1H), 7.50 (brs, 1H), 7.42 (s, 1H), 6.75 (s, 1H); ^{13}C NMR (150 MHz, DMSO-d_6): δ = 167.23, 154.81, 152.78, 149.39, 148.74, 144.66, 142.48, 139.50, 134.99, 132.70, 128.25, 127.77, 127.19, 118.83, 117.28, 115.59, 112.48, 111.77, 110.14; HRMS (ESI-TOF): m/z calcd for $C_{24}H_{17}N_3O_2$: 366.1237 $(M+H)^+$; found: 366.1238.

5c: ^{1}H NMR (600 MHz, DMSO-d_6): δ = 8.54 (m, 3H), 8.47 (d, J = 12 Hz, 1H), 8.16 (brs, 1H), 8.15 (d, J = 6 Hz, 2H), 8.10–8.07 (m, 5H), 8.00 (d, J = 6 Hz, 1H), 7.51 (brs, 1H); ^{13}C NMR (150 MHz, DMSO-d_6): δ = 167.98, 167.20, 155.01, 151.43, 149.35, 144.47, 141.78, 139.12, 135.21, 132.87, 128.35, 127.75, 127.27, 123.37, 119.94, 118.76, 116.21, 112.08; HRMS (ESI-TOF): m/z calcd for $C_{22}H_{14}N_4OS$: 383.0961 $(M+H)^+$; found: 383.0960.

5d: ^{1}H NMR (600 MHz, DMSO-d_6): δ = 8.58 (s, 1H), 8.56 (d, J = 6 Hz, 2H), 8.44 (s, 1H), 8.41 (s, 1H), 8.16 (brs,1H), 8.15 (d, J = 6 Hz, 2H), 8.09 (d, J = 6 Hz, 2H), 8.06 (d, J = 6 Hz, 2H), 7.56 (s, 1H), 7.51 (s, 1H); ^{13}C NMR (150 MHz, DMSO-d_6): δ = 167.19, 159.87, 155.32, 149.11, 146.41, 142.04, 141.50, 138.94, 135.23, 132.80, 128.99, 128.35, 127.90, 127.28, 120.01, 119.00, 118.75, 112.03; HRMS (ESI-TOF): m/z calcd for $C_{22}H_{14}N_4O_2$: 367.1189 $(M+H)^+$; found: 367.1183.

5e: ^{1}H NMR (600 MHz, DMSO-d_6): δ = 8.51 (d, J = 6 Hz, 2H), 8.45 (d, J = 6 Hz, 1H), 8.41 (d, J = 1.5 Hz, 1H), 8.15 (brs, 1H), 8.09 (d, J = 3 Hz, 4H), 8.03 (d, J = 6 Hz, 2H),7.96 (d, J = 12 Hz, 2H), 7.50 (brs, 1H), 7.42 (s, 1H), 7.11 (d, J = 1 Hz, 1H), 4.23 (s, 3H); ^{13}C NMR (150 MHz, DMSO-d_6): δ = 167.25, 154.25, 151.18, 148.53, 143.60, 142.73, 139.54, 135.02, 132.83, 132.38, 128.36, 128.00, 127.09, 125.79, 119.09, 118.81 117.64, 111.75, 36.47; HRMS (ESI-TOF): m/z calcd for $C_{23}H_{17}N_5O$: 380.1506 $(M+H)^+$; found: 380.1504.

5f: ^{1}H NMR (600 MHz, DMSO-d_6): δ = 8.60 (s, 1H), 8.53 (d, J = 6 Hz, 2H), 8.50 (s, 1H), 8.36 (s, 1H), 8.20 (d, J = 6 Hz, 2H), 8.16 (brs, 1H), 8.09 (d, J = 12 Hz, 2H), 8.05 (d, J = 12 Hz, 2H), 7.53 (brs, 1H), 4.50 (s, 3H); ^{13}C NMR (150 MHz, DMSO-d_6): δ = 167.18, 155.05, 149.18, 147.61, 142.36, 139.00, 135.62, 135.17, 134.48, 132.85, 128.20, 127.91, 127.39, 120.20, 119.50, 118.75, 118.45, 112.0, 37.96; HRMS (ESI-TOF): m/z calcd for $C_{22}H_{16}N_6O$: 381.1458 $(M+H)^+$; found: 381.1457.

5 g: ^{1}H NMR (600 MHz, DMSO-d_6): δ = 8.46 (d, J = 12 Hz, 2H), 8.28 (s, 1H), 8.16 (brs, 1H), 8.12 (m, 3H), 8.08 (d, J = 12 Hz, 2H), 8.00 (d, J = 3 Hz, 1H), 7.94 (s, 1H), 7.86 (s, d, J = 3 Hz, 1H), 7.51 (brs, 1H), 7.40 (s, 1H), 6.75 (s, 1H); ^{13}C NMR (150 MHz, DMSO-d_6): δ = 167.29, 166.58, 155.80, 153.00, 149.26, 148.55, 144.50, 144.08, 139.78, 139.67, 134.90, 133.78, 128.77, 127.77, 127.13, 126.48, 120.88, 116.62, 114.92, 112.43, 109.89; HRMS (ESI-TOF): m/z calcd for $C_{25}H_{17}N_3O_2S$: 424.1114 $(M+H)^+$; found: 424.1116.

5 h: ^{1}H NMR (600 MHz, DMSO-d_6): δ = 8.52 (s, 1H), 8.45 (d, J = 12 Hz, 2H), 8.27 (s, 1H), 8.15 (brs, 1H), 8.12 (m, 3H), 8.04 (s, 1H), 7.93 (m, 3H), 7.94 (s, 1H), 7.84 (s, 1H), 7.50 (brs, 1H), 7.39 (s, 1H), 6.74 (s, 1H); ^{13}C NMR (150 MHz, DMSO-d_6): δ = 167.28, 155.89, 153.03, 152.14, 150.21, 149.21, 148.51, 144.48, 139.81, 138.18, 134.88, 128.25, 128.17, 127.68, 127.13, 124.35, 122.81, 116.45, 114.76, 112.42, 109.84; HRMS (ESI-TOF): m/z calcd for $C_{25}H_{17}N_3O_3$: 408.1343 $(M+H)^+$; found: 408.1350.

5i: ^{1}H NMR (600 MHz, $CDCl_3$): δ = 8.28 (d, J = 12 Hz, 2H), 7.96 (s, 1H), 7.85 (s, 1H), 7.82 (d, J = 12 Hz, 2H), 7.78 (d, J = 6 Hz, 2H), 7.61 (s, 1H), 7.58–7.52 (m, 3H), 7.27 (s, 1H), 6.62 (s, 1H); ^{13}C NMR (150 MHz, $CDCl_3$): δ = 154.94, 153.20, 150.02, 149.62, 143.12, 142.98, 137.76, 132.07, 128.92, 128.75, 127.18, 126.63, 118.43, 116.77, 115.67, 112.07, 111.76, 109.01; HRMS (ESI-TOF): m/z calcd for $C_{22}H_{14}N_2O$: 323.1179 $(M+H)^+$; found: 323.1182.

5j: ^{1}H NMR (600 MHz, DMSO-d_6): δ = 8.37 (d, J = 12 Hz, 2H), 8.31 (s, 1H), 8.15 (s, 1H), 8.12 (s, 1H), 8.11 (d, J = 12 Hz, 2H), 8.05 (d, J = 6 Hz, 1H), 8.00 (d, J = 6 Hz, 1H), 7.94 (s, 1H), 7.86 (s, 1H), 7.37 (s, 1H), 6.74 (s, 1H); ^{13}C NMR (150 MHz, DMSO-d_6): δ = 166.48, 164.37, 156.18, 152.55, 149.47, 144.83, 144.51, 144.09, 141.89, 139.04, 133.99, 127.67, 126.58, 123.05, 120.95, 114.96, 113.28, 112.53, 110.20; HRMS (ESI-TOF): m/z calcd for $C_{21}H_{13}N_3OS_2$: 388.0573 $(M+H)^+$; found: 388.0574.

5 k: ^{1}H NMR (600 MHz, DMSO-d_6): δ = 8.54 (d, J = 12 Hz, 2H), 8.34 (s, 1H), 8.18 (d, J = 12 Hz, 2H), 8.11 (s, 1H), 8.07 (d, J = 12 Hz, 2H), 8.03 (d, J = 12 Hz, 3H), 7.94 (s, 1H), 7.41 (s, 1H), 6.74 (s, 1H); ^{13}C NMR (150 MHz, DMSO-d_6): δ = 160.11, 154.69, 152.94, 149.45, 149.31, 144.53, 142.68, 135.00, 134.00, 132.68, 127.74, 127.26, 126.28, 118.86, 116.79, 115.05, 112.42, 111.64, 109.90; HRMS (ESI-TOF): m/z calcd for $C_{23}H_{14}N_6O$: 391.1302 $(M+H)^+$; found: 391.1315.

4.2. Scheme for synthesis of compounds 5m–5o

Carboxylic acid **4a** (1 g, 2.7 mmol.) was dissolved in dry DCM (100 mL) and oxalyl chloride (0.5 mL, 5 mmol) followed by DMF (1 drop) were added. The reaction was stirred at room temperature overnight. Then, the solvent was removed in vacuo and the remaining solid was redissolved in dry DCM (100 mL). The solution was poured onto a solution of (a) methylamine and DIPEA (1:1) (25 mL); (b) methanesulfonamide (300 mg, 3.15 mmol) and DIPEA (10 mL) or (c) hydrazine and DIPEA (1:1) (25 mL) and the reaction mixture was stirred for 30 min. Then, the organic layer was washed with water, separated, dried and evaporated under vacuo to afford **5l**, **5m** and **5n** respectively. The products were purified by prep TLC using DCM/MeOH (85:15) as eluent.

5l: ^{1}H NMR (600 MHz, DMSO-d_6): δ = 8.63 (m, 2H), 8.53 (d, J = 12 Hz, 2H), 8.35 (s, 1H), 8.14 (d, J = 12 Hz, 2H), 8.11 (s, 1H), 8.04 (m, 3H), 7.94 (s, 1H), 7.42 (s, 1H), 6.74 (s, 1H), 2.84 (s, 3H); ^{13}C NMR (150 MHz, DMSO-d_6): δ = 165.92, 154.82, 152.78, 149.39, 148.70, 144.66, 142.48, 139.29, 135.19, 132.70, 127.83, 127.77, 127.24, 118.83, 117.25, 115.55, 112.48, 111.77, 110.13; HRMS (ESI-TOF): m/z calcd for $C_{24}H_{17}N_3O_2$: 380.1393 $(M+H)^+$; found: 380.1394.

5m: ^{1}H NMR (600 MHz, DMSO-d_6): δ = 8.54 (d, J = 6 Hz, 2H), 8.32 (s, 1H), 8.12 (d, J = 6 Hz, 2H), 8.08 (s, 1H), 8.01 (m, 4H), 7.94 (brs, 1H), 7.93 (s, 1H), 7.40 (s, 1H), 6.74 (m, 1H), 2.89 (s, 3H); ^{13}C NMR (150 MHz, DMSO-d_6): δ = 169.75, 154.73, 152.86, 149.32, 144.57, 142.58, 140.75, 137.93, 132.68, 129.74, 129.00, 127.76, 126.34, 118.85, 117.10, 115.40, 112.43, 111.68, 109.98, 43.13; HRMS (ESI-TOF): m/z calcd for $C_{24}H_{17}N_3O_4S$: 444.1012 $(M+H)^+$; found: 444.1017.

5n: ^{1}H NMR (600 MHz, DMSO-d_6): δ = 9.96 (s, 1H), 8.54 (d, J = 12 Hz, 2H), 8.35 (s, 1H), 8.14 (d, J = 6 Hz, 2H), 8.11 (s, 1H), 8.03 (d, J = 12 Hz, 3H), 7.94 (s, 1H), 7.41 (s, 1H), 6.75 (s, 1H), 4.57 (s, 2H); ^{13}C NMR (150 MHz, DMSO-d_6): δ = 165.11, 154.81, 152.77, 149.39, 148.69, 144.66, 142.48, 139.34, 134.01, 132.70, 127.76, 127.27, 118.82, 117.24, 115.55, 112.47, 111.77, 110.13; HRMS (ESI-TOF): m/z calcd for $C_{23}H_{16}N_4O_2$: 381.1346 $(M+H)^+$; found: 381.1358.

4.3. Synthesis of 7a

To a solution of 4-bromo-2-(4-cyanophenyl)pyridine (200 mg, 0.77 mmol) in dry DME (3 mL) was added 4-aminocarbonyl phenyl boronic acid (152 mg, 0.80 mmol.) and water (1 mL). Then, K_2CO_3 (320 mg, 2.3 mmol) and $Pd(PPh_3)_4$ (36 mg, 0.03 mmol) were added and the reaction heated at 85 °C overnight. The reaction mixture was evaporated, adsorbed over silica gel and purified by column chromatography using EtOAc as eluent to afford **7a** as a white solid (160 mg). ^{1}H NMR (600 MHz, DMSO-d_6): δ = 8.82 (d, J = 6 Hz, 1H), 8.45 (m, 3H), 8.13 (brs, 1H), 8.06 (m, 4H), 7.84 (d, J = 6 Hz, 1H), 7.49 (brs, 1H); ^{13}C NMR (150 MHz, DMSO-d_6): δ = 167.25, 154.98, 150.54, 147.61, 142.84, 139.54, 134.89, 132.69, 128.25, 127.66, 127.09, 121.28, 118.83, 111.60; HRMS (ESI-TOF): m/z calcd for $C_{19}H_{13}N_3O$: 300.1131 $(M+H)^+$; found: 300.1132.

4.4. Synthesis of **7b**

To a solution of 2-bromo-6-(furan-2-yl)pyridine (280 mg, 1.25 mmol.) in dry DME (3 mL) was added 4-cyanophenyl boronic acid (220 mg, 1.3 mmol.) and water (1 mL). Then, K_2CO_3 (520 mg, 3.75 mmol.) and $Pd(PPh_3)_4$ (60 mg, 0.05 mmol.) were added and the reaction heated at 85 °C overnight. The reaction mixture was evaporated, adsorbed over silica gel and purified by column chromatography using Hex/EtOAc (8:2) as eluent to afford **7b** as a white solid (180 mg). ^{1}H NMR (600 MHz, $CDCl_3$): δ = 8.23 (d, J = 6 Hz, 2H), 7.86 (t, J = 6 Hz, 1H), 7.80 (m, 1H), 7.73 (d, J = 6 Hz, 1H), 7.66 (d, J = 6 Hz, 1H), 7.59 (s, 1H), 7.22 (s, 1H), 6.60 (m, 1H); ^{13}C NMR (150 MHz, $CDCl_3$): δ = 154.24, 153.10, 149.15, 143.11, 142.84, 137.26, 132.05, 127.04, 118.42, 117.52, 111.69, 108.78; HRMS (ESI-TOF): m/z calcd for $C_{16}H_{10}N_2O$: 247.0866 $(M+H)^+$; found: 247.0866.

4.4.1. General Procedure for compounds **10a–c**

To a solution of furancarboximidine **8** (250 mg, 1.72 mmol) in IPA (20 mL) was added Na (45 mg, 2 mmol) and the reaction was refluxed for 2 h. Afterwards, **2** (500 mg, 1.72 mmol) was added and the mixture was refluxed overnight. Then, it was evaporated to dryness under vacuum, dissolved in DCM:MeOH (8:2) and filtered through a pad of silica gel. The filtrate was evaporated to dryness to give a red oil. Carboxylic acid **9** was precipitated using EtOAc:Hex (1:1) as a yellow solid (55%). This material was carried on without further purification. **9** (200 mg, 0.55 mmol) was dissolved in DCM (20 mL) and oxalyl chloride (0.2 mL, 36 mmol) followed by 1 drop of DMF. The reaction was stirred at room temperature overnight. Solvent was removed in vacuo and the remaining solid was redissolved in DCM (50 mL). The solution was poured onto a NH_4OH solution (50 mL) and the reaction mixture was stirred for 30 min. The organic layer was separated, dried and evaporated under vacuo to afford a brown oil which was purified to obtain pyrimidine **10**.

10a: ^{1}H NMR (600 MHz, DMSO-d_6): δ = 8.66 (s, 1H), 8.65 (d, J = 2 Hz, 2H), 8.55 (d, J = 12 Hz, 2H), 8.18 (s, 1H), 8.10 (m, 4H), 8.03 (s, 1H), 7.60 (s, 1H), 7.55 (s, 1H), 6.79 (s, 1H); ^{13}C NMR (150 MHz, DMSO-d_6): δ = 167.24, 163.91, 162.60, 157.33, 151.72, 146.12, 140.41, 138.39, 136.65, 132.89, 128.20, 128.04, 127.35, 118.55, 114.35, 113.49, 112.61, 111.30; HRMS (ESI-TOF): m/z calcd for $C_{22}H_{14}N_4O_2$: 367.1189 $(M+H)^+$; found: 367.1202.

10b: ^{1}H NMR (400 MHz, DMSO-d_6): δ = 8.35 (d, 2H), 8.22 (m, 1H), 8.10 (d, 2H), 7.82 (bs, 2H), 7.90 (m, 4H), 7.80 (d, 2H), 7.50 (m, 3H); HRMS (ESI-TOF): m/z calcd for $C_{22}H_{16}N_4O$: 377.1402 $(M+H)^+$; found: 377.1482.

10c: ^{1}H NMR (400 MHz, DMSO-d_6): δ = 8.66 (s, 1H), 8.65 (d, J = 2 Hz, 2H), 8.55 (d, J = 12 Hz, 2H), 8.18 (s, 1H), 8.10 (m, 4H), 8.03 (s, 1H), 7.60 (s, 1H), 7.55 (s, 1H), 6.79 (s, 1H); HRMS (ESI-TOF): m/z calcd for $C_{22}H_{16}N_4O$: 382.1555 $(M+H)^+$; found: 382.1482.

Author contributions

The manuscript was written through contributions of all authors. All authors have given approval to the final version of the manuscript.

Notes

This is manuscript number 29684 from the Scripps Research Institute.

Acknowledgments

This work was supported by the Skaggs Institute for Chemical Biology, the National Institutes of Health (R35 CA197582 to P.K.V., and CTSA TL1TR002551 to N.T.J), and the Seventh Framework Program of the European Union (REA Grant Agreement No. 623155 to P.O.M.).

A. Supplementary data

Supplementary data (supplementary figures, biological protocols, sensogram data, compound characterizations, and expanded synthetic procedures anf molecular formula strings) associated with this article can be found, in the online version, at https://doi.org/10.1016/j.bmc.2018.07.019.

References

1. Adhikary S, Eilers M. Transcriptional regulation and transformation by Myc proteins. *Nat Rev Mol Cell Biol.* 2005;6:635–645.
2. Eilers M, Eisenman RN. Myc's broad reach. *Genes Dev.* 2008;22:2755–2766.
3. Varlakhanova NV, Knoepfler PS. Acting locally and globally: Myc's ever-expanding roles on chromatin. *Cancer Res.* 2009;69:7487–7490.
4. Gabay M, Li Y, Felsher DW. MYC activation is a hallmark of cancer initiation and maintenance. *Cold Spring Harb Perspect Med.* 2014;4:a014241.
5. Dang CV. MYC on the path to cancer. *Cell.* 2012;149:22–35.
6. Ruggero D. The role of Myc-induced protein synthesis in cancer. *Cancer Res.* 2009;69:8839–8843.
7. Kress TR, Sabò A, Amati B. MYC: connecting selective transcriptional control to global RNA production. *Nat Rev Cancer.* 2015;15:593–607.
8. Conacci-Sorrell M, McFerrin L, Eisenman RN. An overview of MYC and its interactome. *Cold Spring Harb Perspect Med.* 2014;4:a014357.
9. McKeown MR, Bradner JE. Therapeutic strategies to inhibit MYC. *Cold Spring Harb Perspect Med.* 2014;4:a014266.
10. Hart JR, Garner AL, Yu J, et al. Inhibitor of MYC identified in a Krohnke pyridine library. *Proc Natl Acad Sci USA.* 2014;111:12,556–12,561.
11. Lerner MB, Pan D, Gao Y, et al. Large scale commercial fabrication of high quality graphene-based assays for biomolecule detection. *Sens Actuators, B.* 2017;239:1261–1267.
12. Wang L, Estrela P, Huq E, et al. Fabrication of BioFET linear array for detection of protein interactions. *Microelectron Eng.* 2010;87:753–755.
13. Kerkhoff E, Bister K, Klempnauer KH. Sequence-specific DNA binding by Myc proteins. *PNAS.* 1991;88:4323–4327.
14. Hu J, Banerjee A, Goss DJ. Assembly of B/HLH/Z proteins C-Myc, Max, and Mad1 with cognate DNA: importance of protein-protein and protein-DNA interactions. *Biochemistry.* 2005;44:11,855–11,863.
15. Bos TJ, Monteclaro FS, Mitsunobu F, et al. Efficient transformation of chicken embryo fibroblasts by C-jun requires structural modification in coding and noncoding sequences. *Genes Dev.* 1990;4:1677–1687.
16. Fieber W, Schneider ML, Matt T, Krautler B, Konrat R, Bister K. Structure, Function, and Dynamics of the Dimerization and DNA-binding Domain of Oncogenic Transcription Factor c-MYC. *J Mol Biol.* 2001;307:1395–1410.
17. Peterson LA. Reactive metabolites in the biotransformation of molecules containing a furan ring. *Chem Res Toxicol.* 2013;26:6–25.

UNIVERSITAT ROVIRA I VIRGILI
GOLD-CATALYZED INTERMOLECULAR REACTIONS OF ALKYNES WITH ALKENES: NOVEL REACTIVITIES AND GLOBAL MECHANISTIC PICTURE
María Elena de Orbe Izquierdo

UNIVERSITAT ROVIRA I VIRGILI
GOLD-CATALYZED INTERMOLECULAR REACTIONS OF ALKYNES WITH ALKENES: NOVEL REACTIVITIES AND GLOBAL MECHANISTIC PICTURE
María Elena de Orbe Izquierdo

UNIVERSITAT ROVIRA I VIRGILI
GOLD-CATALYZED INTERMOLECULAR REACTIONS OF ALKYNES WITH ALKENES: NOVEL REACTIVITIES AND GLOBAL MECHANISTIC PICTURE
María Elena de Orbe Izquierdo

UNIVERSITAT
ROVIRA i VIRGILI